THE ROLE OF DNA REPAIR PATHWAYS IN RESISTANCE TO CHEMOTHERAPY AND RADIOTHERAPY IN CANCER

EDITED BY: José Díaz-Chávez, Rosa Maria Bermudez-Cruz and David Y. Lee

PUBLISHED IN: Frontiers in Oncology and Frontiers in Cell and Developmental Biology

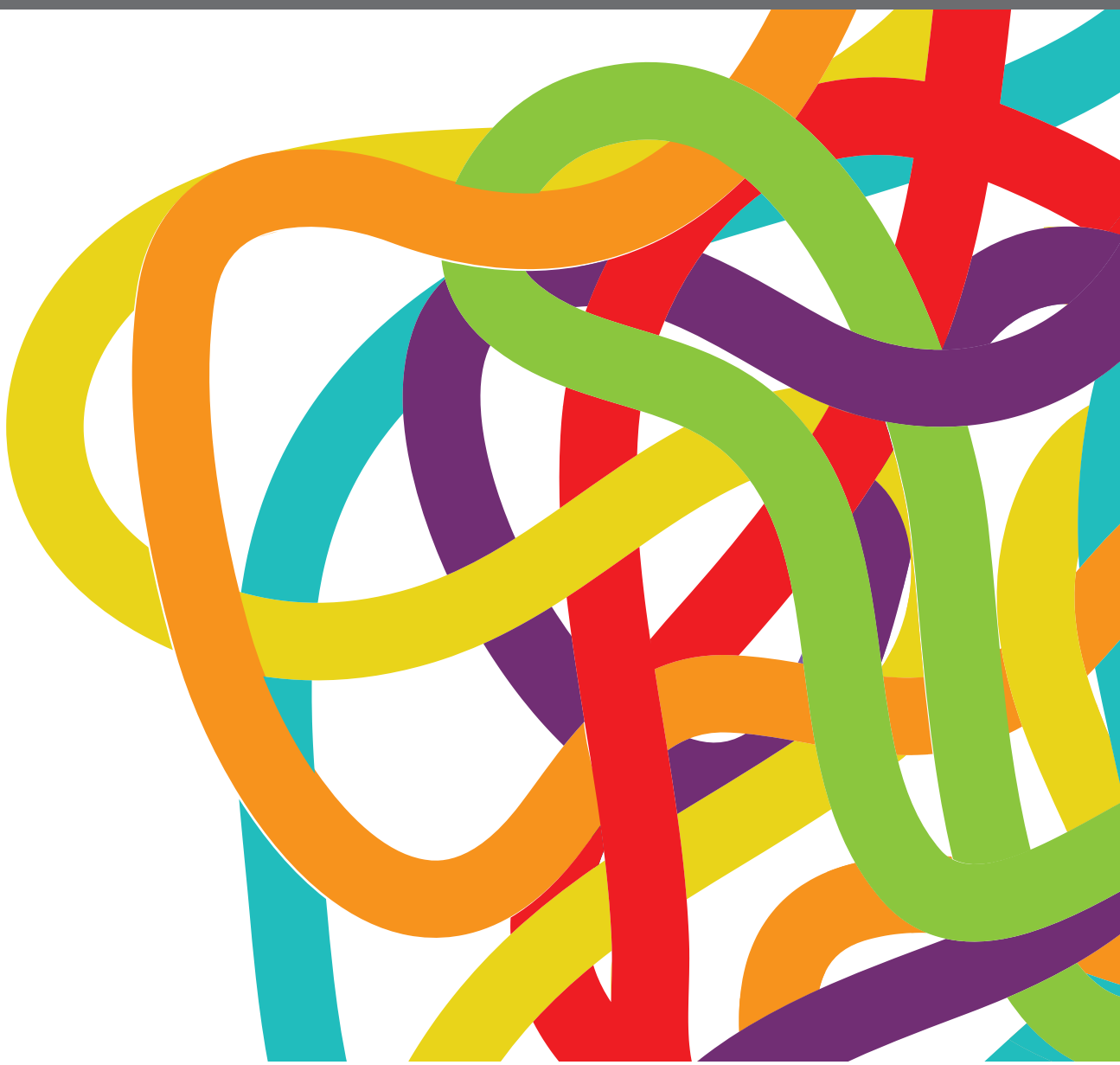

frontiers Research Topics

ISSN 1664-8714
ISBN 978-2-88976-048-0
DOI 10.3389/978-2-88976-048-0

About Frontiers

Frontiers is more than just an open-access publisher of scholarly articles: it is a pioneering approach to the world of academia, radically improving the way scholarly research is managed. The grand vision of Frontiers is a world where all people have an equal opportunity to seek, share and generate knowledge. Frontiers provides immediate and permanent online open access to all its publications, but this alone is not enough to realize our grand goals.

Frontiers Journal Series

The Frontiers Journal Series is a multi-tier and interdisciplinary set of open-access, online journals, promising a paradigm shift from the current review, selection and dissemination processes in academic publishing. All Frontiers journals are driven by researchers for researchers; therefore, they constitute a service to the scholarly community. At the same time, the Frontiers Journal Series operates on a revolutionary invention, the tiered publishing system, initially addressing specific communities of scholars, and gradually climbing up to broader public understanding, thus serving the interests of the lay society, too.

Dedication to Quality

Each Frontiers article is a landmark of the highest quality, thanks to genuinely collaborative interactions between authors and review editors, who include some of the world's best academicians. Research must be certified by peers before entering a stream of knowledge that may eventually reach the public - and shape society; therefore, Frontiers only applies the most rigorous and unbiased reviews.
Frontiers revolutionizes research publishing by freely delivering the most outstanding research, evaluated with no bias from both the academic and social point of view. By applying the most advanced information technologies, Frontiers is catapulting scholarly publishing into a new generation.

What are Frontiers Research Topics?

Frontiers Research Topics are very popular trademarks of the Frontiers Journals Series: they are collections of at least ten articles, all centered on a particular subject. With their unique mix of varied contributions from Original Research to Review Articles, Frontiers Research Topics unify the most influential researchers, the latest key findings and historical advances in a hot research area! Find out more on how to host your own Frontiers Research Topic or contribute to one as an author by contacting the Frontiers Editorial Office: frontiersin.org/about/contact

THE ROLE OF DNA REPAIR PATHWAYS IN RESISTANCE TO CHEMOTHERAPY AND RADIOTHERAPY IN CANCER

Topic Editors:
José Díaz-Chávez, Instituto Nacional de Cancerología (INCAN), Mexico
Rosa Maria Bermudez-Cruz, Centro de Investigaciones y Estudios Avanzados, Instituto Politécnico Nacional de México (CINVESTAV), Mexico
David Y. Lee, University of New Mexico, United States

Citation: Díaz-Chávez, J., Bermudez-Cruz, R. M., Lee, D. Y., eds. (2022). The Role of DNA Repair Pathways in Resistance to Chemotherapy and Radiotherapy in Cancer. Lausanne: Frontiers Media SA. doi: 10.3389/978-2-88976-048-0

Table of Contents

frontiers | Frontiers in Oncology

EDITORIAL
published: 08 April 2022
doi: 10.3389/fonc.2022.894357

Editorial: The Role of DNA Repair Pathways in Resistance to Chemotherapy and Radiotherapy in Cancer

David Y. Lee[1], *Rosa María Bermúdez-Cruz*[2] *and José Díaz-Chávez*[3*]

[1] Department of Internal Medicine, Division of Hematology/Oncology, Section of Radiation Oncology, University of New Mexico School of Medicine and Comprehensive Cancer Center, Albuquerque, NM, United States, [2] Departamento de Genética y Biología Molecular, Centro de Investigación y de Estudios Avanzados (CINVESTAV-IPN), Ciudad de México, Mexico, [3] Unidad de Investigación Biomédica en Cáncer, Instituto de Investigaciones Biomédicas, Universidad Nacional Autónoma de México (UNAM)/Instituto Nacional de Cancerología (INCan), Ciudad de México, Mexico

Keywords: DNA repair pathways, cancer, chemoresistance, radioresistance, DNA damage response

Editorial on the Research Topic:

The Role of DNA Repair Pathways in Resistance to Chemotherapy and Radiotherapy in Cancer

OPEN ACCESS

Edited and reviewed by:
Tao Liu,
University of New South Wales, Australia

***Correspondence:**
José Díaz-Chávez
jdiazchavez03@gmail.com

Specialty section:
This article was submitted to Molecular and Cellular Oncology, a section of the journal Frontiers in Oncology

Received: *11 March 2022*
Accepted: *18 March 2022*
Published: *08 April 2022*

Citation:
Lee DY, Bermúdez-Cruz RM and Díaz-Chávez J (2022) Editorial: The Role of DNA Repair Pathways in Resistance to Chemotherapy and Radiotherapy in Cancer. Front. Oncol. 12:894357. doi: 10.3389/fonc.2022.894357

INTRODUCTION

Over the past decade, there has been enormous progress in treating cancer patients with the continued development of novel targeted therapies (1), the advent of immunotherapy (2), and novel radiation therapy technologies (3). However, resistance to radiation therapy and chemotherapy continues to be a major problem in our field, for which many patients ultimately succumb to the disease. Although we celebrate the approval of each new targeted therapy, we invariable find that cancer cells develop resistance to each one. Furthermore, it is still very difficult to predict who will respond to immunotherapy. Therefore, the search for radiation therapy sensitizers continues.

Through our Research Topic, several principles have emerged that may guide us in the future to overcome this resistance. First, some biomarkers may predict who will be more resistant to radiation and/or chemotherapy. Zhang et al. showed that nasopharyngeal carcinoma patients with elevated levels of LCN2 (Lipocalin 2) showed resistance to radiation therapy. We could consider treatment intensification for these patients with LCN2 elevation by considering higher radiation doses or the addition of novel targeted therapies. Similarly, Fang et al. demonstrated that increased levels of NTGN1 (neuroligin 1) predicted resistance to cisplatin treatment in epithelial ovarian cancer cells, identifying a subgroup of patients for treatment intensification with additional systemic agents. Huang et al. utilized epithelial-mesenchymal transformation and DNA repair gene panels to classify colorectal cancer patients, which may guide treatment selection of chemotherapy vs immunotherapy to optimize treatment response.

Second, some pathways can ameliorate existing treatments by synergistic effect or through synthetic lethal interactions. Rose et al. prepared a wonderful review on the role of PARP inhibitors, specifically in the setting of tumors harboring BRCA1/2 mutations. The synthetic lethal interaction between PARP inhibitor and BRCA1/2 mutations represent one of the successful translation of basic research (4). Cancers with defects or mutations in the homologous recombination (HR) DNA repair pathway also

respond to radiation therapy. Therefore, the PARP inhibitor and radiation therapy combination should be considered to obtain a durable response. Interestingly, Sabbatino et al. observed that patients with intrahepatic cholangiocarcinoma harboring BAP1 (BRCA1 Associated Protein 1) mutation may be sensitive to a PARP inhibitor. This is because BAP1 interacts with BRCA1, and BAP1 mutation likely alters the HR DNA repair pathway. Thus, consideration should be given for a potential role to PARP inhibitors in situations with alternations in the HR pathway, not just BRCA1/2 mutations.

The synergistic effect between temozolomide and mifepristone was shown by Llaguno-Munive et al. Mifepristone, an antihormonal agent, can enhance the effects of temozolomide by decreasing the levels of VEGF (vascular endothelial growth factor) and P-glycoprotein in murine orthotopic glioblastoma model. Since mifepristone would be repurposed for glioblastoma treatment, this drug represents a potential target for rapid clinical translation. Whether mifepristone and temozolomide can be combined with radiation therapy safely would be an important question to address. Similarly, Hong et al. demonstrated that the inhibition of thioredoxin reductase 1 by isodeoxyelephantopin synergistically enhanced the effect of cisplatin in colon cancer cells. Thus, the addition of new agents such as mifepristone or thioredoxin reductase 1 inhibitor to existing treatment can lead to synergistic effects and overcome or delay potential chemo/radiation resistance.

Third, there are potential novel pathways and inhibitors that can modulate the effect of radiation or chemotherapy. The role of non-coding RNAs and exosomes in radiation and chemotherapy response was addressed by Zhang et al. and Zhong et al., respectively. While a role for non-coding RNAs was shown in neck and head cancer radiotherapy, exosomes, vesicles which also transport non-coding RNAs plus protein are suggested to play a role in drug resistance in cancer. Concerning chemo/radiation resistance, these two areas of research, poorly studied, hold the potential to dramatically alter our understanding of chemo/radiation resistance. How the RAS oncogenic pathway impinges on the DNA repair pathway and subsequent therapeutic resistance is addressed by Caceres-Gutierrez et al. with the recent approval of RAS G12C mutant inhibitor (5), one could consider how this inhibitor could be combined with radiation therapy in lung and pancreas patients who frequently harbor this mutation. Wang et al. provide evidence for alternations in DNA damage repair pathways in esophageal squamous cell carcinomas, and Carlos-Reyes et al. describe biological adaptations of tumor cells to radiation therapy along with implications of such adaptation in patients outcome.

Avery et al. reviewed the role of GLI1 (glioma Family Zinc Finger 1) as a therapeutic target in cancer. One of the GLI1 inhibitors, Vismodegib, has shown a dramatic effect on unresectable basal cell carcinomas of the skin (6). Clinically, we are now able to convert some of the unresectable basal cell carcinoma patients to surgery by shrinking the tumor. Questions still remain on the duration of Vismodegib treatment before resistance develops, the extent of surgical resection, and radiation therapy's role in the optimal management of basal cell carcinoma patients. Then, Lagunas-Rangel et al. provide a list of natural compounds that target DNA repair pathways. Currently, there has been significant difficulty in developing novel radiation therapy sensitizers, and the list of natural compounds provides an excellent starting point.

A fourth approach to sensitize drug-resistant cancers has been by including PDT (photodynamic therapy) in different types of cancer treatment (7). Gemcitabine has been described to cause DNA damage and is used to control hepatic cancer cells (8). Yang et al. in this particular case, have shown that cholangiocarcinoma cells resistant to gemcitabine and exposed to PDT display apoptosis, viability is reduced, and they are arrested in the G1 cell cycle phase.

In summary, our Research Topic has illuminated our understanding of radiation and chemotherapy resistance mechanisms, also some novel biomarkers to predict such resistance, novel pathways that interact by synergistic or synthetic lethal interactions, and potential inhibitors and pathways that may enhance the effect of radiation and/or chemotherapy.

AUTHOR CONTRIBUTIONS

All authors listed have made a substantial, direct, and intellectual contribution to the Research Topic and approved it for publication.

ACKNOWLEDGMENTS

We are grateful to all the authors and reviewers of this Frontiers Research Topic for their excellent contribution. We also thank the editorial team at Frontiers for their invaluable support.

REFERENCES

1. Mangat PK, Halabi H, Bruinooge SS, Garrett-Mayer E, Alva A, Janeway KA. Rationale and Design of the Targeted Agent and Profiling Utilization Registry (TAPUR) Study. *JCO Precis Oncol* (2018) 2018:10.1200/PO.18.00122. doi: 10.1200/PO.18.00122
2. Sharma P, Siddiqui BA, Anandhan S, Yadav SS, Subudhi SK, Gao J, et al. The Next Decade of Immune Checkpoint Therapy. *Cancer Discovery* (2021) 11:838–57. doi: 10.1158/2159-8290.CD-20-1680
3. Chandra RA, Keane FK, Voncken FEM, Thomas CRJr. Contemporary Radiotherapy: Present and Future. *Lancet* (2021) 398:171–84. doi: 10.1016/S0140-6736(21)00233-6
4. Poveda A, Floquet A, Ledermann JA, Asher R, Penson RT, Oza AM. Olaparib Tablets as Maintenance Therapy in Patients With Platinum-Sensitive Relapsed Ovarian Cancer and a BRCA1/2 Mutation (SOLO2/ENGOT-Ov21): A Final Analysis of a Double-Blind, Randomised, Placebo-Controlled, Phase 3 Trial. *Lancet Oncol* (2021) 22:6208–311. doi: 10.1016/S1470-2045(21)00073-5
5. Hong DS, Fakih MG, Strickler JH, Desai J, Durm GA, Shapiro GI, et al. KRAS^{G12C} Inhibition With Sotorasib in Advanced Solid Tumors. *N Engl J Med* (2020) 383:1207–17. doi: 10.1056/NEJMoa1917239
6. Tay EY, Teoh YL, Yeo MS. Hedgehog Pathway Inhibitors and Their Utility in Basal Cell Carcinoma: A Comprehensive Review of Current Evidence. *Dermatol Ther (Heidelb)* (2019) 9:33–49. doi: 10.1007/s13555-018-0277-7
7. Chilakamarthi U, Giribabu L. Photodynamic Therapy: Past, Present and Future. *Chem Rec* (2017) 17:775–802. doi: 10.1002/tcr.201600121
8. Hailan WAQ, Abou-Tarboush FM, Al-Anazi KM, Ahmad A, Qasem A, Farah MA. Gemcitabine Induced Cytotoxicity, DNA Damage and Hepatic Injury in

Laboratory Mice. *Drug Chem Toxicol* (2020) 43:158–64. doi: 10.1080/01480545.2018.1504957

Conflict of Interest: The authors declare that the research was conducted in the absence of any commercial or financial relationships that could be construed as a potential conflict of interest.

Publisher's Note: All claims expressed in this article are solely those of the authors and do not necessarily represent those of their affiliated organizations, or those of the publisher, the editors and the reviewers. Any product that may be evaluated in this article, or claim that may be made by its manufacturer, is not guaranteed or endorsed by the publisher.

frontiers in Cell and Developmental Biology

REVIEW
published: 09 September 2020
doi: 10.3389/fcell.2020.564601

PARP Inhibitors: Clinical Relevance, Mechanisms of Action and Tumor Resistance

*Maddison Rose[1], Joshua T. Burgess[1], Kenneth O'Byrne[1,2], Derek J. Richard[1] and Emma Bolderson[1]**

[1] Cancer & Ageing Research Program, School of Biomedical Sciences, Institute of Health and Biomedical Innovation, Translational Research Institute, Queensland University of Technology, Brisbane, QLD, Australia, [2] Princess Alexandra Hospital, Brisbane, QLD, Australia

OPEN ACCESS

Edited by:
José Díaz-Chávez, National Cancer Institute (INCAN), Mexico

Reviewed by:
Kai Fu, Central South University, China
Helen E. Bryant, The University of Sheffield, United Kingdom

***Correspondence:**
Emma Bolderson
emma.bolderson@qut.edu.au

Specialty section:
This article was submitted to Molecular and Cellular Oncology, a section of the journal Frontiers in Cell and Developmental Biology

Received: *22 May 2020*
Accepted: *13 August 2020*
Published: *09 September 2020*

Citation:
Rose M, Burgess JT, O'Byrne K, Richard DJ and Bolderson E (2020) PARP Inhibitors: Clinical Relevance, Mechanisms of Action and Tumor Resistance. Front. Cell Dev. Biol. 8:564601. doi: 10.3389/fcell.2020.564601

The Poly (ADP-ribose) polymerase (PARP) family has many essential functions in cellular processes, including the regulation of transcription, apoptosis and the DNA damage response. PARP1 possesses Poly (ADP-ribose) activity and when activated by DNA damage, adds branched PAR chains to facilitate the recruitment of other repair proteins to promote the repair of DNA single-strand breaks. PARP inhibitors (PARPi) were the first approved cancer drugs that specifically targeted the DNA damage response in BRCA1/2 mutated breast and ovarian cancers. Since then, there has been significant advances in our understanding of the mechanisms behind sensitization of tumors to PARP inhibitors and expansion of the use of PARPi to treat several other cancer types. Here, we review the recent advances in the proposed mechanisms of action of PARPi, biomarkers of the tumor response to PARPi, clinical advances in PARPi therapy, including the potential of combination therapies and mechanisms of tumor resistance.

Keywords: BRCA, PARP inhibitors, DNA damage, DNA repair, cancer, targeted therapy

INTRODUCTION

Cancer is a large subset of diseases characterized by the uncontrollable growth of abnormal cells. Globally, there are 17 million new cancer diagnoses each year, with an estimated 9.6 million cancer-related deaths occurring in 2018, placing an enormous burden on health care systems (Bray et al., 2018). The advances in targeted cancer therapies have gained significant momentum in recent years, although chemotherapy treatment regimens remain the gold standard in the treatment of several cancer types. Chemotherapeutic agents are designed to target rapidly dividing cells; however, the major disadvantage of this treatment type is that the drugs are unable to discriminate between malignant and non-malignant cells. Therefore, chemotherapy patients often experience off-target toxicity and detrimental side effects due to the impact of chemotherapy on healthy tissues. The most commonly experienced side effects are nausea and vomiting, with greater than 90% of chemotherapy patients requiring anti-emetic medications whilst undergoing treatment (Lorusso et al., 2017). Additional patient reported side effects include fatigue, generalized pain

and other gastrointestinal disturbances (Pearce et al., 2017). In contrast, targeted therapies directly target cancer-specific mutations and abnormalities to inhibit tumor growth and progression, while minimizing the effects on surrounding non-malignant tissue. Targeted therapies are often associated with more favorable patient outcomes, given they are significantly less likely to result in off-target side effects.

PARP Poly (ADP-ribose) polymerases are a family of 17 proteins involved in several cellular processes, including the stress response, chromatin remodeling, DNA repair and apoptosis (Krishnakumar and Kraus, 2010; Pines et al., 2012; Hu et al., 2014; Zhao Q. et al., 2019). The most well recognized and characterized member of the PARP protein family is PARP1, initially identified for its role in the detection and repair of single-strand DNA breaks (Fisher et al., 2007; Hanzlikova et al., 2016; Heeke et al., 2018). More recent evidence suggests that PARP1 may also have a role in alternative DNA repair pathways, including nucleotide excision repair, non-homologous end joining (both classical and alternative), homologous recombination and DNA mismatch repair (Wang et al., 2006; Haince et al., 2008; Sugimura et al., 2008; Bryant et al., 2009; Boehler et al., 2011; Rulten et al., 2011; Pines et al., 2012; Fenton et al., 2013; Min W. et al., 2013; Beck et al., 2014).

The first member of the PARP protein family was discovered in 1963 during investigations of an enzyme that was activated by nicotinamide mononucleotide (NMN) in a DNA dependent manner and hypothesized to have involvement in a PolyA producing reaction (Chambon et al., 1963). However, later studies revealed that the resulting molecule did not possess PolyA characteristics, given it had the adenylic moiety of ATP and the ribose and phosphate moieties of NMN. Thereby, suggesting the enzyme had transglycosidase activity which catalyzes the polymerization of nicotinamide adenine dinucleotide (NAD) intermediates to form an ADP-ribose polymer, via the simultaneous formation of ribose-ribose bonds and removal of the nicotinamide residues (Chambon et al., 1969). In 1967, numerous studies further identified and characterized this ADP-ribose polymer producing enzyme (Fujimura et al., 1967; Hasegawa et al., 1967; Nishizuka et al., 1967; Reeder et al., 1967; Sugimura et al., 1967). Reeder et al. (1967) and Sugimura et al. (1967) independently identified the reactant product as the negatively charged polymer termed poly(ADP-ribose) (PAR).

Poly (ADP-ribose) polymerase (PARP) inhibitors (PARPi) are a novel class of anti-cancer therapies which compete with NAD^+ for the catalytically active site of PARP molecules. PARPi have shown to be effective in the treatment of homologous recombination repair (HR) deficient tumors. Specifically, PARP inhibitors have been used to target tumors with mutations in the essential HR genes, Breast Cancer Associated 1 and 2 (BRCA1 and BRCA2) (Fong et al., 2009, 2010; Coleman et al., 2019; Tuli et al., 2019). Several PARP inhibitors have been approved for the treatment of BRCA-mutated ovarian, breast and pancreatic cancer. In addition, there are currently 269 clinical trials registered on clinicaltrials.gov examining the use of PARP inhibitors as an anti-cancer therapy in chemo-resistant germline or somatic BRCA1/2 mutated breast, ovarian, lung, and pancreatic cancers (Dockery et al., 2017).

PARP1 and SINGLE-STRAND BREAK REPAIR (SSBR)

PARP1 is vital for the repair of single-strand breaks (Fisher et al., 2007; Hanzlikova et al., 2016). Since single-strand breaks are also produced as an intermediate of Base-Excision Repair (BER); PARP is also sometimes considered to be required for BER, as suggested by several studies (Dantzer et al., 1999, 2000). However, there is contradictory evidence for the sensitivity of PARP1 deficient or PARP1 inhibited cells to agents that induce base damage (de Murcia et al., 1997; Dantzer et al., 1999; Vodenicharov et al., 2000; Allinson et al., 2003; Pachkowski et al., 2009). Another study found that PARP was not required to repair base damage but was required to repair hydrogen peroxide-induced single-strand breaks (Strom et al., 2011). There is also some evidence that PARP1 dependent and independent pathways of SSBR may exist with one study showing that PARP1 was required for SSBR in G1 but not S phase of the cell cycle. In contrast PARPi inhibited SSBR in all phases of the cell cycle (Godon et al., 2008).

DNA damage is rapidly detected through the conserved N-terminal DNA-damage sensing and binding domain of PARP (Ali et al., 2012). Subsequently, PARP1 catalyzes the post-translational polymerization of ADP-ribose units (PARs) from NAD^+ molecules onto target proteins via covalent linkages to acidic residues (Bian et al., 2019). PARP1 activation enables the auto-PARylation of PARP1 itself at serine, tyrosine and glutamic acid residues within the PARP1 auto-modification domain. This auto-PARylation further activates PARP1 and enables the PARylation of histones and other chromatin-associated proteins (Chaudhuri and Nussenzweig, 2017). Collectively, this auto- and hetero-modification recruits additional DNA repair molecules, such as XRCC1 to the site of damage, promoting the effective repair of DNA (**Figure 1a**) (Liu et al., 2017).

PARP2 and PARP3 also have roles in DNA repair processes and share partial redundancy with PARP1 in some of these roles. Demonstrating this redundancy, PARP2 deficient mice display post-replicative genomic instability and PARP1 and PARP2 double mutant mice are embryonic lethal (Ménissier de Murcia et al., 2003). PARP2 also has a role in SSBR and has an overlapping role with PARP1 for recruitment of XRCC1 (Hanzlikova et al., 2017). In addition, PARP3 deficient cells also display genome instability and delayed repair of single-strand breaks, but no radiosensitivity (Boehler et al., 2011). PARP1, PARP2, and PARP3 share structural similarities and were also shown to be activated in a similar manner through DNA-dependent catalytic activation through a local destabilization of the catalytic domain (Langelier et al., 2014).

DNA DOUBLE-STRAND BREAK REPAIR PATHWAYS

Targeted therapies, such as PARPi, have greater specificity and less off-target side effects than traditional therapies, such as chemotherapy or radiation treatment, and can lead to more favorable outcomes in cancer patients. As mentioned previously,

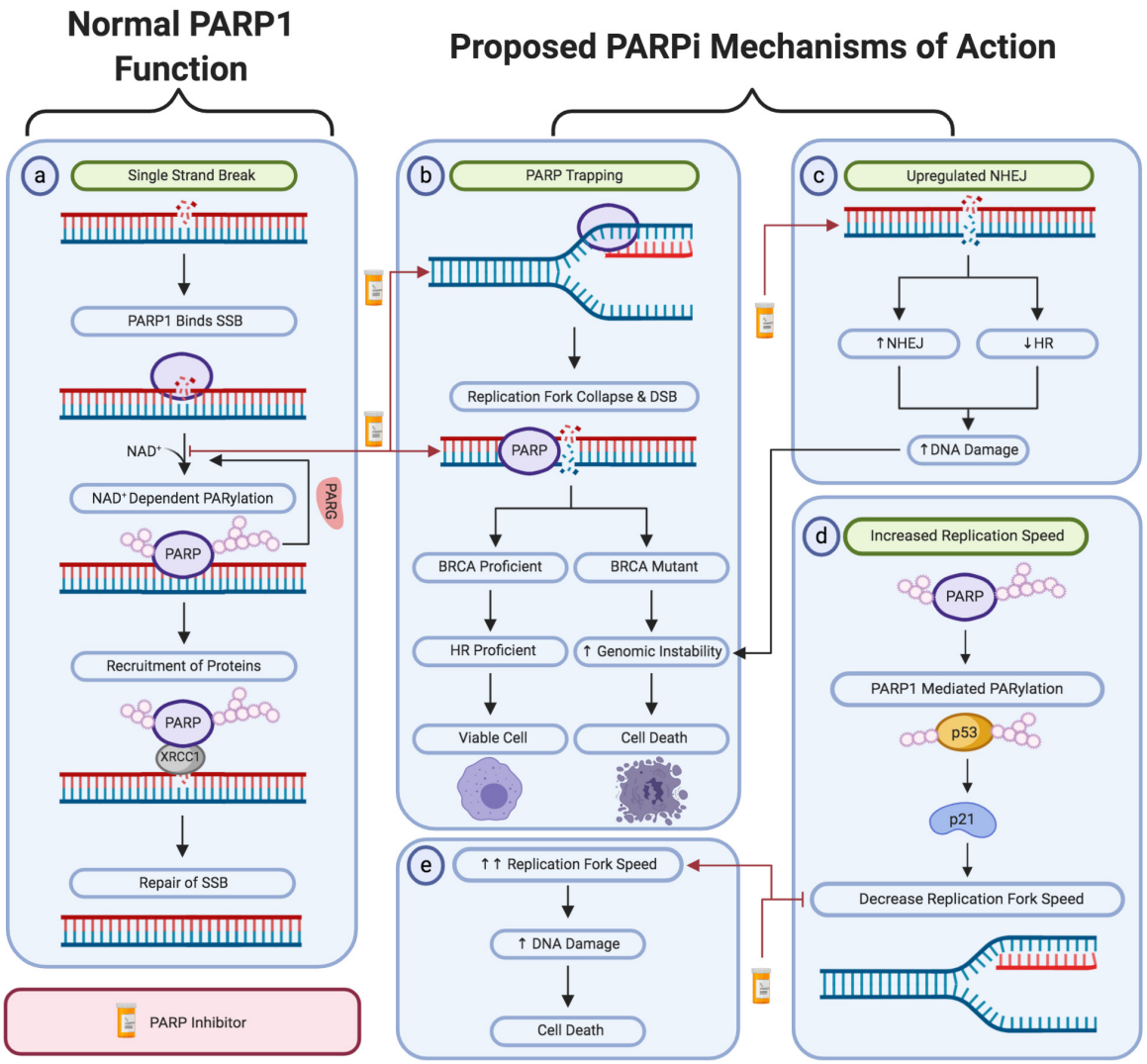

FIGURE 1 | A schematic representation of PARP1 activity in single-strand break repair and the proposed mechanism of action of PARP inhibitors. **(a)** The activity of PARP1 in the repair of oxidative stress-induced single-strand breaks via the base excision repair pathway. The proposed PARPi-induced: **(b)** PARP trapping mechanism. **(c)** Upregulation of non-homologous end joining activity and downregulation of homologous recombination repair. **(d,e)** Loss of negative regulation of replication fork speed. Created with Biorender.

PARPi have been found to target tumors with defects in the HR pathway due to BRCA1 or BRCA2 mutations but have little toxicity on normal cells with functional HR. The two main pathways of DNA double strand break (DSB) repair are briefly described below.

Homologous Recombination Repair

Although HR is considered the least error-prone form of DSB repair, it is restricted to the S and G2 phases of the cell cycle due to the requirement of a template sister chromatid (Brandsma and Gent, 2012).

HR is a complex process, requiring a myriad of proteins. The MRN-complex, composed of MRE11, Rad50 and Nbs1 has several roles in the DNA damage response. Most well recognized, is the role of the MRN-complex as a sensor of DSB to initiate HR following their detection (Krajewska et al., 2015). The MRN-complex is rapidly recruited to the sites of DSBs, facilitating the recruitment and full activation of the ATM kinase and initiates the subsequent ATM-mediated phosphorylation of each member of the MRN-complex. This then promotes further recruitment of the MRN-complex and initiates ATM-dependent downstream signaling (Cassani et al., 2019). The MRN-complex, in conjunction with CtIP, then initiates the 5′ to 3′ nucleolytic resection of the DNA to produce a 3′ overhang of single-stranded DNA (Zhu et al., 2008; Yun and Hiom, 2009; Brandsma and Gent, 2012). This end strand resection is further mediated by other exonuclease proteins, such as Exo1.

The resulting 3′ overhang is then bound by a RPA heterotrimer at a high affinity, mediating the removal of a secondary structure and protecting the section of ssDNA (Chen et al., 2013).

Subsequently, the BRCA1 and BRCA2-mediated displacement of RPA by Rad51 occurs, forming a helical nucleoprotein filament on the single-stranded DNA (Jensen et al., 2010). This filament locates a homologous sequence of DNA and catalyzes strand invasion to form a Holliday junction intermediate (Hiom, 2001). The 3′ end of the invading strand is then used to prime DNA synthesis and extend the region of homology. The resulting Holliday junction is resolved, primarily by the BTR complex, consisting of Bloom's syndrome helicase (BLM), topoisomerase IIIα, RMI1, and RMI2 (Xue et al., 2013). Holliday junction dissolution signals the completion of HR activity, indicating the effective repair of the dsDNA break (Matos and West, 2014; Ma et al., 2017).

Non-homologous End Joining

Unlike HR, non-homologous end joining (NHEJ) does not require a homologous template for the repair of DSBs and directly ligates DNA ends (Khanna and Jackson, 2001; Davis and Chen, 2013). Furthermore, it is active throughout all phases of the cell cycle (Mao et al., 2008).

Given the lack of a template strand, NHEJ is considered to be a comparatively error prone DSB repair mechanism, associated with an increased prevalence of nucleotide insertions and deletions and therefore, a greater probability for genomic instability (Bassing and Alt, 2004). NHEJ is initiated by the binding of a Ku heterodimer, composed of the Ku70 and Ku80 proteins, to a DSB (Sishc and Davis, 2017). The Ku70/80 heterodimer then acts as a scaffold protein to recruit and activate DNA-dependent protein kinase (DNA-PKcs) at the site of damage and produce a catalytically active complex. DNA-PKcs mediated bridging across the break enables DNA resection or gap-filling by several known enzymes. The Ligase IV/XRCC4 complex then ligates the DNA ends back together (Sharma et al., 2016).

PARP INHIBITORS – SYNTHETIC LETHALITY

Poly (ADP-ribose) polymerases (PARP) inhibitors (PARPi) are a class of anti-cancer drugs which compete with nicotinamide (NAD^+) for the catalytically active site of PARP molecules. Inhibition of PARP activity was initially demonstrated in 1971, following treatment of HeLa cells with thymidine and nicotinamide (Preiss et al., 1971). Several later studies identified numerous benzamides as inhibiting PARP activity via NAD^+ competition. However, these compounds were considered clinically unviable due to their low potency and specificity (Purnell and Whish, 1980; Canan Koch et al., 2002; Skalitzky et al., 2003). Although PARP1 is generally considered the major target of PARPi, due to the structural similarity of the NAD-binding domain of some of the PARP family members, some PARPi also inhibit the activity of other PARPs, including PARP2 and PARP3 and some other off-target effects on kinases have also been observed (Murai et al., 2012b; Antolin et al., 2020).

PARPi have been shown to be effective against homologous recombination repair deficient tumors in a synthetically lethal interaction. Synthetic lethality is where loss of one gene is compatible with cell viability; however, simultaneous disruption of two genes results in cell death (Geenen et al., 2018). The synthetic lethality between PARP inhibition and BRCA mutation or depletion was first observed in 2005, where it was originally hypothesized that inhibition of PARP1 activity would lead to replication fork collapse and the subsequent HR-dependent repair of these forks. Therefore, given that BRCA1/2 mutated tumor cells have disrupted HR activity, the collapsed replication forks are unable to be repaired and cell death occurs (Bryant et al., 2005; Farmer et al., 2005).

There are currently several PARP inhibitors approved for the treatment of BRCA1/2 mutated breast, ovarian, pancreatic and prostate cancers. Due to the relatively low frequency of BRCA1/2 mutations, this limits their applicability to the treatment of 10–15% of breast and ovarian tumors, 4–7% of pancreatic tumors and 1.5% of prostate carcinoma (Bryant et al., 2005; Iqbal et al., 2012; Oh et al., 2019). However, more recent studies suggest that PARP inhibitors may have much wider applications. This includes the treatment of tumors with alternative HR deficiencies or mutations in other DNA damage response genes (Bryant et al., 2005; Turner et al., 2008; Jonsson et al., 2019). Tumors with high levels of oxidative and replicative stress may also be sensitive to PARP inhibitors as a monotherapy, irrespective of HR status (Majuelos-Melguizo et al., 2015; Kukolj et al., 2017; Schoonen et al., 2017; Michelena et al., 2018).

The indications for which PARP inhibitors have been approved for are summarized below (**Table 1**). In 2014, Olaparib (Lynparza) was the first PARPi approved by the Food and Drug Agency (FDA) and European Medicines Agency (EMA) as a monotherapy for the treatment of advanced, germline BRCA mutated ovarian cancer (Kaufman et al., 2015). In 2017, this was extended to include maintenance therapy of reoccurring ovarian, fallopian and primary peritoneal tumors, regardless of BRCA mutational status (Pujade-Lauraine et al., 2017; Friedlander et al., 2018). Olaparib has also been approved for the treatment of germline BRCA1/2 mutated HER2-negative breast and metastatic pancreatic cancer in 2018 and 2019, respectively (Moore et al., 2018; Golan et al., 2019; Robson et al., 2019). Most recently, Olaparib was approved for the treatment of HRD-positive metastatic castration-resistant prostate cancer (de Bono et al., 2020).

Several other PARP inhibitors, including Rucaparib (Rubraca), Niraparib (Zejula), and Talazoparib (Talzenna) have also been approved for use in various clinical settings. In 2016, Rucaparib was granted an accelerated approval for the treatment of germline or somatic BRCA1/2-mutated advanced ovarian carcinomas, following multiple chemotherapy treatments (Oza et al., 2017). Subsequently, Rucaparib maintenance therapy was approved in 2018 for reoccurring ovarian, fallopian and primary peritoneal, regardless of BRCA mutational status (Coleman et al., 2017). In May 2020, Rucaparib gained FDA approval for the treatment BRCA1/2 mutated metastatic castration-resistant prostate cancer (Abida et al., 2019).

Niraparib was initially approved in 2017 for the maintenance treatment of reoccurring ovarian, fallopian and primary

TABLE 1 | Food and Drug Administration (FDA) and European Medicines Agency (EMA) approval history of PARP inhibitors.

PARP inhibitor	Approving organization	Year of approval	Indication	Mutational requirement	Relevant studies
Olaparib	FDA and EMA	2014	Advanced ovarian carcinoma	Germline BRCA1/2 Mutation	NCT0107662 (Kaufman et al., 2015)
	FDA and EMA	2017	Reoccurring ovarian, fallopian and primary peritoneal carcinoma	Independent of BRCA1/2 Mutational Status	SOLO-2 (Pujade-Lauraine et al., 2017) and Study 19 (Friedlander et al., 2018)
	FDA EMA	2018 2019	HER-2 negative breast cancer	BRCA1/2 Mutated	OlympiAD (Robson et al., 2017)
	FDA EMA	2018 2019	First-line treatment of advanced ovarian, fallopian and primary peritoneal carcinoma	Germline BRCA1/2 Mutation Complete or partial chemotherapy response.	SOLO-1 (Moore et al., 2018)
	FDA	2019	Metastatic pancreatic cancer	BRCA1/2 Mutated	POLO (Golan et al., 2019)
	FDA	2020	First-line treatment of advanced ovarian, fallopian and primary peritoneal carcinoma in combination with Bevacizumab	HRD-Positive Complete or partial chemotherapy response.	PAOLA-1 (Ray-Coquard et al., 2019)
	FDA	2020	Metastatic castration-resistant prostate cancer	HRD-positive	PROfound (de Bono et al., 2020)
Rucaparib	FDA EMA	2016 2018	Advanced ovarian carcinomas, following multiple chemotherapy treatments	BRCA1/2 Mutated	ARIEL2 and Study 10 (Oza et al., 2017)
	FDA EMA	2018 2019	Reoccurring ovarian, fallopian and primary peritoneal carcinoma	Independent of BRCA1/2 Mutational Status	ARIEL3 (Coleman et al., 2017)
	FDA	2020	Metastatic castration-resistant prostate cancer	BRCA1/2 Mutated	TRITON2 (Abida et al., 2019)
Niraparib	FDA and EMA	2017	Reoccurring ovarian, fallopian and primary peritoneal carcinoma	Complete or partial chemotherapy response.	ENGOT-OV16/NOVA Study (Mirza et al., 2016)
	FDA	2019	Reoccurring ovarian, fallopian and primary peritoneal carcinoma	HRD-positive Independent of chemotherapy response	QUADRA Study (Moore et al., 2019)
	FDA and EMA	2020	Advanced ovarian carcinomas and primary peritoneal carcinoma	Independent of biomarker status Complete or partial chemotherapy response.	PRIMA Study (Gonzalez-Martin et al., 2019)
Talazoparib	FDA and EMA	2018	Advanced or metastatic HER2-negative breast cancer	Germline BRCA1/2 Mutated	EMBRACA Study (Ettl et al., 2018)

peritoneal carcinomas, regardless of BRCA mutational status that show a complete or partial chemotherapy response (Mirza et al., 2016). In 2019, this was expanded to the late-line treatment of the aforementioned carcinomas, that were specifically HRD-positive, irrespective of prior sensitivity to chemotherapy (Moore et al., 2019). Subsequently, this was further expanded in 2020 to include the treatment of reoccurring ovarian, fallopian and primary peritoneal carcinomas that have previously shown complete or partial response to chemotherapy, independent of biomarker status (Gonzalez-Martin et al., 2019).

In 2018, Talazoparib was approved for the treatment of germline BRCA1/2-mutated advanced or metastatic HER2-negative breast cancer (Ettl et al., 2018). Since this approval, Talazoparib has not gained approval for the treatment of any further malignancies.

A fifth PARPi, Veliparib (ABT-888) is currently undergoing clinical trials; however, is not yet approved for use in clinical practice (Kummar et al., 2009; Baxter et al., 2020). Lastly, Fluzoparib (HS10160) was initially identified in 2017 as a novel PARPi (Jhan and Andrechek, 2017). Clinical trials for Fluzoparib commenced in 2019 for the treatment of solid tumors, including ovarian, breast, pancreatic and lung cancer (Han et al., 2019; Luo et al., 2019).

PARPi BIOMARKERS

Biomarkers which can predict the PARPi sensitivity of tumors are of great interest within the scientific community. The identification of biomarkers will not only further our understanding of the mechanism by which PARP inhibitors mediate their anti-cancer capacity but may also increase the subset of patients treated with PARP inhibitors. Since their approval in 2014, significant efforts have been made to establish validated biomarkers for PARPi sensitivity, but with little success. As such, germline and somatic BRCA1/2 mutations remain the main predictive biomarkers for the majority of PARP inhibitors (Ganguly et al., 2016). However, in 2019, a Homologous Recombination Deficiency (HRD) assay was approved as biomarker for the use of Niraparib in patients with advanced ovarian cancer.

The BRCA1 and BRCA2 Genes

The Breast Cancer Susceptibility Genes, BRCA1 and BRCA2, have well established roles in the maintenance of genomic stability. Germline mutations in the tumor suppressor BRCA1 and BRCA2 genes have been strongly associated with an increased risk of breast and ovarian cancer (Antoniou et al., 2003; Brekelmans et al., 2006). Specifically, it is estimated

that a woman's lifetime risk of developing breast or ovarian cancer without a BRCA mutation is approximately 12 and 1.3%, respectively (Kotsopoulos, 2018; Pasanisi and Bruno, 2018). However, in women carrying a harmful BRCA1 mutation this is elevated to 60% lifetime risk of developing breast cancer and 44% risk of developing ovarian cancer (Cavanagh and Rogers, 2015). Similarly, it is estimated that women carrying harmful BRCA2 mutations have a 26 and 17% lifetime risk of inheriting breast and ovarian cancer, respectively (Kuchenbaecker et al., 2017). These mutations are of substantial prevalence, with between 1/400 and 1/800 people carrying a harmful BRCA1/2 mutation (Hall et al., 2009).

Collectively, more than 3500 pathogenic BRCA1/2 mutations have been identified (Godet and Gilkes, 2017). Many of the BRCA1 mutations are frame shift mutations which have a deleterious effect on BRCA1 protein expression, resulting in a non-functional or missense protein. In individuals that have inherited a single mutated BRCA1/2 allele, the wild-type allele is often somatically mutated or silenced as they age (Godet and Gilkes, 2017). This second event often leaves the individual without a functional BRCA1/2 allele and significantly increases the mutation burden within their cells (Petrucelli et al., 2010). BRCA2 frame shift mutations have been shown to frequently result in premature truncation of proteins. Many of these mutations render the BRCA2 gene ineffective and the cells are unable to perform HR repair of stalled replication forks or DSBs.

Under current guidelines, women presenting with breast or ovarian tumors are routinely tested for hereditary mutations in BRCA1/2 and this guides whether they are treated with PARP inhibitors. A recent study showed that over 40% of BRCA1/2 mutations were somatic, suggesting that the tumors should also be tested, to identify more patients that would benefit from PARP inhibitor treatment (Vos et al., 2020.) However, growing evidence suggests that BRCA1/2 mutational status does not always accurately correlate with PARPi sensitivity (Jonsson et al., 2019) and there is a need to find more accurate predictive PARPi biomarkers.

A recent study of ovarian cancer samples, from patients treated with Olaparib maintenance therapy, indicated that Olaparib also significantly improved survival outcomes in patients who lacked BRCA1/2 mutations; but harbored other DDR gene mutations. This indicates that alternative DDR proteins, beyond BRCA1/2, may have the capacity to be an effective PARPi biomarker (Hodgson et al., 2018). Several HR repair mutations have been identified as potential prospective PARPi biomarkers, including ATM, FANC A/F, CHK2, RAD51B/C and CDK12 (Mateo et al., 2015; Criscuolo et al., 2019).

Homologous Recombination Deficiency Score

Homologous recombination deficiency score is defined as the unweighted sum of the loss of heterozygosity (LOH) score, telomeric-allelic imbalance (TAI) score and large-scale state transitions (LST) score. HRD score has been previously identified as a predictive biomarker for tumor response to neoadjuvant chemotherapy treatment (Telli et al., 2016). Tumors with BRCA1/2 mutations are recognized to have the highest HRD scores; however, tumors with homologous recombination repair defects have also been shown to have intermediate HRD scores (Hodgson et al., 2018). Given tumors with HR deficiencies have been shown to be more sensitive to PARP inhibitors than HR proficient tumors, it was hypothesized that HRD score may be an effective PARPi biomarker. However, studies have shown mixed outcomes about the applicability of HRD score as a PARPi biomarker. Several studies have been conducted examining the link between HRD score and Progression Free Survival (PFS) in BRCA wild-type tumors. PFS is defined as the period of time in which a tumor does not worsen following a treatment regime. Hurley et al. (2019) showed that higher HRD scores did correlate with significantly greater PFS following Niraparib treatment in BRCA wild-type ovarian cancer. However, an earlier study indicated that HRD status did not strongly correlate with tumor shrinkage following Veliparib treatment (Mirza et al., 2016; Hurley et al., 2019).

Furthermore, several observational studies have been conducted to investigate potential predictive biomarkers of PARPi response; however, significant research is required to validate these targets prior to them being implicated in clinical practice. These include biomarkers other than gene mutations, including hypermethylation of the promoter regions of BRCA1 and RAD51, hypermethylation of H0XA9 in circulating DNA, high expression of Ku80 and low 53BP1 expression (Montavon et al., 2012; Kondrashova et al., 2018).

PROPOSED MECHANISMS OF ACTION OF PARP INHIBITORS

The underlying mechanism of action by which PARP inhibitors induce their anti-cancer activities has yet to be fully uncovered. However, recent findings have significantly improved our understanding of PARPi activity, and several broadly recognized theories have emerged, although a consensus is yet to be reached.

Inhibiting Single Strand Break Repair

PARP1 has been identified to have an essential role in Single-Strand Break Repair (SSBR). Therefore, it was initially hypothesized that PARP inhibitors may induce lethality by impairing the repair of DNA single-strand breaks and leading to the accumulation of damage (Bryant et al., 2005). However, other studies suggest that the synthetic lethality induced by PARP inhibitors is not due to the inhibition of SSBR. Supporting this, there is little evidence that PARP inhibitors lead to the accumulation of DNA single-strand breaks (Gottipati et al., 2010). In addition, siRNA-mediated depletion of XRCC1, a key protein in the SSBR response, did not increase sensitivity to PARP depletion via PARP1 siRNA (Nazarkina et al., 2007; Patel et al., 2011). Although, XRCC1 depletion did increase the sensitivity to two PARP inhibitors, Olaparib and Veliparib, in cellular cytotoxic assays (Horton et al., 2014). This is consistent with findings that genetically inhibiting PARP is significantly less cytotoxic than utilizing a PARPi, which may be expected to be similarly cytotoxic

if the mechanism of PARPi toxicity was due to inhibiting SSBR (Murai et al., 2012a). In light of the above, this suggested that PARPi sensitivity may be mediated via other mechanisms in addition to inhibiting SSBR.

Replication Fork Stalling and PARP Trapping

It is well recognized that PARP activation is required at the site of stalled replication forks to facilitate MRE11-mediated restart of replication (Bryant et al., 2009; Koppensteiner et al., 2014). DNA DSBs are likely to arise following the collision of the replication fork with a DNA lesion or single strand break (Liao et al., 2018). Based on these findings, it was hypothesized that PARP inhibitors may induce tumor cell death because stalled replication forks are unable to be restarted in PARP inhibited homologous recombination repair-deficient cells. This is supported by the evidence that PARP inhibitors are synthetically lethal with tumors which possess either HR or fork stabilization defects (Liao et al., 2018).

The PARP trapping mechanism of PARP inhibitors is also linked to replication fork stalling and is one of the most well-established theories. This proposed mechanism also offers insight into why inhibiting PARP activity is significantly more cytotoxic than genetically removing PARP1 through methods such as small-interfering RNA (siRNA) technologies (Murai et al., 2012a). The initial PARP trapping theory proposed that PARP inhibitors competitively bind to the NAD^+ binding domain on PARP1. This results in PARP1 becoming trapped on the DNA due to the inability to auto-PARylate PARP1 (Shen et al., 2013). There is strong evidence supporting this theory, including the observation that PARP1-DNA complexes pre-exposed to a PARPi had less ability to dissociate following NAD^+ induced auto-modification of PARP1. Therefore, indicating that the PARPi mechanism could involve PARP trapping to some extent (Hopkins et al., 2015).

Given PARP1's involvement in single strand break repair, it was proposed that PARP1 trapping results in a DNA lesion that cannot be bypassed by replication forks (Farmer et al., 2005). Subsequently, leading to the formation of DSBs and stalled replication forks at the site of damage, as the cell progresses through S-phase (Solier and Pommier, 2014). DSBs can only be repaired through homologous recombination (HR) repair or non-homologous end joining (NHEJ). As previously discussed, HR is essential for the error-free repair of DSBs and requires functional BRCA1/2 proteins (Offit, 2006; Palomba et al., 2014; Vos et al., 2018; Bu et al., 2019). In HR deficient tumors, such as BRCA1/2 mutated tumors, the inhibition of PARP yields DSBs which can only be repaired through NHEJ. NHEJ mediates the direct re-ligation of DNA lesions without the requirement of a homologous template. This direct re-joining increases the incidence of catastrophic genomic instability which may result in cell death. Furthermore, PARPi-induced collapsed replication forks cannot be repaired by NHEJ, resulting in death in HR-deficient tumor cells (**Figure 1b**) (Min A. et al., 2013).

Several studies have examined the correlation between PARP-trapping and tumor sensitivity. The main evidence supporting this mechanism is that the PARP-trapping activity of PARP inhibitors correlates with their cell line toxicity (from the most to the least potent): Talazoparib > > Niraparib > Olaparib = Rucaparib > > Veliparib (Murai et al., 2012a; Murai et al., 2014a). This mirrors the cytotoxicity observed in tumor cell lines, with Talazoparib being active at nanomolar concentrations and Veliparib remaining inactive at 100 μM.

A recent study used a modified proximity ligation assay to detect chromatin-trapped PARP1 and concluded that PARP1 trapping correlated with cellular toxicity in both non-malignant and tumor cells, which may limit the therapeutic advantage of potent trapping activity. It was also observed that three different PARP inhibitors caused similar tumor growth inhibition, regardless of their PARP-trapping potency, suggesting that PARP-trapping may not entirely mediate the anti-cancer activity of PARP inhibitors (Hopkins et al., 2019). Consistent with the conclusions from this study, the link between PARP-trapping and tumor toxicity remains unclear in clinical studies. Veliparib, which was determined to have the lowest PARP-trapping activity, was shown to have a response rate of 47% in patients with platinum-resistant or partially platinum-sensitive BRCA-mutated epithelial ovarian cancer (Vergote et al., 2015). This was comparable to the response rate of platinum sensitive/resistant or BRCA-mutated ovarian tumors to Niraparib (40%) (Sandhu et al., 2013), Olaparib (46%) (Fong et al., 2010), and Talazoparib (42%) (de Bono et al., 2017).

Therefore, although it is tempting to speculate that PARP-trapping mediates its anti-cancer activity, there is a lack of clinical evidence to support this theory. Specifically, the extent of each PARP inhibitor's PARP:DNA trapping capacity does not correlate clearly with the overall toxicity of each drug in the clinic, suggesting that other factors are also involved.

Activation of the Non-homologous End Joining Repair Pathway

Several studies have suggested that the synthetically lethal interaction between BRCA1 and PARP inhibition is due to the upregulation of NHEJ activity in HR-deficient tumor cells. This hyper-activation of NHEJ increases the likelihood of catastrophic genomic instability and subsequent cell death (George et al., 2017). This was initially hypothesized following the finding that PARPi treatment increases the phosphorylation of DNA-PK substrates, consequently promoting NHEJ activity (**Figure 1c**) (Patel et al., 2011). In support of this theory, studies have shown that anionic poly (ADP-ribose) (pADPr) scaffolds produced by PARP1 activation directly interact with Ku70 and Ku80 to inhibit classical NHEJ (Scott et al., 2015). Thereby, inhibiting PARP1's activity removes this negative regulation to promote the upregulation of NHEJ activity. Furthermore, Veliparib treatment was also shown to enhance NHEJ activity in BRCA-deficient ovarian carcinoma cell lines (Patel et al., 2011). This was further supported by another study which demonstrated that depletion of several NHEJ proteins, including DNA-PK and Ku80, induced PARPi resistance in previously sensitive cell-based models (Choi et al., 2016).

Shieldin has been recently identified as a 53BP1 effector complex that is recruited to DSBs via the ATM-RNF8-RNF16-53BP1-RIF1 axis (Dev et al., 2018). Shieldin recruitment at the site of damage has been shown to promote NHEJ activity, fusion of unfinished telomeres and class-switch recombination (CSR) (Greenberg, 2018). Deletion or inhibition of Shieldin, 53BP1, RIF1 or REV7 has been shown to correlate with increased PARPi resistance (Xu et al., 2015; Francica and Rottenberg, 2018; Gupta et al., 2018). Furthermore, a recent study demonstrated TRIP13 ATPase acts as a negative regulator of REV7 via catalyzing the conformational transformation of REV7 to an inactive state. It was also observed that tumors with elevated expression of TRIP13 ATPase possessed significant Olaparib resistance, mediated by the down regulation of REV7 activity (Clairmont et al., 2020). Given the finding that Shieldin activity directly promotes NHEJ, this correlation supports the hypothesis that PARPi lethality is due to the hyper-activation of NHEJ activity.

In contrast, simultaneous treatment with a DNA-dependent protein kinase (DNA PKcs) inhibitor (AZD7648) and a PARPi (Olaparib) has been shown to have synergistic effects in BRCA mutated tumor cells (Fok et al., 2019). It was hypothesized that this was due to the catastrophic genomic instability induced by concurrent inhibition of NHEJ via the DNA PK inhibitor and the pre-existing HR defect of these cells. This finding suggests that the PARPi mechanism is not fully described by the NHEJ activation theory, given that suppression of NHEJ would be predicted to induce PARPi resistance in these circumstances.

Disrupted Processing of Okazaki Fragments and Replication Fork Speed

It was recently demonstrated that inhibition or depletion of the replication fork regulators, FEN1 and LIG1, results in PARP1 accumulation, thereby enabling XRCC1-mediated processing (Hanzlikova et al., 2018). Supporting a role for PARP1 in responding to unligated Okazaki fragments, it has also been found that PARPi therapy increased replication fork progression speed by 1.4-fold (**Figures 1d,e**) (Maya-Mendoza et al., 2018). This suggests an underlying mechanism of PARPi toxicity could be the result of DSBs occurring as a result of high-speed replication (Maya-Mendoza et al., 2018; Quinet and Vindigni, 2018). Based on these findings, it was also recently proposed that increased replication speed may result in the accumulation of replication-associated single-stranded DNA (ssDNA) gaps (Cong et al., 2019). It was hypothesized that these cytotoxic ssDNA gaps were attributed to PARP1's role in processing Okazaki fragments or the reversal of stalled replication forks. Therefore, inhibiting the action of PARP within these processes would result in the formation of short single-stranded gaps in the DNA sequence. Although not yet well recognized, this theory does possess significant supporting evidence. This includes the substantially increased prevalence of ssDNA gaps following PARPi treatment in BRCA-deficient tumor cell lines, in comparison to those that were BRCA-wild type. Furthermore, significantly less ssDNA gaps were observed in PARPi resistant cell models, demonstrating that PARPi sensitivity correlates with the level of ssDNA gaps induced by PARPi treatment (Cong et al., 2019).

Disruption of the Role of PARP1 in Transcription

In addition to roles in DNA repair, PARP1 also regulates the transcription of several proteins, by mechanisms such as regulating chromatin structure and histone PARylation, directly acting as transcriptional co-regulator and direct binding to transcription sites (Schiewer and Knudsen, 2014). As such, PARP1 also regulates the transcription of several proteins implicated in cancer cell survival, including p53 and NF-κB (Stanisavljevic et al., 2011; Lee et al., 2012). Therefore, inhibition of PARP1 using PARPi could also lead to the inhibition of oncogenes regulated by PARP-dependent transcription. An example of this is the sensitization of Ewing's sarcoma by PARPi, in part due to the inhibition of PARP-dependent transcription of ETS gene fusions such as EWS-FLI-1 (Brenner et al., 2012). PARPi treatment also reduces the transcription of DDX21, which leads to the inhibition of rDNA transcription and ribosome biogenesis in BRCA1/2 proficient breast cancers leading to reduced cancer growth (Kim et al., 2019).

In conclusion, multiple mechanisms have been proposed to mediate PARPi toxicity in BRCA1/2 mutated tumors since their initial discovery and clinical application. However, it is not yet established whether one or several of these mechanisms mediate the anti-tumor effects induced by PARPi therapy and further study is required to increase our understanding. It is considered likely that PARPi-induced inhibition of the repair of DNA single-strand breaks and PARP-trapping contributes to the collapse of replications forks, but that other mechanisms are also likely to be involved.

PARPi RESISTANCE

A major complication associated with anti-cancer therapies is the development of acquired resistance in tumors. Human and rodent models have shown that the extent of initial responsiveness to PARPi therapy correlates with the severity of resistance. Therefore, this suggests that individuals who are more likely to see a substantial effect during initial PARPi treatment are most likely to experience poor long-term sensitivity.

Restoration of HR Activity

One of the most well-established mechanisms of acquired PARPi resistance is through the restoration of HR capacity. Through restoring HR capacity, DSBs can be effectively repaired, and the tumor cell continues to survive. This mainly occurs as a result of reversion mutations or the suppression of NHEJ activity.

Reversion Mutations

The most frequent method by which HR is restored is by the reactivation of BRCA1/2 due to secondary mutations. These reversion mutations have been identified in patients diagnosed with both germline and somatic BRCA1/2 mutated breast and ovarian carcinomas (Shroff et al., 2018). A study of high-grade ovarian cancers showed BRCA reversion mutations were identified in the circulating cell-free DNA of 18 and 13% of platinum-refractory and platinum-resistant tumors, respectively.

Furthermore, the presence of a BRCA1/2 reversion mutation was shown to have decreased the PFS induced by Rucaparib treatment from 9 to 1.8 months (Lin et al., 2019). This provided the first clinical evidence that intragenic deletions of BRCA1/2 contribute to the development of PARPI resistant tumors.

Open reading frame (ORF) mutations result in BRCA function being restored due to the removal of the initial delirious mutation and subsequently, result in HR being reactivated (Christie et al., 2017). These reversion mutations have been observed in both patient samples and cellular based studies. For instance, a 55-year-old woman was diagnosed with an ER+ metastatic breast cancer that initially showed sensitivity to Olaparib treatment due to a V1283fs*2 mutation in BRCA2, which is a recognized loss of function mutation. However, after approximately 10 months of treatment the patient's primary tumor showed Olaparib resistance. A circulating tumor DNA assay was conducted on the patient's blood sample and a secondary BRCA2 D1280_N1288 deletion mutation was detected. This mutation is predicted to restore the ORF function via the deletion of the V1283fs*2 BRCA2 mutation, without the removal of critical components of the gene (Gornstein et al., 2018). Therefore, creating a functional isotype of BRCA2 which induces PARPi resistance in previously sensitive cellular models by restoring effective HR (Edwards et al., 2008). Similarly, the c.6174d deletion mutation is a BRCA2 mutation frequently observed in the Ashkenazi Jewish population, which results in truncated BRCA2 protein and confers PARPi sensitivity (Wang and Figg, 2008). Several intragenic mutations which cause the deletion of the c.6174d mutation and subsequently restore the ORF function have been identified in cellular models (Edwards et al., 2008).

However, further genetic testing of BRCA status following acquired PARPi resistance is infrequent, resulting in the cause of resistance commonly remaining undiagnosed (Jiang et al., 2019). This is often disadvantageous to the patient as knowledge of these mutations may guide treatment opportunities. For instance, treatment with the chemotherapeutic agent, 6-Thioguanine, has been shown to be effective at overcoming PARPi resistance induced by BRCA2 reversion mutations (Issaeva et al., 2010). Similar reversion mutations have been observed in patients who were previously sensitive to PARPi therapy due to mutations in RAD51C or RAD51D (Kondrashova et al., 2017).

Suppression of Non-homologous End Joining

Several papers have shown that defective HR resulting from BRCA1 mutations can be reactivated due to concomitant disruption of genes which regulate NHEJ (Noordermeer and van Attikum, 2019). Depletion of 53BP1, a protein involved in the activation of NHEJ, rescues BRCA1-deficient HR and decreases hypersensitivity to PARP inhibitors (Bouwman et al., 2010). Furthermore, as discussed above, the Shieldin complex has been identified as a 53BP1 effector complex. Reduced expression of Shieldin has been observed in numerous breast carcinomas exhibiting acquired PARPi resistance. In addition, REV7 localize to the site of damage following a DSB and is known to promote NHEJ activity and suppress HR (Xu et al., 2015). Inhibition of REV7 via shRNA has been shown to inhibit NHEJ and consequently, promote HR. This shRNA mediated inhibition of REV7 induces PARPi resistance and rescue cells from Olaparib-induced cytotoxicity (Clements et al., 2019). In support of this theory, elevated expression of TRIP13 ATPase has been identified in a large cohort of PARPi resistant BRCA1 mutated carcinomas. As previously discussed, TRIP13 ATPase indirectly suppresses NHEJ activity via the down regulation of REV7. Increased Olaparib sensitivity was also observed in TRIP13 depleted cellular models; therefore, further supporting the hypothesis that TRIP13 ATPase is involved in mediating sensitivity to PARP inhibitors via regulating NHEJ activity (Clairmont et al., 2020).

microRNAs are small, highly conserved regions of non-coding RNA, recognized to have a role in regulating gene expression (Macfarlane and Murphy, 2010). A recent screen revealed that increased expression of miR6-22, miR644, miR-492, miR-613, miR-577, and miR-126 were associated with PARPi resistance (Choi et al., 2014, 2016). However, only over-expression of miR-622 was shown to desensitize BRCA-mutated breast and ovarian cancer cell lines to Olaparib and Veliparib treatment. It was proposed that this desensitization is due to the miR-622 mediated down regulation of Ku 70/80 expression; thereby, blocking NHEJ activity and promoting HR activity (Choi et al., 2016). Collectively, the above findings support the hypothesis that down regulation of NHEJ may play a role in PARPi resistance due to upregulation of HR activity.

Increased Drug Efflux

Increased drug efflux is where there is an increase in the rate which compounds, such as PARP inhibitors, are removed from cells. There is some evidence which suggests that PARPi resistance may be due to increased expression of drug efflux transporter genes. It is hypothesized that this is specifically mediated by the ATP Binding Cassette Subfamily B Member 1 and 2 (Abc1a/b) genes, with one study showing that expression of Abcb1a/b was increased by 2- to 85- fold in Olaparib resistant breast cancers (Rottenberg et al., 2008). Furthermore, Abc1a/b expression was shown to be correlated with resistance to Olaparib and Rucaparib treatment in ovarian cancer cell lines. This resistance was reversed following treatment with Verapamil or Elacridar, two commonly prescribed Abcb1a/b inhibitors (Vaidyanathan et al., 2016). However, Abcb1a/b over-expression was not shown to induce resistance to treatment with Veliparib or AZD2461, an Olaparib analog, AZD2461 indicating that this is unlikely to be the sole mechanism of PARPi resistance (Vaidyanathan et al., 2016).

Stabilization of Stalled Replication Forks

The stabilization of stalled replication forks inhibits their collapse and the subsequent creation of double stranded breaks (Taglialatela et al., 2017). Pre-clinical evidence has indicated that this stabilization may contribute to the acquired PARPi resistance experienced by patients. This was initially proposed by Chaudhuri et al. (2016), following the discovery that depletion of the MLL3/4 complex protein, PTIP, prevents PARPi induced replication fork stalling in BRCA-deficient cells. Following its localization at the site of replication, PTIP recruits MRE11 to the site of damage to promote the degradation of stalled replication

forks. Consequently, restarting the stalled replication fork and improving resection at the site (Ying et al., 2012; Chaudhuri et al., 2016). Therefore, depletion of PTIP inhibits the recruitment of MRE11 to the stalled replication fork to minimize degradation of the nascent strand of DNA. This results in less replication fork collapse associated DSBs in BRCA1/2 deficient cells and confers PARPi resistance.

EZH2 is a histone methyltransferase and catalytic subunit of PRC2, proposed to contribute to PARPi efficiency (Yamaguchi et al., 2018). PARP1 is known to activate and PARylate EZH2, causing it to dissociate from PRC2 and later, degrade. Following replication fork stalling, EZH2 localizes to the fork and promotes the methylation of histone H3. This methylation facilitates the recruitment of a nuclease, MUS81, to the replication fork to promote replication fork degradation (Rondinelli et al., 2017). Depletion, or deactivation, of EZH2 or MUS81 has been shown to induce PARPi resistance by promoting replication fork stabilization.

Down-Regulation of PARG Protein Expression

As previously discussed, PARP1 undergoes auto-PARylation promote its full activation and promote the PARylation of other chromatin-associated proteins. PARylation has been well characterized as a reversible post-translational modification, with Poly (ADP-ribose) glycohydrolase (PARG) identified as the primary PAR degrading enzyme (Miwa and Sugimura, 1971). PARG functions via hydrolyzing the ribose-ribose bond to produce adenosine diphosphate (ADP) ribose (Miwa et al., 1974).

In vitro and *vivo* findings have demonstrated PARG depletion is a common occurrence in PARPi resistant BRCA2-deficent mouse mammary tumor models (Gogola et al., 2018). Given PARPi have been proposed to significantly inhibit PARylation, it is hypothesized that depletion or inactivation of PARG enables PAR accumulation to maintain adequate PARP function, preventing PARP trapping and promoting PARPi resistance. However, further study is required to determine whether changes in PARG levels is a mechanism of PARPi resistance in human cancers.

Notably, several PARG inhibitors (PARGi) are currently undergoing pre-clinical development. Several studies have shown promising anti-tumor outcomes when utilizing combination PARPi/PARGi treatment in PARPi-resistant glioblastoma and cellular models (Houl et al., 2019).

COMBINATION TREATMENTS

Given high dosage requirements and the prevalence of acquired PARPi resistance, combination therapies are of significant interest to minimize dosage requirements and increase drug efficiency.

PARP Inhibitors and Alkylating Agents

Cytotoxic chemotherapy using alkylating agents remains one of the most frequently utilized anti-cancer therapies. Alkylating agents are a class of chemotherapeutic drugs which induce cell death by directly adding additional alkyl groups to the bases of DNA, most frequently via the N7 position on guanine residues (Damia and D'Incalci, 1998). This results in significant intra- and inter- strand linking at the alkylated residues to induce DNA damage. In cancer cells, undergoing rapid growth, this leads to inhibition of DNA replication, cell division and subsequent cell death. Alkylating agents frequently utilized in cancer therapy include the platinum compounds Cisplatin and Carboplatin, and Temozolomide. Platinum compounds crosslink the purine bases within DNA, inducing DNA damage.

Although these drugs initially show beneficial anti-cancer activity, most tumors develop acquired or *de novo* mutations resulting in chemo-resistance and poor patient outcomes. Furthermore, many patients require high dosages for effective tumor size reduction following the administration of chemotherapy alone. This results in a large proportion of patients experiencing adverse side effects, which decreases their quality of life during treatment. Therefore, there is a clear requirement for combination therapies in order to decrease the dosage of chemotherapy. PARP inhibitors have been demonstrated to be novel chemotherapeutics and chemopotentiators.

Early studies of PARP inhibitors with platinum chemotherapy showed higher levels of myelosuppression and it was suggested that this could be linked to the trapping ability of PARP inhibitors. Therefore, it was proposed that, due to its lower PARP trapping activity, Veliparib may be less myelotoxic than other PARP inhibitors. The Phase III VELIA trial recently showed that Veliparib in combination with chemotherapy for first-line and maintenance treatment of stage III or IV high-grade serous ovarian cancer significantly improved progression-free survival (PFS) (Coleman et al., 2019). Furthermore, the phase III BROCADE3 trial showed that 34% of HER2-negative, BRCA-mutated breast cancer patients treated with Veliparib, Carboplatin, and Paclitaxel were progression free at 24 months, compared to 20% of patients treated with Carboplatin and Paclitaxel alone (Han et al., 2017). To further support this, the Phase III PAOLA trial showed Veliparib in combination with Carboplatin or Paclitaxel in HER2-negative advanced or metastatic germline BRCA-mutated breast cancer significantly improved PFS without notably increasing toxicity (Ray-Coquard et al., 2019). Additionally, the Phase III PRIMA study of recurrent platinum sensitive BRCA-mutated ovarian cancer patients showed that Niraparib significantly improved median progression free survival following platinum-based chemotherapy, in comparison to patients treated with a placebo. Patients with BRCA wild-type tumors showed a PFS of 13.8 months following Niraparib maintenance therapy, in comparison to 8.2 months for those administered a placebo (Gonzalez-Martin et al., 2019). This demonstrates the effectiveness of maintenance PARPi treatment following chemotherapy in ovarian tumor, regardless of BRCA status (Gonzalez-Martin et al., 2019).

The alkylating agent Temozolomide acts by adding methyl groups to guanine at the O6 and N7, and adenines at the N3 positions, leading to single-strand breaks (SSBs) at the N7 methylated guanines and N3 methylated adenines (Zhang et al., 2012). These Temozolomide-induced SSBs require PARP1

for repair and therefore induce PARP1-recruitement, which is subsequently trapped in the presence of PARP inhibitors (Murai et al., 2014b). In light of this increased PARP1 trapping in the presence of Temozolomide, it is proposed that the synergy observed between the two treatments is dependent upon inhibition of PARP's catalytic activity and trapping potential of PARP inhibitors. This is supported by preclinical studies which show that Talazoparib and Olaparib have a greater synergistic affect with Temozolomide than Veliparib or genetic inactivation of PARP1/2 (Murai et al., 2014b). As previously discussed, increased PARP trapping has been proposed to contribute toward myelosuppression and in support of this, a phase II clinical trial combining Rucaparib and Temozolomide, observed increased myelosuppression patients with metastatic melanoma (Plummer et al., 2013). It has since been suggested that this combination treatment will require a truncated PARPi treatment schedule, to minimize the negative effects on bone marrow function.

PARP Inhibitors and Topoisomerase I Inhibitors

Topoisomerase I (TOP1) is an enzyme that functions to reduce torsional stain on the DNA helix by the induction of single-strand breaks. Inhibition of topoisomerase I by the Camptothecin related compounds, Topotecan or Irinotecan, traps TOP1 on the DNA leading to single-strand breaks that are then converted into double-strand breaks during the S-phase of the cell cycle resulting in tumor cell death (Xu and Her, 2015). In contrast to alkylating agents, the synergistic effects of topoisomerase inhibitors and PARP inhibitors do not depend on the PARP-trapping activity. Instead the synergy is suggested to result from 3 main mechanisms, firstly, the inhibition of TOP1-PARylation, which is required for the release of trapped TOP1 (Malanga and Althaus, 2004). Secondly, the inhibition of HR and stimulation of NHEJ (Maede et al., 2014) and thirdly, the inhibition of tyrosyl-DNA-phosphodiesterase 1 (TDP1), which is the enzyme required for the cleavage of TOP1-covalently linked complexes from the DNA (Das et al., 2014). It remains to be determined whether this combination confers a therapeutic advantage in the clinic compared to either inhibitor alone.

PARP Inhibitors and WEE1 Kinase Inhibitors

WEE1 kinase is a critical cell cycle regulator protein, involved in G2-M cell cycle arrest prior to mitotic entry. Therefore, inhibition of WEE1 promotes the rapid progression through the cell cycle to inevitably produce genomic instability which subsequently results in mitotic catastrophe and cell death (Matheson et al., 2016). Initial investigations of WEE1i/PARPi simultaneous combination treatments showed disappointing outcomes, due to overwhelming toxicity to non-malignant cells being poorly tolerated in mouse studies. However, sequential WEE1i/PARPi treatment was shown to have significant additive anti-tumor effects in xenograft models, whilst minimizing replication stress induced in non-malignant tissue; therefore, decreasing off-target toxicity (Fang et al., 2019). Furthermore, low dose WEE1i and PARPi combination treatment has shown to act as a radiosensitizer in pancreatic cancer and KRAS-mutated NSCLC models (Karnak et al., 2014; Parsels et al., 2018).

PARP Inhibitors and PI3k Inhibitors

Phosphoinositide 3-kinases (PI3ks) are a class of enzyme involved in numerous cellular processes, including proliferation, intracellular trafficking and differentiation. The use of PI3k inhibitors in cancer therapy has been well established, given the PI3k pathway has been suggested to be one of the most commonly activated pathways in cancer cells (Liu et al., 2009). In cellular Ovarian cancer models, combination treatment with a PI3ki, Buparlsib, and Olaparib has been shown to significantly inhibit cellular proliferation by downregulating BRCA1/2 expression. This effect was observed in BRCA wild-type cell lines which did not possess PIK3CA mutations, providing a rationale for the use of this combination in a wider cohort of tumors independent of their mutational status (Wang et al., 2016). Furthermore, cellular and xenograft models have shown promising results for the use of PARPi and PI3ki combination therapy in the treatment of PTEN/p53-deficient prostate cancer models (González-Billalabeitia et al., 2014). Similar down-regulation of BRCA1/2 and subsequent PARPi sensitivity has also been observed in BRCA-wildtype TNBC cellular studies following treatment with a Buparlsib and Olaparib combination (Ibrahim et al., 2012).

PARP Inhibitors and Radiation

PARP inhibitors have been shown to radio-sensitize tumor cells in several studies, irrespective of BRCA status (Zhao W. et al., 2019). It is proposed that the underlying mechanism for this sensitization is that PARP inhibitors inhibit the repair of radiation-induced single-strand breaks, leading to replication fork collapse and subsequent DSBs in S-phase (Dungey et al., 2008).

Several clinical trials have been conducted to establish the efficacy of radiation therapy in combination with PARPi treatment; however, clinical data from these studies have not yet been published. A phase II trial in patients with brain metastases from non-small cell lung cancer, combining whole brain radiotherapy with Veliparib, observed no clinical benefit over whole brain radiotherapy plus a placebo (Chabot et al., 2017).

PARP Inhibitors and Immunotherapy

Immunotherapies are an emerging class of cancer therapy, showing promising results as both monotherapies and combination therapies. During the initiation of the innate immune response, pattern recognition receptors (PRRs) recognize pathogen-associated molecular patterns (PAMPs), and damage-associated molecular patterns (DAMPs) (Amarante-Mendes et al., 2018). PAMPs are small molecule motifs conserved within a class of microbes; therefore, are not stimulated by PARPi treatment. However, DAMPs are endogenous molecules released from host cells during damaging or death related cellular events (Huang et al., 2015). Cytosolic DNA, which arises due to nuclear damage or loss-of-function mutations in DNA degrading proteins, has been identified as a DAMP which can bind to cyclic guanosine monophosphate (GMP)–

adenosine monophosphate (AMP) synthase (cGAS) to induce a conformational change in cGAS (Li and Chen, 2018). This conformational change results in the conversion of guanosine triphosphate (GTP) and ATP to the second messenger, cyclic GMP-AMP. GMP-AMP is then able to act as an endogenous ligand for Stimulator of IFN Gene (STING), which activates numerous transcription factors to stimulate an innate immune response (Kato et al., 2017).

Based on evidence of an interaction between the DNA damage response and the immune system, it has been suggested that PARPi therapy may have positive implications for the anti-cancer immune response (Li and Chen, 2018). It is now well recognized that tumors with mutations in DNA damage response genes are more sensitive to immunotherapies (Samstein and Riaz, 2018). For instance, a study of patients diagnosed with advanced urothelial carcinomas demonstrated that the presence of mutations in DNA damage response genes increased the response to PD-1/PD-L1 blockade therapies by 4.2-fold (Vidotto et al., 2019). To further expand on the above findings, preclinical studies showed that Talazoparib and Veliparib treatment induced catastrophic DNA damage which activated cGAS (Chabanon et al., 2019; Pantelidou et al., 2019).

Interestingly, a recent study demonstrated that PARPi treatment induced STING activation in cellular models deficient of BRCA2 via shRNA technology; however, this was not observed in BRCA-proficient cells (Reisländer et al., 2019). These findings were controversial; given they suggest that immune checkpoint inhibitors were unlikely to be effective in combination with PARP inhibitors in HR-proficient individuals.

Several clinical trials are currently underway investigating the effects of PARP inhibitors in combination with PD-1 inhibitors. Results from a Phase I study were 49 patient's suffering from solid tumors were treated with a combination of a PARPi and Tislelizumab showed 20% of patients achieved an objective response. Furthermore, 32% of patients entered a state of stable disease, where the tumor did not show any increase in size (Friedlander et al., 2019).

PARP Inhibitors and Drugs Targeting Epigenetic Modifications: DNA Methyltransferase Inhibitors (DNMTi)

DNA methyltransferases (DNMTs) are a conserved family of enzymes, responsible for the transfer of methyl groups via *S*-adenosyl methionine (SAM). DNMTs have a vital role in gene silencing, transcriptional activation and post-transcriptional gene regulation (Lyko, 2018). Deregulated DNMT function has been associated with numerous components of cancer development, including silencing of tumor suppressor genes and hypermethylation of cancer-associated genes. For instance, hypermethylation of the retinoblastoma gene promoter region has been observed in a significant number of unilateral retinoblastoma cancers (Robertson, 2001). Dysregulation of DNMT activity, and subsequent hypermethylation of promoter regions, has been identified as a key component in acute myeloid leukemia initiation and progression (Yang et al., 2019). Furthermore, hypermethylation of promoter regions has also been observed in 56% of breast and 15–30% ovarian cancers (de Almeida et al., 2019; Hentze et al., 2019).

Given the clear link between excessive DMNT activity and tumorigenesis, the development of DNMT inhibitors offered a promising, targeted anti-cancer therapy via inhibiting the methylation of DNA residues. Currently, two DNMT inhibitors, Azacytidine (Vidazaand) and Decitabine (Dacogen), that have received FDA and European Medicines Agency approval for the treatment of acute myeloid leukemia and myelodysplasia syndrome. However, impartial or no response is experienced by greater than 50% of patients undergoing DNMT inhibitor therapy. This indicates the need for a more targeted, potent approach to DNMT inhibitor therapy. Reversing the gene expression changes associated with DNA methylation abnormalities in cancer is one proposed mechanism for the clinical efficacy of DNMTis (Baylin and Jones, 2011). It has also been determined that DNMTi can be incorporated into replicating DNA in place of cytosine bases. Once added to DNA, these can then covalently bind DNMTs, effectively trapping DNMT on the DNA leading to cell death (Chovanec et al., 2018). It has been observed that PARP can bind to DNMT and therefore treatment with both PARPi and DNMTi increase PARP trapping on the DNA. DMNT inhibitors have also been shown to increase the accumulation of reactive oxygen species (ROS). This increase in oxidative stress activates cellular kinase activity to promote PARP1 binding at the site of damage. Therefore, promoting the trapping of PARP1 at site of damage via PARP inhibitors and the subsequent replication fork collapse (Pulliam et al., 2018).

Recent pre-clinical cellular and xenograft breast cancer and AML studies using a PARPi and DNMT inhibitor (DNMTi) combination have shown promising outcomes, including decreased clonogenic formation and increased cytotoxicity (Muvarak et al., 2016). Furthermore, a recent study demonstrated that combination Guadecitabine and Talazoparib therapy enhanced PARPi trapping activity in cellular assays, and decreased tumor growth in ovarian and TNBC xenograph models (Pulliam et al., 2018). The PARPi:DNMTi combination therapy has not yet been trialed in the clinic but a phase I/II trial is currently recruiting patients to assess the efficacy of Talazoparib in combination with the DNMTi, Decitabine, for treatment of acute myeloid leukemia.

CLINICAL SIGNIFICANCE: PARP INHIBITORS AS A CANCER THERAPY

PARP inhibitors have shown promising results in both clinical trials and practice for the treatment of ovarian, breast, prostate and pancreatic cancers. There are currently 286 clinical trials registered on clinicaltrials.gov investigating PARPi therapies.

Ovarian Cancer

As discussed previously, BRCA1/2 mutations have been identified in approximately 10–15% of ovarian cancers (Bryant et al., 2005). The benefit of PARP inhibitors as a maintenance therapy for ovarian cancer has been well established, since the approval of Olaparib in 2014 (reviewed in Franzese et al., 2019).

However, recent studies have shown that PARPi can also have clinical benefit as a first line therapy in ovarian cancer treatment.

In the recent PRIMA phase III randomized trial, 733 patients with newly diagnosed ovarian cancer were treated with Niraparib or placebo, following a response to platinum-based chemotherapy. The study outcomes showed that median PFS was significantly longer in the niraparib-treated group than in the placebo group (21.9 months vs. 10.4 months). Significantly, this increase in PFS was higher in HR deficient tumors but an increase in PFS was still observed in HR proficient tumors (Gonzalez-Martin et al., 2019).

The recent VELIA Trial aimed to assess Veliparib as a font line therapy for Ovarian cancer. Over 1000 women with newly diagnosed ovarian cancer were assigned first line therapy of chemotherapy plus either Veliparib or placebo followed by maintenance therapy of Veliparib or placebo. Veliparib was found to extend median progression free survival by 7 months over all (24 months vs. 17 months). The PFS was improved further in patients with BRCA mutations (35 months vs. 22 months), suggesting that PARPi could be an efficient front-line therapy for ovarian cancer (Coleman et al., 2019).

Breast Cancer

Approximately 5–10% of breast cancer cases are due to inherited genomic alterations. Similar to ovarian cancer, the majority are caused by BRCA1/2 mutations (Lee et al., 2020). For individuals with a BRCA1/2 mutation, the risk of developing breast cancer is 69 and 62%, respectively. However, the risk for individuals without a BRCA mutation is as low as 12% (Armstrong et al., 2019). The phase III OlympiAD trial demonstrated that maintenance therapy with Olaparib significantly increased PFS in patients with metastatic HER2-negative BRCA-mutated breast cancer, in comparison to standard chemotherapy (Robson et al., 2017, 2019). Given these findings, Olaparib was approved by the FDA in 2018 for the treatment of metastatic HER2-negative BRCA-mutated breast cancer following chemotherapy (Le and Gelmon, 2018). In 2018, the TALA study provided the first evidence that Talazoparib could induce a complete pathological response as a monotherapy treatment in the treatment of BRCA-mutated breast cancer. This was further supported by the phase III EMBRACA study which demonstrated that Talazoparib monotherapy had significantly greater PFS in patients with metastatic HER2-negative BRCA-mutated breast cancer in comparison to standard chemotherapy treatment (Litton et al., 2018). Given this, the FDA approved Talazoparib as the second PARPi for the treatment of breast cancer (Litton et al., 2018). Additionally, patient-reported studies have shown PARPi therapy offered significantly greater patient quality of life during treatment in comparison to several standard therapies (Ettl et al., 2018; Hurvitz et al., 2018). Collectively, these findings highlight the potential of PARP inhibitors as viable breast cancer treatment.

Prostate Cancer

Prostate cancer accounts for 7.1% of all cancer diagnoses in men, although contributes to an unproportionable 13.3% of cancer related deaths (Crawford, 2003). Improvements have been made for treatment options, although a radical prostatectomy remains the gold standard treatment. Radical prostatectomies are minimally invasive procedures, although many patients experience long-term side effects that significantly decrease their quality of life (Chin, 2009). Therefore, there is a clear requirement for alternative treatment options to be made available. The application of PARP inhibitors in the treatment of prostate cancer was initiated in 2015 following the finding that 19.6% of prostate cancers had BRCA1, BRCA2 or ATM mutations (Mandelker et al., 2017). Currently, numerous clinical trials are being completed to investigate the effectiveness of PARPi mono- and combination therapies in the treatment of prostate cancer. The phase II TOPARP study showed that following treatment with 400 mg Olaparib, 54.3% of patients with DNA repair mutated, castration-resistant prostate cancer had a composite response at a two-year follow up (Mateo et al., 2020). The Phase II Galahad study investigated the effect of Niraparib treatment in patients suffering from metastatic castration-resistant prostate cancer which possessed a DDR defect. The results demonstrated that 65% of patients diagnoses with a BRCA1/2-mutated prostate carcinoma, and 31% of patients with alternative DDR gene mutated prostate cancers, achieved a composite response (Smith et al., 2019).

Pancreatic Cancer

Pancreatic cancer is recognized to be one of the most common cause of cancer-associated deaths worldwide, with the 5-year survival rate being a mere 9% (Rawla et al., 2019). Due to its asymptomatic progression, most patients do not present until advanced-stage disease. Although surgical and adjuvant pancreatic cancer treatments are advancing, the 5-year survival statistics continue to worsen (Brunner et al., 2019). This highlights the urgent need for the development of effective, targeted anti-cancer therapies to improve patient survival (Brunner et al., 2019). BRCA1/2 mutations have been identified in 4–7% of pancreatic cancer patients. Furthermore, these mutations have been correlated with poorer survival outcomes in pancreatic cancer patients (Iqbal et al., 2012). The recent POLO trial showed that in patients with chemotherapy responsive BRCA1/2-mutated tumors, 22.1% of patients treated with Olaparib did not have any tumor progression after two years. In contrast, only 9.6% of patients treated with the placebo showed no tumor progression. Furthermore, the median PFS was determined to be 7.4 and 3.8 months following Olaparib and control drug treatments, respectively (Golan et al., 2019). This clinical trial provided the first evidence for the effectiveness of PARP inhibitors in the treatment of pancreatic cancer and subsequently resulted in the FDA approval of Olaparib for the treatment of germline BRCA1/2-mutated metastatic pancreatic adenocarcinomas.

Lung Cancer

Lung cancer accounts for 2.09 million of annual cancer diagnoses and is the leading cause of worldwide cancer-associated deaths (Cao and Chen, 2019). DDR mutations are evident in a significant proportion of lung cancer patients, including mutations in

ATM, PTEN, MRE11, and FANCA (Mamdani et al., 2019). Most notably, 5% of lung cancers have been identified to be BRCA1/2-mutated. Collectively, these findings provide a rationale for the use of PARP inhibitors in the treatment of lung cancer. However, the phase II STOMP trial demonstrated that maintenance Olaparib monotherapy for small cell lung cancer (SCLC) did not significantly increase PFS or overall survival, in comparison to a placebo. Subsequently, the phase I/II clinical trial examining the effectiveness of an Olaparib/Temozolomide combination treatment in reoccurring SCLC demonstrated that 41.7% of participants had a complete pathological response (Farago et al., 2019).

PARP inhibitors are well recognized to induce radio-sensitization in various cancer subtypes. However, cellular and xenograft-based studies provided the first evidence that Talazoparib sensitizes a significant proportion of NSCLC models to ionizing radiation. A similar effect was also observed following Veliparib treatment; however, to a lesser extent. Given Talazoparib has a significantly greater PARP trapping capacity, it is hypothesized that PARP trapping may be the underlying mechanism by which sensitivity to radiation is induced (Laird et al., 2018). Fluzoparib has been identified as a novel PARPi, in the early stages of preliminary clinical trials (Wang et al., 2019). Fluzoparib has shown promising results in Phase I/II lung cancer clinical trials as a radiosensitizer and in combination with SHR-1316, a PD-L1 inhibitor (Luo et al., 2019).

Acute Myeloid Leukemia

Acute myeloid leukemia (AML) is the most common cause of adult leukemia, contributing to 80% of adult leukemia diagnoses (Yamamoto and Goodman, 2008). Although BRCA1/2 mutations are not characteristic of AML, several pre-clinical studies have demonstrated genomic mutations which provide a rationale for PARPi use in AML therapy (reviewed in Faraoni et al., 2019). It was initially shown that microsatellite instability-positive AML cellular models exhibited down-regulation and mutation of the HR genes CtIP and MRE11 (Gaymes et al., 2013). Furthermore, Olaparib and Veliparib hypersensitivity has been demonstrated in patient-derived myeloproliferative neoplasms irrespective of BRCA1/2 mutational status. However, greater PARPi sensitivity was observed in samples which possessed a DNA damage repair defect (Pratz et al., 2016).

Several AML-inducing fusion proteins have been shown to confer PARPi sensitivity in cellular models. For instance, Olaparib has been shown to have significant additive effects on the anti-tumor activity of two chemotherapy drugs, Doxorubicin and Cytarabine, in MLL-AF9-positive mouse models (Stavropoulou et al., 2018). AML1-ETO and PML-RARα are well recognized AML-associated fusion proteins, shown to promote leukemogenesis (Singh et al., 2017). Esposito et al. (2015) demonstrated that AML1-ETO or PML-RARα positive models possessed PARPi sensitivity due to a jeopardized DDR and the down-regulation of HR genes, shown to be mediated by HOXA9 activity (Esposito et al., 2015). There are currently several clinical trials underway to investigate PARPi use in AML patients; however, the majority of these are still in the recruitment phase and results are not yet available.

PARP1 REGULATING PROTEINS AS POTENTIAL NEW BIOMARKERS OR THERAPEUTIC TARGETS

Given the growing prevalence of PARPi resistance, it is essential that alternative PARP inhibiting mechanisms are investigated to improve treatment opportunities. Recent research has shown PARP1 activity is regulated by physical interactions with several other proteins, including HPF1, YB-1, Sam68, Banf1, TRIP12 and, as discussed earlier, PARG (Alemasova et al., 2016; Gibbs-Seymour et al., 2016; Sun et al., 2016; Gogola et al., 2018; Bolderson et al., 2019; Gatti et al., 2020). Therefore, modulation of these PARP1 regulatory proteins may provide an alternate method of downregulating PARP1 activity or modulating the sensitivity of tumor cells to PARP inhibitors.

Histone PARylation factor 1 (HPF1) has been shown to have an essential role in enabling the *trans* ADP-ribosylation of histones by PARP1 during the DNA damage response at serine residues (Gibbs-Seymour et al., 2016; Leidecker et al., 2016; Bonfiglio et al., 2017). HPF1 was also identified to be involved in the inhibition of PARP1 hyper-automotification induced by DNA damage, which may have a role in maintaining genomic stability (Gibbs-Seymour et al., 2016). Lastly, in *vitro* findings by Gibbs-Seymour et al. (2016) demonstrated that depletion of HPF1 induces sensitivity to PARPi treatment and other DNA damaging agents. Collectively, these findings suggest that HPF1 is involved in maintaining appropriate PARP1 activity, particularly by upregulating PARP1's activity during the DNA damage response.

Furthermore, YB-1 (Y-box-binding protein) has also been shown to physically interact with PARP1 and PARP2 to promote the auto-PARylation of PARP and inhibit PARG-mediated PAR degradation (Alemasova et al., 2016). Subsequently, YB-1 was identified as a co-factor of PARP1 and shown to counteract the inhibition of PARylation induced by low dosages of PARPi in *vitro* (Alemasova et al., 2018). However, it was also shown that YB-1 was unable to entirely inhibit the effects of high dosages of PARPi (Alemasova et al., 2018). Together, these findings indicate that YB-1 plays a key role in the regulation of PARP1 activity via the regulation of PARP1/2 auto-PARylation.

Src-associated substrate during mitosis 68 kDa (Sam68) is a protein shown to localize at DNA lesions following damage. A physical interaction between Sam68 and PARP1 has been observed; however, similar interactions were not observed between Sam68 and PARP2, PARP3, PARP5a or PARP5b (Sun et al., 2016). Supporting its role as a positive regulator of PARP1 depletion of Sam68 in mice models resulted in impaired PARP1 activation, PAR chain development and activation of PAR dependent signaling, including the NF-κB pathway (Fu et al., 2016a,b). Sam68 depletion also resulted in similar phenotypes to those observed following PARP1 depletion (Sun et al., 2016). The role of Sam68 in PARPi sensitivity has not been examined to date.

In summary, these findings suggest that Sam68 is a key regulator of PARP1 activation and subsequent downstream regulating.

We recently identified that Barrier to Autointegration Factor 1, Banf1 is a negative regulator of PARP1 activity (Bolderson et al., 2019). Banf1 was found to bind to the NAD^+ binding domain of PARP1 and inhibit it's auto-PARylation and activity toward histone substrates following oxidative stress. The role of Banf1 in the response of tumors to PARPi remains to be determined.

A recent study identified the ubiquitin E3 ligase TRIP12 as a regulator of PARP1 stability and PARPi-induced PARP trapping. As such, depletion of TRIP12 leads to an increase in PARPi-induced PARP trapping and induces replication stress, DNA damage and results in cell death. Hence, the levels of TRIP12 protein could be an important consideration for the sensitivity of tumor cells to PARPi (Gatti et al., 2020).

Given their role in the regulation of PARP stability and activity, modulation of HPF1, YB-1, Sam68, Banf1 and TRIP12 may provide novel combination therapies to potentiate the effect of existing PARP inhibitors or provide alternative targets for the development of new PARP inhibiting drugs. It is also possible that these regulators could act as biomarkers for the response of tumors to PARPi. However, the safety and efficiency of these targets in humans remains to be established.

CONCLUSION

Since their discovery half a century ago, the PARP protein family has been proposed to have multiple functions in cellular processes; including transcription, cell death and DNA repair. In particular, knowledge of the basic biology and roles of PARP1 in DNA repair pathways led to the development of PARPi, for the targeted treatment of BRCA-mutated cancers. The potential of PARPi therapy in a variety of cancer subtypes has been highlighted by the significant numbers of preclinical studies and clinical trials, demonstrating their superior efficacy over traditional chemotherapies in some cancers. Studies have also established the substantial anti-tumor benefits of utilizing PARPi in combination with other anti-cancer agents to induce significant tumor regression. However, although the clinical relevance of PARPi is clear, the underlying mechanisms of PARPi activity remain elusive; therefore, limiting our understanding of potential targets for PARPi tumor biomarkers and pathways of therapy resistance. Further studies of the mechanism of action of PARPi are required, along with the validation and approval of additional biomarkers to ensure that PARPi therapy is utilized to provide maximal patient benefit.

AUTHOR CONTRIBUTIONS

All the authors contributed to writing and editing the manuscript. MR made the figure.

FUNDING

This work was supported by a grant from the Princess Alexandra Hospital Research Foundation and a Queensland Senior Clinical Research Fellowship (KO'B). JB is supported by an Advance Queensland Early-career Research Fellowship.

REFERENCES

Abida, W., Campbell, D., Patnaik, A., Sautois, B., Shapiro, J., Vogelzang, N. J., et al. (2019). 846PD - Preliminary results from the TRITON2 study of rucaparib in patients (pts) with DNA damage repair (DDR)-deficient metastatic castration-resistant prostate cancer (mCRPC): updated analyses. *Ann. Oncol.* 30, v327–v328. doi: 10.1093/annonc/mdz248.003

Alemasova, E. E., Moor, N. A., Naumenko, K. N., Kutuzov, M. M., Sukhanova, M. V., Pestryakov, P. E., et al. (2016). Y-box-binding protein 1 as a non-canonical factor of base excision repair. *Biochim. Biophys. Acta* 1864, 1631–1640. doi: 10.1016/j.bbapap.2016.08.012

Alemasova, E. E., Naumenko, K. N., Kurgina, T. A., Anarbaev, R. O., and Lavrik, O. I. (2018). The multifunctional protein YB-1 potentiates PARP1 activity and decreases the efficiency of PARP1 inhibitors. *Oncotarget* 9, 23349–23365. doi: 10.18632/oncotarget.25158

Ali, A. A. E., Timinszky, G., Arribas-Bosacoma, R., Kozlowski, M., Hassa, P. O., Hassler, M., et al. (2012). The zinc-finger domains of PARP1 cooperate to recognize DNA strand breaks. *Nat. Struct. Mol. Biol.* 19, 685–692. doi: 10.1038/nsmb.2335

Allinson, S. L., Dianova, I. I., and Dianov, G. L. (2003). Poly(ADP-ribose) polymerase in base excision repair: always engaged, but not essential for DNA damage processing. *Acta Biochim. Pol.* 50, 169–179. doi: 10.18388/abp.2003_3724

Amarante-Mendes, G. P., Adjemian, S., Branco, L. M., Zanetti, L. C., Weinlich, R., and Bortoluci, K. R. (2018). Pattern recognition receptors and the host cell death molecular machinery. *Front. Immunol.* 9:2379. doi: 10.3389/fimmu.2018.02379

Antolin, A. A., Ameratunga, M., Banerji, U., Clarke, P. A., Workman, P., and Al-Lazikani, B. (2020). The kinase polypharmacology landscape of clinical PARP inhibitors. *Sci. Rep.* 10:2585. doi: 10.1038/s41598-020-59074-4

Antoniou, A., Pharoah, P. D. P., Narod, S., Risch, H. A., Eyfjord, J. E., Hopper, J. L., et al. (2003). Average risks of breast and ovarian cancer associated with BRCA1 or BRCA2 mutations detected in case Series unselected for family history: a combined analysis of 22 studies. *Am. J. Hum. Genet.* 72, 1117–1130. doi: 10.1086/375033

Armstrong, N., Ryder, S., Forbes, C., Ross, J., and Quek, R. G. (2019). A systematic review of the international prevalence of BRCA mutation in breast cancer. *Clin. Epidemiol.* 11, 543–561. doi: 10.2147/CLEP.S206949

Bassing, C. H., and Alt, F. W. (2004). The cellular response to general and programmed DNA double strand breaks. *DNA Repair* 3, 781–796. doi: 10.1016/j.dnarep.2004.06.001

Baxter, P. A., Su, J. M., Onar-Thomas, A., Billups, C. A., Li, X. N., Poussaint, T. Y., et al. (2020). A Phase I/II Study of Veliparib (ABT-888) with Radiation and Temozolomide in newly diagnosed diffuse pontine glioma: a pediatric brain tumor consortium study. *Neuro Oncol.* 22, 875–885. doi: 10.1093/neuonc/noaa016

Baylin, S. B., and Jones, P. A. (2011). A decade of exploring the cancer epigenome - biological and translational implications. *Nat. Rev. Cancer* 11, 726–734. doi: 10.1038/nrc3130

Beck, C., Boehler, C., Guirouilh Barbat, J., Bonnet, M. E., Illuzzi, G., Ronde, P., et al. (2014). PARP3 affects the relative contribution of homologous recombination and nonhomologous end-joining pathways. *Nucleic Acids Res.* 42, 5616–5632. doi: 10.1093/nar/gku174

Bian, C., Zhang, C., Luo, T., Vyas, A., Chen, S. H., Liu, C., et al. (2019). NADP(+) is an endogenous PARP inhibitor in DNA damage response and tumor suppression. *Nat. Commun.* 10:693. doi: 10.1038/s41467-019-08530-5

Boehler, C., Gauthier, L. R., Mortusewicz, O., Biard, D. S., Saliou, J. M., Bresson, A., et al. (2011). Poly(ADP-ribose) polymerase 3 (PARP3), a newcomer in cellular

response to DNA damage and mitotic progression. *Proc. Natl. Acad. Sci. U.S.A.* 108, 2783–2788. doi: 10.1073/pnas.1016574108

Bolderson, E., Burgess, J. T., Li, J., Gandhi, N. S., Boucher, D., Croft, L. V., et al. (2019). Barrier-to-autointegration factor 1 (Banf1) regulates poly [ADP-ribose] polymerase 1 (PARP1) activity following oxidative DNA damage. *Nat. Commun.* 10:5501. doi: 10.1038/s41467-019-13167-5

Bonfiglio, J. J., Fontana, P., Zhang, Q., Colby, T., Gibbs-Seymour, I., Atanassov, I., et al. (2017). Serine ADP-Ribosylation depends on HPF1. *Mol. Cell* 65, 932.e6–940.e6. doi: 10.1016/j.molcel.2017.01.003

Bouwman, P., Aly, A., Escandell, J. M., Pieterse, M., Bartkova, J., van der Gulden, H., et al. (2010). 53BP1 loss rescues BRCA1 deficiency and is associated with triple-negative and BRCA-mutated breast cancers. *Nat. Struct. Mol. Biol.* 17, 688–695. doi: 10.1038/nsmb.1831

Brandsma, I., and Gent, D. C. (2012). Pathway choice in DNA double strand break repair: observations of a balancing act. *Genome Integr.* 3:9. doi: 10.1186/2041-9414-3-9

Bray, F., Ferlay, J., Soerjomataram, I., Siegel, R. L., Torre, L. A., and Jemal, A. (2018). Global cancer statistics 2018: GLOBOCAN estimates of incidence and mortality worldwide for 36 cancers in 185 countries. *CA Cancer J. Clin.* 68, 394–424. doi: 10.3322/caac.21492

Brekelmans, C. T., Seynaeve, C., Menke-Pluymers, M., Bruggenwirth, H. T., Tilanus-Linthorst, M. M., Bartels, C. C., et al. (2006). Survival and prognostic factors in BRCA1-associated breast cancer. *Ann. Oncol.* 17, 391–400. doi: 10.1093/annonc/mdj095

Brenner, J. C., Feng, F. Y., Han, S., Patel, S., Goyal, S. V., Bou-Maroun, L. M., et al. (2012). PARP-1 inhibition as a targeted strategy to treat Ewing's sarcoma. *Cancer Res.* 72, 1608–1613. doi: 10.1158/0008-5472.CAN-11-3648

Brunner, M., Wu, Z., Krautz, C., Pilarsky, C., Grutzmann, R., and Weber, G. F. (2019). Current clinical strategies of pancreatic cancer treatment and open molecular questions. *Int. J. Mol. Sci.* 20:4543. doi: 10.3390/ijms20184543

Bryant, H. E., Petermann, E., Schultz, N., Jemth, A. S., Loseva, O., Issaeva, N., et al. (2009). PARP is activated at stalled forks to mediate Mre11-dependent replication restart and recombination. *EMBO J.* 28, 2601–2615. doi: 10.1038/emboj.2009.206

Bryant, H. E., Schultz, N., Thomas, H. D., Parker, K. M., Flower, D., Lopez, E., et al. (2005). Specific killing of BRCA2-deficient tumours with inhibitors of poly(ADP-ribose) polymerase. *Nature* 434, 913–917. doi: 10.1038/nature03443

Bu, H., Chen, J., Li, Q., Hou, J., Wei, Y., Yang, X., et al. (2019). BRCA mutation frequency and clinical features of ovarian cancer patients: a report from a Chinese study group. *J. Obstet. Gynaecol. Res.* 45, 2267–2274. doi: 10.1111/jog.14090

Canan Koch, S. S., Thoresen, L. H., Tikhe, J. G., Maegley, K. A., Almassy, R. J., Li, J., et al. (2002). Novel tricyclic poly(ADP-ribose) polymerase-1 inhibitors with potent anticancer chemopotentiating activity: design, synthesis, and X-ray cocrystal structure. *J. Med. Chem.* 45, 4961–4974. doi: 10.1021/jm020259n

Cao, M., and Chen, W. (2019). Epidemiology of lung cancer in China. *Thorac. Cancer* 10, 3–7. doi: 10.1111/1759-7714.12916

Cassani, C., Vertemara, J., Bassani, M., Marsella, A., Tisi, R., Zampella, G., et al. (2019). The ATP-bound conformation of the Mre11-Rad50 complex is essential for Tel1/ATM activation. *Nucleic Acids Res.* 47, 3550–3567. doi: 10.1093/nar/gkz038

Cavanagh, H., and Rogers, K. M. (2015). The role of BRCA1 and BRCA2 mutations in prostate, pancreatic and stomach cancers. *Hered Cancer Clin. Pract.* 13:16. doi: 10.1186/s13053-015-0038-x

Chabanon, R. M., Muirhead, G., Krastev, D. B., Adam, J., Morel, D., Garrido, M., et al. (2019). PARP inhibition enhances tumor cell-intrinsic immunity in ERCC1-deficient non-small cell lung cancer. *J. Clin. Invest.* 129, 1211–1228. doi: 10.1172/JCI123319

Chabot, P., Hsia, T.-C., Ryu, J.-S., Gorbunova, V., Belda-Iniesta, C., Ball, D., et al. (2017). Veliparib in combination with whole-brain radiation therapy for patients with brain metastases from non-small cell lung cancer: results of a randomized, global, placebo-controlled study. *J. Neurooncol.* 131, 105–115. doi: 10.1007/s11060-016-2275-x

Chambon, P., Weill, J. D., and Mandel, P. (1963). Nicotinamide mononucleotide activation of new DNA-dependent polyadenylic acid synthesizing nuclear enzyme. *Biochem. Biophys. Res. Commun.* 11, 39–43. doi: 10.1016/0006-291x(63)90024-x

Chambon, P., Weill, J. D., Strosser, M., and Mandel, P. (1969). On the formation of a novel Adenylic compound by enzymatic extracts of liver nuclei. *Biochem. Biophys. Res. Commun.* 25, 638–643. doi: 10.1016/0006-291x(66)90502-x

Chaudhuri, A., Callen, E., Ding, X., Gogola, E., Duarte, A. A., Lee, J.-E., et al. (2016). Replication fork stability confers chemoresistance in BRCA-deficient cells. *Nature* 535, 382–387. doi: 10.1038/nature18325

Chaudhuri, A., and Nussenzweig, A. (2017). The multifaceted roles of PARP1 in DNA repair and chromatin remodelling. *Nat. Rev. Mol. Cell. Biol.* 18, 610–621. doi: 10.1038/nrm.2017.53

Chen, H., Lisby, M., and Symington, L. S. (2013). RPA coordinates DNA end resection and prevents formation of DNA hairpins. *Mol. Cell* 50, 589–600. doi: 10.1016/j.molcel.2013.04.032

Chin, J. L. (2009). Measuring quality of life after radical prostatectomy from the patient's perspective. *Can. Urol. Assoc. J.* 3, 453–453. doi: 10.5489/cuaj.1172

Choi, Y. E., Meghani, K., Brault, M.-E., Leclerc, L., He, Yizhou, J., et al. (2016). Platinum and PARP inhibitor resistance due to overexpression of MicroRNA-622 in BRCA1-mutant ovarian cancer. *Cell Rep.* 14, 429–439. doi: 10.1016/j.celrep.2015.12.046

Choi, Y. E., Pan, Y., Park, E., Konstantinopoulos, P., De, S., D'Andrea, A., et al. (2014). MicroRNAs down-regulate homologous recombination in the G1 phase of cycling cells to maintain genomic stability. *eLife* 3:e02445. doi: 10.7554/eLife.02445

Chovanec, M., Taza, F., Kalra, M., Hahn, N., Nephew, K. P., Spinella, M. J., et al. (2018). Incorporating DNA Methyltransferase Inhibitors (DNMTis) in the treatment of genitourinary malignancies: a systematic review. *Target Oncol.* 13, 49–60. doi: 10.1007/s11523-017-0546-x

Christie, E. L., Fereday, S., Doig, K., Pattnaik, S., Dawson, S. J., and Bowtell, D. D. L. (2017). Reversion of BRCA1/2 Germline mutations detected in circulating tumor DNA from patients with high-grade serous ovarian cancer. *J. Clin. Oncol.* 35, 1274–1280. doi: 10.1200/JCO.2016.70.4627

Clairmont, C. S., Sarangi, P., Ponnienselvan, K., Galli, L. D., Csete, I., Moreau, L., et al. (2020). TRIP13 regulates DNA repair pathway choice through REV7 conformational change. *Nat. Cell Biol.* 22, 87–96. doi: 10.1038/s41556-019-0442-y

Clements, K. E., Hale, A., Tolman, N. J., Nicolae, C. M., Sharma, A., Thakar, T., et al. (2019). Identification of regulators of poly-ADP-ribose polymerase (PARP) inhibitor response through complementary CRISPR knockout and activation screens. *bioRxiv* [Preprint]. doi: 10.1101/871970

Coleman, R. L., Fleming, G. F., Brady, M. F., Swisher, E. M., Steffensen, K. D., Friedlander, M., et al. (2019). Veliparib with first-line chemotherapy and as maintenance therapy in Ovarian cancer. *N. Engl. J. Med.* 381, 2403–2415. doi: 10.1056/NEJMoa1909707

Coleman, R. L., Oza, A. M., Lorusso, D., Aghajanian, C., Oaknin, A., Dean, A., et al. (2017). Rucaparib maintenance treatment for recurrent ovarian carcinoma after response to platinum therapy (ARIEL3): a randomised, double-blind, placebo-controlled, phase 3 trial. *Lancet* 390, 1949–1961. doi: 10.1016/S0140-6736(17)32440-6

Cong, K., Kousholt, A. N., Peng, M., Panzarino, N., Lee, W. T. C., Nayak, S., et al. (2019). PARPi synthetic lethality derives from replication-associated single-stranded DNA gaps. *bioRxiv* [Preprint]. doi: 10.1101/781989

Crawford, E. D. (2003). Epidemiology of prostate cancer. *Urology* 62, 3–12. doi: 10.1016/j.urology.2003.10.013

Criscuolo, D., Morra, F., Giannella, R., Cerrato, A., and Celetti, A. (2019). Identification of novel biomarkers of homologous recombination defect in DNA repair to predict sensitivity of prostate cancer cells to PARP-Inhibitors. *Int. J. Mol. Sci.* 20:3100. doi: 10.3390/ijms20123100

Damia, G., and D'Incalci, M. (1998). Mechanisms of resistance to alkylating agents. *Cytotechnology* 27, 165–173. doi: 10.1023/A:1008060720608

Dantzer, F., de La Rubia, G., Menissier-De Murcia, J., Hostomsky, Z., de Murcia, G., and Schreiber, V. (2000). Base excision repair is impaired in mammalian cells lacking Poly(ADP-ribose) polymerase-1. *Biochemistry* 39, 7559–7569. doi: 10.1021/bi0003442

Dantzer, F., Schreiber, V., Niedergang, C., Trucco, C., Flatter, E., De La Rubia, G., et al. (1999). Involvement of poly(ADP-ribose) polymerase in base excision repair. *Biochimie* 81, 69–75. doi: 10.1016/s0300-9084(99)80040-6

Das, B. B., Huang, S.-Y. N., Murai, J., Rehman, I., Amé, J.-C., Sengupta, S., et al. (2014). PARP1-TDP1 coupling for the repair of topoisomerase I-induced DNA damage. *Nucleic Acids Res.* 42, 4435. doi: 10.1093/nar/gku088

Davis, A. J., and Chen, D. J. (2013). DNA double strand break repair via non-homologous end-joining. *Transl. Cancer Res.* 2, 130–143. doi: 10.3978/j.issn.2218-676X.2013.04.02

de Almeida, B. P., Apolonio, J. D., Binnie, A., and Castelo-Branco, P. (2019). Roadmap of DNA methylation in breast cancer identifies novel prognostic biomarkers. *BMC Cancer* 19:219. doi: 10.1186/s12885-019-5403-0

de Bono, J., Mateo, J., Fizazi, K., Saad, F., Shore, N., Sandhu, S., et al. (2020). Olaparib for metastatic castration-resistant prostate cancer. *N. Engl. J. Med.* 382, 2091–2102. doi: 10.1056/NEJMoa1911440

de Bono, J., Ramanathan, R. K., Mina, L., Chugh, R., Glaspy, J., Rafii, S., et al. (2017). Phase I, dose-escalation, two-part trial of the PARP inhibitor talazoparib in patients with advanced germline BRCA1/2 mutations and selected sporadic cancers. *Cancer Discov.* 7, 620–629. doi: 10.1158/2159-8290.CD-16-1250

de Murcia, J. M., Niedergang, C., Trucco, C., Ricoul, M., Dutrillaux, B., Mark, M., et al. (1997). Requirement of poly(ADP-ribose) polymerase in recovery from DNA damage in mice and in cells. *Proc. Natl. Acad. Sci. U.S.A.* 94, 7303–7307. doi: 10.1073/pnas.94.14.7303

Dev, H., Chiang, T.-W. W., Lescale, C., de Krijger, I., Martin, A. G., Pilger, D., et al. (2018). Shieldin complex promotes DNA end-joining and counters homologous recombination in BRCA1-null cells. *Nat. Cell Biol.* 20, 954–965. doi: 10.1038/s41556-018-0140-1

Dockery, L. E., Gunderson, C. C., and Moore, K. N. (2017). Rucaparib: the past, present, and future of a newly approved PARP inhibitor for ovarian cancer. *Onco Targets Ther.* 10, 3029–3037. doi: 10.2147/OTT.S114714

Dungey, F. A., Löser, D. A., and Chalmers, A. J. (2008). Replication-dependent radiosensitization of human glioma cells by inhibition of Poly(ADP-Ribose) polymerase: mechanisms and therapeutic potential. *Int. J. Radiat. Oncol. Biol. Phys.* 72, 1188–1197. doi: 10.1016/j.ijrobp.2008.07.031

Edwards, S. L., Brough, R., Lord, C. J., Natrajan, R., Vatcheva, R., Levine, D. A., et al. (2008). Resistance to therapy caused by intragenic deletion in BRCA2. *Nature* 451, 1111–1115. doi: 10.1038/nature06548

Esposito, M. T., Zhao, L., Fung, T. K., Rane, J. K., Wilson, A., Martin, N., et al. (2015). Synthetic lethal targeting of oncogenic transcription factors in acute leukemia by PARP inhibitors. *Nat. Med.* 21, 1481–1490. doi: 10.1038/nm.3993

Ettl, J., Quek, R. G. W., Lee, K. H., Rugo, H. S., Hurvitz, S., Goncalves, A., et al. (2018). Quality of life with talazoparib versus physician's choice of chemotherapy in patients with advanced breast cancer and germline BRCA1/2 mutation: patient-reported outcomes from the EMBRACA phase III trial. *Ann. Oncol.* 29, 1939–1947. doi: 10.1093/annonc/mdy257

Fang, Y., McGrail, D. J., Sun, C., Labrie, M., Chen, X., Zhang, D., et al. (2019). Sequential therapy with PARP and WEE1 inhibitors minimizes toxicity while maintaining efficacy. *Cancer Cell* 35, 851–867.e7. doi: 10.1016/j.ccell.2019.05.001

Farago, A. F., Yeap, B. Y., Stanzione, M., Hung, Y. P., Heist, R. S., Marcoux, J. P., et al. (2019). Combination olaparib and temozolomide in relapsed small-cell lung cancer. *Cancer Discov.* 9, 1372–1387. doi: 10.1158/2159-8290.CD-19-0582

Faraoni, I., Giansanti, M., Voso, M. T., Lo-Coco, F., and Graziani, G. (2019). Targeting ADP-ribosylation by PARP inhibitors in acute myeloid leukaemia and related disorders. *Biochem. Pharmacol.* 167, 133–148. doi: 10.1016/j.bcp.2019.04.019

Farmer, H., McCabe, N., Lord, C. J., Tutt, A. N. J., Johnson, D. A., Richardson, T. B., et al. (2005). Targeting the DNA repair defect in BRCA mutant cells as a therapeutic strategy. *Nature* 434, 917–921. doi: 10.1038/nature03445

Fenton, A. L., Shirodkar, P., Macrae, C. J., Meng, L., and Koch, C. A. (2013). The PARP3- and ATM-dependent phosphorylation of APLF facilitates DNA double-strand break repair. *Nucleic Acids Res.* 41, 4080–4092. doi: 10.1093/nar/gkt134

Fisher, A. E., Hochegger, H., Takeda, S., and Caldecott, K. W. (2007). Poly(ADP-ribose) polymerase 1 accelerates single-strand break repair in concert with poly(ADP-ribose) glycohydrolase. *Mol. Cell. Biol.* 27, 5597–5605. doi: 10.1128/MCB.02248-06

Fok, J. H. L., Ramos-Montoya, A., Vazquez-Chantada, M., Wijnhoven, P. W. G., Follia, V., James, N., et al. (2019). AZD7648 is a potent and selective DNA-PK inhibitor that enhances radiation, chemotherapy and olaparib activity. *Nat. Commun.* 10:5065. doi: 10.1038/s41467-019-12836-9

Fong, P. C., Boss, D. S., Yap, T. A., Tutt, A., Wu, P., Mergui-Roelvink, M., et al. (2009). Inhibition of poly(ADP-ribose) polymerase in tumors from BRCA mutation carriers. *N. Engl. J. Med.* 361, 123–134. doi: 10.1056/NEJMoa0900212

Fong, P. C., Yap, T. A., Boss, D. S., Carden, C. P., Mergui-Roelvink, M., Gourley, C., et al. (2010). Poly(ADP)-ribose polymerase inhibition: frequent durable responses in BRCA carrier ovarian cancer correlating with platinum-free interval. *J. Clin. Oncol.* 28, 2512–2519. doi: 10.1200/JCO.2009.26.9589

Francica, P., and Rottenberg, S. (2018). Mechanisms of PARP inhibitor resistance in cancer and insights into the DNA damage response. *Genome Med.* 10:101. doi: 10.1186/s13073-018-0612-8

Franzese, E., Centonze, S., Diana, A., Carlino, F., Guerrera, L. P., Di Napoli, M., et al. (2019). PARP inhibitors in ovarian cancer. *Cancer Treat Rev.* 73, 1–9. doi: 10.1016/j.ctrv.2018.12.002

Friedlander, M., Matulonis, U., Gourley, C., du Bois, A., Vergote, I., Rustin, G., et al. (2018). Long-term efficacy, tolerability and overall survival in patients with platinum-sensitive, recurrent high-grade serous ovarian cancer treated with maintenance olaparib capsules following response to chemotherapy. *Br. J. Cancer* 119, 1075–1085. doi: 10.1038/s41416-018-0271-y

Friedlander, M., Meniawy, T., Markman, B., Mileshkin, L., Harnett, P., Millward, M., et al. (2019). Pamiparib in combination with tislelizumab in patients with advanced solid tumours: results from the dose-escalation stage of a multicentre, open-label, phase 1a/b trial. *Lancet Oncol.* 20, 1306–1315. doi: 10.1016/S1470-2045(19)30396-1

Fu, K., Sun, X., Wier, E. M., Hodgson, A., Hobbs, R. P., and Wan, F. (2016a). Sam68/KHDRBS1-dependent NF-kappaB activation confers radioprotection to the colon epithelium in gamma-irradiated mice. *eLife* 5:e21957. doi: 10.7554/eLife.21957

Fu, K., Sun, X., Wier, E. M., Hodgson, A., Liu, Y., Sears, C. L., et al. (2016b). Sam68/KHDRBS1 is critical for colon tumorigenesis by regulating genotoxic stress-induced NF-kappaB activation. *eLife* 5:e15018. doi: 10.7554/eLife.15018

Fujimura, S., Hasegawa, S., Shimizu, Y., and Sugimura, T. (1967). Polymerization of the adenosine 5'-diphosphate-ribose moiety of nicotinamide-adenine dinucleotide by nuclear enzyme. I. Enzymatic reactions. *Biochim. Biophys. Acta* 145, 247–259. doi: 10.1016/0005-2787(67)90043-3

Ganguly, B., Dolfi, S. C., Rodriguez-Rodriguez, L., Ganesan, S., and Hirshfield, K. M. (2016). Role of biomarkers in the development of PARP inhibitors. *Biomark. Cancer* 8(Suppl. 1), 15–25. doi: 10.4137/BIC.S36679

Gatti, M., Imhof, R., Huang, Q., Baudis, M., and Altmeyer, M. (2020). The ubiquitin ligase TRIP12 limits PARP1 trapping and constrains PARP inhibitor efficiency. *Cell Rep.* 32:107985. doi: 10.1016/j.celrep.2020.107985

Gaymes, T. J., Mohamedali, A. M., Patterson, M., Matto, N., Smith, A., Kulasekararaj, A., et al. (2013). Microsatellite instability induced mutations in DNA repair genes CtIP and MRE11 confer hypersensitivity to poly (ADP-ribose) polymerase inhibitors in myeloid malignancies. *Haematologica* 98, 1397–1406. doi: 10.3324/haematol.2012.079251

Geenen, J. J. J., Linn, S. C., Beijnen, J. H., and Schellens, J. H. M. (2018). PARP inhibitors in the treatment of triple-negative breast cancer. *Clin. Pharmacokinet.* 57, 427–437. doi: 10.1007/s40262-017-0587-4

George, A., Kaye, S., and Banerjee, S. (2017). Delivering widespread BRCA testing and PARP inhibition to patients with ovarian cancer. *Nat. Rev. Clin. Oncol.* 14, 284–296. doi: 10.1038/nrclinonc.2016.191

Gibbs-Seymour, I., Fontana, P., Rack, J. G. M., and Ahel, I. (2016). HPF1/C4orf27 Is a PARP-1-Interacting Protein that Regulates PARP-1 ADP-Ribosylation Activity. *Mol. Cell* 62, 432–442. doi: 10.1016/j.molcel.2016.03.008

Godet, I., and Gilkes, D. M. (2017). BRCA1 and BRCA2 mutations and treatment strategies for breast cancer. *Integr. Cancer Sci. Ther.* 4:10.15761/ICST.1000228. doi: 10.15761/ICST.1000228

Godon, C., Cordelieres, F. P., Biard, D., Giocanti, N., Megnin-Chanet, F., Hall, J., et al. (2008). PARP inhibition versus PARP-1 silencing: different outcomes in terms of single-strand break repair and radiation susceptibility. *Nucleic Acids Res.* 36, 4454–4464. doi: 10.1093/nar/gkn403

Gogola, E., Duarte, A. A., de Ruiter, J. R., Wiegant, W. W., Schmid, J. A., de Bruijn, R., et al. (2018). Selective Loss of PARG restores PARylation and counteracts PARP inhibitor-mediated synthetic lethality. *Cancer Cell* 33, 1078–1093.e12. doi: 10.1016/j.ccell.2018.05.008

Golan, T., Hammel, P., Reni, M., Van Cutsem, E., Macarulla, T., Hall, M. J., et al. (2019). Maintenance Olaparib for Germline BRCA-mutated metastatic pancreatic cancer. *N. Engl. J. Med.* 381, 317–327. doi: 10.1056/NEJMoa1903387

González-Billalabeitia, E., Seitzer, N., Song, S. J., Song, M. S., Patnaik, A., Liu, X.-S., et al. (2014). Vulnerabilities of PTEN-TP53-deficient prostate cancers

to compound PARP-PI3K inhibition. *Cancer Discov.* 4, 896–904. doi: 10.1158/2159-8290.CD-13-0230

Gonzalez-Martin, A., Pothuri, B., Vergote, I., DePont Christensen, R., Graybill, W., Mirza, M. R., et al. (2019). Niraparib in patients with newly diagnosed advanced ovarian cancer. *N. Engl. J. Med.* 381, 2391–2402. doi: 10.1056/NEJMoa1910962

Gornstein, E. L., Sandefur, S., Chung, J. H., Gay, L. M., Holmes, O., Erlich, R. L., et al. (2018). BRCA2 reversion mutation associated with acquired resistance to olaparib in estrogen receptor-positive breast cancer detected by genomic profiling of tissue and liquid biopsy. *Clin. Breast Cancer* 18, 184–188. doi: 10.1016/j.clbc.2017.12.010

Gottipati, P., Vischioni, B., Schultz, N., Solomons, J., Bryant, H. E., Djureinovic, T., et al. (2010). Poly(ADP-ribose) polymerase is hyperactivated in homologous recombination-defective cells. *Cancer Res.* 70, 5389–5398. doi: 10.1158/0008-5472.CAN-09-4716

Greenberg, R. A. (2018). Assembling a protective shield. *Nat. Cell Biol.* 20, 862–863. doi: 10.1038/s41556-018-0152-x

Gupta, R., Somyajit, K., Narita, T., Maskey, E., Stanlie, A., Kremer, M., et al. (2018). DNA repair network analysis reveals shieldin as a key regulator of NHEJ and PARP inhibitor sensitivity. *Cell* 173, 972–988.e23. doi: 10.1016/j.cell.2018.03.050

Haince, J. F., McDonald, D., Rodrigue, A., Dery, U., Masson, J. Y., Hendzel, M. J., et al. (2008). PARP1-dependent kinetics of recruitment of MRE11 and NBS1 proteins to multiple DNA damage sites. *J. Biol. Chem.* 283, 1197–1208. doi: 10.1074/jbc.M706734200

Hall, M. J., Reid, J. E., Burbidge, L. A., Pruss, D., Deffenbaugh, A. M., Frye, C., et al. (2009). BRCA1 and BRCA2 mutations in women of different ethnicities undergoing testing for hereditary breast-ovarian cancer. *Cancer* 115, 2222–2233. doi: 10.1002/cncr.24200

Han, H., Dieras, V., Robson, M. E., Palacova, M., Marcom, P. K., Jager, A., et al. (2017). Efficacy and tolerability of veliparib (V; ABT-888) in combination with carboplatin (C) and paclitaxel (P) vs placebo (Plc) plus C/P in patients (pts) with *BRCA1* or *BRCA2* mutations and metastatic breast cancer: a randomized, phase 2 study. *Cancer Res.* 77:S2-05-S2-05. doi: 10.1158/1538-7445.SABCS16-S2-05

Han, Y., Chen, M. K., Wang, H. L., Hsu, J. L., Li, C. W., Chu, Y. Y., et al. (2019). Synergism of PARP inhibitor fluzoparib (HS10160) and MET inhibitor HS10241 in breast and ovarian cancer cells. *Am. J. Cancer Res.* 9, 608–618.

Hanzlikova, H., Gittens, W., Krejcikova, K., Zeng, Z., and Caldecott, K. (2016). Overlapping roles for PARP1 and PARP2 in the recruitment of endogenous XRCC1 and PNKP into oxidized chromatin. *Nucleic Acids Res.* 45, 2546–2557. doi: 10.1093/nar/gkw1246

Hanzlikova, H., Gittens, W., Krejcikova, K., Zeng, Z., and Caldecott, K. W. (2017). Overlapping roles for PARP1 and PARP2 in the recruitment of endogenous XRCC1 and PNKP into oxidized chromatin. *Nucleic Acids Res.* 45, 2546–2557.

Hanzlikova, H., Kalasova, I., Demin, A. A., Pennicott, L. E., Cihlarova, Z., and Caldecott, K. W. (2018). The Importance of Poly(ADP-Ribose) Polymerase as a Sensor of Unligated Okazaki Fragments during DNA Replication. *Mol. Cell* 71, 319–331.e3. doi: 10.1016/j.molcel.2018.06.004

Hasegawa, S., Fujimura, S., Shimizu, Y., and Sugimura, R. (1967). The polymerization of adenosine 5'-diphosphate-ribose moiety of NAD by nuclear enzyme. II. Properties of the reaction product. *Biochim. Biophys. Acta* 149, 369–376. doi: 10.1016/0005-2787(67)90165-7

Heeke, A. L., Pishvaian, M. J., Lynce, F., Xiu, J., Brody, J. R., Chen, W.-J., et al. (2018). Prevalence of homologous recombination-related gene mutations across multiple cancer types. *JCO Precis. Oncol.* 2018:10.1200/PO.17.00286. doi: 10.1200/PO.1217.00286

Hentze, J. L., Høgdall, C. K., and Høgdall, E. V. (2019). Methylation and ovarian cancer: Can DNA methylation be of diagnostic use? *Mol. Clin. Oncol.* 10, 323–330. doi: 10.3892/mco.2019.1800

Hiom, K. (2001). Recombination: homologous recombination branches out. *Curr. Biol.* 11, R278–R280. doi: 10.1016/s0960-9822(01)00138-5

Hodgson, D. R., Dougherty, B. A., Lai, Z., Fielding, A., Grinsted, L., Spencer, S., et al. (2018). Candidate biomarkers of PARP inhibitor sensitivity in ovarian cancer beyond the BRCA genes. *Br. J. Cancer* 119, 1401–1409. doi: 10.1038/s41416-018-0274-8

Hopkins, T. A., Ainsworth, W. B., Ellis, P. A., Donawho, C. K., Digiammarino, E. L., Panchal, S. C., et al. (2019). PARP1 trapping by PARP inhibitors drives cytotoxicity in both cancer cells and healthy bone marrow. *Mol. Cancer Res.* 17, 409–419. doi: 10.1158/1541-7786.MCR-18-0138

Hopkins, T. A., Shi, Y., Rodriguez, L. E., Solomon, L. R., Donawho, C. K., DiGiammarino, E. L., et al. (2015). Mechanistic dissection of PARP1 trapping and the impact on *in vivo* tolerability and efficacy of PARP inhibitors. *Mol. Cancer Res.* 13, 1465–1477. doi: 10.1158/1541-7786.MCR-15-0191-T

Horton, J. K., Stefanick, D. F., Prasad, R., Gassman, N. R., Kedar, P. S., and Wilson, S. H. (2014). Base excision repair defects invoke hypersensitivity to PARP inhibition. *Mol. Cancer Res.* 12, 1128–1139. doi: 10.1158/1541-7786.MCR-13-0502

Houl, J. H., Ye, Z., Brosey, C. A., Balapiti-Modarage, L. P. F., Namjoshi, S., Bacolla, A., et al. (2019). Selective small molecule PARG inhibitor causes replication fork stalling and cancer cell death. *Nat. Commun.* 10:5654. doi: 10.1038/s41467-019-13508-4

Hu, Y., Petit, S. A., Ficarro, S. B., Toomire, K. J., Xie, A., Lim, E., et al. (2014). PARP1-driven poly-ADP-ribosylation regulates BRCA1 function in homologous recombination-mediated DNA repair. *Cancer Discov.* 4, 1430–1447. doi: 10.1158/2159-8290.CD-13-0891

Huang, J., Xie, Y., Sun, X., Zeh, H. J. III, Kang, R., Lotze, M. T., et al. (2015). DAMPs, ageing, and cancer: the 'DAMP Hypothesis'. *Ageing Res. Rev.* 24(Pt A), 3–16. doi: 10.1016/j.arr.2014.10.004

Hurley, R. M., Wahner Hendrickson, A. E., Visscher, D. W., Ansell, P., Harrell, M. I., Wagner, J. M., et al. (2019). 53BP1 as a potential predictor of response in PARP inhibitor-treated homologous recombination-deficient ovarian cancer. *Gynecol. Oncol.* 153, 127–134. doi: 10.1016/j.ygyno.2019.01.015

Hurvitz, S. A., Quek, R. G. W., Turner, N. C., Telli, M. L., Rugo, H. S., Mailliez, A., et al. (2018). Quality of life with talazoparib after platinum or multiple cytotoxic non-platinum regimens in patients with advanced breast cancer and germline BRCA1/2 mutations: patient-reported outcomes from the ABRAZO phase 2 trial. *Eur. J. Cancer* 104, 160–168. doi: 10.1016/j.ejca.2018.09.003

Ibrahim, Y. H., Garcia-Garcia, C., Serra, V., He, L., Torres-Lockhart, K., Prat, A., et al. (2012). PI3K inhibition impairs BRCA1/2 expression and sensitizes BRCA-proficient triple-negative breast cancer to PARP inhibition. *Cancer Discov.* 2, 1036–1047. doi: 10.1158/2159-8290.CD-11-0348

Iqbal, J., Ragone, A., Lubinski, J., Lynch, H. T., Moller, P., Ghadirian, P., et al. (2012). The incidence of pancreatic cancer in BRCA1 and BRCA2 mutation carriers. *Br. J. Cancer* 107, 2005–2009. doi: 10.1038/bjc.2012.483

Issaeva, N., Thomas, H. D., Djureinovic, T., Jaspers, J. E., Stoimenov, I., Kyle, S., et al. (2010). 6-thioguanine selectively kills BRCA2-defective tumors and overcomes PARP inhibitor resistance. *Cancer Res.* 70, 6268–6276. doi: 10.1158/0008-5472.CAN-09-3416

Jensen, R. B., Carreira, A., and Kowalczykowski, S. C. (2010). Purified human BRCA2 stimulates RAD51-mediated recombination. *Nature* 467, 678–683. doi: 10.1038/nature09399

Jhan, J. R., and Andrechek, E. R. (2017). Triple-negative breast cancer and the potential for targeted therapy. *Pharmacogenomics* 18, 1595–1609. doi: 10.2217/pgs-2017-0117

Jiang, X., Li, X., Li, W., Bai, H., and Zhang, Z. (2019). PARP inhibitors in ovarian cancer: sensitivity prediction and resistance mechanisms. *J. Cell. Mol. Med.* 23, 2303–2313. doi: 10.1111/jcmm.14133

Jonsson, P., Bandlamudi, C., Cheng, M. L., Srinivasan, P., Chavan, S. S., Friedman, N. D., et al. (2019). Tumour lineage shapes BRCA-mediated phenotypes. *Nature* 571, 576–579. doi: 10.1038/s41586-019-1382-1

Karnak, D., Engelke, C. G., Parsels, L. A., Kausar, T., Wei, D., Robertson, J. R., et al. (2014). Combined inhibition of Wee1 and PARP1/2 for radiosensitization in pancreatic cancer. *Clin. Cancer Res.* 20, 5085–5096. doi: 10.1158/1078-0432.CCR-14-1038

Kato, K., Omura, H., Ishitani, R., and Nureki, O. (2017). Cyclic GMP–AMP as an endogenous second messenger in innate immune signaling by cytosolic DNA. *Annu. Rev. Biochem.* 86, 541–566. doi: 10.1146/annurev-biochem-061516-044813

Kaufman, B., Shapira-Frommer, R., Schmutzler, R. K., Audeh, M. W., Friedlander, M., Balmaña, J., et al. (2015). Olaparib monotherapy in patients with advanced cancer and a germline BRCA1/2 mutation. *J. Clin. Oncol.* 33, 244–250. doi: 10.1200/jco.2014.56.2728

Khanna, K. K., and Jackson, S. P. (2001). DNA double-strand breaks: signaling, repair and the cancer connection. *Nat. Genet.* 27, 247–254. doi: 10.1038/85798

Kim, D. S., Camacho, C. V., Nagari, A., Malladi, V. S., Challa, S., and Kraus, W. L. (2019). Activation of PARP-1 by snoRNAs controls ribosome biogenesis and cell growth via the RNA Helicase DDX21. *Mol. Cell* 75, 1270–1285.e14. doi: 10.1016/j.molcel.2019.06.020

Kondrashova, O., Nguyen, M., Shield-Artin, K., Tinker, A. V., Teng, N. N. H., Harrell, M. I., et al. (2017). Secondary somatic mutations restoring RAD51C and RAD51D associated with acquired resistance to the PARP inhibitor Rucaparib in high-grade ovarian carcinoma. *Cancer Discov.* 7, 984–998. doi: 10.1158/2159-8290.CD-17-0419

Kondrashova, O., Topp, M., Nesic, K., Lieschke, E., Ho, G.-Y., Harrell, M. I., et al. (2018). Methylation of all BRCA1 copies predicts response to the PARP inhibitor rucaparib in ovarian carcinoma. *Nat. Commun.* 9:3970. doi: 10.1038/s41467-018-05564-z

Koppensteiner, R., Samartzis, E. P., Noske, A., von Teichman, A., Dedes, I., Gwerder, M., et al. (2014). Effect of MRE11 loss on PARP-inhibitor sensitivity in endometrial cancer *in vitro*. *PLoS One* 9:e100041. doi: 10.1371/journal.pone.0100041

Kotsopoulos, J. (2018). BRCA mutations and breast cancer prevention. *Cancers* 10:524. doi: 10.3390/cancers10120524

Krajewska, M., Fehrmann, R. S. N., de Vries, E. G. E., and van Vugt, M. A. T. M. (2015). Regulators of homologous recombination repair as novel targets for cancer treatment. *Front. Genet.* 6:96. doi: 10.3389/fgene.2015.00096

Krishnakumar, R., and Kraus, W. L. (2010). The PARP side of the nucleus: molecular actions, physiological outcomes, and clinical targets. *Mol. Cell* 39, 8–24. doi: 10.1016/j.molcel.2010.06.017

Kuchenbaecker, K. B., Hopper, J. L., Barnes, D. R., Phillips, K. A., Mooij, T. M., Roos-Blom, M. J., et al. (2017). Risks of breast, ovarian, and contralateral breast cancer for BRCA1 and BRCA2 mutation carriers. *JAMA* 317, 2402–2416. doi: 10.1001/jama.2017.7112

Kukolj, E., Kaufmann, T., Dick, A. E., Zeillinger, R., Gerlich, D. W., and Slade, D. (2017). PARP inhibition causes premature loss of cohesion in cancer cells. *Oncotarget* 8, 103931–103951. doi: 10.18632/oncotarget.21879

Kummar, S., Kinders, R., Gutierrez, M. E., Rubinstein, L., Parchment, R. E., Phillips, L. R., et al. (2009). Phase 0 clinical trial of the poly (ADP-ribose) polymerase inhibitor ABT-888 in patients with advanced malignancies. *J. Clin. Oncol.* 27, 2705–2711. doi: 10.1200/JCO.2008.19.7681

Laird, J. H., Lok, B. H., Ma, J., Bell, A., de Stanchina, E., Poirier, J. T., et al. (2018). Talazoparib is a potent radiosensitizer in small cell lung cancer cell lines and xenografts. *Clin. Cancer Res.* 24, 5143–5152. doi: 10.1158/1078-0432.CCR-18-0401

Langelier, M. F., Riccio, A. A., and Pascal, J. M. (2014). PARP-2 and PARP-3 are selectively activated by 5' phosphorylated DNA breaks through an allosteric regulatory mechanism shared with PARP-1. *Nucleic Acids Res.* 42, 7762–7775. doi: 10.1093/nar/gku474

Le, D., and Gelmon, K. A. (2018). Olaparib tablets for the treatment of germ line BRCA-mutated metastatic breast cancer. *Expert Rev. Clin. Pharmacol.* 11, 833–839. doi: 10.1080/17512433.2018.1513321

Lee, A., Moon, B. I., and Kim, T. H. (2020). BRCA1/BRCA2 pathogenic variant breast cancer: treatment and prevention strategies. *Ann. Lab. Med.* 40, 114–121. doi: 10.3343/alm.2020.40.2.114

Lee, M. H., Na, H., Kim, E. J., Lee, H. W., and Lee, M. O. (2012). Poly(ADP-ribosyl)ation of p53 induces gene-specific transcriptional repression of MTA1. *Oncogene* 31, 5099–5107. doi: 10.1038/onc.2012.2

Leidecker, O., Bonfiglio, J. J., Colby, T., Zhang, Q., Atanassov, I., Zaja, R., et al. (2016). Serine is a new target residue for endogenous ADP-ribosylation on histones. *Nat. Chem. Biol.* 12, 998–1000. doi: 10.1038/nchembio.2180

Li, T., and Chen, Z. J. (2018). The cGAS-cGAMP-STING pathway connects DNA damage to inflammation, senescence, and cancer. *J. Exp. Med.* 215, 1287–1299. doi: 10.1084/jem.20180139

Liao, H., Ji, F., Helleday, T., and Ying, S. (2018). Mechanisms for stalled replication fork stabilization: new targets for synthetic lethality strategies in cancer treatments. *EMBO Rep.* 19:e46263. doi: 10.15252/embr.201846263

Lin, K. K., Harrell, M. I., Oza, A. M., Oaknin, A., Ray-Coquard, I., Tinker, A. V., et al. (2019). BRCA reversion mutations in circulating tumor DNA Predict primary and acquired resistance to the PARP inhibitor rucaparib in high-grade ovarian carcinoma. *Cancer Discov.* 9, 210–219. doi: 10.1158/2159-8290.CD-18-0715

Litton, J. K., Rugo, H. S., Ettl, J., Hurvitz, S. A., Goncalves, A., Lee, K. H., et al. (2018). Talazoparib in patients with advanced breast cancer and a Germline BRCA mutation. *N. Engl. J. Med.* 379, 753–763. doi: 10.1056/NEJMoa1802905

Liu, L., Kong, M., Gassman, N. R., Freudenthal, B. D., Prasad, R., Zhen, S., et al. (2017). PARP1 changes from three-dimensional DNA damage searching to one-dimensional diffusion after auto-PARylation or in the presence of APE1. *Nucleic Acids Res.* 45, 12834–12847. doi: 10.1093/nar/gkx1047

Liu, P., Cheng, H., Roberts, T. M., and Zhao, J. J. (2009). Targeting the phosphoinositide 3-kinase pathway in cancer. *Nat. Rev. Drug Discov.* 8, 627–644. doi: 10.1038/nrd2926

Lorusso, D., Bria, E., Costantini, A., Di Maio, M., Rosti, G., and Mancuso, A. (2017). Patients' perception of chemotherapy side effects: expectations, doctor–patient communication and impact on quality of life – An Italian survey. *Eur. J. Cancer Care* 26:e12618. doi: 10.1111/ecc.12618

Luo, J., Dai, X., Hu, H., Chen, J., Zhao, L., Yang, C., et al. (2019). Fluzoparib increases radiation sensitivity of non-small cell lung cancer (NSCLC) cells without BRCA1/2 mutation, a novel PARP1 inhibitor undergoing clinical trials. *J. Cancer Res. Clin. Oncol.* 146, 721–737. doi: 10.1007/s00432-019-03097-6

Lyko, F. (2018). The DNA methyltransferase family: a versatile toolkit for epigenetic regulation. *Nat. Rev. Genet.* 19, 81–92. doi: 10.1038/nrg.2017.80

Ma, C. J., Gibb, B., Kwon, Y., Sung, P., and Greene, E. C. (2017). Protein dynamics of human RPA and RAD51 on ssDNA during assembly and disassembly of the RAD51 filament. *Nucleic Acids Res.* 45, 749–761. doi: 10.1093/nar/gkw1125

Macfarlane, L. A., and Murphy, P. R. (2010). MicroRNA: biogenesis, function and role in cancer. *Curr. Genomics* 11, 537–561. doi: 10.2174/138920210793175895

Maede, Y., Shimizu, H., Fukushima, T., Kogame, T., Nakamura, T., Miki, T., et al. (2014). Differential and common DNA repair pathways for topoisomerase I- and II-targeted drugs in a genetic DT40 repair cell screen panel. *Mol. Cancer Ther.* 13, 214–220. doi: 10.1158/1535-7163.mct-13-0551

Majuelos-Melguizo, J., Rodriguez, M. I., Lopez-Jimenez, L., Rodriguez-Vargas, J. M., Marti Martin-Consuegra, J. M., Serrano-Saenz, S., et al. (2015). PARP targeting counteracts gliomagenesis through induction of mitotic catastrophe and aggravation of deficiency in homologous recombination in PTEN-mutant glioma. *Oncotarget* 6, 4790–4803. doi: 10.18632/oncotarget.2993

Malanga, M., and Althaus, F. R. (2004). Poly(ADP-ribose) reactivates stalled DNA topoisomerase I and Induces DNA strand break resealing. *J. Biol. Chem.* 279, 5244–5248. doi: 10.1074/jbc.C300437200

Mamdani, H., Chen, J., Kim, S., Ibrahim, Y., Asad, M. F. B., Nieva, J. J., et al. (2019). DNA damage response and repair (DDR) gene mutations and correlation with tumor mutation burden (TMB) in non-small cell lung cancer (NSCLC). *J. Clin. Oncol.* 37, 9100–9100. doi: 10.1200/JCO.2019.37.15_suppl.9100

Mandelker, D., Zhang, L., Kemel, Y., Stadler, Z. K., Joseph, V., Zehir, A., et al. (2017). Mutation detection in patients with advanced cancer by universal sequencing of cancer-related genes in tumor and normal DNA vs Guideline-Based Germline testing. *JAMA* 318, 825–835. doi: 10.1001/jama.2017.11137

Mao, Z., Bozzella, M., Seluanov, A., and Gorbunova, V. (2008). DNA repair by nonhomologous end joining and homologous recombination during cell cycle in human cells. *Cell Cycle* 7, 2902–2906. doi: 10.4161/cc.7.18.6679

Mateo, J., Carreira, S., Sandhu, S., Miranda, S., Mossop, H., Perez-Lopez, R., et al. (2015). DNA-repair defects and olaparib in metastatic prostate cancer. *N. Engl. J. Med.* 373, 1697–1708. doi: 10.1056/NEJMoa1506859

Mateo, J., Porta, N., Bianchini, D., McGovern, U., Elliott, T., Jones, R., et al. (2020). Olaparib in patients with metastatic castration-resistant prostate cancer with DNA repair gene aberrations (TOPARP-B): a multicentre, open-label, randomised, phase 2 trial. *Lancet Oncol.* 21, 162–174. doi: 10.1016/S1470-2045(19)30684-9

Matheson, C. J., Backos, D. S., and Reigan, P. (2016). Targeting WEE1 Kinase in Cancer. *Trends Pharmacol. Sci.* 37, 872–881. doi: 10.1016/j.tips.2016.06.006

Matos, J., and West, S. C. (2014). Holliday junction resolution: regulation in space and time. *DNA Repair* 19, 176–181. doi: 10.1016/j.dnarep.2014.03.013

Maya-Mendoza, A., Moudry, P., Merchut-Maya, J. M., Lee, M., Strauss, R., and Bartek, J. (2018). High speed of fork progression induces DNA replication stress and genomic instability. *Nature* 559, 279–284. doi: 10.1038/s41586-018-0261-5

Ménissier de Murcia, J., Ricoul, M., Tartier, L., Niedergang, C., Huber, A., Dantzer, F., et al. (2003). Functional interaction between PARP-1 and PARP-2 in chromosome stability and embryonic development in mouse. *EMBO J.* 22, 2255–2263. doi: 10.1093/emboj/cdg206

Michelena, J., Lezaja, A., Teloni, F., Schmid, T., Imhof, R., and Altmeyer, M. (2018). Analysis of PARP inhibitor toxicity by multidimensional fluorescence microscopy reveals mechanisms of sensitivity and resistance. *Nat. Commun.* 9:2678. doi: 10.1038/s41467-018-05031-9

Min, A., Im, S. A., Yoon, Y. K., Song, S. H., Nam, H. J., Hur, H. S., et al. (2013). RAD51C-deficient cancer cells are highly sensitive to the PARP inhibitor olaparib. *Mol. Cancer Ther.* 12, 865–877. doi: 10.1158/1535-7163.MCT-12-0950

Min, W., Bruhn, C., Grigaravicius, P., Zhou, Z. W., Li, F., Kruger, A., et al. (2013). Poly(ADP-ribose) binding to Chk1 at stalled replication forks is required for S-phase checkpoint activation. *Nat. Commun.* 4:2993. doi: 10.1038/ncomms3993

Mirza, M. R., Monk, B. J., Herrstedt, J., Oza, A. M., Mahner, S., Redondo, A., et al. (2016). Niraparib maintenance therapy in platinum-sensitive, recurrent ovarian cancer. *N. Engl. J. Med.* 375, 2154–2164. doi: 10.1056/NEJMoa1611310

Miwa, M., and Sugimura, T. (1971). Splitting of the ribose-ribose linkage of poly(adenosine diphosphate-robose) by a calf thymus extract. *J. Biol. Chem.* 246, 6362–6364.

Miwa, M., Tanaka, M., Matsushima, T., and Sugimura, T. (1974). Purification and properties of glycohydrolase from calf thymus splitting ribose-ribose linkages of poly(adenosine diphosphate ribose). *J. Biol. Chem.* 249, 3475–3482.

Montavon, C., Gloss, B. S., Warton, K., Barton, C. A., Statham, A. L., Scurry, J. P., et al. (2012). Prognostic and diagnostic significance of DNA methylation patterns in high grade serous ovarian cancer. *Gynecol. Oncol.* 124, 582–588. doi: 10.1016/j.ygyno.2011.11.026

Moore, K., Colombo, N., Scambia, G., Kim, B.-G., Oaknin, A., Friedlander, M., et al. (2018). Maintenance Olaparib in patients with newly diagnosed advanced ovarian cancer. *N. Engl. J. Med.* 379, 2495–2505. doi: 10.1056/NEJMoa1810858

Moore, K. N., Secord, A. A., Geller, M. A., Miller, D. S., Cloven, N., Fleming, G. F., et al. (2019). Niraparib monotherapy for late-line treatment of ovarian cancer (QUADRA): a multicentre, open-label, single-arm, phase 2 trial. *Lancet Oncol.* 20, 636–648. doi: 10.1016/S1470-2045(19)30029-4

Murai, J., Huang, S. Y., Das, B. B., Renaud, A., Zhang, Y., Doroshow, J. H., et al. (2012b). Trapping of PARP1 and PARP2 by Clinical PARP Inhibitors. *Cancer Res.* 72, 5588–5599. doi: 10.1158/0008-5472.CAN-12-2753

Murai, J., Huang, S. Y., Renaud, A., Zhang, Y., Ji, J., Takeda, S., et al. (2014b). Stereospecific PARP trapping by BMN 673 and comparison with olaparib and rucaparib. *Mol. Cancer Ther.* 13, 433–443. doi: 10.1158/1535-7163.MCT-13-0803

Murai, J., Huang, S.-Y. N., Das, B. B., Renaud, A., Zhang, Y., Doroshow, J. H., et al. (2012a). Trapping of PARP1 and PARP2 by Clinical PARP Inhibitors. *Cancer Res.* 72, 5588. doi: 10.1158/0008-5472.CAN-12-2753

Murai, J., Zhang, Y., Morris, J., Ji, J., Takeda, S., Doroshow, J. H., et al. (2014b). Rationale for poly(ADP-ribose) polymerase (PARP) inhibitors in combination therapy with camptothecins or temozolomide based on PARP trapping versus catalytic inhibition. *J. Pharmacol. Exp. Ther.* 349, 408–416. doi: 10.1124/jpet.113.210146

Muvarak, N. E., Chowdhury, K., Xia, L., Robert, C., Choi, E. Y., Cai, Y., et al. (2016). Enhancing the cytotoxic effects of PARP inhibitors with DNA demethylating agents–A potential therapy for cancer. *Cancer Cell* 30, 637–650. doi: 10.1016/j.ccell.2016.09.002

Nazarkina, Z. K., Khodyreva, S. N., Marsin, S., Lavrik, O. I., and Radicella, J. P. (2007). XRCC1 interactions with base excision repair DNA intermediates. *DNA Repair* 6, 254–264. doi: 10.1016/j.dnarep.2006.10.002

Nishizuka, Y., Ueda, K., Nakazawa, K., and Hayaishi, O. (1967). Studies on the polymer of adenosine diphosphate ribose. I. Enzymic formation from nicotinamide adenine dinuclotide in mammalian nuclei. *J. Biol. Chem.* 242, 3164–3171.

Noordermeer, S. M., and van Attikum, H. (2019). PARP inhibitor resistance: a tug-of-war in BRCA-mutated cells. *Trends Cell Biol.* 29, 820–834. doi: 10.1016/j.tcb.2019.07.008

Offit, K. (2006). BRCA mutation frequency and penetrance: new data, old debate. *J. Natl. Cancer Inst.* 98, 1675–1677. doi: 10.1093/jnci/djj500

Oh, M., Alkhushaym, N., Fallatah, S., Althagafi, A., Aljadeed, R., Alsowaida, Y., et al. (2019). The association of BRCA1 and BRCA2 mutations with prostate cancer risk, frequency, and mortality: a meta-analysis. *Prostate* 79, 880–895. doi: 10.1002/pros.23795

Oza, A. M., Tinker, A. V., Oaknin, A., Shapira-Frommer, R., McNeish, I. A., Swisher, E. M., et al. (2017). Antitumor activity and safety of the PARP inhibitor rucaparib in patients with high-grade ovarian carcinoma and a germline or somatic BRCA1 or BRCA2 mutation: integrated analysis of data from Study 10 and ARIEL2. *Gynecol. Oncol.* 147, 267–275. doi: 10.1016/j.ygyno.2017.08.022

Pachkowski, B. F., Tano, K., Afonin, V., Elder, R. H., Takeda, S., Watanabe, M., et al. (2009). Cells deficient in PARP-1 show an accelerated accumulation of DNA single strand breaks, but not AP sites, over the PARP-1-proficient cells exposed to MMS. *Mutat. Res.* 671, 93–99. doi: 10.1016/j.mrfmmm.2009.09.006

Palomba, G., Budroni, M., Olmeo, N., Atzori, F., Ionta, M. T., Pisano, M., et al. (2014). Triple-negative breast cancer frequency and type of BRCA mutation: clues from Sardinia. *Oncol. Lett.* 7, 948–952. doi: 10.3892/ol.2014.1834

Pantelidou, C., Sonzogni, O., De Oliveria Taveira, M., Mehta, A. K., Kothari, A., Wang, D., et al. (2019). PARP inhibitor efficacy depends on CD8 $^{+}$ T-cell recruitment via intratumoral STING pathway activation in BRCA-deficient models of triple-negative breast cancer. *Cancer Discov.* 9, 722–737. doi: 10.1158/2159-8290.Cd-18-1218

Parsels, L. A., Karnak, D., Parsels, J. D., Zhang, Q., Velez-Padilla, J., Reichert, Z. R., et al. (2018). PARP1 trapping and DNA replication stress enhance radiosensitization with combined WEE1 and PARP inhibitors. *Mol. Cancer Res.* 16, 222–232. doi: 10.1158/1541-7786.mcr-17-0455

Pasanisi, P., and Bruno, E. (2018). Breast cancer in BRCA mutations carriers: is it time for a "lifestyle" primary prevention? *Epidemiol. Prev.* 42, 369–371. doi: 10.19191/EP18.5-6.P369.107

Patel, A. G., Sarkaria, J. N., and Kaufmann, S. H. (2011). Nonhomologous end joining drives poly(ADP-ribose) polymerase (PARP) inhibitor lethality in homologous recombination-deficient cells. *Proc. Natl. Acad. Sci. U.S.A.* 108, 3406–3411. doi: 10.1073/pnas.1013715108

Pearce, A., Haas, M., Viney, R., Pearson, S.-A., Haywood, P., Brown, C., et al. (2017). Incidence and severity of self-reported chemotherapy side effects in routine care: a prospective cohort study. *PLoS One* 12:e0184360. doi: 10.1371/journal.pone.0184360

Petrucelli, N., Daly, M. B., and Feldman, G. L. (2010). Hereditary breast and ovarian cancer due to mutations in BRCA1 and BRCA2. *Genet. Med.* 12, 245–259. doi: 10.1097/GIM.0b013e3181d38f2f

Pines, A., Vrouwe, M. G., Marteijn, J. A., Typas, D., Luijsterburg, M. S., Cansoy, M., et al. (2012). PARP1 promotes nucleotide excision repair through DDB2 stabilization and recruitment of ALC1. *J. Cell Biol.* 199, 235–249. doi: 10.1083/jcb.201112132

Plummer, R., Lorigan, P., Steven, N., Scott, L., Middleton, M., Wilson, R., et al. (2013). A phase II study of the potent PARP inhibitor, Rucaparib (PF-01367338, AG014699), with temozolomide in patients with metastatic melanoma demonstrating evidence of chemopotentiation. *Cancer Chemother. Pharmacol.* 71, 1191–1199. doi: 10.1007/s00280-013-2113-1

Pratz, K. W., Koh, B. D., Patel, A. G., Flatten, K. S., Poh, W., Herman, J. G., et al. (2016). Poly (ADP-Ribose) polymerase inhibitor hypersensitivity in aggressive myeloproliferative neoplasms. *Clin. Cancer Res.* 22, 3894–3902. doi: 10.1158/1078-0432.ccr-15-2351

Preiss, J., Schlaeger, R., and Hilz, H. (1971). Specific inhibition of poly adpribose polymerase by thymidine and nicotinamide in HeLa cells. *FEBS Lett.* 19, 244–246. doi: 10.1016/0014-5793(71)80524-0

Pujade-Lauraine, E., Ledermann, J. A., Selle, F., Gebski, V., Penson, R. T., Oza, A. M., et al. (2017). Olaparib tablets as maintenance therapy in patients with platinum-sensitive, relapsed ovarian cancer and a BRCA1/2 mutation (SOLO2/ENGOT-Ov21): a double-blind, randomised, placebo-controlled, phase 3 trial. *Lancet Oncol.* 18, 1274–1284. doi: 10.1016/S1470-2045(17)304692

Pulliam, N., Fang, F., Ozes, A. R., Tang, J., Adewuyi, A., Keer, H., et al. (2018). An effective epigenetic-PARP inhibitor combination therapy for breast and ovarian cancers independent of BRCA mutations. *Clin. Cancer Res.* 24, 3163–3175. doi: 10.1158/1078-0432.CCR-18-0204

Purnell, M. R., and Whish, W. J. (1980). Novel inhibitors of poly(ADP-ribose) synthetase. *Biochem. J.* 185, 775–777. doi: 10.1042/bj1850775

Quinet, A., and Vindigni, A. (2018). Superfast DNA replication causes damage in cancer cells. *Nature* 559, 186–187. doi: 10.1038/d41586-018-05501-6

Rawla, P., Sunkara, T., and Gaduputi, V. (2019). Epidemiology of pancreatic cancer: global trends, etiology and risk factors. *World J. Oncol.* 10, 10–27. doi: 10.14740/wjon1166

Ray-Coquard, I., Pautier, P., Pignata, S., Perol, D., Gonzalez-Martin, A., Berger, R., et al. (2019). Olaparib plus bevacizumab as first-line maintenance in ovarian cancer. *N. Engl. J. Med.* 381, 2416–2428. doi: 10.1056/NEJMoa1911361

Reeder, R. H., Ueda, K., Honjo, T., Nishizuka, Y., and Hayaishi, O. (1967). Studies on the polymer of adenosine diphosphate ribose. II. Characterization of the polymer. *J. Biol. Chem.* 242, 3172–3179.

Reisländer, T., Lombardi, E. P., Groelly, F. J., Miar, A., Porru, M., Di Vito, S., et al. (2019). BRCA2 abrogation triggers innate immune responses potentiated by treatment with PARP inhibitors. *Nat. Commun.* 10:3143. doi: 10.1038/s41467-019-11048-5

Robertson, K. D. (2001). DNA methylation, methyltransferases, and cancer. *Oncogene* 20, 3139–3155. doi: 10.1038/sj.onc.1204341

Robson, M., Im, S. A., Senkus, E., Xu, B., Domchek, S. M., Masuda, N., et al. (2017). Olaparib for metastatic breast cancer in patients with a Germline BRCA mutation. *N. Engl. J. Med.* 377, 523–533. doi: 10.1056/NEJMoa1706450

Robson, M. E., Tung, N., Conte, P., Im, S. A., Senkus, E., Xu, B., et al. (2019). OlympiAD final overall survival and tolerability results: olaparib versus chemotherapy treatment of physician's choice in patients with a germline BRCA mutation and HER2-negative metastatic breast cancer. *Ann. Oncol.* 30, 558–566. doi: 10.1093/annonc/mdz012

Rondinelli, B., Gogola, E., Yücel, H., Duarte, A. A., van de Ven, M., van der Sluijs, R., et al. (2017). EZH2 promotes degradation of stalled replication forks by recruiting MUS81 through histone H3 trimethylation. *Nat. Cell Biol.* 19, 1371–1378. doi: 10.1038/ncb3626

Rottenberg, S., Jaspers, J. E., Kersbergen, A., van der Burg, E., Nygren, A. O. H., Zander, S. A. L., et al. (2008). High sensitivity of BRCA1-deficient mammary tumors to the PARP inhibitor AZD2281 alone and in combination with platinum drugs. *Proc. Natl. Acad. Sci. U.S.A.* 105, 17079–17084. doi: 10.1073/pnas.0806092105

Rulten, S. L., Fisher, A. E., Robert, I., Zuma, M. C., Rouleau, M., Ju, L., et al. (2011). PARP-3 and APLF function together to accelerate nonhomologous end-joining. *Mol. Cell* 41, 33–45. doi: 10.1016/j.molcel.2010.12.006

Samstein, R. M., and Riaz, N. (2018). The DNA damage response in immunotherapy and radiation. *Adv. Radiat. Oncol.* 3, 527–533. doi: 10.1016/j.adro.2018.08.017

Sandhu, S. K., Schelman, W. R., Wilding, G., Moreno, V., Baird, R. D., Miranda, S., et al. (2013). The poly(ADP-ribose) polymerase inhibitor niraparib (MK4827) in BRCA mutation carriers and patients with sporadic cancer: a phase 1 dose-escalation trial. *Lancet Oncol.* 14, 882–892. doi: 10.1016/S1470-2045(13)70240-7

Schiewer, M. J., and Knudsen, K. E. (2014). Transcriptional roles of PARP1 in cancer. *Mol. Cancer Res.* 12, 1069–1080. doi: 10.1158/1541-7786.MCR-13-0672

Schoonen, P. M., Talens, F., Stok, C., Gogola, E., Heijink, A. M., Bouwman, P., et al. (2017). Progression through mitosis promotes PARP inhibitor-induced cytotoxicity in homologous recombination-deficient cancer cells. *Nat. Commun.* 8:15981. doi: 10.1038/ncomms15981

Scott, C. L., Swisher, E. M., and Kaufmann, S. H. (2015). Poly (ADP-ribose) polymerase inhibitors: recent advances and future development. *J. Clin. Oncol.* 33, 1397–1406. doi: 10.1200/JCO.2014.58.8848

Sharma, M. K., Imamichi, S., Fukuchi, M., Samarth, R. M., Tomita, M., and Matsumoto, Y. (2016). In cellulo phosphorylation of XRCC4 Ser320 by DNA-PK induced by DNA damage. *J. Radiat. Res.* 57, 115–120. doi: 10.1093/jrr/rrv086

Shen, Y., Rehman, F. L., Feng, Y., Boshuizen, J., Bajrami, I., Elliott, R., et al. (2013). BMN 673, a novel and highly potent PARP1/2 inhibitor for the treatment of human cancers with DNA repair deficiency. *Clin. Cancer Res.* 19, 5003–5015. doi: 10.1158/1078-0432.CCR-13-1391

Shroff, R. T., Hendifar, A., McWilliams, R. R., Geva, R., Epelbaum, R., Rolfe, L., et al. (2018). Rucaparib monotherapy in patients with pancreatic cancer and a known deleterious BRCA Mutation. *JCO Precis. Oncol.* 2018:10.1200/PO.17.00316. doi: 10.1200/PO.17.00316

Singh, A. A., Mandoli, A., Prange, K. H., Laakso, M., and Martens, J. H. (2017). AML associated oncofusion proteins PML-RARA, AML1-ETO and CBFB-MYH11 target RUNX/ETS-factor binding sites to modulate H3ac levels and drive leukemogenesis. . *Oncotarget* 8, 12855–12865. doi: 10.18632/oncotarget.14150

Sishc, B. J., and Davis, A. J. (2017). The role of the core non-homologous end joining factors in carcinogenesis and cancer. *Cancers* 9:81. doi: 10.3390/cancers9070081

Skalitzky, D. J., Marakovits, J. T., Maegley, K. A., Ekker, A., Yu, X.-H., Hostomsky, Z., et al. (2003). Tricyclic Benzimidazoles as Potent Poly(ADP-ribose) Polymerase-1 Inhibitors. *J. Med. Chem.* 46, 210–213. doi: 10.1021/jm0255769

Smith, M. R., Sandhu, S. K., Kelly, W. K., Scher, H. I., Efstathiou, E., Lara, P., et al. (2019). Phase II study of niraparib in patients with metastatic castration-resistant prostate cancer (mCRPC) and biallelic DNA-repair gene defects (DRD): preliminary results of GALAHAD. *J. Clin. Oncol.* 37, 202–202. doi: 10.1200/JCO.2019.37.7

Solier, S., and Pommier, Y. (2014). The nuclear gamma-H2AX apoptotic ring: implications for cancers and autoimmune diseases. *Cell. Mol. Life Sci.* 71, 2289–2297. doi: 10.1007/s00018-013-1555-2

Stanisavljevic, J., Porta-de-la-Riva, M., Batlle, R., de Herreros, A. G., and Baulida, J. (2011). The p65 subunit of NF-kappaB and PARP1 assist Snail1 in activating fibronectin transcription. *J. Cell Sci.* 124(Pt 24), 4161–4171. doi: 10.1242/jcs.078824

Stavropoulou, V., Peters, A., and Schwaller, J. (2018). Aggressive leukemia driven by MLL-AF9. *Mol. Cell. Oncol.* 5:e1241854. doi: 10.1080/23723556.2016.1241854

Strom, C. E., Johansson, F., Uhlen, M., Szigyarto, C. A., Erixon, K., and Helleday, T. (2011). Poly (ADP-ribose) polymerase (PARP) is not involved in base excision repair but PARP inhibition traps a single-strand intermediate. *Nucleic Acids Res.* 39, 3166–3175. doi: 10.1093/nar/gkq1241

Sugimura, K., Takebayashi, S., Taguchi, H., Takeda, S., and Okumura, K. (2008). PARP-1 ensures regulation of replication fork progression by homologous recombination on damaged DNA. *J. Cell Biol.* 183, 1203–1212. doi: 10.1083/jcb.200806068

Sugimura, T., Fujimura, S., Hasegawa, S., and Kawamura, Y. (1967). Polymerization of the adenosine 5'-diphosphate ribose moiety of NAD by rat liver nuclear enzyme. *Biochim. Biophys. Acta* 138, 438–441. doi: 10.1016/0005-2787(67)90507-2

Sun, X., Fu, K., Hodgson, A., Wier, E. M., Wen, M. G., Kamenyeva, O., et al. (2016). Sam68 is required for DNA damage responses via regulating Poly(ADP-ribosyl)ation. *PLoS Biol.* 14:e1002543. doi: 10.1371/journal.pbio.1002543

Taglialatela, A., Alvarez, S., Leuzzi, G., Sannino, V., Ranjha, L., Huang, J.-W., et al. (2017). Restoration of Replication Fork Stability in BRCA1- and BRCA2-Deficient Cells by Inactivation of SNF2-Family Fork Remodelers. *Mol. Cell* 68, 414–430.e8. doi: 10.1016/j.molcel.2017.09.036

Telli, M. L., Timms, K. M., Reid, J., Hennessy, B., Mills, G. B., Jensen, K. C., et al. (2016). Homologous recombination deficiency (HRD) score predicts response to platinum-containing neoadjuvant chemotherapy in patients with triple-negative breast cancer. *Clin. Cancer Res.* 22, 3764–3773. doi: 10.1158/1078-0432.CCR-15-2477

Tuli, R., Shiao, S. L., Nissen, N., Tighiouart, M., Kim, S., Osipov, A., et al. (2019). A phase 1 study of veliparib, a PARP-1/2 inhibitor, with gemcitabine and radiotherapy in locally advanced pancreatic cancer. *EBioMedicine* 40, 375–381. doi: 10.1016/j.ebiom.2018.12.060

Turner, N. C., Lord, C. J., Iorns, E., Brough, R., Swift, S., Elliott, R., et al. (2008). A synthetic lethal siRNA screen identifying genes mediating sensitivity to a PARP inhibitor. *EMBO J.* 27, 1368–1377. doi: 10.1038/emboj.2008.61

Vaidyanathan, A., Sawers, L., Gannon, A.-L., Chakravarty, P., Scott, A. L., Bray, S. E., et al. (2016). ABCB1 (MDR1) induction defines a common resistance mechanism in paclitaxel- and olaparib-resistant ovarian cancer cells. *Br. J. Cancer* 115, 431–441. doi: 10.1038/bjc.2016.203

Vergote, I., Brize, A., Lisyanskaya, A., and Lichinitser, M. (2015). Randomized phase III study comparing paclical-carboplatin with paclitaxel-carboplatin in patients with recurrent platinum-sensitive epithelial ovarian cancer. *J. Clin. Oncol.* 33, 5517–5517. doi: 10.1200/jco.2015.33.15_suppl.5517

Vidotto, T., Nersesian, S., Graham, C., Siemens, D. R., and Koti, M. (2019). DNA damage repair gene mutations and their association with tumor immune regulatory gene expression in muscle invasive bladder cancer subtypes. *J. Immunother. Cancer* 7:148. doi: 10.1186/s40425-019-0619-8

Vodenicharov, M. D., Sallmann, F. R., Satoh, M. S., and Poirier, G. G. (2000). Base excision repair is efficient in cells lacking poly(ADP-ribose)

polymerase 1. *Nucleic Acids Res.* 28, 3887–3896. doi: 10.1093/nar/28.20.3887

Vos, J. R., Fakkert, I. E., de Hullu, J. A., van Altena, A. M., Sie, A. S., Ouchene, H., et al. (2020). Universal tumor DNA BRCA1/2 testing of ovarian cancer: prescreening PARPi treatment and genetic predisposition. *J. Natl. Cancer Inst.* 112, 161–169. doi: 10.1093/jnci/djz080

Vos, S., van Diest, P. J., and Moelans, C. B. (2018). A systematic review on the frequency of BRCA promoter methylation in breast and ovarian carcinomas of BRCA germline mutation carriers: mutually exclusive, or not? *Crit. Rev. Oncol. Hematol.* 127, 29–41. doi: 10.1016/j.critrevonc.2018.05.008

Wang, D., Li, C., Zhang, Y., Wang, M., Jiang, N., Xiang, L., et al. (2016). Combined inhibition of PI3K and PARP is effective in the treatment of ovarian cancer cells with wild-type PIK3CA genes. *Gynecol. Oncol.* 142, 548–556. doi: 10.1016/j.ygyno.2016.07.092

Wang, L., Yang, C., Xie, C., Jiang, J., Gao, M., Fu, L., et al. (2019). Pharmacologic characterization of fluzoparib, a novel poly(ADP-ribose) polymerase inhibitor undergoing clinical trials. *Cancer Sci.* 110, 1064–1075. doi: 10.1111/cas.13947

Wang, M., Wu, W., Wu, W., Rosidi, B., Zhang, L., Wang, H., et al. (2006). PARP-1 and Ku compete for repair of DNA double strand breaks by distinct NHEJ pathways. *Nucleic Acids Res.* 34, 6170–6182. doi: 10.1093/nar/gkl840

Wang, W., and Figg, W. D. (2008). Secondary BRCA1 and BRCA2 alterations and acquired chemoresistance. *Cancer Biol. Ther.* 7, 1004–1005. doi: 10.4161/cbt.7.7.6409

Xu, G., Chapman, J. R., Brandsma, I., Yuan, J., Mistrik, M., Bouwman, P., et al. (2015). REV7 counteracts DNA double-strand break resection and affects PARP inhibition. *Nature* 521, 541–544. doi: 10.1038/nature14328

Xu, Y., and Her, C. (2015). Inhibition of topoisomerase (DNA) I (TOP1): DNA damage repair and anticancer therapy. *Biomolecules* 5, 1652–1670. doi: 10.3390/biom5031652

Xue, X., Raynard, S., Busygina, V., Singh, A. K., and Sung, P. (2013). Role of replication protein A in double holliday junction dissolution mediated by the BLM-Topo IIIα-RMI1-RMI2 protein complex. *J. Biol. Chem.* 288, 14221–14227. doi: 10.1074/jbc.M113.465609

Yamaguchi, H., Du, Y., Nakai, K., Ding, M., Chang, S. S., Hsu, J. L., et al. (2018). EZH2 contributes to the response to PARP inhibitors through its PARP-mediated poly-ADP ribosylation in breast cancer. *Oncogene* 37, 208–217. doi: 10.1038/onc.2017.311

Yamamoto, J. F., and Goodman, M. T. (2008). Patterns of leukemia incidence in the United States by subtype and demographic characteristics, 1997–2002. *Cancer Causes Control* 19, 379–390. doi: 10.1007/s10552-007-9097-2

Yang, X., Wong, M. P. M., and Ng, R. K. (2019). Aberrant DNA methylation in acute myeloid leukemia and its clinical implications. *Int. J. Mol. Sci.* 20:4576. doi: 10.3390/ijms20184576

Ying, S., Hamdy, F. C., and Helleday, T. (2012). Mre11-dependent degradation of stalled DNA replication forks is prevented by BRCA2 and PARP1. *Cancer Res.* 72, 2814–2821. doi: 10.1158/0008-5472.CAN-11-3417

Yun, M. H., and Hiom, K. (2009). CtIP-BRCA1 modulates the choice of DNA double-strand-break repair pathway throughout the cell cycle. *Nature* 459, 460–463. doi: 10.1038/nature07955

Zhang, J., Stevens, F. G. M., and Bradshaw, D. T. (2012). Temozolomide: mechanisms of action, repair and resistance. *Curr. Mol. Pharmacol.* 5, 102–114. doi: 10.2174/1874467211205010102

Zhao, Q., Lan, T., Su, S., and Rao, Y. (2019). Induction of apoptosis in MDA-MB-231 breast cancer cells by a PARP1-targeting PROTAC small molecule. *Chem. Commun.* 55, 369–372. doi: 10.1039/c8cc07813k

Zhao, W., Hu, H., Mo, Q., Guan, Y., Li, Y., Du, Y., et al. (2019). Function and mechanism of combined PARP-1 and BRCA genes in regulating the radiosensitivity of breast cancer cells. *Int. J. Clin. Exp. Pathol.* 12, 3915–3920.

Zhu, Z., Chung, W.-H., Shim, E. Y., Lee, S. E., and Ira, G. (2008). Sgs1 Helicase and two nucleases Dna2 and Exo1 Resect DNA double-strand break ends. *Cell* 134, 981–994. doi: 10.1016/j.cell.2008.08.037

Conflict of Interest: KO'B and DR are founders of CARP Pharmaceuticals. EB, DR, and KO'B are founders of Carpe Vitae Pharmaceuticals. EB, JB, KO'B, and DR are inventors on patent applications filed by Queensland University of Technology.

The remaining author declares that the research was conducted in the absence of any commercial or financial relationships that could be construed as a potential conflict of interest.

frontiers in Cell and Developmental Biology

ORIGINAL RESEARCH
published: 22 September 2020
doi: 10.3389/fcell.2020.580517

Isodeoxyelephantopin Inactivates Thioredoxin Reductase 1 and Activates ROS-Mediated JNK Signaling Pathway to Exacerbate Cisplatin Effectiveness in Human Colon Cancer Cells

Lin Hong[1,2†], Jundixia Chen[2†], Fang Wu[1†], Fengjiao Wu[2], Xin Shen[2], Peisen Zheng[2], Rongrong Shao[2], Kongqin Lu[3], Zhiguo Liu[2], Daoxing Chen[2], Guang Liang[2], Yuepiao Cai[2], Peng Zou[1,2,4] and Yiqun Xia[1*]*

[1] The First Affiliated Hospital of Wenzhou Medical University, Wenzhou Medical University, Wenzhou, China, [2] Cancer and Anticancer Drug Research Center, School of Pharmaceutical Sciences, Wenzhou Medical University, Wenzhou, China, [3] Zhuji Institute of Biomedicine, School of Pharmaceutical Sciences, Wenzhou Medical University, Zhuji, China, [4] Wenzhou University-Wenzhou Medical University Collaborative Innovation Center of Biomedical, Wenzhou, China

Colon cancer is one of the leading causes of cancer-related death in the world. The development of new drugs and therapeutic strategies for patients with colon cancer are urgently needed. Isodeoxyelephantopin (ESI), a sesquiterpene lactone isolated from the medicinal plant *Elephantopus scaber* L., has been reported to exert antitumor effects on several cancer cells. However, the molecular mechanisms underlying the action of ESI is still elusive. In the present study, we found that ESI potently suppressed cell proliferation in human colon cancer cells. Furthermore, our results showed that ESI treatment markedly increased cellular reactive oxygen species (ROS) levels by inhibiting thioredoxin reductase 1 (TrxR1) activity, which leads to activation of the JNK signaling pathway and eventually cell death in HCT116 and RKO cells. Importantly, we found that ESI markedly enhanced cisplatin-induced cytotoxicity in HCT116 and RKO cells. Combination of ESI and cisplatin significantly increased the production of ROS, resulting in activation of the JNK signaling pathway in HCT116 and RKO cells. *In vivo*, we found that ESI combined with cisplatin significantly suppressed tumor growth in HCT116 xenograft models. Together, our study provide a preclinical proof-of-concept for ESI as a potential strategy for colon cancer treatment.

Keywords: isodeoxyelephantopin, oxidative stress, thioredoxin reductase 1, cisplatin, JNK

Abbreviations: ROS, reactive oxygen species; TrxR1, thioredoxin reductase 1; JNK, c-Jun N-terminal kinase; NAC, *N*-acetyl-L-cysteine; DCFH-DA, 2′,7′-dichlorofluorescin diacetate; MDA, malondialdehyde; DTNB, 5,5'-dithiobis(2-nitrobenzoic acid); CI, combination index.

OPEN ACCESS

Edited by:
José Díaz-Chávez, National Institute of Cancerology (INCAN), Mexico

Reviewed by:
Parvez Khan, University of Nebraska Medical Center, United States
Yulin Ren, The Ohio State University, United States

***Correspondence:**
Peng Zou
zoupeng@wmu.edu.cn
Yiqun Xia
yiqunxia@yeah.net

† These authors have contributed equally to this work

Specialty section:
This article was submitted to Molecular and Cellular Oncology, a section of the journal Frontiers in Cell and Developmental Biology

Received: *06 July 2020*
Accepted: *28 August 2020*
Published: *22 September 2020*

Citation:
Hong L, Chen J, Wu F, Wu F, Shen X, Zheng P, Shao R, Lu K, Liu Z, Chen D, Liang G, Cai Y, Zou P and Xia Y (2020) Isodeoxyelephantopin Inactivates Thioredoxin Reductase 1 and Activates ROS-Mediated JNK Signaling Pathway to Exacerbate Cisplatin Effectiveness in Human Colon Cancer Cells. Front. Cell Dev. Biol. 8:580517. doi: 10.3389/fcell.2020.580517

INTRODUCTION

Colon cancer is a significant public health problem and one of the leading causes of cancer-related death in the world. Despite advances in surgery, radiation therapy and chemotherapy, the overall survival rate of patients with colon cancer is still not optimistic (Arnold et al., 2017). Therefore, novel therapeutic strategies for patients with colon cancer are urgently needed. Natural products have been used for treatment or prevention of various human diseases for centuries, particularly in cancer therapy (Newman and Cragg, 2016). *Elephantopus scaber* L. is a traditional medicinal herb with multiple medicinal uses. In Chinese medicine, the extract of this plant is used as an antiviral, antidiuretic, and antibacterial agent as well as in the treatment of bronchitis, hepatitis, and arthralgia (Poli et al., 1992; Rajesh and Latha, 2001; Li et al., 2004). Isodeoxyelephantopin (ESI), a sesquiterpene lactone isolated from *Elephantopus scaber* L, has been reported to exert antitumor effects in several malignant carcinomas (Yan et al., 2013; Verma et al., 2019). A previous study demonstrated that ESI induces cell cycle arrest at G2/M phase in T47D cells (Kabeer et al., 2014). ESI was also found to inhibit the growth of human chronic myeloid leukemia cells by inhibiting NF-κB activation and NF-κB-regulated gene expression (Ichikawa et al., 2006). In lung cancer cells, ESI favored cell survival by activating protective autophagy (Wang et al., 2017). However, the antitumor effects of ESI on colon cancer has not been reported till now, and the molecular mechanisms underlying the action of ESI is still elusive.

Cisplatin is one of the most successful chemotherapeutics and has been widely used in clinics for the treatment of cancer (Wang and Lippard, 2005). The mechanism of action of cisplatin has been broadly studied in the past decades. It is generally agreed that DNA is a major target for cisplatin (Jung and Lippard, 2007; Basu and Krishnamurthy, 2010). Various signal transduction pathways and molecules, including p53, Nrf2, MAPK, and PD-L1, are involved in the process of cisplatin-induced cell death (Bragado et al., 2007; Fournel et al., 2019; Liao et al., 2019). However, many patients rapidly acquire resistance to cisplatin treatment during therapy, and the molecular mechanisms of cisplatin resistance remains enigmatic (Ahmed et al., 2018; Roy et al., 2018; Cruz-Bermudez et al., 2019; Su et al., 2019). It has been suggested that cisplatin in combination with other herb compounds is more effective than cisplatin alone (Wang J. et al., 2018; Wang Y. et al., 2018). Therefore, it is interesting to investigate the synergistic effect of cisplatin in combination with ESI for the treatment of colon cancer.

In this study, we investigated the molecular mechanisms underlying the action of ESI in human colon cancer cells. We observed that ESI significantly inhibited TrxR1 activity and increased the accumulation of ROS, which leads to activation of the JNK signaling pathway and eventually cell death in HCT116 and RKO cells. Importantly, we found that ESI significantly enhanced cisplatin-induced cytotoxicity in HCT116 and RKO cells. Moreover, ESI in combination with cisplatin markedly suppressed tumor growth in HCT116 xenograft models. Together, our data provide new insight into the mechanisms of antitumor action of ESI, and suggest that ESI might be a potential candidate for the treatment of colon cancer.

RESULTS

ESI Treatment Increases ROS Levels in Human Colon Cancer Cells

We first tested the cytotoxic effect of ESI (**Figure 1A**) on the viability of colon cancer cells and normal cells. As shown in **Figures 1B,C**, there were significant reductions in the viability of two colon cancer cell lines upon ESI treatment, but has little effect on normal MPM and NRK-52E cells. Next, we set out to investigate the molecular mechanisms underlying the action of ESI. Recent studies showed that ROS generation plays an important role in the antitumor action of some natural compounds (Dias et al., 2018; Liu et al., 2018). Therefore, we measured the intracellular ROS levels after ESI treatment. Time-course results showed that ESI treatment markedly induced ROS generation in HCT116 and RKO cells (**Figures 1D,E**). In addition, we found that treatment with ESI for 2 h caused a dose-dependent increase in ROS levels (**Figure 1F**). To determine the role of ROS in mediating the antitumor effect of ESI, the ROS scavenger NAC was used in our experiment. We found that pretreatment with NAC markedly reversed ESI-induced increase in ROS levels and cell death rate in HCT116 and RKO cells (**Figures 1G–J**). These data suggest that ROS generation plays an essential role in ESI-induced cytotoxicity in colon cancer cells.

ESI Inactivates TrxR1 in Human Colon Cancer Cells

Thioredoxin reductase 1 is a key regulator of cellular redox balance and accumulating evidence suggest that ROS accumulation may be increased when TrxR1 activity is inhibited (Duan et al., 2016; Dagnell et al., 2018; Zheng et al., 2019). Therefore, we tested the inhibitory effect of ESI on TrxR1 activity in colon cancer cells. Using an endpoint insulin reduction assay to quantify inhibition of TrxR1 activity, we found that ESI treatment inhibited the TrxR1 activity in a time- and dose-dependent manner in HCT116 and RKO cells (**Figures 2A,B**). Remarkably, we found that ESI directly inhibited the TrxR1 protein activity in a dose-dependent manner (**Figure 2C**). The densitometric analysis of Western blot bands showed that the expression level of TrxR1 did not significantly change after treated with ESI (**Figures 2D,E**). In addition, we performed a molecular simulation of ESI-TrxR1 complex using docking software. As shown in **Figure 2F**, the key residues around ESI included Gly499, Sec498, Cys497, Gly496, Gln494, Leu493, Ile492, Ser404 and Lys29. Thus, the proposed reaction mechanism for ESI is to block the adjacent C-terminal active site residues Cys and Sec of TrxR1, which is expected to effectively suppress TrxR1 activity (Xu et al., 2016). To further address the physiological relevance of TrxR1-mediated ESI cytotoxicity, we knocked down TrxR1 expression by using siRNA in HCT116 cells. The TrxR1 knockdown by siRNA resulted in an appreciable increase in ESI-induced cell death in HCT116 cells (**Figure 2G**).

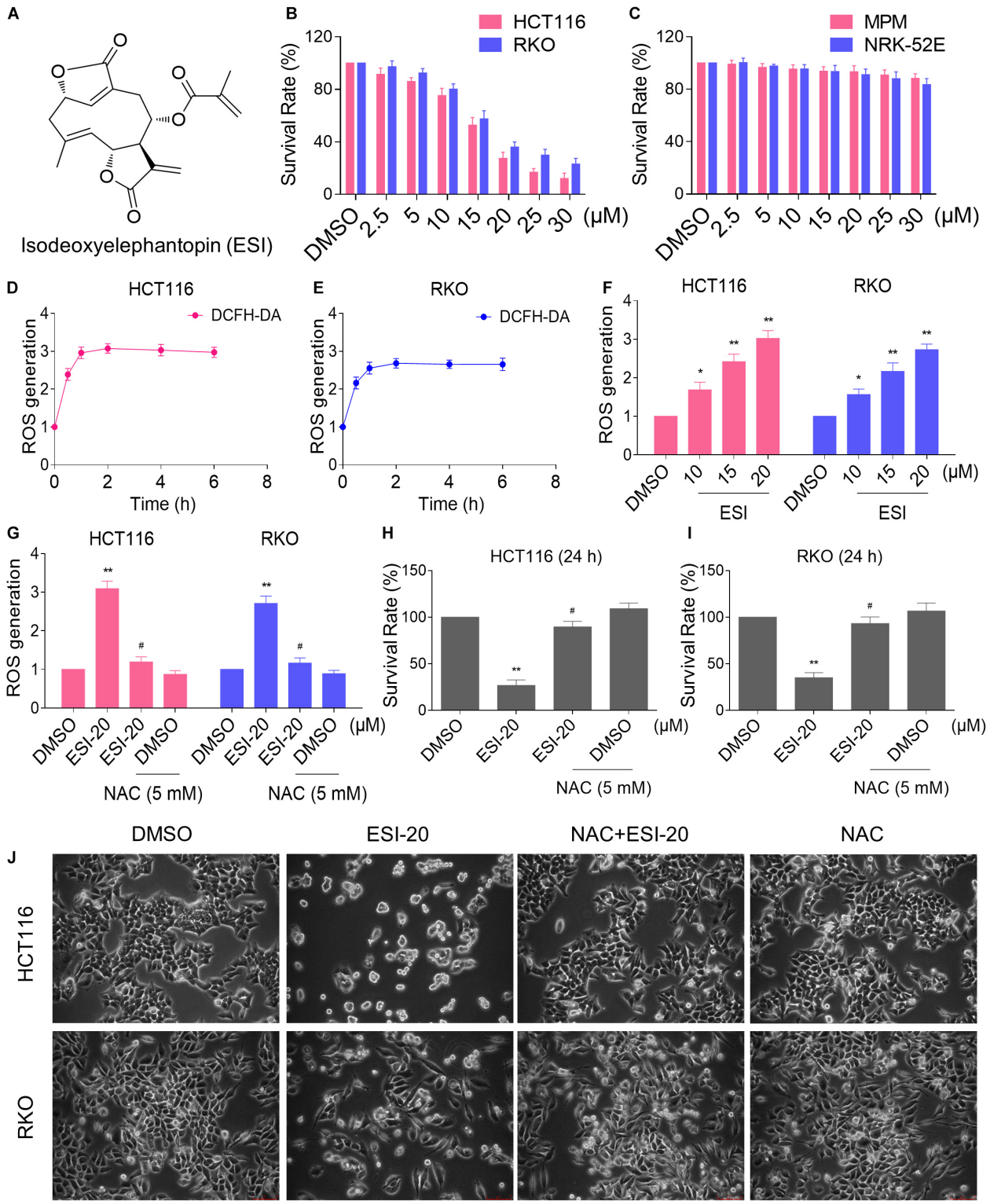

FIGURE 1 | ESI inhibits cell proliferation and increases ROS levels in HCT116 and RKO cells. **(A)** Chemical structure of ESI. **(B)** Cell viability was measured in HCT116 and RKO cells after treated with ESI for 24 h. **(C)** Cell viability was measured in MPM and NRK-52E cells after treated with ESI for 24 h. **(D,E)** Intracellular ROS levels were measured in HCT116 and RKO cells after treated with ESI (20 μM) for indicated time periods. **(F)** Intracellular ROS levels were measured in HCT116 and RKO cells after treated with ESI for 2 h. **(G)** Cells were pretreated with NAC (5 mM) for 2 h before exposure to ESI. Intracellular ROS levels were measured after treated with ESI (20 μM) for 2 h. **(H,I)** Cells were pretreated with NAC (5 mM) for 2 h before exposure to ESI. Cell viability was measured after treated with ESI for 24 h. **(J)** Cells were pretreated with NAC (5 mM) for 2 h and cell morphology was observed after treated with ESI for 24 h. Data from three technical replicates ($^{*}p < 0.05$, $^{**}p < 0.01$ versus DMSO group, $^{\#}p < 0.05$ versus ESI-20 group).

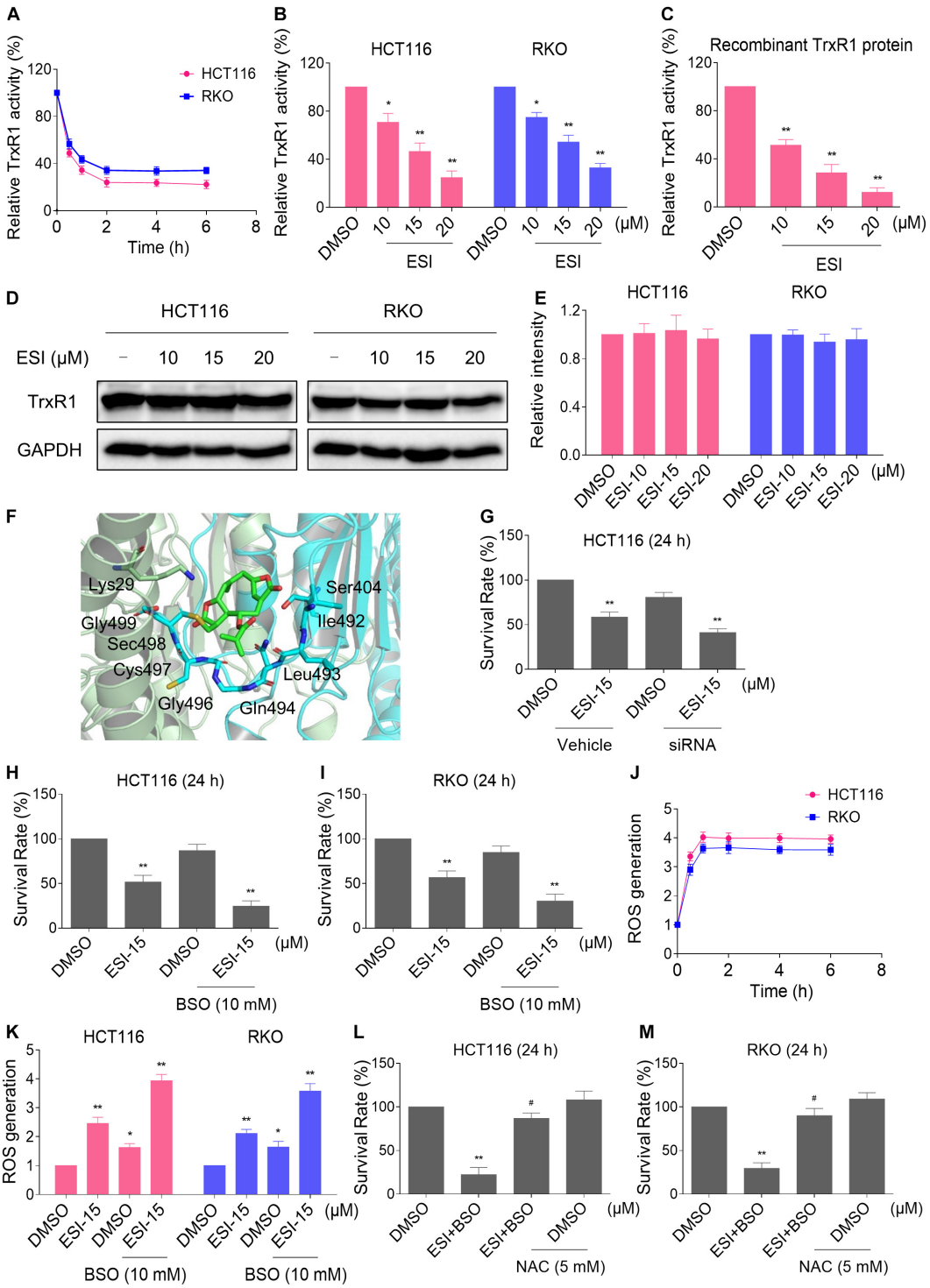

FIGURE 2 | ESI inhibits TrxR1 activity in HCT116 and RKO cells. **(A)** TrxR1 activity was measured by the endpoint insulin reduction assay after treated with ESI (20 μM) for indicated time periods. **(B)** TrxR1 activity was measured by the endpoint insulin reduction assay after treated with ESI for 2 h. **(C)** TrxR1 protein activity was measured by the DTNB assay after treated with ESI for 2 h. **(D,E)** HCT116 and RKO cells were treated with ESI for 12 h and then lysed for Western blot analyses with the indicated antibodies. The intensities of TrxR1 and GAPDH bands were quantified using ImageJ software. TrxR1 protein levels were normalized to GAPDH. **(F)** Molecular docking of ESI with TrxR1 protein was carried out with the docking software. **(G)** HCT116 cells transfected with TrxR1 siRNA or control siRNA were treated with ESI for 24 h. Cell viability was measured using a methyl thiazolyl tetrazolium assay. **(H,I)** Cell viability was measured after treated with ESI or BSO alone or their combination for 24 h. **(J)** Intracellular ROS levels were measured after treated with ESI (15 μM) and BSO (10 mM) combination for indicated time periods. **(K)** Intracellular ROS levels were measured after treated with ESI or BSO alone or their combination for 2 h. **(L,M)** Cells were pretreated with NAC (5 mM) for 2 h and cell viability was measured after treated with ESI (15 μM) and BSO (10 mM) combination for 24 h. Data from three technical replicates (*$p < 0.05$, **$p < 0.01$ versus DMSO group, $^{\#}p < 0.05$ versus ESI+BSO group).

Glutathione (GSH) is the most abundant antioxidant in cells, and plays a critical role in cellular antioxidant defenses. GSH acting in concert with its dependent enzymes, known as the GSH system, which is another redox regulatory network in cells besides the thioredoxin system, and it also acts as a backup of the thioredoxin system (Du et al., 2012; Harris et al., 2015). L-Buthionine-sulfoximine (BSO) is a sulfoximine which reduces levels of GSH and is being investigated as an adjunct with chemotherapy in the treatment of cancer (Lien et al., 2016; Rashmi et al., 2018). Therefore, we set out to evaluate the synergistic effects of ESI and BSO. Using the MTT assay, we found that ESI in combination with BSO exhibited a synergistic effect against both HCT116 and RKO cells (**Figures 2H,I**). Furthermore, compared with ESI or BSO treatment alone, the combined treatment greatly increased ROS levels in HCT116 and RKO cells (**Figures 2J,K**). To investigate the role of ROS in the combined treatment-induced cell death, the cells were treated with the combination of ESI and BSO after pretreated with antioxidant NAC. As shown in **Figures 2L,M**, NAC pretreatment significantly attenuated the combined treatment-induced cytotoxicity in both HCT116 and RKO cells. Taken together, these data indicate that ESI induces ROS-mediated cell death by inhibiting TrxR1 activity.

ESI Activates JNK Signaling Pathway in Human Colon Cancer Cells

In the presence of ROS, the oxidized thioredoxin (Trx) form is released and subsequently activates apoptosis signal-regulating kinase 1 to induce cell death via activation of the JNK signaling pathway (Jin et al., 2015; Mantzaris et al., 2016). Therefore, we set out to determine whether the JNK signaling pathway was activated in HCT116 and RKO cell lines when treated with ESI. As shown in **Figures 3A–C**, the JNK signaling pathway was indeed activated in both cell lines. In addition, ESI treatment increased the phosphorylation of JNK in a dose-dependently manner (**Figures 3D–F**). We next sought to

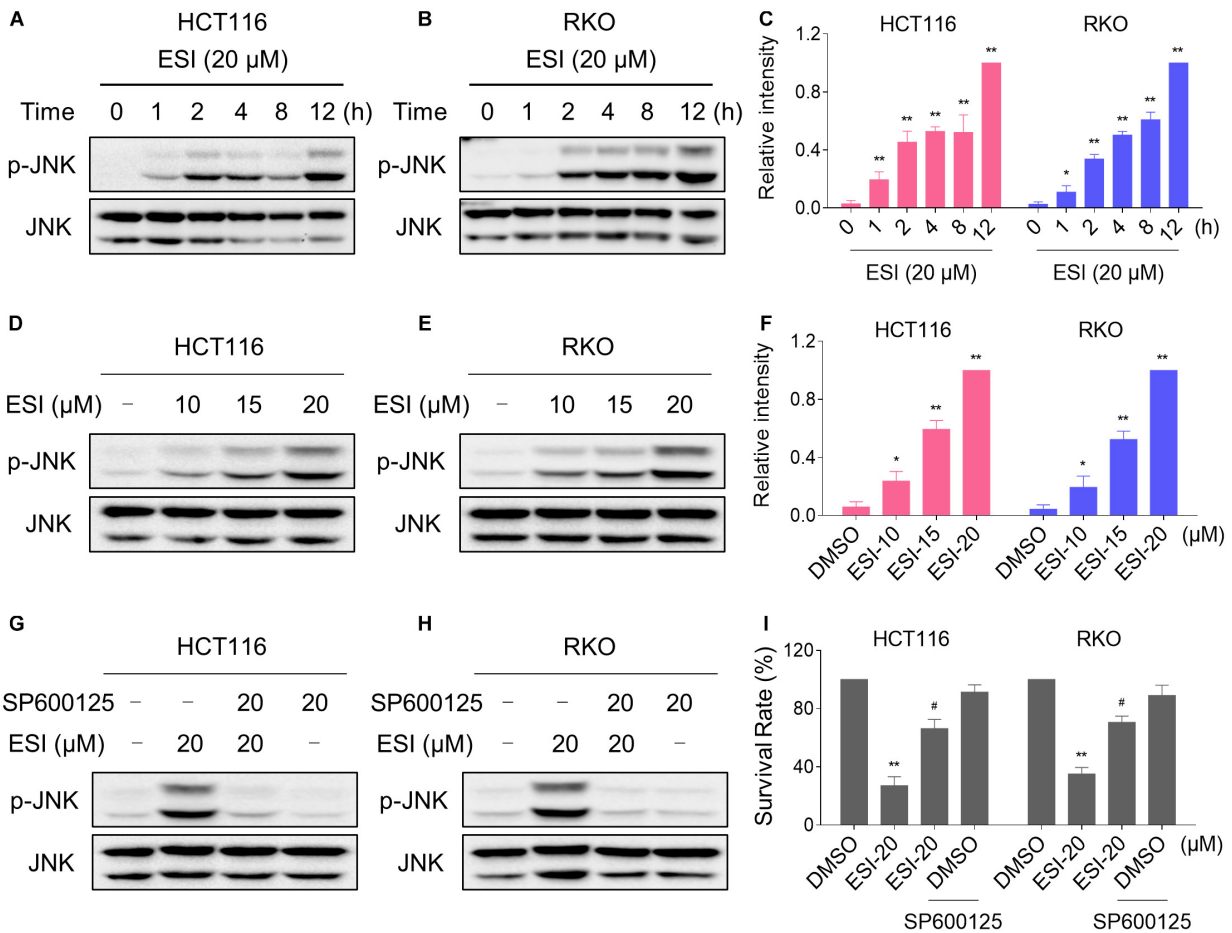

FIGURE 3 | ESI activates JNK signaling pathway in HCT116 and RKO cells. **(A–C)** Cells were treated with ESI for indicated time periods and then lysed for Western blot analyses with the indicated antibodies. The intensities of p-JNK and JNK bands were quantified using ImageJ software. p-JNK protein levels were normalized to JNK. **(D–F)** Cells were treated with ESI for 12 h and then lysed for Western blot analyses with the indicated antibodies. **(G,H)** Cells were pretreated with SP600125 (20 μM) for 2 h before exposure to ESI. Cell lysates were blotted with the indicated antibodies after treated with ESI for 12 h. **(I)** Cells were pretreated with SP600125 (20 μM) for 2 h and cell viability was measured after treated with ESI for 24 h. Data from three technical replicates (*$p < 0.05$, **$p < 0.01$ versus DMSO group, #$p < 0.05$ versus ESI-20 group).

determine the role of JNK signaling pathway in mediating ESI-induced cell death in HCT116 and RKO cells. As shown in **Figures 3G,H**, the phosphorylation of JNK induced by ESI was greatly reversed when pre-treated with SP600125 (a JNK inhibitor). This was associated with an appreciable reduction in ESI-induced cell death in HCT116 and RKO cells, indicating that JNK activation is essential for ESI-induced cell death in colon cancer cells (**Figure 3I**).

We next investigated the relationship between ROS generation and JNK activation in colon cancer cells. As shown in **Figures 4A–C**, the phosphorylation of JNK induced by ESI was significantly reversed when pre-treated with NAC. To further extend this observation, we measured the level of JNK phosphorylation in HCT116 and RKO cells after treated with ESI and BSO combination. As shown in **Figures 4D–F**, ESI and BSO synergistically increased the level of JNK phosphorylation in both cell lines. Moreover, the combined treatment-induced phosphorylation of JNK was markedly reversed by NAC pretreatment in both HCT116 and RKO cells (**Figures 4G–I**). Together, these findings indicate that the JNK signaling pathway is a downstream effector of ROS induced by the combined treatment in colon cancer cells.

ESI and Cisplatin Combination Increases ROS Levels in Human Colon Cancer Cells

Several studies showed that some ROS inducers can sensitize the tumor cells to cisplatin (Yang et al., 2017; Sun et al., 2018; Hsu et al., 2019; Zhang et al., 2019). Therefore, we set out to determine

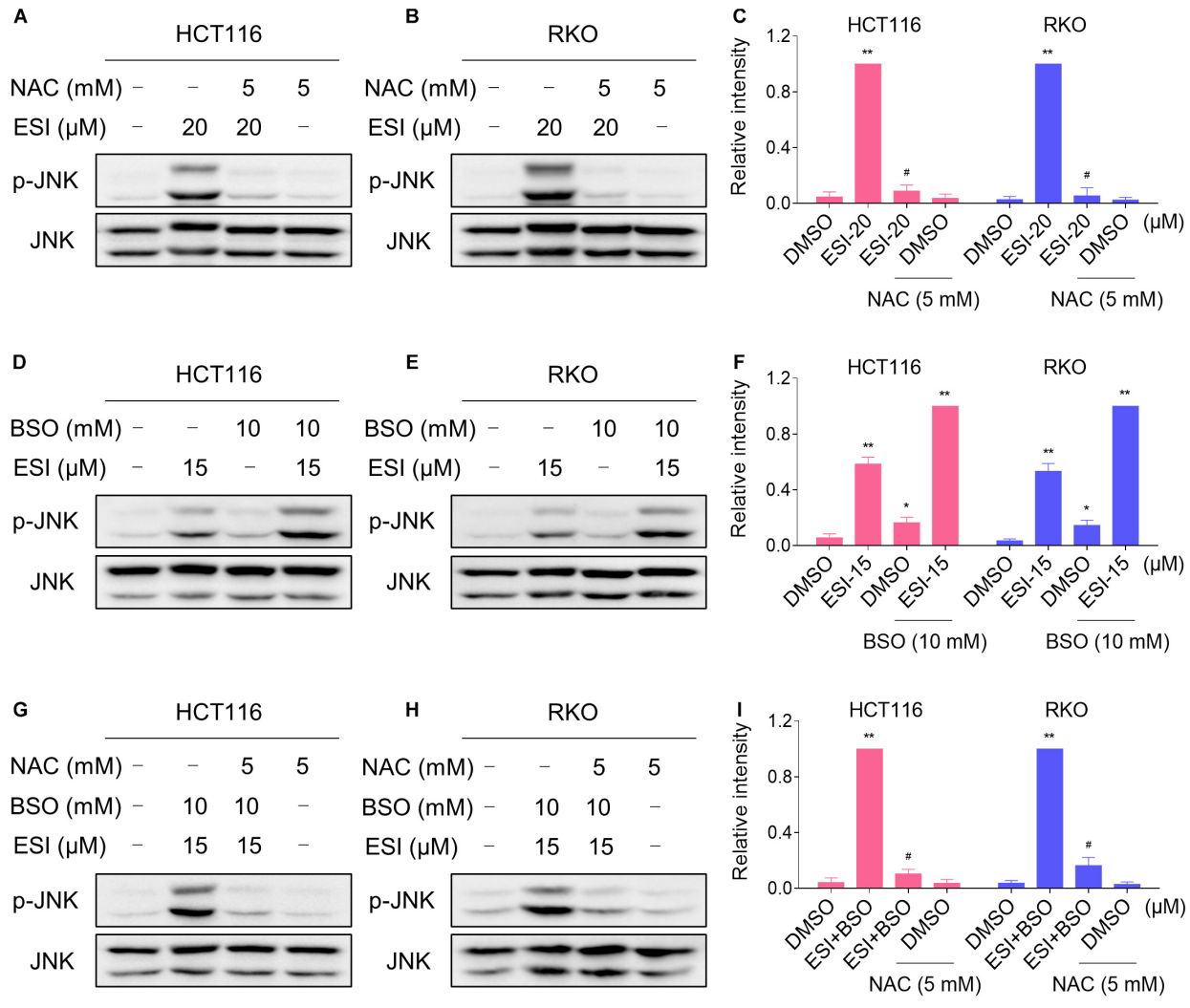

FIGURE 4 | ESI activates ROS-dependent JNK signaling pathway in HCT116 and RKO cells. **(A–C)** Cells were pretreated with NAC (5 mM) for 2 h before exposure to ESI. Cell lysates were blotted with the indicated antibodies after treated with ESI for 12 h. **(D–F)** Cells were treated with ESI or BSO alone or their combination for 12 h and then lysed for Western blot analyses with the indicated antibodies. **(G–I)** Cells were pretreated with NAC (5 mM) for 2 h and cell lysates were blotted with the indicated antibodies after treated with ESI (15 μM) and BSO (10 mM) combination for 12 h. Data from three technical replicates (*$p < 0.05$, **$p < 0.01$ versus DMSO group, $^{\#}p < 0.05$ versus ESI-20 or ESI+BSO group).

the synergistic effects of ESI and cisplatin. Using the MTT assay, we found that 15 μM ESI greatly increased the cytotoxicity of cisplatin in HCT116 and RKO cells (**Figures 5A,C**). The CI values were calculated from the MTT assay and suggested that ESI in combination with cisplatin exhibited a synergistic effect against both HCT116 and RKO cells (**Figures 5B,D**). Since ROS generation plays a critical role in ESI-induced cell death, we set out to determine whether ROS was upregulated in the HCT116 and RKO cell lines when treated with ESI and cisplatin combination. As shown in **Figure 5E**, ESI and cisplatin synergistically increased the levels of ROS in both cell lines.

Excessive amounts of ROS can cause oxidative damage to lipids and DNA (Park et al., 2018; Srinivas et al., 2018). Using an immunofluorescence assay, we found that combined treatment with ESI and cisplatin resulted in a significant accumulation of nuclear 53BP1 foci in HCT116 and RKO cells (**Figure 5F**). In addition, the combined treatment-induced accumulation of ROS and nuclear 53BP1 foci were markedly reversed by NAC pretreatment in both cell lines (**Figures 5G,H**). To further investigate the role of ROS in the combined treatment-induced cell death, the cells were treated with the combination of ESI and cisplatin after pre-treated with antioxidant NAC. As shown in **Figure 5I**, NAC pretreatment greatly attenuated the combined treatment-induced cytotoxicity in both HCT116 and RKO cells. Taken together, these data indicate that ESI and cisplatin combination induces ROS-mediated cell death in colon cancer cells.

ESI and Cisplatin Cooperated to Activate ROS-Dependent JNK Signaling Pathway

We next tested if the JNK signaling pathway was activated in HCT116 and RKO cell lines when treated with ESI and cisplatin. As shown in **Figures 6A–C**, ESI in combination with cisplatin increased the level of JNK phosphorylation in a time-dependently manner. Moreover, ESI and cisplatin synergistically increased the level of JNK phosphorylation in both cell lines (**Figures 6D–F**). We then attempted to investigate the relationship between ROS generation and JNK activation induced by the combined treatment in HCT116 and RKO cells. As shown in **Figures 6G–I**, the combined treatment-induced phosphorylation of JNK was markedly reversed by NAC pretreatment in both cell lines, indicating that activation of the JNK signaling pathway is due to accumulation of intracellular ROS in colon cancer cells.

ESI and Cisplatin Cooperated to Inhibit Tumor Growth of HCT116 Xenografts in Nude Mice

To extend our finding *in vivo*, we inoculated HCT116 cells into the athymic mice subcutaneously. The mice were equally divided into four groups (six mice/group) and received the following treatments: (1) control vehicle; (2) ESI (10 mg/kg); (3) cisplatin (4 mg/kg); (4) ESI (10 mg/kg) plus cisplatin (4 mg/kg). As shown in **Figures 7A–C**, 10 mg/kg ESI or 4 mg/kg cisplatin treatment effectively reduced tumor growth of HCT116 xenografts. Remarkably, the combined treatment with ESI and cisplatin showed stronger inhibitory effect on tumor growth in nude mice. Mechanistically, ESI and cisplatin synergistically inhibited the expression of Ki-67 and increased the level of γ-H2A.X in the tumor tissues (**Figure 7D**). Furthermore, we found that ESI in combination with cisplatin markedly increased the level of MDA, a marker of oxidative stress, in the tumor tissues (**Figure 7E**). These *in vivo* data support our findings in cell culture experiments and further strengthen the hypotheses that the generation of ROS is critical for the synergistic effect of ESI and cisplatin.

DISCUSSION

Colon cancer is one of the leading causes of cancer-related deaths worldwide. Chemotherapy remains an important therapeutic strategy for colon cancer. However, the application of conventional chemotherapeutic drugs is limited due to drug resistance and toxicities (Rabik and Dolan, 2007; Al-Batran et al., 2019; Pan et al., 2019). Therefore, the development of more effective drugs and/or drug combinations for colon cancer has high priority. Here, we investigated the effect and mechanism of ESI in colon cancer cells. We found that ESI potently inhibited the growth of colon cancer cells *in vitro* and in nude mice. Remarkably, we verified TrxR1 was a target of ESI and showed that ESI induced ROS generation by inhibiting TrxR1 activity. In addition, we showed that ESI has synergistic effects with the frontline chemotherapeutic agent cisplatin, suggesting that such a combinatorial treatment might be a more effective strategy for colon cancer treatment.

Under physiological conditions, ROS production and elimination is tightly regulated. Compared with normal cells, cancer cells usually generate and maintain higher ROS levels due to distorted metabolism (Glasauer and Chandel, 2014; Schieber and Chandel, 2014). Elevated ROS levels render cancer cells more sensitive to agents that increases ROS generation. Therefore, manipulating ROS levels by redox modulation is a useful strategy to selectively kill cancer cells (Trachootham et al., 2009; Gorrini et al., 2013). In the present study, we showed that ESI treatment resulted in a significant increase in intracellular ROS levels, and that pretreatment with NAC significantly reversed ESI-induced ROS generation and cell death, indicating that ROS play an important role in the antitumor activity of ESI. We also identified the downstream effector of ROS induced by ESI in the cell death process. We found that ESI treatment concomitantly activated the JNK signaling pathway, as indicated by increased phosphorylation of JNK. Moreover, we found that pretreatment with NAC markedly reversed ESI-induced phosphorylation of JNK in colon cancer cells, suggesting that ROS acts as an upstream signaling molecule involved in ESI-induced activation of the JNK signaling pathway.

Understanding the molecular mechanism underlying the antitumor action of ESI may optimize the design of ESI-based therapies. TrxR1 is a selenoprotein that functions to reduce the oxidoreductase Trx in a NADPH dependent manner, and plays a critical role in regulating the cellular redox balance (Arner, 2017). Accumulating evidence indicates that intracellular ROS levels may be increased when the TrxR1 activity is chemically inhibited

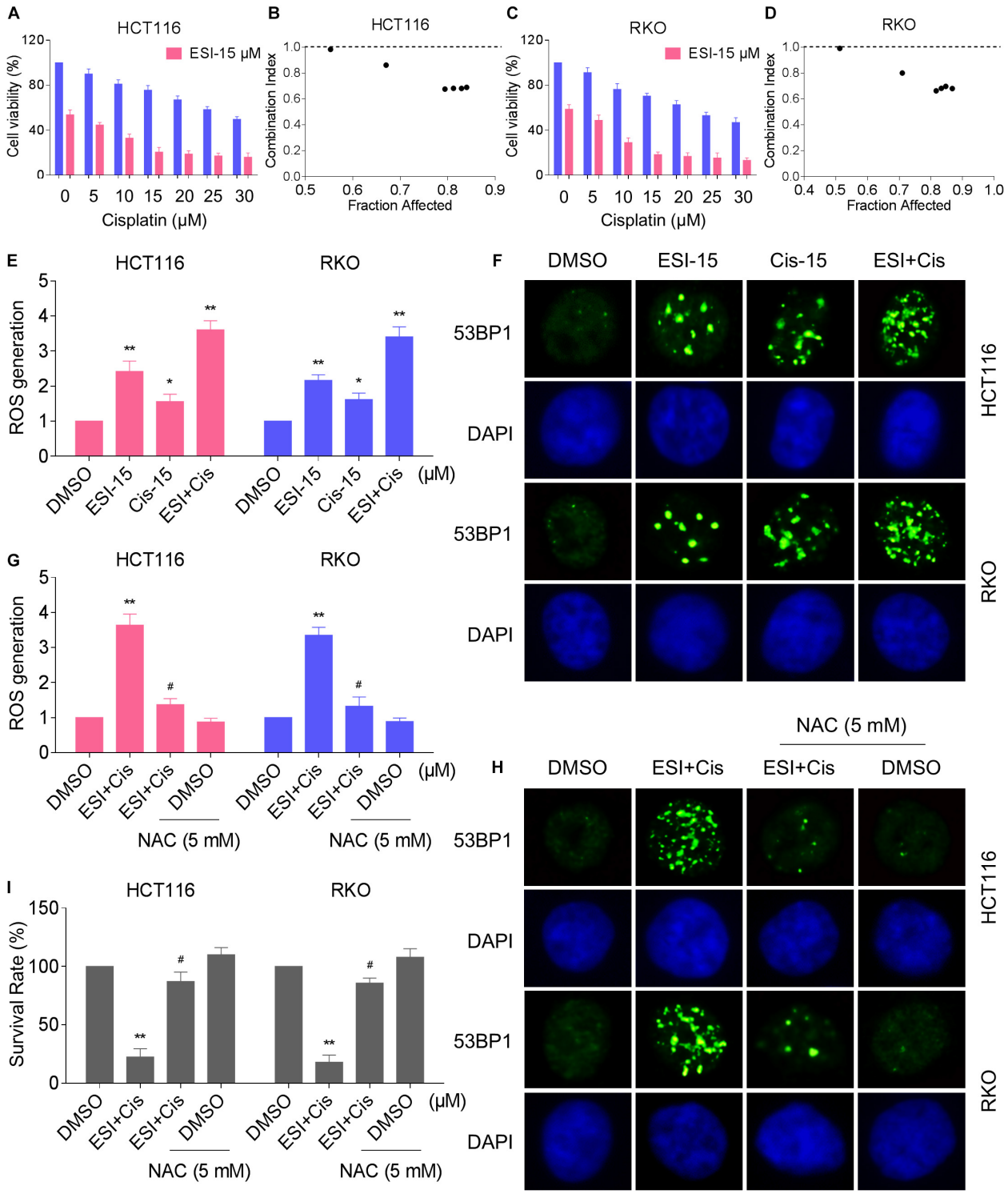

FIGURE 5 | ESI and cisplatin combination increases ROS levels in HCT116 and RKO cells. **(A,C)** Cell viability was measured after treated with ESI or cisplatin alone or their combination for 24 h. **(B,D)** Combination index (CI) values were calculated from the MTT assays using Calcusyn software. **(E)** Intracellular ROS levels were measured after treated with ESI (15 μM) or cisplatin (15 μM) alone or their combination (15 μM ESI and 15 μM cisplatin) for 2 h. **(F)** The nuclear foci formation of 53BPI was detected after treated with ESI (15 μM) or cisplatin (15 μM) alone or their combination (15 μM ESI and 15 μM cisplatin) for 20 h. **(G)** Cells were pretreated with NAC (5 mM) for 2 h and intracellular ROS levels were measured after treated with ESI (15 μM) and cisplatin (15 μM) combination for 2 h. **(H)** Cells were pretreated with NAC (5 mM) for 2 h and nuclear foci formation of 53BPI was detected after treated with ESI (15 μM) and cisplatin (15 μM) combination for 20 h. **(I)** Cells were pretreated with NAC (5 mM) for 2 h and cell viability was measured after treated with ESI (15 μM) and cisplatin (15 μM) combination for 24 h. Data from three technical replicates (*$p < 0.05$, **$p < 0.01$ versus DMSO group, $^{\#}p < 0.05$ versus ESI+Cis group).

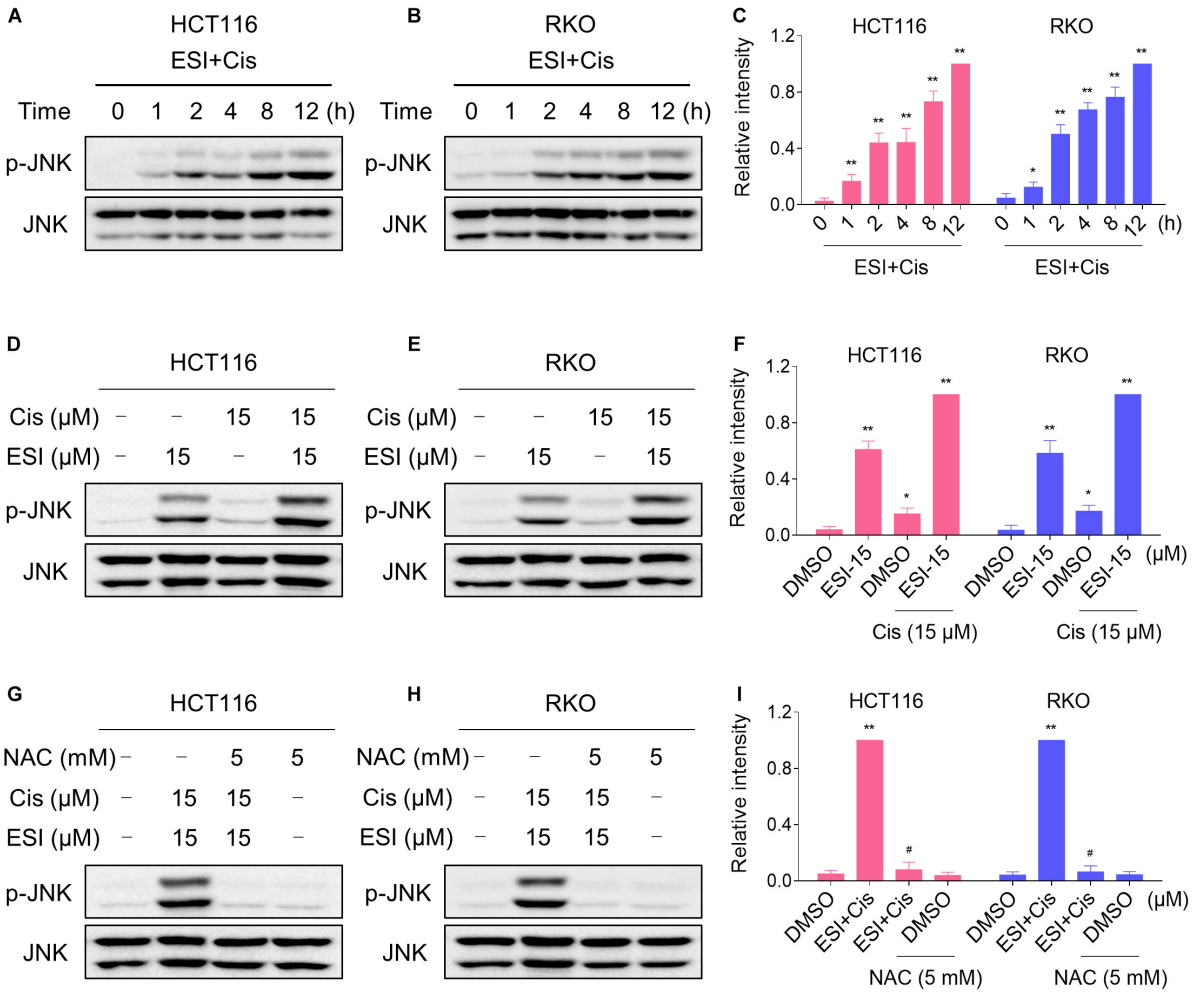

FIGURE 6 | ESI and cisplatin cooperated to activate ROS-dependent JNK signaling pathway. **(A–C)** Cells were treated with ESI (15 μM) and cisplatin (15 μM) combination for indicated time periods and then lysed for Western blot analyses with the indicated antibodies. **(D–F)** Cells were treated with ESI or cisplatin alone or their combination for 12 h and then lysed for Western blot analyses with the indicated antibodies. **(G–I)** Cells were pretreated with NAC (5 mM) for 2 h and cell lysates were blotted with the indicated antibodies after treated with ESI (15 μM) and cisplatin (15 μM) combination for 12 h. Data from three technical replicates (*$p < 0.05$, **$p < 0.01$ versus DMSO group, $^{\#}p < 0.05$ versus ESI+Cis group).

(Duan et al., 2016; Dagnell et al., 2018; Zheng et al., 2019). Accordingly, we found that TrxR1 activity in colon cancer cells was decreased with increasing ESI concentration. In addition, we demonstrated that ESI directly inhibited the TrxR1 protein activity in a dose-dependent manner. The densitometric analysis of Western blot bands revealed that ESI treatment does not affect the expression of TrxR1 in colon cancer cells. Furthermore, we found that TrxR1 knockdown sensitized cells to ESI, which was consistent with previous studies (Duan et al., 2016; Yao et al., 2020). The thioredoxin and GSH systems play important roles in regulating the cellular redox balance (Du et al., 2012; Harris et al., 2015; Kengen et al., 2018). Interestingly, we found that BSO significantly enhanced ESI-induced cell death in HCT116 and RKO cells via promoting generation of ROS, indicating that a combination therapy inhibiting both thioredoxin and GSH systems may become an effective way to treat colon cancer. Further insight into the roles of other antioxidant systems such as Nrf2 and GPX4, and how they act both alone and together, will provide important clues into more effective therapies for cancer patients.

A number of physical treatments or antitumor drugs, such as exemestane (Nuvoli et al., 2018), sorafenib (Roh et al., 2017), cisplatin (Pan et al., 2019), osimertinib (Tang et al., 2017), and irradiation (He et al., 2015), act, at least in part, through the generation of ROS. In this study, we showed that ESI significantly enhanced cisplatin-induced cell death in HCT116 and RKO cells via promoting generation of ROS and activation of the JNK signaling pathway. In addition, we demonstrated that ESI enhanced DNA damage induced by cisplatin based on increased formation of nuclear 53BP1 foci. The observation that ESI sensitizes the response of colon cancer cells to cisplatin may provide a promising strategy for colon

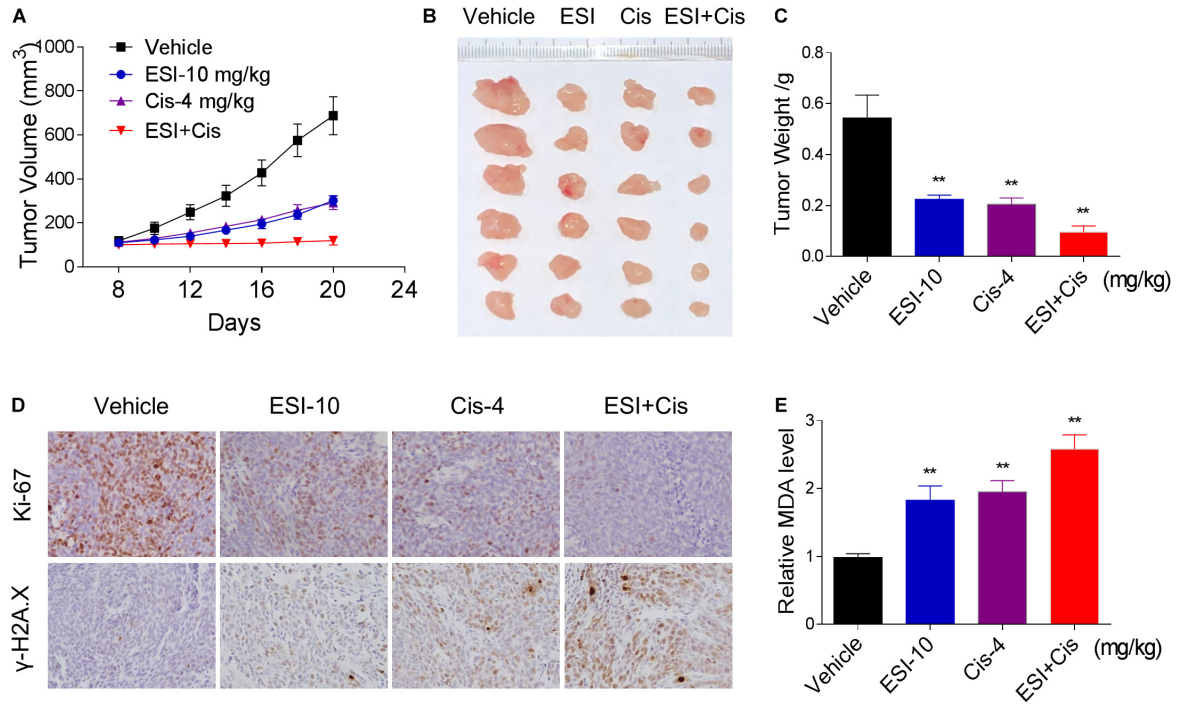

FIGURE 7 | ESI and cisplatin cooperated to inhibit tumor growth of HCT116 xenografts in nude mice. **(A,B)** ESI (10 mg/kg) and cisplatin (4 mg/kg) combined treatment significantly decreased tumor volume and tumor weight **(C)** of HCT116 human colon cancer xenografts in nude mice. **(D)** The levels of Ki-67 and γH2A.X in tumor tissues. **(E)** MDA levels in tumor tissues (**$p < 0.01$ versus Vehicle group).

cancer treatment: combination of ESI with existing oxidative stress-causing antitumor drugs or physical treatments, such as ionizing radiation (IR) and photodynamic therapy (PDT).

In conclusion, we have discovered a novel small molecule inhibitor of TrxR1, and showed that ESI induced cell death through ROS-mediated JNK signaling pathway in colon cancer cells. Our findings clearly demonstrated that ESI can be developed as a novel anticancer drug for the treatment of colon cancer. Furthermore, we found that ESI significantly enhanced the antitumor activity of cisplatin *in vitro* and *in vivo*. These findings provided new insight into the molecular mechanisms of antitumor action of ESI, which may provide potential therapies for the treatment of colon cancer.

MATERIALS AND METHODS

Materials

Isodeoxyelephantopin (ESI) was purchased from Chengdu Herbpurify Co., Ltd. (Chengdu, China). ESI was dissolved in dimethyl sulfoxide (DMSO). JNK inhibitor SP600125 was obtained from Selleck Chemicals (Houston, TX, United States). L-Buthionine-sulfoximine (BSO) was purchased from Aladdin Industrial Corporation (Shanghai, China). NAC was purchased from Sigma (St. Louis, MO, United States). Antibodies of p-JNK and JNK were purchased from Cell Signaling Technology (Danvers, MA, United States). Antibodies of TrxR1 and GAPDH were purchased from Santa Cruz Biotechnology (Santa Cruz, CA, United States). Antibodies of Ki-67 and γ-H2A.X antibody were purchased from Abcam (Cambridge, MA, United States). The 53BP1 antibody was purchased from Novus Biologicals (Littleton, CO, United States).

Cell Culture

HCT116, RKO and NRK-52E cell lines were obtained from the Cell Bank of Shanghai Institute of Biochemistry and Cell Biology, Chinese Academy of Sciences. HCT116 cells were grown in McCoy's 5A medium plus 10% fetal bovine serum (FBS). RKO cells were grown in minimum essential medium plus 10% FBS. NRK-52E cells were grown in DMEM plus 10% FBS. Mouse peritoneal macrophage (MPM) cells were obtained as previously described (Zhao et al., 2015). All the cells were cultured in a humidified incubator with 5% CO_2 at 37°C.

Cell Viability Assay

Approximately 8,000 cells per well were seeded in 96-well plates and incubated overnight. Next, the cells were treated with ESI or cisplatin alone or their combination for 24 h. Cell viability was measured using a methyl thiazolyl tetrazolium assay. The drug interaction was evaluated by using the CI according to the Chou-Talalay method (Chou, 2010).

Measurement of Intracellular ROS

The fluorescent probe 2′,7′-dichlorofluorescin diacetate (DCFH-DA) was employed to detect intracellular ROS levels. Briefly, cells were plated in 6-well plates and incubated overnight. Cells were

treated with ESI or cisplatin alone or their combination for the indicated times. Next, the cells were stained with 10 μM DCFH-DA for 30 min before collecting. For quantitative assessment of intracellular ROS levels, the cells were collected and analyzed by FACSCalibur flow cytometer.

Western Blot Analysis

Cells were seeded in 6-well plates and incubated overnight. After various treatments, the cells were washed once with 1 ml of phosphate-buffered saline and lysed using cell lysis buffer. The same amount of lysate proteins were separated by 10% SDS-PAGE and electroblotted onto PVDF transfer membranes. The blots were blocked with five percent non-fat milk in TBST for 2 h at room temperature. Then incubated with specific primary antibodies overnight at 4°C. HRP-conjugated secondary antibodies and ECL substrate (Bio-Rad, Hercules, CA, United States) were used for detection.

Measurement of TrxR1 Activity

Cells were seeded in 6-well plates and incubated overnight. Next, the cells were treated with ESI for the indicated time periods and lysed with lysis buffer. TrxR1 activity in cell lysates was measured using an endpoint insulin reduction assay as previously described (Zou et al., 2016). The TrxR1 (14638, Cayman Chemical, MI, United States) activity was determined at room temperature using the DTNB assay. The NADPH-reduced TrxR1 (170 nM) protein was treated with varying concentrations of ESI for the indicated time in a 96-well plates. A master mixture of Tris-EDTA buffer (1 mM EDTA, 50 mM Tris-HCl, pH 7.5) containing NADPH (200 μM) and DTNB (2 mM) was added. The linear increase in absorbance at 412 nm during the initial 3 min was recorded.

Transient Transfection of Small Interfering RNA (siRNA)

The siRNA duplexes used in this study were obtained from Sigma (St. Louis, MO, United States). The sequences of siRNA were described previously (Zou et al., 2016). Sense 5′-(CUUUGCAGCUGCGCUCAAA)dTdT-3′, antisense 5′-(UUUGAGCGCAGCUGCAAAG)dT dT-3′. The siRNA duplexes targeting TrxR1 were transduced into HCT116 cells. Forty-eight hours post-transduction, the cells were washed with complete media and plated with or without ESI for 24 h for assessing cell survival.

Docking of ESI to the TrxR1 Structural Model

The crystal structure of rat TrxR1 (PDB code 3EAN, chainA and chain B) was used for present docking study as described previously (Cheng et al., 2009; Liu et al., 2019). The center co-ordination of dock pocket was set as 1.49, 5.74, and 159.58. A grid box size of 60 × 60 × 60 points with a spacing of 0.375 Å between the grid points was implemented. The default parameters were used for running the docking simulation.

Immunofluorescence Staining

Cells were seeded on sterile cover glasses placed in the 6-well plates and incubated overnight. Next, the cells were treated with ESI or cisplatin alone or their combination for 20 h. For immunofluorescence, the cells were stained with a primary antibody (53BP1, 1:2,000 dilution) overnight at 4°C. Next, the cells were incubated with a DyLight 488 conjugated secondary antibody for 1.5 h at room temperature. The images were obtained using a Leica fluorescence microscope.

Immunohistochemistry Staining

For immunohistochemistry, 5-μm sections from paraformaldehyde-fixed paraffin-embedded tissues were deparaffinized in xylenes solvent and rehydrated through a graded alcohol series. Immunohistochemistry analyses of Ki-67 and γ-H2A.X were performed according to the protocol described previously (He et al., 2019).

Xenograft Experiments

Five-week-old athymic BALB/c nude mice (total $n = 24$) were used for *in vivo* experiments. All animals used in this study were handled according to the Institutional Animal Care and Use Committee (IACUC) guidelines, Wenzhou Medical University. The animals were housed at a constant room temperature with a 12 h light/12 h dark cycle and fed a standard rodent diet and water. HCT116 cells (5×10^6 cells in 100 μl of phosphate-buffered saline) were injected subcutaneously into the right back of nude mice. The mice were treated with ESI, cisplatin, or the combination by intraperitoneal (i.p.) injection once every other day at the indicated doses. The tumor volumes were measured to observe dynamic changes in tumor growth and calculated according to the formula: $V\ (mm^3) = 0.5 \times D \times d^2$, where D and d are the longest and the shortest diameters, respectively. At the end of the experiment, all nude mice were sacrificed, and the tumor tissues were removed and measured.

MDA Assay

Malondialdehyde is a terminal product of lipid peroxidation. For the MDA assay, tissue proteins of tumor xenograft were homogenized in ice-cold RIPA buffer. The protein concentrations were determined using the Bradford assay (Bio-Rad, Hercules, CA, United States). The MDA levels were detected according to the protocol described previously (Zou et al., 2016).

Statistical Analysis

The data are expressed as means ± standard error of the mean (SEM). Significant differences between control and experimental groups were determined by t-test analyses using statistical software, GraphPad Prism 5.0. A probability (P) value of <0.05 was considered statistically significant.

DATA AVAILABILITY STATEMENT

All datasets presented in this study are included in the article/supplementary material.

ETHICS STATEMENT

The animal study was reviewed and approved by the Institutional Animal Care and Use Committee (IACUC) guidelines, Wenzhou Medical University.

AUTHOR CONTRIBUTIONS

YX and PZo designed the study. YX and PZo supervised the study and wrote the manuscript. LH and JC performed the experiments. FaW, FeW, XS, PZh, RS, KL, ZL, DC, GL, and YC collected and analyzed the data. All authors contributed to the article and approved the submitted version.

FUNDING

Financial support from the National Natural Science Foundation of China (81603153 and 81503107), Zhejiang Provincial Natural Science Foundation (LY20H310004 and LY17B020008), National College Students Innovation and Entrepreneurship Training Program (201910343025), and the Zhejiang Provincial College Students' Technological Innovation Training Program (2019R413015) are gratefully acknowledged.

REFERENCES

Ahmed, E. M., Bandopadhyay, G., Coyle, B., and Grabowska, A. (2018). A HIF-independent, CD133-mediated mechanism of cisplatin resistance in glioblastoma cells. *Cell Oncol.* 41, 319–328. doi: 10.1007/s13402-018-0374-8

Al-Batran, S. E., Homann, N., Pauligk, C., Goetze, T. O., Meiler, J., Kasper, S., et al. (2019). Perioperative chemotherapy with fluorouracil plus leucovorin, oxaliplatin, and docetaxel versus fluorouracil or capecitabine plus cisplatin and epirubicin for locally advanced, resectable gastric or gastro-oesophageal junction adenocarcinoma (FLOT4): a randomised, phase 2/3 trial. *Lancet* 393, 1948–1957.

Arner, E. S. J. (2017). Targeting the selenoprotein thioredoxin reductase 1 for anticancer therapy. *Adv. Cancer Res.* 136, 139–151. doi: 10.1016/bs.acr.2017.07.005

Arnold, M., Sierra, M. S., Laversanne, M., Soerjomataram, I., Jemal, A., and Bray, F. (2017). Global patterns and trends in colorectal cancer incidence and mortality. *Gut* 66, 683–691. doi: 10.1136/gutjnl-2015-310912

Basu, A., and Krishnamurthy, S. (2010). Cellular responses to Cisplatin-induced DNA damage. *J. Nucleic Acids* 2010, 201367.

Bragado, P., Armesilla, A., Silva, A., and Porras, A. (2007). Apoptosis by cisplatin requires p53 mediated p38alpha MAPK activation through ROS generation. *Apoptosis* 12, 1733–1742. doi: 10.1007/s10495-007-0082-8

Cheng, Q., Sandalova, T., Lindqvist, Y., and Arner, E. S. (2009). Crystal structure and catalysis of the selenoprotein thioredoxin reductase 1. *J. Biol. Chem.* 284, 3998–4008. doi: 10.1074/jbc.m807068200

Chou, T. C. (2010). Drug combination studies and their synergy quantification using the Chou-Talalay method. *Cancer Res.* 70, 440–446. doi: 10.1158/0008-5472.can-09-1947

Cruz-Bermudez, A., Laza-Briviesca, R., Vicente-Blanco, R. J., Garcia-Grande, A., Coronado, M. J., Laine-Menendez, S., et al. (2019). Cisplatin resistance involves a metabolic reprogramming through ROS and PGC-1alpha in NSCLC which can be overcome by OXPHOS inhibition. *Free Radic. Biol. Med.* 135, 167–181. doi: 10.1016/j.freeradbiomed.2019.03.009

Dagnell, M., Schmidt, E. E., and Arner, E. S. J. (2018). The A to Z of modulated cell patterning by mammalian thioredoxin reductases. *Free Radic. Biol. Med.* 115, 484–496. doi: 10.1016/j.freeradbiomed.2017.12.029

Dias, R. B., De Araujo, T. B. S., De Freitas, R. D., Rodrigues, A., Sousa, L. P., Sales, C. B. S., et al. (2018). beta-Lapachone and its iodine derivatives cause cell cycle arrest at G2/M phase and reactive oxygen species-mediated apoptosis in human oral squamous cell carcinoma cells. *Free Radic. Biol. Med.* 126, 87–100. doi: 10.1016/j.freeradbiomed.2018.07.022

Du, Y., Zhang, H., Lu, J., and Holmgren, A. (2012). Glutathione and glutaredoxin act as a backup of human thioredoxin reductase 1 to reduce thioredoxin 1 preventing cell death by aurothioglucose. *J. Biol. Chem.* 287, 38210–38219. doi: 10.1074/jbc.m112.392225

Duan, D., Zhang, J., Yao, J., Liu, Y., and Fang, J. (2016). Targeting thioredoxin reductase by parthenolide contributes to inducing apoptosis of HeLa cells. *J. Biol. Chem.* 291, 10021–10031. doi: 10.1074/jbc.m115.700591

Fournel, L., Wu, Z., Stadler, N., Damotte, D., Lococo, F., Boulle, G., et al. (2019). Cisplatin increases PD-L1 expression and optimizes immune check-point blockade in non-small cell lung cancer. *Cancer Lett.* 464, 5–14. doi: 10.1016/j.canlet.2019.08.005

Glasauer, A., and Chandel, N. S. (2014). Targeting antioxidants for cancer therapy. *Biochem. Pharmacol.* 92, 90–101. doi: 10.1016/j.bcp.2014.07.017

Gorrini, C., Harris, I. S., and Mak, T. W. (2013). Modulation of oxidative stress as an anticancer strategy. *Nat. Rev. Drug Discov.* 12, 931–947. doi: 10.1038/nrd4002

Harris, I. S., Treloar, A. E., Inoue, S., Sasaki, M., Gorrini, C., Lee, K. C., et al. (2015). Glutathione and thioredoxin antioxidant pathways synergize to drive cancer initiation and progression. *Cancer Cell* 27, 211–222. doi: 10.1016/j.ccell.2014.11.019

He, L., Lai, H., and Chen, T. (2015). Dual-function nanosystem for synergetic cancer chemo-/radiotherapy through ROS-mediated signaling pathways. *Biomaterials* 51, 30–42. doi: 10.1016/j.biomaterials.2015.01.063

He, W., Cao, P., Xia, Y., Hong, L., Zhang, T., Shen, X., et al. (2019). Potent inhibition of gastric cancer cells by a natural compound via inhibiting TrxR1 activity and activating ROS-mediated p38 MAPK pathway. *Free Radic. Res.* 53, 104–114. doi: 10.1080/10715762.2018.1558448

Hsu, J. H., Chang, P. M., Cheng, T. S., Kuo, Y. L., Wu, A. T., Tran, T. H., et al. (2019). Identification of Withaferin A as a potential candidate for anti-cancer therapy in non-small cell lung cancer. *Cancers* 11:1003. doi: 10.3390/cancers11071003

Ichikawa, H., Nair, M. S., Takada, Y., Sheeja, D. B., Kumar, M. A., Oommen, O. V., et al. (2006). Isodeoxyelephantopin, a novel sesquiterpene lactone, potentiates apoptosis, inhibits invasion, and abolishes osteoclastogenesis through suppression of nuclear factor-kappaB (nf-kappaB) activation and nf-kappaB-regulated gene expression. *Clin. Cancer Res.* 12, 5910–5918. doi: 10.1158/1078-0432.ccr-06-0916

Jin, R., Gao, Y., Zhang, S., Teng, F., Xu, X., Aili, A., et al. (2015). Trx1/TrxR1 system regulates post-selected DP thymocytes survival by modulating ASK1-JNK/p38 MAPK activities. *Immunol. Cell Biol.* 93, 744–752. doi: 10.1038/icb.2015.36

Jung, Y., and Lippard, S. J. (2007). Direct cellular responses to platinum-induced DNA damage. *Chem. Rev.* 107, 1387–1407. doi: 10.1021/cr068207j

Kabeer, F. A., Sreedevi, G. B., Nair, M. S., Rajalekshmi, D. S., Gopalakrishnan, L. P., and Prathapan, R. (2014). Isodeoxyelephantopin from *Elephantopus scaber* (Didancao) induces cell cycle arrest and caspase-3-mediated apoptosis in breast carcinoma T47D cells and lung carcinoma A549 cells. *Chin. Med.* 9:14. doi: 10.1186/1749-8546-9-14

Kengen, J., Deglasse, J. P., Neveu, M. A., Mignion, L., Desmet, C., Gourgue, F., et al. (2018). Biomarkers of tumour redox status in response to modulations of glutathione and thioredoxin antioxidant pathways. *Free Radic. Res.* 52, 256–266. doi: 10.1080/10715762.2018.1427236

Li, Y., Ooi, L. S., Wang, H., But, P. P., and Ooi, V. E. (2004). Antiviral activities of medicinal herbs traditionally used in southern mainland China. *Phytother. Res.* 18, 718–722. doi: 10.1002/ptr.1518

Liao, W., Wang, Z., Fu, Z., Ma, H., Jiang, M., Xu, A., et al. (2019). p62/SQSTM1 protects against cisplatin-induced oxidative stress in kidneys by mediating the

cross talk between autophagy and the Keap1-Nrf2 signalling pathway. *Free Radic. Res.* 53, 800–814. doi: 10.1080/10715762.2019.1635251

Lien, E. C., Lyssiotis, C. A., Juvekar, A., Hu, H., Asara, J. M., Cantley, L. C., et al. (2016). Glutathione biosynthesis is a metabolic vulnerability in PI(3)K/Akt-driven breast cancer. *Nat. Cell Biol.* 18, 572–578. doi: 10.1038/ncb3341

Liu, N., Wang, K. S., Qi, M., Zhou, Y. J., Zeng, G. Y., Tao, J., et al. (2018). Vitexin compound 1, a novel extraction from a Chinese herb, suppresses melanoma cell growth through DNA damage by increasing ROS levels. *J. Exp. Clin. Cancer Res.* 37:269.

Liu, R., Shi, D., Zhang, J., Li, X., Han, X., Yao, X., et al. (2019). Virtual screening-guided discovery of thioredoxin reductase inhibitors. *Toxicol. Appl. Pharmacol.* 370, 106–116. doi: 10.1016/j.taap.2019.03.014

Mantzaris, M. D., Bellou, S., Skiada, V., Kitsati, N., Fotsis, T., and Galaris, D. (2016). Intracellular labile iron determines H2O2-induced apoptotic signaling via sustained activation of ASK1/JNK-p38 axis. *Free Radic. Biol. Med.* 97, 454–465. doi: 10.1016/j.freeradbiomed.2016.07.002

Newman, D. J., and Cragg, G. M. (2016). Natural products as sources of new drugs from 1981 to 2014. *J. Nat. Prod.* 79, 629–661. doi: 10.1021/acs.jnatprod.5b01055

Nuvoli, B., Camera, E., Mastrofrancesco, A., Briganti, S., and Galati, R. (2018). Modulation of reactive oxygen species via ERK and STAT3 dependent signalling are involved in the response of mesothelioma cells to exemestane. *Free Radic. Biol. Med.* 115, 266–277. doi: 10.1016/j.freeradbiomed.2017.12.008

Pan, C., Jin, L., Wang, X., Li, Y., Chun, J., Boese, A. C., et al. (2019). Inositol-triphosphate 3-kinase B confers cisplatin resistance by regulating NOX4-dependent redox balance. *J. Clin. Invest.* 130, 2431–2445. doi: 10.1172/jci124550

Park, H., Jeong, Y. J., Han, N. K., Kim, J. S., and Lee, H. J. (2018). Oridonin enhances radiation-induced cell death by promoting DNA damage in non-small cell lung cancer cells. *Int. J. Mol. Sci.* 19:2378. doi: 10.3390/ijms19082378

Poli, A., Nicolau, M., Simoes, C. M., Nicolau, R. M., and Zanin, M. (1992). Preliminary pharmacologic evaluation of crude whole plant extracts of Elephantopus scaber. Part I: in vivo studies. *J. Ethnopharmacol.* 37, 71–76. doi: 10.1016/0378-8741(92)90005-c

Rabik, C. A., and Dolan, M. E. (2007). Molecular mechanisms of resistance and toxicity associated with platinating agents. *Cancer Treat. Rev.* 33, 9–23. doi: 10.1016/j.ctrv.2006.09.006

Rajesh, M. G., and Latha, M. S. (2001). Hepatoprotection by Elephantopus scaber Linn. *in CCl4*-induced liver injury. *Ind. J. Physiol. Pharmacol.* 45, 481–486.

Rashmi, R., Huang, X., Floberg, J. M., Elhammali, A. E., Mccormick, M. L., Patti, G. J., et al. (2018). Radioresistant cervical cancers are sensitive to inhibition of glycolysis and redox metabolism. *Cancer Res.* 78, 1392–1403. doi: 10.1158/0008-5472.can-17-2367

Roh, J. L., Kim, E. H., Jang, H., and Shin, D. (2017). Aspirin plus sorafenib potentiates cisplatin cytotoxicity in resistant head and neck cancer cells through xCT inhibition. *Free Radic. Biol. Med.* 104, 1–9. doi: 10.1016/j.freeradbiomed.2017.01.002

Roy, S., Kar, M., Saha, A., Padhi, S., and Banerjee, B. (2018). Role of beta-catenin in cisplatin resistance, relapse and prognosis of head and neck squamous cell carcinoma. *Cell. Oncol.* 41, 185–200. doi: 10.1007/s13402-017-0365-1

Schieber, M., and Chandel, N. S. (2014). ROS function in redox signaling and oxidative stress. *Curr Biol.* 24, R453–R462.

Srinivas, U. S., Tan, B. W. Q., Vellayappan, B. A., and Jeyasekharan, A. D. (2018). ROS and the DNA damage response in cancer. *Redox Biol.* 25:101084. doi: 10.1016/j.redox.2018.101084

Su, Y., Yang, W., Jiang, N., Shi, J., Chen, L., Zhong, G., et al. (2019). Hypoxia-elevated circELP3 contributes to bladder cancer progression and cisplatin resistance. *Int. J. Biol. Sci.* 15, 441–452. doi: 10.7150/ijbs.26826

Sun, Y., Miao, H., Ma, S., Zhang, L., You, C., Tang, F., et al. (2018). FePt-Cys nanoparticles induce ROS-dependent cell toxicity, and enhance chemo-radiation sensitivity of NSCLC cells in vivo and in vitro. *Cancer Lett.* 418, 27–40. doi: 10.1016/j.canlet.2018.01.024

Tang, Z. H., Cao, W. X., Su, M. X., Chen, X., and Lu, J. J. (2017). Osimertinib induces autophagy and apoptosis via reactive oxygen species generation in non-small cell lung cancer cells. *Toxicol. Appl. Pharmacol.* 321, 18–26. doi: 10.1016/j.taap.2017.02.017

Trachootham, D., Alexandre, J., and Huang, P. (2009). Targeting cancer cells by ROS-mediated mechanisms: a radical therapeutic approach? *Nat. Rev. Drug Discov.* 8, 579–591. doi: 10.1038/nrd2803

Verma, S. S., Rai, V., Awasthee, N., Dhasmana, A., Rajalaksmi, D. S., Nair, M. S., et al. (2019). Isodeoxyelephantopin, a Sesquiterpene lactone induces ROS generation, suppresses NF-kappaB activation, modulates LncRNA expression and exhibit activities against breast cancer. *Sci. Rep.* 9:17980.

Wang, D., and Lippard, S. J. (2005). Cellular processing of platinum anticancer drugs. *Nat. Rev. Drug Discov.* 4, 307–320. doi: 10.1038/nrd1691

Wang, J., Tian, L., Khan, M. N., Zhang, L., Chen, Q., Zhao, Y., et al. (2018). Ginsenoside Rg3 sensitizes hypoxic lung cancer cells to cisplatin via blocking of NF-kappaB mediated epithelial-mesenchymal transition and stemness. *Cancer Lett.* 415, 73–85. doi: 10.1016/j.canlet.2017.11.037

Wang, Y., Hao, F., Nan, Y., Qu, L., Na, W., Jia, C., et al. (2018). PKM2 inhibitor Shikonin overcomes the Cisplatin resistance in bladder cancer by inducing necroptosis. *Int. J. Biol. Sci.* 14, 1883–1891. doi: 10.7150/ijbs.27854

Wang, Y., Zhang, J., Huang, Z. H., Huang, X. H., Zheng, W. B., Yin, X. F., et al. (2017). Isodeoxyelephantopin induces protective autophagy in lung cancer cells via Nrf2-p62-keap1 feedback loop. *Cell Death Dis* 8:e2876. doi: 10.1038/cddis.2017.265

Xu, J., Cheng, Q., and Arner, E. S. (2016). Details in the catalytic mechanism of mammalian thioredoxin reductase 1 revealed using point mutations and juglone-coupled enzyme activities. *Free Radic. Biol. Med.* 94, 110–120. doi: 10.1016/j.freeradbiomed.2016.02.013

Yan, G. R., Tan, Z., Wang, Y., Xu, M. L., Yu, G., Li, Y., et al. (2013). Quantitative proteomics characterization on the antitumor effects of isodeoxyelephantopin against nasopharyngeal carcinoma. *Proteomics* 13, 3222–3232. doi: 10.1002/pmic.201300152

Yang, C., Lim, W., Bazer, F. W., and Song, G. (2017). Myricetin suppresses invasion and promotes cell death in human placental choriocarcinoma cells through induction of oxidative stress. *Cancer Lett.* 399, 10–19.

Yao, J., Duan, D., Song, Z. L., Zhang, J., and Fang, J. (2020). Sanguinarine as a new chemical entity of thioredoxin reductase inhibitor to elicit oxidative stress and promote tumor cell apoptosis. *Free Radic. Biol. Med.* 152, 659–667. doi: 10.1016/j.freeradbiomed.2020.01.008

Zhang, T., Zheng, P., Shen, X., Shao, R., Wang, B., Shen, H., et al. (2019). Curcuminoid WZ26, a TrxR1 inhibitor, effectively inhibits colon cancer cell growth and enhances cisplatin-induced cell death through the induction of ROS. *Free Radic. Biol. Med.* 141, 93–102. doi: 10.1016/j.freeradbiomed.2019.06.005

Zhao, C., Zhang, Y., Zou, P., Wang, J., He, W., Shi, D., et al. (2015). Synthesis and biological evaluation of a novel class of curcumin analogs as anti-inflammatory agents for prevention and treatment of sepsis in mouse model. *Drug Des. Devel. Ther.* 9, 1663–1678. doi: 10.2147/dddt.s75862

Zheng, X., Chen, Y., Bai, M., Liu, Y., Xu, B., Sun, R., et al. (2019). The antimetastatic effect and underlying mechanisms of thioredoxin reductase inhibitor ethaselen. *Free Radic. Biol. Med.* 131, 7–17. doi: 10.1016/j.freeradbiomed.2018.11.030

Zou, P., Xia, Y., Ji, J., Chen, W., Zhang, J., Chen, X., et al. (2016). Piperlongumine as a direct TrxR1 inhibitor with suppressive activity against gastric cancer. *Cancer Lett.* 375, 114–126. doi: 10.1016/j.canlet.2016.02.058

Conflict of Interest: The authors declare that the research was conducted in the absence of any commercial or financial relationships that could be construed as a potential conflict of interest.

frontiers in Oncology

ORIGINAL RESEARCH
published: 05 October 2020
doi: 10.3389/fonc.2020.581814

Mifepristone as a Potential Therapy to Reduce Angiogenesis and P-Glycoprotein Associated With Glioblastoma Resistance to Temozolomide

*Monserrat Llaguno-Munive[1,2], Sebastián León-Zetina[1], Inés Vazquez-Lopez[1], María del Pilar Ramos-Godinez[3], Luis A. Medina[4,5] and Patricia Garcia-Lopez[1]**

[1] Laboratorio de Farmacología, Subdirección de Investigación Básica, Instituto Nacional de Cancerología, Mexico City, Mexico, [2] Posgrado en Ciencias Biomédicas, Universidad Nacional Autónoma de México, Mexico City, Mexico, [3] Departamento de Patología Quirúrgica, Instituto Nacional de Cancerología, Mexico City, Mexico, [4] Unidad de Investigación Biomédica en Cáncer INCan-UNAM, Instituto Nacional de Cancerología, Mexico City, Mexico, [5] Instituto de Física, Universidad Nacional Autónoma de México, Coyoacán, Mexico City, Mexico

OPEN ACCESS

Edited by:
Rosa Maria Bermudez-Cruz, National Polytechnic Institute of Mexico (CINVESTAV), Mexico

Reviewed by:
Keith R. Laderoute, SRI International, United States
Eduardo J. Salustiano, Federal University of Rio de Janeiro, Brazil

***Correspondence:**
Patricia Garcia-Lopez
pgarcia_lopez@yahoo.com.mx

Specialty section:
This article was submitted to Molecular and Cellular Oncology, a section of the journal Frontiers in Oncology

Received: *09 July 2020*
Accepted: *08 September 2020*
Published: *05 October 2020*

Citation:
Llaguno-Munive M, León-Zetina S, Vazquez-Lopez I, Ramos-Godinez MP, Medina LA and Garcia-Lopez P (2020) Mifepristone as a Potential Therapy to Reduce Angiogenesis and P-Glycoprotein Associated With Glioblastoma Resistance to Temozolomide. Front. Oncol. 10:581814. doi: 10.3389/fonc.2020.581814

Glioblastoma, the most common primary central nervous system tumor, is characterized by extensive vascular neoformation and an area of necrosis generated by rapid proliferation. The standard treatment for this type of tumor is surgery followed by chemotherapy based on temozolomide and radiotherapy, resulting in poor patient survival. Glioblastoma is known for strong resistance to treatment, frequent recurrence and rapid progression. The aim of this study was to evaluate whether mifepristone, an antihormonal agent, can enhance the effect of temozolomide on C6 glioma cells orthotopically implanted in Wistar rats. The levels of the vascular endothelial growth factor (VEGF), and P-glycoprotein (P-gp) were examined, the former a promoter of angiogenesis that facilitates proliferation, and the latter an efflux pump transporter linked to drug resistance. After a 3-week treatment, the mifepristone/temozolomide regimen had decreased the level of VEGF and P-gp and significantly reduced tumor proliferation (detected by PET/CT images based on 18F-fluorothymidine uptake). Additionally, mifepristone proved to increase the intracerebral concentration of temozolomide. The lower level of O6-methylguanine-DNA-methyltransferase (MGMT) (related to DNA repair in tumors) previously reported for this combined treatment was herein confirmed. After the mifepristone/temozolomide treatment ended, however, the values of VEGF, P-gp, and MGMT increased and reached control levels by 14 weeks post-treatment. There was also tumor recurrence, as occurred when administering temozolomide alone. On the other hand, temozolomide led to 100% mortality within 26 days after beginning the drug treatment, while mifepristone/temozolomide enabled 70% survival 60–70 days and 30% survived over 100 days, suggesting that mifepristone could possibly act as a chemo-sensitizing agent for temozolomide.

Keywords: glioblastoma, temozolomide, mifepristone, drug resistance, angiogenesis, P-gp

INTRODUCTION

Glioblastoma is the most frequent primary neoplasm of the central nervous system and the most aggressive brain tumor, with a life expectancy of 14–15 months post-diagnosis (1–3). It is characterized by uncontrolled cell proliferation, highly diffuse infiltration, resistance to apoptosis, robust angiogenesis, and DNA repair mechanisms contributing to drug resistance. The standard treatment for glioblastoma is surgery followed by chemotherapy based on temozolomide and radiotherapy, which leads to poor patient survival.

The growth of glioblastoma is associated with its capacity to maintain a balanced expression of proteins that control the cell cycle and allow for proliferation, motility and vascular neoformation. Furthermore, it is able to avoid recognition by the immune system. Reports in the Cancer Genome Atlas (TCGA) identify three main pathways participating in the pathogenesis of glioma: (RTK)/RAS/(PI3K), p53, and retinoblastoma (4).

A major factor in the strong resistance of tumors to temozolomide treatment is the overexpression of enzyme O6-methylguanine-DNA-methyltransferase (MGMT), which participates in the repair of temozolomide-induced DNA damage. Our group previously demonstrated that mifepristone enhances the temozolomide-induced decrease in orthotopic glioblastoma tumors by increasing apoptosis and reducing levels of MGMT (thus impeding repair of DNA damage) (5).

Among other pathways of glioma resistance to treatment described in the literature are those that contribute to angiogenesis, the formation of new blood vessels from a pre-existing vascular network. Several studies have correlated increased tumor vascularization with a lower rate of patient survival. Indeed, in the absence of angiogenesis, tumors cannot grow beyond a size of 1–2 mm^3 (6). One of the main promoters of angiogenesis is hypoxia, which stimulates the synthesis of the most important mediator in angiogenesis, the vascular endothelial growth factor (VEGF). The receptors of VEGF are reported to be over-expressed in glioblastoma (7, 8). Among the strategies for inhibiting the expression of VEGF is the use of bevacizumab, a humanized monoclonal antibody. Two phase III studies on this drug have showed that the addition of bevacizumab to standard treatment (radiotherapy–temozolomide) for patients with newly diagnosed glioblastoma, was associated with a 4-month increase in progression-free survival without a significant effect on overall survival. Moreover, there was an increase in adverse events associated with bevacizumada (9, 10), emphasizing the need to seek new pharmacological strategies.

Another pathway involved in glioblastoma is related to the blood–brain barrier (BBB). Many promising chemotherapeutic agents have had great difficulty in overcoming the mechanisms of the BBB. On one hand, it is a physical barrier comprised of tight junctions between endothelial cells and a lack of fenestrae. In addition, it is an active efflux system that transports a wide range of antineoplastic drugs (e.g., temozolomide) out of the brain. The best known of these transporters is P-glycoprotein (P-gp), a membrane protein belonging to the superfamily of ATP-binding cassette (ABC) transporters. The blocking of these transport proteins might be useful in the treatment of glioblastoma (11–14).

To date, the search for new treatments against glioblastoma has not improved the survival of patients. An attractive strategy is the repositioning of approved drugs for use in combination with standard therapy. One attractive candidate for repositioning is mifepristone, a synthetic steroid that serves as an abortifacient drug based on anti-progestational and anti-glucocorticoid action. Mifepristone reportedly has antiproliferative effects in breast (15, 16), cervix (17), endometrium (18), ovary (19), and prostate cancer (20), can cross the BBB, and provides palliative effects on brain tumors such as meningiomas (21) and glioblastoma (22). Additionally, it is considered safe (with few adverse effects) and has a low cost. Besides reducing levels of MGMT (5), mifepristone is reported to diminish the activity of P-gp in human leukemia cancer cells (23) and a gastric cancer cell line (24). However, whether or not mifepristone is an inhibitor of P-gp on glioma cells or in the efflux transport system mediated by P-gp in the BBB has not yet been established. Likewise, there are no reports, to our knowledge, on its effect on temozolomide treatment.

Mifepristone may serve as a chemo-sensitizing drug, considering the descriptions in the literature of its inhibition of multiple targets in cancer cells. The aim of the present study was to evaluate the capacity of a mifepristone/temozolomide treatment in an orthotopic rat model of glioblastoma to modulate angiogenesis, reduce P-gp levels in the glioma tumors and increase the intracerebral concentration of temozolomide. Since tumors initially sensitive to chemotherapy often develop resistance, tumor recurrence was monitored after the combined treatment ended. Finally, the MGMT level was quantified as a parameter of DNA repair in tumor cells.

MATERIALS AND METHODS

Drugs and Reagents

Mifepristone and temozolomide were provided by Sigma Chemical Co. (St. Louis, MO, United States). Dulbecco's modified Eagle's medium (DMEM), FBS (fetal bovine serum), and EDTA (Ethylenediaminetetracetic acid) were purchased from Gibco-BRL (Grand Island, NY, United States). LC-MS/MS grade methanol was acquired from J.T.Baker. Acetic acid was of analytical grade. High-quality water for the solutions was processed with a Milli-Q Reagent Water System (Continental Water Systems, El Paso, TX, United States). A stock solution of temozolomide was prepared in DMSO at a final concentration of 4% and mifepristone was reconstituted in polyethylene glycol/saline solution. All standard solutions were stored at −20°C until use.

Animals

Male Wistar rats (230–250 g) were obtained from the Faculty of Medicine of the UNAM, Mexico City, Mexico. The animals were kept in pathogen-free conditions on a 12–12 h light/dark cycle, with adequate temperature and humidity. All procedures for the care and handling of the animals were reviewed and approved by the Ethics Committee of the "Instituto Nacional

de Cancerología" (INCan, Mexico City, Mexico), (Ref. No. 010/17/IBI-CEI/601/10), and were in accordance with the Mexican Federal Regulation for Animal Experimentation and Care (NOM-062-ZOO-1999, Ministry of Agriculture, Mexico).

Tumor Cell Implantation

The rat glioma C6 cell line was supplied by the American Type Culture Collection (ATCC, Rockville, United States). These cells were maintained under sterile conditions in DMEM medium (Gibco, Grand Island, NY, United States) supplemented with 5% fetal bovine serum and incubated at 37°C in a 5% CO_2 atmosphere.

The effect of Mif/Tz on tumor growth was evaluated on C6 glioma cells orthotopically implanted in Wistar rats. Each animal was anesthetized with a combination of tiletamine hydrochloride (10 mg/kg) and acepromazine maleate (0.4 mg/kg) administered subcutaneously (sc), then placed in a stereotactic device for surgery. The tumor cell implantation was performed according to Llaguno et al. (5). Briefly, after fastening the head in the frame, a midline incision was made and bregma was identified. The skull was then drilled at the coordinates of 2.0 mm right from bregma and 6 mm deep (hippocampus). C6 cells were harvested, washed and diluted in DMEM to a concentration of 7.5×10^5 in a volume of 3 μL. Employing an infusion pump, these cells were slowly implanted at a depth of 6 mm from the dura mater. The sham group was surgically opened and instead of implanting cancer cells, culture medium was injected.

Treatments

At 2 weeks post-surgery, the rats were randomly divided into six groups: (A) negative control (without surgery and without treatment, (B) sham surgery (in the absence of glioma cells and drug treatments) and four groups with the surgical implantation of cancer cells: (C) without drug treatment (vehicle control), (D) temozolomide alone (Tz), (E) mifepristone alone (Mif), (F) mifepristone/temozolomide (Mif/Tz). Tz was administered at a dose of 5 mg/kg ip and Mif at a dose of 10 mg/kg sc. The drugs were given for five consecutive days (Monday–Friday) during 3 weeks.

Determination of Tumor Growth

Brain tumor proliferation was measured by capturing images with a microPET/CT scanner (Albira ARS, Oncovision, Spain) at 2, 5, 7, 9, and 14 weeks post-surgery. For this purpose, 300 μCi of 18F-fluorothymidine (18F-FLT) were administered into the caudal vein. Another method of tracking tumor growth was by monitoring animal weight. Rats were weighed three times/week throughout the experiment, recording the global survival of each group.

Histological Analysis

The rats were euthanized and perfused with saline solution followed by 4% paraformaldehyde. Brains were removed and immersed in 4% paraformaldehyde for 2 weeks. The brain tissue was embedded in paraffin and sliced into sections (2 mm thick) on the coronal plane for the subsequent analysis with Eosin and Hematoxylin (H&E) and microvessel density immunohistochemical was evaluated with CD31 marker (#77699, Cell Signalling Technology).

Molecular Analysis

At the end of the study, the rats were sacrificed and the tumor was removed. The brain tissue was homogenized with a lysis buffer containing protease inhibitors (Cat. 78440; Thermo Scientist, TM). The samples were centrifuged at 10,000 *g* at 4°C and the supernatant was recovered. The proteins were quantified with the BCA (bicinchoninic acid) assay and separated by electrophoresis on 4–20% gradient gel (Mini-Protean TGX 456-1094, Bio-Rad Laboratories, Inc, United States). Colored markers (Bio-Rad, CA, United States) were included to establish size. For each sample, 40 g of protein were used. Following the transfer of the proteins onto PVDF membranes (Amersham, United Kingdom), the latter were blocked for 2 h at room temperature with 5% non-fat dry milk. The antibodies employed were anti-MGMT (sc-166528, 1:1000, Santa Cruz Biotechnology, TX, United States), P-gp (12683, 1:500, Cell Signalling Technology) and β-actin (sc-69879, 1:1000; Santa Cruz Biotechnology, TX, United States). After washing, the membranes were incubated with IRDye® 800 CW goat anti-mouse or IRDye® 680RD goat anti-rabbit secondary antibodies (1:15000; LI-COR, Inc.) for 1 h. The membranes were scanned on an Odyssey Imaging System and their intensity of fluorescence was measured with Image Studio software. In each figure, representative blot images were selected from the same gel. For the evaluation of angiogenesis, the relative concentration of VEGF was assessed with an Elisa kit according to the manufacturer's instructions (human VEGF, ENZ-KIT156-0001, Enzo Life Sciences, Inc).

Determination of Temozolomide in Rat Brain Tissue

Male Wistar rats (200–230 g) were divided into groups for two drug treatments ($n = 6$ each): (1) Tz (30 mg/kg, ip) and (2) Mif/Tz (60 mg/kg, sc, and 30 mg/kg, ip, respectively). For the second group, mifepristone was administered 2 h before temozolomide. In both groups, rats were euthanized 45 min after Tz was given. The tissues were weighed and kept at −70°C to await use.

The concentration of temozolomide was ascertained by chromatography on an LC-MS system (Agilent Agilent Technologies, Infinity 1260) with an autosampler temperature of 4°C. The separation was carried out at 25°C on an Agilent Zorbax SB-C18 column (1.8 μm, 2.1 mm × 50 mm) utilising a linear elution with (A) water (containing 0.5% acetic acid and 10 mM ammonium acetate) and (B) methanol as the mobile phase (10/90). The flow rate was set at 0.3 ml/min with an injection volume of 5 μl.

Mass spectrometry was performed on an Agilent QQQ Detector (Agilent Technologies, Infinity 1260) in the positive ESI mode with nitrogen as the solvent. The capillary voltage was 3.0 kV and the dissolvation temperature 350°C. Quantification was achieved by using multiple reactions monitoring of the transitions of m/z 195.10–137.95 for temozolomide, and m/z 181.10–124.0 for theophylline as the internal standard.

Individual stock solutions of temozolomide (1 mg/ml) and theophylline (1 mg/ml) were prepared in separate volumetric flasks and dissolved in acid methanol (acetic acid 0.5% and methanol v/v, 20/80) for temozolomide and pure methanol for theophylline. Intermediate and final working solutions containing temozolomide were prepared in acid methanol and theophylline solutions were prepared in water. Calibration standards were prepared at following concentrations: 50, 100, 500, 1000, 2000, and 5000 ng/ml.

The internal standard solution (1000 ng/ml in water) was added to small slices of the brain (400 mg; 50 µl 1 M HCL and temozolomide working solutions for the calibration standards). The slices were individually homogenized before adding ethyl acetate and mixing for 5 min. The samples were centrifuged at 14000 rpm for 15 min at 4°C. The supernatant was transferred to an Eppendorf tube, ethyl acetate was added, and centrifugation was performed at 14,000 rpm. The supernatant was transferred to an Eppendorf tube and evaporated to dryness under a stream of nitrogen at 24°C. Afterward, 200 µl of acid methanol was added to the dry residue and injected into the chromatographic system.

Statistical Analysis

Data are expressed as the mean ± SD. Statistical significance was determined with one-way analysis of variance (ANOVA) on SPSS Base 20.0 software (SPSS Inc, Chicago, IL, United States). When necessary, the comparison of means was Bonferroni adjusted. In all cases, significance was considered at $p < 0.05$.

RESULTS

Animal Body Weight

During the first 2 weeks post-implantation of C6 cells, all animals continued to gain weight. Subsequently, the negative control and sham group gained weight while the untreated, Tz and Mif groups rapidly lost weight, similar to data previously reported by our group (5). The rats in the Mif/Tz group maintained their weight throughout the experiment (**Figure 1**).

Histological and Immunohistochemical Analysis

In the histological examination, applying H&E stain, we observed typical characteristics of glioblastoma in without treatment group, as hypercellularity, infiltration of tumor cells and mitosis. The tissue of the animals treated with Tz or Mif showed lesser hypercellularity and mitosis; however, the effect was more evident at 5 weeks post-surgery (at the end of the 3-weeks drug treatment period) with a considerable decrease infiltration of tumoral cells and inflammation cells, as well as the absence of pseudopalisading necrosis (**Figure 2**). These results are consistent with previously reported.

Expression of VEGF

At the end of 3 weeks drug treatment the rats were sacrificed to evaluated CD31 marker and VEGF expression. Vascular density was determined by CD31 marker, we observed that Mif and Tz decrease the vascular density compared to without treatment group; however, this decrease was greater in Mif/Tz group, these results were corroborated with the quantification of VEGF (**Figure 3A**). VEGF expression is closely related to angiogenesis. Compared to the sham group, the untreated animals with implanted cancer cells displayed a significantly higher level of VEGF. Compared to the latter group, the level of VEGF declined (but not significantly) in animals receiving either Tz or Mif, and was significantly lower in the Mif/Tz group (**Figure 3B**).

Expression of P-gp

Western blot data and band intensity analysis revealed that the protein expression of P-gp (**Figure 4**) was downregulated at the

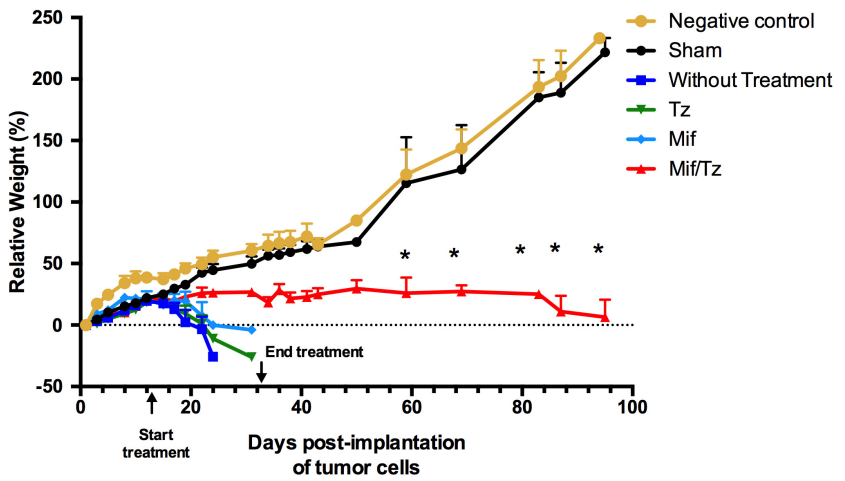

FIGURE 1 | Tumor growth in the orthotopic rat model of glioma was evaluated by comparing animals weight between groups: negative control (●) and sham surgery (●); and in four groups with implanted glioma cancer cells, one without drug treatment (■) and the other given temozolomide only (Tz) (●), mifepristone only (Mif) (♦), and mifepristone/temozolomide (Mif/Tz) (●). Each point of the graphic represents the mean ± SEM of six animals. *Significant difference ($p < 0.05$) between Mif/Tz and sham.

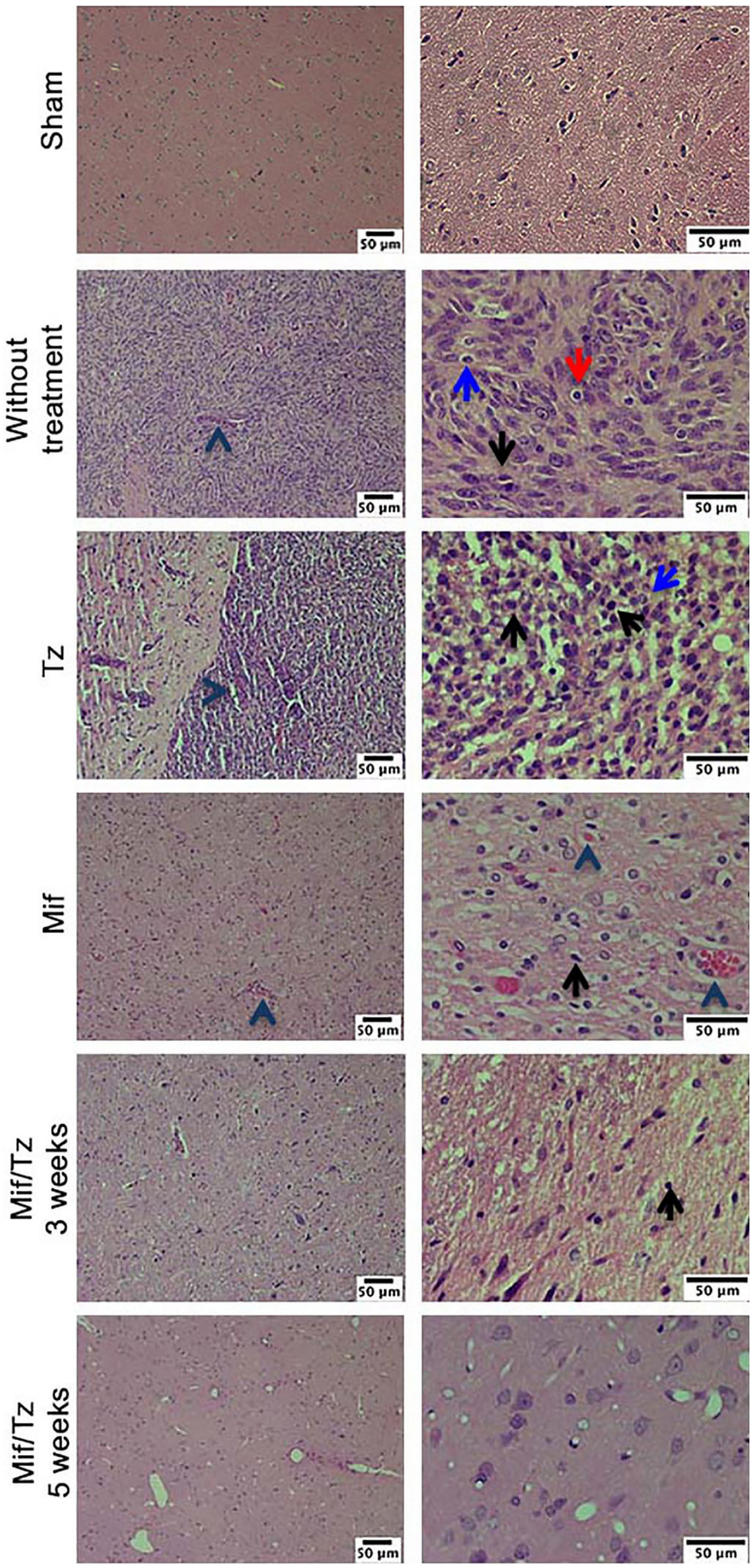

FIGURE 2 | Hematoxylin and eosin (H&E) staining analysis of glioma tissue. Hyperbasophilic cells (black arrow), hyperchromatics cells (red arrow), vessel proliferation (arrowhead), mitosis (blue arrow). The images are representative of three animals per treatment Scale bars = 50 µm.

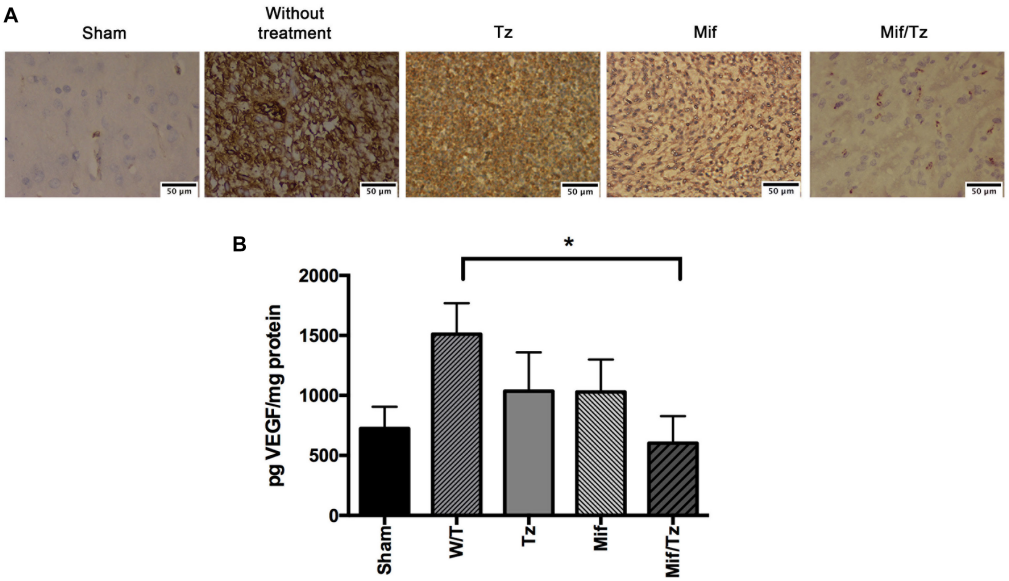

FIGURE 3 | (A) Immunohistochemical staining of CD31 marker. Vessel density was assessed by immunostaining for CD31 positive glioma cell nuclei in rats implanted with glioma. The images are representative of three animals per treatment. Scale bar 50 μm. **(B)** Expression of VEGF at the end of the 3-week drug treatment, showing a significantly lower level in the mifepristone/temozolomide (Mif/Tz)-treated group versus the untreated (W/T) group, both with implanted cancer cells. Data are expressed as the mean ± SD from eight independent experiments. *Significant difference ($p < 0.05$) between the Mif/Tz and W/T group.

end of the 3-week drug treatment (5 weeks post-surgery) in the Mif rats compared to the Tz and untreated groups. On the other hand, the Mif/Tz regimen caused an even greater reduction in this protein.

Accumulation of Temozolomide in Brain Tissue

The accumulation of temozolomide in brain tissue was determined by LC-MS analysis after treatment with Mif/Tz or Tz (**Figure 5**). Typical chromatograms obtained after the extraction of temozolomide in brain tissue from the groups of Tz and Mif/Tz are shown in **Figure 5A**. A significant two-fold greater intracerebral level of temozolomide was found in the brain tissue of the Mif/Tz versus Tz group (14820 ± 3852 vs 7136 ± 981 ng/g brain tissue); **Figure 5B**; $p < 0.05$.

Therapeutic Effect of Mifepristone/Temozolomide on Tumor Size

PET/CT scans were performed at 5, 7, 9, and 14 weeks post-implantation of tumor cells (the Mif/Tz treatments were given during week 2–5). In the images, the presence of red reflects the 18F-FLT uptake and thus the relative size of the tumor. The 18F-FLT uptake was higher at 5 weeks (3-week drug treatment). By 7 weeks post-surgery (2 weeks after the end of drug treatment), the 18F-FLT uptake had dropped drastically. At 9 weeks, however, 18F-FLT uptake appeared again, and can be observed at about the similar level at 14 weeks (**Figure 6A**). This suggests a tumor cell growth again at 9 weeks, indicating a possible tumor recurrence that remains stable at 14 weeks post-surgery. The 18F-FLT uptake was also measured as total lesion proliferation (TLP). At 7 weeks post-surgery a significant decrease of TLP was observed. Moreover, at 9 and 14 weeks post-surgery (4 and 9 weeks after the end of drug treatment), the TLP increased again (**Figure 6B**). The average survival time for rats was similar in the untreated, Tz or Mif groups, being 25–35 days. Contrarily, 70% of the Mif/Tz animals survived 60–70 days and approximately 30% survived over 100 days (**Figure 6C**).

Histological Examination During Tumor Recurrence

Within the pathological characteristics of glioblastoma are an increase of necrosis, mitosis, and pleomorphism as well as a vascularity proliferation. As shown in **Figure 7**, these characteristics decreased with the treatment of Mif/Tz (5 weeks), in the 7 weeks groups (2 weeks after the end of treatment) we observed some hyperchromatic cells and a decrease of hypercellularity; however, at 9 and 14 weeks pseudopalisading, necrosis, mitotic activity and vascular proliferation increased. A close correlation was observed with the molecular images of the same groups.

Effect of Mifepristone/Temozolomide on VEGF During Tumor Recurrence

The brain tissue was processed for immunohistochemical assays with CD31 marker. At 5-weeks, Mif/Tz group showed a decrease in vessel density compared to without treatment group; however, there is an increase in positive cells at 9 and 14 weeks post-surgery (4 and 9 weeks after the end of drug treatment), interestingly, the density of positive cells was less compared to the group without

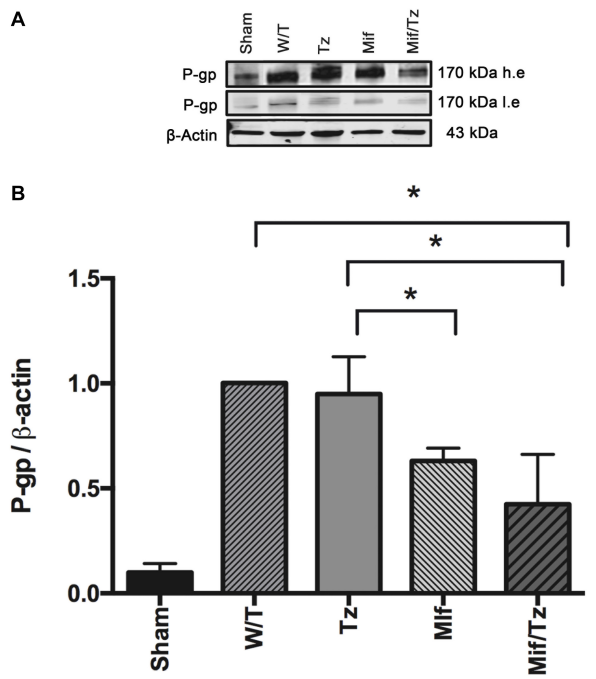

FIGURE 4 | The quantification of P-gp levels at the end of the 3-week drug treatment evidenced a significant downregulation in the rats given mifepristone (Mif) or mifepristone/temozolomide (Mif/Tz) compared to those receiving no drug treatment (W/T) or temozolomide (Tz). **(A)** Representative Western blot; h.e., high exposure; l.e., low exposure. **(B)** densitometric analysis of the P-gp protein. Data are expressed as the mean ± SD from three independent experiments. *Significant difference ($p < 0.05$).

treatment (**Figure 8A**). The VEGF levels at the end of the 3-week Mif/Tz treatment (at 5 weeks post-surgery) was significantly lower than that found in the untreated group and the same as that of the sham animals. However, this reduced level in the Mif/Tz group was reversed after drug treatment ended, during tumor recurrence at 9 and 14 weeks post-surgery (4 and 9 weeks after the end of drug treatment), this parameter increased in the Mif/Tz group, being similar to the value of the untreated group (**Figure 8B**).

Effect of Mifepristone/Temozolomide on P-gp Levels During Tumor Recurrence

Evaluation of the expression of P-gp by Western blot at the end of the 3-week drug treatment period (at 5 weeks post-surgery) showed a significantly lower level for Mif/Tz-treated versus untreated rats (**Figure 9**). This reduced level in the Mif/Tz group was reversed after drug treatment ended, gradually rising until reaching the level of the untreated group at 14 weeks.

Effect of Mifepristone/Temozolomide on the Level of MGMT During Tumor Recurrence

At 5 weeks post-surgery, the expression of MGMT was lower in healthy sham rats compared to the untreated animals with implanted cancer cells. This point in time corresponds to the end of the drug treatments, at which time the combination regimen of mifepristone/temozolomide produced a significant decrease in the level of MGMT, in agreement with a our previous report (5). This effect was reversed at weeks 9 and 14, corresponding to the time of tumor recurrence (**Figure 10**).

DISCUSSION

Although there have been advances in the treatments of some cancers, the molecules recently developed for glioblastoma therapy have shown little success in improving patient prognosis and survival. Glioblastoma is currently treated with surgery followed by chemotherapy with temozolomide and radiotherapy,

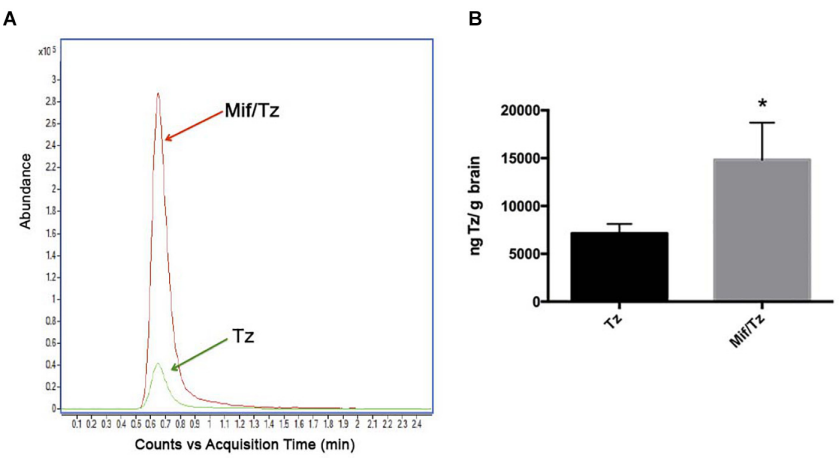

FIGURE 5 | (A) Based on typical chromatograms of temozolomide in brain tissue, there was a significantly higher concentration of temozolomide (Tz) in rats given a pre-treatment of 60 mg/kg of mifepristone (Mif) followed by 30 mg/kg of Tz (red line) than in animals receiving only 30 mg/kg of Tz (green line). **(B)** Bar graph illustration of the Tz uptake in rat brain tissue ($n = 6 \pm$ SD). *Significant difference ($p < 0.05$).

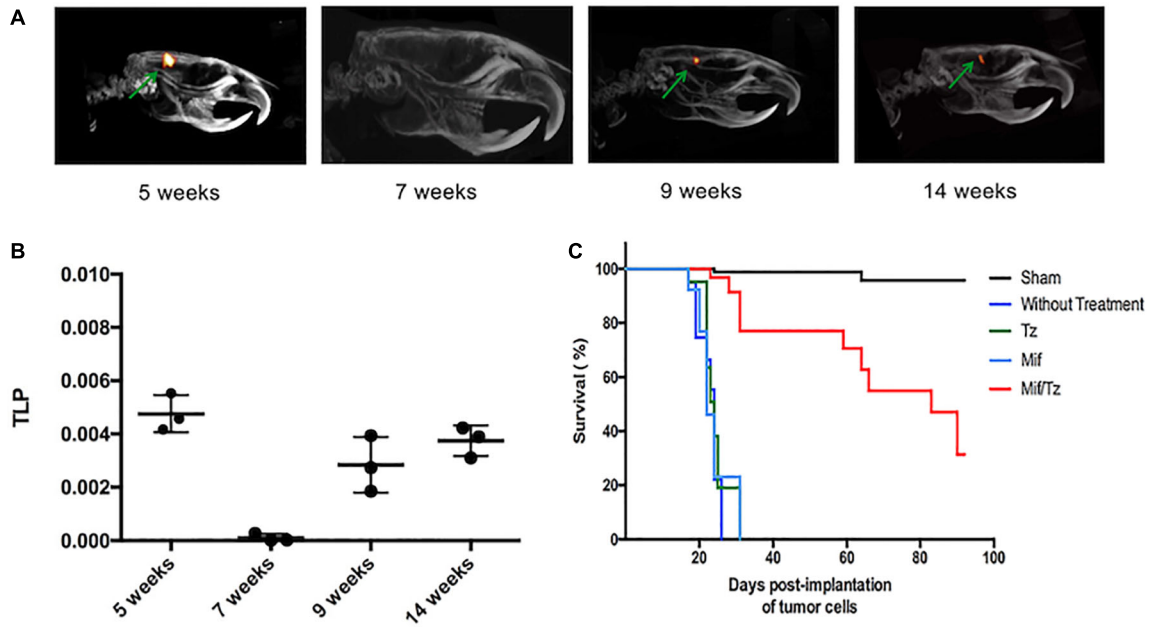

FIGURE 6 | Proliferative activity in the orthotopic model of glioma evaluated by PET/CT images showing tumor uptake of 18F-FLT. **(A)** The images reveal the relative tumor size at 5, 7, 9, and 14 weeks post-surgery. Drug treatments were given from weeks 2–5. **(B)** The activity proliferative of tumors measured as total proliferation (TLP). **(C)** Survival analysis for 100 days after tumor cells implantation.

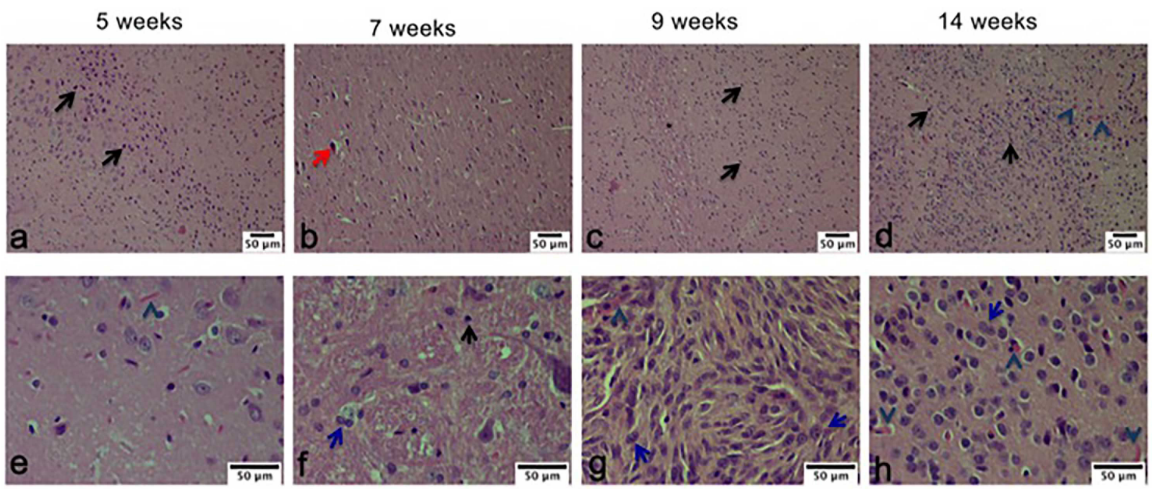

FIGURE 7 | Hematoxylin and eosin (H&E) staining analysis of glioma tissue. The images are representative of three animals per treatment. Hyperbasophilic cells (black arrow), Hyperchromatics cells (red arrow), vessel proliferation (arrowhead), mitosis (blue arrow). Scale bars = 50 µm.

resulting in a post-diagnostic median survival time of only 1-2 years. Among the main problems in glioblastoma treatment are rapid proliferation, the limited capacity of drugs to cross the BBB, and other mechanisms related to the resistance of cancer cells to chemotherapy. Thus, new strategies are necessary (1).

It has reported that the antitumor activity of temozolomide is schedule-dependent, with multiple administrations being more effective than a single treatment. In clinical use, the recommended dose of temozolomide is 75 mg/m^2, daily until with a maximum of 49 doses and in the dose of maintenance of 200 mg/m^2 given for five consecutive days every 28-day cycle (5/28 days) (9, 10).

The scheme of drug treatments used presently is similar to that used in patients. In our study, temozolomide was administered for only three weeks because it is the average survival time of the rats with the individual treatments.

The dose of temozolomide was calculated based on several reports in the literature and in our previous work. The doses

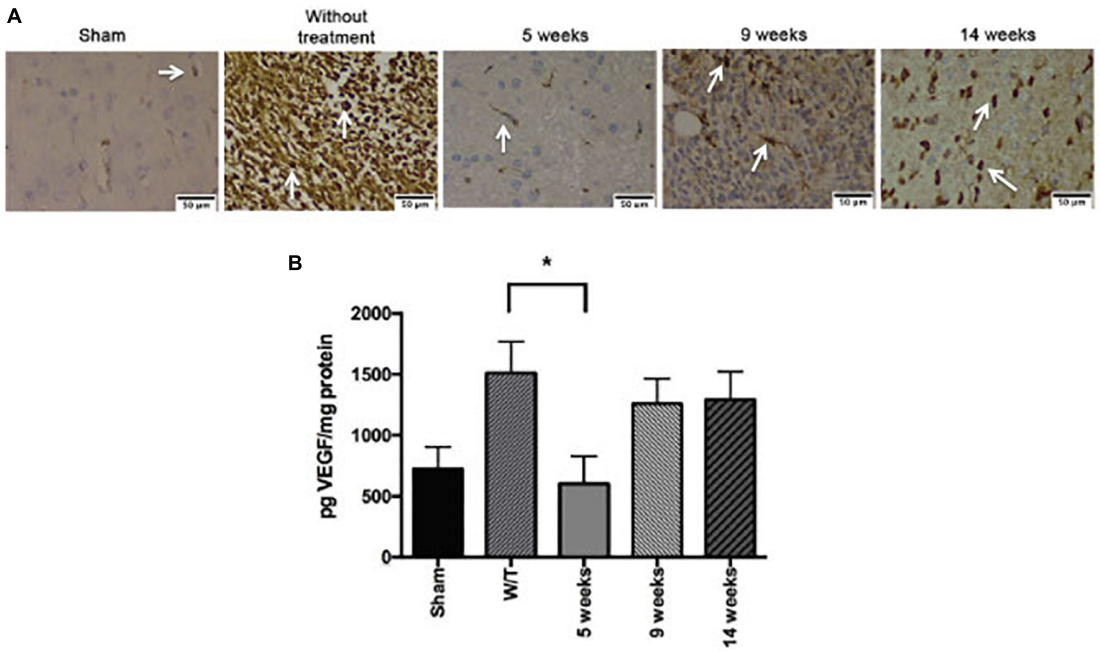

FIGURE 8 | Effect of mifepristone/temozolomide on VEGF during tumor recurrence. **(A)** Immunohistochemical stainings with CD31 marker. Vessel density was assessed by immunostaining for CD31 positive glioma cell nuclei in rats implanted with glioma. The images are representative of three animals per treatment. Scale bar 50 μm. **(B)** Expression of VEGF in the sham-operated rats, implant-operated animals with no drug treatment (W/T), and at 5, 9 and 14 weeks post-surgery (the mifepristone/temozolomide (Mif/Tz) treatment were given only during weeks 2–5). Compared to the W/T rats, the Mif/Tz animals showed a lower level of VEGF at 5 weeks and a similar level at the time of tumour recurrence, at 9 and 14 weeks post-surgery. Data are expressed as the mean ± SD from five independent experiments. * Significant difference ($p < 0.05$) between the Mif/Tz and W/T group.

of temozolomide used in the present work is compared to metronomic doses of 2 mg/kg every day for 16 days reported by Kim et al. (25), the authors observed a significant effect on the tumor volume and microvessel density. Moreover there were no signs of toxicity with drug administration, such as body weight loss. Other study also showed similar results using temozolomide at dose of 5 mg/kg/day (26), showing a significant decrease on tumor growth. These results correlate with our previous findings where we used temozolomide 5 mg/kg/day × 21 days, there was a significant decrease on tumor growth measured as the proliferative activity in tumors (5).

In the case of mifepristone, we used a total dose of 150 mg/kg (10mg/kg × 5 days/3 weeks) in rats according with our previous report (5), On the other hand, several reports support that using low dose of the drugs it is more probably to find a synergistic effect when the drugs are combined. This is important in cancer because many studies looking for a synergistic effect more than an additive effect due to the side effects of chemotherapy.

The antihormonal agent mifepristone has been investigated in regard to different types of cancer, both hormone- and non-hormone-dependent (27). Mifepristone acts as an antagonist of progestins, glucocorticoids and androgens through the respective receptors. It reportedly inhibits cell growth in non-hormone-dependent cancer cells, such as MDA-MB-321 (breast cancer) (28) and LNCaP (prostate cancer) (29), which are negative for progesterone, estrogen and androgen receptors.

Previous studies in our laboratory demonstrated the chemo-sensitizing effect of mifepristone in combination with temozolomide in a xenograft and an orthotopic glioma model (5, 30). The current study evaluated two possible molecular mechanisms in this chemo-sensitizing effect: the inhibition of VEGF and CD31 marker to reduce angiogenesis and of P-gp to facilitate the capacity of temozolomide to cross the BBB (**Figure 11**).

A significant difference in weight was observed between the animals administered mifepristone/temozolomide and those given temozolomide only, mifepristone only, or without treatment animals. This result could be due to the decrease in tumor growth as was observed in the previous reports (5). Typical features of glioblastoma were seen in the H&E images shown; in the group without treatment, there was an increase in hypercellularity and vascular proliferation, which was diminished with the Mif/Tz treatment. A mechanism that has been little explored in cancer-induced weight loss is the modification of metabolic changes involved in cachexia. Cachexia is a complex metabolic disorder that impacts about 80% of patients with advanced cancers (31). Griffith et al. (32) reported body weight loss in glioma patients (32), studies on cachexia symptoms induced by glioblastoma have rarely been reported; Recently Cui et al. (33) demonstrated cachexia manifestations in an orthotopic glioma murine model (33); however, is necessary a metabolic pathway analysis during glioma cachexia. It has been reported that mifepristone impact

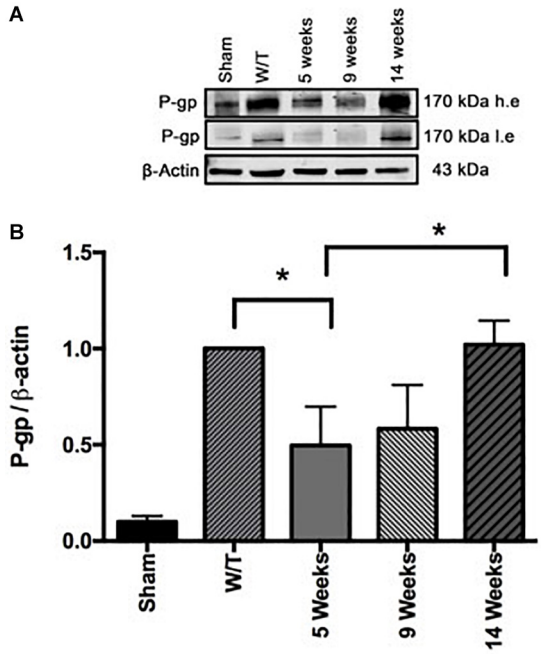

FIGURE 9 | (A) Comparison of the levels of P-gp (determined by Western Blot) in the sham-operated rats and two groups of implant-operated animals: one with no drug treatment (W/T) and the other given mifepristone/temozolomide (Mif/Tz) at 5 weeks post-surgery (corresponding to the end of the 3-week drug treatment), and 9, 14 weeks (corresponding to 4 and 9 weeks after the end of drug treatment), h.e., high exposure; l.e., low exposure. **(B)** The densitometer analysis (n = 3). Data represent the mean ± SD of three independent experiments. *Significant difference ($p < 0.05$) between the Mif/Tz rats at 5 and 14 weeks.

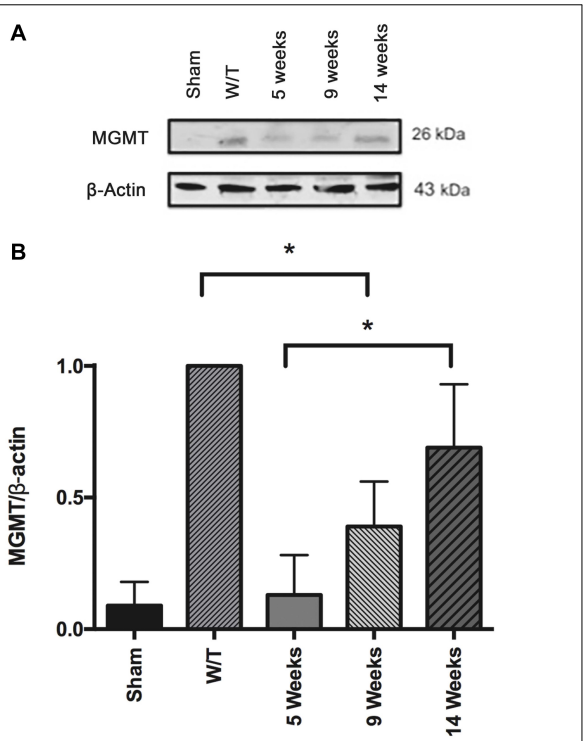

FIGURE 10 | (A) Comparison of the level of the DNA repair enzyme, MGMT, determined by Western blot in the sham-operated rats and two groups of implant-operated animals: one with no drug treatment (W/T) and the other given mifepristone/temozolomide (Mif/Tz) at 5 weeks post-surgery (corresponding to the end of the 3-week drug treatment) and 9 and 14 weeks after surgery. A lower level of MGMT was found in the Mif/Tz versus W/T group at 5 weeks post-surgery, an effect that was gradually reversed. **(B)** Densitometer analysis (n = 3). Data is expressed as the mean ± SD of three independent experiment. * Significant difference ($p < 0.05$).

in cancer cachexia by blocking the interaction of cortisol and induction of zinc-alpha2-glycoprotein (ZAG) expression in adipose tissue (34). On the other hand, cachexia is characterized by systemic inflammation and it has been reported that mifepristone reduced the expression of nuclear transcription factors, including NF-kB (35), a central mediator of pro-inflammatory gene induction. With these antecedents, it is interesting to investigate, in the future, the possible modulation of cachexia by mifepristone/temozolomide treatment.

The tumor microenvironment is known to play a key role in resistance to treatment. In particular, a hypoxic microenvironment is closely related to chemo- and radio-resistance by modulating different mechanisms including angiogenesis (36). Glioma tumors are known to elevate levels of VEGF and its corresponding receptor, the activation of which is related to angiogenesis. Without angiogenesis, tumor growth would be severely limited.

Due to the importance of VEGF in the physiopathology of glioblastoma, one of the strategies to improve patient survival is to diminish its expression. Unfortunately, this strategy has not yet been fruitful. In the current effort, we observed that there was an additive effect by temozolamide and mifepristone in the inhibition of VEGF levels, the Mif/Tz rats exhibited a lower expression of VEGF compared to the other animals with implanted cancer cells, including the untreated, Tz and Mif groups. This results correlated with immunohistochemical studies with CD31 marker, vessel density was decreased in Tz and Mif groups; however, a lower vessel density was observed in Mif/Tz group. Hence, the combined treatment may contribute to an effective strategy for overcoming the resistance of glioblastoma tumors. It is known that the endothelial cells in the vascular bed of tumor are more susceptible to chemotherapeutic agents than resting endothelium, because they have significantly higher proliferation rates than the normal endothelium in the rest of the body. In addition metronomic chemotherapy, which is the continuous administration of the chemotherapeutic agent at a low dose, it exposes endothelial cells in tumor beds to drugs, inducing angiogenesis and apoptosis in endothelial cells before tumor cells (25). Therefore, it is possible that an additive apoptotic effect of Mif/Tz on vascular endothelial cells contribute to antitumor efficacy of the combined drugs.

On the other hand, recently it has been described that temozolomide is able to decrease the expression of VEGF levels at therapeutic or higher doses on U87 glioblastoma cells (37). The authors demonstrated that temozolomide added at doses below its therapeutic dose is not able to induce apoptosis in cells. But it is capable of inducing apoptosis when was introduced in therapeutic dose or above. In our work, the consecutive

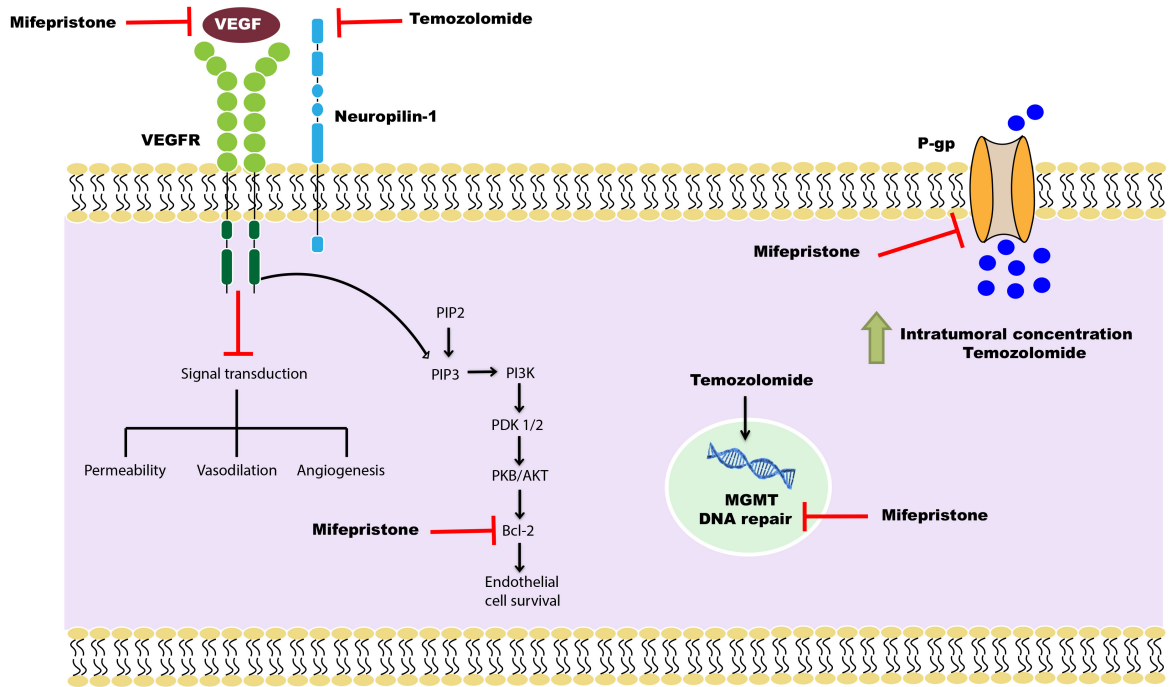

FIGURE 11 | Schematic portrayal of the possible mechanisms of the combination mifepristone/temozolomide treatment that improved the effect found with temozolomide alone. The mechanisms studied were: (1) the inhibition of angiogenesis, measured as reduced levels of VEGF; (2) the attenuation of DNA repair, evaluated as a decrease in MGMT; and (3) the increased capacity of temozolomide to pass through the BBB, assessed as a lower P-gp level and a higher concentration of temozolomide in brain cells. As described in a previous report by our group (5), mifepristone diminishes the level of anti-apoptotic protein Bcl-2 and impedes endothelial cell survival in tumors. This may be the mechanism by which mifepristone/temozolomide herein lowered the level of VEGF. The treatment with mifepristone or temozolomide alone decreased the levels of VEGF to a lesser extent, perhaps by the blockade of autocrine VEGF signaling through specific down-regulation of NRP-1. Additionally, a decline in the expression P-gp was found when administering mifepristone/temozolomide. Thus, this combination treatment may allow for an enhanced intratumoral concentration of temozolomide and contribute to greater tumor cell death. The latter was evidenced by lower tumor proliferation during the drug treatment period. As can be appreciated, mifepristone appears to sensitize glioblastoma cells to the effects of temozolomide.

doses of Mif/Tz administered to the animals could lead to a cumulative dose reaching therapeutic doses that may contribute to an additive effect in the reduction of VEGF levels.

Hernandez-Hernandez et al. described a progesterone-induced increase in the expression of VEGF in the astrocytoma U373 cell line, and a mifepristone-induced reversal of the increase by recruitment of the steroid receptor coactivator (SRC-1) (38). Another possible mechanism leading to a lower level of VEGF is through the regulation of Bcl-2, a protein family composed of cell death regulators. It has been implicated in the differentiation of several cell types, including neuronal, epithelial and hematopoietic cells, as well as in the survival of endothelial cells (39). Karl et al. described pro-angiogenic activity by Bcl-2 based on its ability to activate the NF-κB signaling pathway and elicit expression of the pro-angiogenic CXCL8 and CXCL1 chemokines in endothelial cells (40). According to a previous report by our group, mifepristone reduces Bcl-2 expression in glioma cells (5). Therefore, the diminished VEGF level observed herein could possibly be related to a decrease in Bcl-2 induced by mifepristone.

The BBB, on the other hand, has been the greatest problem for many promising drugs developed to treat glioblastoma. The brain microvascular endothelium is peculiar, characterized by a lack of fenestrations and adherens junctions and by the presence of drug efflux transporters, such as P-glycoprotein (P-gp, Abcb1), the multidrug resistance proteins (MRPs, Abcc1) and breast cancer resistance protein (BCRP, Abcg2) (41). Several researches have focused on the role of inhibition of drug efflux transporters to improve chemotherapy response. P-glycoprotein is the best-characterized molecule of the class of efflux pump transporters, forming part of the BBB by removing drugs from the brain. This protein is expressed by endothelial cells in both healthy brain tissue and gliomas, and a key role has been attribute to it in the chemoresistance of several types of tumors (e.g., gliomas) (42). Consequently, it probably contributes to a low concentration of temozolomide in glioma tumor cells.

The present study found a significant drop in the level of P-gp in the Mif/Tz group. A decrease the levels of P-gp in patients should be able to enhance the intracellular distribution of temozolomide in brain tissue and trigger greater tumor cell death. Various transcription factors (in addition to transcriptional/translational regulation) are involved in regulation of efflux pump transporters (43). This protein is known to be regulated by a nuclear receptor, the pregnane

X receptor (PXR) (44–46), which mediates the activation of several genes by xenobiotics, including several ABC transporters. Although the *PXR* promoter has not yet been characterized, dexamethasone is reported to boost *PXR* mRNA levels in primary cultures of human hepatocytes and rat hepatoma H4IIE cells, an effect blocked by mifepristone, suggesting that the GR pathway is involved in the regulation of these transporters (47, 48).

On an other hand it has been reported that glioblastoma is characterized by aberrant activation of inflammatory responses; von Wedel-Parlow et al., reported that the pro-inflammatory cytokines interleukin-1 (IL-1b) and tumor necrosis factor-a (TNF-alpha) affect the expression of cerebral ABC-transporters in primary endothelial cells, the anti-inflammatory glucocorticoid hydrocortisone leads to a induction of Abcg2 (BCRP) and Abcc1 (MRP) mRNA in microvascular endothelial cells whereas Abcb1 (P-gp)gene expression is down-regulated (49). It has been reported that mifepristone decreased the levels of of TNF-alpha in rats exposed to Paraquat (50), and in endometrial epithelial and stromal cells reduced the secretion of IL-6 and TNF-alpha (51). However, more research is necessary to better understand the regulation and the role of mifepristone in efflux pump transporters.

Other strategy to improve treatment response is blocking the drug efflux transporters. Gooijer et al., reported an accumulation about 1.5 fold more of temozolomide in the brain by P-gp and BCRP inhibitors (52). These drug efflux transporters might be possible target of mifepristone to improve the efficacy of temozolomide against glioblastoma.

In the current contribution, the participation of mifepristone in the inhibition of drug efflux transporters was explored indirectly by evaluating the intracerebral concentration of temozolomide, representing a direct and indirect approach, respectively. The Mif/Tz rats exhibited a significantly lower level of P-gp and an increased intracerebral concentration of temozolomide compared to the Tz group. These results are consistent with the findings published by various authors. Mifepristone inhibits the activity of P-gp in a gastric cell line SGC7901/VCR (37) and in KG1a leukemia cells (23), enhances doxorubicin cellular accumulation in resistant human K562 leukemia cells (53), and increases the concentration of cisplatin in the tumors of mice given a combined cisplatin/mifepristone treatment (54). Hence, the blocking of drug efflux transporters by mifepristone could possibly increase the intracellular bioavailability of temozolomide in brain and tumor cells of patients, which should improve the therapeutic response.

Other drug efflux transporters that plays an important role in treatment resistance is MRP and blocking it could be an important strategy, it has been reported that mifepristone exhibited selective MRP1 inhibition (55). Hence, the blocking of drug efflux transporters by mifepristone could possibly increase the concentration of temozolomide in brain and consequently tumor cells can increase the disposition to drug.

In the second part of the present investigation, tumor growth after of the mifepristone/temozolomide treatment was monitored with a microPET/CT scanner measuring 18F-FLT uptake (**Figure 6**). There was a remarkable decrease at 7 week post-implantation with molecular imaging showing no proliferative activity. Afterward, new proliferation was observed at 9 week post-surgery, indicating tumor relapse. Nevertheless, the animals maintained a constant body weight and the proliferative activity did not rise by the next measurement at 14 weeks. The H&E images shown in the group at 7 weeks, there was a decrease in hypercellularity and vascular proliferation. However, after the end of the drug treatment, an infiltration of neoplastic cells with a hyperchromatic nucleus was observed again, in addition to an increase in the mitotic index and pseudopalisading. Despite being observed again these typical features of glioblastoma, which are associated with a poor prognosis, the animals survided longer. These results were corroborated with molecular images where it was observed tumor recurrence at week 9. Moreover, 70% of rats given mifepristone/temozolomide survived 60–70 days and approximately 30% survived over 100 days. In glioblastoma patients, a relapsed tumor inevitably causes 100% mortality.

Another molecular mechanism explored presently was the effect of the Mif/Tz treatment on MGMT, which is related to DNA repair in tumor cells. Glioblastoma stem cells are reported to express high levels of MGMT (56) and P-gp, in both cases generating more resistance to temozolomide, and therefore a greater probability of tumor relapse (57). Several studies have suggested that stem cells may be responsible for resistance and recurrence in glioblastoma. In such a case, a challenge in the treatment of glioblastoma would be the removal not only of the tumor cells, but also the glioblastoma stem cells.

O6-methylguanine-DNA-methyltransferase was found to significantly decrease by the end of the 3-week Mif/Tz treatment, thus confirming a previous finding by our group. Indeed, MGMT followed the same pattern as VEGF and P-gp. All three parameters were found to decrease during the Mif/Tz treatment, and then increase afterward. Within 14 weeks, all three of these molecules reached levels similar to the control group. In our study drug treatment were given only by 3 weeks; we did not observed adverse effects associated with the administration of mifepristone. The decrease of weight gain in the animals was due to implantation of tumor cells. In according to the literature, several clinical studies of mifepristone in patients with breast cancer (58), meningioma (59), and non-small cell lung cancer (60) have demonstrated that mifepristone has tolerable side effect, including nausea, lethargy, anorexia, fatigue, and hot flashes; even when mifepristone has been taken daily for long periods of time, it has mild adverse effects; therefore, the long-term administration of mifepristone may be feasible and well tolerated; we proposed in the near future to test this possibility and to evaluate whether mifepristone offers greater benefits during tumor recurrence. According to the current results, mifepristone could possibly contribute to the modulation of tumor relapse in glioblastoma by decreasing the levels of VEGF, MGMT, and P-gp. Further research is needed to explore other mechanisms of drug resistance of glioblastoma tumors.

CONCLUSION

Mifepristone herein improved the effect of temozolomide. The mifepristone/temozolomide combination produced a

sharply lower expression of VEGF, CD31, P-gp, and MGMT compared to the other groups with implanted cancer cells, including the untreated animals and those given mifepristone or temozolomide alone. Moreover, the combination treatment increased the intracerebral concentration of temozolomide and diminished tumor proliferation. The present results strongly suggest that mifepristone could serve as part of a strategy to overcome the resistance of glioblastoma tumors to temozolomide. Future research is required to determine whether the mifepristone/temozolomide regimen can regulate glioma stem cells and inhibit the mechanisms related to tumor relapse.

DATA AVAILABILITY STATEMENT

The datasets generated for this study are available on request to the corresponding author.

ETHICS STATEMENT

The animal study was reviewed and approved by Ethics Committee of the "Instituto Nacional de Cancerología" (INCan, Mexico City, Mexico) (Ref No. 010-17-IBICB601-10).

AUTHOR CONTRIBUTIONS

ML-M participated in the experimental procedures for tumor cell implantation, helped with data processing, and performed the analysis of the results. SL-Z and MR-G designed the histological experiments. IV-L contributed to the LC/MS experiments for quantification of temozolomide in brain tissue. LM carried out the evaluation of the tumor growth by molecular imaging. PG-L planned and supervised the entire study. All authors read and approved the final version of the manuscript.

FUNDING

This work was partially financed by CONACYT (Mexico) through grant CB-258823.

ACKNOWLEDGMENTS

We thank MD Adriana Méndez Bernal for the description of the histological assays and Bruce Allan Larsen for proofreading the manuscript.

REFERENCES

1. Johnson DR, O'Neill BP. Glioblastoma survival in the United States before and during the temozolomide era. *J Neurooncol*. (2012) 107:359–64. doi: 10.1007/s11060-011-0749-4
2. Thakkar JP, Dolecek TA, Horbinski C, Ostrom QT, Lightner DD, Barnholtz-Sloan JS, et al. Epidemiologic and molecular prognostic review of glioblastoma. *Cancer Epidemiol Biomarkers Prev*. (2014) 23:1985–96. doi: 10.1158/1055-9965.EPI-14-0275
3. Witthayanuwat S, Pesee M, Supaadirek C, Supakalin N, Thamronganantasakul K, Krusun S. Survival analysis of glioblastoma multiforme. *Asian Pac J Cancer Prev*. (2018) 19:2613–7. doi: 10.22034/APJCP.2018.19.9.2613
4. Wang H, Xu T, Jiang Y, Xu H, Yan Y, Fu D, et al. The challenges and the promise of molecular targeted therapy in malignant gliomas. *Neoplasia*. (2015) 17:239–55. doi: 10.1016/j.neo.2015.02.002
5. Llaguno-Munive M, Romero-Pina M, Serrano-Bello J, Medina LA, Uribe-Uribe N, Salazar AM, et al. Mifepristone overcomes tumor resistance to temozolomide associated with DNA damage repair and apoptosis in an orthotopic model of glioblastoma. *Cancers*. (2019) 11:16. doi: 10.3390/cancers11010016
6. Nishida N, Yano H, Nishida T, Kamura T, Kojiro M. Angiogenesis in cancer. *Vasc Health Risk Manag*. (2006) 2:213–9. doi: 10.2147/vhrm.2006.2.3.213
7. Machein MR, Plate KH. VEGF in brain tumors. *J Neurooncol*. (2000) 50:109–20.
8. Kaur B, Khwaja FW, Severson EA, Matheny SL, Brat DJ, Van Meir EG. Hypoxia and the hypoxia-inducible-factor pathway in glioma growth and angiogenesis. *Neuro Oncol*. (2005) 7:134–53. doi: 10.1215/S1152851704001115
9. Gilbert MR, Dignam JJ, Armstrong TS, Wefel JS, Blumenthal DT, Vogelbaum MA, et al. A randomized trial of bevacizumab for newly diagnosed glioblastoma. *N Engl J Med*. (2014) 370:699–708. doi: 10.1056/NEJMoa1308573
10. Chinot OL, Wick W, Mason W, Henriksson R, Saran F, Nishikawa R, et al. Bevacizumab plus radiotherapy-temozolomide for newly diagnosed glioblastoma. *N Engl J Med*. (2014) 370:709–22. doi: 10.1056/NEJMoa1308345
11. Louis DN. Molecular pathology of malignant gliomas. *Annu Rev Pathol*. (2006) 1:97–117. doi: 10.1146/annurev.pathol.1.110304.100043
12. Schaich M, Kestel L, Pfirrmann M, Robel K, Illmer T, Kramer M, et al. A MDR1 (ABCB1) gene single nucleotide polymorphism predicts outcome of temozolomide treatment in glioblastoma patients. *Ann Oncol*. (2009) 20:175–81. doi: 10.1093/annonc/mdn548
13. Agarwal S, Manchanda P, Vogelbaum MA, Ohlfest JR, Elmquist WF. Function of the blood-brain barrier and restriction of drug delivery to invasive glioma cells: findings in an orthotopic rat xenograft model of glioma. *Drug Metab Dispos*. (2013) 41:33–9. doi: 10.1124/dmd.112.048322
14. Da Ros M, De Gregorio V, Iorio AL, Giunti L, Guidi M, de Martino M, et al. Glioblastoma chemoresistance: the double play by microenvironment and blood-brain barrier. *Int J Mol Sci*. (2018) 19:2879. doi: 10.3390/ijms19102879
15. Gaddy VT, Barrett JT, Delk JN, Kallab AM, Porter AG, Schoenlein PV. Mifepristone induces growth arrest, caspase activation, and apoptosis of estrogen receptor-expressing, antiestrogen-resistant breast cancer cells. *Clin Cancer Res*. (2004) 10:5215–25. doi: 10.1158/1078-0432.CCR-03-0637
16. Liu R, Shi P, Nie Z, Liang H, Zhou Z, Chen W, et al. Mifepristone suppresses basal triple-negative breast cancer stem cells by down-regulating KLF5 expression. *Theranostics*. (2016) 6:533–44. doi: 10.7150/thno.14315
17. Segovia-Mendoza M, Jurado R, Mir R, Medina LA, Prado-Garcia H, Garcia-Lopez P. Antihormonal agents as a strategy to improve the effect of chemo-radiation in cervical cancer: in vitro and in vivo study. *BMC Cancer*. (2015) 15:21. doi: 10.1186/s12885-015-1016-4
18. Moe BT, Vereide AB, Orbo A, Jaeger R, Sager G. Levonorgestrel, medroxyprogesterone and progesterone cause a concentration-dependent reduction in endometrial cancer (Ishikawa) cell density, and high concentrations of progesterone and mifepristone act in synergy. *Anticancer Res*. (2009) 29:1047–52.
19. Goyeneche AA, Caron RW, Telleria CM. Mifepristone inhibits ovarian cancer cell growth in vitro and in vivo. *Clin Cancer Res*. (2007) 13:3370–9. doi: 10.1158/1078-0432.CCR-07-0164
20. Ritch SJ, Brandhagen BN, Goyeneche AA, Telleria CM. Advanced assessment of migration and invasion of cancer cells in response to mifepristone therapy using double fluorescence cytochemical labeling. *BMC Cancer*. (2019) 19:376. doi: 10.1186/s12885-019-5587-3
21. Touat M, Lombardi G, Farina P, Kalamarides M, Sanson M. Successful treatment of multiple intracranial meningiomas with the antiprogesterone

receptor agent mifepristone (RU486). *Acta Neurochir*. (2014) 156:1831–5. doi: 10.1007/s00701-014-2188-4
22. Check JH, Wilson C, Cohen R, Sarumi M. Evidence that mifepristone, a progesterone receptor antagonist, can cross the blood brain barrier and provide palliative benefits for glioblastoma multiforme grade IV. *Anticancer Res*. (2014) 34:2385–8.
23. Fardel O, Courtois A, Drenou B, Lamy T, Lecureur V, le Prise PY, et al. Inhibition of P-glycoprotein activity in human leukemic cells by mifepristone. *Anticancer Drugs*. (1996) 7:671–7. doi: 10.1097/00001813-199608000-00008
24. Li DQ, Wang ZB, Bai J, Zhao J, Wang Y, Hu K, et al. Reversal of multidrug resistance in drug-resistant human gastric cancer cell line SGC7901/VCR by antiprogestin drug mifepristone. *World J Gastroenterol*. (2004) 10:1722–5. doi: 10.3748/wjg.v10.i12.1722
25. Kim JT, Kim JS, Ko KW, Kong DS, Kang CM, Kim MH, et al. Metronomic treatment of temozolomide inhibits tumor cell growth through reduction of angiogenesis and augmentation of apoptosis in orthotopic models of gliomas. *Oncol Rep*. (2006) 16:33–9.
26. Sun C, Yu Y, Wang L, Wu B, Xia L, Feng F, et al. Additive antiangiogenesis effect of ginsenoside Rg3 with low-dose metronomic temozolomide on rat glioma cells both in vivo and in vitro. *J Exp Clin Cancer Res*. (2016) 35:32. doi: 10.1186/s13046-015-0274-y
27. Tieszen CR, Goyeneche AA, Brandhagen BN, Ortbahn CT, Telleria CM. Antiprogestin mifepristone inhibits the growth of cancer cells of reproductive and non-reproductive origin regardless of progesterone receptor expression. *BMC Cancer*. (2011) 11:207. doi: 10.1186/1471-2407-11-207
28. Liang Y, Hou M, Kallab AM, Barrett JT, El Etreby F, Schoenlein PV. Induction of antiproliferation and apoptosis in estrogen receptor negative MDA-231 human breast cancer cells by mifepristone and 4-hydroxytamoxifen combination therapy: a role for TGFbeta1. *Int J Oncol*. (2003) 23:369–80.
29. El Etreby MF, Liang Y, Lewis RW. Induction of apoptosis by mifepristone and tamoxifen in human LNCaP prostate cancer cells in culture. *Prostate*. (2000) 43:31–42. doi: 10.1002/(sici)1097-0045(20000401)43:1<31::aid-pros5>3.0.co;2-#
30. Llaguno-Munive M, Medina LA, Jurado R, Romero-Pina M, Garcia-Lopez P. Mifepristone improves chemo-radiation response in glioblastoma xenografts. *Cancer Cell Int*. (2013) 13:29. doi: 10.1186/1475-2867-13-29
31. Pin F, Barreto R, Couch ME, Bonetto A, O'Connell TM. Cachexia induced by cancer and chemotherapy yield distinct perturbations to energy metabolism. *J Cachexia Sarcopenia Muscle*. (2019) 10:140–54. doi: 10.1002/jcsm.12360
32. Griffith JL, Hochberg FH. Anorexia and weight loss in glioma patients. *Psychosomatics*. (1988) 29:335–7. doi: 10.1016/S0033-3182(88)72373-7
33. Cui P, Shao W, Huang C, Wu CJ, Jiang B, Lin D. Metabolic derangements of skeletal muscle from a murine model of glioma cachexia. *Skelet Muscle*. (2019) 9:3. doi: 10.1186/s13395-018-0188-4
34. Russell ST, Tisdale MJ. The role of glucocorticoids in the induction of zinc-alpha2-glycoprotein expression in adipose tissue in cancer cachexia. *Br J Cancer*. (2005) 92:876–81. doi: 10.1038/sj.bjc.6602404
35. Boopalan T, Arumugam A, Parada J, Saltzstein E, Lakshmanaswamy R. Receptor activator for nuclear factor-kappaB ligand signaling promotes progesterone-mediated estrogen-induced mammary carcinogenesis. *Cancer Sci*. (2015) 106:25–33. doi: 10.1111/cas.12571
36. Tate MC, Aghi MK. Biology of angiogenesis and invasion in glioma. *Neurotherapeutics*. (2009) 6:447–57. doi: 10.1016/j.nurt.2009.04.001
37. Mirabdaly S, Elieh Ali Komi D, Shakiba Y, Moini A, Kiani A. Effects of temozolomide on U87MG glioblastoma cell expression of CXCR4, MMP2, MMP9, VEGF, anti-proliferatory cytotoxic and apoptotic properties. *Mol Biol Rep*. (2020) 47:1187–97. doi: 10.1007/s11033-019-05219-2
38. Hernandez-Hernandez OT, Gonzalez-Garcia TK, Camacho-Arroyo I. Progesterone receptor and SRC-1 participate in the regulation of VEGF, EGFR and Cyclin D1 expression in human astrocytoma cell lines. *J Steroid Biochem Mol Biol*. (2012) 132:127–34. doi: 10.1016/j.jsbmb.2012.04.005
39. Mabeta P. Oncosuppressors and oncogenes: role in haemangioma genesis and potential for therapeutic targeting. *Int J Mol Sci*. (2018) 19:1192. doi: 10.3390/ijms19041192
40. Karl E, Warner K, Zeitlin B, Kaneko T, Wurtzel L, Jin T, et al. Bcl-2 acts in a proangiogenic signaling pathway through nuclear factor-kappaB and CXC chemokines. *Cancer Res*. (2005) 65:5063–9. doi: 10.1158/0008-5472.CAN-05-0140
41. Ueno M, Nakagawa T, Wu B, Onodera M, Huang CL, Kusaka T, et al. Transporters in the brain endothelial barrier. *Curr Med Chem*. (2010) 17:1125–38. doi: 10.2174/092986710790827816
42. Toth K, Vaughan MM, Peress NS, Slocum HK, Rustum YM. MDR1 P-glycoprotein is expressed by endothelial cells of newly formed capillaries in human gliomas but is not expressed in the neovasculature of other primary tumors. *Am J Pathol*. (1996) 149:853–8.
43. Scotto KW. Transcriptional regulation of ABC drug transporters. *Oncogene*. (2003) 22:7496–511. doi: 10.1038/sj.onc.1206950
44. Whyte-Allman SK, Hoque MT, Jenabian MA, Routy JP, Bendayan R. Xenobiotic nuclear receptors pregnane X receptor and constitutive androstane receptor regulate antiretroviral drug efflux transporters at the blood-testis barrier. *J Pharmacol Exp Ther*. (2017) 363:324–35. doi: 10.1124/jpet.117.243584
45. Bauer B, Hartz AM, Fricker G, Miller DS. Pregnane X receptor up-regulation of P-glycoprotein expression and transport function at the blood-brain barrier. *Mol Pharmacol*. (2004) 66:413–9. doi: 10.1124/mol.66.3
46. Narang VS, Fraga C, Kumar N, Shen J, Throm S, Stewart CF, et al. Dexamethasone increases expression and activity of multidrug resistance transporters at the rat blood-brain barrier. *Am J Physiol Cell Physiol*. (2008) 295:C440–50. doi: 10.1152/ajpcell.00491.2007
47. Kliewer SA, Goodwin B, Willson TM. The nuclear pregnane X receptor: a key regulator of xenobiotic metabolism. *Endocr Rev*. (2002) 23:687–702. doi: 10.1210/er.2001-0038
48. Pascussi JM, Drocourt L, Fabre JM, Maurel P, Vilarem MJ. Dexamethasone induces pregnane X receptor and retinoid X receptor-alpha expression in human hepatocytes: synergistic increase of CYP3A4 induction by pregnane X receptor activators. *Mol Pharmacol*. (2000) 58:361–72. doi: 10.1124/mol.58.2.361
49. von Wedel-Parlow M, Wolte P, Galla HJ. Regulation of major efflux transporters under inflammatory conditions at the blood-brain barrier in vitro. *J Neurochem*. (2009) 111:111–8. doi: 10.1111/j.1471-4159.2009.06305.x
50. Hong GL, Cai QQ, Tan JP, Jiang XZ, Zhao GJ, Wu B, et al. Mifepristone-inducible recombinant adenovirus attenuates paraquat-induced lung injury in rats. *Hum Exp Toxicol*. (2015) 34:32–43. doi: 10.1177/0960327114532381
51. Che X, Wang J, He J, Guo X, Li T, Zhang X. The new application of mifepristone in the relief of adenomyosis-caused dysmenorrhea. *Int J Med Sci*. (2020) 17:224–33. doi: 10.7150/ijms.39252
52. de Gooijer MC, de Vries NA, Buckle T, Buil LCM, Beijnen JH, Boogerd W, et al. Improved brain penetration and antitumor efficacy of temozolomide by inhibition of ABCB1 and ABCG2. *Neoplasia*. (2018) 20:710–20. doi: 10.1016/j.neo.2018.05.001
53. Lecureur V, Fardel O, Guillouzo A. The antiprogestatin drug RU 486 potentiates doxorubicin cytotoxicity in multidrug resistant cells through inhibition of P-glycoprotein function. *Lett*. (1994) 335:187–91. doi: 10.1016/0014-5793(94)01186-9
54. Jurado R, Lopez-Flores A, Alvarez A, Garcia-Lopez P. Cisplatin cytotoxicity is increased by mifepristone in cervical carcinoma: an in vitro and in vivo study. *Oncol Rep*. (2009) 22:1237–45. doi: 10.3892/or_00000560
55. Sampson A, Peterson BG, Tan KW, Iram SH. Doxorubicin as a fluorescent reporter identifies novel MRP1 (ABCC1) inhibitors missed by calcein-based high content screening of anticancer agents. *Biomed Pharmacother*. (2019) 118:109289. doi: 10.1016/j.biopha.2019.109289
56. Pistollato F, Abbadi S, Rampazzo E, Persano L, Della Puppa A, Frasson C, et al. Intratumoral hypoxic gradient drives stem cells distribution and MGMT expression in glioblastoma. *Stem Cells*. (2010) 28:851–62. doi: 10.1002/stem.415
57. Eramo A, Ricci-Vitiani L, Zeuner A, Pallini R, Lotti F, Sette G, et al. Chemotherapy resistance of glioblastoma stem cells. *Cell Death Differ*. (2006) 13:1238–41. doi: 10.1038/sj.cdd.4401872

58. Klijn JG, de Jong FH, Bakker GH, Lamberts SW, Rodenburg CJ, Alexieva-Figusch J. Antiprogestins, a new form of endocrine therapy for human breast cancer. *Cancer Res*. (1989) 49:2851–6.
59. Grunberg SM, Weiss MH, Russell CA, Spitz IM, Ahmadi J, Sadun A, et al. Long-term administration of mifepristone (RU486): clinical tolerance during extended treatment of meningioma. *Cancer Invest*. (2006) 24:727–33. doi: 10.1080/07357900601062339
60. Check JH, Check D, Poretta T. Mifepristone extends both length and quality of life in a patient with advanced non-small cell lung cancer that has progressed despite chemotherapy and a check-point inhibitor. *Anticancer Res*. (2019) 39:1923–6. doi: 10.21873/anticanres.13301

Conflict of Interest: The authors declare that the research was conducted in the absence of any commercial or financial relationships that could be construed as a potential conflict of interest.

frontiers in Oncology

ORIGINAL RESEARCH
published: 16 October 2020
doi: 10.3389/fonc.2020.575711

A Comprehensive Analysis of Alterations in DNA Damage Repair Pathways Reveals a Potential Way to Enhance the Radio-Sensitivity of Esophageal Squamous Cell Cancer

*Guangchao Wang[1], Shichao Guo[1], Weimin Zhang[2], Zhangfu Li[1], Jiancheng Xu[1], Dan Li[1], Yan Wang[2] and Qimin Zhan[1,2]**

[1] State Key Laboratory of Molecular Oncology, National Cancer Center/National Clinical Research Center for Cancer/Cancer Hospital, Chinese Academy of Medical Sciences and Peking Union Medical College, Beijing, China, [2] Key Laboratory of Carcinogenesis and Translational Research (Ministry of Education/Beijing), Laboratory of Molecular Oncology, Peking University Cancer Hospital & Institute, Beijing, China

OPEN ACCESS

Edited by:
Rosa Maria Bermudez-Cruz, National Polytechnic Institute of Mexico (CINVESTAV), Mexico

Reviewed by:
Jan Theys, Maastricht University, Netherlands
Vandna Kukshal, Washington University School of Medicine in St. Louis, United States

***Correspondence:**
Qimin Zhan
zhanqimin@bjmu.edu.cn

Specialty section:
This article was submitted to Molecular and Cellular Oncology, a section of the journal Frontiers in Oncology

Received: *24 June 2020*
Accepted: *24 September 2020*
Published: *16 October 2020*

Citation:
Wang G, Guo S, Zhang W, Li Z, Xu J, Li D, Wang Y and Zhan Q (2020) A Comprehensive Analysis of Alterations in DNA Damage Repair Pathways Reveals a Potential Way to Enhance the Radio-Sensitivity of Esophageal Squamous Cell Cancer. Front. Oncol. 10:575711. doi: 10.3389/fonc.2020.575711

Esophageal squamous cell cancer (ESCC) is a common malignancy with a poor 5-year overall survival in China. Altered DNA damage repair (DDR) pathways are associated with a predisposition to cancer and contribute to therapeutic response and resistance in cancers. However, alterations of DDR pathway genes in ESCC are still largely unknown. In this study, we employed genome sequencing data of 192 samples, comparative genomic hybridization data of 123 cases, and gene expression microarray data of 119 patients to firstly perform a comprehensive analysis of the gene alterations of 7 DDR pathways in ESCC. Gene mutations and copy number variations (CNVs) were observed in all 7 DDR pathways, and especially, CNVs were the dominant alteration types. Compared with other pathways, two DNA double-strand break (DSB) repair pathways homologous recombination (HR) and non-homologous end joining (NHEJ), carried significant gene mutations and CNVs especially gene amplifications. Most genes including *RAD54B*, *NBS1*, *RAD51B*, and *PRKDC* were significantly amplified and over-expressed in ESCC. Amplification and high expression of DSB repair pathway genes were associated with poorer overall survival. Gene set variation analysis further showed that DSB repair pathways were up-regulated in ESCC. Besides, we firstly demonstrated that combination of mirin and NU7441, two inhibitors for HR and NHEJ respectively, with ionizing radiation treatment significantly enhanced DSBs, reduced clonogenic cell survival, inhibited cell proliferation, and promoted cell apoptosis in ESCC cells with DSB pathway gene amplification. These findings suggest that DSB repair pathways were significantly altered in ESCC and inhibiting DSB repair pathways might enhance the radio-sensitivity of ESCC with DSB repair up-regulation.

Keywords: DNA damage repair pathways, esophageal squamous cell cancer, homologous recombination, non-homologous end joining, mirin, NU7441, radio-sensitivity

INTRODUCTION

Esophageal cancer, principally comprising of two pathological types: esophageal squamous cell cancer (ESCC) and esophageal adenocarcinoma, is a global problem and the sixth leading cause of cancer mortality annually worldwide. The overall 5-year survival of patients with esophageal cancer ranges from 15 to 25%. ESCC accounts for 70% of cases of esophageal cancer globally and is the dominant type of esophageal cancer in China (1, 2). Recently, the diagnosis and treatment of ESCC have been improved, but the prognosis is still poor (1). The underlying mechanisms involved in tumorigenesis and progression of ESCC remain much less explored.

DNA damage repair (DDR) genes have crucial roles in maintaining genomic stability of human cells. According to biochemical and mechanistic criteria, DDR genes can be grouped into seven main functional pathways. Base excision repair (BER) and nucleotide excision repair (NER) are involved in DNA base damage repair, while mismatch repair (MMR) mainly corrects base mis-pairs. Homologous recombination (HR) and non-homologous end joining (NHEJ) are two pathways which contribute to DNA double-strand break (DSB) repair. In addition, the Fanconi anemia (FA) pathway is associated with the repair of DNA inter-strand crosslinks in the genome, and specialized DNA polymerases in trans-lesion synthesis (TLS) pathway synthesize DNA to bypass unrepaired DNA lesions (3, 4). Dysregulation of DDR pathways is an important determinant of cancer risk, progression, and therapeutic response (4). Up-regulation of DDR pathways are linked to cause resistance to DNA-damaging radiotherapy and chemotherapy. Especially, activation of DSB repair genes is one of the reasons for cancer radio-and chemo-resistance (4–11).

In ESCC, polymorphisms of BER genes were reported to be probably associated with the susceptibility to ESCC (12, 13). Genetic variants in NER genes were linked to exert an impact on survival outcomes of Chinese ESCC patients (14, 15). Moreover, genetic polymorphisms of *XRCC6* and *XRCC5*, two genes in NHEJ pathway, were related to higher risk of ESCC (16). In addition, promoter hypermethylation of the MMR gene *MLH1*, which is important for maintenance of genomic stability, may be a predictor of prognosis for male ESCC patients (17). However, the genetic alterations of DDR pathway genes in ESCC remain to be further investigated.

In the present study, we employed data from previously published studies to perform a comprehensive analysis of genetic alterations of DDR pathway genes in ESCC. Two DSB repair pathways, HR and NHEJ, showed significant gene mutations and amplifications. We investigated the gene expression profile of HR and NHEJ pathways with GSE53624 dataset, and found that most of genes were over-expressed in ESCC. Then, gene set variation analysis (GSVA) was conducted to analyze the pathway activity changes of HR and NHEJ, and DSB repair pathways were observed to be up-regulated in ESCC. We finally investigated the effect of combination of mirin and NU7441 with ionizing radiation (IR) treatment on ESCC cell phenotypes, and found that mirin and NU7441 could enhance the radio-sensitivity of ESCC cells with DSB pathway gene amplification. These findings suggest that alterations of DSB repair pathways might be involved in ESCC radio-resistance, and mirin and NU7441 might have potential application in ESCC treatment.

MATERIALS AND METHODS

Data Collection and Processing

A workflow was designed to identify the gene alterations in DDR pathways (**Figure 1**). Our group previously published two

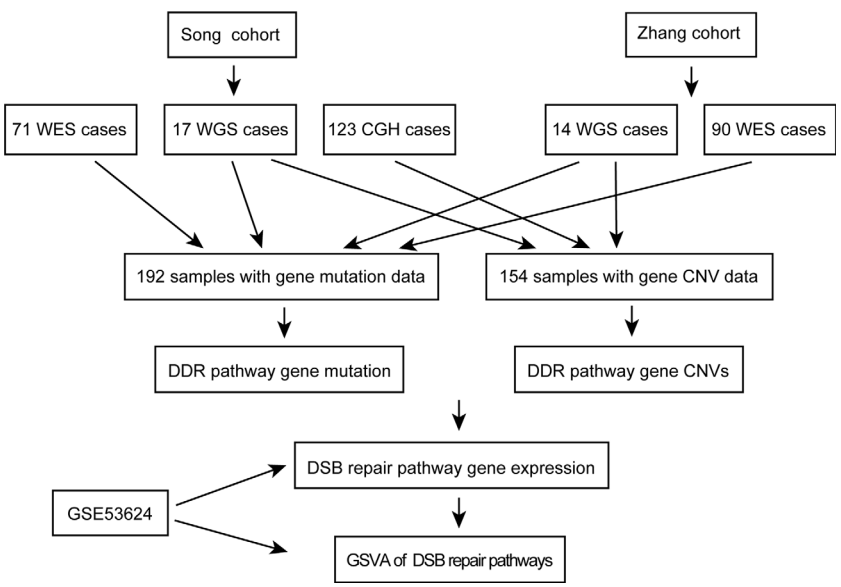

FIGURE 1 | The workflow of data analysis in this study.

studies to identify genomic alterations including gene mutations and copy number variations (CNVs) in ESCC (18, 19), and these two datasets were used to identify genomic alterations of DDR pathway genes. Two ESCC cohorts consist of a total of 262 cases, including 161 from whole-exome sequencing (WES), 31 from whole-genome sequencing (WGS), and 123 from comparative genomic hybridization (CGH) analysis. The data processing has been described in previous studies (18, 19). As the sequencing of both Song and Zhang cohorts was conducted in BGI, and the data of two cohorts has similar sequencing depth and coverage, we integrated the gene mutation data of two cohorts. Besides, we combined the gene CNV data generated by WGS and CGH. Consequently, we obtained 192 ESCC samples with gene mutation data, and 154 ESCC cases with CNV data. The clinical characteristics of two groups of ESCC patients were summarized in **Table 1**.

Additionally, in order to analyze the mRNA expression of DSB repair pathway genes in ESCC, we downloaded GSE53624 dataset, the mRNA expression profile of paired cancer, and adjacent normal tissues from 119 ESCC patients (20), from GEO (Gene Expression Omnibus, https://www.ncbi.nlm.nih.gov/geo/) database. To extract gene expression information of DDR genes in GSE53624, we re-annotated probes from Agilent-038314 CBC Homo sapiens lncRNA + mRNA microarray V2.0 platform (https://www.ncbi.nlm.nih.gov/geo/query/acc.cgi?acc=GPL18109). Human protein-coding transcript sequences (release 29) were downloaded from GENCODE (https://www.gencodegenes.org/) database. All probes in Agilent-038314 platform were then re-annotated as follow: 1, All probes sequences were aligned to human protein-coding transcript sequences with BLASTN. 2, The probes that were matched to one transcript or multiple transcripts from same genes were reserved. 3, The max expression value of multiple probes that were mapped to the same gene was calculated to represent the expression level of the gene. The clinical characteristics of 119 ESCC patients in GSE53624 were summarized in **Table 1**.

TABLE 1 | The clinical characteristics of esophageal squamous cell cancer (ESCC) patients in this study.

Clinical characteristics	Total cases (Mutation cohort)	Total cases (CNV cohort)	Total cases (GSE53624)
Gender			
Male	170	122	98
Female	22	32	21
Age	[a]		
	104 (>=59)	84 (>=58)	66 (>=59)
	87 (<59)	70 (<58)	53 (<59)
TNM stage			
I+II	106	86	53
III	86	68	66
N stage			
N = 0	102	79	54
N > 0	90	75	65
T stage			
T1+T2	48	31	28
T3+T4	144	123	91
Drinking status			
Drinker	17	33	74
Non-drinker	175	121	45
Smoking status			
Smoker	153	104	80
Non-smoker	39	50	39
Survival	[b]	[c]	
Status			
Death	84	73	73
Survival	84	78	46
Median survival time (days)	902	751	32.2 (months)

[a]*Age information of one ESCC patient is missing.*
[b]*Survival information of 24 ESCC patients is missing.*
[c]*Survival information of three ESCC patients is missing.*

Cell Lines

The human ESCC cell lines YES2 and KYSE30 were obtained from Y. Shimada's lab in Kyoto University. YES2 and KYSE30 cells were cultured in Roswell Park Memorial Institute (RPMI) 1640 medium (Gibco, Thermo Fisher Scientific, USA) supplemented with 10% fetal bovine serum (FBS), and were grown at 37°C in humidified air with 5% CO_2. The source of YES2 and KYSE30 cell lines have been recently authenticated and tested for mycoplasma contamination, and no contamination was found.

Gene Set Variation Analysis

GSVA, using a nonparametric approach to transform a gene-by-sample matrix into a gene set-by-sample matrix, facilitates to determine the variation of pre-defined gene set activities over the samples based on gene expression data (21). Expression values of DSB repair pathway genes were used to perform GSVA *via* R "GSVA" package with the following parameters: method = "gsva," mx.diff = "TRUE," and kcdf = "Gaussian."

Immunofluorescence Analysis of γ-H2AX Expression

A total of 1×10^4 YES2 and KYSE30 cells were seeded into confocal dishes for 24 h prior to treatment with mirin (Selleckchem, Houston, TX, USA) (50 μM) and NU7441 (Selleckchem, Houston, TX, USA) (5 μM). After treatment with inhibitors for 1 h, cells were exposed to 6 Gy of IR. Then, cells were cultured with inhibitors for 24 h. Subsequently, cells were fixed with 4% paraformaldehyde in phosphate-buffered saline (PBS) for 10 min at room temperature, then were permeabilized with PBST (0.5% Triton X-100 in PBS) for 10 min on ice. Nonspecific binding was blocked with 1% bovine serum albumin (BSA) in PBST for 30 min. Then, the cells were incubated in the diluted antibody against γ-H2AX (ab26350, Abcam) in 1% BSA (1:200) in a humidified chamber for overnight at 4°C and followed by incubation with Alexa Fluor 488-conjugated secondary antibody (ZSGB-BIO, Beijing, China) in PBS for 1 h at room temperature in the dark. Immunofluorescence images were taken by using laser-scanning confocal microscope (Leica Microsystems Heidelberg GmbH, Am Friedensplatz 3, Germany).

Clonogenic Assay

To assess how combination of inhibitors with IR treatment affects clonogenic cell survival, YES2, and KYSE30 cells were seeded into six-well plates at a density of 1,500 and 1,000 cells per well, respectively. The cells were incubated for 10 days. Then, cells were treated with mirin (50 μM) and NU7441 (5 μM) for 1 h

and irradiated afterward once with 6 Gy. After incubation with inhibitors for an additional 3 days, the cells were fixed with methanol for 5 min, and stained with 0.05% crystal violet (Sigma Chemical Company, St. Louis, MO, USA) for 5 min. Colonies were counted by using ImageJ 1.52V software.

Cell Proliferation Assay

To examine the effect of combination of inhibitors with IR treatment on cell proliferation, YES2 and KYSE30 cells were seeded into 96-well plates at a density of 5,000 cells per well for 24 h. Then, cells were incubated with mirin (50 μM) and NU7441 (5 μM) for 1 h, followed by being exposed to 6 Gy of IR. Subsequently, the optical density (OD) value at 490 nm was detected after 0, 24, 48, 72, and 96 h with a microplate reader (iMark^{TM}, BIO-RAD) after treatment with [3-(4,5-dimethylthiazol-2-yl)-5-(3-carboxymethoxyphenyl)-2-(4-sulfophenyl)-2H-tetrazolium, inner salt] (MTS) (Promega) solution (10% MTS in RPMI 1640 medium) for 1 h. The experiment was repeated three times, and the ratio of OD value (hours 24–96) to the average value of 0 h was calculated and plotted as MTS curves.

Cell Apoptosis Assay

A total of 2×10^5 YES2 and KYSE30 cells were seeded into 6 cm dishes and cultured for 24 h. Subsequently, cells were treated with mirin (50 μM) and NU7441 (5 μM) for 1 h, and were then exposed to 6 Gy of IR. After being cultured with inhibitors for 24 h, cells were collected and stained with annexin V and propidium iodide (PI) according to the manufacturer's instruction provided in Annexin V-FITC/PI apoptosis assay kit (NEOBIOSCIENCE, Shenzhen, China). Flow cytometry (BD LSR) was used to determine the percentage of apoptotic cells.

Statistical Analysis

All statistical tests and graphing were performed by R 3.6.0 and GraphPad Prism 7.0. All of the experiments in this study were independently performed in triplicate, and the data was presented as mean ± standard deviation (S.D.). Fisher's exact test was applied to gene mutation enrichment analysis. Survival curves were performed by Kaplan-Meier method, and the differences between the curves were estimated by log-rank test. Welch's unequal variances *t*-test was used to compare the GSVA scores in ESCC and normal samples, and to analyze the correlations between the GSVA scores and clinical characteristics of ESCC patients. ESCC patients were divided into two groups (high and low groups) according to the median value of gene expression or GSVA scores, and survival analysis was conducted by Kaplan-Meier method. Besides, the correlations between gene expression and clinical characteristics of ESCC patients were analyzed with Fisher's exact test. The other statistical analyses were performed with Student's *t*-test. Each *P* was two-sided, and $P < 0.05$ was considered statistically significant.

RESULTS

In order to investigate the landscape of genetic alterations in DDR pathways, we defined a "core DDR" gene set of 79 DNA repair pathway-specific genes (genes annotated to more than one specific DDR pathway were not included), encompassing 7 major DDR pathways: BER, NER, MMR, HR, NHEJ, FA, and TLS (**Table 2**) (3, 22).

DNA Damage Repair Pathway Genes Were Mutated in Esophageal Squamous Cell Cancer

Firstly, we investigated the non-silent somatic mutation profile of DDR pathway genes in ESCC. As shown in **Figure 2A**, we observed that gene mutation occurred in all 7 DDR pathways and 44 genes were mutated. There were three genes (*POLB*, *LIG1*, and *LIG3*) mutated in BER pathway, each of which only carried one mutation. In NER pathway, both *XPC* and *ERCC6* had two mutations and *ERCC2* had one mutation. Similarly, three genes (*PMS2*, *MSH2*, and *MSH6*) in MMR pathway each had one mutation event and *MLH1* was mutated in two samples. In HR pathway, *BRCA1/2* showed four mutation events (2.1%, 4/192). We also observed that MRE11-RAD50-NBS1 (MRN) complex genes, which play important roles in the sensing, processing and repair of DSBs (23), were mutated in four ESCC patients. Besides, *RBBP8*, *PALB2*, *WRN*, and *BARD1* were mutated in more than one ESCC case. In NHEJ pathway, another pathway involved in repairing DSBs, *PRKDC*, which encodes the catalytic subunit of the DNA-dependent protein kinase (DNA-PK), carried the most frequent mutations (3.1%, 6/192). Furthermore, both *TP53BP1* and *LIG4* had two mutations. *FANCM* was the highest frequently mutated gene of FA pathway (2.6%, 5/192), and *REV3L* was the most frequently (2.1%, 4/192) mutated gene in TLS pathway. Interestingly, we observed that most ESCC samples only had one DDR gene mutation, indicating a mutually exclusive tendency.

TABLE 2 | Gene lists of seven DNA damage repair (DDR) pathways.

BER	NER	MMR	HR	NHEJ	FA	TLS
UNG	*XPC*	*PMS2*	*XRCC3*	*XRCC6*	*UBE2T*	*SHPRH*
TDP1	*XPA*	*PMS1*	*XRCC2*	*XRCC5*	*FANCM*	*REV3L*
TDG	*POLE3*	*MSH6*	*TOP3A*	*XRCC4*	*FANCL*	*REV1*
POLB	*POLE*	*MSH3*	*SLX1A*	*PRKDC*	*FANCI*	*POLQ*
PARP1	*ERCC6*	*MSH2*	*SHFM1*	*POLM*	*FANCD2*	*POLN*
FEN1	*ERCC5*	*MLH3*	*RBBP8*	*POLL*	*FANCC*	*POLK*
APEX2	*ERCC4*	*MLH1*	*RAD52*	*NHEJ1*	*FANCB*	*POLH*
APEX1	*ERCC2*	*EXO1*	*RAD51*	*LIG4*	*FANCA*	*POLI*
LIG1	*ERCC1*		*RAD50*	*TP53BP1*	*FANCE*	
LIG3	*CUL5*		*PALB2*		*FANCF*	
			NBS1		*FANCG*	
			MUS81			
			MRE11			
			GEN1			
			EME1			
			BRIP1			
			BRCA2			
			BRCA1			
			BLM			
			BARD1			
			RAD51B			
			RAD54B			
			WRN			

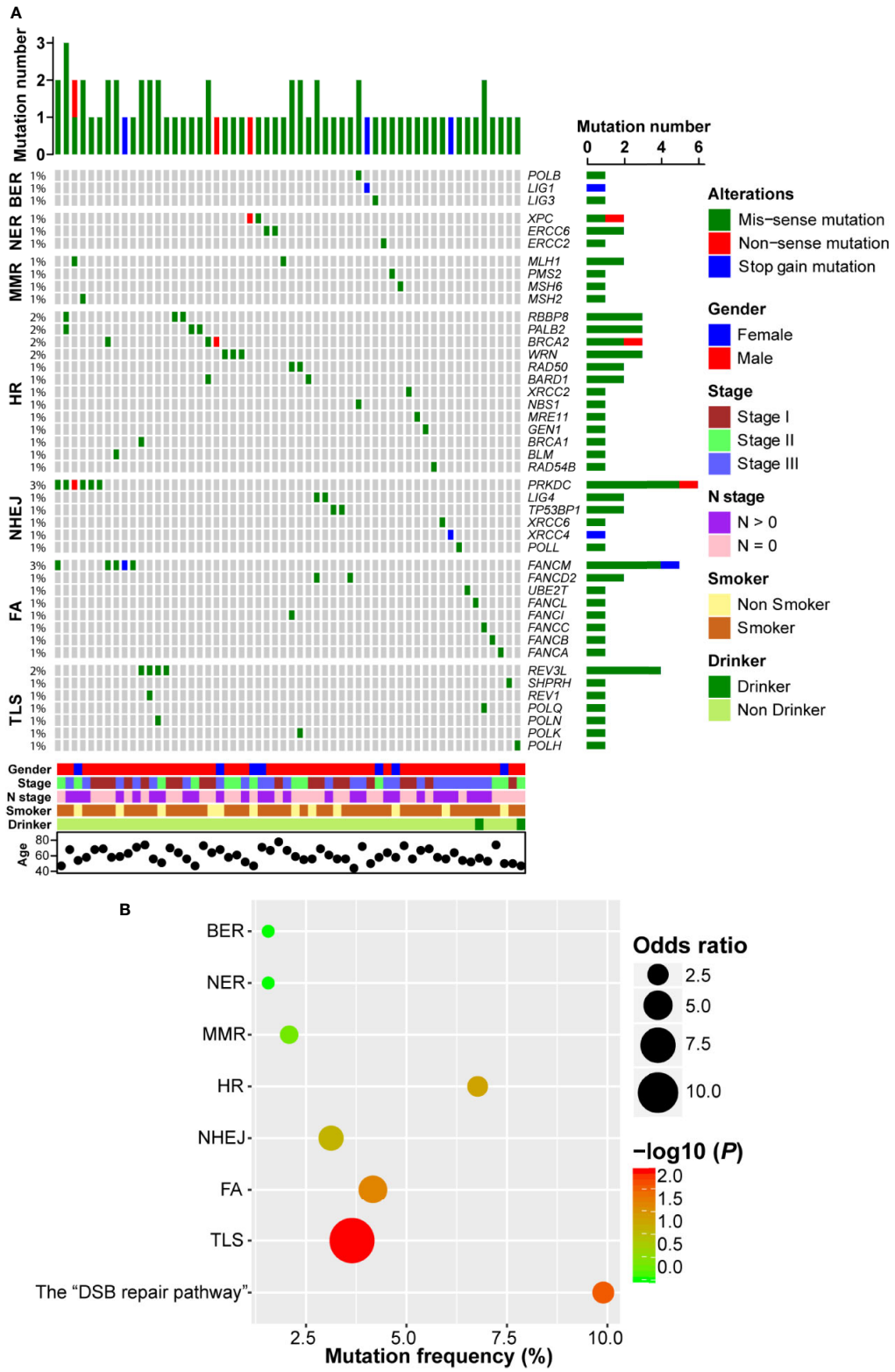

FIGURE 2 | DNA damage repair (DDR) pathway genes were mutated in esophageal squamous cell cancer (ESCC). **(A)** A complex heatmap that shows the non-silent gene mutation profile in DDR pathways (genes and samples with no gene mutations are removed). The top panel presents the number of gene mutations in each of ESCC samples, and the right panel shows the number of gene mutations in each gene. **(B)** A bubble plot that depicts the gene mutation enrichment analysis result of DDR pathways.

In order to further evaluate the significantly mutated DDR pathways, we performed pathway enrichment analysis. As shown in **Figure 2B**, BER, NER, and MMR pathway mutations were not enriched. Gene mutations in FA and TLS pathways were significantly enriched (P = 0.022 and P = 0.004, respectively). Similarly, HR and NHEJ pathways tended to be enriched in ESCC (P = 0.05 and P = 0.08, respectively). We combined HR and NHEJ as the "DSB repair pathway" and conducted enrichment analysis. The result showed that the "DSB repair pathway" mutation was significantly enriched in ESCC (P = 0.009; **Figure 2B**).

DNA Damage Repair Pathway Genes Had Notable Copy Number Variations in Esophageal Squamous Cell Cancer

Next, we identified the CNV profile of DDR pathway genes in ESCC. As the complex heatmap in **Figure 3A** shown, CNVs occurred in all of DDR pathway genes, and 74.7% (115/154) of ESCC samples possessed at least one gene CNV in DDR pathways. In BER pathway, genes were mainly amplified rather than deleted. Both *POLB* and *TDP1* were amplified in 10.4% (16/154) of cases and the incidence of amplification of *APEX1/2* was 14.3% (22/154). Besides, *PARP1* revealed 5.8% (9/154) of amplification frequency and 0.6% (1/154) of deletion frequency. On the contrary, some genes in NER pathway had more deletions instead of amplifications. *CUL5* had the highest deletion frequency (9.1%, 14/154), and *ERCC1* and *ERCC2* had the same CNV profile (3.9% of amplification and 6.5% of deletion) due to proximal genomic location. Gene polymorphisms of *XPA* and *XPC* were reported to be associated with increasing risk of ESCC (15). We observed that *XPA* was amplified in 8 ESCC patients (5.2%) and deleted in 2 ESCC cases (1.3%), whereas the incidences of amplification and deletion of *XPC* were 1.3% (2/154) and 5.2% (8/154), respectively. *MLH1*, one of the important genes in MMR process, was observed to be deleted in 5.2% (8/154) of ESCC cases. Other genes in MMR pathway mainly had more amplifications than deletions.

Interestingly, we found that most of HR pathway genes were mainly amplified. The most amplified gene was *RAD54B* (22.7%, 35/154) which is related to multiple cancers (24–26). However, how *RAD54B* links to ESCC is unclear. *NBS1*, which encodes one of important proteins in MRN complex, was amplified in 21.4% (33/154) of ESCC patients. Cheng and colleagues reported that *XRCC3* was up-regulated in ESCC and was a potential target to improve the radiotherapy effect of ESCC (8). We observed that *XRCC3* was amplified in 11.7% (18/154) of ESCC cases, indicating that up-regulation of *XRCC3* might be due to gene amplification. Other genes such as *SHFM1*, *RAD52*, *RAD51B*, and *MUS81* were also remarkably amplified in ESCC with the frequency 16.2% (25/154), 12.3% (19/154), 11% (17/154), and 10.4% (16/154), respectively. In NHEJ pathway, *PRKDC* was one of significantly amplified DDR pathway genes with the amplification frequency 21.4% (33/154). Another notably amplified gene was *POLM* (13.6%, 21/154), which has not been studied in cancers yet. Besides, *XRCC6* had more amplification events (5.8%, 9/154) than deletions (1.9%, 3/154) (**Figure 3A**).

Additionally, *FANCD2*, carrying the most CNVs in FA pathway, was mainly deleted in 11% (17/154) of ESCC cases. Conversely, *FANCL*, *FANCM*, *FACC*, *UBE2T*, and *FANCI* obviously had more amplification events. In TLS pathway, although *POLQ* did not have significant mutation events, this gene was obviously amplified in ESCC (14.9%, 23/154). Similarly, the main CNV type of *POLH* and *REV1* was deletion. *REV3L*, the most mutated gene in TLS pathway, carried 8 (5.2%) amplification events (**Figure 3A**).

Given the fact that HR and NHEJ, the DSB repair pathways, had significant gene amplifications, we were interested to investigate the correlation between amplification of DSB repair pathways and clinical characteristics of ESCC patients. Survival analysis showed that ESCC samples with amplification of HR or NHEJ pathway had shorter overall survival (P = 0.0501 and P = 0.2876, respectively; **Figure 3B**). Similarly, we found that ESCC patients with the "DSB repair pathway" amplification had poorer overall survival (P = 0.0956; **Figure 3B**). Besides, MRN complex gene amplification was associated with shorter overall survival (P = 0.0413; **Figure 3C**). In addition, we performed survival analysis of DSB repair pathway genes with amplification frequency more than 10%. As presented in **Figure 3D**, amplification of *RAD54B* or *RAD51B* was related to poorer overall survival (P = 0.0313 and P = 0.0146, respectively).

Double-Strand Break Repair Pathway Genes Were Up-Regulated in Esophageal Squamous Cell Cancer

We next analyzed gene expression of DSB repair pathways in GSE53624 dataset. Interestingly, we observed that most of genes were up-regulated in ESCC samples compared with normal tissues (**Figure 4A**). Both *RAD54B* and *RAD51B* were significantly over-expressed in ESCC (P < 0.0001 and P < 0.0001, respectively; **Figure 4B**). Similarly, *MRE11* and *NBS1*, two MRN complex genes, and the most amplified NHEJ pathway gene *PRKDC* were also markedly up-regulated in ESCC (P < 0.0001, P = 0.0174, and P < 0.0001, respectively; **Figure 4B**).

We also investigated the correlations between expression of DSB repair pathway genes and clinical traits of ESCC patients. Survival analysis showed that high expression of five genes including *RAD51B*, *MUS81*, *TOP3A*, *GEN1*, and *TP53BP1* were related to shorter overall survival (P = 0.0091, P = 0.0275, P = 0.0011, P = 0.0179, and P = 0.0060, respectively; **Figure 4C**). **Table 3** summarized the correlation between gene expression and clinical characteristics. We found that gene expression of *RAD51B* and *TOP3A* was associated with TNM stage (P = 0.043 and P = 0.043, respectively). Besides, *XRCC5* expression was related to lymph node metastasis (P = 0.027).

Gene Set Variation Analysis Showed Up-Regulation of Double-Strand Break Repair Pathways in Esophageal Squamous Cell Cancer

In order to further compare the activities of DSB repair pathways between ESCC and normal tissues, we conducted GSVA based on expression of DSB repair pathway genes. We observed that pathway activities of HR, NHEJ and the combined "DSB repair pathway"

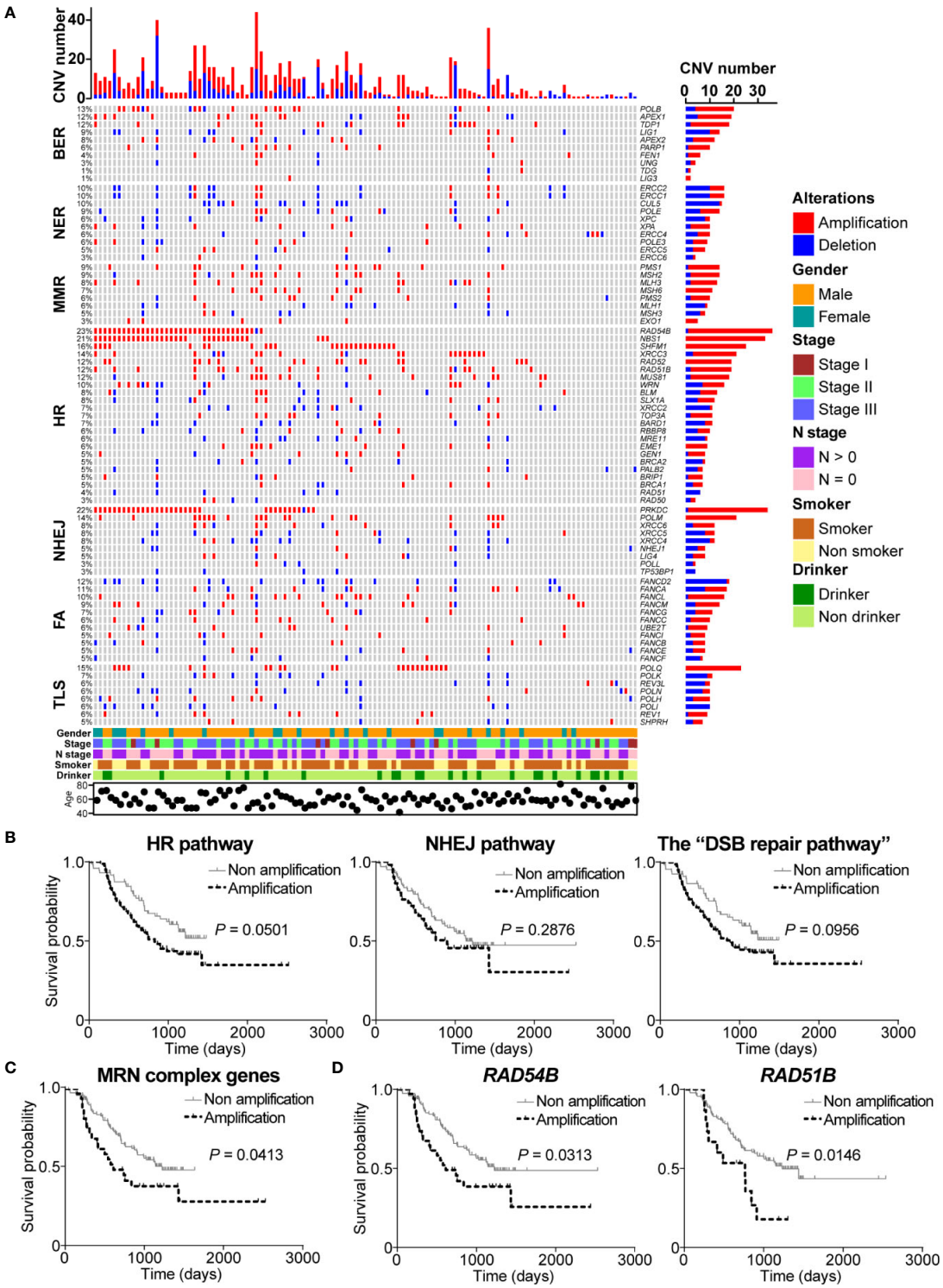

FIGURE 3 | DNA damage repair (DDR) pathway genes had significant copy number variations (CNVs) in esophageal squamous cell cancer (ESCC). **(A)** A complex heatmap that shows the gene CNV profile in DDR pathways (samples with no CNVs are removed). The top panel presents the number of gene CNVs in each of ESCC samples, and the right panel shows the number of gene CNVs in each gene. **(B)** Amplification of homologous recombination (HR), non-homologous end joining (NHEJ), and the "DSB repair pathway" was associated with poorer overall survival. The amplification of MRE11-RAD50-NBS1 (MRN) complex genes **(C)**, *RAD54B*, and *RAD51B* **(D)** was related to shorter overall survival.

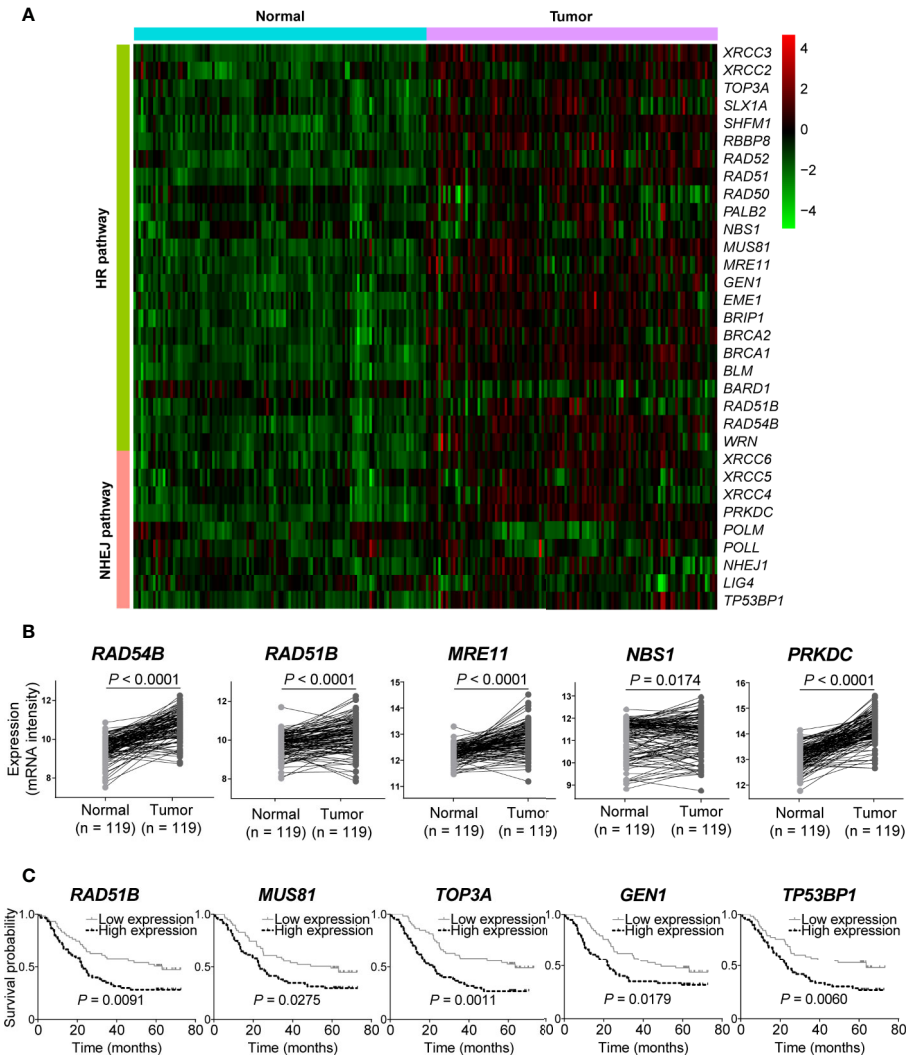

FIGURE 4 | The messenger RNA (mRNA) expression level of double-strand break (DSB) repair pathway genes was up-regulated in esophageal squamous cell cancer (ESCC). **(A)** A heatmap that depicts the mRNA expression profile of DSB repair pathway genes in ESCC and normal tissues from GSE53624 dataset. **(B)** Student's *t*-test analysis showed that *RAD54B*, *RAD51B*, *MRE11*, *NBS1*, and *PRKDC* were up-regulated in ESCC with statistically significant *P* values. ESCC patients were divided into two groups based on the median expression values of DSB repair pathway genes, and survival analysis was then performed. High expression of *RAD51B*, *MUS81*, *TOP3A*, *GEN1*, and *TP53BP1* was associated with poorer overall survival of ESCC patients **(C)**.

were all significantly up-regulated in ESCC based on GSVA scores ($P < 0.0001$, $P < 0.0001$, and $P < 0.0001$, respectively; **Figures 5A, B**). Moreover, survival analysis showed that high pathway activities of HR, NHEJ, and the "DSB repair pathway" were associated with poorer overall survival ($P = 0.0186$, $P = 0.0187$, and $P = 0.0180$, respectively; **Figure 5C**). Besides, the GSVA scores of NHEJ pathway were higher in ESCC cases with lymph node metastasis ($P = 0.0004$; **Figure 5D**). Similarly, the GSVA scores of NHEJ pathway in ESCC stage III group were higher than stage I and II group ($P = 0.0334$; **Figure 5D**). The GSVA scores of the "DSB repair pathway" were obviously increased in ESCC cases with lymph node metastasis ($P = 0.0468$; **Figure 5D**).

Combination of Mirin and NU7441 With Ionizing Radiation Treatment Significantly Enhanced DNA Double-Strand Breaks, Reduced Clonogenic Cell Survival, Inhibited Cell Proliferation, and Promoted Cell Apoptosis in Esophageal Squamous Cell Cancer Cells

Although radiotherapy is one of the effective treatments for ESCC, some ESCC patients often show no response or encounter adverse effects as a result of tumor radio-resistance (27, 28). As IR can induce a variety of DNA damages especially double-strand breaks, HR and

TABLE 3 | The correlations between gene expression of homologous recombination (HR) and non-homologous end joining (NHEJ) pathways and clinical characteristics of esophageal squamous cell cancer (ESCC) patients in GSE53624 dataset.

	Gender	Age	TNM stage	N stage	T stage	Drinking status	Smoking status
XRCC3	0.814	0.582	0.582	0.582	0.518	0.706	0.697
XRCC2	0.480	0.713	0.855	0.359	0.670	0.451	0.697
TOP3A	0.814	0.098	**0.043**	0.142	0.829	0.348	0.175
SLX1A	0.632	1.000	0.855	1.000	0.829	0.059	0.697
SHFM1	0.097	0.141	0.713	1.000	0.829	0.188	0.847
RBBP8	0.814	1.000	0.855	0.582	0.394	1.000	0.562
RAD52	1.000	0.855	0.359	0.464	1.000	0.706	0.697
RAD51	0.814	1.000	0.582	1.000	0.200	0.348	0.081
RAD50	0.632	0.462	0.855	0.272	0.829	0.573	0.847
PALB2	0.814	1.000	0.359	0.272	0.518	0.091	0.562
NBS1	0.632	0.141	0.462	0.855	1.000	0.573	0.333
MUS81	1.000	0.270	0.582	0.464	1.000	0.851	0.242
MRE11	0.632	0.713	0.855	0.714	0.394	0.451	0.697
GEN1	0.480	0.855	0.855	0.272	0.130	1.000	0.562
EME1	0.632	0.462	0.855	1.000	0.518	0.348	0.333
BRIP1	0.632	0.270	1.000	0.272	0.280	0.573	0.562
BRCA2	0.238	0.141	0.855	0.855	0.200	1.000	0.562
BRCA1	0.238	0.713	1.000	0.855	0.518	0.091	0.081
BLM	1.000	0.855	1.000	0.359	0.394	0.451	0.562
BARD1	0.814	0.855	0.199	0.066	1.000	1.000	0.847
RAD51B	1.000	0.359	**0.043**	0.142	1.000	0.348	0.847
RAD54B	0.480	1.000	0.270	0.855	0.518	0.573	**0.033**
WRN	0.814	0.713	0.855	0.272	0.518	0.091	**0.033**
XRCC6	0.337	0.359	0.582	0.714	1.000	1.000	1.000
XRCC5	0.632	1.000	0.582	**0.027**	0.280	0.573	0.175
XRCC4	1.000	0.582	0.582	0.464	1.000	0.851	0.847
PRKDC	0.814	1.000	0.855	0.142	0.280	0.573	0.081
POLM	0.480	0.270	0.359	0.714	1.000	0.851	1.000
POLL	1.000	0.855	0.359	0.272	0.829	0.573	0.847
NHEJ1	0.632	0.359	0.359	0.272	0.051	0.706	0.847
LIG4	0.337	0.141	0.582	1.000	0.200	1.000	0.242
TP53BP1	0.337	0.199	0.582	0.464	0.670	0.573	0.847

Statistically significant P values were in bold.

NHEJ pathways play an important role in causing radio-resistance (5, 7, 29). In this study, we observed that HR and NHEJ pathway genes were significantly up-regulated in ESCC. Accordingly, we assumed that inhibition of HR and NHEJ pathways might enhance the radiosensitivity of ESCC with DSB repair pathway up-regulation. In HR pathway, the MRN complex is essential for sensing and signaling from DNA double-strand breaks and promoting homology-dependent DNA repair (23). As mentioned above, two MRN complex genes *MRE11* and *NBS1* were up-regulated in ESCC. DNA-PK, a protein kinase complex composed of a Ku70/Ku80 heterodimer and a catalytic subunit encoded by *PRKDC*, plays a crucial role in facilitating NHEJ repair for DNA double-strand breaks and was identified as a potential anticancer target (30, 31). Similarly, over-expression of *PRKDC* was identified in ESCC. Therefore, mirin and NU7441, the highly potent and selective inhibitors for MRN complex and DNA-PK respectively (32–34), were utilized to assess whether inhibition of DSB repair pathways could improve the radiosensitivity of ESCC cell lines with altered DSB repair pathways.

We found that most DSB repair pathway genes were amplified in YES2 and KYSE30 cells according to the result of WGS on ESCC cell lines previously conducted in our laboratory (data not published). Therefore, we used YES2 and KYSE30 cells to investigate the effects of mirin and NU7441. We firstly tested if mirin and NU7441 could induce DSBs. As phosphorylation of H2AX (γ-H2AX) is a hall marker of DSBs (35), we conducted an immunofluorescence assay to determine the number of γ-H2AX foci after 24 h of treatment with IR and inhibitors in ESCC cells. The level of γ-H2AX had a little increasing following 6 Gy IR treatment alone, whereas both mirin and NU7441 enhanced γ-H2AX recruitment and combination of two inhibitors led to the higher level of γ-H2AX (**Figures 6A, B**), indicating that inhibiting DSB repair pathways could enhance IR-inducing DSBs in ESCC cells.

Next, to investigate the effect of mirin and NU7441 on clonogenic cell survival of ESCC cells, we conducted clonogenic assay. IR treatment alone did not have a significant influence on clonogenic survival of both YE2 and KYSE30 cells (**Figures 7A, B**). Combining IR with mirin or NU7441 treatment showed notable reduction in clonogenic survival of ESCC cells, and combination of mirin and NU7441 with IR treatment led to the lowest number of colonies in both cells (**Figures 7A, B**). We performed MTS assay in a 96 h interval to detect how mirin and NU7441 treatment affects cell proliferation. As shown in **Figure 7C**, compared with negative control, the proliferation of ESCC cells did not obviously decrease with IR treatment alone. Interestingly, we observed that combining IR with mirin or NU7441 showed significant inhibition of cell proliferation. Moreover, combination of two inhibitors presented the strongest inhibition ability (**Figure 7C**). Apoptosis is considered as one of the main forms of cell death induced by IR. We

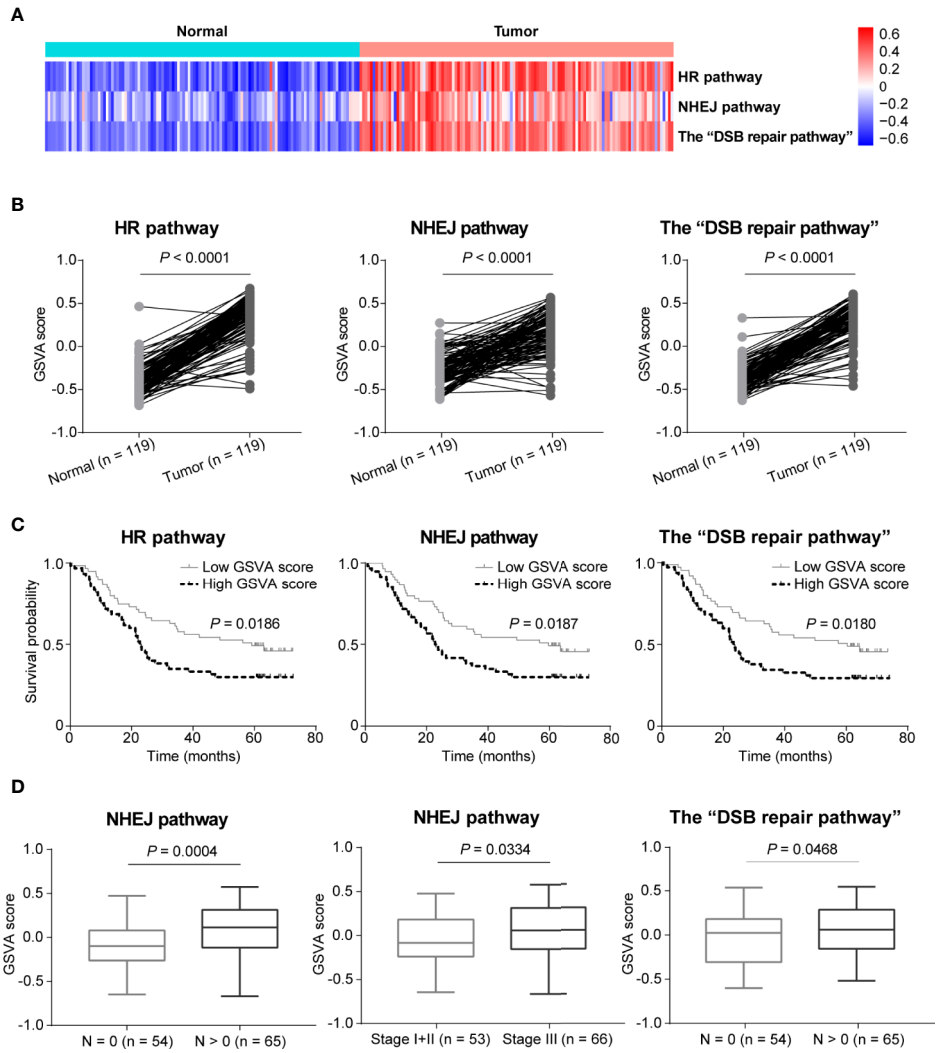

FIGURE 5 | The activities of double-strand break (DSB) repair pathways were up-regulated in esophageal squamous cell cancer (ESCC) as determined by gene set variation analysis (GSVA). **(A)** A heatmap that shows the GSVA scores of homologous recombination (HR), non-homologous end joining (NHEJ), and the "DSB repair pathway" in each ESCC or normal sample. **(B)** Welch's unequal variances *t*-test result showed that the activities of HR, NHEJ and the "DSB repair pathway" were significantly up-regulated in ESCC based on the GSVA scores. ESCC patients were divided into two groups based on the median GSVA scores of HR, NHEJ and the "DSB repair pathway" respectively, and survival analysis was then performed. High activities of HR, NHEJ, and the "DSB repair pathway" were associated with shorter overall survival **(C)**. **(D)** Compared to ESCC patients with N = 0, the GSVA scores of NHEJ and the "DSB repair pathway" were significantly higher in ESCC cases with N > 0. Besides, the GSVA scores of NHEJ in ESCC samples of stage III were significantly higher than ESCC patients of stage I and II.

investigated the effect of IR, mirin and NU7441 on apoptosis in ESCC cells. Similarly, 6 Gy IR treatment alone had a little effect on promoting ESCC cell apoptosis (**Figures 7D, E**). The apoptosis rates were obviously increased in groups combining IR with mirin or NU7441 treatment (**Figures 7D, E**). Furthermore, the synergistic effect of mirin and NU7441 dramatically promoted cell apoptosis (**Figures 7D, E**).

DISCUSSION

Personalized care has become a key part of developing effective treatment guidelines for human cancer. One of the most important aspects of precision medicine in cancer is matching patients and treatments based on the genomic features of an individual and their tumor (36). As genomics-driven precision medicine extends beyond somatic mutations, comprehensive cancer sequencing to identify structural and copy number variations, as well as abnormal expression is becoming increasingly relevant to guide cancer therapy (37). Although diagnosis and treatment of ESCC have been improved, the prognosis is still poor. The development of ESCC is the result of a complex process with several steps implicated in multiple gene alterations (1, 2, 38). Thus, better patient stratification is needed to develop personalized treatment strategies for ESCC. Genomics-driven precision medicine may fulfill this urgent need.

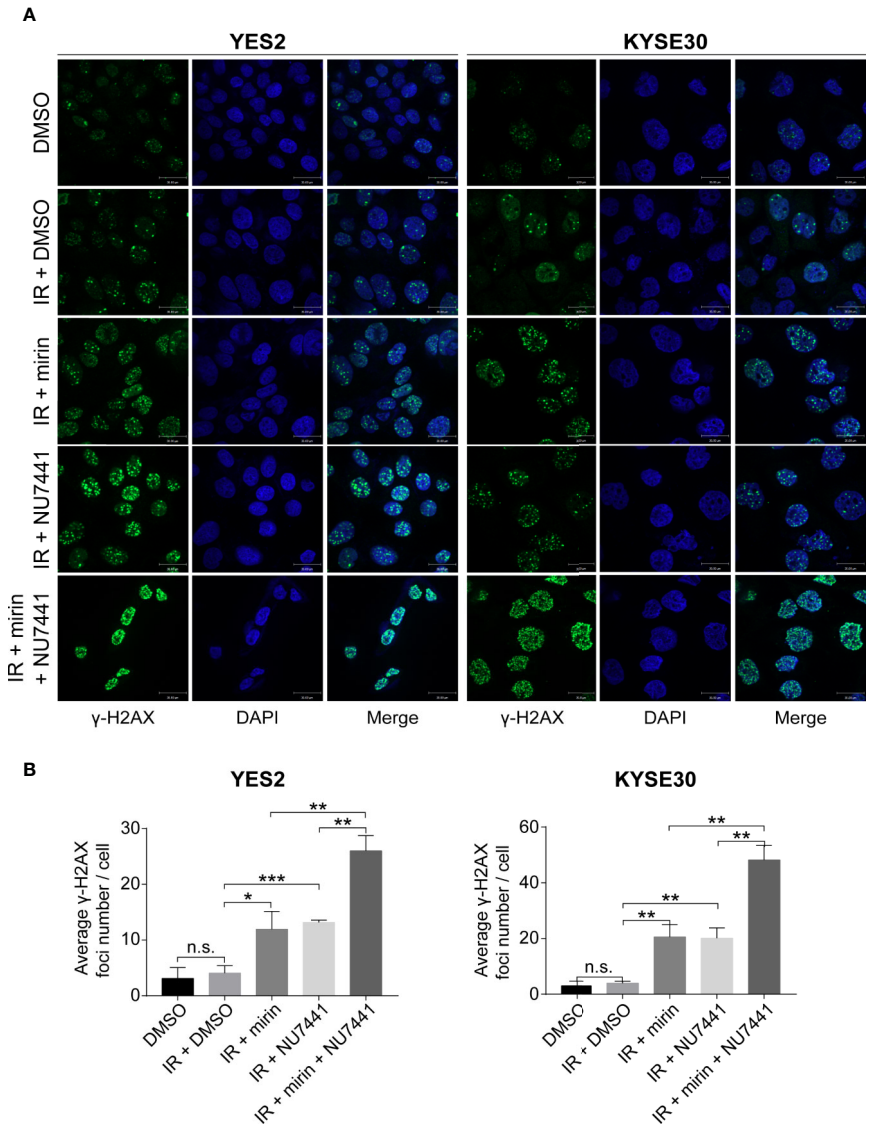

FIGURE 6 | Combination of mirin and NU7441 with ionizing radiation (IR) treatment significantly enhanced double-strand breaks (DSBs) in esophageal squamous cell cancer (ESCC) cells. **(A, B)** DSBs were indicated by immunostaining with γ-H2AX. Combinations of mirin (50 μM) or/and NU7441 (5 μM) with IR (6 Gy) treatment significantly improved the number of γ-H2AX foci in both YES2 and KYSE30 cells. Scale bar = 30 μm. All the experiments were independently performed in triplicate. The error bars represent the standard deviation and *P* values were evaluated by Student's *t*-test. $^{*}P \leq 0.05$, $^{**}P \leq 0.01$, $^{***}P \leq 0.001$, n.s. $P > 0.05$.

One hallmark of cancer is genomic instability induced by various insults that lead to DNA damage (39). DDR plays a critical role on the protection of genomic stability to prevent from tumorigenesis. Alterations in DDR pathways play important roles in the development of cancers. In melanoma, gene up-regulation in DDR pathways is associated with tumor metastasis (40). DDR gene mutations were linked to immune-related gene expression in ovarian cancer and muscle invasive bladder cancer (41, 42). DDR was also reported to be involved in cancer metabolism. Activated DDR increases nucleotide synthesis and anabolic glucose metabolism, while reduces glutamine anaplerosis (43). Besides, up-regulated DDR pathways is one of important factors that trigger resistance to radiotherapy and chemotherapy (4–6). Therefore, identification of alterations in DDR pathways is helpful for better understanding the mechanisms of cancer progression. Moreover, targeting altered DDR pathways could be an effective way for cancer treatment (4, 5). Gene polymorphisms in BER, NER and NHEJ pathway genes have been reported to be related to higher risk of ESCC (12–16). However, the alterations in DDR pathways, including gene mutations, CNVs, and abnormal expression, are still largely unknown in ESCC, and how alterations in DDR pathways contribute to ESCC needs to be further explored.

In this study, we firstly performed a comprehensive analysis of genomic alterations in DDR pathways with previously published sequencing data. Mutations in DDR pathway genes are associated

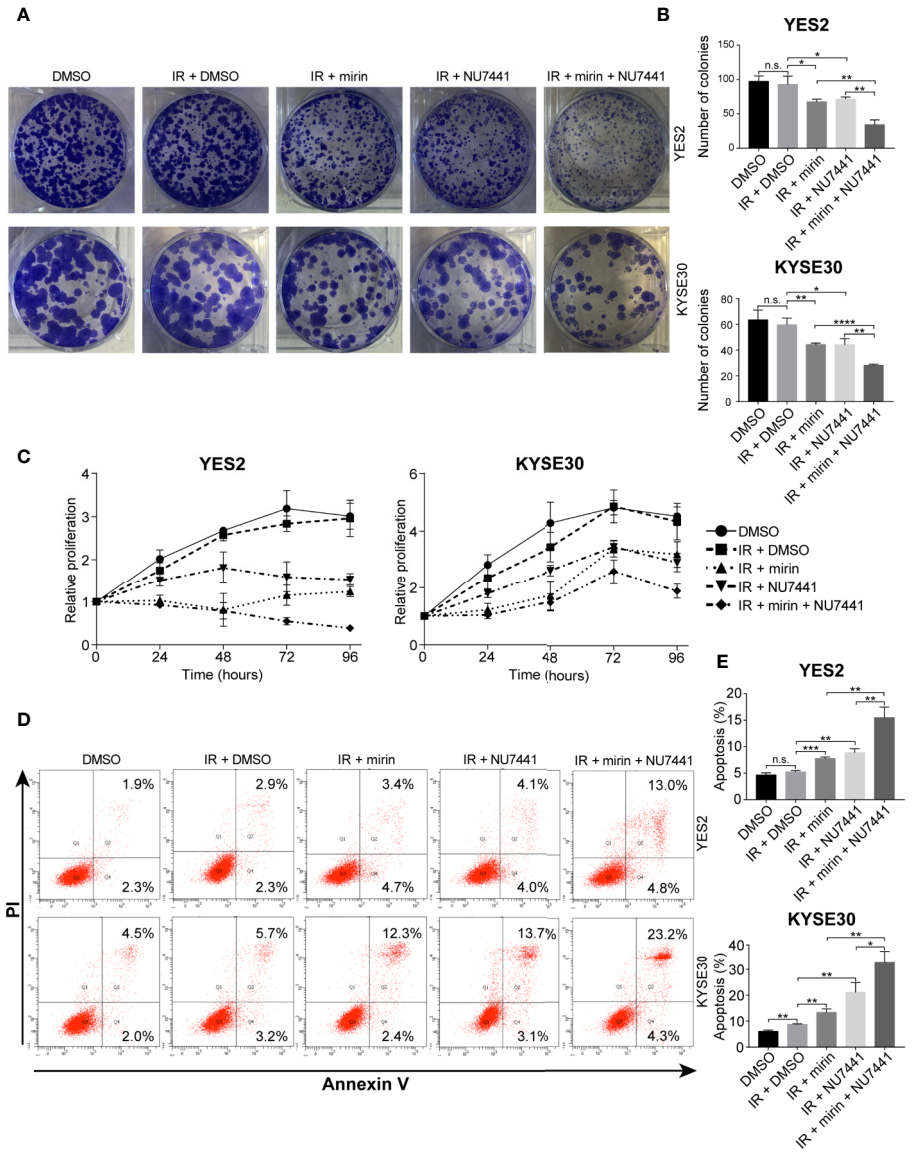

FIGURE 7 | Combination of mirin and NU7441 with ionizing radiation (IR) treatment significantly reduced clonogenic cell survival, inhibited cell proliferation and promoted cell apoptosis in esophageal squamous cell cancer (ESCC) cells. **(A, B)** Clonogenic cell survival with combinations of inhibitors and IR (6 Gy) treatment was investigated by clonogenic assay. Combinations of mirin (50 μM) or/and NU7441 (5 μM) with IR treatment significantly reduced number of colonies of both YES2 and KYSE30 cells. **(C)** Cell proliferation was measured at 24, 48, 72, and 96 h after treatment with inhibitors and IR (6 Gy) by MTS assay. Combinations of mirin (50 μM) or/and NU7441 (5 μM) with IR treatment significantly inhibited proliferation of both YES2 and KYSE30 cells. **(D, E)** Flow cytometric analysis was applied to detect the effect of combinations of inhibitors and IR (6 Gy) treatment on cell apoptosis. Combinations of mirin (50 μM) or/and NU7441 (5 μM) with IR treatment significantly promoted cell apoptosis of both YES2 and KYSE30 cells. All the experiments were independently performed in triplicate. The error bars represent the standard deviation and *P* values were evaluated by Student's *t*-test. $^{*}P \leq 0.05$, $^{**}P \leq 0.01$, $^{***}P \leq 0.001$, $^{****}P \leq 0.0001$, n.s. $P > 0.05$.

with human cancers (4, 44, 45). Although somatic mutations were observed in DDR pathway genes in ESCC, the mutation rate was low. Polymorphisms of BER pathway genes were reported to be associated with risk of ESCC (13), and frequent mutations of MMR pathway genes occurred in colorectal cancer and were associated with the etiology of colorectal cancer (45). However, no significant mutations in BER and MMR pathways were identified in ESCC. Interestingly, Two DSB repair pathways HR and NHEJ carried most gene mutations. Contrast to the gene mutation profile, CNVs especially amplification was observed to be the dominant alteration type in DDR pathways. Amplification of DDR pathway genes was reported to play a crucial role in cancer progression (9, 26, 46). We observed that obvious gene amplification occurred in multiple DDR pathways in ESCC. Similar to the gene mutation profile, HR and NHEJ had a significant gene amplification profile. Previous studies

demonstrated that DSB repair pathway genes were over-expressed in cancers and high expression of these genes was associated with cancer development and resistance to chemotherapy and radiotherapy (8, 10, 11, 25, 26, 47, 48). However, how altered DSB repair pathways contribute to ESCC is much less explored. We found that amplification of DSB repair pathways was associated with poorer overall survival. Gain of MRN complex genes, *RAD54B* and *RAD51B*, whose alterations were reported to be involved in cancer progression (9, 47, 48), was related to poorer overall survival. The NHEJ pathway gene *PRKDC*, which is linked to the development of multiple cancers (10, 31, 49), was also significantly amplified in ESCC. Nevertheless, how amplification of these genes contributes to the development of ESCC is still unclear. CNVs are important factors that can affect gene expression (50). We observed that DSB repair pathway genes, especially the genes with notable amplification such as *RAD54B, RAD51B, NBS1* and *PRKDC*, were up-regulated in ESCC. GSVA result further showed that DSB repair pathways were obviously up-regulated in ESCC, and high pathway activities of DSB repair pathways were related to shorter overall survival and lymph node metastasis. These findings suggest that alterations in DSB repair pathways might play important roles in the development of ESCC.

Although radiotherapy is widely used for ESCC treatment, locoregional disease persists or recurs in 40 to 60% of patients owing to the ability of ESCC cells to become radio-resistant (51, 52). Thus, it is critical to well understand the underlying mechanisms of radio-resistance in ESCC and find the ways to improve the effectiveness of radiotherapy. As up-regulated DDR pathways confer therapeutic resistance in cancers, discovery and development of targeted agents that abrogate specific proteins in DDR pathways is a promising strategy for developing precise cancer treatments. Hitherto, many inhibitors that target specific DDR pathways have been developed (4). However, only a few DDR inhibitors have been used for ESCC treatment. (53–55). Whether targeting DSB repair is an effective strategy for ESCC treatment is much less explored. It is known that up-regulation of DSB repair pathway genes is one of the reasons for cancer radio-resistance. Therefore, targeting DSB repair pathways is a potential effective strategy to enhance radio-sensitivity (4–6, 8, 11). As one of the most famous examples of HR inhibitors, mirin was developed against endonuclease activity of MRE11 and used to effectively inhibit multiple cancers (32, 56, 57). Similarly, NU7441, a highly selective inhibitor for DNA-PK, blocked NHEJ of radiation-induced DSBs and enhanced cancer radio-sensitivity (33, 34, 58, 59). However, whether mirin and NU7441 could affect the radio-sensitivity of ESCC with DSB repair pathway up-regulation is still unclear. We made the first demonstration that combination of mirin and NU7441 with IR treatment significantly enhanced the radio-sensitivity of ESCC cells with DSB repair pathway gene amplification. This result provides a basis for exploring precision medicine strategies for ESCC treatment. Nevertheless, the effect of mirin and NU7441 on xenograft tumors in mice needs to be explored in the future.

In conclusion, this is the first report to comprehensively identify the alterations of DDR pathways in ESCC, and demonstrated that altered DSB repair pathway genes might contribute to ESCC progression. However, the molecular functions of these genes in ESCC should be further studied. We also firstly revealed two DSB repair pathway inhibitors mirin and NU7441 could obviously improve the radio-sensitivity of ESCC cells with DSB repair pathway gene amplification, showing the potential clinical application in ESCC treatment.

DATA AVAILABILITY STATEMENT

Publicly available datasets were analyzed in this study. This data can be found here: European Genome-phenome Archive (https://www.ebi.ac.uk/ega/, accession number EGAS00001000709), NCBI Sequence Read Archive (https://www.ncbi.nlm.nih.gov/sra, accession number SRA112617) and Gene Expression Omnibus (https://www.ncbi.nlm.nih.gov/geo/, accession number GSE54995 and GSE53624). Additionally, gene mutation and clinical information within this study can be found in the supplementary materials of the previously published studies (https://www.nature.com/articles/nature13176) (https://www.cell.com/ajhg/fulltext/S0002-9297(15)00100-7).

ETHICS STATEMENT

Our research was approved by the Ethics Committee of Cancer Hospital Chinese Academy of Medical Sciences and Peking Union Medical College.

AUTHOR CONTRIBUTIONS

GW collected, analyzed, interpreted data, performed experiments, and wrote the manuscript. SG interpreted data and provided support. WZ, ZL, JX, DL, and YW provided supervision and support. QZ conceived the concept, designed the study, wrote the manuscript, and took responsibility for the whole manuscript. All authors contributed to the article and approved the submitted version.

FUNDING

This work was supported by the National Natural Science Foundation of China (81830086 and 81988101), Beijing Municipal Commission of Health and Family Planning Project (PXM2018_026279_000005).

ACKNOWLEDGMENTS

We gratefully thank Mr. Xiao Liang for technical service of fluorescence microscope and Mr. Tao Xu for assistance with flow cytometry analysis. In addition, we thank Dr. Y. Shimada from Kyoto University for providing ESCC cell lines.

REFERENCES

1. Pennathur A, Gibson MK, Jobe BA, Luketich JD. Oesophageal carcinoma. *Lancet* (2013) 381:400–12. doi: 10.1016/S0140-6736(12)60643-6
2. Smyth EC, Lagergren J, Fitzgerald RC, Lordick F, Shah MA, Lagergren P, et al. Oesophageal cancer. *Nat Rev Dis Primers* (2017) 3:17048. doi: 10.1038/nrdp.2017.48
3. Knijnenburg TA, Wang L, Zimmermann MT, Chambwe N, Gao GF, Cherniack AD, et al. Genomic and Molecular Landscape of DNA Damage Repair Deficiency across The Cancer Genome Atlas. *Cell Rep* (2018) 23:239–54 e6. doi: 10.1016/j.celrep.2018.03.076
4. Curtin NJ. DNA repair dysregulation from cancer driver to therapeutic target. *Nat Rev Cancer* (2012) 12:801–17. doi: 10.1038/nrc3399
5. Begg AC, Stewart FA, Vens C. Strategies to improve radiotherapy with targeted drugs. *Nat Rev Cancer* (2011) 11:239–53. doi: 10.1038/nrc3007
6. Srivastava M, Raghavan SC. DNA double-strand break repair inhibitors as cancer therapeutics. *Chem Biol* (2015) 22:17–29. doi: 10.1016/j.chembiol.2014.11.013
7. Todorovic V, Prevc A, Zakelj MN, Savarin M, Brozic A, Groselj B, et al. Mechanisms of different response to ionizing irradiation in isogenic head and neck cancer cell lines. *Radiat Oncol* (2019) 14:214. doi: 10.1186/s13014-019-1418-6
8. Cheng J, Liu W, Zeng X, Zhang B, Guo Y, Qiu M, et al. XRCC3 is a promising target to improve the radiotherapy effect of esophageal squamous cell carcinoma. *Cancer Sci* (2015) 106:1678–86. doi: 10.1111/cas.12820
9. Berlin A, Lalonde E, Sykes J, Zafarana G, Chu KC, Ramnarine VR, et al. NBN gain is predictive for adverse outcome following image-guided radiotherapy for localized prostate cancer. *Oncotarget* (2014) 5:11081–90. doi: 10.18632/oncotarget.2404
10. Sun G, Yang L, Dong C, Ma B, Shan M, Ma B. PRKDC regulates chemosensitivity and is a potential prognostic and predictive marker of response to adjuvant chemotherapy in breast cancer patients. *Oncol Rep* (2017) 37:3536–42. doi: 10.3892/or.2017.5634
11. Ihara M, Ashizawa K, Shichijo K, Kudo T. Expression of the DNA-dependent protein kinase catalytic subunit is associated with the radiosensitivity of human thyroid cancer cell lines. *J Radiat Res* (2019) 60:171–7. doi: 10.1093/jrr/rry097
12. Yang X, Zhu H, Qin Q, Yang Y, Yang Y, Cheng H, et al. Genetic variants and risk of esophageal squamous cell carcinoma: a GWAS-based pathway analysis. *Gene* (2015) 556:149–52. doi: 10.1016/j.gene.2014.11.049
13. Hao B, Wang H, Zhou K, Li Y, Chen X, Zhou G, et al. Identification of genetic variants in base excision repair pathway and their associations with risk of esophageal squamous cell carcinoma. *Cancer Res* (2004) 64:4378–84. doi: 10.1158/0008-5472.CAN-04-0372
14. Zhang R, Zhou F, Cheng L, Yu A, Zhu M, Wang M, et al. Genetic variants in nucleotide excision repair pathway predict survival of esophageal squamous cell cancer patients receiving platinum-based chemotherapy. *Mol Carcinog* (2018) 57:1553–65. doi: 10.1002/mc.22877
15. Yang PW, Hsieh CY, Kuo FT, Huang PM, Hsu HH, Kuo SW, et al. The survival impact of XPA and XPC genetic polymorphisms on patients with esophageal squamous cell carcinoma. *Ann Surg Oncol* (2013) 20:562–71. doi: 10.1245/s10434-012-2622-x
16. Li K, Yin X, Yang H, Yang J, Zhao J, Xu C, et al. Association of the genetic polymorphisms in XRCC6 and XRCC5 with the risk of ESCC in a high-incidence region of North China. *Tumori* (2015) 101:24–9. doi: 10.5301/tj.5000206
17. Wu D, Chen X, Xu Y, Wang H, Yu G, Jiang L, et al. Prognostic value of MLH1 promoter methylation in male patients with esophageal squamous cell carcinoma. *Oncol Lett* (2017) 13:2745–50. doi: 10.3892/ol.2017.5759
18. Song Y, Li L, Ou Y, Gao Z, Li E, Li X, et al. Identification of genomic alterations in oesophageal squamous cell cancer. *Nature* (2014) 509:91–5. doi: 10.1038/nature13176
19. Zhang L, Zhou Y, Cheng C, Cui H, Cheng L, Kong P, et al. Genomic analyses reveal mutational signatures and frequently altered genes in esophageal squamous cell carcinoma. *Am J Hum Genet* (2015) 96:597–611. doi: 10.1016/j.ajhg.2015.02.017
20. Li J, Chen Z, Tian L, Zhou C, He MY, Gao Y, et al. LncRNA profile study reveals a three-lncRNA signature associated with the survival of patients with oesophageal squamous cell carcinoma. *Gut* (2014) 63:1700–10. doi: 10.1136/gutjnl-2013-305806
21. Hanzelmann S, Castelo R, Guinney J. GSVA: gene set variation analysis for microarray and RNA-seq data. *BMC Bioinf* (2013) 14:7. doi: 10.1186/1471-2105-14-7
22. Scarbrough PM, Weber RP, Iversen ES, Brhane Y, Amos CI, Kraft P, et al. A Cross-Cancer Genetic Association Analysis of the DNA Repair and DNA Damage Signaling Pathways for Lung, Ovary, Prostate, Breast, and Colorectal Cancer. *Cancer Epidemiol Biomarkers Prev* (2016) 25:193–200. doi: 10.1158/1055-9965.EPI-15-0649
23. van den Bosch M, Bree RT, Lowndes NF. The MRN complex: coordinating and mediating the response to broken chromosomes. *EMBO Rep* (2003) 4:844–9. doi: 10.1038/sj.embor.embor925
24. McManus KJ, Barrett IJ, Nouhi Y, Hieter P. Specific synthetic lethal killing of RAD54B-deficient human colorectal cancer cells by FEN1 silencing. *Proc Natl Acad Sci U S A* (2009) 106:3276–81. doi: 10.1073/pnas.0813414106
25. Xu C, Liu D, Mei H, Hu J, Luo M. Knockdown of RAD54B expression reduces cell proliferation and induces apoptosis in lung cancer cells. *J Int Med Res* (2019) 47:5650–9. doi: 10.1177/0300060519869423
26. Zhang Z, Li X, Han Y, Ji T, Huang X, Gao Q, et al. RAD54B potentiates tumor growth and predicts poor prognosis of patients with luminal A breast cancer. *BioMed Pharmacother* (2019) 118:109341. doi: 10.1016/j.biopha.2019.109341
27. Minsky BD, Pajak TF, Ginsberg RJ, Pisansky TM, Martenson J, Komaki R, et al. INT 0123 (Radiation Therapy Oncology Group 94-05) phase III trial of combined-modality therapy for esophageal cancer: high-dose versus standard-dose radiation therapy. *J Clin Oncol* (2002) 20:1167–74. doi: 10.1200/JCO.2002.20.5.1167
28. Sakakura C, Miyagawa K, Fukuda KI, Nakashima S, Yoshikawa T, Kin S, et al. Frequent silencing of RUNX3 in esophageal squamous cell carcinomas is associated with radioresistance and poor prognosis. *Oncogene* (2007) 26:5927–38. doi: 10.1038/sj.onc.1210403
29. Santivasi WL, Xia F. Ionizing radiation-induced DNA damage, response, and repair. *Antioxid Redox Signal* (2014) 21:251–9. doi: 10.1089/ars.2013.5668
30. Burma S, Chen DJ. Role of DNA-PK in the cellular response to DNA double-strand breaks. *DNA Repair (Amst)* (2004) 3:909–18. doi: 10.1016/j.dnarep.2004.03.021
31. Goodwin JF, Kothari V, Drake JM, Zhao S, Dylgjeri E, Dean JL, et al. DNA-PKcs-Mediated Transcriptional Regulation Drives Prostate Cancer Progression and Metastasis. *Cancer Cell* (2015) 28:97–113. doi: 10.1016/j.ccell.2015.06.004
32. Dupre A, Boyer-Chatenet L, Sattler RM, Modi AP, Lee JH, Nicolette ML, et al. A forward chemical genetic screen reveals an inhibitor of the Mre11-Rad50-Nbs1 complex. *Nat Chem Biol* (2008) 4:119–25. doi: 10.1038/nchembio.63
33. Hardcastle IR, Cockcroft X, Curtin NJ, El-Murr MD, Leahy JJ, Stockley M, et al. Discovery of potent chromen-4-one inhibitors of the DNA-dependent protein kinase (DNA-PK) using a small-molecule library approach. *J Med Chem* (2005) 48:7829–46. doi: 10.1021/jm050444b
34. Zhao Y, Thomas HD, Batey MA, Cowell IG, Richardson CJ, Griffin RJ, et al. Preclinical evaluation of a potent novel DNA-dependent protein kinase inhibitor NU7441. *Cancer Res* (2006) 66:5354–62. doi: 10.1158/0008-5472.CAN-05-4275
35. Peng A, Lewellyn AL, Schiemann WP, Maller JL. Repo-man controls a protein phosphatase 1-dependent threshold for DNA damage checkpoint activation. *Curr Biol* (2010) 20:387–96. doi: 10.1016/j.cub.2010.01.020
36. Dizman N, Philip EJ, Pal SK. Genomic profiling in renal cell carcinoma. *Nat Rev Nephrol* (2020) 16:435–51. doi: 10.1038/s41581-020-0301-x
37. Aung KL, Fischer SE, Denroche RE, Jang GH, Dodd A, Creighton S, et al. Genomics-Driven Precision Medicine for Advanced Pancreatic Cancer: Early Results from the COMPASS Trial. *Clin Cancer Res* (2018) 24:1344–54. doi: 10.1158/1078-0432.CCR-17-2994
38. Lin DC, Wang MR, Koeffler HP. Genomic and Epigenomic Aberrations in Esophageal Squamous Cell Carcinoma and Implications for Patients. *Gastroenterology* (2018) 154:374–89. doi: 10.1053/j.gastro.2017.06.066
39. Hanahan D, Weinberg RA. Hallmarks of cancer: the next generation. *Cell* (2011) 144:646–74. doi: 10.1016/j.cell.2011.02.013
40. Broustas CG, Lieberman HB. DNA damage response genes and the development of cancer metastasis. *Radiat Res* (2014) 181:111–30. doi: 10.1667/RR13515.1

41. Tian W, Shan B, Zhang Y, Ren Y, Liang S, Zhao J, et al. Association between DNA damage repair gene somatic mutations and immune-related gene expression in ovarian cancer. *Cancer Med* (2020) 9:2190–200. doi: 10.1002/cam4.2849
42. Vidotto T, Nersesian S, Graham C, Siemens DR, Koti M, damage repair gene mutations DNA. and their association with tumor immune regulatory gene expression in muscle invasive bladder cancer subtypes. *J Immunother Cancer* (2019) 7:148. doi: 10.1186/s40425-019-0619-8
43. Turgeon MO, Perry NJS, Poulogiannis G. DNA Damage, Repair, and Cancer Metabolism. *Front Oncol* (2018) 8:15:15. doi: 10.3389/fonc.2018.00015
44. Tubbs A, Nussenzweig A. Endogenous DNA Damage as a Source of Genomic Instability in Cancer. *Cell* (2017) 168:644–56. doi: 10.1016/j.cell.2017.01.002
45. Li SKH, Martin A. Mismatch Repair and Colon Cancer: Mechanisms and Therapies Explored. *Trends Mol Med* (2016) 22:274–89. doi: 10.1016/j.molmed.2016.02.003
46. Tamilzhalagan S, Muthuswami M, Periasamy J, Lee MH, Rha SY, Tan P, et al. Upregulated, 7q21-22 amplicon candidate gene SHFM1 confers oncogenic advantage by suppressing p53 function in gastric cancer. *Cell Signal* (2015) 27:1075–86. doi: 10.1016/j.cellsig.2015.02.010
47. Ho V, Chung L, Singh A, Lea V, Abubakar A, Lim SH, et al. Overexpression of the MRE11-RAD50-NBS1 (MRN) complex in rectal cancer correlates with poor response to neoadjuvant radiotherapy and prognosis. *BMC Cancer* (2018) 18:869. doi: 10.1186/s12885-018-4776-9
48. Yang MH, Chang SY, Chiou SH, Liu CJ, Chi CW, Chen PM, et al. Overexpression of NBS1 induces epithelial-mesenchymal transition and co-expression of NBS1 and Snail predicts metastasis of head and neck cancer. *Oncogene* (2007) 26:1459–67. doi: 10.1038/sj.onc.1209929
49. Cornell L, Munck JM, Alsinet C, Villanueva A, Ogle L, Willoughby CE, et al. DNA-PK-A candidate driver of hepatocarcinogenesis and tissue biomarker that predicts response to treatment and survival. *Clin Cancer Res* (2015) 21:925–33. doi: 10.1158/1078-0432.CCR-14-0842
50. Henrichsen CN, Chaignat E, Reymond A. Copy number variants, diseases and gene expression. *Hum Mol Genet* (2009) 18:R1–8. doi: 10.1093/hmg/ddp011
51. Tachimori Y, Kanamori N, Uemura N, Hokamura N, Igaki H, Kato H. Salvage esophagectomy after high-dose chemoradiotherapy for esophageal squamous cell carcinoma. *J Thorac Cardiovasc Surg* (2009) 137:49–54. doi: 10.1016/j.jtcvs.2008.05.016
52. Zhou S, Ye W, Ren J, Shao Q, Qi Y, Liang J, et al. MicroRNA-381 increases radiosensitivity in esophageal squamous cell carcinoma. *Am J Cancer Res* (2015) 5:267–77.
53. Zhan L, Qin Q, Lu J, Liu J, Zhu H, Yang X, et al. Novel poly (ADP-ribose) polymerase inhibitor, AZD2281, enhances radiosensitivity of both normoxic and hypoxic esophageal squamous cancer cells. *Dis Esophagus* (2016) 29:215–23. doi: 10.1111/dote.12299
54. Miyamoto K, Minegaki T, Tanahashi M, Yamamoto A, Moriyama Y, Wada A, et al. Synergistic Effects of Olaparib and DNA-damaging Agents in Oesophageal Squamous Cell Carcinoma Cell Lines. *Anticancer Res* (2019) 39:1813–20. doi: 10.21873/anticanres.13288
55. Shi Q, Shen LY, Dong B, Fu H, Kang XZ, Yang YB, et al. The identification of the ATR inhibitor VE-822 as a therapeutic strategy for enhancing cisplatin chemosensitivity in esophageal squamous cell carcinoma. *Cancer Lett* (2018) 432:56–68. doi: 10.1016/j.canlet.2018.06.010
56. Petroni M, Sardina F, Infante P, Bartolazzi A, Locatelli E, Fabretti F, et al. MRE11 inhibition highlights a replication stress-dependent vulnerability of MYCN-driven tumors. *Cell Death Dis* (2018) 9:895. doi: 10.1038/s41419-018-0924-z
57. Berte N, Piee-Staffa A, Piecha N, Wang M, Borgmann K, Kaina B, et al. Targeting Homologous Recombination by Pharmacological Inhibitors Enhances the Killing Response of Glioblastoma Cells Treated with Alkylating Drugs. *Mol Cancer Ther* (2016) 15:2665–78. doi: 10.1158/1535-7163.MCT-16-0176
58. Geng W, Tian D, Wang Q, Shan S, Zhou J, Xu W, et al. DNAPKcs inhibitor increases the sensitivity of gastric cancer cells to radiotherapy. *Oncol Rep* (2019) 42:561–70. doi: 10.3892/or.2019.7187
59. Dong J, Ren Y, Zhang T, Wang Z, Ling CC, Li GC, et al. Inactivation of DNA-PK by knockdown DNA-PKcs or NU7441 impairs non-homologous end-joining of radiation-induced double strand break repair. *Oncol Rep* (2018) 39:912–20. doi: 10.3892/or.2018.6217

Conflict of Interest: The authors declare that the research was conducted in the absence of any commercial or financial relationships that could be construed as a potential conflict of interest.

frontiers in Oncology

REVIEW
published: 19 November 2020
doi: 10.3389/fonc.2020.598174

Natural Compounds That Target DNA Repair Pathways and Their Therapeutic Potential to Counteract Cancer Cells

Francisco Alejandro Lagunas-Rangel and Rosa María Bermúdez-Cruz *

Department of Genetics and Molecular Biology, Centro de Investigación y de Estudios Avanzados del Instituto Politécnico Nacional (CINVESTAV), Mexico City, Mexico

Resistance to current cancer treatments is an important problem that arises through various mechanisms, but one that stands out involves an overexpression of several factors associated with DNA repair. To counteract this type of resistance, different drugs have been developed to affect one or more DNA repair pathways, therefore, to test different compounds of natural origin that have been shown to induce cell death in cancer cells is paramount. Since natural compounds target components of the DNA repair pathways, they have been shown to promote cancer cells to be resensitized to current treatments. For this and other reasons, natural compounds have aroused great curiosity and several research projects are being developed around the world to establish combined treatments between them and radio or chemotherapy. In this work, we summarize the effects of different natural compounds on the DNA repair mechanisms of cancer cells and emphasize their possible application to re-sensitize these cells.

Keywords: DNA damage, radioresistance, chemoresistance, sensitization, treatment

OPEN ACCESS

Edited by:
Zhe-Sheng Chen,
St. John's University, United States

Reviewed by:
Bernd Kaina,
Johannes Gutenberg University Mainz, Germany
Samir Gorasiya,
St. John's University, United States

***Correspondence:**
Rosa María Bermúdez-Cruz
roberm@cinvestav.mx

Specialty section:
This article was submitted to Molecular and Cellular Oncology, a section of the journal Frontiers in Oncology

Received: *24 August 2020*
Accepted: *23 October 2020*
Published: *19 November 2020*

Citation:
Lagunas-Rangel FA and Bermúdez-Cruz RM (2020) Natural Compounds That Target DNA Repair Pathways and Their Therapeutic Potential to Counteract Cancer Cells. Front. Oncol. 10:598174. doi: 10.3389/fonc.2020.598174

INTRODUCTION

Day by day we are exposed to chemical carcinogens in the environment, ultraviolet (UV) radiation, ionizing radiation, and also those substances produced in our body during cellular metabolism that attack and produce a variety of DNA injuries. Each lesion favors the development of alterations in DNA and chromosomes, which favors oncogenic transformation and tumor progression. In order to reduce the number of changes in the genome and its instability, cells have several pathways of response to damage and DNA repair proteins that eliminate these lesions (1). DNA adducts, such as those created by alkylating agents, can be cleaved and repaired by base excision repair (BER) or by nucleotide excision repair (NER), depending on whether it is necessary to remove only a nitrogenous base or a nucleotide (2). Also, O-6-methylguanine-DNA methyltransferase (MGMT), an alkyltransferase, eliminates alkylations (3). Mismatch repair (MMR) is a system for repairing the insertion, deletion, and misincorporation of bases that can arise during DNA replication and recombination. While, direct double-strand breaks are repaired by non-homologous end joining, those associated with replication are repaired by homologous recombination. Other repair pathways active during replication include the Fanconi anemia repair pathway, endonuclease-mediated repair, and RecQ-mediated repair (2, 4).

Several cancer cells in contrast to normal cells have one or more DNA repair pathways defective during carcinogenesis, leading to a greater reliance on the remaining pathways and at the same time accumulating mutations during the process (5). Examples of these are the silencing of MGMT in approximately 40% of glioblastomas (6) and the downregulation of MMR genes in colon cancer (7, 8). However, some types of cancer overexpress DNA repair genes and this makes them more resistant to the treatments currently used, causing what is known as resistance (9). Resistance to current cancer treatments is a major problem that requires the search for new compounds that can re-sensitize cancer cells. We speak of resistance when a cancer cell develops the ability to resist radio and chemotherapy, and this can be achieved through various mechanisms such as regulation of the entry and exit of drugs, inhibition of cell death, alterations in metabolism and degradation of drugs, epigenetic factors, and improved DNA repair (10). In terms of its effects on DNA repair, DNA repair inhibitors have been shown to increase the efficacy of anticancer drugs and several works have illustrated the sensitizing efficacy of natural compounds in various cancers (11). Natural compounds are biologically active substances present in plants, fungi, bacteria, and other organisms that affect DNA repair, and are classified mainly according to their chemical structure into terpenes, carotenoids, phenolic compounds (**Table 1**): phenolic acids, flavonoids, stilbenes, coumarins, tannins; alkaloids, nitrogen compounds; organosulfates: isothiocyanates and indoles, allyl sulfates. Flavonoids are further divided into chalcones, flavanones, flavones, flavonols, flavanols, isoflavones, and anthocyanins (12). In this work, we summarize the effects of different natural compounds on the DNA repair mechanisms of cancer cells and emphasize their possible application to re-sensitize these cells to radio and chemotherapy (**Figure 1**).

RESVERATROL

Resveratrol is a natural polyphenolic compound, specifically a stilbene, which is found in significant amounts in grapes, berries, peanuts, and other plant sources, as well as in red wine. This compound has become very popular due to its multiple reported properties that include inflammation-mediating, cardioprotective, antioxidant, and anti-cancer, among other things (13). As an anti-cancer compound, low-dose resveratrol accelerates non-mutagenic repair of DNA damage in mouse embryonic stem cells exposed to ionizing radiation (14). Similarly, resveratrol in mouse embryonic fibroblasts was shown to help maintain genomic stability after chemical and ionizing radiation damage by allowing greater repair efficiency of double-strand breaks and less replicative stress (15). Furthermore, resveratrol was shown to significantly reduce DNA damage from arsenic compounds in non-cancerous mammalian cells by enhancing repair activities, especially if used prior to exposure (16). Resveratrol causes DNA damage and activates the repair mechanisms in various cancer cell lines such as prostate cancer cells, colon cancer cells, and breast cancer cells (17, 18). Indeed, head and neck squamous cell carcinoma cells as well as breast cancer cells receive more DNA damage than their normal counterparts (19, 20). Non-small cell lung cancer cells have shown DNA damage after treatment with resveratrol, which was potentiated by the pemetrexed antifolate that destabilizes ERCC1 protein, an essential nuclease in the BER pathway and, to a lesser extent, in double-stranded DNA breaks and in crosslink repair, by inhibiting p38 MAPK activity (21). Resveratrol has been shown to affect different DNA repair pathways in MCF7 breast cancer cells by reducing the expression of several genes involved in this activity and where mismatch repair and homologous recombination stand out such as most affected (22). Resveratrol made breast cancer cells more susceptible to cisplatin, and specifically in cisplatin-resistant MCF7 cells, resveratrol was able to re-sensitize cells by decreasing several key components of the homologous recombination pathway (23). Etoposide in combination with resveratrol treatments were more effective than either chemical alone given as treatment to stop cell proliferation and eliminate non-small-cell lung cancer cells by suppressing the expression of the XRCC1 protein (DNA repair protein within NER or BER pathway) (24). The same happened in sphere cultures of cervical cancer cells treated with this combination, but in this case a strong decrease in the expression of the RAD51 protein (DNA repair protein within HR pathway) was reported (25). Resveratrol potentiates the effects of temozolomide on glioblastoma cells by negatively regulating the NF-κB pathway and thereby causing a reduction in MGMT expression (26). Resveratrol switched radioresistant prostate cancer cells back to sensitive phenotype by inhibiting ATM phosphorylation and its target protein H2AX, causing cell cycle arrest and subsequently cell death (27). Resveratrol also radiosensitized glioma stem cells by causing an accumulation of DNA damage that impairs their self-renewal and potency (28). By the same mechanism, resveratrol together with capsaicin made radiosensitive pancreatic tumor cells more susceptible to the effect of radiation (29). In colon cancer cells resistant to 5-fluorouracil, resveratrol in conjunction with 1,3-bis(2-chloroethyl)-1-nitrosourea (BCNU) managed to induce apoptosis and re-sensitize the cells by decreasing the levels of FEN1 and PCNA (30). The same decrease in both proteins was observed in cigarette smoke-induced breast cancer cells treated with resveratrol alone, where it was also detailed that p21 levels increased and affected the binding of FEN1 to PCNA, thus inhibiting the long patch base excision repair pathway. Other components of this pathway, such as DNA-ligase-I and polymerases (β, δ, ϵ) were also decreased (31). Despite the fact that melanoma cells have an increased expression of APE/REF1, especially those resistant to dacarbazine, it has been shown that resveratrol can sensitize them by inhibiting REF1-activated AP-1 DNA bindings (32). As can be seen from the data referred, resveratrol is an important candidate despite somewhat solubility issues that affect its bioavailability.

CURCUMIN

Curcumin is a bright yellow hydrophobic polyphenol present in the rhizome of turmeric (*Curcuma longa*) and to which antimicrobial, anti-inflammatory, antioxidant, immunomodulatory, renoprotective,

TABLE 1 | Structural classification of natural compounds targeting DNA repair pathways in cancer cells.

Class	Active metabolite	Structure
Phenolic compounds	Curcumin	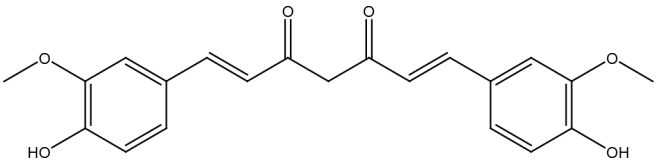
	Epigallocatechin gallate (EGCG)	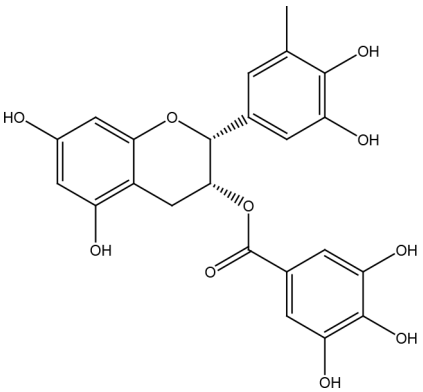
	Genistein	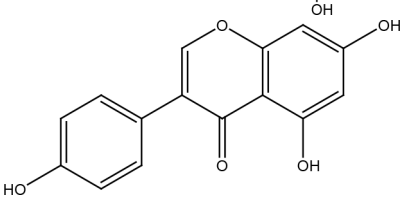
	Quercetin	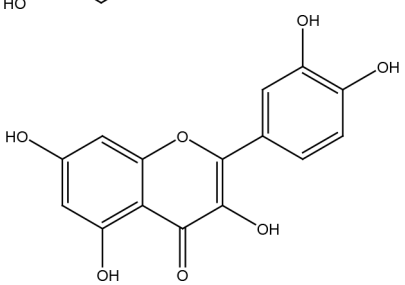
	Resveratrol	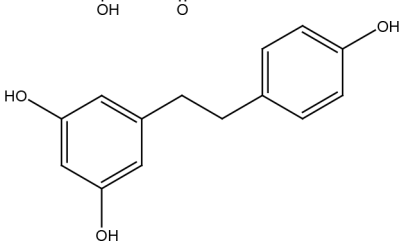
	Honokiol	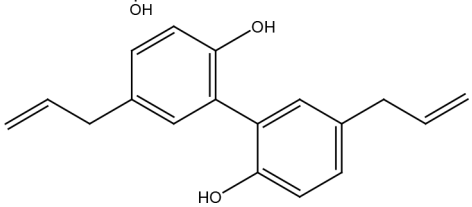

(Continued)

TABLE 1 | Continued

Class	Active metabolite	Structure
	Ellagic acid	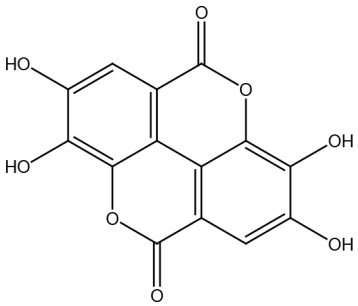
	Kaempferol	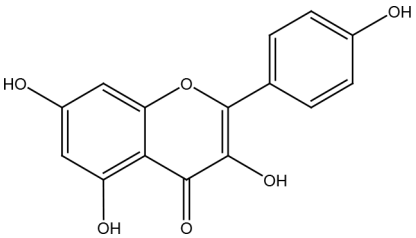
	Isoorientin	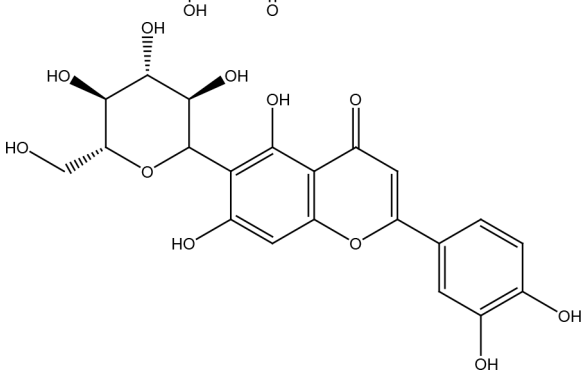
	Ferrulic acid	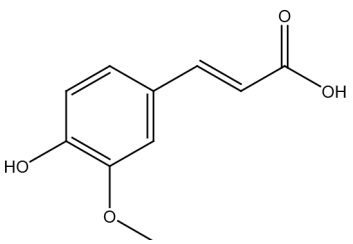
Terpenoids	Celastrol	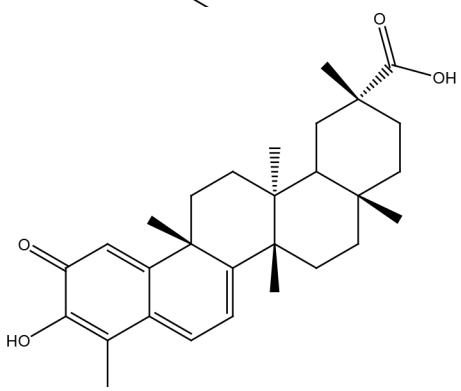

(Continued)

TABLE 1 | Continued

Class	Active metabolite	Structure
	β-Carotene	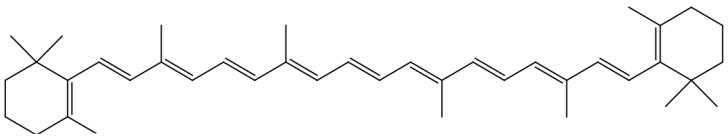
	Triptolide	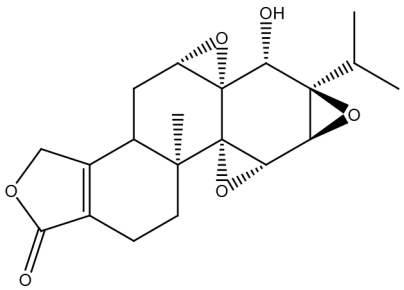
	Cantharidin	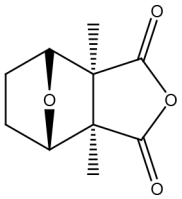
	β-Thujaplicin	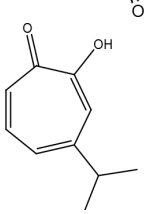
	Retigeric acid B	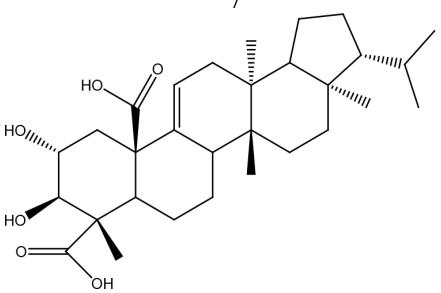
	Thymoquinone	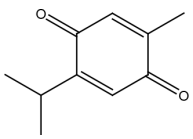
	Withanolide D	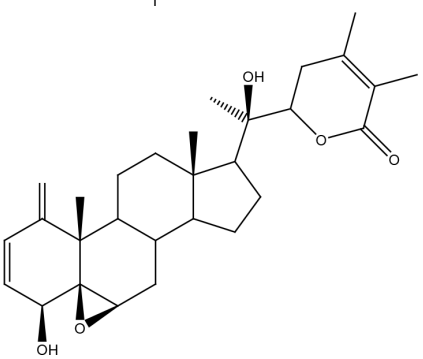

(Continued)

TABLE 1 | Continued

Class	Active metabolite	Structure
	Garcinol	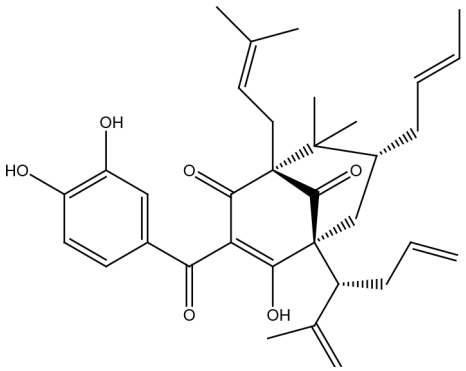
Nitrogen-containing alkaloids	Berberine	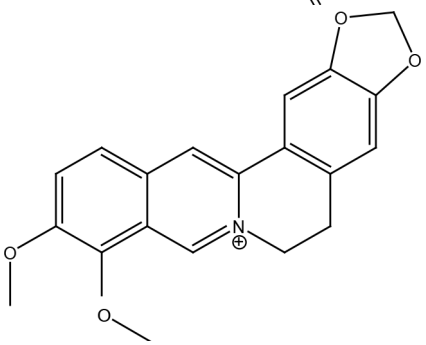
	Capsaicin	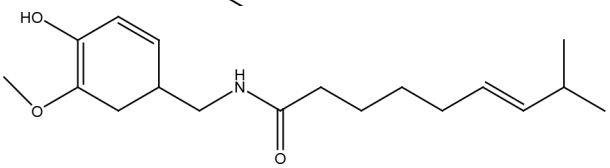
	Harmine	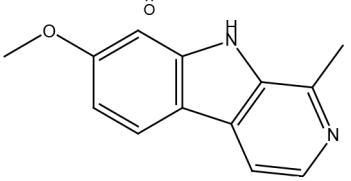

hepatoprotective, hypoglycemic, and anti-cancer effects have been attributed (33). Curcumin's ability to affect multiple pathways makes it an extremely powerful anticancer agent. Furthermore, curcumin has shown multiple effects on DNA repair systems, both in healthy cells and cancer cells. Curcumin prevents DNA damage in lymphocytes of people chronically exposed to arsenic and improves its repair capacity. Thus, it induces an increase in the proteins of the base excision repair and non-homologous end joining pathways and collaborates to avoid carcinogenesis (34). Also, in murine models, curcumin reduced cyclobutane and pyrimidine dimers produced after exposure to UVB radiation and delayed skin carcinogenesis (35). In cancer cells, curcumin blocks both non-homologous end joining and homologous recombination pathways: by inhibiting the acetyltransferase activity of CBP on histone at double strand breaks thus preventing the recruitment of KU70/KU80 proteins and p300 on BRCA1 promoter and causing downregulation of its expression. ATR kinase activity is also inhibited by curcumin, causing cell cycle arrest in the G2 phase (36, 37). It has also been seen that mismatch repair is important in curcumin activity because cells deficient in this system, particularly when MSH2 and MLH1 proteins are affected, show a greater sensitivity to it. The difference is that the competent cells of the mismatch repair system can activate CHK1 and arrest in the G2/M phase before inducing apoptosis, whereas the deficient cells go directly to apoptosis (38). In gastric cancer cells, curcumin induces DNA damage that is reflected by overexpression of DNA-PKcs, ATM, ATR, HDAC1, p21, and GADD45A along with activation of the p53 pathway, which consequently suppresses phosphorylation of Rb and expression of cyclin E, thus stopping the cell cycle and causing a general demethylation of DNA by repressing the expression of DNMT1 thus allowing the re-expression of tumor suppressor genes (39). The same effect on DNMT1 was reported in curcumin-treated breast cancer cells, but the effects were different between cell lines. For example, in HCC-38 cells, the curcumin-dependent decrease in DNMT1 together with the inhibition of miR-29b caused an increase in TET1 (a methylcytosine dioxygenase that plays an important role in the demethylation of DNA) allowing

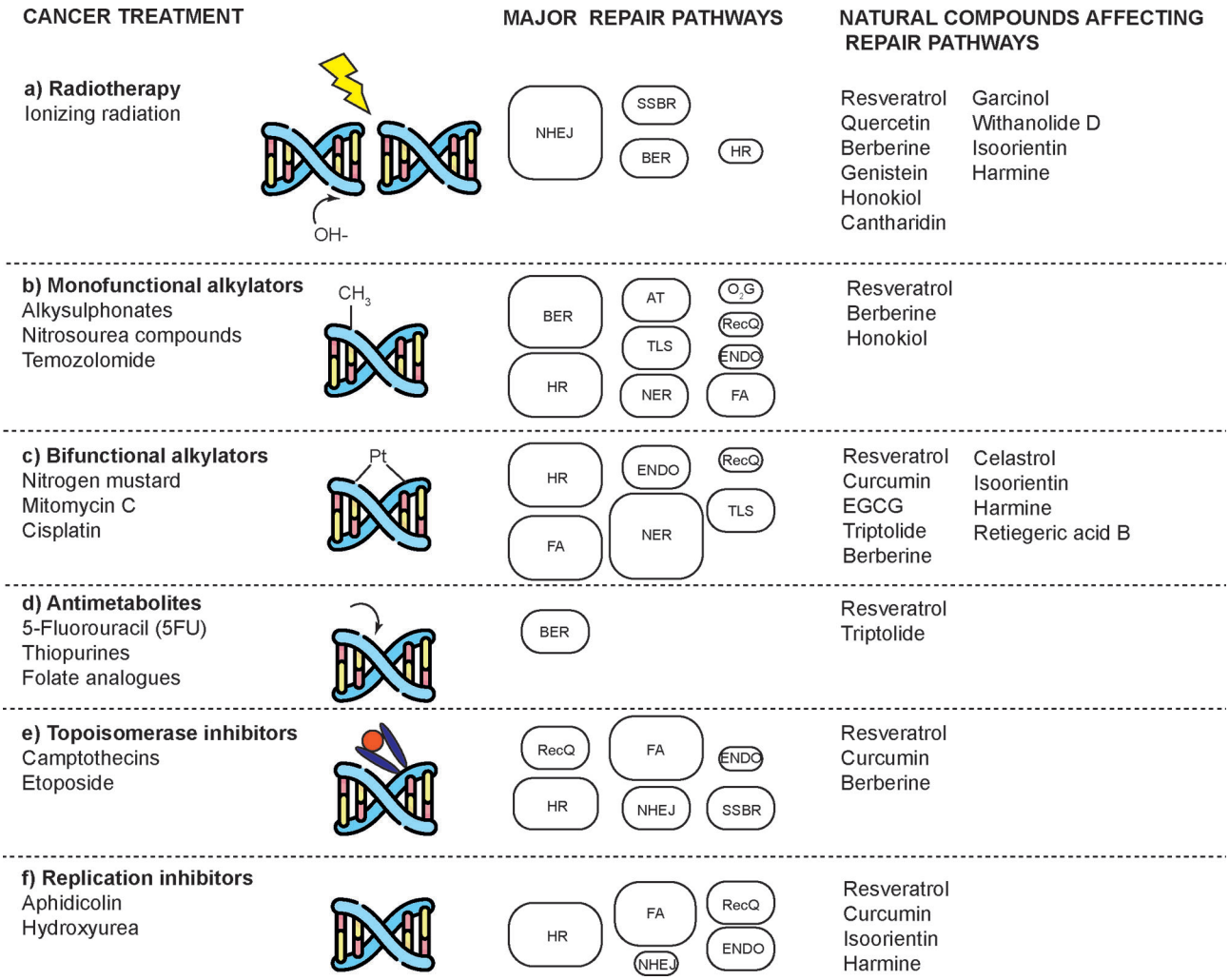

FIGURE 1 | Natural compounds that enhance the effects of radio and chemotherapy by affecting DNA repair mechanisms in cancer cells. DNA damaging agents used in cancer treatment induce a diverse spectrum of toxic lesions. These injuries are recognized by a variety of DNA repair pathways that are specific to the injury but are complementary in some respects. Natural compounds enhance the effects of these toxic agents by preventing proper DNA repair and inducing cell death. DNA repair pathways involved are: base-excision repair (BER), nucleotide-excision repair (NER), alkyltransferases (ATs), mismatch repair (MMR), non-homologous end joining (NHEJ), homologous recombination (HR), endonuclease mediated repair (ENDO), Fanconi anaemia repair (FA), DNA dioxygenases (O2G), and RecQ-mediated repair (RecQ). The size of the boxes represents the relative contribution of each repair mechanism in each type of damage caused by a type of treatment. Modified according to (2).

BRCA1 re-expression, but this did not occur in T47D cells (40). It is also important to note that the response to DNA damage triggered by curcumin and varies according to the BRCA1 mutation status in triple negative breast cancer cells, but regardless of this, in all cases it leads to apoptosis (41). In curcumin-treated MCF-7 breast cancer cells, a decrease in FEN1 (long patch BER pathway) was observed as a result of overexpression of NRF2 and its positioning on the promoter of this gene, thus collaborating to prevent cell proliferation (42). In lung cancer cells, curcumin reduces the levels of some DNA repair proteins such as BRCA1, MGMT, MDC1, and 14-3-3σ, but elevates DNA damage proteins such as phosphorylated p53 and γH2AX, thus causing cytotoxicity, condensation of the nucleus, and DNA damage (43). Meanwhile, curcumin causes DNA damage in cervical cancer cells and increases levels of BRCA1, MGMT, MDC1, p53, DNA-PKcs, MDM2, PARP, and the phosphorylated forms of ATM, ATR, and H2AX (44). In contrast, RAD51 foci formation was also decreased in lymphoma cells and breast cancer cells treated with curcumin (45, 46).

On the other hand, the ability of curcumin to reverse chemoresistance in various cancers is remarkable. In combination with cisplatin, curcumin prevents the activation of p38 MAPK through MKP1 phosphatase activity consequently affecting the expression of XRCC1, making lung cancer cells more sensitive to the cytotoxic effects of this chemotherapeutic agent (47). A decrease in thymidine phosphorylase, ERCC1 and RAD51 can also be observed with this combination and with

mitomycin C and curcumin, which is due to the inhibition of ERK1/2 activity and an increase in their ubiquitin-mediated 26S proteasome degradation (48, 49). As a complementary medicine to carboplatin, curcumin reduces its adverse effects by selectively activating nucleotide excision repair and homologous recombination in bone marrow cells through positive regulation of BRCA1, BRCA2, and ERCC1 expression, but it has the opposite effect on malignant cells (50). Together with quinacrine, curcumin binds DNA more efficiently, being able to cause further damage to breast cancer stem cells and preventing their repair by lowering the expression of DDB2, Polβ, Polδ, PolH, Rad51, Fen1, XRCC1, CHK1, and RPA proteins (51). Curcumin increases the apoptotic effects of cisplatin on cisplatin-resistant lung adenocarcinoma cells by inhibiting FANCD2 monoubiquitination and, therefore, also preventing activation of the Fanconi anemia/BRCA pathway that enables DNA repair by homologous recombination (52). The same effect was reported in multiple myeloma cells treated with melphalan and curcumin (53). Curcumin sensitizes colon cancer cells to radiation by modifying the expression of several genes, highlighting an overexpression of CCNH and XRCC5 along with low expression of LIG4 and PNKP (54). Hydroxyurea, camptothecin, and cisplatin were shown to be more efficient in lymphoma cells when combined with curcumin (45). In the same way, PARP inhibitors and DNA-PK inhibitors together with curcumin showed a synergistic effect to induce DNA damage, apoptosis, and mitotic cell catastrophe in different cancer cell lines (36, 45, 46). This, in part, due to the inhibition of topoisomerase II and the reduction in the expression of WRN, FEN1, APE1, DNA ligase III, and XRCC1 (55).

(−)-EPIGALLOCATECHIN-3-GALLATE

The main polyphenolic component of green tea (*Camellia sinensis*) extracts is epigallocatechin gallate (EGCG), an ester of epigallocatechin and gallic acid, and a type of catechin. Biological effects that have been reported for EGCG are antioxidant, anti-inflammatory, neuroprotective, cardioprotective, and anti-cancer (56). In terms of anti-cancer effects, among the many activities that EGCG has (57), some of them are related to its effect on DNA repair systems. EGCG is a compound capable of inhibiting the activity of the ERCC1/XPF protein in non-small cell lung cancer cell lines, blocking the intrastrand crosslink repair, and thus enhancing the cytotoxic activities of cisplatin, preventing proliferation and increasing cellular death (58). Furthermore, EGCG selectively decreased MGMT levels in glioblastoma multiforme cells by preventing translocation of β-catenin to the nucleus, thereby avoiding the removal of temozolomide-produced O6-methylguanine and helping to resensitize cells resistant to this drug. In contrast, EGCG improved MGMT expression in non-tumor glial cells by inhibiting DNMT1 and allowing demethylation of its promoter (59). Normal human leucocytes with continuous low-dose EGCG treatments show less DNA damage (single and double chain mutations, adducts, and mutations) when exposed to genotoxic agents such as bleomycin and some heterocyclic amines (60, 61).

TRIPTOLIDE

Triptolide is a diterpene triepoxide obtained from the Chinese medicinal plant *Tripterygium wilfordii* Hook F, commonly known as lei gong teng or thunder god vine. This compound has a variety of bioactivities and pharmacological effects such as anti-microbial, anti-inflammatory, neuroprotective, cardiovascular, immunosuppressive, and recently anti-cancer (62). The anticancer effects of triptolide are time and dose dependent, varying according to cell type, but where its effects on DNA repair mechanisms stand out, most often culminating in apoptosis of cells. First, triptolide was shown to affect the nucleotide excision repair pathway by selectively inhibiting the ATPase activity of XPB helicase, thus allowing for a malfunction of the TFIIH holocomplex and preventing filling of the gaps after damage excision (63). Then, triptolide was reported to inhibit the double-stranded DNA damage response in breast cancer cells through post-transcriptional downregulation of ATM, which causes a reduction in the levels of γH2AX (64). The same was observed in melanoma cell lines along with decreased levels of ATR, BRCA-1, DNA-PKcs, MGMT, and p53 (65). Meanwhile, in murine B−cell lymphoma cells and acute lymphoblastic leukemia cells, triptolide induces DNA double strand breaks with upregulation of γH2AX and RAD51, which culminates in caspase-3 dependent apoptosis and helps enhance the effects of PARP1 and PI3K inhibitors, as well as re-sensitizing cytarabine- and doxorubicin-resistant leukemia cells (66, 67). Triptolide was shown to cause a decrease in the levels of PARP1, XRCC1, and RAD51 proteins in triple negative breast cancer cells, affecting single-strand break repair, base excision repair, and homologous recombination pathways (64). Furthermore, this natural compound causes cells accumulate DNA damage, stopping their growth, and being arrested in the S phase of the cell cycle, as well as presenting a greater sensitivity to chemotherapeutic agents such as cisplatin and doxorubicin (64, 68). Lung cancer cells showed an increase in ATM phosphorylation after combined treatment of cisplatin with triptolide, which led to the activation of apoptotic genes such as PUMA (69). Likewise, triptolide showed synergy with oxaliplatin in pancreatic cancer cell lines by producing a decrease in the expression of key proteins in the nucleotide excision repair pathway such as XPA, XPB, XPC, ERCC1, XPD, and XPF, but unlike breast cancer cells, here showing an increase in the levels of γH2AX and, therefore, also of DNA double strand breaks (70).

QUERCETIN

Quercetin is a flavonoid found in a variety of foods, including fruits and vegetables such as apples, berries, capers, grapes, onions, shallots, tea, and tomatoes, as well as many seeds such

as nuts, flowers, bark, and leaves (71). Quercetin is known for its anti-inflammatory, antihypertensive, vasodilatory, anti-hypercholesterolemic, anti-atherosclerotic, antioxidant and, more recently, anti-cancer effects (72). Quercetin following a 1,2-dimethylhydrazine dihydrochloride (DMD) induced colon carcinogenesis protocol allowed decreased production of 8-oxoguanine and apurine/pyrimidine sites by increasing levels of the BER proteins OGG1, APE1, and XRCC1, and positively modulate NRF2 signaling with a higher antioxidant response (73). Also in response to oxidative damage to colon cells by H_2O_2, an increase in OGG1 was observed (74). In prostate cancer cells, quercetin significantly reduced the expression of ATM, PARP1, and DNA-PKcs (75). Quercetin suppresses the repair of double-stranded DNA breaks and improves the radiosensitivity of ovarian cancer cells through activation of ATM and the p53-dependent endoplasmic reticulum stress pathway (76). Meanwhile, in some colorectal cancer, cervical cancer and breast cancer cell lines, quercetin acted as a radiosensitizer by blocking ATM activation and its downstream signaling, thereby prolonging the persistence of damage and inducing apoptosis (77). Quercetin can potentiate the effects of PARP inhibitors, preventing efficient repair of DNA damage, and where inhibition of BRCA2 activity plays an important role during the passage of single-strand breaks to double-strand breaks during DNA replication (78).

BERBERINE

Berberine is an isoquinoline alkaloid isolated mainly from the Chinese herb *Coptis chinensis*, although it is also present in other plants of the genus *Berberis*. It has a wide range of pharmacological properties such as anti-inflammatory, antibiotic, antitumor, antiarrhythmic functions, and it can regulate blood lipids and glucose levels (79). Berberine has been shown to induce oxidative DNA damage and alter RAD51 expression in ovarian cancer cells, breast cancer cells, and osteosarcoma cells, but not in normal cells, thereby causing increased DNA damage and longer, with abundant γH2AX, ATM, and p53 foci (80–82). This property has been important in radiosensitizing breast cancer cells and esophageal cancer cells (82, 83). Furthermore, it showed synergy with PARP inhibitors to induce cellular apoptosis (80). Also, berberine was able to increase the sensitivity of triple negative breast cancer cells to cisplatin, camptothecin, and methyl methanesulfonate by attenuating XRCC1-mediated repair of base excision and subsequently increasing double-stranded DNA breaks (84).

GENISTEIN

Genistein is a multifunctional isoflavonoid whose best-known source is soy-based foods. Genistein has been shown to modulate various pathways involved with obesity, metabolic syndrome, and cancer (85). In normal skin, genistein reduces the formation of cyclobutane pyrimidine dimers caused by UVB radiation (86), and in rats treated with genistein, BRCA1 expression was elevated and tumorigenesis caused by 7,12-dimethylbenz [a] anthracene (DMBA) was reduced (87). Genistein inhibited both homologous recombination repair and non-homologous end joining pathway in glioblastoma cells and sarcoma cells after the damage caused by the radiation of carbon ions. This can be explained by considering that genistein prevents the phosphorylation of DNA-PKcs and KU80, and it delays the formation of RAD51 foci (88, 89). The same happened with X-ray therapy and a combined treatment of genistein and IGF1R inhibitor AG1024 in prostate cancer cells (90). Genistein has also been shown to reduce AP-1 levels and sensitize these cells to doxorubicin nanoparticles (91). Interestingly, normal liver cells were protected from damage by ionizing radiation using low concentrations of genistein (92).

OTHER COMPOUNDS

Thymoquinone is the main active component of *Nigella sativa Linn* seed extracts and has been shown to possess antineoplastic properties. This compound induces DNA damage and apoptosis in glioblastoma cells where shortening of telomeres is involved by a DNA-PKcs-dependent mechanism (93). Honokiol is a biphenolic compound with a powerful antineoplastic activity which is obtained from the *Magnolia officinalis* plant. It is more toxic in tumor cells than in normal cells and has been reported to inhibit the activity of the X family polymerases (β and λ), affecting the base excision repair pathway and making various cancer cells more susceptible to the effect of bleomycin and temozolomide (94). Ellagic acid obtained from various fruits and vegetables is a polyphenolic compound that can reduce MGMT expression in glioblastoma cells and together with anti-angiogenic therapy with bevacizumab (which also affects DNA repair by reducing the expression of ERCC-1 and XRCC-1) improves the radiosensitivity of tumors (95, 96). Celastrol is a polyphenolic compound isolated mainly from plants in the *Celastraceae* family. Celastrol has been shown to exhibit significant antioxidant, anti-inflammatory, and antineoplastic activities. For this last aspect, celastrol promotes a reduction in cancer cells of the monoubiquitinated FANCD2 protein, promoting its degradation by the proteasome and affecting the activation of the DNA damage-induced Fanconi anemia pathway and the downstream pathways. Thus, enhancing the effects of crosslinking agents such as cisplatin (97). Cantharidin is a substance of the terpenoid class that is secreted by many species of blister beetles, and which has been observed to sensitize pancreatic cancer cells to the effects of ionizing radiation by increasing levels of phosphorylated H2AX and affecting the expression of UBE2T, RPA1, GTF2H5, LIG1, POLD3, RMI2, XRCC1, PRKDC, FANCI, FAAP100, RAD50, RAD51D, RAD51B, and DMC1, which are important for repair by homologous recombination and non-homologous end joining pathway (98). In bladder cancer cells, decreased phosphorylated ATR and H2AX, as well as total levels of DNA-PK, PARP, MGMT, BRAC1, and MDC1 were observed with this compound

(99). Garcinol, a polyisoprenylated benzophenone derivative of the fruit rind *Garcinia indica*, sensitizes cervical cancer cells to ionizing radiation by inhibiting non-homologous end joining pathway by preventing chromatin remodeling, especially histone acetylation (100, 101). Gastric cancer cells treated with high doses of β-carotene showed a significant decrease in the KU70 and KU80 proteins (102). Androgen receptor-target DNA repair genes were epigenetically repressed in androgen-sensible prostate cells after treatment with 3,3'-diindolylmethane, a compound derived from indole-3-carbinol and found in cruciferous vegetables such as broccoli, brussels sprouts, cabbage, and kale (103). Kaempferol inhibited the expression of DNA-PKcs, MDC1, MGMT, p53, 14-3-3, phosphorylated forms of ATM and ATR in promyelocytic leukemia cells but increased phosphorylated p53 and H2AX. Kaempferol is a flavonoid found in vegetables and fruits such as berries, grapefruit, and *Ginkgo biloba* (104). Luteolin, a flavonoid enriched in various vegetables and plants such as carrots, broccoli, and parsley, reduced phosphorylation levels of ATM, CHK2, and H2AX in oral squamous cell carcinoma cells (105). In lung squamous carcinoma cells, luteolin caused an increase in the levels of MHT1, OGG1, and AP-1 (106). Withanolide D, a compound obtained from *Withania somnifera*, was shown to improve the radiosensitivity of different cancer cell lines by inhibiting DNA damage *via* non-homologous end joining repair pathway (107). Isoorientin is a flavonoid extracted from many plant species, such as flax straw, watery leaf, *Gypsophila elegans*, *Phyllostachys pubescens*, *Patrinia*, and *Drosophyllum lusitanicum*. Meanwhile, harmine is a tricyclic β-carboline alkaloid that was originally isolated from *Peganum harmala* seeds. Both compounds inhibited repair by homologous recombination in hepatoma cells, without affecting normal cells, by inhibiting the ATM-downstream signaling pathways and therefore enhancing the effects of ionizing radiation, hydroxyurea, mitomycin C, olaparib, and camptothecin (108, 109). Ferulic acid potentiated the effects of PARP inhibitors on breast cancer cells by reducing the formation of RAD51 foci and lengthening the time that double-stranded DNA breaks remain unrepaired (110). Capsaicin, the main bioactive compound found in chili peppers of the *Capsicum* genus, downregulates the ERCC1 protein in lung cancer cells by promoting its proteasomal degradation, thereby enhancing the cytotoxic effects of the EGFR inhibitor erlotinib (111, 112). β-Thujaplicin, a natural monoterpenoid found in the wood of trees in the *Cupressaceae* family, sensitized osteosarcoma cells to damage caused by ionizing radiation, as it inhibits the formation of RAD51 foci and keeps RPA phosphorylated (113). Retiegeric acid B potentiates the effects of cisplatin on hormone-refractory prostate cancer cells by affecting nucleotide excision repair, particularly ERCC1, TFB5, and RPA1 proteins, and mismatch repair, presumably MSH2 and MSH6 proteins (114).

CONCLUSIONS

Natural compounds have been be used with other drugs to make cancer cells more sensitive to radiation therapy and different chemotherapeutic agents, even reversing the resistance mechanisms that these cells may have developed. Since increasing the levels of genes involved in DNA repair is a mechanism used by many cancer cells to resist the effects of radio and chemotherapy, the fact that natural compounds can affect the DNA repair pathways makes them candidates to reverse cases of resistance and thus, perhaps contribute to the improvement of patients to allow their survival time to be longer. Despite this potential, there are currently very few clinical trials testing these compounds in combination with chemotherapy or radiotherapy, mainly due to all the challenges that this entails [revised in (115)], including shortages of funds due to lack of patentability and manufacturing difficulties. It is necessary to continue studying different natural compounds and their effects on DNA repair systems in order to implement them in current treatment strategies, establish the appropriate doses and times, and decipher the mechanisms of action by which they carry out their effects.

AUTHOR CONTRIBUTIONS

FL-R compiled the information, wrote the manuscript, made the figures and tables, RB-C reviewed and corrected the manuscript as well as obtained funding. All authors contributed to the article and approved the submitted version.

REFERENCES

1. Roos WP, Thomas AD, Kaina B. DNA damage and the balance between survival and death in cancer biology. *Nat Rev Cancer* (2016) 16:20–33. doi: 10.1038/nrc.2015.2
2. Helleday T, Petermann E, Lundin C, Hodgson B, Sharma RA. DNA repair pathways as targets for cancer therapy. *Nat Rev Cancer* (2008) 8:193–204. doi: 10.1038/nrc2342
3. Mitra S. MGMT: A personal perspective. *DNA Repair (Amst)* (2007) 6:1064–70. doi: 10.1016/j.dnarep.2007.03.007
4. Kelley MR, Fishel ML. Overview of DNA repair pathways, current targets, and clinical trials bench to clinic. In: *DNA Repair in Cancer Therapy*. Elsevier (2016). p. 1–54. doi: 10.1016/B978-0-12-803582-5.00001-2
5. Torgovnick A, Schumacher B. DNA repair mechanisms in cancer development and therapy. *Front Genet* (2015) 6:157. doi: 10.3389/fgene.2015.00157
6. Hegi ME, Diserens A-C, Gorlia T, Hamou M-F, de Tribolet N, Weller M, et al. MGMT Gene Silencing and Benefit from Temozolomide in Glioblastoma. *N Engl J Med* (2005) 352:997–1003. doi: 10.1056/NEJMoa043331
7. Peltomaki P. Deficient DNA mismatch repair: a common etiologic factor for colon cancer. *Hum Mol Genet* (2001) 10:735–40. doi: 10.1093/hmg/10.7.735
8. Christmann M, Kaina B. Transcriptional regulation of human DNA repair genes following genotoxic stress: trigger mechanisms, inducible responses and genotoxic adaptation. *Nucleic Acids Res* (2013) 41:8403–20. doi: 10.1093/nar/gkt635

9. O'Connor MJ. Targeting the DNA Damage Response in Cancer. *Mol Cell* (2015) 60:547–60. doi: 10.1016/j.molcel.2015.10.040
10. Ramos P, Bentires-Alj M. Mechanism-based cancer therapy: resistance to therapy, therapy for resistance. *Oncogene* (2015) 34:3617–26. doi: 10.1038/onc.2014.314
11. Khatoon E, Banik K, Harsha C, Sailo BL, Thakur KK, Khwairakpam AD, et al. Phytochemicals in cancer cell chemosensitization: Current knowledge and future perspectives. *Semin Cancer Biol* (2020). doi: 10.1016/j.semcancer.2020.06.014
12. Rejhová A, Opattová A, Čumová A, Slíva D, Vodička P. Natural compounds and combination therapy in colorectal cancer treatment. *Eur J Med Chem* (2018) 144:582–94. doi: 10.1016/j.ejmech.2017.12.039
13. Rauf A, Imran M, Butt MS, Nadeem M, Peters DG, Mubarak MS. Resveratrol as an anti-cancer agent: A review. *Crit Rev Food Sci Nutr* (2018) 58:1428–47. doi: 10.1080/10408398.2016.1263597
14. Denissova NG, Nasello CM, Yeung PL, Tischfield JA, Brenneman MA. Resveratrol protects mouse embryonic stem cells from ionizing radiation by accelerating recovery from DNA strand breakage. *Carcinogenesis* (2012) 33:149–55. doi: 10.1093/carcin/bgr236
15. Matsuno Y, Atsumi Y, Alauddin M, Rana MM, Fujimori H, Hyodo M, et al. Resveratrol and its Related Polyphenols Contribute to the Maintenance of Genome Stability. *Sci Rep* (2020) 10:5388. doi: 10.1038/s41598-020-62292-5
16. Roy M, Sinha D, Mukherjee S, Paul S, Bhattacharya RK. Protective effect of dietary phytochemicals against arsenite induced genotoxicity in mammalian V79 cells. *Indian J Exp Biol* (2008) 46:690–7.
17. Hsieh T-c, Huang Y-c, Wu JM. Control of prostate cell growth, DNA damage and repair and gene expression by resveratrol analogues, in vitro. *Carcinogenesis* (2011) 32:93–101. doi: 10.1093/carcin/bgq230
18. Colin DJ, Limagne E, Ragot K, Lizard G, Ghiringhelli F, Solary É, et al. The role of reactive oxygen species and subsequent DNA-damage response in the emergence of resistance towards resveratrol in colon cancer models. *Cell Death Dis* (2014) 5:e1533–3. doi: 10.1038/cddis.2014.486
19. Tyagi A, Gu M, Takahata T, Frederick B, Agarwal C, Siriwardana S, et al. Resveratrol Selectively Induces DNA Damage, Independent of Smad4 Expression, in Its Efficacy against Human Head and Neck Squamous Cell Carcinoma. *Clin Cancer Res* (2011) 17:5402–11. doi: 10.1158/1078-0432.CCR-11-1072
20. Kala R, Shah HN, Martin SL, Tollefsbol TO. Epigenetic-based combinatorial resveratrol and pterostilbene alters DNA damage response by affecting SIRT1 and DNMT enzyme expression, including SIRT1-dependent γ-H2AX and telomerase regulation in triple-negative breast cancer. *BMC Cancer* (2015) 15:672. doi: 10.1186/s12885-015-1693-z
21. Chen R-S, Ko J-C, Chiu H-C, Wo T-Y, Huang Y-J, Tseng S-C, et al. Pemetrexed downregulates ERCC1 expression and enhances cytotoxicity effected by resveratrol in human nonsmall cell lung cancer cells. *Naunyn Schmiedebergs Arch Pharmacol* (2013) 386:1047–59. doi: 10.1007/s00210-013-0905-9
22. Leon-Galicia I, Diaz-Chavez J, Garcia-Villa E, Uribe-Figueroa L, Hidalgo-Miranda A, Herrera LA, et al. Resveratrol induces downregulation of DNA repair genes in MCF-7 human breast cancer cells. *Eur J Cancer Prev* (2013) 22:11–20. doi: 10.1097/CEJ.0b013e328353edcb
23. Leon-Galicia I, Diaz-Chavez J, Albino-Sanchez M, Garcia-Villa E, Bermudez-Cruz R, Garcia-Mena J, et al. Resveratrol decreases Rad51 expression and sensitizes cisplatin−resistant MCF−7 breast cancer cells. *Oncol Rep* (2018) 39:3025–33. doi: 10.3892/or.2018.6336
24. Ko J-C, Syu J-J, Chen J-C, Wang T-J, Chang P-Y, Chen C-Y, et al. Resveratrol Enhances Etoposide-Induced Cytotoxicity through Down-Regulating ERK1/2 and AKT-Mediated X-ray Repair Cross-Complement Group 1 (XRCC1) Protein Expression in Human Non-Small-Cell Lung Cancer Cells. *Basic Clin Pharmacol Toxicol* (2015) 117:383–91. doi: 10.1111/bcpt.12425
25. Ruíz G, Valencia-González HA, León-Galicia I, García-Villa E, García-Carrancá A, Gariglio P. Inhibition of RAD51 by siRNA and Resveratrol Sensitizes Cancer Stem Cells Derived from HeLa Cell Cultures to Apoptosis. *Stem Cells Int* (2018) 2018:1–11. doi: 10.1155/2018/2493869
26. Zhang X. Resveratrol reverses temozolomide resistance by downregulation of MGMT in T98G glioblastoma cells by the NF-κB-dependent pathway. *Oncol Rep* (2012) 27:2050–6. doi: 10.3892/or.2012.1715
27. Chen Y-A, Lien H-M, Kao M-C, Lo U-G, Lin L-C, Lin C-J, et al. Sensitization of Radioresistant Prostate Cancer Cells by Resveratrol Isolated from Arachis hypogaea Stems. *PloS One* (2017) 12:e0169204. doi: 10.1371/journal.pone.0169204
28. Wang L, Long L, Wang W, Liang Z. Resveratrol, a potential radiation sensitizer for glioma stem cells both in vitro and in vivo. *J Pharmacol Sci* (2015) 129:216–25. doi: 10.1016/j.jphs.2015.11.001
29. Vendrely V, Amintas S, Noel C, Moranvillier I, Lamrissi I, Rousseau B, et al. Combination treatment of resveratrol and capsaicin radiosensitizes pancreatic tumor cells by unbalancing DNA repair response to radiotherapy towards cell death. *Cancer Lett* (2019) 451:1–10. doi: 10.1016/j.canlet.2019.02.038
30. Das D, Preet R, Mohapatra P, Satapathy SR, Kundu CN. 1,3-Bis(2-chloroethyl)-1-nitrosourea enhances the inhibitory effect of Resveratrol on 5-fluorouracil sensitive/resistant colon cancer cells. *World J Gastroenterol* (2013) 19:7374. doi: 10.3748/wjg.v19.i42.7374
31. Mohapatra P, Satapathy SR, Das D, Siddharth S, Choudhuri T, Kundu CN. Resveratrol mediated cell death in cigarette smoke transformed breast epithelial cells is through induction of p21Waf1/Cip1 and inhibition of long patch base excision repair pathway. *Toxicol Appl Pharmacol* (2014) 275:221–31. doi: 10.1016/j.taap.2014.01.011
32. Yang S. Alterations in the expression of the apurinic/apyrimidinic endonuclease-1/redox factor-1 (APE/Ref-1) in human melanoma and identification of the therapeutic potential of resveratrol as an APE/Ref-1 inhibitor. *Mol Cancer Ther* (2005) 4:1923–35. doi: 10.1158/1535-7163.MCT-05-0229
33. Devassy JG, Nwachukwu ID, Jones PJH. Curcumin and cancer: barriers to obtaining a health claim. *Nutr Rev* (2015) 73:155–65. doi: 10.1093/nutrit/nuu064
34. Roy M, Sinha D, Mukherjee S, Biswas J. Curcumin prevents DNA damage and enhances the repair potential in a chronically arsenic-exposed human population in West Bengal, India. *Eur J Cancer Prev* (2011) 20:123–31. doi: 10.1097/CEJ.0b013e328341017a
35. Tsai K-D, Lin J-C, Yang S, Tseng M-J, Hsu J-D, Lee Y-J, et al. Curcumin Protects against UVB-Induced Skin Cancers in SKH-1 Hairless Mouse: Analysis of Early Molecular Markers in Carcinogenesis. *Evid Based Complement Altern Med* (2012) 2012:1–11. doi: 10.1155/2012/593952
36. Ogiwara H, Ui A, Shiotani B, Zou L, Yasui A, Kohno T. Curcumin suppresses multiple DNA damage response pathways and has potency as a sensitizer to PARP inhibitor. *Carcinogenesis* (2013) 34:2486–97. doi: 10.1093/carcin/bgt240
37. Sahu RP, Batra S, Srivastava SK. Activation of ATM/Chk1 by curcumin causes cell cycle arrest and apoptosis in human pancreatic cancer cells. *Br J Cancer* (2009) 100:1425–33. doi: 10.1038/sj.bjc.6605039
38. Jiang Z, Jin S, Yalowich JC, Brown KD, Rajasekaran B. The Mismatch Repair System Modulates Curcumin Sensitivity through Induction of DNA Strand Breaks and Activation of G2-M Checkpoint. *Mol Cancer Ther* (2010) 9:558–68. doi: 10.1158/1535-7163.MCT-09-0627
39. Tong R, Wu X, Liu Y, Liu Y, Zhou J, Jiang X, et al. Curcumin-Induced DNA Demethylation in Human Gastric Cancer Cells Is Mediated by the DNA-Damage Response Pathway. *Oxid Med Cell Longev* (2020) 2020:1–13. doi: 10.1155/2020/2543504
40. Al-Yousef N, Shinwari Z, Al-Shahrani B, Al-Showimi M, Al-Moghrabi N. Curcumin induces re−expression of BRCA1 and suppression of γ synuclein by modulating DNA promoter methylation in breast cancer cell lines. *Oncol Rep* (2020) 43:827–38. doi: 10.3892/or.2020.7473
41. Guney Eskiler G, Sahin E, Deveci Ozkan A, Cilingir Kaya OT, Kaleli S. Curcumin induces DNA damage by mediating homologous recombination mechanism in triple negative breast cancer. *Nutr Cancer* (2020) 72:1057–66. doi: 10.1080/01635581.2019.1670216
42. Chen B, Zhang Y, Wang Y, Rao J, Jiang X, Xu Z. Curcumin inhibits proliferation of breast cancer cells through Nrf2-mediated down-regulation of Fen1 expression. *J Steroid Biochem Mol Biol* (2014) 143:11–8. doi: 10.1016/j.jsbmb.2014.01.009
43. Ting C-Y, Wang H-E, Yu C-C, Liu H-C, Liu Y-C, Chiang I-T. Curcumin Triggers DNA Damage and Inhibits Expression of DNA Repair Proteins in Human Lung Cancer Cells. *Anticancer Res* (2015) 35:3867–73.
44. Shang H-S, Chang C-H, Chou Y-R, Yeh M-Y, Au M-K, Lu H-F, et al. Curcumin causes DNA damage and affects associated protein expression in HeLa human cervical cancer cells. *Oncol Rep* (2016) 36:2207–15. doi: 10.3892/or.2016.5002
45. Zhao Q, Guan J, Qin Y, Ren P, Zhang Z, Lv J, et al. Curcumin sensitizes lymphoma cells to DNA damage agents through regulating

Rad51-dependent homologous recombination. *BioMed Pharmacother* (2018) 97:115–9. doi: 10.1016/j.biopha.2017.09.078
46. Choi YE, Park E. Curcumin enhances poly(ADP-ribose) polymerase inhibitor sensitivity to chemotherapy in breast cancer cells. *J Nutr Biochem* (2015) 26:1442–7. doi: 10.1016/j.jnutbio.2015.07.015
47. Tung C-L, Jian Y-J, Chen J-C, Wang T-J, Chen W-C, Zheng H-Y, et al. Curcumin downregulates p38 MAPK-dependent X-ray repair cross-complement group 1 (XRCC1) expression to enhance cisplatin-induced cytotoxicity in human lung cancer cells. *Naunyn Schmiedebergs Arch Pharmacol* (2016) 389:657–66. doi: 10.1007/s00210-016-1235-5
48. Tsai M-S, Weng S-H, Kuo Y-H, Chiu Y-F, Lin Y-W. Synergistic Effect of Curcumin and Cisplatin via Down-Regulation of Thymidine Phosphorylase and Excision Repair Cross-Complementary 1 (ERCC1). *Mol Pharmacol* (2011) 80:136–46. doi: 10.1124/mol.111.071316
49. Ko J-C, Tsai M-S, Weng S-H, Kuo Y-H, Chiu Y-F, Lin Y-W. Curcumin enhances the mitomycin C-induced cytotoxicity via downregulation of MKK1/2–ERK1/2-mediated Rad51 expression in non-small cell lung cancer cells. *Toxicol Appl Pharmacol* (2011) 255:327–38. doi: 10.1016/j.taap.2011.07.012
50. Chen X, Wang J, Fu Z, Zhu B, Wang J, Guan S, et al. Curcumin activates DNA repair pathway in bone marrow to improve carboplatin-induced myelosuppression. *Sci Rep* (2017) 7:17724. doi: 10.1038/s41598-017-16436-9
51. Nayak D, Tripathi N, Kathuria D, Siddharth S, Nayak A, Bharatam PV, et al. Quinacrine and curcumin synergistically increased the breast cancer stem cells death by inhibiting ABCG2 and modulating DNA damage repair pathway. *Int J Biochem Cell Biol* (2020) 119:105682. doi: 10.1016/j.biocel.2019.105682
52. Chen P, Li J, Jiang H-G, Lan T, Chen Y-C. Curcumin reverses cisplatin resistance in cisplatin-resistant lung caner cells by inhibiting FA/BRCA pathway. *Tumour Biol* (2015) 36:3591–9. doi: 10.1007/s13277-014-2996-4
53. Xiao H, Xiao Q, Zhang K, Zuo X, Shrestha UK. Reversal of multidrug resistance by curcumin through FA/BRCA pathway in multiple myeloma cell line MOLP-2/R. *Ann Hematol* (2010) 89:399–404. doi: 10.1007/s00277-009-0831-6
54. Yang G, Qiu J, Wang D, Tao Y, Song Y, Wang H, et al. Traditional Chinese Medicine Curcumin Sensitizes Human Colon Cancer to Radiation by Altering the Expression of DNA Repair-related Genes. *Anticancer Res* (2018) 38:131–6. doi: 10.21873/anticanres.12200
55. Molla S, Hembram KC, Chatterjee S, Nayak D, Sethy C, Pradhan R, et al. PARP inhibitor Olaparib Enhances the Apoptotic Potentiality of Curcumin by Increasing the DNA Damage in Oral Cancer Cells through Inhibition of BER Cascade. *Pathol Oncol Res* (2019) 26(4):2091–103. doi: 10.1007/s12253-019-00768-0
56. Chu C, Deng J, Man Y, Qu Y. Green Tea Extracts Epigallocatechin-3-gallate for Different Treatments. *BioMed Res Int* (2017) 2017:1–9. doi: 10.1155/2017/5615647
57. Min K-J, Kwon TK. Anticancer effects and molecular mechanisms of epigallocatechin-3-gallate. *Integr Med Res* (2014) 3:16–24. doi: 10.1016/j.imr.2013.12.001
58. Heyza J, Arora S, Zhang H, Conner K, Lei W, Floyd A, et al. Targeting the DNA Repair Endonuclease ERCC1-XPF with Green Tea Polyphenol Epigallocatechin-3-Gallate (EGCG) and Its Prodrug to Enhance Cisplatin Efficacy in Human Cancer Cells. *Nutrients* (2018) 10:1644. doi: 10.3390/nu10111644
59. Xie C-R, You C-G, Zhang N, Sheng H-S, Zheng X-S. Epigallocatechin Gallate Preferentially Inhibits O 6 -Methylguanine DNA-Methyltransferase Expression in Glioblastoma Cells Rather than in Nontumor Glial Cells. *Nutr Cancer* (2018) 70:1339–47. doi: 10.1080/01635581.2018.1539189
60. Glei M, Pool-Zobel BL. The main catechin of green tea, (–)-epigallocatechin-3-gallate (EGCG), reduces bleomycin-induced DNA damage in human leucocytes. *Toxicol In Vitro* (2006) 20:295–300. doi: 10.1016/j.tiv.2005.08.002
61. Arimoto-Kobayashi S, Inada N, Sato Y, Sugiyama C, Okamoto K, Hayatsu H, et al. Inhibitory Effects of (–)-Epigallocatechin Gallate on the Mutation, DNA Strand Cleavage, and DNA Adduct Formation by Heterocyclic Amines. *J Agric Food Chem* (2003) 51:5150–3. doi: 10.1021/jf0302761
62. Li X-J, Jiang Z-Z, Zhang L. Triptolide: Progress on research in pharmacodynamics and toxicology. *J Ethnopharmacol* (2014) 155:67–79. doi: 10.1016/j.jep.2014.06.006
63. Titov DV, Gilman B, He Q-L, Bhat S, Low W-K, Dang Y, et al. XPB, a subunit of TFIIH, is a target of the natural product triptolide. *Nat Chem Biol* (2011) 7:182–8. doi: 10.1038/nchembio.522
64. Deng Y, Li F, He P, Yang Y, Yang J, Zhang Y, et al. Triptolide sensitizes breast cancer cells to Doxorubicin through the DNA damage response inhibition. *Mol Carcinog* (2018) 57:807–14. doi: 10.1002/mc.22795
65. Chueh F-S, Chen Y-L, Hsu S-C, Yang J-S, Hsueh S-C, Ji B-C, et al. Triptolide induced DNA damage in A375.S2 human malignant melanoma cells is mediated via reduction of DNA repair genes. *Oncol Rep* (2013) 29:613–8. doi: 10.3892/or.2012.2170
66. Guan J, Zhao Q, Lv J, Zhang Z, Sun S, Mao W. Triptolide induces DNA breaks, activates caspase-3-dependent apoptosis and sensitizes B-cell lymphoma to poly(ADP-ribose) polymerase 1 and phosphoinositide 3-kinase inhibitors. *Oncol Lett* (2017) 14:4965–70. doi: 10.3892/ol.2017.6771
67. Zhao H, Shi P, Deng M, Jiang Z, Li Y, Kannappan V, et al. Low dose triptolide reverses chemoresistance in adult acute lymphoblastic leukemia cells via reactive oxygen species generation and DNA damage response disruption. *Oncotarget* (2016) 7:85515–28. doi: 10.18632/oncotarget.13454
68. Zhang Z, Sun C, Zhang L, Chi X, Ji J, Gao X, et al. Triptolide interferes with XRCC1/PARP1-mediated DNA repair and confers sensitization of triple-negative breast cancer cells to cisplatin. *BioMed Pharmacother* (2019) 109:1541–6. doi: 10.1016/j.biopha.2018.11.008
69. Wang G, Wang X, Xu X. Triptolide potentiates lung cancer cells to cisplatin-induced apoptosis by selectively inhibiting the NER activity. *Biomark Res* (2015) 3:17. doi: 10.1186/s40364-015-0043-2
70. Modi S, Kir D, Giri B, Majumder K, Arora N, Dudeja V, et al. Minnelide Overcomes Oxaliplatin Resistance by Downregulating the DNA Repair Pathway in Pancreatic Cancer. *J Gastrointest Surg* (2016) 20:13–24. doi: 10.1007/s11605-015-3000-3
71. Li Y, Yao J, Han C, Yang J, Chaudhry M, Wang S, et al. Quercetin, Inflammation and Immunity. *Nutrients* (2016) 8:167. doi: 10.3390/nu8030167
72. Anand David A, Arulmoli R, Parasuraman S. Overviews of biological importance of quercetin: A bioactive flavonoid. *Pharmacogn Rev* (2016) 10:84. doi: 10.4103/0973-7847.194044
73. Darband SG, Sadighparvar S, Yousefi B, Kaviani M, Ghaderi-Pakdel F, Mihanfar A, et al. Quercetin attenuated oxidative DNA damage through NRF2 signaling pathway in rats with DMH induced colon carcinogenesis. *Life Sci* (2020) 253:117584. doi: 10.1016/j.lfs.2020.117584
74. Min K, Ebeler SE. Quercetin inhibits hydrogen peroxide-induced DNA damage and enhances DNA repair in Caco-2 cells. *Food Chem Toxicol* (2009) 47:2716–22. doi: 10.1016/j.fct.2009.07.033
75. Noori-Daloii MR, Momeny M, Yousefi M, Shirazi FG, Yaseri M, Motamed N, et al. Multifaceted preventive effects of single agent quercetin on a human prostate adenocarcinoma cell line (PC-3): implications for nutritional transcriptomics and multi-target therapy. *Med Oncol* (2011) 28:1395–404. doi: 10.1007/s12032-010-9603-3
76. Gong C, Yang Z, Zhang L, Wang Y, Gong W, Liu Y. Quercetin suppresses DNA double-strand break repair and enhances the radiosensitivity of human ovarian cancer cells via p53-dependent endoplasmic reticulum stress pathway. *Onco Targets Ther* (2017) 11:17–27. doi: 10.2147/OTT.S147316
77. Lin C, Yu Y, Zhao H, Yang A, Yan H, Cui Y. Combination of quercetin with radiotherapy enhances tumor radiosensitivity in vitro and in vivo. *Radiother Oncol* (2012) 104:395–400. doi: 10.1016/j.radonc.2011.10.023
78. Maeda J, Roybal EJ, Brents CA, Uesaka M, Aizawa Y, Kato TA. Natural and glucosyl flavonoids inhibit poly(ADP-ribose) polymerase activity and induce synthetic lethality in BRCA mutant cells. *Oncol Rep* (2014) 31:551–6. doi: 10.3892/or.2013.2902
79. Song D, Hao J, Fan D. Biological properties and clinical applications of berberine. *Front Med* (2020) 14(5):564–82. doi: 10.1007/s11684-019-0724-6
80. Hou D, Xu G, Zhang C, Li B, Qin J, Hao X, et al. Berberine induces oxidative DNA damage and impairs homologous recombination repair in ovarian cancer cells to confer increased sensitivity to PARP inhibition. *Cell Death Dis* (2017) 8:e3070–0. doi: 10.1038/cddis.2017.471
81. Liu Z, Liu Q, Xu B, Wu J, Guo C, Zhu F, et al. Berberine induces p53-dependent cell cycle arrest and apoptosis of human osteosarcoma cells by inflicting DNA damage. *Mutat Res Mol Mech Mutagen* (2009) 662:75–83. doi: 10.1016/j.mrfmmm.2008.12.009

82. Wang J, Liu Q, Yang Q. Radiosensitization effects of berberine on human breast cancer cells. *Int J Mol Med* (2012) 30:1166–72. doi: 10.3892/ijmm.2012.1095
83. Liu Q, Jiang H, Liu Z, Wang Y, Zhao M, Hao C, et al. Berberine Radiosensitizes Human Esophageal Cancer Cells by Downregulating Homologous Recombination Repair Protein RAD51. *PloS One* (2011) 6: e23427. doi: 10.1371/journal.pone.0023427
84. Gao X, Wang J, Li M, Wang J, Lv J, Zhang L, et al. Berberine attenuates XRCC1-mediated base excision repair and sensitizes breast cancer cells to the chemotherapeutic drugs. *J Cell Mol Med* (2019) 23:6797–804. doi: 10.1111/jcmm.14560
85. Mukund V, Mukund D, Sharma V, Mannarapu M, Alam A. Genistein: Its role in metabolic diseases and cancer. *Crit Rev Oncol Hematol* (2017) 119:13–22. doi: 10.1016/j.critrevonc.2017.09.004
86. Moore JO, Wang Y, Stebbins WG, Gao D, Zhou X, Phelps R, et al. Photoprotective effect of isoflavone genistein on ultraviolet B-induced pyrimidine dimer formation and PCNA expression in human reconstituted skin and its implications in dermatology and prevention of cutaneous carcinogenesis. *Carcinogenesis* (2006) 27:1627–35. doi: 10.1093/carcin/bgi367
87. Cabanes A. Prepubertal estradiol and genistein exposures up-regulate BRCA1 mRNA and reduce mammary tumorigenesis. *Carcinogenesis* (2003) 25:741–8. doi: 10.1093/carcin/bgh065
88. Liu X, Li P, Hirayama R, Niu Y, Liu X, Chen W, et al. Genistein sensitizes glioblastoma cells to carbon ions via inhibiting DNA-PKcs phosphorylation and subsequently repressing NHEJ and delaying HR repair pathways. *Radiother Oncol* (2018) 129:84–94. doi: 10.1016/j.radonc.2018.04.005
89. Liu XX, Sun C, Jin XD, Li P, Zheng XG, Zhao T, et al. Genistein sensitizes sarcoma cells in vitro and in vivo by enhancing apoptosis and by inhibiting DSB repair pathways. *J Radiat Res* (2016) 57:227–37. doi: 10.1093/jrr/rrv091
90. Tang Q, Ma J, Sun J, Yang L, Yang F, Zhang W, et al. Genistein and AG1024 synergistically increase the radiosensitivity of prostate cancer cells. *Oncol Rep* (2018) 40:579–88. doi: 10.3892/or.2018.6468
91. Wang G, Zhang D, Yang S, Wang Y, Tang Z, Fu X. Co-administration of genistein with doxorubicin-loaded polypeptide nanoparticles weakens the metastasis of malignant prostate cancer by amplifying oxidative damage. *Biomater Sci* (2018) 6:827–35. doi: 10.1039/C7BM01201B
92. Song L, Ma L, Cong F, Shen X, Jing P, Ying X, et al. Radioprotective effects of genistein on HL-7702 cells via the inhibition of apoptosis and DNA damage. *Cancer Lett* (2015) 366:100–11. doi: 10.1016/j.canlet.2015.06.008
93. Gurung RL, Lim SN, Khaw AK, Soon JFF, Shenoy K, Mohamed Ali S, et al. Thymoquinone Induces Telomere Shortening, DNA Damage and Apoptosis in Human Glioblastoma Cells. *PloS One* (2010) 5:e12124. doi: 10.1371/journal.pone.0012124
94. Gowda ASP, Suo Z, Spratt TE. Honokiol Inhibits DNA Polymerases β and λ and Increases Bleomycin Sensitivity of Human Cancer Cells. *Chem Res Toxicol* (2017) 30:715–25. doi: 10.1021/acs.chemrestox.6b00451
95. Çetin A, Biltekin B, Degirmencioglu S. Ellagic Acid Enhances the Antitumor Efficacy of Bevacizumab in an In Vitro Glioblastoma Model. *World Neurosurg* (2019) 132:e59–65. doi: 10.1016/j.wneu.2019.08.257
96. Gao H, Xue J, Zhou L, Lan J, He J, Na F, et al. Bevacizumab radiosensitizes non-small cell lung cancer xenografts by inhibiting DNA double-strand break repair in endothelial cells. *Cancer Lett* (2015) 365:79–88. doi: 10.1016/j.canlet.2015.05.011
97. Wang G-Z, Liu Y-Q, Cheng X, Zhou G-B. Celastrol induces proteasomal degradation of FANCD2 to sensitize lung cancer cells to DNA crosslinking agents. *Cancer Sci* (2015) 106:902–8. doi: 10.1111/cas.12679
98. Xu M-D, Liu S-L, Zheng B-B, Wu J, Wu M-Y, Zhang Y, et al. The radiotherapy-sensitization effect of cantharidin: Mechanisms involving cell cycle regulation, enhanced DNA damage, and inhibited DNA damage repair. *Pancreatology* (2018) 18:822–32. doi: 10.1016/j.pan.2018.08.007
99. Hsia T-C, Lin J-H, Hsu S-C, Tang N-Y, Lu H-F, Wu S-H, et al. Cantharidin induces DNA damage and inhibits DNA repair-associated protein levels in NCI-H460 human lung cancer cells. *Environ Toxicol* (2015) 30:1135–43. doi: 10.1002/tox.21986
100. Oike T, Ogiwara H, Torikai K, Nakano T, Yokota J, Kohno T. Garcinol, a Histone Acetyltransferase Inhibitor, Radiosensitizes Cancer Cells by Inhibiting Non-Homologous End Joining. *Int J Radiat Oncol* (2012) 84:815–21. doi: 10.1016/j.ijrobp.2012.01.017
101. Lagunas-Rangel FA. Current role of mammalian sirtuins in DNA repair. *DNA Repair (Amst)* (2019) 80:85–92. doi: 10.1016/j.dnarep.2019.06.009
102. Park Y, Choi J, Lim JW, Kim H. β-Carotene-induced apoptosis is mediated with loss of Ku proteins in gastric cancer AGS cells. *Genes Nutr* (2015) 10:17. doi: 10.1007/s12263-015-0467-1
103. Palomera-Sanchez Z, Watson GW, Wong CP, Beaver LM, Williams DE, Dashwood RH, et al. The phytochemical 3,3′-diindolylmethane decreases expression of AR-controlled DNA damage repair genes through repressive chromatin modifications and is associated with DNA damage in prostate cancer cells. *J Nutr Biochem* (2017) 47:113–9. doi: 10.1016/j.jnutbio.2017.05.005
104. Wu L-Y, Lu H-F, Chou Y-C, Shih Y-L, Bau D-T, Chen J-C, et al. Kaempferol Induces DNA Damage and Inhibits DNA Repair Associated Protein Expressions in Human Promyelocytic Leukemia HL-60 Cells. *Am J Chin Med* (2015) 43:365–82. doi: 10.1142/S0192415X1550024X
105. Tjioe KC, Tostes Oliveira D, Gavard J. Luteolin Impacts on the DNA Damage Pathway in Oral Squamous Cell Carcinoma. *Nutr Cancer* (2016) 68:838–47. doi: 10.1080/01635581.2016.1180411
106. Leung HW-C, Wu C-H, Lin C-H, Lee H-Z. Luteolin induced DNA damage leading to human lung squamous carcinoma CH27 cell apoptosis. *Eur J Pharmacol* (2005) 508:77–83. doi: 10.1016/j.ejphar.2004.12.032
107. Lacombe J, Cretignier T, Meli L, Wijeratne EMK, Veuthey J-L, Cuendet M, et al. Withanolide D Enhances Radiosensitivity of Human Cancer Cells by Inhibiting DNA Damage Non-homologous End Joining Repair Pathway. *Front Oncol* (2020) 9:1468. doi: 10.3389/fonc.2019.01468
108. Huang D, Jin L, Li Z, Wu J, Zhang N, Zhou D, et al. Isoorientin triggers apoptosis of hepatoblastoma by inducing DNA double-strand breaks and suppressing homologous recombination repair. *BioMed Pharmacother* (2018) 101:719–28. doi: 10.1016/j.biopha.2018.02.142
109. Zhang L, Zhang F, Zhang W, Chen L, Gao N, Men Y, et al. Harmine suppresses homologous recombination repair and inhibits proliferation of hepatoma cells. *Cancer Biol Ther* (2015) 16:1585–92. doi: 10.1080/15384047.2015.1078021
110. Choi YE, Park E. Ferulic acid in combination with PARP inhibitor sensitizes breast cancer cells as chemotherapeutic strategy. *Biochem Biophys Res Commun* (2015) 458:520–4. doi: 10.1016/j.bbrc.2015.01.147
111. Chen J-C, Ko J-C, Yen T-C, Chen T-Y, Lin Y-C, Ma P-F, et al. Capsaicin enhances erlotinib-induced cytotoxicity via AKT inactivation and excision repair cross-complementary 1 (ERCC1) down-regulation in human lung cancer cells. *Toxicol Res (Camb)* (2019) 8:459–70. doi: 10.1039/C8TX00346G
112. Li L, Wang H, Yang ES, Arteaga CL, Xia F. Erlotinib Attenuates Homologous Recombinational Repair of Chromosomal Breaks in Human Breast Cancer Cells. *Cancer Res* (2008) 68:9141–6. doi: 10.1158/0008-5472.CAN-08-1127
113. Zhang L, Peng Y, Uray IP, Shen J, Wang L, Peng X, et al. Natural product β-thujaplicin inhibits homologous recombination repair and sensitizes cancer cells to radiation therapy. *DNA Repair (Amst)* (2017) 60:89–101. doi: 10.1016/j.dnarep.2017.10.009
114. Liu Y, Yue C, Li J, Wu J, Wang S, Sun D, et al. Enhancement of cisplatin cytotoxicity by Retigeric acid B involves blocking DNA repair and activating DR5 in prostate cancer cells. *Oncol Lett* (2017) 15:2871–80. doi: 10.3892/ol.2017.7664
115. Paller CJ, Denmeade SR, Carducci MA. Challenges of conducting clinical trials of natural products to combat cancer. *Clin Adv Hematol Oncol* (2016) 14:447–55.

Conflict of Interest: The authors declare that the research was conducted in the absence of any commercial or financial relationships that could be construed as a potential conflict of interest.

frontiers in Oncology

CASE REPORT
published: 27 November 2020
doi: 10.3389/fonc.2020.567289

Case Report: BAP1 Mutation and RAD21 Amplification as Predictive Biomarkers to PARP Inhibitor in Metastatic Intrahepatic Cholangiocarcinoma

Francesco Sabbatino[1,2], Luigi Liguori[3], Umberto Malapelle[4], Francesca Schiavi[5], Vincenzo Tortora[3], Valeria Conti[1,6], Amelia Filippelli[1,6], Giampaolo Tortora[7], Cristina R. Ferrone[8] and Stefano Pepe[1,2]*

[1] Department of Medicine, Surgery and Dentistry "Scuola Medica Salernitana", University of Salerno, Salerno, Italy, [2] Oncology Unit, University Hospital San Giovanni di Dio e Ruggi D'Aragona, Salerno, Italy, [3] Department of Clinical Medicine and Surgery, University of Naples "Federico II", Naples, Italy, [4] Public Health, University of Naples "Federico II", Naples, Italy, [5] Familial Cancer Clinic and Oncoendocrinology, Veneto Institute of Oncology IOV–IRCCS, Padua, Italy, [6] Clinical Pharmacology and Pharmacogenetics Unit, University Hospital "San Giovanni di Dio e Ruggi D'Aragona", Salerno, Italy, [7] Oncologia Unit, Fondazione Policlinico Universitario A. Gemelli IRCCS, Università Cattolica Del Sacro Cuore, Roma, Italy, [8] Department of Surgery, Massachusetts General Hospital, Harvard Medical School, Boston, MA, United States

OPEN ACCESS

Edited by:
Rosa Maria Bermudez-Cruz, National Polytechnic Institute of Mexico (CINVESTAV), Mexico

Reviewed by:
Mohamed H. Abdel-Rahman, The Ohio State University, United States
Giovanni Gaudino, Retired, Bellinzona, Switzerland
David Y. Lee, University of New Mexico, United States

***Correspondence:**
Francesco Sabbatino
fsabbatino@unisa.it

Specialty section:
This article was submitted to Molecular and Cellular Oncology, a section of the journal Frontiers in Oncology

Received: *29 May 2020*
Accepted: *30 October 2020*
Published: *27 November 2020*

Citation:
Sabbatino F, Liguori L, Malapelle U, Schiavi F, Tortora V, Conti V, Filippelli A, Tortora G, Ferrone CR and Pepe S (2020) Case Report: BAP1 Mutation and RAD21 Amplification as Predictive Biomarkers to PARP Inhibitor in Metastatic Intrahepatic Cholangiocarcinoma. Front. Oncol. 10:567289. doi: 10.3389/fonc.2020.567289

Introduction: Intrahepatic cholangiocarcinoma (ICC) is a rare hepatobiliary cancer characterized by a poor prognosis and a limited response to conventional therapies. Currently chemotherapy is the only therapeutic option for patients with Stage IV ICC. Due to the poor response rate, there is an urgent need to identify novel molecular targets to develop novel effective therapies. Precision oncology tests utilizing targeted next-generation sequencing (NGS) platforms have rapidly entered into clinical practice. Profiling the genome and transcriptome of cancer to identify potentially targetable oncogenic pathways may guide the clinical care of the patient.

Case presentation: We present a 56-year-old male patient affected with metastatic ICC, whose cancer underwent several precision oncology tests by different NGS platforms. A novel BAP1 mutation (splice site c.581-17_585del22) and a RAD21 amplification were identified by a commercial available platform on a metastatic lesion. No germline BAP1 mutations were identified. Several lines of evidences indicate that PARP inhibitor administration might be an effective treatment in presence of BAP1 and/or RAD21 alterations since both BAP1 and RAD21 are involved in the DNA repair pathway, BAP1 interacts with BRCA1 and BRCA1-mediated DNA repair pathway alterations enhance the sensitivity to PARP inhibitor administration. In this case, after failing conventional therapies, patient was treated with PARP inhibitor olaparib. The patient had a partial response according to RECIST criteria with an overall survival of 37.2 months from the time of diagnosis of his ICC. Following 11.0 months on olaparib treatment, sustained stable disease control is ongoing. The patient is still being treated with olaparib and no significant toxicity has been reported.

Conclusion: These findings have clinical relevance since we have shown PARP inhibitor as a potential treatment for ICC patients harboring BAP1 deletion and RAD21 amplification. We have also highlighted the utility of NGS platforms to identify targetable mutations within a cancer.

Keywords: BAP1, precision oncology, cholangio carcinoma, Poly ADP ribose polymerase (PARP) inhibitor, RAD21, olaparib

INTRODUCTION

Cholangiocarcinoma (CCA) is historically classified by location into intrahepatic, perihilar (or Klatskintumor) and distal cancers. Intrahepatic cholangiocarcinoma (ICC) is the second most common primary intrahepatic tumor, with an estimated incidence of 1.6 per 100,000/year in the United States (1). Unfortunately, ICC carries an extremely poor prognosis with an overall 5-year survival of 5–15% (1). For patients with early stage ICC, surgical resection of the cancer and removal of local lymph nodes remains the only curative option (2). However, even with a complete resection, most patients succumb to both loco-regional and distant metastases (3). Unfortunately, most patients present with advanced disease. Palliative chemotherapy is of limited efficacy (4), highlighting the urgent need for novel effective therapies.

Different cancers express different oncogenic alterations which drive tumor progression. Several lines of evidences demonstrate that some of these alterations can be effectively targeted by tailored targeted agents, improving the overall survival of treated patients (5). These results have increased the use of precision oncology tests by targeted next-generation sequencing (NGS) platforms into clinical practice, to inform clinicians in making appropriate therapeutic decisions (6). Unselected ICC patients have been often included in "basket" trials (7), most of which have unfortunately failed to demonstrate a clinical benefit (7). As a result, there is a high interest to identifying oncogenic alterations in ICC to design potentially effective strategies in biomarker-enriched populations.

NGS of ICC has already allowed identification of molecular alterations which are involved in ICC carcinogenesis such as those in *KRAS*, *BRAF*, *IDH1, IDH2*, *EGFR*, *FGFR2*, *ROS1*, *ARID1A*, *PBRM1*, *BRCA1*, and *BAP1* (8–16). FGFR kinase inhibitors have demonstrated anti-tumor activity in ICC patients harboring activating FGFR2 gene fusions (17–19). However, no effective therapeutic strategies have currently changed the standard of care of ICC patients harboring different types of alterations.

Here, we describe the case of a chemorefractory patient with ICC harboring BAP1 mutation and RAD21 amplification. The patient was successfully treated with the PARP inhibitor olaparib.

CASE PRESENTATION

In March 2017, a 56-year-old Caucasian male was admitted to San Giovanni di Dio and Ruggi D'Aragona University Hospital for mild abdominal pain and nausea. The patient's past medical history included i) Hodgkin's lymphoma of the spleen in 1987, treated with splenectomy and radiotherapy; ii) myocardial infarction in 2006, treated with coronary angioplasty; and iii) myocardial infarction in 2012, treated with multiple coronary artery bypass grafting. He was also a former-smoker. Patient did not present with any ICC risk factors including biliary lithiasis, alcoholic liver disease, chronic hepatitis B or C infections, or primary sclerosing cholangitis. His family history was negative for any inherited-familial cancers. Abdominal ultrasound and computed tomography (CT) scan revealed a 10 cm intrahepatic lesion in the left lobe of the liver, as well as stable right basal lung thickening (**Figure 1A**). The latter was already described in a previous chest CT scan. Ultrasound guided biopsy of the liver mass demonstrated ICC (CK7+, CK19+, HepPar1-, AFP-). In April 2017, the patient underwent a left hepatectomy and sub-total gastrectomy and cholecystectomy. Histological examination demonstrated a Stage II ICC with vascular invasion [TNM staging, American Joint Committee on Cancer (AJCC) 8th edition]. Post operatively he was seen by the multidisciplinary team. Genomic analysis of *NRAS*, *KRAS* and *BRAF V600* by polymerase chain reaction (PCR) sequencing, as well as immunohistochemical (IHC) staining for detection of HER2 amplification were performed on ICC tumor tissue. Both analyses did not show any type of alteration (**Supplementary Table 1**). Further genomic testing of *EGFR* was performed by sanger sequencing, but no alterations were found in exons 18, 19, 20, and

Abbreviations: AFP, alpha fetoprotein; AJCC, American Joint Committee on Cancer; ARID1A, AT-rich interactive domain-containing protein 1A; ATM, ataxia-telangiectasia mutated; ATR, ataxia telangiectasia and Rad3-related protein; BAP1, BRCA1 associated protein 1; BRAF, v-raf murine sarcoma viral oncogene homolog B1; BRCA1, Breast cancer type 1 susceptibility protein; CCA, Cholangiocarcinoma; CDK12, Cyclin Dependent Kinase 12; CHEK1-CHEK2, Checkpoint kinase 1-2; CK7, Cytokeratin 7; CK19, Cytokeratin 19; CT, computed tomography; EGFR, Epidermal Growth Factor Receptor; EMA, European Medicines Agency; ERCC1, excision repair cross-complementation group 1; FANC, Fanconi anaemia complementation group; FDA, Food and Drug Administration; FEN1, Flap endonuclease 1; FFPE, formalin fixed paraffin embedded; FGFR2, Fibroblast Growth Factor Receptor 2; 5-FU, 5-fluorouracil; HepPar1, Hepatocyte Paraffin 1; HER2, Human epidermal growth factor receptor 2; HR, homologous recombination; ICC, Intrahepatic cholangiocarcinoma; IDH1/IDH2, Isocitrate Dehydrogenase 1/2; IHC, immunohistochemical; KRAS, Kirsten ras oncogene homolog; LOH, loss of heterozygosity; MSS, Microsatellite Stable; NBN, Nibrin; NGS, next-generation sequencing; NRAS, neuroblastoma; RAS, viral oncogene homolog; RPA1, Replication protein A 70 kDa DNA-binding subunit; NTRK, neurotrophic receptor tyrosine kinase 1; PARP, poly ADP ribose polymerase; PCR, polymerase chain reaction; PR, partial response; PBRM1, Polybromo 1; PCR, polymerase chain reaction; PD, progression of disease; POLB, DNA Polymerase Beta; PRKDC, Protein Kinase; DNA-Activated, Catalytic Subunit; PTA, percutaneous thermal ablation; RAD51-RAD54, radiation-repair genes 51–54; RECIST, Response evaluation criteria in solid tumors; ROS1, ROS proto-oncogene 1receptor tyrosine kinase; STR, Short Tandem Repeat.

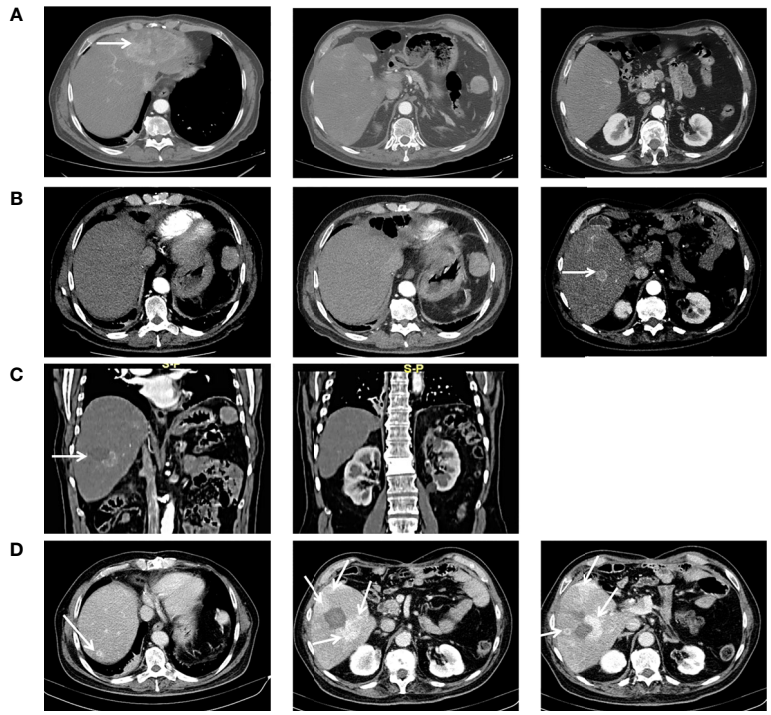

FIGURE 1 | Chest CT-scan performed at diagnosis in March 2017 **(A)**, in October 2017 following first relapse **(B)**, in February 2018 at tumor progression following first percutaneous thermal ablation **(C)**, in May 2018 at tumor progression following second percutaneous thermal ablation and before starting chemotherapy with cisplatin and gemcitabine **(D)**. Arrows indicate tumor lesion.

21 (**Supplementary Table 1**). In October 2017, a whole body CT scan demonstrated a 2.0 cm local recurrence in segment V of the liver (**Figure 1B**). Patient received a percutaneous thermal ablation (PTA) of the lesion. In February 2018, a whole body CT scan demonstrated a new 3.6 cm local recurrence in segment V of the liver, close to the previously treated lesion (**Figure 1C**) for which patient received a new PTA. In May 2018, a whole body CT scan demonstrated a new local recurrence in segment V of liver and multiple lesions in segment VII and VIII (**Figure 1D**). He then started a chemotherapeutic regimen with cisplatin (25 mg/m^2) followed by gemcitabine (1,000 mg/m^2), each administered on days 1 and 8 every 3 weeks. Due to his poor prognosis, patient requested additional testing of the ICC specimen. An IHC analysis of ROS1 rearrangements and NTRK fusions did not demonstrate any alterations (**Supplementary Table 2**). A Short Tandem Repeat (STR) analysis by PCR of *BAT25*, *BAT26*, *D2S123*, *D5S346*, *D17S250*, *NR-21*, and *MONO-27* showed a Microsatellite Stable (MSS) tumor profile. Lastly an IHC analysis of MSH2, MSH6, PMS2, and MLH1 demonstrated no alterations of the mismatch repair system (**Supplementary Table 2**). Following six cycles of cisplatin and gemcitabine, in September 2018, a whole-body CT scan demonstrated a stable disease (according to RECIST criteria v 1.1). The patient received an additional PTA of the lesions in segments V, VII, and VIII of the liver. In February 2019, the CT scan demonstrated progression of disease (PD) (according to RECIST criteria v 1.1) due to the development of multiple small lesions localized at the hepatic dome and around the area of previous PTA, long with a large bone metastasis to the 12th vertebral body and a left upper lobe pulmonary nodule (**Figure 2A**). Based on the availability of additional formalin fixed tumor tissue obtained from a novel tumor biopsy, three different NGS platform studies were requested by the patient: Oncomine Comprehensive Assay (implemented at Istituto Tumori Milano, Milan, Italy) (**Table 1**), Oncofocus test [Oncologica® UK ltd (Cambridge, UK)] (**Table 2**) and Foundation One CDx [Foundation Medicine (Cambridge, MA)] (**Table 3**). Both the Oncomine Comprehensive Assay and the Oncofocus test did not detect any alterations of analyzed genes. In contrast the Foundation One CDx demonstrated the presence of a deletion in *BAP1* (splice site c.581-17_585del22) and amplification of *RAD21*. Analysis of *BAP1* by sanger sequencing on primary ICC tumor tissue confirmed the presence of BAP1 (splice site 581-17_585del22) alteration (**Figure 3**). In contrast no alterations were identified in *BAP1* from nucleic acids extracted from buffy coat (**Figure 3**). Because of the involvement of RAD21 in the DNA repair pathway, the interaction of BAP1 with BRCA1 and the enhanced sensitivity to PARP inhibitor administration in presence of alterations in the BRCA1-mediated DNA repair pathway, it was decided first to treat the patient with FOLFIRI every 2 weeks [irinotecan 180 mg/m^2, folinic acid 400 mg/m^2, 5-fluorouracil (5-FU) 400 mg/m^2 intravenous infusion bolus, then 5-FU 2400 mg/m^2 intravenous infusion over 46 h] and then to start a PARP inhibitor. FOLFIRI is a conventional second-line chemotherapy regimen for ICC. In addition, irinotecan is a DNA-damaging agent. Following six cycles of FOLFIRI, in June 2019, a whole-body CT scan demonstrated PD (**Figure 2B**). A third-

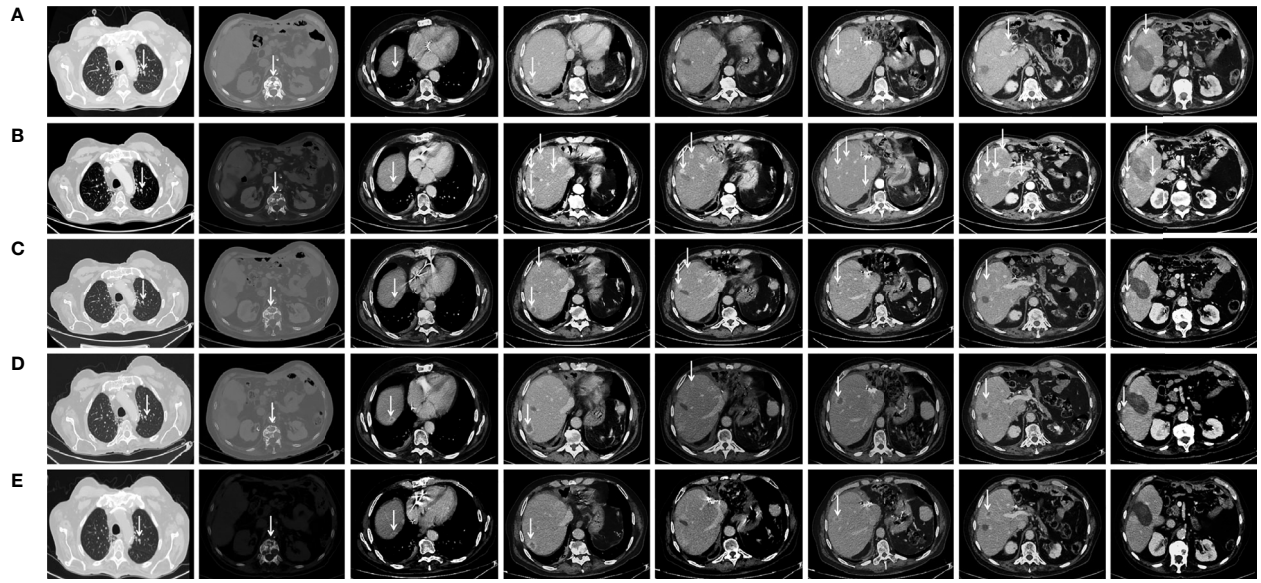

FIGURE 2 | Chest CT-scan performed at diagnosis in February 2019 at tumor progression following chemotherapy with cisplatin and gemcitabine and a third percutaneous thermal ablation and before to start treatment with FOLFIRI **(A)**, in June 2019 at tumor progression following six cycles of FOLFIRI administration and before to start treatment with olaparib **(B)**, in September 2019 following three cycles of olaparib **(C)**, in November 2019 following six cycles of olaparib **(D)**, and in February 2020 following 11 cycles of olaparib **(E)**. Arrows indicate tumor lesion.

TABLE 1 | Oncomine Comprehensive Assay.

March 1st, 2019								
NGS: Hot spot Cancer Panel with PGM (Personal Genome Machine) Ion Torrent technology [Thermo Fisher Scientific Life Technologies (Waltham, MA)]								
ABL1	AKT1	ALK	APC	ATM	BRAF	CDH1	CDKN2A	CSF1R
CTNNB1	EGFR	ERBB2	ERBB4	EZH2	FBXW7	FGFR1	FGFR2	FGFR3
FLT3	GNA11	GNAQ	GNAS	HNF1A	HRAS	IDH1	IDH2	JAK2
JAK3	KDR (VEGFR2)	KIT	KRAS	MET	MLH1	MPL	NOTCH1	NPM1
NRAS	PDGFRA	PIK3CA	PTEN	PTPN11	RB1	RET	SMAD4	SMARCB1
SMO	SRC	STK11	TP53	VHL				
Results: No hot spot mutations detected.								

line therapy of off-label use with the PARP inhibitor olaparib at 800 mg/die and palliative radiotherapy (10 Gy) on the vertebral lesion was begun. In September 2019, a whole-body CT scan demonstrated a partial response (PR) (**Figure 2C**). The latter was confirmed on successive restaging scans in November 2019 (**Figure 2D**) and February 2020 (**Figure 2E**). Following 11 cycles of olaparib, the progression free survival has been 11.0 months. Currently, the patient has an overall survival of 37.2 months from the time of diagnosis of his ICC and has continued treatment with olaparib. He is in good health conditions and no treatment-related adverse events have been reported.

DISCUSSION AND CONCLUSIONS

Novel effective therapies are urgently needed for metastatic ICC patients. The current clinical case has provided for the first-time evidence that ICC patients carrying a BAP1 deletion and RAD21 amplification might benefit from a PARP inhibitor treatment. *BAP1* is a tumor suppressor gene which modulates several pathways including cell death, cell differentiation, DNA damage response and gluconeogenesis (20–28). In mediating DNA damage response, BAP1 interacts with BRCA1 (20, 21). BRCA1 plays a key role in the DNA repair mechanism as well as in cell cycle regulation (29). Germline heterozygous mutations in *BAP1* cause an autosomal dominant condition known as BAP1-cancer syndrome which confers a high susceptibility to the development of several malignancies including mesothelioma, uveal melanoma, renal, cholangio and breast carcinomas (30–38). In the clinical case we have described, we identified a novel mutation in *BAP1* (c.581-17_585del22). The variant was somatic and not detected in the germline. We have examined several databases (Cosmic, GenBank, ClinVar) and c.581-17_585del22 mutation was not identified. Some literature data reported a similar deletion of *BAP1* with a pathogenic value (39, 40). Somatic mutations in *BAP1* are reported to drive

TABLE 2 | Oncofocus test.

March 2nd, 2019

NGS: Oncofocus test (Oncologica® UK ltd (Cambridge, UK)

A2M	ABCB5	ACACA	ACADM	ACBD5	ACTG2	ADAM32	ADAMTS16	AES	AFAP1	AFF3	AGAP3	AGBL4	AGGF1	AGK
AGTRAP	AHCYL1	AKAP12	AKAP13	AKAP9	AKT1	AKT2	AKT3	ALK	AP3B1	AR	ARAF	ARHGEF2	ARID1A	ARMC10
ARMT1	ASIC2	ATAD2	ATAD5	ATF7IP	ATG7	ATIC	ATM	ATP1B1	ATR	ATRNL1	ATRX	AXL	B4GALT1	BAG4
BAIAP2L1	BAP1	BBS9	BCAM	BCAN	BCL2L11	BCR	BEND5	BICC1	BICD2	BIN2	BIRC6	BRAF	BRCA1	BRCA2
BRD3	BRD4	BTAF1	BTBD1	BTF3L4	BTK	C11orf95	C7orf73	C8ORF34	C9orf153	CAD	CAND1	CAPRIN1	CAPZA2	CARS
CASP7	CBL	CCAR2	CCDC170	CCDC6	CCDC88A	CCDC91	CCND1	CCND2	CCND3	CCNE1	CCNY	CD44	CD74	CDC27
CDK12	CDK2	CDK4	CDK5RAP2	CDK6	CDKN1B	CDKN2A	CDKN2B	CEL	CEP85L	CEP89	CHD9	CHEK1	CHEK2	CHTOP
CIC	CIITA	CIT	CLCN6	CLIP1	CLIP2	CLIP4	CLTC	CNTLN	CNTRL	COL14A1	COX5A	CPSF6	CREB3L2	CREB5
CREBBP	CSF1R	CTNNB1	CUL1	CUX1	DAB2	DAB2IP	DCTN1	DDR2	DIP2C	DNAJB1	DTD1	DYM	DYNC1I2	DYNC2H1
EBF1	EGFR	EIF3E	ELAVL3	EML4	EPHB2	EPS15	ERBB2	ERBB3	ERBB4	ERC1	ERCC2	ERG	ERLIN2	ERP44
ERVK3_1	ESR1	ESRP1	ETV1	ETV4	ETV5	ETV6	EZH2	EZR	FAM114A2	FAM131B	FAM76A	FANCA	FANCD2	FANCI
FA1	FBXO28	FBXW7	FCHSD1	FGF3	FGFR1	FGFR19	FGFR1OP	FGFR1OP2	FGFR2	FGFR3	FGFR4	FGR	FP1L1	FKBP15
FLT3	FN1	FNDC3B	FOXL2	FOXP1	FXR1	FYCO1	GABBR2	GATA2	GATM	GFPT1	GHR	GIT2	GLIS3	GNA11
GNAI1	GNAQ	GNAS	GNS	GOLGA4	GOLGA5	GOLGB1	GOPC	GRB7	GRHL2	GTF2I	GTF2IRD1	GTF3C2	H3F3A	HACL1
HERPUD1	HIP1	HIST1H3B	HLA_A	HMGA2	NHNF1A	HOMER1	HOOK3	HRAS	IDH1	IDH2	IGF1R	IRF2BP2	JAK1	JAK2
JAK3	JAKMIP1	KANK1	KANK2	KCNQ5	KCTD1	KCTD7	KDELR2	KDM7A	KDR	KIAA1468	KIAA1549	KIAA1598	KIF5B	KIT
KLC1	KLHL7	KNSTRN	KRAS	KTN1	LMNA	LRIG3	LRRFIP1	LSM12	LSM14A	LYN	MACF1	MAD1L1	MAGOH	MAP2K1
MAP2K2	MAP2K4	MAPK1	MAX	MBIP	MCFD2	MDM2	MDM4	MED12	MEMO1	MET	MGEA5	MIR143HG	MKRN1	MLH1
MPRIP	MRE11A	MRPL24	MRPS33	MSH2	MSH6	MSN	MTFHD1L	MTMR12	MTOR	MYB	MYBL1	MYC	MYCL	MYCN
MYD88	MYH13	MYH9	MYO18A	MYO5A	MYRIP	MZT1	NACC2	NAV1	NBN	NCOA1	NCOA4	NCOR2	NDE1	NF1
NF2	NFASC	NFIB	NFKB2	NIN	NOL4	NOTCH1	NOTCH2	NOTCH3	NOTCH4	NPC2	NPM1	NRAS	NRG1	NSD1
NTM	NTRK1	NTRK2	NTRK3	NUB1	NUDCD3	NUP214	NUTM1	OFD1	OPHN1	OXR1	PALB2	PAPD7	PAPSS1	PARK2
PAX5	PAX8	PCDHGA1	PCM1	PCNX	PDE10A	PDE4DIP	PDE7A	PDGFRA	PDGFRB	PDHX	PDP1	PDZRN3	PHEB	PIK3CA
PIK3CB	PIK3R1	PLAG1	PLIN3	PMS2	POLE	POLH	PPARG	PPFIBP1	PPHLN1	PPL	PPM1G	PPP2R1A	PPP4R3B	PRKACA
PRKACB	PRKAR1A	PRKG2	PSMD11	PSPH	PTCH1	PTEN	PTPN11	PTPN3	PTPRK	PTPRZ1	PWWP2A	QKI	RABEP1	RABGAP1L
RAC1	RAD18	RAD50	RAD51	RAD51B	RAD51C	RAD51D	RAF1	RANBP2	RB1	RBMS3	RBPMS	RELA	RET	RHOA
RICTOR	RNF11	RNF130	RNF213	RNF43	ROS1	RP2	RSPO2	RSPO3	RUFY2-	SART3	SCAF11	SDC4	SDCCAG3	SEC16A
SEC31A	SEC61G	SETD2	SF3B1	SHROOM4	SHTN1	SLC12A7	SLC26A4	SLC34A2	SLC3A2	SLC45A3	SLMAP	SLX4	SMAD4	SMARCA4
SMARCB1	SMOP	SND1	SNHG7	SNX19	SOX6	SPAG9	SPECC1	SPECC1L	SPOP	SPTBN1	SQSTM1	SRC	SRGAP3	SSBP2
STAT3	STK11	STK32B	STRN	STRN3	SUGCT	TACC1	TACC3	TANK	TAX1BP1	TBL1XR1	TENM4	TERF2	TERT	TPM1
TFG	TMEM106B	TMEM178B	TMPRSS2	TNIP1	TNKS2	TOP1	TP53	TP53BP1	TPM3	TPM4	TPR	TRAF1	TRAK1	TRIM24
TRIM27	TRIM33	TRIM4	TRIO	TRIP11	TRMT61B	TSC1	TSC2	TSEN2	TTLL7	TXLNA	TYK2	U2AF1	UBE2L3	UBN2
USP10	VAMP2	VCL	VOPP1	WASF2	WDR48	WHSC1L1	WIPF2	XPO1	YAP1	YTHDF3	YWHAE	ZC3HAV1	ZCCHC8	ZEB2
ZKSCAN1	ZKSCAN5	ZMYM2	ZMYND8	ZNF226	ZNF703	ZSCAN30								

Results:

- Mutations: No actionable variant detected
- Copy Number Variations: No actionable variant detected
- Fusion Genes: No actionable variant detected

TABLE 3 | Foundation One CDx.

March 7nd, 2019

DNA GENE LIST: ENTIRE CODING SEQUENCE FOR THE DETECTION OF BASE SUBSTITUTIONS, INSERTION/ DELETIONS, AND COPY NUMBER ALTERATIONS Foundation One CDx [Foundation Medicine (Cambridge, MA)]

ABL1	ACVR1B	AKT1	AKT2	AKT3	ALK	ALOX12B	AMER1 (FAM123B)	APC	AR	ARAF	ARFRP1
ARID1A	ASXL1	ATM	ATR	ATRX	AURKA	AURKB	AXIN1	AXL	BAP1	BARD1	BCL2
BCL2L1	BCL2L2	BCL6	BCOR	BCORL1	BRAF	BRCA1	BRCA2	BRD4	BRIP1	BTG1	BTG2
BTK	C11orf30 (EMSY)	C17orf39 (GID34)	CALR	CARD11	CASP8	CBFB	CBL	CCND1	CCND2	CCND3	CCNE1
CD22	CD274 (PD-L1)	CD70	CD79A	CD79B	CDC73	CDH1	CDK12	CDK4	CDK6	CDK8	CDKN1A
CDKN1B	CDKN2A	CDKN2B	CDKN2C	CEBPA	CHEK1	CHEK2	CIC	CREBBP	CRKL	CSF1R	CSF3R
CTCF	CTNNA1	CTNNB1	CUL3	CUL4A	CXCR4	CYP17A1	DAXX	DDR1	DDR2	DIS3	DNMT3A
DOT1L	EED	EGFR	EP300	EPHA3	EPHB1	EPHB4	ERBB2	ERBB3	ERBB4	ERCC4	ERG
ERRFI1	ESR1	EZH2	FAM46C	FANCA	FANCC	FANCG	FANCL	FAS	FBXW7	FGF10	FGF12
FGF14	FGF19	FGF23	FGF3	FGF4	FGF6	FGFR1	FGFR2	FGFR3	FGF4	FH	FLCN
FLT1	FLT3	FOXL2	FUBP1	GABRA6	GATA3	GATA4	GATA6	GNA11	GNA13	GNAQ	GNAS
GRM3	GSK3B	H3F3A	HDAC1	HGF	HNF1A	HRAS	HSD3B1	ID3	IDH1	IDH2	IGF1R
IKBKE	IKZF1	INPP4B	IRF2	IRF4	IRS2	JAK1	JAK2	JAK3	JUN	KDM5A	KDM5C
KDM6A	KDR	KEAP1	KEL	KIT	KLHL6	KMT2A (MLL)	KMT2D (MLL2)	KRAS	LTK	LYN	MAF
MAP2K1 (MEK1)	MAP2K2 (MEK2)	MAP2K4	MAP3K1	MAP3K13	MAPK1	MCL1	MDM2	MDM4	MED12	MEF2B	MEN1
MEERTK	MET	MITF	MKNK1	MLH1	MPL	MRE11A	MSH2	MSH3	NBN	NF1	NF2
NFE2L2	NFKBIA	NKX2-1	NOTCH1	NOTCH2	NOTCH3	NPM1	NRAS	NSD3 (WHSC1L1)	NT5C2	NTRK1	NTK2
NTRK3	P2RY8	PALB2	PARK2	PARP1	PARP2	PARP3	PAX5	PBRM1	PRKAR1A	PRKCI	PTCH1
PTEN	PTPN11	PTPRO	QKI	RAC1	RAD21	RAD51	RAD51B	RAD51C	RAD51D	RAD52	RAD54L
RAF1	RARA	RB1	RBM10	REL	RET	SF3B1	SGK1	SMAD2	SMAD4	SMARCA4	SMARCB1
SMO	SNCAIP	SOCS1	SYK	TBX3	TEK	TET2	TGFBR2	TIPARP	TNFAIP3	TNFRSF14	TP53
TSC1	TSC2	TYRO3	U2AF1	VEGFA	VHL	WHSC1	WT1	XPO1			

DNA GENE LIST: FOR THE DETECTION OF SELECT REARRANGEMENTS

ALK	BCL2	BCR	BRAF	BRCA1	BRCA2	CD74	EGFR	ETV4	ETV5	ETV6	EWSR1
EZR	FGFR1	FGFR2	FGFR3	KIT	KMT2A (MLL)	MSH2	MYB	MYC	NOTCH2	NTRK1	NTRK2
NUTM1	PGFRA	RAF1	RARA	RET	ROS1	RSPO2	SDC4	SLC34A2	TERC	TERT	TMPRSS2

Results:

- **BAP1: Splice site 581-17_585del22**
- **RAD21: amplification**

carcinogenesis in mesothelioma, lung adenocarcinoma and melanoma (30, 32, 34, 41). BAP1 mutations occur in 10–32% of ICC cases (10, 14, 30, 42–49). As a tumor suppressor gene, BAP1 seems to follow a classic two-hit model (Knudson model) in which probably the first hit involves loss of heterozygosity (LOH) induced by 3p21 deletion. The latter occurs in almost 50–75% of ICCs (36). A subsequent mutation occurring in the remaining allele might lead to impairment of protein function and/or homeostasis (36). Protein function impairment by c.581-17_585del22 is most likely to reflect a deletion in the 3'-splice site of *BAP1*. Previously a c.581(-5)_c.590delACTAGGGCCCTGGGG mutation has been reported causing a premature truncation of BAP1 (50). This type of alterations that disrupt the nuclear localizations signal (aminoacids 717-722) of *BAP1* are predicted to be inactivating (14, 51).

As BAP1 interacts with BRCA1, several lines of evidence indicate that alterations in the BRCA-mediated DNA repair pathway confers sensitivity to PARP inhibitor administration (52). PARP inhibitors act through synthetic lethality, whereby genetic DNA repair defects are enhanced by drug-induced defects in a compensatory pathway (53). Carriers of heterozygous BRCA1/2 mutations are sensitive to PARP inhibitor treatment as they lose the wild-type allele during tumorigenesis and thereby become deficient of the homologous recombination (HR) pathway of double-strand break DNA repair by BRCA1/2-null status. Four PARP inhibitors, olaparib, rucaparib, niraparib, and talazoparib, have been approved by the U.S. Food and Drug Administration (FDA) and by the European Medicines Agency (EMA). In 2014, olaparib was approved as maintenance therapy for platinum-sensitive advanced ovarian cancer with germline mutations in BRCA1/2. In 2016, rucaparib was approved for advanced ovarian cancer with both germline and somatic BRCA1/2 mutations. In 2017 and 2018, olaparib, rucaparib, and niraparib were approved for the maintenance treatment of recurrent, epithelial ovarian, fallopian tube, or primary peritoneal cancer irrespective of the BRCA status. Last, in 2018, olaparib and talazoparib were approved for HER2-negative locally advanced or metastatic breast cancer with germline BRCA1/2 mutations. Besides in ovarian and breast cancer, PARP inhibitor efficacy has also been

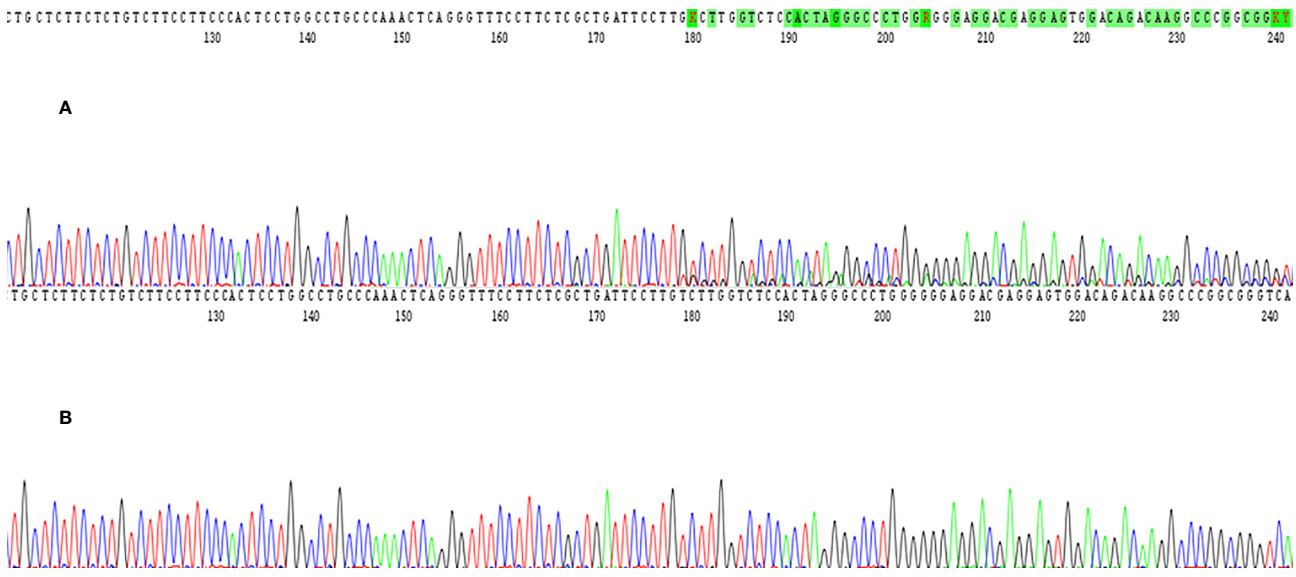

FIGURE 3 | The figure shows BAP1 molecular analysis performed on tumor tissue samples and buffy coat by using sanger sequencing platform. In details, c. 581-17_585del22 mutation was found only in tumor tissue specimen **(A)** while nucleic acids extracted from buffy coat did not harbor this mutation **(B)**.

demonstrated in other types of cancer including prostate and pancreatic cancer, and small cell lung carcinoma, irrespective of the BRCA status (54–61). It has become clear that any form of HR deficiency in tumors that phenocopies BRCA1/2 mutations, often referred to as BRCAness, may sensitize cells to PARP inhibitors (62). Indeed mutations in DNA damage response genes such as *ATM*, *PRKDC*, *ATR*, *RPA1*, *DSS1*, *NBN*, *RAD51*, *RAD54*, *CHEK1*, *CHEK2*, FANC genes, *ERCC1*, *POLB*, *FEN1*, and *CDK12* have shown synthetic lethality in combination with PARP inhibitors (63–67).

BAP1 is a HR DNA repair component and its loss sensitizes cancer cells to DNA repair defects (28). Currently, further investigations are needed to establish the real efficacy of PARP inhibitor on BAP1 mutated cancer cells. Some studies on various types of BAP1 mutated cancer cell lines demonstrated the potential efficacy of PARP inhibitors (68–70). A synergistic effect of PARP inhibitor and gemcitabine is described in BAP1 deficient cholangiocarcinoma cell lines (71). As a result, PARP inhibitors are currently under investigation alone or in combination with other therapies in cancer patients harboring a BAP1 mutant tumor including ICC (ClinicalTrials.gov Identifier: NCT03207347, NCT03786796, NCT03531840, and NCT03375307).

In the current clinical case, we have shown that PARP inhibitor administration can be potentially effective in BAP1 mutated ICC. Chemotherapeutic agents, such as platinum compounds which induce double-strand DNA breaks, are usually utilized prior to PARP inhibition in order to enhance DNA damage and induce PARP inhibition-mediated cell death (72). In addition PARP inhibitors are currently administered after obtaining a disease control with platinum compounds (73, 74). In the present clinical case, the PARP inhibitor olaparib was effective in controlling tumor progression, even though the patient did not benefit from FOLFIRI administration, a combination of 5-FU and topoisomerase I inhibitor irinotecan. Irinotecan exerts its anticancer effects through induction of single- and double-strand DNA breaks. 5-FU is an antimetabolite drug that exerts its anticancer effects through inhibition of DNA synthesis by inhibition of thymidylate synthase and incorporation of its metabolites into RNA and DNA. One could speculate that efficacy to PARP inhibitor was not enhanced by FOLFIRI administration, but rather by the previous administration of cisplatin. Additional studies are needed to define the timing and schedule of DNA damaging agents for PARP inhibitor enhancement in BAP1 deficient tumors.

In addition to BAP1 mutations, many other molecular alterations have been described in ICC such as *KRAS*, *BRAF*, *IDH1*, *IDH2*, *EGFR*, *FGFR2*, *ROS1*, *ARID1A*, *PBRM1*, and *BRCA1* (8–16). These types of alterations are frequently mutually exclusive (8–16). In the current clinical case, BAP1 mutation is not associated with KRAS, BRAF, IDH1, IDH2, EGFR, FGFR2, ROS1, ARID1A, PBRM1, and BRCA1 alterations but with a RAD21 amplification. Further studies are needed to validate this type of association. *RAD21* is a gene involved in the repair of DNA double-strand breaks, as well as in chromatid cohesion during mitosis (75, 76). Amplification of *RAD21* is described in approximately 1.23% of cases reported in the AACR Project Genomics Evidence Neoplasia Information Exchange (AACR Project GENIE), including invasive breast carcinoma, prostate adenocarcinoma, lung adenocarcinoma and colon adenocarcinoma having the greatest prevalence (77). However, no prior data exists regarding RAD21 amplification in ICC. Whether RAD21 amplification might enhance the activity of a PARP inhibitor in BAP1 mutant ICC should be further investigated.

Both BAP1 and RAD21 alterations were detected by utilizing NGS analysis. Patient's tumor tissue underwent analysis by several precision oncology testing methods to identify potentially oncogenic alterations. However, most of the tests performed did not detect any alterations. By comparing the results from the two most extensive tumor genomic profiles *BAP1* was analyzed in both: the Foudation One CDx and Oncofocus test. However only the Foudation One CDx test was able to detect BAP1 and RAD21 alterations. These findings are likely to reflect the different methods utilized to detect potentially oncogenic alterations, the regions of the genes included in the analysis, the potential tumor heterogeneity especially with a low allele frequency of the variants and the percentage of tumor cells in the sample tested. Since there is no targeted regions for BAP1 it is unlikely that different NGS platforms only test selected exons. In our case the novel mutation c.581-17_585del22 of BAP1 was localized on exon 8 of *BAP1*, at the boundary of intron 7. Most of the NGS platforms include 20-25bp in the vicinity of exons. However the Oncofocus® Test did not detect the c.581-17_585del22 alteration of BAP1 alteration most likely because this region of the gene was not included in the analysis. In contrast, the Foundation One CDx platform included in the analysis the full exonic region of *BAP1* besides including also *RAD21* in the analysis. Foundation One CDx report contains information only about the genomic findings without allele frequency values. As limit of detection range at non-homopolymer context (insertion up to 42 bp and deletion up to 276 bp) is 6–10%, we can assume that the BAP1 c.581-17_585del mutated allele was present with a higher variant fraction in the metastatic tumor tissue analyzed. In addition, direct sequencing has a reported limit of detection of approximately 20% mutant alleles. In our case BAP1 sanger sequencing on primary ICC tumor tissue showed the unbalanced presence of the mutated allele, even if it is not possible to have a quantitative value, as with NGS or digital PCR, we can hypothesize an allele frequency close to the limit of detection. Therefore, we can assume that BAP1 c.581-17_585del mutated allele occurred with a high allele frequency, early in ICC oncogenesis.

In conclusion, genomic characterization of ICC tumors by NGS analysis can identify potential targetable oncogenic alterations in ICC, providing the possibility to improve patient survival. Specifically, BAP1 deletion and RAD21 amplification were identified and effectively targeted by PARP inhibitor administration. These results warrant further studies to define the role of PARP inhibitor in ICC harboring BAP1 and RAD21 alterations.

DATA AVAILABILITY STATEMENT

The original contributions presented in the study are included in the article/**Supplementary Material**. Further inquiries can be directed to the corresponding author.

ETHICS STATEMENT

Written informed consent was obtained from the patient for publication of this case report and any accompanying images.

AUTHOR CONTRIBUTIONS

Conception and design: FSa, SP, and UM. Acquisition of data: LL, VT, and FSa. Analysis and interpretation of data: FSa, AF, VC, FSc, and UM. Writing, review, and/or revision of the manuscript: FSa, LL, and CF. Administrative, technical, or material support (i.e., reporting or organizing data, constructing databases): LL, and VT. Study supervision: SP. Other (contributed clinical and pathological material; discussed results and implications of findings): SP, GT, and CF. All authors contributed to the article and approved the submitted version.

FUNDING

The work was supported by Ministero dell'Università e della Ricerca (Progetti di Rilevante Interesse Nazionale (PRIN), 2017, CODICE 2017PHRC8X_003) (to SP).

ACKNOWLEDGEMENTS

The authors wish to gratefully acknowledge the patient for allowing us to publish his clinical case.

SUPPLEMENTARY MATERIAL

The Supplementary Material for this article can be found online at: https://www.frontiersin.org/articles/10.3389/fonc.2020.567289/full#supplementary-material

REFERENCES

1. Massarweh NN, El-Serag HB. Epidemiology of Hepatocellular Carcinoma and Intrahepatic Cholangiocarcinoma. *Cancer Control* (2017) 24:1–11. doi: 10.1177/1073274817729245 1073274817729245.
2. Bridgewater J, Galle PR, Khan SA, Llovet JM, Park J-W, Patel T, et al. Guidelines for the diagnosis and management of intrahepatic cholangiocarcinoma. *J Hepatol* (2014) 60:1268–89. doi: 10.1016/j.jhep.2014.01.021
3. Rahnemai-Azar AA, Weisbrod A, Dillhoff M, Schmidt C, Pawlik TM. Intrahepatic cholangiocarcinoma: Molecular markers for diagnosis and prognosis. *Surg Oncol* (2017) 26:125–37. doi: 10.1016/j.suronc.2016.12.009
4. Valle J, Wasan H, Palmer DH, Cunningham D, Anthoney A, Maraveyas A, et al. Cisplatin plus gemcitabine versus gemcitabine for biliary tract cancer. *N Engl J Med* (2010) 362:1273–81. doi: 10.1056/NEJMoa0908721
5. Fujimura T, Fujisawa Y, Kambayashi Y, Aiba S. Significance of BRAF Kinase Inhibitors for Melanoma Treatment: From Bench to Bedside. *Cancers (Basel)* (2019) 11:1342. doi: 10.3390/cancers11091342
6. Schwartzberg L, Kim ES, Liu D, Schrag D. Precision Oncology: Who, How, What, When, and When Not? *Am Soc Clin Oncol Educ Book* (2017) 37:160–9. doi: 10.1200/EDBK_174176
7. Valle JW, Lamarca A, Goyal L, Barriuso J, Zhu AX. New Horizons for Precision Medicine in Biliary Tract Cancers. *Cancer Discov* (2017) 7:943–62. doi: 10.1158/2159-8290.CD-17-0245

8. Arai Y, Totoki Y, Hosoda F, Shirota T, Hama N, Nakamura H, et al. Fibroblast growth factor receptor 2 tyrosine kinase fusions define a unique molecular subtype of cholangiocarcinoma. *Hepatology* (2014) 59:1427–34. doi: 10.1002/hep.26890
9. Gu T-L, Deng X, Huang F, Tucker M, Crosby K, Rimkunas V, et al. Survey of tyrosine kinase signaling reveals ROS kinase fusions in human cholangiocarcinoma. *PloS One* (2011) 6:e15640. doi: 10.1371/journal.pone.0015640
10. Jiao Y, Pawlik TM, Anders RA, Selaru FM, Streppel MM, Lucas DJ, et al. Exome sequencing identifies frequent inactivating mutations in BAP1, ARID1A and PBRM1 in intrahepatic cholangiocarcinomas. *Nat Genet* (2013) 45:1470–3. doi: 10.1038/ng.2813
11. Moeini A, Sia D, Bardeesy N, Mazzaferro V, Llovet JM. Molecular Pathogenesis and Targeted Therapies for Intrahepatic Cholangiocarcinoma. *Clin Cancer Res* (2016) 22:291–300. doi: 10.1158/1078-0432.CCR-14-3296
12. Saha SK, Parachoniak CA, Ghanta KS, Fitamant J, Ross KN, Najem MS, et al. Mutant IDH inhibits HNF-4α to block hepatocyte differentiation and promote biliary cancer. *Nature* (2014) 513:110–4. doi: 10.1038/nature13441
13. Yoshikawa D, Ojima H, Iwasaki M, Hiraoka N, Kosuge T, Kasai S, et al. Clinicopathological and prognostic significance of EGFR, VEGF, and HER2 expression in cholangiocarcinoma. *Br J Cancer* (2008) 98:418–25. doi: 10.1038/sj.bjc.6604129
14. Chan-On W, Nairismägi M-L, Ong CK, Lim WK, Dima S, Pairojkul C, et al. Exome sequencing identifies distinct mutational patterns in liver fluke-related and non-infection-related bile duct cancers. *Nat Genet* (2013) 45:1474–8. doi: 10.1038/ng.2806
15. Andrici J, Goeppert B, Sioson L, Clarkson A, Renner M, Stenzinger A, et al. Loss of BAP1 Expression Occurs Frequently in Intrahepatic Cholangiocarcinoma. *Med (Baltimore)* (2016) 95:e2491. doi: 10.1097/MD.0000000000002491
16. Sia D, Hoshida Y, Villanueva A, Roayaie S, Ferrer J, Tabak B, et al. Integrative molecular analysis of intrahepatic cholangiocarcinoma reveals 2 classes that have different outcomes. *Gastroenterology* (2013) 144:829–40. doi: 10.1053/j.gastro.2013.01.001
17. Javle M, Lowery M, Shroff RT, Weiss KH, Springfeld C, Borad MJ, et al. Phase II Study of BGJ398 in Patients With FGFR-Altered Advanced Cholangiocarcinoma. *J Clin Oncol* (2018) 36:276–82. doi: 10.1200/JCO.2017.75.5009
18. Nakanishi Y, Akiyama N, Tsukaguchi T, Fujii T, Sakata K, Sase H, et al. The fibroblast growth factor receptor genetic status as a potential predictor of the sensitivity to CH5183284/Debio 1347, a novel selective FGFR inhibitor. *Mol Cancer Ther* (2014) 13:2547–58. doi: 10.1158/1535-7163.MCT-14-0248
19. Goyal L, Shi L, Liu LY, Fece de la Cruz F, Lennerz JK, Raghavan S, et al. TAS-120 Overcomes Resistance to ATP-Competitive FGFR Inhibitors in Patients with FGFR2 Fusion-Positive Intrahepatic Cholangiocarcinoma. *Cancer Discov* (2019) 9:1064–79. doi: 10.1158/2159-8290.CD-19-0182
20. Jensen DE, Rauscher FJ. BAP1, a candidate tumor suppressor protein that interacts with BRCA1. *Ann N Y Acad Sci* (1999) 886:191–4. doi: 10.1111/j.1749-6632.1999.tb09414.x
21. Jensen DE, Proctor M, Marquis ST, Gardner HP, Ha SI, Chodosh LA, et al. BAP1: a novel ubiquitin hydrolase which binds to the BRCA1 RING finger and enhances BRCA1-mediated cell growth suppression. *Oncogene* (1998) 16:1097–112. doi: 10.1038/sj.onc.1201861
22. Baughman JM, Rose CM, Kolumam G, Webster JD, Wilkerson EM, Merrill AE, et al. NeuCode Proteomics Reveals Bap1 Regulation of Metabolism. *Cell Rep* (2016) 16:583–95. doi: 10.1016/j.celrep.2016.05.096
23. Bononi A, Giorgi C, Patergnani S, Larson D, Verbruggen K, Tanji M, et al. BAP1 regulates IP3R3-mediated Ca2+ flux to mitochondria suppressing cell transformation. *Nature* (2017) 546:549–53. doi: 10.1038/nature22798
24. Eletr ZM, Wilkinson KD. An emerging model for BAP1's role in regulating cell cycle progression. *Cell Biochem Biophys* (2011) 60:3–11. doi: 10.1007/s12013-011-9184-6
25. Machida YJ, Machida Y, Vashisht AA, Wohlschlegel JA, Dutta A. The deubiquitinating enzyme BAP1 regulates cell growth via interaction with HCF-1. *J Biol Chem* (2009) 284:34179–88. doi: 10.1074/jbc.M109.046755
26. Ruan H-B, Han X, Li M-D, Singh JP, Qian K, Azarhoush S, et al. O-GlcNAc transferase/host cell factor C1 complex regulates gluconeogenesis by modulating PGC-1α stability. *Cell Metab* (2012) 16:226–37. doi: 10.1016/j.cmet.2012.07.006
27. Xu J, Kadariya Y, Cheung M, Pei J, Talarchek J, Sementino E, et al. Germline Mutation of Bap1 Accelerates Development of Asbestos-Induced Malignant Mesothelioma. *Cancer Res* (2014) 74:4388–97. doi: 10.1158/0008-5472.CAN-14-1328
28. Yu H, Pak H, Hammond-Martel I, Ghram M, Rodrigue A, Daou S, et al. Tumor suppressor and deubiquitinase BAP1 promotes DNA double-strand break repair. *Proc Natl Acad Sci USA* (2014) 111:285–90. doi: 10.1073/pnas.1309085110
29. Yoshida K, Miki Y. Role of BRCA1 and BRCA2 as regulators of DNA repair, transcription, and cell cycle in response to DNA damage. *Cancer Sci* (2004) 95:866–71. doi: 10.1111/j.1349-7006.2004.tb02195.x
30. Di Nunno V, Frega G, Santoni M, Gatto L, Fiorentino M, Montironi R, et al. BAP1 in solid tumors. *Future Oncol* (2019) 15:2151–62. doi: 10.2217/fon-2018-0915
31. Carbone M, Yang H, Pass HI, Krausz T, Testa JR, Gaudino G. BAP1 and cancer. *Nat Rev Cancer* (2013) 13:153–9. doi: 10.1038/nrc3459
32. Cheung M, Talarchek J, Schindeler K, Saraiva E, Penney LS, Ludman M, et al. Further evidence for germline BAP1 mutations predisposing to melanoma and malignant mesothelioma. *Cancer Genet* (2013) 206:206–10. doi: 10.1016/j.cancergen.2013.05.018
33. Pilarski R, Rai K, Cebulla C, Abdel-Rahman M. BAP1 Tumor Predisposition Syndrome, in: *GeneReviews®*. Seattle (WA: University of Washington, Seattle. Available at: http://www.ncbi.nlm.nih.gov/books/NBK390611/ (Accessed July 28, 2020).
34. Abdel-Rahman MH, Pilarski R, Cebulla CM, Massengill JB, Christopher BN, Boru G, et al. Germline BAP1 mutation predisposes to uveal melanoma, lung adenocarcinoma, meningioma, and other cancers. *J Med Genet* (2011) 48:856–9. doi: 10.1136/jmedgenet-2011-100156
35. Carbone M, Flores EG, Emi M, Johnson TA, Tsunoda T, Behner D, et al. Combined Genetic and Genealogic Studies Uncover a Large BAP1 Cancer Syndrome Kindred Tracing Back Nine Generations to a Common Ancestor from the 1700s. *PloS Genet* (2015) 11:e1005633. doi: 10.1371/journal.pgen.1005633
36. Murali R, Wiesner T, Scolyer RA. Tumours associated with BAP1 mutations. *Pathology* (2013) 45:116–26. doi: 10.1097/PAT.0b013e32835d0efb
37. Kobrinski DA, Yang H, Kittaneh M. BAP1: role in carcinogenesis and clinical implications. *Transl Lung Cancer Res* (2020) 9:S60–6. doi: 10.21037/tlcr.2019.11.24
38. Carbone M, Ferris LK, Baumann F, Napolitano A, Lum CA, Flores EG, et al. BAP1 cancer syndrome: malignant mesothelioma, uveal and cutaneous melanoma, and MBAITs. *J Transl Med* (2012) 10:179. doi: 10.1186/1479-5876-10-179
39. Ewens KG, Kanetsky PA, Richards-Yutz J, Purrazzella J, Shields CL, Ganguly T, et al. Chromosome 3 status combined with BAP1 and EIF1AX mutation profiles are associated with metastasis in uveal melanoma. *Invest Ophthalmol Vis Sci* (2014) 55:5160–7. doi: 10.1167/iovs.14-14550
40. Ewens KG, Lalonde E, Richards-Yutz J, Shields CL, Ganguly A. Comparison of Germline versus Somatic BAP1 Mutations for Risk of Metastasis in Uveal Melanoma. *BMC Cancer* (2018) 18:1172. doi: 10.1186/s12885-018-5079-x
41. Masoomian B, Shields JA, Shields CL. Overview of BAP1 cancer predisposition syndrome and the relationship to uveal melanoma. *J Curr Ophthalmol* (2018) 30:102–9. doi: 10.1016/j.joco.2018.02.005
42. Bogenberger JM, DeLeon TT, Arora M, Ahn DH, Borad MJ. Emerging role of precision medicine in biliary tract cancers. *NPJ Precis Oncol* (2018) 2:21. doi: 10.1038/s41698-018-0064-z
43. Simbolo M, Fassan M, Ruzzenente A, Mafficini A, Wood LD, Corbo V, et al. Multigene mutational profiling of cholangiocarcinomas identifies actionable molecular subgroups. *Oncotarget* (2014) 5:2839–52. doi: 10.18632/oncotarget.1943
44. Fujimoto A, Furuta M, Shiraishi Y, Gotoh K, Kawakami Y, Arihiro K, et al. Whole-genome mutational landscape of liver cancers displaying biliary phenotype reveals hepatitis impact and molecular diversity. *Nat Commun* (2015) 6:6120. doi: 10.1038/ncomms7120
45. Ross JS, Wang K, Gay L, Al-Rohil R, Rand JV, Jones DM, et al. New routes to targeted therapy of intrahepatic cholangiocarcinomas revealed by next-

generation sequencing. *Oncologist* (2014) 19:235–42. doi: 10.1634/theoncologist.2013-0352
46. Churi CR, Shroff R, Wang Y, Rashid A, Kang HC, Weatherly J, et al. Mutation Profiling in Cholangiocarcinoma: Prognostic and Therapeutic Implications. *PloS One* (2014) 9:e115383. doi: 10.1371/journal.pone.0115383
47. Zou S, Li J, Zhou H, Frech C, Jiang X, Chu JSC, et al. Mutational landscape of intrahepatic cholangiocarcinoma. *Nat Commun* (2014) 5:5696. doi: 10.1038/ncomms6696
48. Sia D, Losic B, Moeini A, Cabellos L, Hao K, Revill K, et al. Massive parallel sequencing uncovers actionable FGFR2 – PPHLN1 fusion and ARAF mutations in intrahepatic cholangiocarcinoma. *Nat Commun* (2015) 6:6087. doi: 10.1038/ncomms7087
49. Borad MJ, Champion MD, Egan JB, Liang WS, Fonseca R, Bryce AH, et al. Integrated genomic characterization reveals novel, therapeutically relevant drug targets in FGFR and EGFR pathways in sporadic intrahepatic cholangiocarcinoma. *PloS Genet* (2014) 10:e1004135. doi: 10.1371/journal.pgen.1004135
50. Farshidfar F, Zheng S, Gingras M-C, Newton Y, Shih J, Robertson AG, et al. Integrative Genomic Analysis of Cholangiocarcinoma Identifies Distinct IDH-Mutant Molecular Profiles. *Cell Rep* (2017) 18:2780–94. doi: 10.1016/j.celrep.2017.02.033
51. Ventii KH, Devi NS, Friedrich KL, Chernova TA, Tighiouart M, Van Meir EG, et al. BRCA1-associated protein-1 is a tumor suppressor that requires deubiquitinating activity and nuclear localization. *Cancer Res* (2008) 68:6953–62. doi: 10.1158/0008-5472.CAN-08-0365
52. Kamel D, Gray C, Walia JS, Kumar V. PARP Inhibitor Drugs in the Treatment of Breast, Ovarian, Prostate and Pancreatic Cancers: An Update of Clinical Trials. *Curr Drug Targets* (2018) 19:21–37. doi: 10.2174/1389450118666170711151518
53. Lord CJ, Ashworth A. PARP inhibitors: Synthetic lethality in the clinic. *Science* (2017) 355:1152–8. doi: 10.1126/science.aam7344
54. Weaver AN, Yang ES. Beyond DNA Repair: Additional Functions of PARP-1 in Cancer. *Front Oncol* (2013) 3:290. doi: 10.3389/fonc.2013.00290
55. Sonnenblick A, de Azambuja E, Azim HA, Piccart M. An update on PARP inhibitors–moving to the adjuvant setting. *Nat Rev Clin Oncol* (2015) 12:27–41. doi: 10.1038/nrclinonc.2014.163
56. Mirza MR, Pignata S, Ledermann JA. Latest clinical evidence and further development of PARP inhibitors in ovarian cancer. *Ann Oncol* (2018) 29:1366–76. doi: 10.1093/annonc/mdy174
57. Franzese E, Centonze S, Diana A, Carlino F, Guerrera LP, Napoli MD, et al. PARP inhibitors in ovarian cancer. *Cancer Treat Rev* (2019) 73:1–9. doi: 10.1016/j.ctrv.2018.12.002
58. Keung MYT, Wu Y, Vadgama JV. PARP Inhibitors as a Therapeutic Agent for Homologous Recombination Deficiency in Breast Cancers. *J Clin Med* (2019) 8:435. doi: 10.3390/jcm8040435
59. Mateo J, Lord CJ, Serra V, Tutt A, Balmaña J, Castroviejo-Bermejo M, et al. de Bono JS. A decade of clinical development of PARP inhibitors in perspective. *Ann Oncol* (2019) 30:1437–47. doi: 10.1093/annonc/mdz192
60. Pant S, Maitra A, Yap TA. PARP inhibition — opportunities in pancreatic cancer. *Nat Rev Clin Oncol* (2019) 16:595–6. doi: 10.1038/s41571-019-0257-6
61. Pilié PG, Gay CM, Byers LA, O'Connor MJ, Yap TA. PARP Inhibitors: Extending Benefit Beyond BRCA-Mutant Cancers. *Clin Cancer Res* (2019) 25:3759–71. doi: 10.1158/1078-0432.CCR-18-0968
62. Lord CJ, Ashworth A. BRCAness revisited. *Nat Rev Cancer* (2016) 16:110–20. doi: 10.1038/nrc.2015.21
63. Bryant HE, Helleday T. Inhibition of poly (ADP-ribose) polymerase activates ATM which is required for subsequent homologous recombination repair. *Nucleic Acids Res* (2006) 34:1685–91. doi: 10.1093/nar/gkl108
64. McCabe N, Turner NC, Lord CJ, Kluzek K, Białkowska A, Swift S, et al. Deficiency in the Repair of DNA Damage by Homologous Recombination and Sensitivity to Poly(ADP-Ribose) Polymerase Inhibition. *Cancer Res* (2006) 66:8109–15. doi: 10.1158/0008-5472.CAN-06-0140
65. Murai J, Huang SN, Das BB, Renaud A, Zhang Y, Doroshow JH, et al. Trapping of PARP1 and PARP2 by Clinical PARP Inhibitors. *Cancer Res* (2012) 72:5588–99. doi: 10.1158/0008-5472.CAN-12-2753
66. Postel-Vinay S, Bajrami I, Friboulet L, Elliott R, Fontebasso Y, Dorvault N, et al. A high-throughput screen identifies PARP1/2 inhibitors as a potential therapy for ERCC1-deficient non-small cell lung cancer. *Oncogene* (2013) 32:5377–87. doi: 10.1038/onc.2013.311
67. Bajrami I, Frankum JR, Konde A, Miller RE, Rehman FL, Brough R, et al. Genome-wide Profiling of Genetic Synthetic Lethality Identifies CDK12 as a Novel Determinant of PARP1/2 Inhibitor Sensitivity. *Cancer Res* (2014) 74:287–97. doi: 10.1158/0008-5472.CAN-13-2541
68. Peña-Llopis S, Vega-Rubín-de-Celis S, Liao A, Leng N, Pavía-Jiménez A, Wang S, et al. BAP1 loss defines a new class of renal cell carcinoma. *Nat Genet* (2012) 44:751–9. doi: 10.1038/ng.2323
69. Parrotta R, Okonska A, Ronner M, Weder W, Stahel R, Penengo L. Felley-Bosco E. A Novel BRCA1-Associated Protein-1 Isoform Affects Response of Mesothelioma Cells to Drugs Impairing BRCA1-Mediated DNA Repair. *J Thorac Oncol* (2017) 12:1309–19. doi: 10.1016/j.jtho.2017.03.023
70. Rathkey D, Khanal M, Murai J, Zhang J, Sengupta M, Jiang Q, et al. Sensitivity of Mesothelioma Cells to PARP Inhibitors Is Not Dependent on BAP1 but Is Enhanced by Temozolomide in Cells With High-Schlafen 11 and Low-O6-methylguanine-DNA Methyltransferase Expression. *J Thorac Oncol* (2020) 15:843–59. doi: 10.1016/j.jtho.2020.01.012
71. Parasramka M, Yan IK, Wang X, Nguyen P, Matsuda A, Maji S, et al. BAP1 dependent expression of long non-coding RNA NEAT-1 contributes to sensitivity to gemcitabine in cholangiocarcinoma. *Mol Cancer* (2017) 16:22. doi: 10.1186/s12943-017-0587-x
72. Mylavarapu S, Das A, Roy M. Role of BRCA Mutations in the Modulation of Response to Platinum Therapy. *Front Oncol* (2018) 8:16. doi: 10.3389/fonc.2018.00016
73. Pennington KP, Walsh T, Harrell MI, Lee MK, Pennil CC, Rendi MH, et al. Germline and somatic mutations in homologous recombination genes predict platinum response and survival in ovarian, fallopian tube, and peritoneal carcinomas. *Clin Cancer Res* (2014) 20:764–75. doi: 10.1158/1078-0432.CCR-13-2287
74. Wang ZC, Birkbak NJ, Culhane AC, Drapkin R, Fatima A, Tian R, et al. Profiles of Genomic Instability in High-Grade Serous Ovarian Cancer Predict Treatment Outcome. *Clin Cancer Res* (2012) 18:5806–15. doi: 10.1158/1078-0432.CCR-12-0857
75. Peters J-M, Nishiyama T. Sister Chromatid Cohesion. *Cold Spring Harb Perspect Biol* (2012) 4:a011130. doi: 10.1101/cshperspect.a011130
76. Hill VK, Kim J-S, Waldman T. Cohesin Mutations in Human Cancer. *Biochim Biophys Acta* (2016) 1866:1–11. doi: 10.1016/j.bbcan.2016.05.002
77. AACR Project GENIE Consortium. AACR Project GENIE: Powering Precision Medicine through an International Consortium. *Cancer Discov* (2017) 7:818–31. doi: 10.1158/2159-8290.CD-17-0151

Conflict of Interest: UM reports personal fees (as speaker bureau or advisor) from Boehringer Ingelheim, AstraZeneca, Roche, MSD, Amgen and Merck, unrelated to the current work.

The remaining authors declare that the research was conducted in the absence of any commercial or financial relationships that could be construed as a potential conflict of interest.

frontiers in Oncology

ORIGINAL RESEARCH
published: 15 January 2021
doi: 10.3389/fonc.2020.595182

A Combined Epithelial Mesenchymal Transformation and DNA Repair Gene Panel in Colorectal Cancer With Prognostic and Therapeutic Implication

Xiaoliang Huang[1,2†], Jungang Liu[1,2,3†], Haizhou Liu[4†], Xianwei Mo[1,2], Yongsheng Meng[1,2], Lihua Zhang[1,2], Yuqing Deng[1,2], Yawei Zhang[3] and Weizhong Tang[1,2*]*

[1] Division of Colorectal & Anal Surgery, Department of Gastrointestinal Surgery, Guangxi Medical University Cancer Hospital, Nanning, China, [2] Guangxi Clinical Research Center for Colorectal Cancer, Nanning, China, [3] Department of Environmental Health Sciences, Yale School of Public Health, New Haven, CT, United States, [4] Department of Research, Guangxi Medical University Cancer Hospital, Nanning, China

Background: Epithelial mesenchymal transformation (EMT) and DNA repair status represent intrinsic features of colorectal cancer (CRC) and are associated with patient prognosis and treatment responsiveness. We sought to develop a combined EMT and DNA repair gene panel with potential application in patient classification and precise treatment.

Methods: We comprehensively evaluated the EMT and DNA repair patterns of 1,652 CRC patients from four datasets. Unsupervised clustering was used for classification. The clinical features, genetic mutation, tumor mutation load, and chemotherapy as well as immunotherapy sensitivity among different clusters were systematically compared. The least absolute shrinkage and selection operator regression method was used to develop the risk model.

Results: Three distinct CRC clusters were determined. Clustet1 was characterized by down-regulated DNA repair pathways but active epithelial markers and metabolism pathway and had intermediate prognosis. Clustet2 was characterized by down-regulated both epithelial markers and DNA repair pathways and had poor outcome. Clustet3 presented with activation of DNA repair pathway and epithelial markers had favorable prognosis. Clustet1 might benefit form chemotherapy and Clustet3 had a higher response rate to immunotherapy. An EMT and DNA repair risk model related to prognosis and treatment response was developed.

Conclusions: This work developed and validated a combined EMT and DNA repair gene panel for CRC classification, which may be an effective tool for survival prediction and treatment guidance in CRC patients.

Keywords: DNA repair, epithelial to mesenchymal transition, colorectal cancer, immunotherapy, metabolism

OPEN ACCESS

Edited by:
David Y. Lee, University of New Mexico, United States

Reviewed by:
Clarissa Ribeiro Reily Rocha, Federal University of São Paulo, Brazil
Jorg Kobarg, Campinas State University, Brazil

***Correspondence:**
Weizhong Tang
tangweizhong@gxmu.edu.cn
Yawei Zhang
yawei.zhang@yale.edu

[†]These authors have contributed equally to this work

Specialty section:
This article was submitted to Molecular and Cellular Oncology, a section of the journal Frontiers in Oncology

Received: *15 August 2020*
Accepted: *23 November 2020*
Published: *15 January 2021*

Citation:
Huang X, Liu J, Liu H, Mo X, Meng Y, Zhang L, Deng Y, Zhang Y and Tang W (2021) A Combined Epithelial Mesenchymal Transformation and DNA Repair Gene Panel in Colorectal Cancer With Prognostic and Therapeutic Implication. Front. Oncol. 10:595182. doi: 10.3389/fonc.2020.595182

BACKGROUND

Colorectal cancer (CRC) remains a major cause of cancer-related mortality worldwide despite advancements in tumor screening, early diagnosis, and curative resection (1). Staging based on the tumor, nodule, and metastasis (TNM) is generally considered as the main tools for routine prognostication of CRC patients in treatment practice (2, 3). However, heterogeneity of clinical process and treatment response are often observed between individuals in the same stage, which are often attributed to diversity of CRC (4). The diversity of tumors is also manifested at the molecular level. Tumors of the same histological subtype may have different genetic backgrounds and gene expression profile. Tumors of different histological subtype may share common genetic backgrounds and molecular features. Identifying tumor subtypes with different molecular characteristics and clinical outcome is important for the precise treatment of cancer.

In recent years, the molecular classification of CRC has received increasing attention. The international CRC Subtyping Consortium developed a transcriptomic classification of colorectal cancer, which classifies CRC into four biologically distinct consensus molecular subtypes (CMSs). CMS1 and CMS4 tumors have high levels of immune infiltration but antagonistic functional orientation. CMS2 and CMS3 are devoid of immune cell infiltration (5). CMS4 subtype has the worst prognosis. The French national Cartes d'Identite´ des Tumeurs (CIT) program identified six molecular subtypes with distinct clinicopathological characteristics and molecular alterations (6). C1 ($CIN_{ImmuneDown}$) is more frequently chromosomal instability (CIN) and immunosuppression. C2 (dMMR) contains most deficient mismatch repair (dMMR) tumors. C3 (KRASm) is enriched for KRAS-mutant tumors. C4 (CSC) is characterized by presenting cancer stem cell (CSC) phenotype–like gene expression profile as well as up-regulating of the bottom crypt signature. C5 (CIN_{WntUp}) has frequency CNI with up-regulation of Wnt pathway. C6 is enriched for "normal-like'" tumor (7). Nevertheless, some defect limits the clinical application of the above-mentioned classification. There is no consensus on whether classification is associated with treatment response. Besides, tumor classification is based on whole-genome gene expression patterns, which increases the complexity of classification and decreases the feasibility of clinical application. And there is overlap between pathways enriched in different classification, increasing the uncertainty of the interpretation of the results. Selecting characteristic pathways for tumor classification may be a way to simplify the classification process and improve clinical utility, and assess the correlation between classification and treatment response.

Epithelial–mesenchymal transition (EMT) facilitates the acquisition of stem cell characteristics and sustains stem cell-like populations (8). During the process of EMT, cancer cells lose their epithelial morphology and adopt a spindle-shaped and mesenchymal appearance progressively. Activation of EMT provides cancer cells with the enhanced plasticity required for invasion and metastasis (9). In CRC, EMT is strongly associated with tumor proliferation, infiltration, metastasis, tumor budding and drug resistance (10). Patients with active EMT tumor have poor prognosis. However, EMT is a reversible process, which offers new insight for the treatment of tumors (11). Incorporating EMT gene expression profiles into CRC classification may identify a subtype of cancer with high malignancy and therapeutic implications.

DNA repair is a critical system for recognizing and repairing abnormalities in the structure or sequence of DNA. Mutations in DNA repair genes, including mismatch repair (MMR), can impair cells' ability to repair damaged DNA, leading to cell death or genome instability (12). Tumors with aberrant DNA repair pathway have increased mutational and neoantigen burden (13), which in turn were linked with greater tumor infiltration by activated T cells. DNA repair defects are associated with improved clinical response to PD-1 blockade, specifically, in CRC patients with deficient mismatch repair (dMMR) (14).

Therefore, we integrated EMT and DNA repair genes for CRC classification. Three CRC clusters with distinct prognosis and molecular characteristic were determined.

MATERIALS AND METHODS

Clinical Specimens

In the present study, eight cases of CRC samples including two cased of metastatic CRC samples and six cased of non-metastatic CRC samples were obtained from patients at the Guangxi Medical University Cancer Hospital. The samples were subjected to RNA sequencing. All of the patients were pathologically diagnosed as CRC without chemotherapy or radiotherapy before the collection of the tissues. Written informed consents were obtained from all patients. The study was approved by the Ethics and Human Subject Committee of Guangxi Medical University Cancer Hospital. All experiments and methods were performed according to relevant guidelines and regulations formulated by the Guangxi Medical University.

RNA-Seq Analysis

Total RNA was extracted using Trizol reagent (Invitrogen). The construction of RNA-seq library was based on the protocol of the IlluminaTruSeq RNA Sample Preparation Kit (illumina). Finally, RNA-seq analysis was performed by GENE+ company (Beijing, China) using Illumina HiSeqX Ten platforms. After quality control and trimming adaptor, reads were mapped onto human genome GRCh38. RNA-seq data have been deposited in the China National Center for Bioinformation (ID: PRJCA003751).

Data Acquisition and Pre-Processing

Multiplatform genomics data was included in the study, including mRNA expression data, gene somatic mutation data, DNA copy data, and clinical information. For mRNA expression data, we collected the TCGA COAD AND READ datasets and three GEO datasets [GSE39582 (6), GSE17536 (15), and GSE14333 (16)] which meeting the following standard: samples were hybridized to the Affymetrix HGU133 Plus 2·0 (GPL570) platforms, each dataset contains more than 150 cases CRC patients, and information about the prognosis could be gathered. Besides, to analyze the efficiency of immunotherapy,

we also included the "IMvigor" dataset using "IMvigor" package, which was generated from patients with metastatic urothelial cancer treated with anti-PD-L1 drugs (atezolizumab) (17). For TCGA mRNA datasets, the FPKM (fragments per kilobase of exon model per million reads mapped) normalized expression matrix was download form the Genomic Data Commons (GDC, https://portal.gdc.cancer.gov/). For microarray data, the raw "CEL" files were downloaded from GEO (http://www.ncbi.nlm.nih.gov/geo/) and subjected to a robust multiarray averaging method to perform background adjustment and quantile normalization using the "affy" packages (18). The corresponding clinical data was download at the same time. The gene somatic mutation data (MAF files) and DNA copy data (segment file) of TCGA COAD AND READ cohorts were download from GDC.

Generation of EMT and DNA Repair Gene Panel and Unsupervised Clustering

EMT related genes were obtained from published studies and DNA repair related genes were obtained from Molecular Signatures Database (MSigDB) (4, 19, 20). Univariate cox regression was used to screening prognostic genes using GSE39582. Genes with a p-value less than 0.1 was selected for further analysis. Unsupervised clustering analysis was applied to identify characteristic expression patterns based on the expression of EMT and DNA repair gene panel, and patients were classified for further analysis. We use a consensus clustering algorithm to determine the number and stability of clusters (21). The "ConsensuClusterPlus" package was used to perform the above steps with 500 times repetitions to guarantee the stability of classification (22).

Gene Set Variation Analysis (GSVA) and Functional Annotation

To investigate the biological pathways and processes enriched in different clusters, we applied GSVA which reckons the variation of pathway and bioprocess activity in the sample population by adopting unsupervised clustering method (23). The gene set files of "c2.cp.kegg.v6.2.symbols" and "c5.bp.v7.0.symbols" were downloaded from the MSigDB for running GSVA analysis using "GSVA" packages in R software. Adjusted P less than 0.05 was considered as statistically significance.

Development and Validation of EMT and DNA Repair Risk Model

In order to reduce the dimension and pick the most meaningful prognostic indicators, we applied the least absolute shrinkage and selection operator (LASSO) Cox regression model to the EMT and DNA repair gene panel. LASSO is a penalized regression method that determines the regression coefficients by maximizing the log-likelihood function, while limiting the sum of the absolute values of the regression coefficients (24). The regression coefficients estimated by LASSO are sparse and many components are exactly zero. Thus, LASSO automatically deletes unnecessary covariates (25, 26). 10-fold cross validation was used to confirm the suitable tuning parameter (λ) for LASSO regression. The significant genes selected by LASSO were subsequently subjected to stepwise cox regression. The eventual regression model was selected based on the Akaike information criterion (AIC). GSE39582 cohort was served as the training set and the TCGA cohort was served as the validation set. A predicted value was calculated for every patient in the validation set on the basis of the risk model constructed in the training set. The ROC and AUC were used to assess the predictive discrimination ability of the risk model.

Statistical Analysis

The statistically significant differences between non-normally distributed variables was analyzed by the Mann-Whitney U test, and normally distributed variables were reckoned adopting the unpaired Student's t-test. In order to compare more than two groups, used Kruskal-Wallis as non-parametric methods, and adopted one-way ANOVA tests as parametric methods. Spearman and distance correlation analysis were used to calculate the correlation. The survival curves for the prognostic analysis were generated *via* the Kaplan-Meier method and log-rank tests were utilized to identify significance of differences. Use Cox proportional risk model and the "LR forward" stepwise approach to perform univariate and multivariate analyses. Evaluate the survival prediction of accuracy of the prognostic model *via* a time-related receiver operating characteristic curve (ROC) analysis. The R software (version 3.5.0) was used to conduct all statistical analyses, and all statistical P values were two-side, with $p < 0.05$ as statistically significance.

RESULTS

Patient Characteristics and Prognostic Gene Identification

The patient characteristics contained in the datasets used in this study is summarized in **Table 1**. A total of 1,652 CRC patients from TCGA dataset and three GEO datasets (GSE39582, GSE17536, and GSE14333) were retrospectively analyzed in this study. Median age at diagnosis in different datasets ranged from 62 to 68 years. Male patients accounted for 54.48% (900/1652). EMT related genes were obtained from published studies (4, 20) and DNA repair related genes were obtained from MSigDB. We used GSE39582 as training set to identified prognostic gene. 98 genes (DNA repair: 41; EMT: 57) were eventually identified and defined as prognostic EMT and DNA repair genes for further study. Interestingly most of the EMT genes are epithelial markers, which were down-regulated in mesenchymal cells. Detailed information of the 98 genes was listed in **Supplemental Table 1**. The protein interaction network of the 98 genes were shown in **Supplemental Figure 1**.

Identification of Distinct Molecular Clusters Based on EMT and DNA Repair Genes

We divided CRC samples in the GSE39582 into distinct molecular clusters according to 98 prognostic EMT and DNA

TABLE 1 | Baseline characteristics of patients in the discovery and validation cohorts.

Feature	GSE39582 cohort N=566 Number (%)	TCGA cohort N=619 Number (%)	GSE17536 cohort N=177 Number (%)	GSE14333 cohort N=290 Number (%)	All patients N=1652 Number (%)
Age					
Median (IQR)	66.91(17.00)	68.00(18.00)	66.00(18.00)	67.00(17.00)	–
Gender					
Male	310 (54.77)	330 (53.31)	96 (54.24))	164 (56.55)	900 (54.48)
Female	256 (45.23)	289 (46.69)	81 (45.76)	126 (43.45)	752 (45.52)
NA	0	0	0	0	0
T-stage					
Tis	3 (0.53)	1 (0.16)	–	–	4 (0.34)
T0	1 (0.18)	0 (0)	–	–	1 (0.08)
T1	11 (1.94)	20 (3.23)	–	–	31 (2.62)
T2	45 (7.95)	105 (16.96)	–	–	150 (12.66)
T3	367 (64.84)	422 (68.17)	–	–	789 (66.58)
T4	119 (21.02)	70 (11.31)	–	–	189 (15.95)
NA	20 (3.53)	1 (0.16)	–	–	21 (1.77)
N-stage					
N0	302 (53.36)	351 ((56.70)	–	–	653 (55.11)
N1	134 (23.67)	150 (24.23)	–	–	284 (23.97)
N2	98 (17.31)	115 (18.58)	–	–	213 (17.97)
N+	6 (1.06)	0 (0)	–	–	6 (0.51)
NA	26 (4.59)	3 (0.48)			29 (2.45)
M-stage					
M0	482 (85.16)	459 (74.15)	–	–	941 (79.41)
M1	61 (10.78)	87 (14.05)	–	–	148 (12.49)
NA	23 (4.06)	73 (11.79)	–	–	96 (8.10)
TNM				Dukes	–
0	4 (0.71)	0 (0)	0 (0)	A:44 (15.17)	–
I	33 (5.83)	105 (16.96)	24 (13.56)	B:94 (32.41)	–
II	264 (46.64)	227 (36.67)	57 (32.20)	C:91 (31.38)	–
III	205 (36.22)	179 (28.92)	57 (32.20)	D:61 (21.03)	–
IV	60 (10.60)	88 (14.22)	39 (22.03)		–
NA	0 (0)	20 (3.23)	0 (0)	0 (0)	–
MMR status					
dMMR	75 (13.25)	11 (1.78)	–	–	86 (7.26)
pMMR	444 (78.45)	105 (16.96)	–	–	549 (46.33)
NA	47 (8.30)	503 (81.26)	–	–	550 (46.41)

IQR, Interquartile range.

repair genes. The optimal number of clusters was set at 3 (**Figure 1A**), as suggested by Elbow method. The consensus matrix heatmap revealed the identified three clusters (**Figure 1B**). It must be noted that the eventually incorporated EMT genes were principally epithelial cell markers whose expression levels negatively correlate with EMT. As shown in **Figure 1D**, CRC patients of different clusters possessed specific expression patterns of EMT and DNA repair genes. Cluster 1 (EPI^{H}/DNA $repair^{L}$) had increased expression of epithelial markers but down-regulated DNA repair genes. Cluster2 (EPI^{L}/DNA $repair^{L}$) was characterized by low expression of epithelial markers and DNA repair genes. Cluster3 (EPI^{H}/DNA $repair^{H}$) presented with apparent increased expression of epithelial markers and DNA repair genes. We selected recognized DNA repair genes (MLH1, MSH2, PMS1, and PMS2), which are key genes for determining MMR status and widely used in clinical practice (27), and epithelial genes (CDH1 and DSP) as well as mesenchymal genes (VIM, SNAI1, SNAI2, TWIST1, MMP2, and FN1) to analyze their expression among the three clusters (28). As shown in **Supplementary Figure 2**, the expression of DNA repair genes (MLH1, MSH2, PMS1, and PMS2) and epithelial genes (CDH1 and DSP) were significantly increased in the Cluster 3(EPI^{H}/DNA $repair^{H}$) while significantly decreased in the Cluster 2(EPI^{L}/DNA $repair^{L}$). The expression of mesenchymal genes (VIM, SNAI1, SNAI2, TWIST1, MMP2, and FN1) were significantly decreased in the Cluster 3(EPI^{H}/DNA $repair^{H}$) but increased in the Cluster 2(EPI^{L}/DNA $repair^{L}$). These results indicated that DNA repair was active but the EMT was suppressive in Cluster 3, which contrasts with gene expression pattern in Cluster 2. The three Cluster had different survival profiles, with the Cluster 3 having the best prognosis but Cluster 2 having the worst prognosis (**Figure 1C**).

We further validated the 98 genes panel in independent cohort. The first cohort was from TCGA comprised 619 cases of CRC. Three distinct molecular clusters were identified as described above (Cluster 1 (EPI^{H}/DNA $repair^{L}$), Cluster 2(EPI^{L}/DNA $repair^{L}$), and Cluster 3(EPI^{H}/DNA $repair^{H}$), **Figure 1E**). Survival analysis confirmed that cluster have distinct outcomes. Here again, cluster 2 having the worst prognosis (**Figure 1F**). The second cohort was from GSE14333 receive adjuvant chemotherapy.

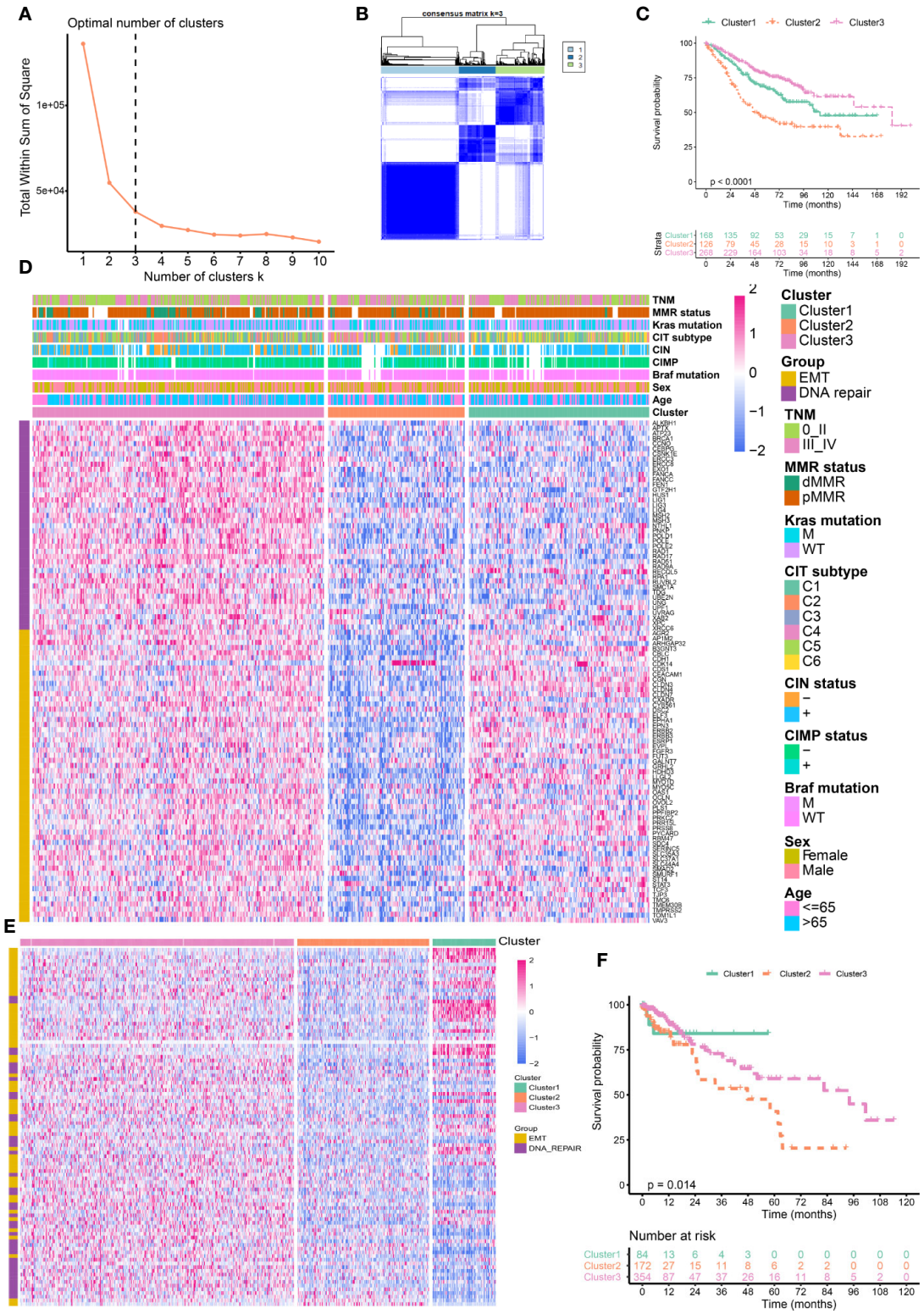

FIGURE 1 | Identification of distinct molecular clusters based on epithelial mesenchymal transformation (EMT) and DNA repair genes. **(A)** The optimal number of clusters determined by Elbow method. **(B)** Consensus matrix for k = 3. **(C)** Overall survival of colorectal cancer (CRC) patients in the three clusters (GSE39582). **(D)** Heatmaps show the expression of 98 EMT and DNA repair genes (GSE39582). **(E)** Heatmaps show the expression of 98 EMT and DNA repair genes (TCGA). **(F)** Overall survival of CRC patients in the three clusters (TCGA).

As shown in **Supplementary Figure 3A**, three distinct molecular clusters were identified and Cluster 2 having the worst prognosis (**Supplementary Figure 3B**). The third validation cohort was from GSE17536 comprised 177 cases of CRC. We also identified three distinct molecular clusters as described above (**Supplementary Figure 3C**). Kaplan–Meier analysis revealed that the three subgroups have distinct outcome, that the Cluster 2 had the worst prognosis while Cluster 1 and Cluster 3 had similar outcome (**Supplementary Figure 3D**).

Correlation of the Clusters With Clinical Characteristics and Classical Classification

The relationships between CRC classifications and clinical characteristics were then investigated by using the GSE39582 (**Figure 2A** and **Supplementary Table 2**). Cluster 1 was associated with lower proportion of BRAF mutation, CpG island methylator phenotype (CIMP) and dMMR. But Cluster 1 has a higher proportion of patients with distal CRC, lymphatic metastasis as well as CIN and mainly enriched in C1, C5, and C6 of CIT subtype. Cluster 2 was associated with high percentage of BRAF mutation, CIMP, T4 stage, distant metastasis, and young patients. Cluster 2 was mainly enriched in C4 of CIT subtype. Cluster 3 had a high percentage of dMMR, node-negative, no distant metastasis and elderly patient. Cluster 3 was mainly concentrated in the C2, C3, and C5 of CIT subtype. **Figure 2B** summarized the relationship between CLT subtype and different clusters. There was no significant difference in the distribution of KRAS mutation, Tp53 mutation and gender among different clusters. We further validated the association by using TCGA dataset. As shown in **Supplementary Figure 4**, We again found that Cluster 2 was associated with a higher proportion of T4 and stage III–IV. But, node-negative CRC and patients without lymphatic invasion (LV) and vessel invasion (VL) have higher percentage in Cluster 3.

Characteristics of Tumor Genome Variation in Different Clusters

TCGA has completed a comprehensive molecular characterization of CRC, thus we analyzed the distribution differences of somatic single nucleotide variants (SNVs) among different clusters based on TCGA dataset. As shown in **Figures 3A–C**, the top three genes with the highest frequency of mutations in cluster1 were APC (82%), TP53 (58%), and KRAS (51%), and those in Cluster2 are APC (72%), TTN (51%), and TP53 (51%), and those in Cluster3 are APC (81%), TP53 (66%), and TTN (47%). There was no significant difference in the frequency of somatic mutations in the three clusters. Tumor mutation burden (TMB) is a measurement of somatic mutation carried by cancer cells and high TMB status presented a durable clinical response to anti-PD-1/PD-L1 immunotherapy in CRC (29). We compared the TMB among different clusters. as shown in **Figure 3D**, the Cluster2 and 3 had the highest TMB while the Cluster1 had the lowest TMB. These results indicated that Cluster2 and 3 might benefit from immunotherapy. Copy number variants (CNVs) are a key component of genetic variation and have a greater impact in the genome than SNVs. We investigated alteration frequency of CNVs among different clusters. A total of 352 genes with significant differences in amplification frequency or deletion frequency among the three clusters were identified. The genes location, amplification frequency and deletion frequency in each cluster was summarized in **Figure 3E**. **Supplementary Figure 5** presented representative genes with significant differences in amplification frequency or deletion frequency among the three clusters. We performed gene enrichment analysis to explore biological processes and pathways involved in aberrant amplification or deletion of genes (**Supplementary Figure 6**). Genes significantly amplified in the Cluster3 were enriched in Defense response to bacterium and Focal adhesion, which indicated that Cluster3 might associate with immune and metastasis. Pathways enrichment analysis suggested that significantly amplified genes in Cluster2 were enriched in Cell cycle and Cell adhesion molecules, indicated that Cluster2 might associate with cell proliferation and metastasis.

Clusters Predicts Therapeutic Benefit of Chemotherapy and Immunotherapy

Adjuvant chemotherapy (ADJC) is the primary treatment strategy for patients with non-metastatic CRC cancer (30). Given that the GSE39582 dataset provided information on chemotherapy in patients, we utilized this dataset to analyze the relationship between EMT and DNA repair gene clusters and ADJC benefit. We used OS to assess treatment outcome. Interestingly, only patients in the Cluster 1 had improved OS after receiving ADJC (**Figure 4A**). No significant difference in OS of patients in Cluster 2 and 3 regardless of whether they received ADJC (**Figures 4B, C**). These results indicated that patients in the Cluster 1 might benefit from chemotherapy.

Immunotherapy has recently emerged as an effective new therapy for CRC. However, immunotherapy is currently indicated only for CRC patients with dMMR, which only account for about 5%–15%. It is crucial to identify CRC patients benefit from immunotherapy. We collected an immunotherapy data set (Imvigor210) to explore whether the clusters could predict the immune treatment benefit. As shown in **Figure 4D**, the proportion of patients achieved a complete response (CR) or partial response (PR) was significantly increased in the Cluster3. These results indicated that patients in the Cluster 3 benefited from immunotherapy at a higher rate.

Biological Pathways and Processes Enriched in Different Clusters

To explore the biological characteristics among these distinct clusters, we performed GSVA enrichment analysis. It should be noted that this was a pathway-level comparison for exploring the biological significance behind the different clusters. It was not a re-phenotyping using a new set of genes. The enrichment analysis results of KEGG pathway showed that Cluster1 was markedly enriched in metabolic pathways such as Retinol Metabolism, Linoleic acid Metabolism, and Arachidonic acid Metabolism (**Figure 5A**). Cluster2 presented enrichment pathways associated with EMT including ECM receptor

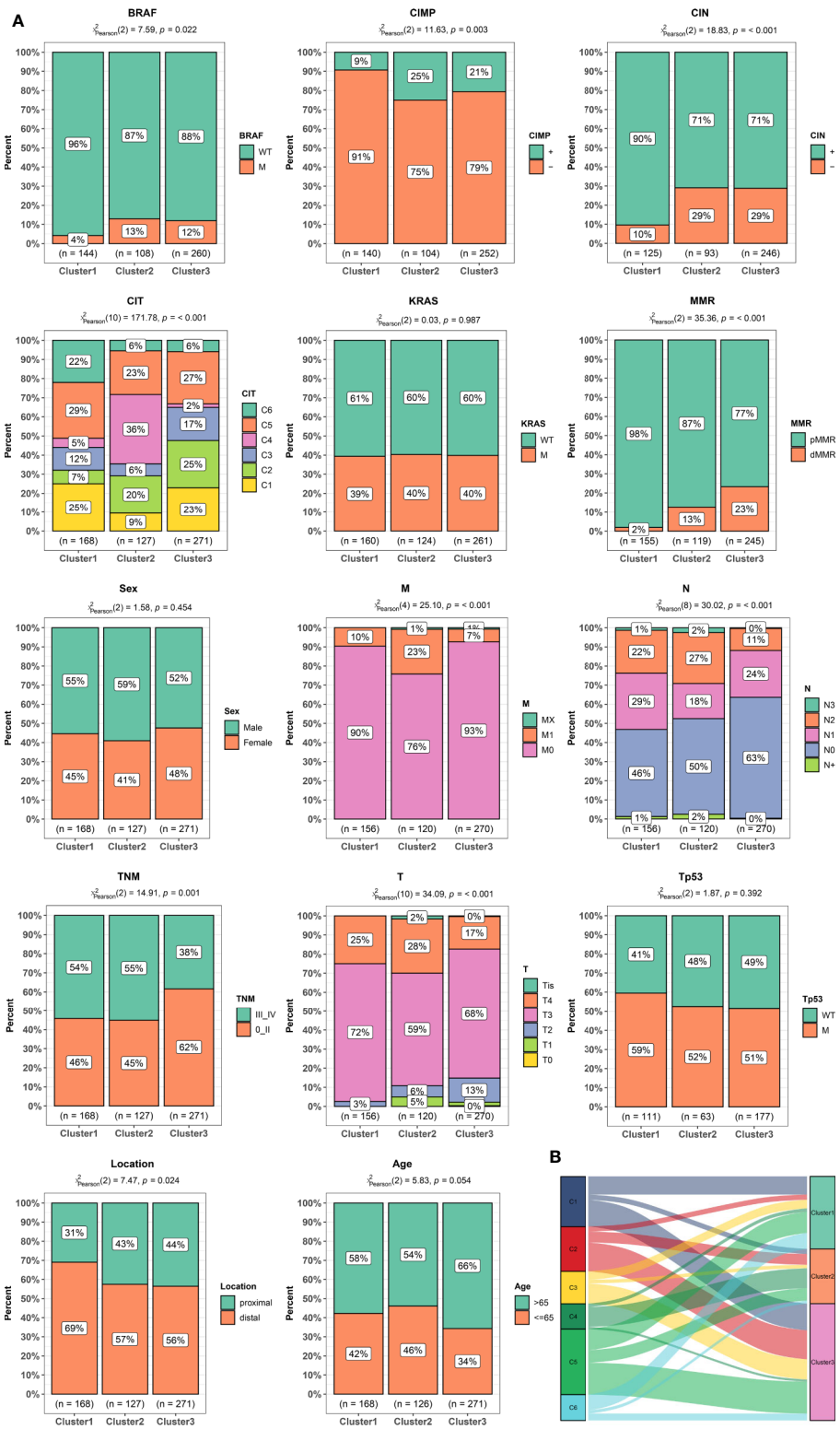

FIGURE 2 | Clinical and molecular characteristics of colorectal cancer (CRC) patients according to the cluster. **(A)** Bar plots showing the proportion of gender, age, stage, tumor localization, KRAS, BRAF, and TP53 mutations, hypermutated phenotype, mismatch repair status (MMR), CpG island methylator phenotype (CIMP), chromosomal instability (CIN), and Cartes d'Identite´ des Tumeurs (CIT) subtypes in different clusters. **(B)** Sankey chart displaying the distribution of C1–C6 CIT subtypes in different clusters.

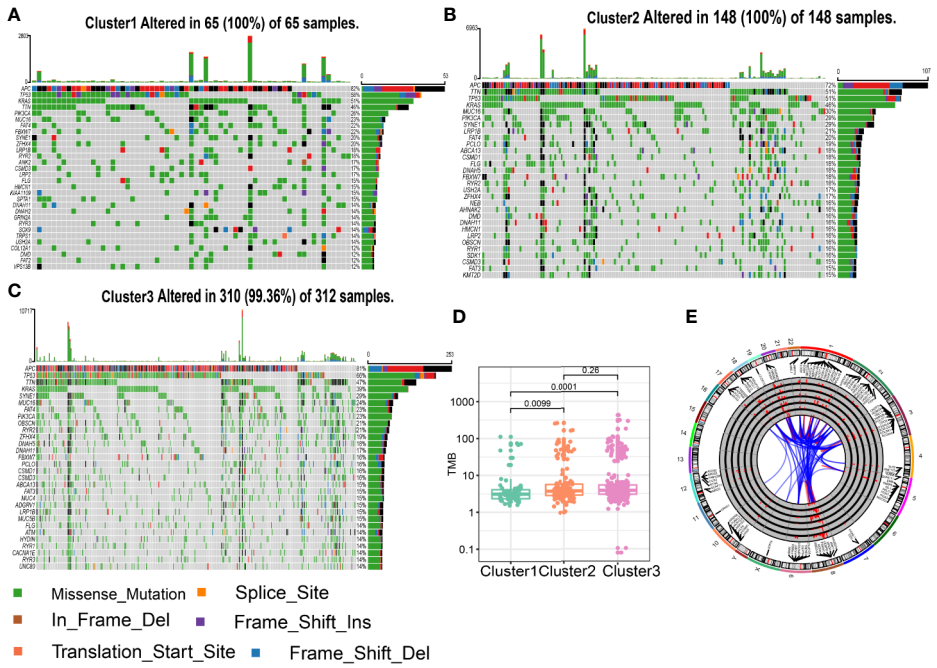

FIGURE 3 | Characteristics of tumor genome variation in different clusters. **(A)** Genes with top 30 mutation frequency in Cluster1. **(B)** Genes with top 30 mutation frequency in Cluster2. **(C)** Genes with top 30 mutation frequency in Cluster3. **(D)** Tumor mutation load (TMB) level in different clusters. **(E)** Circular visualization of the copy number variant (CNV) alteration in each cluster. The outermost circle shows the location of the CNV gene. The histogram shows the frequency of CNV in in different clusters. From outside to inside: genes significant deletion in Cluster1, significant amplification in Cluster1, significant deletion in Cluster2, significant amplification in Cluster2, significant deletion in Cluster3, significant amplification in Cluster3. The link lines dedicated gene interactions.

interactions and Cell adhesion molecules (CAMs). While Cluster3 was prominently related to DNA repair pathways such as DNA Replication, Mismatch Repair and Base excision Repair. **Figure 5B** presented representative pathways and its enrichment scores in different clusters. Again, metabolic pathways had the highest enrichment scores in the Cluster1 and EMT related pathways including extracellular matrix (ECM), Wnt pathways, and TGF-β pathways had the highest enrichment scores in the Cluster2. DNA repair pathways had the highest enrichment scores in the Cluster3. The enrichment scores for the above pathways were significantly different (all $P < 0.05$, **Figure 5B**). We further explored biological processes enriched in distinct clusters. Different clusters had characteristic biological processes (**Supplementary Figure 7**). Biological processes associated with Amino acid transport, Ion transport and Transmission of neural signal were significantly enriched in Cluster1 (**Supplementary Figure 8A**). Cluster2 were enriched in Mesenchymal formation, Immune response and Amino acid transport (**Supplementary Figure 8B**). Besides, biological processes significantly enriched in Cluster3 including RNA processing and DNA repair (**Supplementary Figure 8C**). Based on the above analyses, we were surprised to learn that three clusters had significantly distinct biological characteristics. Cluster1 was characterized by activation of metabolic pathways and Cluster2 was characterized by EMT activation. Cluster3 was characterized by activation of DNA repair.

Construction of EMT and DNA Repair Risk Scores Related to Prognosis and Treatment Response

To develop clinically useful prognostic and efficacy assessment models for individual, we applied the LASSO Cox regression model to the 98 EMT and DNA repair genes for dimension reduction. GSE39582 cohort was served as training set and TCGA cohort were served as validation cohort. As shown in **Figures 6A, B**, the most appropriate tuning parameter λ for LASSO Cox regression analysis was determined to be 0.036 when the partial likelihood deviance was the smallest. The 16 genes with non-zero coefficients in the tuning parameter were selected and subject to stepwise cox regression. Ultimately, nine genes were used to constructed the scoring system. The hazard ratios and P-values of the nine genes in the scoring model were summarized in **Figure 6C**. We compared the expression of nine genes in different clusters, and interestingly, these nine genes were significantly differentially expressed in different clusters (**Supplementary Figure 9**), suggesting that these genes represent characteristics of different clusters. Patients were divided into high-risk and low-risk groups according to the risk score predicted. And survival analysis demonstrated that the EMT and DNA repair risk scores had significant power to distinguish good from poor outcomes in CRC patients ($P<0.001$) (**Figure 6D**). We further validated the scoring model in TCGA cohort. Patients with high-risk had worse outcomes compared

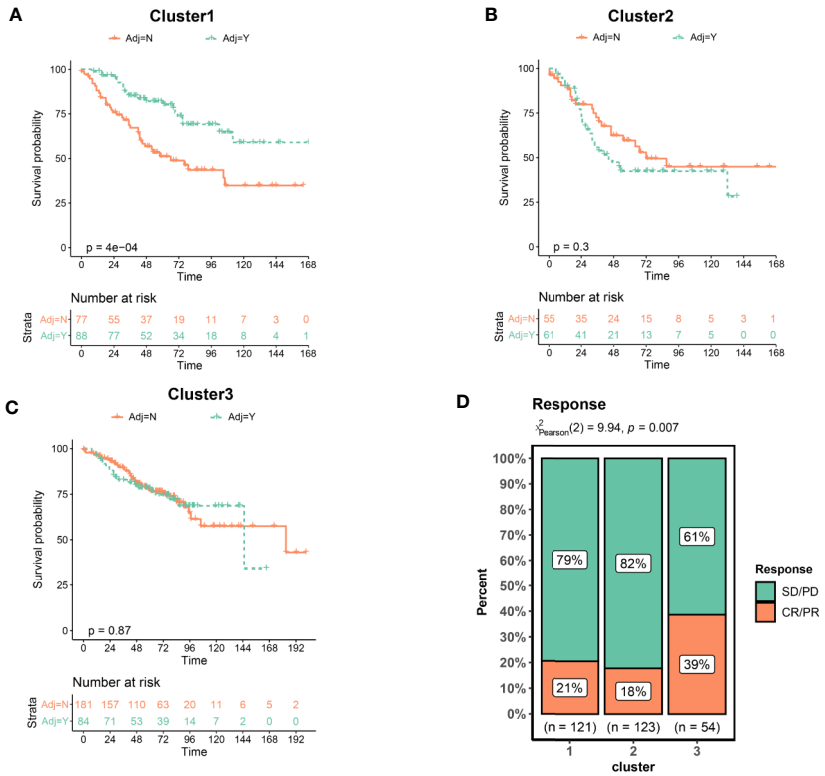

FIGURE 4 | Clusters predicts therapeutic benefit of chemotherapy and immunotherapy. **(A)** Kaplan–Meier curves of overall survival for patients in Cluster1 stratified by receipt of adjuvant chemotherapy. **(B)** Cluster2. **(C)** Cluster3. **(D)** Response rate of patients to immunotherapy. CR, complete response; PR, partial response; SD, stable disease; PD, progressive disease.

with low-risk (**Figure 6E**). ROC curve analysis revealed that the EMT and DNA repair risk scores had similar degree of discrimination in GSE39582 cohort and TCGA cohort (GSE39582: AUC= 0.714; TCGA: AUC=0.696, **Figure 6F**). The correlation between risk scores, gene expression and survival state were present in the **Figures 6G, H**. Next, we analyzed the association between risk scores and cluster. The Cluster 3, with a better prognosis, had the lowest risk score, while Cluster2, with the worst prognosis, had the highest risk score. And Cluster1, with intermediate prognosis, had medium risk score (**Figure 6I**). We further validate the risk scores using in-house data. We found that patients with metastatic CRC had higher risk scores than patients with non-metastatic CRC, but the difference was not statistically significant, possibly because of the small sample size (**Figure 6J**). These results indicated that the risk scores were closely related to prognosis and different clusters had distinct risk scores.

Since the EMT and DNA repair genes clusters were associated with immunotherapeutic response, we investigated whether the risk scores can predict immunotherapeutic benefit. Cluster 3 benefited from immunotherapy at a higher rate. We first compared the levels of risk scores in different clusters based on Imvigor210 cohort. Cluster 3 had lowest risk scores, which indicated that low risk scores predicated immunotherapeutic benefit (**Supplementary Figure 10A**). Besides, the proportion of CR or PR was significantly increased in patients with low risk (**Supplementary Figure 10B**). In patients receiving immunotherapy, patients with low risk had better prognosis than those with high risk (**Supplementary Figure 10C**). These findings suggested that low risk scores predicated immunotherapeutic benefit.

DISCUSSION

With the development of research, we gain a deeper understanding of the biological and molecular characteristics of CRC (31). CRC classification based on characteristic pathways may be a promising way to simplify the classification process and improve clinical utility. Activation of EMT pathways is associated with malignant behavior and drug resistance (32). While activation of DNA repair pathways is a key feature of "hot tumor" and a predictor of immunotherapy (33). In the present study, we identified three distinct CRC clusters based on a combined EMT and DNA repair gene panel.

The three CRC clusters differ significantly in clinical characteristics, prognosis, genomic variation, active pathways, and response to chemotherapy and immunotherapy (**Figure 7**). Clustet1 (EPI^H/DNA $repair^L$) was characterized

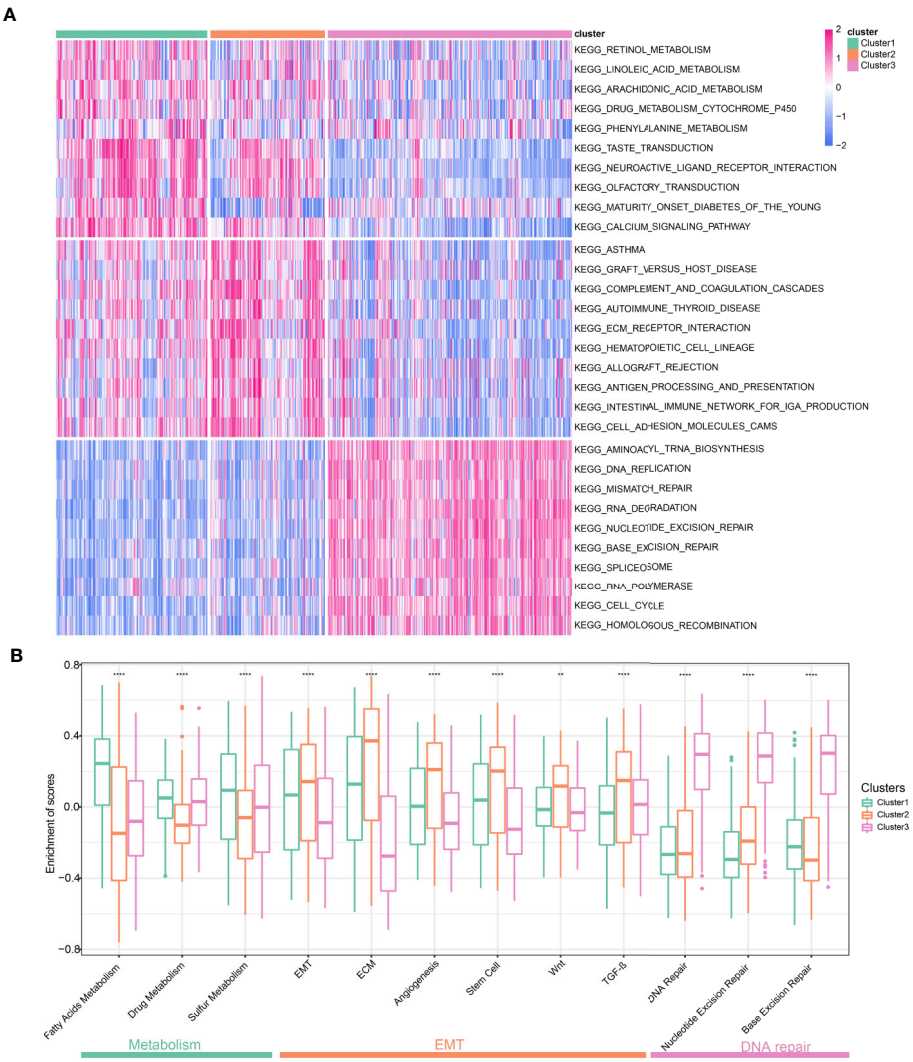

FIGURE 5 | Biological pathways and processes enriched in different Clusters. **(A)** Heatmap of different pathways among the three clusters. Each cluster exhibit 10 of the most distinctive KEGG pathways. **(B)** Comparison representative pathways and its enrichment scores in different clusters.

by down-regulated DNA repair pathways but active epithelial markers and metabolism pathway. Clustet1 has intermediate prognosis and lower proportion of BRAF mutation, CpG island methylator phenotype (CIMP) and dMMR. But Cluster1 has a higher proportion of patients with distal CRC as well as lymphatic metastasis. TMB scores was the lowest in the Cluster1. Patients in the Cluster1 might benefit from chemotherapy but not immunotherapy. Besides, Cluster1 was associated with a moderate EMT and DNA repair risk scores. The Cluster2 (EPI^{L}/DNA $repair^{L}$) was characterized by down-regulated DNA repair and epithelial markers. Clustet2 was associated with the worst prognosis. Cluster 2 has a high percentage of BRAF mutation, CIMP, T4 stage, distant metastasis, and young patients. Clustet2 presented with high TMB and genes significantly amplified in Cluster2 were enriched in Cell cycle and Cell adhesion molecules. Patients in the Cluster2 might not benefit from chemotherapy and immunotherapy. The EMT and DNA repair risk scores was the highest in the Cluster2. The Cluster3 (EPI^{H}/DNA $repair^{H}$) presented with activation of DNA repair pathway and epithelial markers. Patients in Cluster3 had the best prognosis. Cluster 3 had a high percentage of dMMR, node-negative, no distant metastasis, or LV or VL and elderly patient. Clustet3 presented with high TMB and genes significantly amplified in Cluster3 were enriched in Defense response to bacterium and Focal adhesion. Cluster 3 benefited from immunotherapy at a higher rate. The EMT and DNA repair risk scores was the lowest in the Cluster3. Therefore, the identification of three different clusters is of great significance for the accurate treatment of CRC.

Chemotherapy is one of the main treatment strategies for CRC, which is critical for creating surgical opportunities and preventing tumor recurrence (34). Detecting patients who may

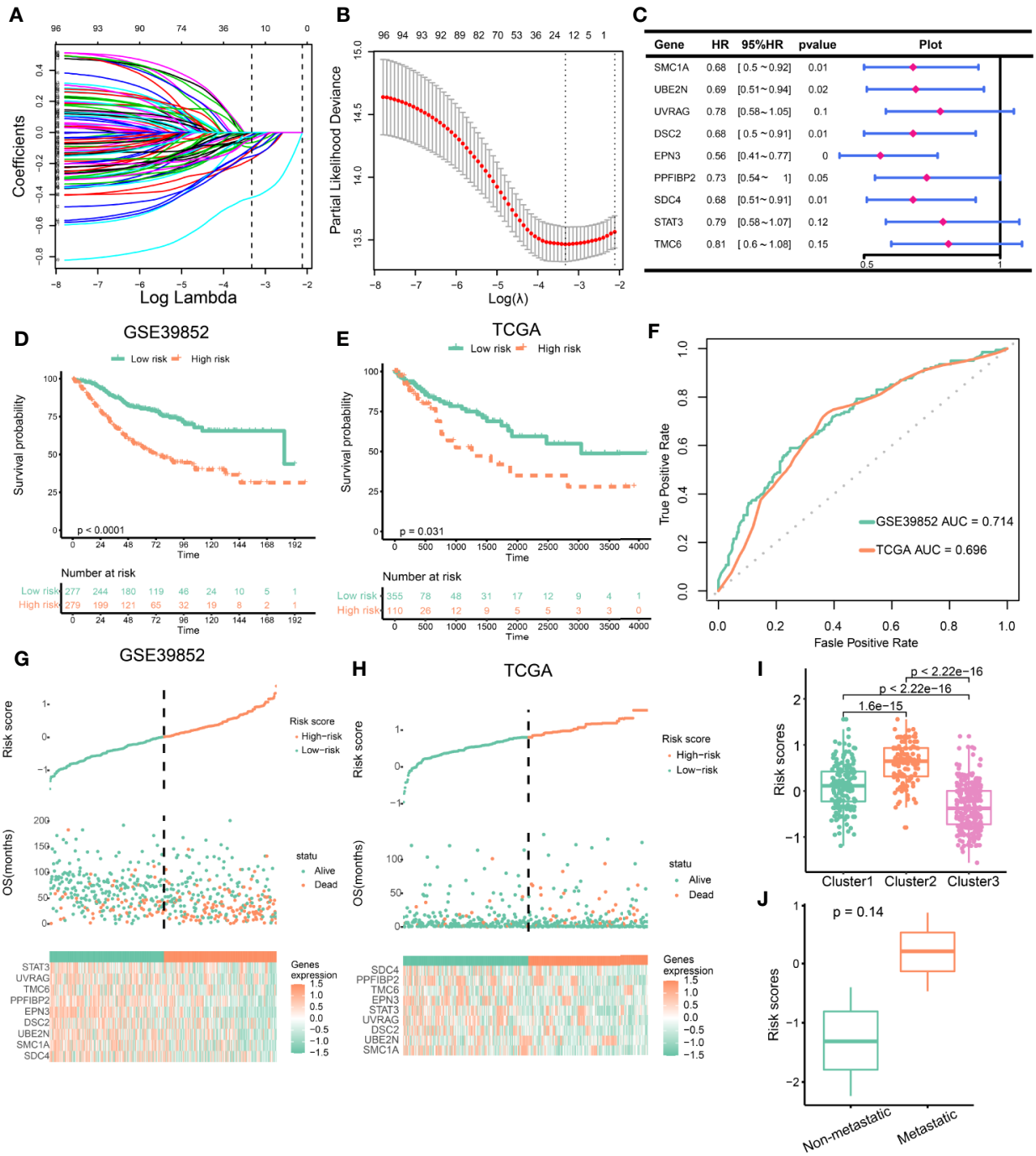

FIGURE 6 | Construction of epithelial mesenchymal transformation (EMT) and DNA repair risk scores. **(A)** LASSO regression coefficient profiles of 98 EMT and DNA repair genes. **(B)** Tuning parameter (λ) selection in the LASSO regression used 10-fold-cross-validation *via* minimum criteria. The black vertical lines are plotted at the optimal λ based on the minimum criteria and 1 standard error for the minimum criteria. **(C)** The hazard ratios and p-values of the 9 genes in the risk model. **(D)** Kaplan–Meier curves of overall survival for patients in GSE39582 stratified by risk scores. **(E)** Kaplan–Meier curves of overall survival for patients in TCGA stratified by risk scores. **(F)** The ROC curves for the risk model in GSE39582 and TCGA. **(G, H)** Construction and analysis of risk scores. The top panels indicate the risk scores of the patients. The middle panels depict the survival statuses and survival times of the patients distributed by risk score. The bottom panels display the heatmap of the expression for the nine genes distributed by risk score. **(G)** GSE39582 cohort; **(H)** TCGA cohort. **(I)** Comparison of risk scores across clusters. **(J)** Risk scores in metastatic VS. non-metastatic colorectal cancer (CRC) patients.

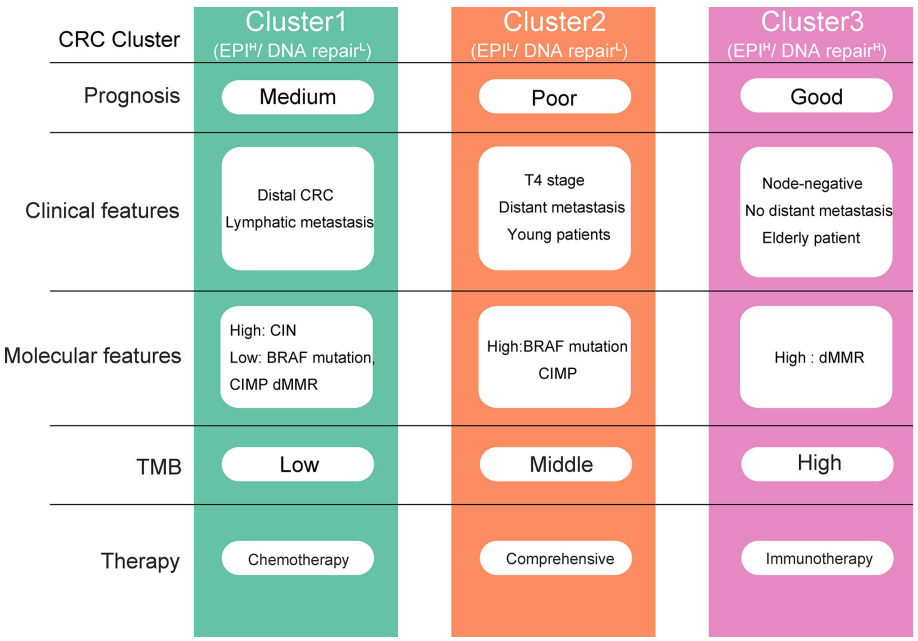

FIGURE 7 | Overview of the characteristics of three colorectal cancer (CRC) clusters. EPI, Epithelial.

benefit from chemotherapy is an important step in precision treatment. Activation of EMT is a recognized factor in the induction of chemotherapy resistance (35). 5-fluorouracil (5-Fu) based chemotherapy is commonly used in convention chemotherapy of CRC (36). The 5-Fu resistance is partially induced by EMT *via* the Akt gene or mediated by Twist, miR-200c, miR-141 (26, 34). Besides, down-regulation of EMT-related miR-200c and miR-141 could induced resistance to oxaliplatin, which is one of the most common drugs in CRC chemotherapy (37). Moreover, EMT is strongly associated with tumor proliferation, infiltration, metastasis, tumor budding (10). Given that Cluster2 presents with activation of EMT, we have reasons to infer that Cluster2 has a poor prognosis and does not benefit from chemotherapy.

Metabolic reprogramming is a hallmark of malignancy (38). To support the rapid proliferation, progression, and metastasis, cancer cells rewire metabolic pathways *via* increased generation of adenosine triphosphate (ATP), macromolecule synthesis, and antioxidant regeneration (39). Abnormal metabolic pathways provide new targets for the treatment of cancer and sensitize cancer chemotherapy (40). For example, increased expression of MUC1 enhanced glycolysis, nonoxidative PPP, and pyrimidine biosynthesis (41). Inhibition of MUC1 sensitizes cancer cell lines to 5-FU (24, 42). Combination of antimetabolic therapy and chemotherapy may yield better response rates (43). Based on our analysis, Cluster1 present with increased metabolism pathways, we speculated that Cluster1 patients may benefit from anti-metabolic therapy and chemotherapy.

Currently, benefits of immunotherapy have received immense research interest because of the impressive long-lasting response seen in several solid tumors (33, 44). In CRC, immune response and survival benefit were limited to mismatch-repair-deficient and microsatellite instability-high (dMMR–MSI-H) CRC patients, who account for only a small percentage of CRC patients (around 8%–15%) (3, 45). Thus, the selection criteria for candidates who are likely to benefit from such regimens requires further investigation. In the present study, we found that patients in the Cluster3 had the highest response rate to immunotherapy (around 40%). Besides, Cluster3 was present with high proportion of dMMR and TMB, which were recognized immunotherapeutic response prediction marker. We infer that patients in Cluster3 may benefit from immunotherapy. In addition, an interesting phenomenon we found was that although Cluster3 had a higher proportion of dMMR, the expression of key MMR genes was elevated. The MMR gene expression products are called MMR proteins, and they exist as heterodimeric complexes for mismatch base identification and subsequent repair (45). Most mutations in the MMR gene interfere with dimerization, leading to proteolytic degradation of the heterodimer, resulting in the loss of obligatory and secondary proteins (27). This assumption may explain why mRNA is elevated but protein expression is down-regulated. Further research is needed to confirm this assumption.

In recent years, the availability of clinical-grade, rapid, and inexpensive benchtop next-generation sequencers, as well as prepackaged analytical software and reagents, has driven the rapid growth and popularity of gene panel assays in clinical laboratories (46). The gene panel amplifies only specific genes and therefore has the advantage of lower cost and faster speed (47). The limitations of gene panel assay are the high investment

in equipment and the cost of sequencing reagents, making it impractical in the case of too small a total specimen volume. In addition, despite the wide application of the technology in recent years, there is still a shortage of experienced professionals. This lack of expertise results in variable quality of analysis and interpretation of the complex data. It is also unclear how to validate, control and charge for these tests, limiting their deployment in hospital laboratories (48).

This study has some limitations. First, the patient population is heterogeneous due to the retrospective nature of this study. Second, the robustness of the predictive value of the gene panel needs further validation in large prospective clinical trials. Third, experimental studies are needed to further elucidate the biological significances of the gene panel. Fourth, although our proposed EMT and DNA repair gene panel has potential clinical applications, such as the development of molecular typing kits for colorectal cancer, many issues remain unresolved, such as further identification of target genes, design of probes and determination of expression thresholds.

CONCLUSION

In conclusion, the present study developed and validated a combined EMT and DNA repair gene panel for CRC classification. Three CRC clusters with distinct characteristics were identified. This gene panel may have clinical application for prognosis estimation and guiding chemotherapy as well as checkpoint inhibitors.

DATA AVAILABILITY STATEMENT

The original contributions presented in the study are included in the article/**Supplementary Material**. Further inquiries can be directed to the corresponding authors.

ETHICS STATEMENT

The studies involving human participants were reviewed and approved by The Ethics and Human Subject Committee of Guangxi Medical University Cancer Hospital. The patients/participants provided their written informed consent to participate in this study.

AUTHOR CONTRIBUTIONS

Conceived and designed the experiments: XH, JL, HL, XM, YZ, and WT. Performed the data collection: XH, JL, HL, LZ, YD, and YM. Analyzed the data: XH, JL, HL, XM, YZ, LZ, YD, and YM. Contributed reagents/materials/analysis tools: HL, XM, YZ, and WT. Contributed to the writing of the manuscript: XH, JL, HL, XM, YZ, WT, LZ, YD, and YM. All authors contributed to the article and approved the submitted version.

FUNDING

This study was funded by the 2019 Guangxi University High-level Innovation Team and the Project of Outstanding Scholars Program, and Guangxi Science and Technology Project (2019AC03004); Guangxi Clinical Research Center for Colorectal Cancer (Guike: AD19245197).

SUPPLEMENTARY MATERIAL

The Supplementary Material for this article can be found online at: https://www.frontiersin.org/articles/10.3389/fonc.2020.595182/full#supplementary-material

SUPPLEMENTARY FIGURE 1 | Protein-protein interaction (PPI) network of the 98 EMT and DNA repair genes. Genes belonging to EMT are represented in red and Genes belonging to DNA repair are represented in blue. The size of a gene is positively correlated with the number of genes it links.

SUPPLEMENTARY FIGURE 2 | Expression of representative EMT and DNA repair genes in the three CRC clusters. DNA repair genes were marked red and epithelial genes were green. Mesenchymal genes were orange.

SUPPLEMENTARY FIGURE 3 | Identification of distinct molecular clusters based on EMT and DNA repair genes using GSE14333 and GSE17536. **(A)** Heatmaps show the expression of 98 EMT and DNA repair genes (GSE14333). **(B)** Survival analysis of CRC patients in the three clusters (GSE14333). **(C)** Heatmaps show the expression of 98 EMT and DNA repair genes (GSE17536). D: Survival analysis of CRC patients in the three clusters (GSE17536).

SUPPLEMENTARY FIGURE 4 | Clinical characteristics of colorectal cancer (CRC) patients according to the cluster (TCGA data). Bar plots showing the proportion of tumor stage, tumor localization, lymphatic invasion (LV) and vessel invasion (VL) in different clusters.

SUPPLEMENTARY FIGURE 5 | Representative genes with significant differences in amplification or deletion frequency among the three clusters.

SUPPLEMENTARY FIGURE 6 | Enrichment analysis of aberrant amplification or deletion of genes. Showing the top five terms with a P value less than 0.05. Left panel: GO biological process; Right panel: KEGG pathways.

SUPPLEMENTARY FIGURE 7 | Heatmap of different biological processes among the three clusters. Each cluster exhibit 30 of the most distinctive GO biological processes.

SUPPLEMENTARY FIGURE 8 | Tree diagram of distinctive GO biological processes in each cluster. Clustering of GO terms according to the common genes contained in the different terms. The closer the two terms are, the more genes they share. **(A)** Cluster1; **(B)** Cluster2; **(C)** Cluster3.

SUPPLEMENTARY FIGURE 9 | The expression of 9 prognostic genes in different clusters.

SUPPLEMENTARY FIGURE 10 | Correlation between risk score and immunotherapy response. **(A)** Comparison of risk scores across clusters based on "IMvigor" dataset. **(B)** Response rate of patients to immunotherapy. Patients were stratified according the risk scores. CR, complete response; PR, partial response; SD, stable disease; PD, progressive disease. **(C)** Kaplan–Meier curves for patients receiving immunotherapy.

REFERENCES

1. Siegel RL, Miller KD, Jemal A. Cancer statistics, 2020. *CA Cancer J Clin* (2020) 70:7–30. doi: 10.3322/caac.21590
2. Edge SB, Compton CC. The American Joint Committee on Cancer: the 7th Edition of the AJCC Cancer Staging Manual and the Future of TNM. *Ann Surg Oncol* (2010) 17:1471–4. doi: 10.1245/s10434-010-0985-4
3. Huang X, Liu J, Wu G, Chen S, Pc FJ, Xie W, et al. Development and Validation of a Nomogram for Preoperative Prediction of Perineural Invasion in Colorectal Cancer. *Med Sci Monit* (2019) 25:1709–17. doi: 10.12659/MSM.914900
4. Piskol R, Huw L, Sergin I, Kljin C, Modrusan Z, Kim D, et al. A Clinically Applicable Gene-Expression Classifier Reveals Intrinsic and Extrinsic Contributions to Consensus Molecular Subtypes in Primary and Metastatic Colon Cancer. *Clin Cancer Res* (2019) 25:4431–42. doi: 10.1158/1078-0432.CCR-18-3032
5. Roelands J, Kuppen PJK, Vermeulen L, Maccalli C, Decock J, Wang E, et al. Immunogenomic Classification of Colorectal Cancer and Therapeutic Implications. *Int J Mol Sci* (2017) 18:2229. doi: 10.3390/ijms18102229
6. Marisa L, de Reynies A, Duval A, Selves J, Gaub MP, Vescovo L, et al. Gene expression classification of colon cancer into molecular subtypes: characterization, validation, and prognostic value. *PloS Med* (2013) 10(5): e1001453. doi: 10.1371/journal.pmed.1001453
7. Sorlie T, Tibshirani R, Parker J, Hastie T, Marron JS, Nobel A, et al. Repeated observation of breast tumor subtypes in independent gene expression data sets. *Proc Natl Acad Sci USA* (2003) 100(14):8418–23. doi: 10.1073/pnas.0932692100
8. Christiansen JJ, Rajasekaran AK. Reassessing epithelial to mesenchymal transition as a prerequisite for carcinoma invasion and metastasis. *Cancer Res* (2006) 66:8319–26. doi: 10.1158/0008-5472.CAN-06-0410
9. Lu W, Kang Y. Epithelial-Mesenchymal Plasticity in Cancer Progression and Metastasis. *Dev Cell* (2019) 49:361–74. doi: 10.1016/j.devcel.2019.04.010
10. Cao H, Xu E, Liu H, Wan L, Lai M. Epithelial-mesenchymal transition in colorectal cancer metastasis: A system review. *Pathol Res Pract* (2015) 211 (8):557–69. doi: 10.1016/j.prp.2015.05.010
11. Feng YL, Chen DQ, Vaziri ND, Guo Y, Zhao YY. Small molecule inhibitors of epithelial-mesenchymal transition for the treatment of cancer and fibrosis. *Med Res Rev* (2020) 40(1):54–78. doi: 10.1002/med.21596
12. Mota MBS, Carvalho MA, Monteiro ANA, Mesquita RD. DNA damage response and repair in perspective: Aedes aegypti, Drosophila melanogaster and Homo sapiens. *Parasit Vectors* (2019) 12(1):533. doi: 10.1186/s13071-019-3792-1
13. Chae YK, Anker JF, Oh MS, Bais P, Namburi S, Agte S, et al. Mutations in DNA repair genes are associated with increased neoantigen burden and a distinct immunophenotype in lung squamous cell carcinoma. *Sci Rep* (2019) 9(1):3235. doi: 10.1038/s41598-019-39594-4
14. Le DT, Uram JN, Wang H, Bartlett BR, Kemberling H, Eyring AD, et al. PD-1 Blockade in Tumors with Mismatch-Repair Deficiency. *N Engl J Med* (2015) 372(26):2509–20. doi: 10.1056/NEJMoa1500596
15. Williams CS, Bernard JK, Demory Beckler M, Almohazey D, Washington MK, Smith JJ, et al. ERBB4 is over-expressed in human colon cancer and enhances cellular transformation. *Carcinogenesis* (2015) 36(7):710–8. doi: 10.1093/carcin/bgv049
16. Jorissen RN, Gibbs P, Christie M, Prakash S, Lipton L, Desai J, et al. Metastasis-Associated Gene Expression Changes Predict Poor Outcomes in Patients with Dukes Stage B and C Colorectal Cancer. *Clin Cancer Res* (2009) 15(24):7642–51. doi: 10.1158/1078-0432.CCR-09-1431
17. Mariathasan S, Turley SJ, Nickles D, Castiglioni A, Yuen K, Wang Y, et al. TGFbeta attenuates tumour response to PD-L1 blockade by contributing to exclusion of T cells. *Nature* (2018) 554(7693):544–8. doi: 10.1038/nature25501
18. Gautier L, Cope L, Bolstad BM, Irizarry RA. affy–analysis of Affymetrix GeneChip data at the probe level. *Bioinformatics* (2004) 20(3):307–15. doi: 10.1093/bioinformatics/btg405
19. Subramanian A, Tamayo P, Mootha V, Mukherjee S, Ebert B, Gillette M, et al. Gene set enrichment analysis: a knowledge-based approach for interpreting genome-wide expression profiles. *Proc Natl Acad Sci USA* (2005) 102 (43):15545–50. doi: 10.1073/pnas.0506580102
20. Kardos J, Chai S, Mose LE, Selitsky SR, Krishnan B, Saito R, et al. Claudin-low bladder tumors are immune infiltrated and actively immune suppressed. *JCI Insight* (2016) 1(3):e85902. doi: 10.1172/jci.insight.85902
21. Nidheesh N, Abdul Nazeer KA, Ameer PM. An enhanced deterministic K-Means clustering algorithm for cancer subtype prediction from gene expression data. *Comput Biol Med* (2017) 91:213–21. doi: 10.1016/j.compbiomed.2017.10.014
22. Wilkerson MD, Hayes DN. ConsensusClusterPlus: a class discovery tool with confidence assessments and item tracking. *Bioinformatics* (2010) 26:1572–3. doi: 10.1093/bioinformatics/btq170
23. Hanzelmann S, Castelo R, Guinney J. GSVA: gene set variation analysis for microarray and RNA-seq data. *BMC Bioinf* (2013) 14:7. doi: 10.1186/1471-2105-14-7
24. Huang X, Liu J, Mo X, Liu H, Wei C, Huang L, et al. Systematic profiling of alternative splicing events and splicing factors in left- and right-sided colon cancer. *Aging (Albany NY)* (2019) 11(19):8270. doi: 10.18632/aging.102319
25. Goeman JJ. L1 penalized estimation in the Cox proportional hazards model. *Biom J* (2010) 52:70–84. doi: 10.1002/bimj.200900028
26. Liu J, Huang X, Yang W, Li C, Li Z, Zhang C, et al. Nomogram for predicting overall survival in stage II-III colorectal cancer. *Cancer Med* (2020) 9(7):2363–71. doi: 10.1002/cam4.2896
27. Luchini C, Bibeau F, Ligtenberg MJL, Singh N, Nottegar A, Bosse T, et al. ESMO recommendations on microsatellite instability testing for immunotherapy in cancer, and its relationship with PD-1/PD-L1 expression and tumour mutational burden: a systematic review-based approach. *Ann Oncol* (2019) 30(8):1232–43. doi: 10.1093/annonc/mdz116
28. Gibbons DL, Creighton CJ. Pan-cancer survey of epithelial-mesenchymal transition markers across the Cancer Genome Atlas. *Dev Dyn* (2018) 247:555–64. doi: 10.1002/dvdy.24485
29. Lu YC, Robbins PF. Targeting neoantigens for cancer immunotherapy. *Int Immunol* (2016) 28:365–70. doi: 10.1093/intimm/dxw026
30. Wilkinson NW, Yothers G, Lopa S, Costantino JP, Petrelli NJ, Wolmark N. Long-term survival results of surgery alone versus surgery plus 5-fluorouracil and leucovorin for stage II and stage III colon cancer: pooled analysis of NSABP C-01 through C-05. A baseline from which to compare modern adjuvant trials. *Ann Surg Oncol* (2010) 17(4):959–66. doi: 10.1245/s10434-009-0881-y
31. Zhou R, Zeng D, Zhang J, Sun H, Wu J, Li N, et al. A robust panel based on tumour microenvironment genes for prognostic prediction and tailoring therapies in stage I-III colon cancer. *EBioMedicine* (2019) 42:420–30. doi: 10.1016/j.ebiom.2019.03.043
32. Wang BD, Lee NH. Aberrant RNA Splicing in Cancer and Drug Resistance. *Cancers (Basel)* (2018) 10(11):458. doi: 10.3390/cancers10110458
33. Ganesh K, Stadler ZK, Cercek A, Mendelsohn RB, Shia J, Segal NH, et al. Immunotherapy in colorectal cancer: rationale, challenges and potential. *Nat Rev Gastroenterol Hepatol* (2019) 16(6):361–75. doi: 10.1038/s41575-019-0126-x
34. Suman S, Das TP, Sirimulla S, Alatassi H, Ankem MK, Damodaran C. Withaferin-A suppress AKT induced tumor growth in colorectal cancer cells. *Oncotarget* (2016) 7(12):13854–64. doi: 10.18632/oncotarget.7351
35. Gurzu S, Silveanu C, Fetyko A, Butiurca V, Kovacs Z, Jung I. Systematic review of the old and new concepts in the epithelial-mesenchymal transition of colorectal cancer. *World J Gastroenterol* (2016) 22(30):6764–75. doi: 10.3748/wjg.v22.i30.6764
36. Vodenkova S, Buchler T, Cervena K, Veskrnova V, Vodicka P, Vymetalkova V. 5-fluorouracil and other fluoropyrimidines in colorectal cancer: Past, present and future. *Pharmacol Ther* (2019) 206:107447. doi: 10.1016/j.pharmthera.2019.107447
37. Zhao X, Fan J, Zhi F, Li A, Li C, Berger AE, et al. Mobilization of epithelial mesenchymal transition genes distinguishes active from inactive lesional tissue in patients with ulcerative colitis. *Hum Mol Genet* (2015) 24(16):4615–24. doi: 10.1093/hmg/ddv192
38. Pavlova NN, Thompson CB. The Emerging Hallmarks of Cancer Metabolism. *Cell Metab* (2016) 23:27–47. doi: 10.1016/j.cmet.2015.12.006
39. Sharma A, Boise LH, Shanmugam M. Cancer Metabolism and the Evasion of Apoptotic Cell Death. *Cancers (Basel)* (2019) 11(8):1144. doi: 10.3390/cancers11081144
40. Guo W, Tan HY, Chen F, Wang N, Feng Y. Targeting Cancer Metabolism to Resensitize Chemotherapy: Potential Development of Cancer

Chemosensitizers from Traditional Chinese Medicines. *Cancers (Basel)* (2020) 12(2):404. doi: 10.3390/cancers12020404
41. Gong W, Ekmu B, Wang X, Lu Y, Wan L. AGR2-induced glucose metabolism facilitated the progression of endometrial carcinoma via enhancing the MUC1/HIF-1alpha pathway. *Hum Cell* (2020) 33(3):790–800. doi: 10.1007/s13577-020-00356-4
42. Trehoux S, Duchene B, Jonckheere N, Van Seuningen I. The MUC1 oncomucin regulates pancreatic cancer cell biological properties and chemoresistance. Implication of p42-44 MAPK, Akt, Bcl-2 and MMP13 pathways. *Biochem Biophys Res Commun* (2015) 456(3):757–62. doi: 10.1016/j.bbrc.2014.12.025
43. Yoshida GJ. Metabolic reprogramming: the emerging concept and associated therapeutic strategies. *J Exp Clin Cancer Res* (2015) 34:111. doi: 10.1186/s13046-015-0221-y
44. Mo X, Huang X, Feng Y, Wei C, Liu H, Ru H, et al. Immune infiltration and immune gene signature predict the response to fluoropyrimidine-based chemotherapy in colorectal cancer patients. *Oncoimmunology* (2020) 9(1):1832347. doi: 10.1080/2162402X.2020.1832347
45. Benatti P, Gafa R, Barana D, Marino M, Scarselli A, Pedroni M, et al. Microsatellite instability and colorectal cancer prognosis. *Clin Cancer Res* (2005) 11(23):8332–40. doi: 10.1158/1078-0432.CCR-05-1030
46. Kamps R, Brandão RD, Bosch BJ, Paulussen AD, Xanthoulea S, Blok MJ, et al. Next-Generation Sequencing in Oncology: Genetic Diagnosis, Risk Prediction and Cancer Classification. *Int J Mol Sci* (2017) 18(2):308. doi: 10.3390/ijms18020308
47. Di Resta C, Ferrari M. Next Generation Sequencing: From Research Area to Clinical Practice. *Ejifcc* (2018) 29:215–20.
48. Kuo FC, Mar BG, Lindsley RC, Lindeman NI. The relative utilities of genome-wide, gene panel, and individual gene sequencing in clinical practice. *Blood* (2017) 130(4):433–9. doi: 10.1182/blood-2017-03-734533

Conflict of Interest: The authors declare that the research was conducted in the absence of any commercial or financial relationships that could be construed as a potential conflict of interest.

frontiers in Oncology

ORIGINAL RESEARCH
published: 02 February 2021
doi: 10.3389/fonc.2020.605777

LCN2 Is a Potential Biomarker for Radioresistance and Recurrence in Nasopharyngeal Carcinoma

Meng-Xia Zhang[1†], Li Wang[2†], Lei Zeng[3] and Zi-Wei Tu[4*]*

[1] State Key Laboratory of Oncology in South China, Department of Nasopharyngeal Carcinoma, Sun Yat-Sen University Cancer Center, Collaborative Innovation Center for Cancer Medicine, Guangzhou, China, [2] Department of Radiotherapy, Eye & ENT Hospital, Fudan University, Shanghai, China, [3] Department of Oncology, The Second Affiliated Hospital of Nanchang University, Nanchang, China, [4] NHC Key Laboratory of Personalized Diagnosis and Treatment of Nasopharyngeal Carcinoma (Jiangxi Cancer Hospital of Nanchang University), Nanchang, China

OPEN ACCESS

Edited by:
David Y. Lee, University of New Mexico, United States

Reviewed by:
Jareer Kassis, Bien-Etre Labs, LLC, United States
Ping Yi, Third Affiliated Hospital of Chongqing Medical University, China

***Correspondence:**
Zi-Wei Tu
tuziwei198803@163.com
Lei Zeng
zlsports100@163.com

[†]These authors have contributed equally to this work

Specialty section:
This article was submitted to Molecular and Cellular Oncology, a section of the journal Frontiers in Oncology

Received: *13 September 2020*
Accepted: *15 December 2020*
Published: *02 February 2021*

Citation:
Zhang M-X, Wang L, Zeng L and Tu Z-W (2021) LCN2 Is a Potential Biomarker for Radioresistance and Recurrence in Nasopharyngeal Carcinoma. Front. Oncol. 10:605777. doi: 10.3389/fonc.2020.605777

Background: Radioresistance-induced local failure, which can result in residual or recurrent tumors, remains one of the major causes of treatment failure in nasopharyngeal carcinoma (NPC). Lipocalin 2 (LCN2) is known to play important roles in cancer initiation, progression, and treatment responses. However, its role in the radioresistance of NPC remains unclear.

Methods: Microarray data from the Gene Expression Omnibus (GEO) was screened for candidate biomarkers relating to the radioresistance of NPC. The expression of LCN2 in NPC cell lines was verified by quantitative real-time PCR (RT-qPCR) and western blotting. The effects of knockdown or overexpression of LCN2 on NPC radiosensitivity were examined using a soft agar colony formation assay and a γH2AX assay. LCN2 expression in NPC specimens was evaluated by immunohistochemistry. Survival outcomes were analyzed. A possible correlation between LCN2 and hypoxia-inducible factor 1-alpha (HIF-1A) was examined by western blotting and a tissue microarray.

Results: LCN2 was highly expressed in the radioresistant NPC cell line CNE2R. Knocking down LCN2 enhanced the radiosensitivity of NPC cells by impairing their ability to repair DNA damage or proliferate, while ectopic expression of LCN2 conferred additional radioresistance to NPC cells. Immunohistochemical analysis of 100 NPC specimens revealed that LCN2 expression was significantly upregulated in radioresistant NPC tissues and was associated with NPC recurrence. Furthermore, a significant correlation between the expression of LCN2 and HIF-1A was detected.

Conclusion: LCN2 is associated with radioresistance and recurrence in NPC and may facilitate the development of a radioresistant phenotype through interacting with HIF-1A. Our data indicate that LCN2 is a promising target for predicting and overcoming radioresistance in NPC.

Keywords: nasopharyngeal carcinoma, lipocalin 2, hypoxia-inducible factor 1-alpha, radioresistance, recurrence

INTRODUCTION

Nasopharyngeal carcinoma (NPC) is a malignancy of the epithelial origin. Although rare in western countries, it is endemic in Southeast Asia and southern China. NPC age-standardized incidence rates are 3.0 and 0.4 per 100,000 population for China and western countries, respectively (1). NPC is one of the most frequently diagnosed malignancies in China (2). Radiotherapy is the primary treatment option for non-metastatic NPC owing to the high sensitivity of this cancer to ionizing radiation and the relatively inaccessible anatomical location of the nasopharynx, which renders surgery difficult to implement. However, the efficacy of radiotherapy and the prognosis of NPC patients are impaired by inherent or acquired radioresistance, which can result in tumor recurrence or distant failure (3). Consequently, investigating the mechanism of radioresistance and identifying biomarkers that can predict radioresistance and outcomes for NPC patients are urgently needed to allow for individualized treatment.

Lipocalin 2 [LCN2; also known as neutrophil gelatinase-associated lipocalin (NGAL)] is a 25-kDa protein belonging to the lipocalin superfamily and is a vital modulator of iron homeostasis (4). A growing number of studies have identified the *LCN2* gene as crucial for various tumor-related processes, including tumorigenesis, tumor progression, and tumor resistance to therapies such as radiotherapy, chemotherapy, endocrine therapy, and targeted therapy (5–12). A previous study has demonstrated that LCN2 is upregulated in lung cancer cells treated with X-ray irradiation and the sensitivity of these lung cancer cells to radiation is enhanced by the silencing of LCN2. Additionally, LCN2 overexpression has been associated with radioresistance in both oral cancer and lung cancer cells and can serve as a predictor of radioresistance (13). These findings indicated that LCN2 may play an important role in the radioresistance of several tumors. NPC is highly sensitive to radiotherapy and is markedly different from other head and neck cancers (*e.g.*, oral cancer). However, the functional role of LCN2 in NPC radioresistance remains largely unknown.

In the current study, we assessed the potential of *LCN2* as a biomarker for NPC radioresistance through analyzing a Gene Expression Omnibus (GEO) data set (GSE48501). Furthermore, we also investigated the relationship between LCN2 and radioresistance, recurrence of NPC. Our results suggested that LCN2 may be an important biomarker for NPC and throw light on the potential mechanisms underlying NPC radioresistance.

MATERIALS AND METHODS

Cell Lines

NPC cell lines (CNE1, HNE1, HNOE1, SUNE1, CNE-2, and its radioresistant cell type CNE2R) were obtained from Sun Yat-Sen University Cancer Center (Guangzhou, China) and maintained in DMEM medium (Invitrogen, California, USA) supplemented with 10% fetal bovine serum (Gibco, New York, USA) and 1% penicillin–streptomycin (HyClone, Utah, USA). All cells were cultured at 37°C in a humidified chamber with 5% CO_2.

Microarray Data Analysis

The mRNA expression profile of gene chip GSE48501 was downloaded from the GEO database (https://www.ncbi.nlm.nih.gov/geo/query/acc.cgi?acc=GSE48501) (14). GSE48501 includes the expression profile of two human radioresistant NPCs and two human radiosensitive NPCs obtained using the Affymetrix Human Genome U133 Plus 2.0 Array platform. Raw data were preprocessed using the Bioconductor package 'affy' as previously described (15). Differentially expressed genes (DEGs) were analyzed using the GEO2R tool (http://www.ncbi.nlm.nih.gov/geo/geo2r/). Adjusted P-value <0.01 was used to select DEGs.

Patients and Tissue Specimens

A total of 100 primary-diagnosed, non-disseminated, paraffin-embedded NPC tissue specimens were obtained from Jiangxi Provincial Hospital of Nanchang University (Nanchang, China) from February 2011 to November 2015 for immunohistochemical analysis. The sensitivity of NPC patients to radiotherapy was defined as previously described (10, 16). In brief, patients with radioresistant NPC were defined as those with incomplete regression of lesions after radical irradiation; residual tumors at more than 6 weeks after the completion of radiotherapy; or local/regional recurrence after radiotherapy. Patients with radiosensitive NPC were defined as those with complete regression after irradiation or without recurrence after the completion of radiotherapy (16). Written informed consent was obtained from all the patients. Approval for NPC tissue use was granted by the Ethics Committee of Jiangxi Provincial Hospital.

Western Blotting

Western blotting was performed to verify the knockdown or overexpression of LCN2 in NPC cells. Cells were rinsed with cold phosphate-buffered saline (PBS) and lysed in RIPA buffer (Beyotime, Shanghai, China). The lysates were then incubated on ice for 30 min and centrifuged at 12,000 rpm for 25 min at 4°C. Equal amounts (40 μg) of protein were separated by 12% sodium dodecyl sulfate–polyacrylamide gradient gel electrophoresis (SDS–PAGE) and transferred onto polyvinylidene difluoride (PVDF) membranes. The membranes were blocked with 5% skimmed milk for 2 h at room temperature and then incubated with a 1:2,000 dilution of an anti-LCN2 rabbit polyclonal antibody (TA322583, Origene, Maryland, USA) for 16 h at 4°C. This was followed by incubation with a 1:5,000 dilution of a horseradish peroxidase-conjugated secondary antibody for 1 h at room temperature on a shaker. An enhanced chemiluminescence reagent (Thermo Scientific, Massachusetts, USA) was used to detect protein signals. GAPDH was used as a loading control.

Quantitative Real-Time PCR

Total RNA was extracted from NPC cells using TRIzol reagent (Invitrogen) according to the manufacturer's instructions. The concentration and quality of the isolated RNA were evaluated using an Agilent 2100 Bioanalyzer (Agilent Technologies, California, USA). First-strand cDNA was reverse-transcribed using the Prime-Script RT Reagent Kit with gDNA Eraser

(TaKaRa, Tokyo, Japan). Quantitative real-time PCR (qPCR) was performed to measure *LCN2* mRNA levels using SYBR Premix Ex Taq II (TaKaRa). The sequences of the primers used were 5′-GCTGACTTCGGAACTAAAGG AGAA-3′ (forward) and 5′-GGGAAGACGATGTGGTTTTCA-3′ (reverse) for *LCN2* and 5′-CATCTCTGCCCCCTCTGCTGA-3′ (forward) and 5′-GGATGACCTTGCCCACAGCCT-3′ (reverse) for *GAPDH*, which was used as an internal control (13). The PCR cycling parameters were as follows: 95°C for 30 s, followed by 40 cycles of 95°C for 20 s, 60°C for 30 s, and 70°C for 2 min. All the reactions were performed in triplicate. Gene expression was normalized that of *GAPDH* and quantified using the 2-ΔΔCt method.

Plasmids, RNA Interference, and Stable Transfection

Human *LCN2* cDNA or a negative control sequence was cloned into a pSin-EF2 retroviral vector (Origene). CNE2R and HNE1 cells stably expressing scrambled or LCN2 short hairpin RNAs (shRNAs) were established by the Sigma shRNA system according to the manufacturer's instructions. The sequences for human LCN2 shRNA-1 and shRNA-2 were 5′-TACAAT GTCACCTCCGTCCTGTTTAGGAA-3′ and 5′-GAGAACCA AGGAGCTGACTTCGGAACTAA-3′, respectively; the non-specific shRNA control sequence was 5′-GCACTACCAGAGC TAACTCAGATAGTACT-3′. The constructed vectors were verified by DNA sequencing and then transfected into 293T cells. The supernatants containing the lentiviruses were collected and purified at 72 h post-transfection. Transfected cells were selected with puromycin (Sigma–Aldrich, St. Louis, MO, USA) at a concentration of 2 μg/ml or neomycin (InvivoGen, Hong Kong, China) at a concentration of 300 μg/ml for 1–2 weeks. To determine transfection efficiency, LCN2 protein levels were assessed by western blotting.

Soft Agar Colony Formation Assay

The soft agar colony formation assay was performed as previously described (17, 18). Briefly, 100, 200, 1×10^3, or 1×10^4 cells were suspended in 2 ml of 0.6% top agar (Sigma–Aldrich) and plated onto 1.2% base agar in 6-well plates and irradiated with a 0-, 2-, 4-, or a 6-Gy dose of 160 kV X-rays (RAD SOURCE, USA). The irradiated cells were cultured for 14 days. Colonies with a diameter of >50 μm were counted and imaged at ×4 magnification using a Nikon ECLIPSE Ti2 inverted fluorescence microscope. The cloning efficiency was calculated by dividing the number of colonies by the number of cells plated. Each measurement was the average ± standard deviation (SD) of three experiments.

γH2AX Assay

Cells were plated in 30-mm dishes and cultured for 72 h at 37°C. To detect irradiation-induced DNA double-strand breaks (DSBs), cells were treated with a 2-Gy dose of irradiation from an external X-ray source (RAD SOURCE) at room temperature and incubated for 0.5 and 24 h. Unirradiated cells served as controls. To detect H2AX phosphorylation, cells were sequentially fixed in 4% formaldehyde (Sigma–Aldrich) for 15 min and 50% methanol in PBS for 10 min. The cells were subsequently blocked with 5% bovine serum albumin for 30 min, incubated with a rabbit monoclonal anti-γH2AX antibody (1:1,000, Cell Signaling Technology, Boston, USA) for 30 min, washed in PBS, incubated with an Alexa 488-conjugated (Molecular Probes, USA) secondary antibody for 30 min, and counterstained with DAPI (Invitrogen). Images were captured using an Olympus FV100 confocal microscope. γH2AX-positive cells were defined as those with more than 20 γH2AX foci. Five random fields per coverslip were selected to calculate the number of γH2AX-positive cells. Assays were performed in triplicate to eliminate intra-assay variability.

Immunohistochemistry

Immunohistochemical analysis of LCN2 was performed on 100 paraffin-embedded NPC specimens. First, tissue slides were baked in an oven at 60°C for 2 h and deparaffinized twice with dimethylbenzene, 10 min each step, and rehydrated with graded ethanol. The slides were then treated with citrate buffer (pH 6.0) under high pressure for antigen retrieval followed by the blocking of endogenous peroxidase activity with 0.3% H_2O_2 for 30 min. Next, the slides were sequentially incubated with an anti-LCN2 antibody (1:100 dilution, Origene) for 16 h at 4°C, a biotinylated anti-rabbit antibody (1:1,000 dilution) for 30 min at room temperature, and a biotinylated secondary antibody for 1 h at 37°C. Finally, the tissue sections were stained with 3,3′-diaminobenzidine tetrahydrochloride (DAB) and counterstained with Harris modified hematoxylin. The immunohistochemical results were scored as the intensity grades multiplied by the positive ratios, as previously reported (19). The scores were classified as 0–3 (no staining, weak staining, moderate staining, and strong staining) for the staining intensity and 0–4 (no staining, <10, 10–50, 50–80, and >80% staining) for the positive ratio. The final scores (0–12) were grouped into no/low expression (≤6) and high expression (>6). The scores were determined blindly by two pathologists.

Statistical Analyses

The data are presented as means ± SD from three independent tests. The Student's *t*-test or the Mann–Whitney *U* test was used to compare the differences between continuous parameters. The distribution of clinicopathological variables between high and low LCN2 expression groups was compared by the chi-square test. Survival curves were constructed using the Kaplan–Meier method and compared using the log-rank test. The endpoints were assessed as follows: local relapse-free survival (LRFS) and nodal relapse-free survival (NRFS) were measured from the date of treatment to the date of the first observation of local and regional recurrence, respectively. Local and regional relapse were defined as relapse-free survival (RFS). Distant metastasis-free survival (DMFS) was measured from the date of treatment to the date of the first observation of distant metastasis. Progression-free survival (PFS) was measured from the date of treatment to either the date of the first observation of local or regional recurrence, or distant metastasis. Overall survival (OS) was measured from the first date of treatment to the date of death due to any cause. Multivariable analysis was conducted using the

Cox proportional hazards model after adjusting for confounding factors such as age, sex, T stage, N stage, and receiving or not induction chemotherapy. The significance of any correlation between LCN2 and HIF-1A expression was determined by Pearson's correlation analysis. All statistical tests were two-sided. Associations were considered statistically significant at *P*-values <0.05. All statistical analyses were performed using SPSS version 26.0 (SPSS IBM, Chicago, USA). The raw data obtained in this study have been uploaded onto the Research Data Deposit (RDD) with the RDD number RDDB2020000932.

RESULTS

LCN2 Was Identified as a Radioresistance-Related Gene in NPC

We manually found a GEO data set (GSE48501), using which, we conducted a comparative analysis of mRNA expression in NPC cell lines CNE2 and CNE2R. The online analysis tool GEO2R showed the upregulation of LCN2 in CNE2R compared to that of CNE2 (**Figure 1A**). A GEO profile was found at GDS3125/212531_at (nih.gov) and demonstrated the responses of radiosensitive and radioresistant tumors to ionizing radiation (time course). Briefly, squamous cell carcinoma-derived xenografts were generated and allowed to grow to a volume of 150–200 mm^3. At that time, tumors were either treated with a 3-Gy dose of irradiation or left untreated and then collected for RNA purification 5 or 24 h later. The overall expression level of LCN2 was higher in the radioresistant squamous cell carcinomas (SCCs) than in the radiosensitive SCCs, in both the irradiated and untreated groups ($P < 0.0001$). In the radiosensitive SCCs, LCN2 expression was significantly upregulated at the 24-h time point after irradiation when compared with that in the untreated group ($P = 0.0441$) (**Figure 1B** and **Supplementary Table 1**).

Validation of LCN2 Expression in NPC Cell Lines

To verify the expression of LCN2 identified in the microarray data, western blotting and RT-qPCR were performed to detect the protein and mRNA levels of LCN2, respectively, in five NPC cell lines (CNE1, CNE2, HNE1, HNOE1, and SUNE1) and one radioresistant NPC cell line (CNE2R). Consistent with the results of the microarray analysis, the highest expression of LCN2 was found in CNE2R cells. Furthermore, LCN2 was also highly expressed in CNE1 and HNE1 cells (**Figures 1C, D**). CNE1 is a highly differentiated NPC-derived squamous cell carcinoma

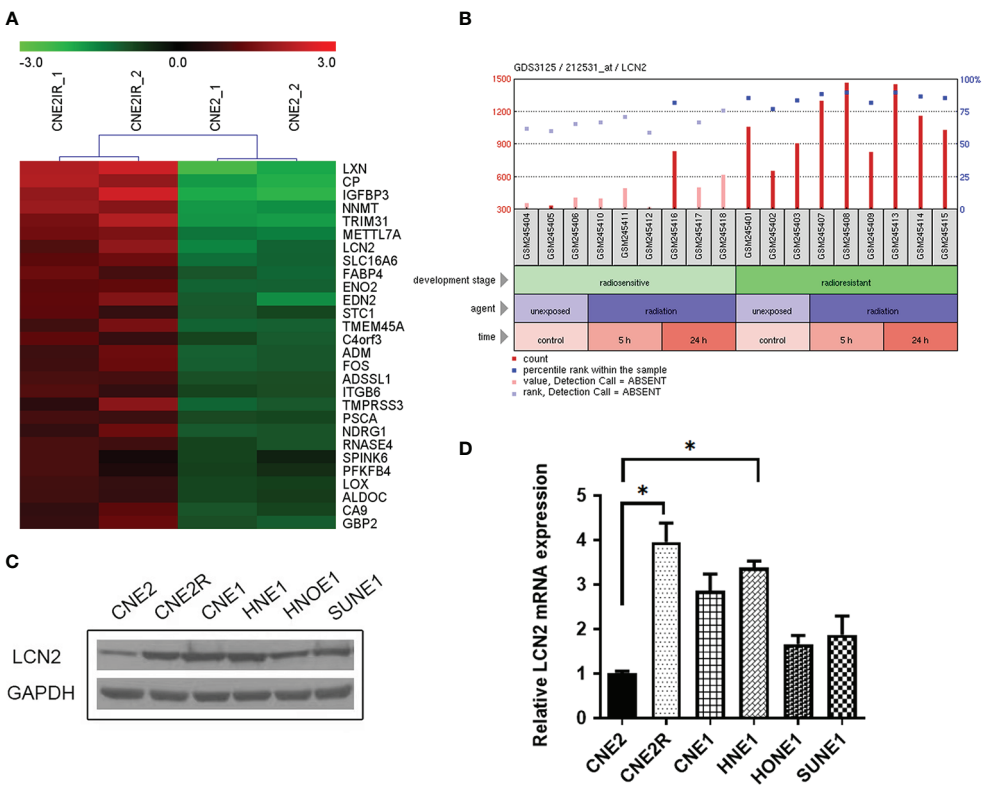

FIGURE 1 | LCN2 was identified as a radioresistance-related gene in nasopharyngeal carcinoma (NPC). **(A)** A heatmap of the overlapping differential expressed genes (DEGs) between the radiosensitive cell line CNE2 and the radioresistant cell line CNE2R in GSE48501. **(B)** The responses of radiosensitive and radioresistant squamous cell carcinomas (SCCs) to ionizing radiation (time course). LCN2 expression was upregulated in both radioresistant and radiosensitive SCCs after irradiation. **(C, D)** Validation of LCN2 expression in NPC cell lines. LCN2 protein **(C)** and mRNA **(D)** levels were examined by western blotting and quantitative real-time PCR (RT-qPCR), respectively. GAPDH was used as an internal control. *$P < 0.05$.

cell line, while HNE1 is an Epstein–Barr virus (EBV)-positive cell line derived from a poorly differentiated squamous carcinoma. According to the law of Bergonié and Tribondeau, highly differentiated tumor cells usually display medium to low sensitivity to radiation (20, 21). In NPC, EBV infection is one of the most important factors contributing to radioresistance (22, 23). Consequently, these results indicate that LCN2 expression is upregulated in radioresistant NPC cells.

LCN2 Regulates the Radiosensitivity of NPC Cells

To determine whether LCN2 levels contribute to NPC radiosensitivity, we generated stable LCN2-knockdown CNE2R and HNE1 cell lines as well as a CNE2 cell line stably overexpressing LCN2. Stable transfections were confirmed by western blotting (**Figures 2A, B**). The colony survival assay is the gold standard method for assessing the radiosensitivity of tumor cells (24). Here, we performed a soft agar colony assay to investigate the effect of LCN2 on cell proliferation after irradiation. We found that, following irradiation at the dose of 2, 4, or 6 Gy, colony-formation rates were markedly reduced in LCN2-depleted CNE2R cells compared with that of control cells (**Figures 2C, E**). Conversely, LCN2-overexpressing cells formed more colonies than control cells (**Figures 2D, F**).

Double-strand breaks (DSBs) constitute the major type of DNA damage caused by irradiation (25), while the DSB repair capacity is closely associated with radiosensitivity (26). Therefore, we conducted a γH2AX [a biomarker of DSBs (27)] assay to examine the phosphorylation status of H2AX in these cells at 0, 0.5, and 24 h post-irradiation. At 24 h after receiving a 2-Gy dose of radiation, the DNA damage repair ability of cells with LCN2 knockdown was significantly attenuated (**Figures 3A, B**), whereas the opposite effect was observed in CNE2 cells stably overexpressing LCN2 (**Figures 3C, D**). These results indicated that LCN2 may regulate NPC radiosensitivity by influencing the DNA damage repair process.

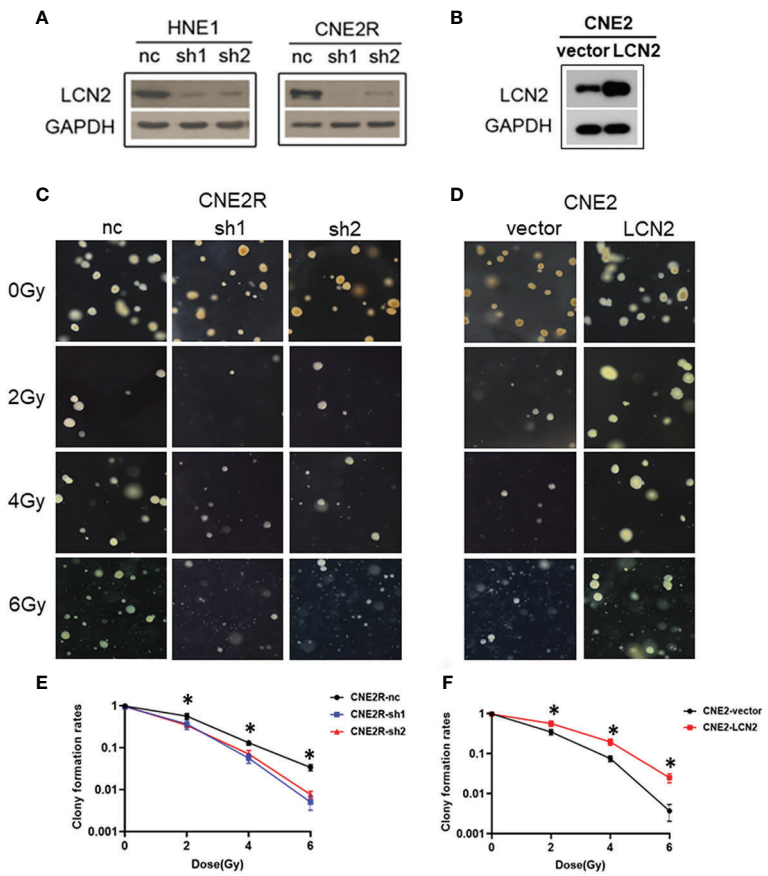

FIGURE 2 | LCN2 regulates the radiosensitivity of nasopharyngeal carcinoma (NPC) cells. **(A, B)** Validation of LCN2 expression in various NPC cell lines. Knockdown or ectopic expression of LCN2 in HNE1, CNE2R, or CNE2 cells was validated by western blotting. **(C, E)** A soft agar colony formation assay was used to assess the radiosensitivity of NPC cells. The colony formation rates were markedly reduced in CNE2R cells with LCN2 knockdown compared with that of control cells following irradiation at the dose of 2, 4, or 6 Gy. *$P < 0.05$. **(D, F)** CNE2 cells overexpressing LCN2 formed more colonies than control cells at the irradiation doses of 2, 4, and 6 Gy. *$P < 0.05$.

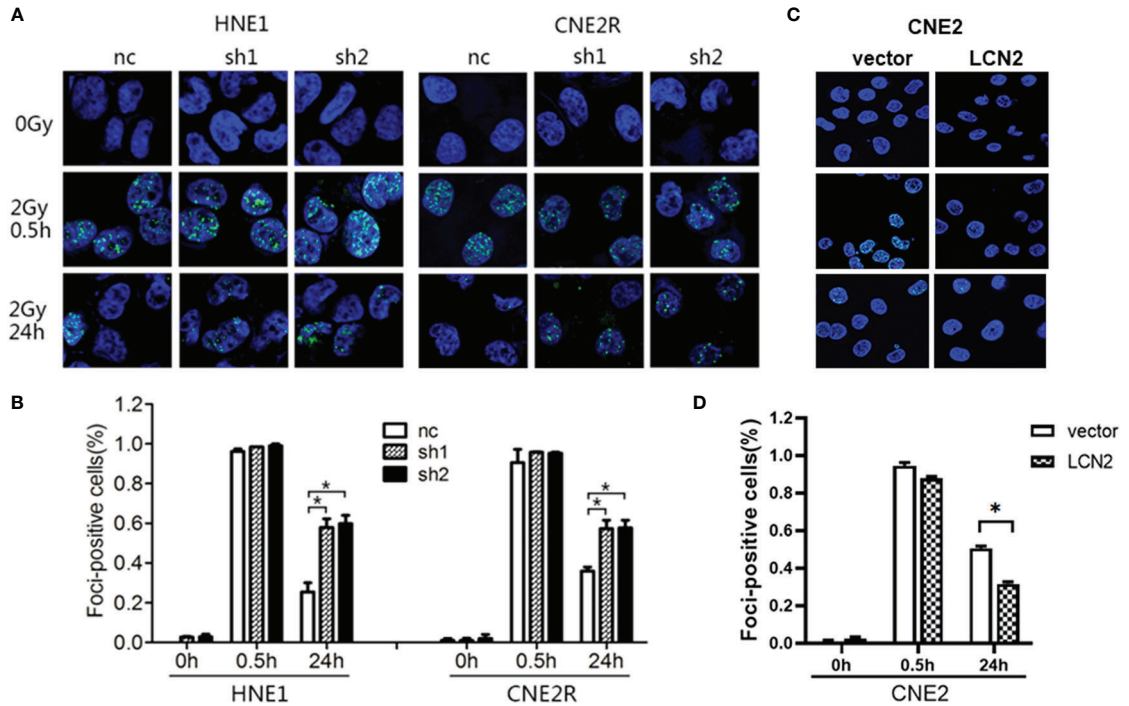

FIGURE 3 | LCN2 regulates the radiosensitivity of nasopharyngeal carcinoma (NPC) cells. **(A, B)** The DNA double-strand break repair capacity was impaired in HNE1 and CNE2R cells with LCN2 knockdown, as evidenced by the greater number of γH2AX-positive LCN2-depleted cells when compared with that of control cells. *$P < 0.05$. **(C, D)** The DNA double-strand break repair capacity was enhanced in LCN2-overexpressing CNE2 cells based on the percentage of γH2AX-positive cells. *$P < 0.05$.

LCN2 Is a Potential Biomarker for Predicting NPC Radioresistance

A total of 14 patients were defined as having radioresistant NPC according to the definition mentioned in the section *Patients and Tissue Specimens*. Immunohistochemical analysis showed that LCN2 expression was significantly higher in radioresistant NPC tissues than in radiosensitive NPC tissues ($P = 0.034$) (**Figure 4A**). The response to radiotherapy is related to the intrinsic characteristics of NPC, including tumor size and infiltration status. Therefore, we compared the potential of using LCN2 expression with that of using T stage, N stage, or UICC stage to discriminate between patients with radioresistant NPC and those with radiosensitive NPC using receiver operating characteristic (ROC) curves. The area under the curve (AUC) values for LCN2 expression, T stage, N stage, and UICC stage were 0.808, 0.634, 0.600, and 0.588, respectively. The sensitivity and specificity of LCN2, T stage, N stage, and UICC stage were 78.6 and 70.9, 64.3% and 55.8, 78.6 and 41.9%, and 71.4 and 40.7%, respectively (**Figure 4B**). These results indicated that the LCN2 expression level was the best predictor of NPC radioresistance among the four indicators.

The Association Between LCN2 Expression and Survival Outcomes in NPC

Next, we assessed whether there was a correlation between LCN2 expression and the clinical parameters of 100 NPC patients. Sections of normal nasopharynx mucosa and NPC tissues stained for LCN2 are shown in **Figures 5A–C**. The expression of LCN2 was not significantly associated with age, sex, T stage, N stage, UICC stage, or whether or not patients had received induction chemotherapy (**Table 1**). High expression of LCN2 was associated with poor LRFS ($P = 0.042$) and RFS ($P = 0.014$), but not with NRFS ($P = 0.212$), DMFS ($P = 0.239$), PFS ($P = 0.918$), or OS ($P = 0.737$) (**Figures 5D–I**). Further multivariate analyses identified LCN2 as an independent and unfavorable prognostic indicator for RFS in NPC patients ($P = 0.022$) (**Table 2**). We also found that LCN2 expression was an independent prognostic factor for LRFS, but with borderline significance ($P = 0.055$). Radioresistance is known to facilitate tumor recurrence to some extent. Consequently, these results indicated that LCN2 overexpression is clinically relevant for NPC recurrence.

The Correlation Between the Expression of LCN2 and HIF-1A

Given that radioresistance is closely related to the hypoxic microenvironment of tumors (28, 29), we speculated that there may be a correlation between the expression of LCN2 and that of hypoxia-related genes. We found that the protein level of HIF-1A, a hypoxia-related factor, was reduced in both HNE1 and CNE2R cells with LCN2 knockdown, while it was increased in CNE2 cells stably overexpressing LCN2 (**Figure 6A**). We also performed a correlation analysis between LCN2 and HIF-1A expression in 23 NPC tissues using a microarray. The results

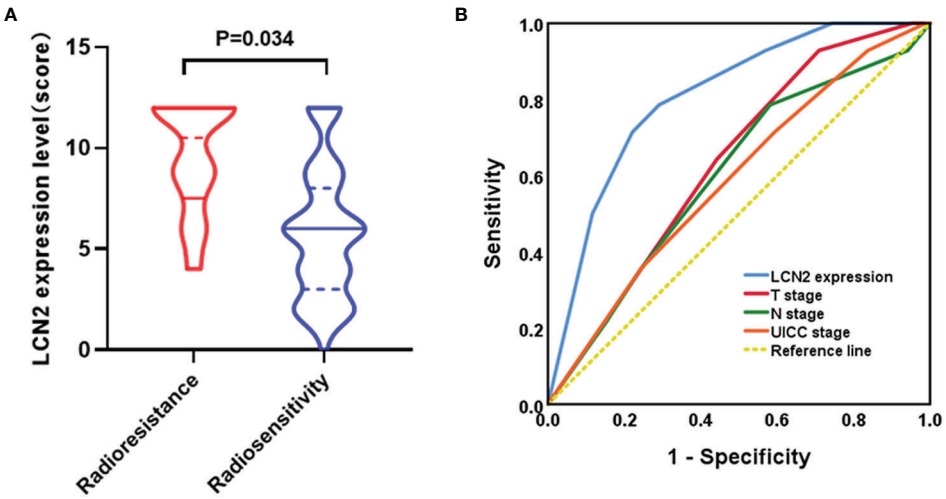

FIGURE 4 | LCN2 is a potential biomarker for predicting nasopharyngeal carcinoma (NPC) radioresistance. **(A)** LCN2 expression was significantly higher in radioresistant NPC tissues than in radiosensitive NPC tissues (P = 0.034). **(B)** Receiver operating characteristic (ROC) curves for the predictive value of using LCN2 expression, T stage, N stage, and UICC stage to discriminate between radioresistant NPC and radiosensitive NPC. The LCN2 level displayed the largest area under the curve (AUC) among the four parameters.

demonstrated that the expression of LCN2 in NPC tissues was positively correlated with that of HIF-1A (Pearson correlation coefficient (r) = 0.5294, P = 0.0094) (**Figure 6B**). These results suggested that LCN2 may regulate NPC radioresistance through interacting with HIF1A.

DISCUSSION

Although several genes, including those associated with cell-cycle control, DNA damage repair, and apoptosis are known to influence the effects of ionizing radiation-induced cell damage, our knowledge of radiation-induced resistance in tumors at the molecular level remains limited. Microarrays have been applied to identify genes involved in the radioresistance of various tumors (30–35). Chang et al. analyzed the gene expression profiles of radioresistant NPC cell lines using a cDNA array and identified at least two genes, *GP96* and *GDF15*, that were involved in the development of radioresistance in NPC (35). In this study, we further identified LCN2 as a radioresistance-related gene in NPC cells using the GEO data set GSE48501 and the online analysis tool GEO2R. Additional functional studies and survival analysis confirmed the key role of LCN2 in the acquisition of a radioresistant phenotype and the recurrence of NPC.

Several studies have reported that the aberrant expression of LCN2 can confer resistance to radiotherapy and chemotherapy in several types of cancer (5–13). Additionally, although increased LCN2 expression was shown to correlate with the apoptosis induced by several reagents in human lung cancer cells, this LCN2 upregulation represented a survival rather than a proapoptotic response (36). Meanwhile, LCN2 was also upregulated in HepG2 cells following irradiation or H_2O_2 treatment (37). The results of these studies suggest that LCN2 protects tumor cells against extracellular stimuli-induced damage, thereby facilitating their survival. Irradiation-induced cell death results from irreparable DNA DSBs, while radiosensitivity is tightly linked to the ability of cells to repair DNA damage after irradiation (38, 39). DSB repair usually begins within 30–60 min of irradiation and peaks after 24 h. γH2AX is a marker for DSB recognition and repair, and the DSB repair efficacy is characterized by the presence of γH2AX foci (40–44). In this study, we found that knocking down LCN2 markedly impaired the DNA DSB repair capability of the NPC cell lines CNE2R and HNE1 and reduced their proliferative ability, which enhanced the sensitivity of these cells to irradiation. Conversely, the overexpression of LCN2 increased the radioresistance of NPC cells. These results suggest that LCN2 may induce radioresistance *via* regulating the DNA DSB repair capability of NPC cells. Cancer cells can activate several pathways to repair DSBs and maintain their proliferation status, thereby promoting tumor radioresistance and recurrence.

Radioresistance frequently underlies tumor recurrence. In line with this phenomenon, our results showed that patients with high LCN2 expression levels had shorter RFS and LRFS. However, studies investigating LCN2 in different head and neck cancers have reported inconsistent results. LCN2 expression was reported to be downregulated in oral cancer, and was further reduced in oral cancer with metastasis (5, 12, 45). In these studies, patients with high levels of LCN2 had better survival outcomes, making LCN2 a good prognostic factor in oral cancer. The mechanism through which LCN2 exerts its anti-tumor effects in oral cancer may be related to a reduction in autophagy mediated through mTOR signaling pathway activation (12). In contrast, LCN2 was reported to be highly expressed in thyroid carcinoma (46, 47) and the silencing of LCN2 attenuated cancer cell survival under conditions of serum deprivation. The discrepancies among these results are partially due to the high heterogeneity among head and neck cancers. One study

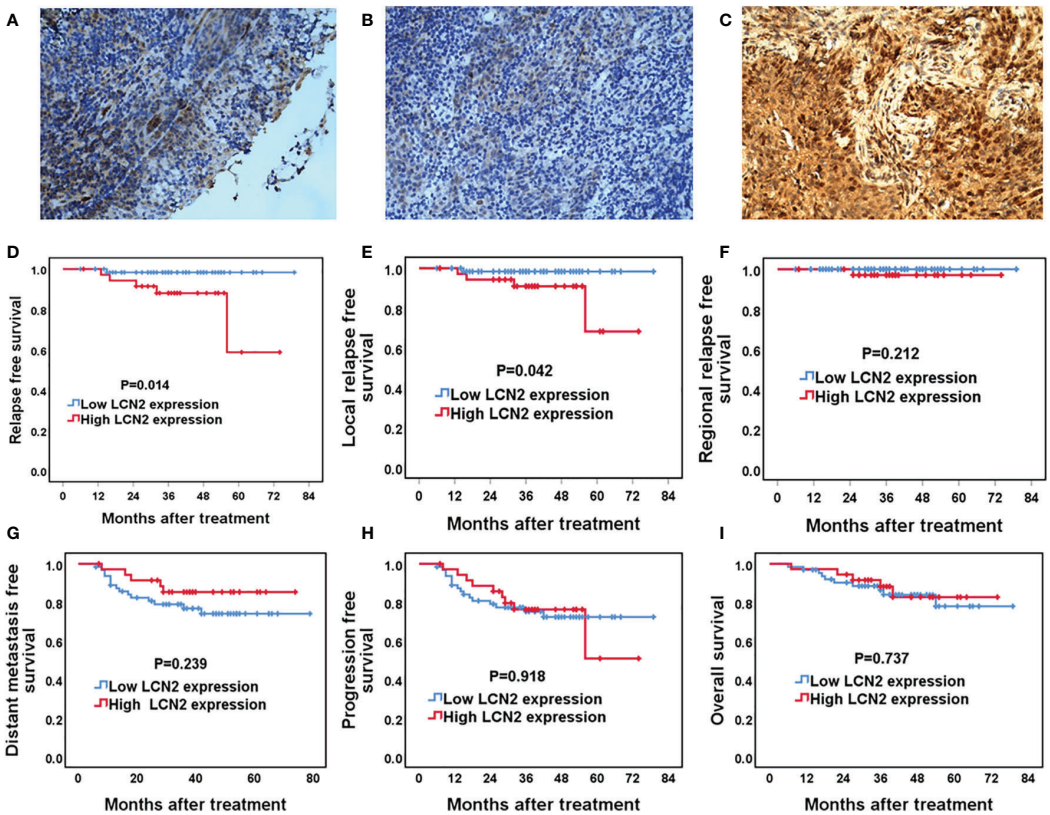

FIGURE 5 | The association between LCN2 expression and survival outcomes in nasopharyngeal carcinoma (NPC) patients. **(A–C)** Representative micrographs (×400) of normal nasopharynx mucosa **(A)**, NPC tissues with low LCN2 expression **(B)**, and NPC tissues with high LCN2 expression **(C)** are shown. **(D–I)** Kaplan–Meier analysis of the 5-year relapse-free survival (RFS), local relapse-free survival (LRFS), regional relapse-free survival (RRFS), distant metastasis-free survival (DMFS), progression-free survival (PFS), and overall survival (OS) between high and low LCN2 expression groups. The RFS and LRFS of patients with high LCN2 expression were significantly lower than those of patients with low LCN2 expression. There were no significant differences in RRFS, DMFS, PFS, or OS between the low and high LCN2 expression groups.

TABLE 1 | The associations between LCN2 expression and clinicopathological parameters.

Variable	Total population	LCN2 expression level		*P*-value
		Low	High	
Sex				0.738
Female	34	21	13	
Male	66	43	23	
Age (y)				0.129
<50	51	29	22	
≥50	49	35	14	
T stage				0.089
T1–3	38	15	53	
T4	26	21	47	
N stage				
N0–1	26	13	39	0.657
N2–3	38	23	61	
UICC stage				
I–III	28	11	39	0.194
IV	36	25	61	
Induction CT				
No	23	9	32	0.260
Yes	41	27	68	

CT, chemotherapy.

demonstrated that survival outcomes for NPC patients with metastasis are generally poor as the biology of NPC differs from that of classic head and neck squamous cell carcinoma (48). NPC tends to be more sensitive to ionizing radiation than other head and neck cancers. Therefore, once NPC becomes resistant to radiotherapy, the treatment outcomes can be poor.

Solid tumors usually have inefficient vasculatures and high energy requirements, resulting in oxygen deprivation (hypoxia) in the tumor microenvironment. Cancer cells can be radioresistant under hypoxic conditions (49, 50). Sørensen et al. reported that, although head and neck cancer cells with HPV infection exhibited markedly greater radiosensitivity than HPV-negative cells, both cell types displayed the same radioresistance potential under hypoxic conditions (51). HIF-1A, which mediates adaptive responses to hypoxia, has been implicated in the induction of biological radioresistance in cancer cells under oxygen deprivation. Most tumor hypoxia adaptations are orchestrated by HIF-1A (52–54). We found that the protein level of HIF-1A was reduced in both HNE1 and CNE2R cells with LCN2 knockdown, but was increased in CNE2 cells stably overexpressing LCN2. Furthermore, we also identified a positive correlation between LCN2 and HIF-1A expression in 23 NPC

TABLE 2 | Multivariate analysis using a Cox proportional hazards model for the RFS and LRFS of NPC patients.

Endpoint	Variables	HR	95% CI	P-value
RFS	Sex (female *vs.* male)	0.990	[0.172–5.697]	0.991
	Age (<50 *vs.* ≥50)	2.212	[0.401–12.215]	0.362
	T stage (T1–3 *vs.* T4)	0.401	[0.068–2.376]	0.314
	N stage (N0–1 *vs.* N2–3)	0.595	[0.097–3.644]	0.575
	Induction CT (no *vs.* yes)	0.823	[0.133–5.085]	0.834
	LCN2 expression (low *vs.* high)	13.925	[1.360–142.548]	**0.026**
LRFS	Sex (female *vs.* male)	0.515	[0.070–3.816]	0.516
	Age (<50 *vs.* ≥50)	4.484	[0.574–35.048]	0.153
	T stage (T1–3 *vs.* T4)	0.151	[0.015–1.484]	0.105
	N stage (N0–1 *vs.* N2–3)	1.179	[0.152–9.150]	0.875
	Induction CT (no *vs.* yes)	1.870	[0.152–22.952]	0.625
	LCN2 expression (low *vs.* high)	12.999	[0.950–177.791]	**0.055**

RFS, relapse-free survival; LRFS, local relapse-free survival; HR, hazard ratio; CI, confidence interval; CT, chemotherapy.
The bold values highlight meaningful p-values with statistical significance or borderline significance.

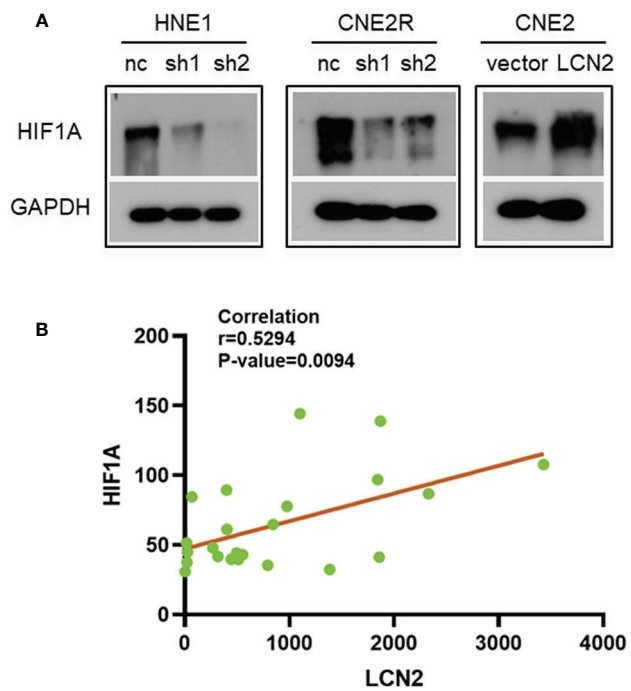

FIGURE 6 | The correlation between the expression of LCN2 and that of hypoxia-inducible factor 1-alpha (HIF-1A). **(A)** The protein level of the hypoxia-related factor HIF-1A was reduced in both HNE1 and CNE2R cells with LCN2 knockdown, but was increased in CNE2 cells stably overexpressing LCN2. **(B)** A significant correlation was detected between LCN2 and HIF-1A expression in 23 NPC tissues using a microarray (Pearson correlation coefficient (r) = 0.5294, P = 0.0094).

tissues. Similarly, Yang and et al. demonstrated that LCN2 significantly enhanced VEGF-induced angiogenesis in human breast cancer and that this effect was mediated through HIF-1A *via* extracellular signal-regulated kinase (Erk) (55). LCN2 expression was also reported to be increased in tumor cells cultured under hypoxic conditions and paralleled the levels of HIF-1A in mouse melanoma cells (56). As HIF-1A is firmly associated with the radioresistance of cancer cells, we think that LCN2 might interact with HIF-1A to facilitate the development of a radioresistant phenotype in NPC. Further studies are warranted to elucidate the mechanism underlying how LCN2 and HIF-1A regulate NPC radioresistance.

This study had several limitations. First, the patient population was relatively small, and these results need to be further verified in a larger cohort. Additionally, no *in vivo* experiments were performed. Finally, we did not further explore the mechanism through which LCN2 exerts its effect on the radioresistance of NPC.

In summary, we demonstrated that LCN2 was positively correlated with the radioresistance of NPC cells. LCN2 was highly expressed in patients with radioresistant NPC. Survival analysis revealed that high LCN2 expression was related to poor RFS and LRFS. Additionally, we identified a positive correlation between LCN2 and HIF-1A expression, which suggested that LCN2 may induce NPC radioresistance through regulating pathways associated with adaptation to hypoxia in the tumor microenvironment. The underlying molecular mechanisms remain to be further elucidated.

DATA AVAILABILITY STATEMENT

The original contributions presented in the study are included in the article/**Supplementary Material**. Further inquiries can be directed to the corresponding authors.

ETHICS STATEMENT

The studies involving human participants were reviewed and approved by the ethics committee of Jiangxi Provincial Hospital. The patients/participants provided their written informed consent to participate in this study.

AUTHOR CONTRIBUTIONS

Z-WT and LZ conceived the study. M-XZ and LW helped to organize and perform the study. Statistical analysis was undertaken by Z-WT. All authors read and approved the final version of the manuscript. M-XZ wrote the manuscript.

FUNDING

This project was supported financially by grants from the Natural Science Foundation of China (81802915, 81660452, and 81660453).

SUPPLEMENTARY MATERIAL

The Supplementary Material for this article can be found online at: https://www.frontiersin.org/articles/10.3389/fonc.2020.605777/full#supplementary-material

REFERENCES

1. Bray F, Ferlay J, Soerjomataram I, Siegel RL, Torre LA, Jemal A. Global cancer statistics 2018: GLOBOCAN estimates of incidence and mortality worldwide for 36 cancers in 185 countries. *CA Cancer J Clin* (2018) 68(6):394–424. doi: 10.3322/caac.21492
2. Wei KR, Zheng RS, Zhang SW, Liang ZH, Li ZM, Chen WQ. Nasopharyngeal carcinoma incidence and mortality in China, 2013. *Chin J Cancer* (2017) 36 (1):90. doi: 10.1186/s40880-017-0257-9
3. Feng XP, Yi H, Li MY, Li XH, Yi B, Zhang PF, et al. Identification of biomarkers for predicting nasopharyngeal carcinoma response to radiotherapy by proteomics. *Cancer Res* (2010) 70(9):3450–62. doi: 10.1158/0008-5472.CAN-09-4099
4. Goetz DH, Holmes MA, Borregaard N, Bluhm ME, Raymond KN, Strong RK. The neutrophil lipocalin NGAL is a bacteriostatic agent that interferes with siderophore-mediated iron acquisition. *Mol Cell* (2002) 10(5):1033–43. doi: 10.1016/s1097-2765(02)00708-6
5. Hiromoto T, Noguchi K, Yamamura M, Zushi Y, Segawa E, Takaoka K, et al. Up-regulation of neutrophil gelatinase-associated lipocalin in oral squamous cell carcinoma: relation to cell differentiation. *Oncol Rep* (2011) 26(6):1415–21. doi: 10.3892/or.2011.1429
6. Zheng LT, Lee S, Yin GN, Mori K, Suk K. Down-regulation of lipocalin 2 contributes to chemoresistance in glioblastoma cells. *J Neurochem* (2009) 111 (5):1238–51. doi: 10.1111/j.1471-4159.2009.06410.x
7. Candido S, Abrams SL, Steelman LS, Lertpiriyapong K, Fitzgerald TL, Martelli AM, et al. Roles of NGAL and MMP-9 in the tumor microenvironment and sensitivity to targeted therapy. *Biochim Biophys Acta* (2016) 1863(3):438–48. doi: 10.1016/j.bbamcr.2015.08.010
8. Cheng G, Sun X, Wang J, Xiao G, Wang X, Fan X, et al. HIC1 silencing in triple-negative breast cancer drives progression through misregulation of LCN2. *Cancer Res* (2014) 74(3):862–72. doi: 10.1158/0008-5472.CAN-13-2420
9. Du ZP, Wu BL, Xie YM, Zhang YL, Liao LD, Zhou F, et al. Lipocalin 2 promotes the migration and invasion of esophageal squamous cell carcinoma cells through a novel positive feedback loop. *Biochim Biophys Acta* (2015) 1853(10 Pt A):2240–50. doi: 10.1016/j.bbamcr.2015.07.007
10. Yu DS, Wu CL, Ping SY, Huang YL, Shen KH. NGAL can alternately mediate sunitinib resistance in renal cell carcinoma. *J Urol* (2014) 192(2):559–66. doi: 10.1016/j.juro.2013.12.049
11. Miyamoto T, Kashima H, Yamada Y, Kobara H, Asaka R, Ando H, et al. Lipocalin 2 Enhances Migration and Resistance against Cisplatin in Endometrial Carcinoma Cells. *PloS One* (2016) 11(5):e0155220. doi: 10.1371/journal.pone.0155220
12. Monisha J, Roy NK, Padmavathi G, Banik K, Bordoloi D, Khwairakpam AD, et al. NGAL is Downregulated in Oral Squamous Cell Carcinoma and Leads to Increased Survival, Proliferation, Migration and Chemoresistance. *Cancers (Basel)* (2018) 10(7):228. doi: 10.3390/cancers10070228
13. Shiiba M, Saito K, Fushimi K, Ishigami T, Shinozuka K, Nakashima D, et al. Lipocalin-2 is associated with radioresistance in oral cancer and lung cancer cells. *Int J Oncol* (2013) 42(4):1197–204. doi: 10.3892/ijo.2013.1815
14. Li XH, Qu JQ, Yi H, Zhang PF, Yi HM, Wan XX, et al. Integrated analysis of differential miRNA and mRNA expression profiles in human radioresistant and radiosensitive nasopharyngeal carcinoma cells. *PloS One* (2014) 9(1): e87767. doi: 10.1371/journal.pone.0087767
15. Mou T, Zhu D, Wei X, Li T, Zheng D, Pu J, et al. Identification and interaction analysis of key genes and microRNAs in hepatocellular carcinoma by bioinformatics analysis. *World J Surg Oncol* (2017) 15(1):63. doi: 10.1186/s12957-017-1127-2
16. To EW, Chan KC, Leung SF, Chan LY, To KF, Chan AT, et al. Rapid clearance of plasma Epstein-Barr virus DNA after surgical treatment of nasopharyngeal carcinoma. *Clin Cancer Res* (2003) 9(9):3254–9.
17. Zhu Y, Ramos da Silva S, He M, Liang Q, Lu C, Feng P, et al. An Oncogenic Virus Promotes Cell Survival and Cellular Transformation by Suppressing Glycolysis. *PloS Pathog* (2016) 12(5):e1005648. doi: 10.1371/journal.ppat.1005648
18. Jones T, Ye F, Bedolla R, Huang Y, Meng J, Qian L, et al. Direct and efficient cellular transformation of primary rat mesenchymal precursor cells by KSHV. *J Clin Invest* (2012) 122(3):1076–81. doi: 10.1172/JCI58530
19. Konno R, Yamakawa H, Utsunomiya H, Ito K, Sato S, Yajima A. Expression of survivin and Bcl-2 in the normal human endometrium. *Mol Hum Reprod* (2000) 6(6):529–34. doi: 10.1093/molehr/6.6.529
20. Vogin G, Foray N. The law of Bergonie and Tribondeau: a nice formula for a first approximation. *Int J Radiat Biol* (2013) 89(1):2–8. doi: 10.3109/09553002.2012.717732
21. Haber AH, Rothstein BE. Radiosensitivity and rate of cell division: "law of Bergonie and Tribondeau". *Science* (1969) 163(3873):1338–9. doi: 10.1126/science.163.3873.1338
22. Lu J, Tang M, Li H, Xu Z, Weng X, Li J, et al. EBV-LMP1 suppresses the DNA damage response through DNA-PK/AMPK signaling to promote radioresistance in nasopharyngeal carcinoma. *Cancer Lett* (2016) 380 (1):191–200. doi: 10.1016/j.canlet.2016.05.032
23. Zhou X, Zheng J, Tang Y, Lin Y, Wang L, Li Y, et al. EBV encoded miRNA BART8-3p promotes radioresistance in nasopharyngeal carcinoma by regulating ATM/ATR signaling pathway. *Biosci Rep* (2019) 39(9):13. doi: 10.1042/BSR20190415
24. Yaromina A, Krause M, Thames H, Rosner A, Krause M, Hessel F, et al. Pre-treatment number of clonogenic cells and their radiosensitivity are major determinants of local tumour control after fractionated irradiation. *Radiother Oncol* (2007) 83(3):304–10. doi: 10.1016/j.radonc.2007.04.020
25. Price BD, D'Andrea AD. Chromatin remodeling at DNA double-strand breaks. *Cell* (2013) 152(6):1344–54. doi: 10.1016/j.cell.2013.02.011
26. Rajpurohit YS, Bihani SC, Waldor MK, Misra HS. Phosphorylation of Deinococcus radiodurans RecA Regulates Its Activity and May Contribute to Radioresistance. *J Biol Chem* (2016) 291(32):16672–85. doi: 10.1074/jbc.M116.736389
27. Bonner WM, Redon CE, Dickey JS, Nakamura AJ, Sedelnikova OA, Solier S, et al. GammaH2AX and cancer. *Nat Rev Cancer* (2008) 8(12):957–67. doi: 10.1038/nrc2523
28. Manoochehri Khoshinani H, Afshar S, Najafi R. Hypoxia: A Double-Edged Sword in Cancer Therapy. *Cancer Invest* (2016) 34(10):536–45. doi: 10.1080/07357907.2016.1245317
29. Horsman MR, Overgaard J. The impact of hypoxia and its modification of the outcome of radiotherapy. *J Radiat Res* (2016) 57 Suppl 1:i90–8. doi: 10.1093/jrr/rrw007
30. Wong YF, Sahota DS, Cheung TH, Lo KW, Yim SF, Chung TK, et al. Gene expression pattern associated with radiotherapy sensitivity in cervical cancer. *Cancer J* (2006) 12(3):189–93. doi: 10.1097/00130404-200605000-00006
31. Ogawa K, Utsunomiya T, Mimori K, Tanaka F, Haraguchi N, Inoue H, et al. Differential gene expression profiles of radioresistant pancreatic cancer cell lines established by fractionated irradiation. *Int J Oncol* (2006) 28(3):705–13.
32. Higo M, Uzawa K, Kouzu Y, Bukawa H, Nimura Y, Seki N, et al. Identification of candidate radioresistant genes in human squamous cell carcinoma cells through gene expression analysis using DNA microarrays. *Oncol Rep* (2005) 14(5):1293–8.
33. Guo WF, Lin RX, Huang J, Zhou Z, Yang J, Guo GZ, et al. Identification of differentially expressed genes contributing to radioresistance in lung cancer cells using microarray analysis. *Radiat Res* (2005) 164(1):27–35. doi: 10.1667/rr3401
34. Fukuda K, Sakakura C, Miyagawa K, Kuriu Y, Kin S, Nakase Y, et al. Differential gene expression profiles of radioresistant oesophageal cancer

cell lines established by continuous fractionated irradiation. *Br J Cancer* (2004) 91(8):1543–50. doi: 10.1038/sj.bjc.6602187
35. Chang JT, Chan SH, Lin CY, Lin TY, Wang HM, Liao CT, et al. Differentially expressed genes in radioresistant nasopharyngeal cancer cells: gp96 and GDF15. *Mol Cancer Ther* (2007) 6(8):2271–9. doi: 10.1158/1535-7163.MCT-06-0801
36. Tong Z, Wu X, Ovcharenko D, Zhu J, Chen CS, Kehrer JP. Neutrophil gelatinase-associated lipocalin as a survival factor. *Biochem J* (2005) 391(Pt 2):441–8. doi: 10.1042/BJ20051020
37. Roudkenar MH, Kuwahara Y, Baba T, Roushandeh AM, Ebishima S, Abe S, et al. Oxidative stress induced lipocalin 2 gene expression: addressing its expression under the harmful conditions. *J Radiat Res* (2007) 48(1):39–44. doi: 10.1269/jrr.06057
38. Christophorou MA, Ringshausen I, Finch AJ, Swigart LB, Evan GII. The pathological response to DNA damage does not contribute to p53-mediated tumour suppression. *Nature* (2006) 443(7108):214–7. doi: 10.1038/nature05077
39. Jackson SP, Bartek J. The DNA-damage response in human biology and disease. *Nature* (2009) 461(7267):1071–8. doi: 10.1038/nature08467
40. Reynolds P, Anderson JA, Harper JV, Hill MA, Botchway SW, Parker AW, et al. The dynamics of Ku70/80 and DNA-PKcs at DSBs induced by ionizing radiation is dependent on the complexity of damage. *Nucleic Acids Res* (2012) 40(21):10821–31. doi: 10.1093/nar/gks879
41. Jakob B, Splinter J, Conrad S, Voss KO, Zink D, Durante M, et al. DNA double-strand breaks in heterochromatin elicit fast repair protein recruitment, histone H2AX phosphorylation and relocation to euchromatin. *Nucleic Acids Res* (2011) 39(15):6489–99. doi: 10.1093/nar/gkr230
42. Lieber MR. The mechanism of double-strand DNA break repair by the nonhomologous DNA end-joining pathway. *Annu Rev Biochem* (2010) 79:181–211. doi: 10.1146/annurev.biochem.052308.093131
43. Schmid TE, Dollinger G, Beisker W, Hable V, Greubel C, Auer S, et al. Differences in the kinetics of gamma-H2AX fluorescence decay after exposure to low and high LET radiation. *Int J Radiat Biol* (2010) 86(8):682–91. doi: 10.3109/09553001003734543
44. Rao VA, Agama K, Holbeck S, Pommier Y. Batracylin (NSC 320846), a dual inhibitor of DNA topoisomerases I and II induces histone gamma-H2AX as a biomarker of DNA damage. *Cancer Res* (2007) 67(20):9971–9. doi: 10.1158/0008-5472.CAN-07-0804
45. Lin CW, Yang WE, Lee WJ, Hua KT, Hsieh FK, Hsiao M, et al. Lipocalin 2 prevents oral cancer metastasis through carbonic anhydrase IX inhibition and is associated with favourable prognosis. *Carcinogenesis* (2016) 37(7):712–22. doi: 10.1093/carcin/bgw050
46. Iannetti A, Pacifico F, Acquaviva R, Lavorgna A, Crescenzi E, Vascotto C, et al. The neutrophil gelatinase-associated lipocalin (NGAL), a NF-kappaB-regulated gene, is a survival factor for thyroid neoplastic cells. *Proc Natl Acad Sci USA* (2008) 105(37):14058–63. doi: 10.1073/pnas.0710846105
47. Volpe V, Raia Z, Sanguigno L, Somma D, Mastrovito P, Moscato F, et al. NGAL controls the metastatic potential of anaplastic thyroid carcinoma cells. *J Clin Endocrinol Metab* (2013) 98(1):228–35. doi: 10.1210/jc.2012-2528
48. Loong HH, Ma BB, Chan AT. Update on the management and therapeutic monitoring of advanced nasopharyngeal cancer. *Hematol Oncol Clin North Am* (2008) 22(6):1267–78. doi: 10.1016/j.hoc.2008.08.012
49. Brown JM, Wilson WR. Exploiting tumour hypoxia in cancer treatment. *Nat Rev Cancer* (2004) 4(6):437–47. doi: 10.1038/nrc1367
50. Kizaka-Kondoh S, Inoue M, Harada H, Hiraoka M. Tumor hypoxia: a target for selective cancer therapy. *Cancer Sci* (2003) 94(12):1021–8. doi: 10.1111/j.1349-7006.2003.tb01395.x
51. Sorensen BS, Busk M, Olthof N, Speel EJ, Horsman MR, Alsner J, et al. Radiosensitivity and effect of hypoxia in HPV positive head and neck cancer cells. *Radiother Oncol* (2013) 108(3):500–5. doi: 10.1016/j.radonc.2013.06.011
52. Harada H, Inoue M, Itasaka S, Hirota K, Morinibu A, Shinomiya K, et al. Cancer cells that survive radiation therapy acquire HIF-1 activity and translocate towards tumour blood vessels. *Nat Commun* (2012) 3:783. doi: 10.1038/ncomms1786
53. Harada H, Kizaka-Kondoh S, Li G, Itasaka S, Shibuya K, Inoue M, et al. Significance of HIF-1-active cells in angiogenesis and radioresistance. *Oncogene* (2007) 26(54):7508–16. doi: 10.1038/sj.onc.1210556
54. Harada H. Hypoxia-inducible factor 1-mediated characteristic features of cancer cells for tumor radioresistance. *J Radiat Res* (2016) 57 Suppl 1:i99–i105. doi: 10.1093/jrr/rrw012
55. Yang J, McNeish B, Butterfield C, Moses MA. Lipocalin 2 is a novel regulator of angiogenesis in human breast cancer. *FASEB J* (2013) 27(1):45–50. doi: 10.1096/fj.12-211730
56. Nakamura I, Hama S, Itakura S, Takasaki I, Nishi T, Tabuchi Y, et al. Lipocalin2 as a plasma marker for tumors with hypoxic regions. *Sci Rep* (2014) 4:7235. doi: 10.1038/srep07235

Conflict of Interest: The authors declare that the research was conducted in the absence of any commercial or financial relationships that could be construed as a potential conflict of interest.

frontiers in Cell and Developmental Biology

REVIEW
published: 11 February 2021
doi: 10.3389/fcell.2020.637435

Role of Non-coding RNAs on the Radiotherapy Sensitivity and Resistance of Head and Neck Cancer: From Basic Research to Clinical Application

*Xixia Zhang and Jing Yang**

Department of Otolaryngology Head and Neck Surgery, Shengjing Hospital of China Medical University, Shenyang, China

OPEN ACCESS

Edited by:
José Díaz-Chávez, National Institute of Cancerology (INCAN), Mexico

Reviewed by:
Zhonghua Wu, The First Affiliated Hospital of China Medical University, China
Jinxin Shi, The First Affiliated Hospital of China Medical University, China

***Correspondence:**
Jing Yang
yangjing7694@126.com

Specialty section:
This article was submitted to Molecular and Cellular Oncology, a section of the journal Frontiers in Cell and Developmental Biology

Received: *03 December 2020*
Accepted: *23 December 2020*
Published: *11 February 2021*

Citation:
Zhang X and Yang J (2021) Role of Non-coding RNAs on the Radiotherapy Sensitivity and Resistance of Head and Neck Cancer: From Basic Research to Clinical Application. Front. Cell Dev. Biol. 8:637435. doi: 10.3389/fcell.2020.637435

Head and neck cancers (HNCs) rank as the sixth common and the seventh leading cause of cancer-related death worldwide, with an estimated incidence of 600,000 cases and 40–50% mortality rate every year. Radiotherapy is a common local therapeutic modality for HNC mainly through the function of ionizing radiation, with approximately 60% of patients treated with radiotherapy or chemoradiotherapy. Although radiotherapy is more advanced and widely used in clinical practice, the 5-year overall survival rates of locally advanced HNCs are still less than 40%. HNC cell resistance to radiotherapy remains one of the major challenges to improve the overall survival in HNC patients. Non-coding RNAs (ncRNAs) are newly discovered functional small RNA molecules that are different from messenger RNAs, which can be translated into a protein. Many previous studies have reported the dysregulation and function of ncRNAs in HNC. Importantly, researchers reported that several ncRNAs were also dysregulated in radiotherapy-sensitive or radiotherapy-resistant HNC tissues compared with the normal cancer tissues. They found that ectopically elevating or knocking down expression of some ncRNAs could significantly influence the response of HNC cancer cells to radiotherapy, indicating that ncRNAs could regulate the sensitivity of cancer cells to radiotherapy. The implying mechanism for ncRNAs in regulating radiotherapy sensitivity may be due to its roles on affecting DNA damage sensation, inducing cell cycle arrest, regulating DNA damage repair, modulating cell apoptosis, etc. Additionally, clinical studies reported that *in situ* ncRNA expression in HNC tissues may predict the response of radiotherapy, and circulating ncRNA from body liquid serves as minimally invasive therapy-responsive and prognostic biomarkers in HNC. In this review, we aimed to summarize the current function and mechanism of ncRNAs in regulating the sensitivity of HNC cancer cells to radiotherapy and comprehensively described the state of the art on the role of ncRNAs in the prognosis prediction, therapy monitoring, and prediction of response to radiotherapy in HNC.

Keywords: head and neck cancer, radiotherapy, non-coding RNA, miRNA, long non-coding RNA, circRNA

INTRODUCTION

Head and neck cancers (HNCs) rank as the sixth common and the seventh leading cause of cancer-related death worldwide, with an estimated incidence of 600,000 cases and 40–50% mortality rate every year (Ferlay et al., 2015; Economopoulou et al., 2016). HNCs are presented mainly by the squamous cell carcinoma originating from the epithelial cells of the oral cavity, nasal cavity, oropharynx, larynx, or hypopharynx (Leemans et al., 2018).

Radiotherapy is a common local therapeutic modality for cancers mainly through the function of ionizing radiation. Ionizing radiation could kill cancer cells via directly damaging the DNA strands of cancer cells to end the infinite proliferative capacity, and also indirectly causes DNA damages in cancer cell through ionizing water to generating highly reactive oxygen species. Radiotherapy is one of the major treatment modalities for HNC, with approximately 60% of patients treated with radiotherapy or chemoradiotherapy (Berrington de Gonzalez et al., 2011). Many high-quality clinical studies have reported that radiotherapy or concurrent chemoradiotherapy could improve the survival for patients with early-stage HNC or locally advanced HNC (Bonner et al., 2010; Caudell et al., 2017; Lacas et al., 2017; Nichols et al., 2019). Although radiotherapy is more advanced and widely used in clinical practice, 5-year overall survival rates of locally advanced HNC are still less than 40% (Pignon et al., 2009). Cancer cell resistance to radiotherapy remains one of the major challenges to improve the overall survival in HNC patients.

Non-coding RNAs (ncRNAs) are newly discovered functional RNA molecules that are different from messenger RNAs, which can be translated into a protein (Mattick and Makunin, 2006; Feng et al., 2019; Dai et al., 2020; Yu et al., 2020). Over the past decades, researchers have discovered multiple kinds of ncRNAs, showing that ncRNAs constitute more than 90% of RNAs transcribed from the human genome DNA (Slack, 2006). Such discovery of numerous ncRNAs has opened up brand-new directions for understanding the normal physiology and the development of diseases. Based on the function difference, ncRNAs are usually divided into two categories: housekeeping and regulatory ncRNAs. The regulatory ncRNAs are mainly composed of miRNAs, circRNAs, and long non-coding RNAs (lncRNA; Chen, 2016; Wu et al., 2017; Yao et al., 2019). In recent years, regulatory RNAs were extensively researched and are revealed to participate in regulating the expression of protein-coding genes at transcriptional, post-transcriptional, as well as translational levels. Emerging studies have reported the key roles of regulatory ncRNAs in various biological processes, disease occurrence, and development.

Many previous studies have reported the dysregulation and function of ncRNAs in HNC (Wang et al., 2018; Jiang et al., 2019; Vo et al., 2019). NcRNAs could regulate the expression of genes associated with cell cycle, cell apoptosis, invasion, and migration, and eventually affect the proliferation, invasion, and metastasis of HNC (Feng et al., 2020; Gu et al., 2020; Huang et al., 2020; Sur et al., 2020; Wang et al., 2020; Zhang et al., 2020). Additionally, researchers reported that several ncRNAs were also dysregulated in radiotherapy-sensitive or radiotherapy-resistant HNC tissues compared with the normal cancer tissues (Zhang et al., 2013; de Jong et al., 2015; Qu et al., 2015a,b; Suh et al., 2015; Xu et al., 2015; Gao et al., 2017a; Hess et al., 2017; Chen et al., 2019; Vahabi et al., 2019; Pasi et al., 2020). They found that ectopically elevating or knocking down expression of some ncRNA could significantly influence the response of HNC cancer cells to radiotherapy, indicating that ncRNAs could regulate the sensitivity of cancer cells to radiotherapy. In this review, we aimed to summarize the current function and mechanism of ncRNAs in regulating the sensitivity of HNC cancer cells to radiotherapy.

RADIATION-INDUCED CELL RESPONSE AND MECHANISM OF RADIOTHERAPY RESISTANCE

Since the discovery of ionizing radiation in 1895, the concept of radiation-based therapy modality was prompted and has been regarded as a major treatment for many types of cancers (Wills, 1904; Alsahafi et al., 2020; Ampil et al., 2020; Plavc et al., 2020; Tao et al., 2020; Sher et al., 2020a,b). Especially, radiotherapy is a crucial treatment for HNC. The radiation-induced cell death is regarded to originate from the damage of two cellular components: DNA and cell membrane.

Upon exposure to radiation, the radiation passed directly through the cell and ionized the DNA, causing lethal DNA damage. Additionally, the radiation can also result in DNA damage through ionizing the intracellular water and inducing the generation of reactive oxygen species (Rothkamm and Löbrich, 2003). These reactive oxygen species could bring various injuries to cells, among which are the DNA double-strand breaks (DSBs), which are one of the most cytotoxic injuries to cells. DSBs, involving breaks in the phosphodiester backbone of both strands of DNA, increase positively with the radiation dose (Hanai et al., 1998; Rothkamm and Löbrich, 2003). It is estimated that each gray unit of radiation could produce 10^5 ionizations per cell, which cause about 40 DSBs, 2,000 single-strand breaks (SSBs), as well as other types of damages in the DNA (Lewanski and Gullick, 2001). When recognizing these complex radiation-induced damages, the cells respond to these damages through multiple signaling pathways. These pathways are involved in modulating important cellular activities such as DNA damage repair, cell-cycle arrest, and apoptosis. In addition, radiation could also function on the cell membrane to mediate cell apoptosis. Mechanistically, radiation activates the enzyme sphingomyelinase, which could hydrolyze plasma-derived sphingomyelin and produce ceramide. Through this process, ceramide could be produced within seconds of radiation exposure. The accumulation of ceramide in cells could initiate cell apoptosis (Obeid et al., 1993; Haimovitz-Friedman et al., 1994;

Abbreviations: ATM, ataxia telangiectasia mutated; ATR, the ataxia telangiectasia mutated and Rad3 related; Bcl-2, B cell lymphoma 2; CHK2, checkpoint kinase 2; DSBs, DNA double-strand breaks; EGFR, epidermal growth factor receptor; EMT, epithelial-to-mesenchymal transition; γ-H2AX, phosphorylated H2AX; HNCs, head and neck cancers; HR, homologous recombination; Jab1, c-Jun activation domain binding protein-1; lncRNA, long non-coding RNAs; MCL1, myeloid cell leukemia 1; ncRNAs, non-coding RNAs; NHEJ, non-homologous end joining; NKILA, NF-κB interacting lncRNA; NPC, nasopharyngeal carcinoma; SSBs, single-strand breaks; UTR, untranslated region.

Jarvis et al., 1994a,b). However, the mechanism on how ceramide initiates apoptosis is still unclear.

In response to radiation exposure, most cells immediately initiate cell apoptosis because of severe DNA damage or the accumulation of ceramide in cells. Such programmed death mechanism could protect cells from propagating genetic mutations to the next generation. Additionally, cells will also initiate the DNA damage repair system, which was developed during the evolution of species. There are two major DNA repair pathways: homologous recombination (HR) and non-homologous end joining (NHEJ; Burgess et al., 2020; Nastasi et al., 2020; Zhao et al., 2020).

The HR repairing system depends on homologous DNA sequences from sister chromatids. This makes HR restricted to phases of the cell cycle where homologous sister chromatids coexist (Zhao et al., 2017). In contrast, NHEJ is a promiscuous repair system that directly ligates two broken ends independent of sequence homology. Hence, NHEJ is not cell cycle dependent and could be initiated at any cell cycle phase (Emerson and Bertuch, 2016). Another important response to DNA damage is cell cycle arrest. Normally, cell cycles pass through the G0 phase, G1 phase, S phase, G2 phase, and M phase. The cell cycle checkpoint pathway regulated the progression of the cell cycle. When sensing DNA damages, cells will stop the cell cycle progression to spare more time for DNA repairing. Overall, these complex cell responses to radiation-induced injury depend on the modulation of various genes.

The sensitivity of cancer cells to radiotherapy depends on the intensity of DNA damage with cells, the cells' ability to balance the expression of genes associated with apoptosis promotion and inhibition, the expression level of genes regulating the induction of cell cycle arrest, and the DNA repair system. Radiotherapy-resistant cancer cells showed obvious tendency to inhibit cell apoptosis and augment the DNA damage repair rate. This adaptation to radiotherapy is closely related with the dysregulated expression of genes in resistant cells. NcRNAs, especially the regulatory ncRNAs, are characterized for their role on regulating gene expression in cancer cells. Because of such an important role, ncRNAs are believed to be associated with radiotherapy resistance and could regulate cell sensitivity to radiotherapy.

IONIZING RADIATION MODULATES NCRNA EXPRESSION PROFILING

The role of ncRNAs on cancer development and progression is one of the hottest topics in cancer cell biology research. With the help of microarray and next-generation technology, researchers have discovered an amount of ncRNAs, such as miRNAs, lncRNAs, and circRNAs, which was differently expressed in cancer tissues compared with the normal tissues. Many of these ncRNAs could significantly regulate the biological behaviors of cancer cell. In HNC, many researchers also focus on the expression and function of ncRNAs. Numerous ncRNAs are reported to modulate HNC proliferation, invasion, metastasis, apoptosis, and other biological processes (Wu et al., 2015; Bao et al., 2018; Vo et al., 2019; Wang S. S. et al., 2019). Recently, researchers also found that these oncogenic or tumor-suppressive ncRNAs could also regulate the sensitivity of cancer cells to radiotherapy. Moreover, they also explore dysregulated ncRNAs expression through comparing radiotherapy-resistant, radiotherapy-sensitive, and normal cancer tissues or cells, so as to discover key ncRNAs that could regulate radiotherapy sensitivity. We summarized the differently expressed ncRNAs in radiotherapy-resistant, radiotherapy-sensitive, and normal cancer tissues or cells as shown in **Table 1** (Qu et al., 2012, 2015a,b; Li et al., 2013; Li B. Y. et al., 2017; Li L. N. et al., 2017; Li et al., 2020; Shiiba et al., 2013; Zhang et al., 2013; Wang et al., 2014, 2016, Wang Z. et al., 2019; de Jong et al., 2015; Lin et al., 2015; Maia et al., 2015; Suh et al., 2015; Sun et al., 2015; Xu et al., 2015; Zhao et al., 2015; Huang et al., 2016, 2018, 2019; Kang et al., 2016; Weng et al., 2016; Wu et al., 2016, 2018; Gao et al., 2017a,b; Han et al., 2017; Hu et al., 2017; Chen H. et al., 2018; Chen et al., 2019; Feng et al., 2018; He et al., 2018; Yang et al., 2018; Kong et al., 2019; Tian et al., 2019; Vahabi et al., 2019; Yi et al., 2019; Gou et al., 2020; Kangboonruang et al., 2020; Shuai and Huang, 2020).

NCRNAS DIRECTLY REGULATE RADIOTHERAPY SENSITIVITY BY MODULATING SPECIFIC PROCESSES

The efficacy of radiotherapy depends mainly on the sensitivity of cancers to radiotherapy. Many factors are found to influence the radiotherapy sensitivity of cancers. Several research groups have discovered that some differentially expressed ncRNAs in HNC could affect radiotherapy sensitivity. Meanwhile, several research groups also discovered differentially expressed ncRNAs in radiation-sensitive and radiation-resistant HNC cancer cells by sequencing and microarray analysis. Some high-regulated ncRNAs in radiation-resistant cancers could decrease the sensitivity of cancer cells to radiotherapy, whereas ncRNAs down-regulated in radiation-resistant cancers could enhance the sensitivity of cancer cells to radiotherapy. These ncRNAs modulate the response of cancer cells to radiotherapy mainly through regulating different genes involved in important processes that are tightly associated with radiotherapy sensitivity. In this section, we mainly describe the effect and molecular mechanisms of ncRNA on regulating radiotherapy sensitivity of HNC cells by DNA damage sensing, cell cycle progression, DNA damage repair, and cell apoptosis of HNC cells.

Affecting DNA Damage Sensation and Inducing Cell Cycle Arrest

In response to DNA damage, cells have evolutionarily developed a mechanism to sense the DNA damage and initiate DNA damage repair. In the process, the ataxia telangiectasia mutated (ATM), an important Ser/Thr kinase, plays a major role in sensing DNA DSBs and initiating a series of cascade responses leading to cell cycle checkpoint activation and DNA repair (Weber and Ryan, 2015; Carrassa and Damia, 2017; **Figures 1**, **2**). After sensing the radiation-induced DNA damage, the main sensor ATM and the ataxia telangiectasia mutated and Rad3

TABLE 1 | Dysregulated ncRNAs in response to radiation in HNC.

Studies	ncRNA	Expression of ncRNA in response to radiation	Cancer type
Qu et al., 2012	miR-205	Up-regulation	NPC
Li et al., 2013	miR-324-3p	Down-regulation	NPC
Zhang et al., 2013	miR-29c	Down-regulation	NPC
Wang et al., 2014	miR-24	Down-regulation	NPC
Lin et al., 2015	miR-378g	Down-regulation	NPC
Qu et al., 2015a	miR-23a	Down-regulation	NPC
Qu et al., 2015b	miR-203	Down-regulation	NPC
Sun et al., 2015	miR-101	Down-regulation	NPC
Xu et al., 2015	miR-185-3p, miR-324-3p	Down-regulation	NPC
Zhao et al., 2015	miR-504	Up-regulation	NPC
Huang et al., 2016	miR-19b-3p	Up-regulation	NPC
Kang et al., 2016	miR-24	Up-regulation	NPC
Wang et al., 2016	miR-24-3p	Up-regulation	NPC
Gao et al., 2017a	miR-138-5p	Down-regulation	NPC
Gao et al., 2017b	ebv-miR-BART7	Up-regulation	NPC
Han et al., 2017	XIST	Up-regulation	NPC
Hu et al., 2017	lncRNA ANRIL	Up-regulation	NPC
Li B. Y. et al., 2017	miR-210	Up-regulation	NPC
Li L. N. et al., 2017	miR-125b	Up-regulation	NPC
Feng et al., 2018	miR-495	Down-regulation	NPC
He et al., 2018	lnRNA PVT1	Up-regulation	NPC
Huang et al., 2018	miR-150	Up-regulation	NPC
Wu et al., 2018	miR-222	Up-regulation	NPC
Chen et al., 2019	CircRNA_000543	Up-regulation	NPC
Kong et al., 2019	miR-193a-3p	Up-regulation	NPC
Tian et al., 2019	miR-483-5p	Up-regulation	NPC
Wang et al., 2018	miR-372	Down-regulation	NPC
Yi et al., 2019	lncRNA PTPRG-AS1	Up-regulation	NPC
Shuai and Huang, 2019	circRNA_001387	Up-regulation	NPC
Maia et al., 2015	miR-296-5p	Up-regulation	Laryngeal cancer
Chen H. et al., 2018	miR-128a	Down-regulation	Laryngeal cancer
Yang et al., 2018	lncRNA-NKILA	Down-regulation	Laryngeal cancer
Shiiba et al., 2013	miR-125b	Down-regulation	Oral cancer
Weng et al., 2016	miR-494-3p	Down-regulation	Oral cancer
Wu et al., 2016	miR-17-5p	Up-regulation	Oral cancer
de Jong et al., 2015	microRNA Expression	Down-regulation	HNC
Suh et al., 2015	miR-196a	Up-regulation	HNC
Huang et al., 2019	LINC00958	Up-regulation	HNC
Vahabi et al., 2019	miR-96-5p	Up-regulation	HNC
Gou et al., 2020	lncRNA BLACAT1	Up-regulation	HNC
Kangboonruang et al., 2020	MALAT1	Up-regulation	HNC
Li et al., 2020	LINC00520	Up-regulation	HNC

HNC, head and neck cancer; NPC, nasopharyngeal carcinoma.

related (ATR) were activated and subsequently activated the cell cycle checkpoint kinases. Usually, ATM activates the checkpoint kinase 2 (CHK2), and ATR is responsible for the activation of CHK1. The activation of CHK1/2 could lead to phosphorylation and inactivation of CDC25A and CDC25C, both of which were involved in dephosphorylation and activation of CDK2 and CDK1, respectively. Inactivation of CDC25A and CDC25C consequently leads to maintenance of CDKs in the phosphorylated and inactivated form, thus inhibiting S phase and M phase entry and eventually inducing cell cycle arrest. Overall, ATM/CHK2 and ATR/CHK1 pathways work coordinately and cooperate to mediating cellular responses to DNA damage and are responsible for the maintenance of genomic stability by inducing cell cycle arrest. In HNC, the function of ATM was reported to be directly and indirectly regulated by several ncRNAs including miRNA and lncRNA. Mansour et al. (2013) reported that miR-421 could directly inhibit the expression of ATM in HNC through binding the ATM' S 3'-untranslated region (UTR). Forced expression of this miRNA could result in a significant cellular ATM deficiency and defect DNA damage repair, and eventually promote the sensitivity of HNC cells to radiotherapy. LncRNA PVT1 was found to be overexpressed in HNC tissues and cell line, and knockdown of PVT1 enhances the radiosensitivity of nasopharyngeal carcinoma (NPC) cell lines (He et al., 2018). Mechanically, knockdown of PVT1 significantly decreased the phosphorylation levels of ATM, p53, and Chk2, causing a decrease in the DNA repair ability of NPC cells after radiotherapy and enhancing their radiosensitivity (He et al., 2018).

Regulating DNA Damage Repair

When DSBs, the most harmful type of DNA damage, occurred in cells, the histone variant H2AX was immediately phosphorylated by the activated ATM (Jackson, 2002; Symington and Gautier, 2011). Therefore, phosphorylated H2AX (γ-H2AX) can be a useful indicator for DSB DNA damage. More importantly, γ-H2AX is responsible for the recruitment of DNA repair associated proteins to initiate the NHEJ or HR repair processes. In NPC cancer, miR-24 has been revealed to directly target H2AX (Wang et al., 2014). It demonstrated that the inhibition of miR-24 results in significant up-regulation of H2AX and thereby renders cancer cells resistant to radiation-induced DNA damage (Wang et al., 2014). Meanwhile, researchers also reported that miR-24 can inhibit the DNA DSB repair by targeting a DNA damage repair associated protein c-Jun activation domain binding protein-1 (Jab1; Wang et al., 2016). Jab 1 was crucial for DSB repair, and deletion of Jab1 resulted in spontaneous DNA fragmentation and increased expression of the γ-H2AX level (Doronkin et al., 2002; Pan et al., 2012, 2013).

Modulation of Cell Apoptosis

When the radiation-induced DNA damage is too lethal to be repaired, cells would initiate an automatic death program like apoptosis to protect genome stability. Therefore, the flexibility of cancer cells to initiate cell apoptosis sometimes may determine whether cancer cells are sensitive to radiotherapy or resistant to it. Some ncRNAs have been reported to influence the sensitivity of cancer cells to radiotherapy through modulation of cell apoptosis. Mechanistically, these ncRNAs mainly function

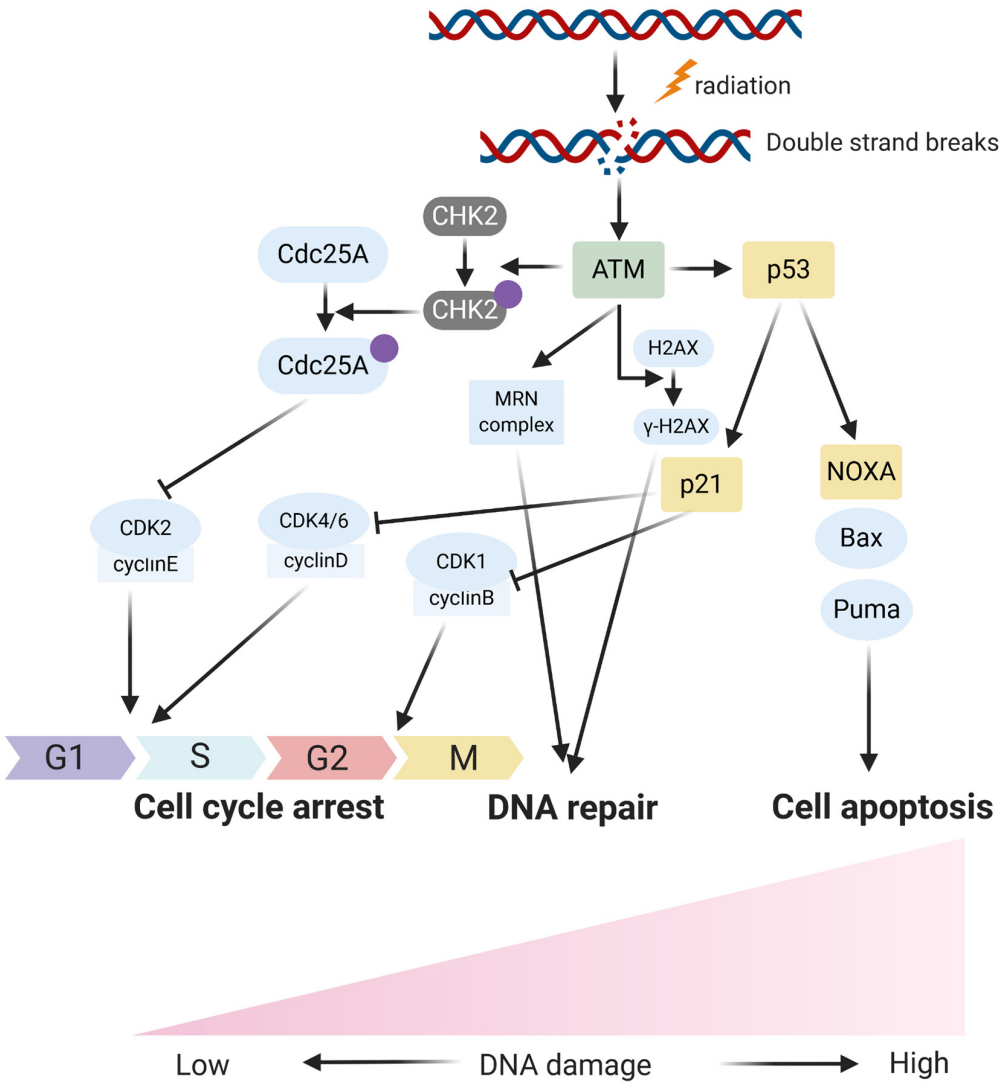

FIGURE 1 | The schematic diagram fors main respones of cells to radiation induced DNA damage.

through regulating the expression of anti-apoptosis or pro-apoptosis members (**Table 2**).

Many ncRNAs could enhance HNC cancer cell sensitivity to radiotherapy through promoting cell apoptosis. MiR-29c was found to target the classical anti-apoptotic proteins B cell lymphoma 2 (Bcl-2) family including myeloid cell leukemia 1 (MCL1) and Bcl-2 itself in human NPC. *In vitro* and *in vivo* studies illustrated that miR-29c could promote cell apoptosis, through which ectopic restoration of miR-29C substantially enhanced the sensitivity of NPC cells to radiotherapy (Zhang et al., 2013). MiR-378g was reported to enhance radiosensitivity, promoting apoptosis in NPC cells via directly targeting SHP-1 (Lin et al., 2015). Overexpression of SHP-1 partially reversed the effect of miR-378g mimics on cell apoptosis and radiosensitivity. MiR-185-3p and miR-324-3p can inhibit NPC cell growth and promote apoptosis partly through targeting SMAD7 (Xu et al., 2015; **Figure 3**).

On the other hand, several miRNAs were reported to inhibit cell apoptosis and enhance HNC cancer cell resistance to radiotherapy. Evidence has shown that PTEN is involved in regulating cell response to radiation-induced cell apoptosis and cell cycle arrest through inhibiting radiation-induced activation of the PI3K-Akt signaling pathway. Several miRNAs including miR-205 and miR-96-5p were reported to be elevated in HNC tissues from NPC patients after radiotherapy, and target PTEN to mediate resistance of HNC cells to radiotherapy (Qu et al., 2012; Vahabi et al., 2019). MiR-504 is found to be up-regulated in NPC radioresistant cells and could directly inhibit the expression of NRF1 and lead to radioresistance in NPC cells. NRF1 inhibition by miR-504 disturbed mitochondrial-mediated oxidative responses, which influence apoptosis of HNC cells and contribute to the resistance of cancer cells to radiation (Zhao et al., 2015). Huang et al. revealed that miR-19b-3p is up-regulated in NPC and could activate NF-κB activity

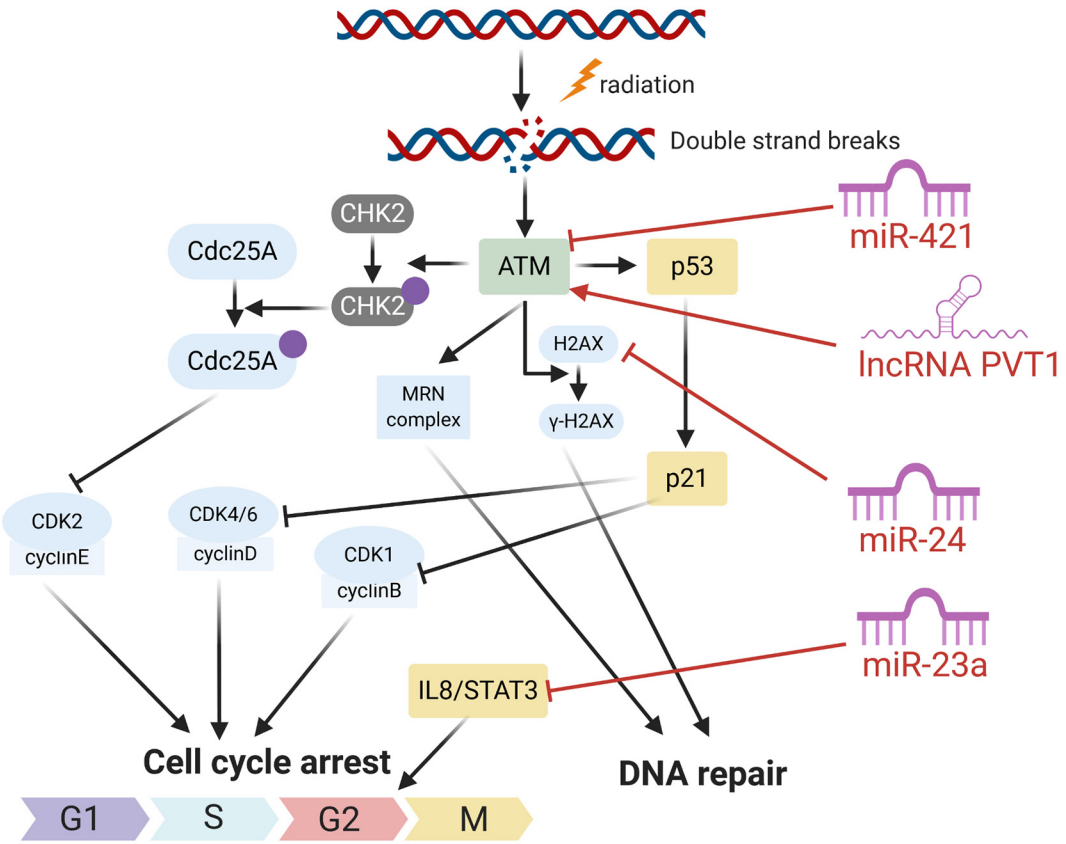

FIGURE 2 | The roles of several ncRNAs on cell respones radiation induced DNA damage.

TABLE 2 | ncRNAs regulating the expression of anti-apoptosis or pro-apoptosis members.

Studies	ncRNA	Cancer type	Target genes	Effects on apoptosis (overexpression)	Effects on radiotherapy (overexpression)
Qu et al., 2012	miR-205	NPC	PTEN	Inhibiting cell apoptosis	Radiotherapy resistance
Zhang et al., 2013	miR-29c	NPC	mcl1 or bcl2	Pro-apoptosis	Radiotherapy sensitive
Wang et al., 2014	miR-24	NPC	H2AX	Pro-apoptosis	Radiotherapy sensitive
Lin et al., 2015	miR-378g	NPC	SHP-1	Pro-apoptosis	Radiotherapy sensitive
Xu et al., 2015	miR-185-3p, miR-324-3p	NPC	SMAD7	Pro-apoptosis	Radiotherapy sensitive
Zhao et al., 2015	miR-504	NPC	NRF1	Inhibiting cell apoptosis	Radiotherapy resistance
Huang et al., 2016	miR-19b-3p	NPC	TNFAIP3/NF-κB axis	Inhibiting cell apoptosis	Radiotherapy resistance
Hu et al., 2017	lncRNA ANRIL	NPC	miR-125a	Inhibiting cell apoptosis	Radiotherapy resistance
Li B. Y. et al., 2017	miR-210	NPC	HIF-1α, CTR1A, ADAMTS5, CAMTA1	Inhibiting cell apoptosis	Radiotherapy resistance
He et al., 2018	lnRNA PVT1	NPC	ATM-P53	Inhibiting cell apoptosis	Radiotherapy resistance
Kong et al., 2019	miR-193a-3p	NPC	SRSF2	Inhibiting cell apoptosis	Radiotherapy resistance
Yi et al., 2019	lncRNA PTPRG-AS1	NPC	miR-194-3p/PRC1	Inhibiting cell apoptosis	Radiotherapy resistance
Yang et al., 2018	lncRNA-NKILA	Laryngeal cancer	NFKB/ikb/p65 Pathway	Pro-apoptosis	Radiotherapy sensitive
Wu et al., 2016	miR-17-5p	Oral cancer	p53	Inhibiting cell apoptosis, G2/M phase arrest	Radiotherapy resistance
Gou et al., 2020	lncRNA BLACAT1	HNC	PSEN	Inhibiting cell apoptosis, G2/M phase arrest	Radiotherapy resistance
Li et al., 2020	LINC00520	HNC	LINC00520/miR-195/HOXA10	Inhibiting cell apoptosis, G2/M phase arrest	Radiotherapy resistance

HNC, head and neck cancer; NPC, nasopharyngeal carcinoma.

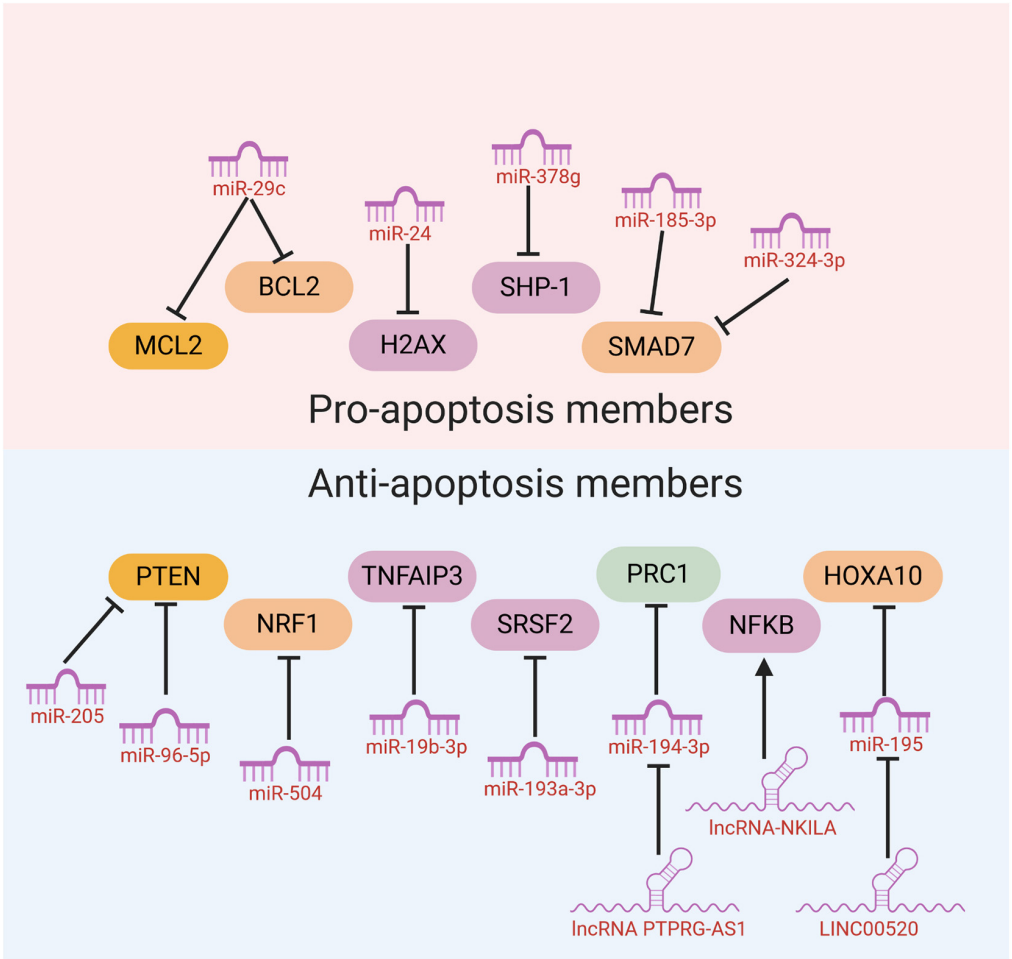

FIGURE 3 | NcRNAs could affect HNC cancer cell sensitivity to radiotherapy through modulation of cell apoptosis.

by targeting TNFAIP3. This miR-19b-3p/TNFAIP3/NF-κB axis could eventually inhibit cancer cell apoptosis and lead to NPC cell radioresistance (Huang et al., 2016). In addition, miR-210, miR-193a-3p, and miR-17-5p were reported to inhibit HNC cell apoptosis and promote cancer cell resistance to radiotherapy (Wu et al., 2016; Li B. Y. et al., 2017; Kong et al., 2019; **Figure 3**).

Recently, evidences have discovered that several lncRNAs and circRNAs could influence cancer cell sensitivity to radiotherapy through modulation of cell apoptosis. These lncRNAs and circRNAs function mainly through alleviating the role of certain miRNAs, which could be bound by lncRNAs and circRNAs through the base-pairing principles. For example, lncRNA ANRIL could function as a miR-125a sponge and negatively modulate miR-125a expression. ANRIL could reverse the inhibited proliferation, induced apoptosis, and enhanced radiosensitivity triggered by miR-125a overexpression (Hu et al., 2017). PTPRG-AS1 was found to specifically bind to miR-194-3p as a competing endogenous RNA, and miR-194-3p negatively regulates PRC1. Silencing PTPRG-AS1 could release the expression of miR-194-3p and resulted in enhanced sensitivity to radiotherapy and cell apoptosis (Yi et al., 2019). The LINC00520 could promote cell resistance to radiotherapy through reversing miR-195/HOXA10 in HNC (Li et al., 2020). CircRNA_000543 could serve as a sponge for miR-9 in NPC. Silencing circRNA_000543 sensitizes NPC cells to radiation by targeting the miR-9/PDGFRB axis (Chen et al., 2019). Additionally, NF-κB interacting lncRNA (NKILA) has been reported to be down-regulated in laryngeal cancer and could enhance the cytotoxicity of radiation through promoting cell apoptosis. Mechanically, lncRNA NKILA functions through combining with NF-κB: IκB complex to inhibit IκB phosphorylation, inhibits p65 nuclear translocation, and finally inhibits NF-κB activation (Yang et al., 2018; **Figure 3**).

Activation of EGFR Signaling

Ionizing radiation activates the epidermal growth factor receptor (EGFR) family of receptor tyrosine kinases, which, in turn, can initiate PI3K/AKT or MAPK pathways.

Through activating the PI3K-AKT pathway, EGFR signaling can prevent radiation-induced apoptosis. EGFR signaling can also promote cancer cell growth by inducing cell cycle progression, which was driven by activation of the

retrovirus associated DNA sequence (RAS)–rapidly accelerated fibrosarcoma (RAF)–mitogen/extracellular signal-regulated kinase (MEK)–ERK pathways. Published data demonstrate that miR-203 is a critical determinant of NPC cells' response to radiotherapy, and reduced miR-203 could promote NPC cell radioresistance by activating IL8/AKT signaling (Qu et al., 2015b). In addition, PTEN is a common inhibitor of AKT and is also a direct target of several miRNAs in HNC, such as miR-205 and miR-96-5p (**Figure 4**).

Epithelial-to-Mesenchymal Transition

Epithelial-to-mesenchymal transition (EMT) is a phenotypic change in which the epithelial cancer cell acquired a fibroblastoid-like morphology. Such transition could result in enhanced tumor cell motility and invasiveness, increased metastatic potential, as well as resistance to radiotherapy or chemotherapy (Marie-Egyptienne et al., 2013). ZEB1, an important EMT marker, could also be regulated by lncRNA NEAT1 in NPC. lncRNA NEAT1 knockdown could sensitize NPC cells to radiation through releasing the expression of miR-204, and eventually enhances the expression of ZEB1, a downstream target of miR-204.

CLINICAL APPLICATION OF NCRNAS AS BIOMARKERS TO RADIOTHERAPY

The *in situ* ncRNA Expression in HNC Tissues Predicting Response of Radiotherapy

It is well known that ncRNAs have shown an important regulatory role on the sensitivity or resistance of HNC cells to radiotherapy. Based on this, ncRNAs expression can be useful biomarkers to identify HNC patients who will be sensitive to radiotherapy and to predict the survival outcomes of HNC patients receiving radiotherapy in clinical practice. One study explored the associations between miR-200b and miR-155 expression in HNC tissues and outcome, and confirmed the prognosis predictive value of candidate miRNAs (Hess et al., 2017). Additionally, some researchers began to build a predictive panel consisting of multiple markers in an attempt to better improve the predictive value. Chen L. et al. (2018) analyzed a large scale of miRNA array profiles and the corresponding clinical records for HNSCC patients (including 509 carcinomas and 44

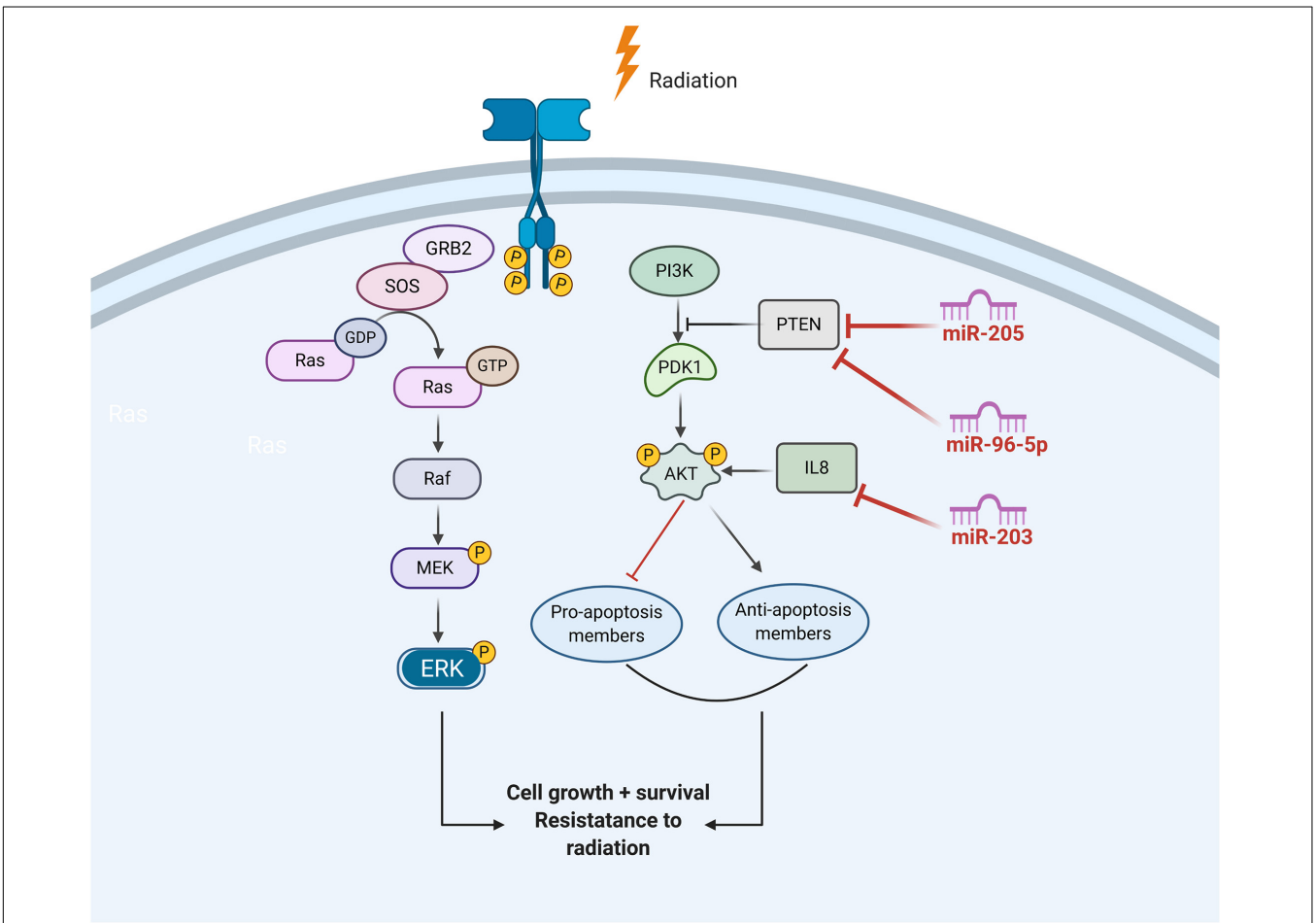

FIGURE 4 | The role of ncRNAs on the regualtion of EGFR signalling in response to radiation induced DNA damage.

normal mucosa specimens) from the TCGA. They established a 5-miRNA signature including miR-99a, miR-31, miR-410, miR-424, and miR-495. Their results showed that this 5-miRNA signature could predict clinical outcomes, and the 5-miRNA signature-based nomogram is useful in predicting radiotherapy response and survival in HNSCC, implying that it might become a promising tool to optimize radiation strategies.

Circulating ncRNAs Serve as Minimally Invasive Therapy-Responsive and Prognostic Biomarkers

Circulating biomarkers in the peripheral blood, such as the biomarker HSP70 in HNSCC patients (Gehrmann et al., 2014), could provide a minimally invasive way to predict therapy response and survival outcomes, as well as monitor the therapy. NcRNAs, especially miRNAs, were reported to show high stability in blood plasma and resistance to RNase activity (Mitchell et al., 2008). This characteristic of miRNA combined with the minimally invasive accessibility of blood sample makes circulating miRNAs useful and attractive biomarkers. Nakashima et al. (2019) reported that the expression of miR-1290 was significantly down-regulated in the plasma of oral squamous cell carcinoma patients as compared to that in healthy volunteers. The patients who showed a poor pathological response to chemoradiotherapy presented a high proportion of miR-1290 down-regulation (Nakashima et al., 2019), suggesting that miR-1290 expression may be useful for guiding treatment decisions in oral squamous cell carcinoma patients receiving radiotherapy. Another research identified eight plasma miRNAs that differentiated significantly between HNC patients and the healthy donors. These candidate miRNAs also showed well therapy-response features and significantly decreased after receiving radiotherapy.

CONCLUSION AND PROSPECTIVE

Radiotherapy is a common therapeutic modality for HNC. Decreased sensitivity or resistance to radiotherapy is still a significant challenge in clinical practice and a barrier to improve the prognosis of HNC patients. With the development of molecular biology and sequencing technology, mounting evidence revealed the important role of ncRNAs on the carcinogenesis, development, and therapy resistance of HNC. These findings were of great significance for the following reasons. First, they highlight the potential of intervening relevant ncRNAs to overcome resistance and re-sensitize cancer cells to the effects of radiotherapy. Second, the ncRNAs could be used as circulating biomarkers in the peripheral blood to predict therapy response and survival outcomes, as well as monitor the therapy.

In the future, more studies are required to further elucidate the potential roles of novel ncRNAs like circRNAs and piRNAs in regulating the sensitivity of HNC cells to radiotherapy. Furthermore, it is still unclear and less studied whether the tumor cells or tumor mesenchymal cells-derived exosomal ncRNAs confer HNC cell resistance characteristics to radiotherapy. These topics will be very interesting and meaningful because circRNAs were more stable than linear RNAs due to their covalently closed loop structures, and exosome encapsulated ncRNAs were less easy to be degraded in the circulation system. These characteristics make circRNAs and exosomal ncRNAs potential biomarker candidates for prognosis prediction and therapy response monitoring. Additionally, with the development of bioinformatics, the integration of ncRNA signature profiling into HNC screening algorithms may help in increasing the specificity of screening patients who will benefit from radiotherapy and improving the prognosis of HNC patients.

AUTHOR CONTRIBUTIONS

JY designed the review. XZ and JY collected the related manuscript. XZ and JY drafted and revised the manuscript. Both authors read and approved the final manuscript.

FUNDING

This study was supported by the 345 Talent project from the Shengjing Hospital of China Medical University, the Natural Science Foundation of Liaoning Province (2014021059).

ACKNOWLEDGMENTS

We would like to acknowledge that figures were created using the © BioRender-biorender.com platform. We would also like to thank members from the Department of Otolaryngology Head and Neck Surgery, Shengjing Hospital of China Medical University for their help on our manuscript.

SUPPLEMENTARY MATERIAL

The Supplementary Material for this article can be found online at: https://www.frontiersin.org/articles/10.3389/fcell.2020.637435/full#supplementary-material

REFERENCES

Alsahafi, E. N., Thavaraj, S., Sarvestani, N., Novoplansky, O., Elkabets, M., Ayaz, B., et al. (2020). EGFR overexpression increases radiotherapy response in HPV-positive head and neck cancer through inhibition of DNA damage repair and HPV E6 downregulation. *Cancer Lett.* 498, 80–97.

Ampil, F. L., Nathan, C. A., and Asarkar, A. (2020). Long-term survival in patients with intermediate-risk head and neck cancer treated with adjuvant radiotherapy. *Oral Oncol.* doi: 10.1016/j.oraloncology.2020.105071 [Epub ahead of print].

Bao, L., You, B., Shi, S., Shan, Y., Zhang, Q., Yue, H., et al. (2018). Metastasis-associated miR-23a from nasopharyngeal carcinoma-derived exosomes mediates angiogenesis by repressing a novel target gene TSGA10. *Oncogene* 37, 2873–2889. doi: 10.1038/s41388-018-0183-186

Berrington de Gonzalez, A., Curtis, R. E., Kry, S. F., Gilbert, E., Lamart, S., et al. (2011). Proportion of second cancers attributable to radiotherapy treatment

in adults: a cohort study in the US SEER cancer registries. *Lancet Oncol.* 12, 353–360. doi: 10.1016/s1470-2045(11)70061-70064

Bonner, J. A., Harari, P. M., Giralt, J., Cohen, R. B., Jones, C. U., Sur, R. K., et al. (2010). Radiotherapy plus cetuximab for locoregionally advanced head and neck cancer: 5-year survival data from a phase 3 randomised trial, and relation between cetuximab-induced rash and survival. *Lancet Oncol.* 11, 21–28. doi: 10.1016/s1470-2045(09)70311-70310

Burgess, J. T., Rose, M., Boucher, D., Plowman, J., Molloy, C., Fisher, M., et al. (2020). The therapeutic potential of DNA Damage repair pathways and genomic stability in lung Cancer. *Front. Oncol.* 10:1256. doi: 10.3389/fonc.2020.01256

Carrassa, L., and Damia, G. (2017). DNA damage response inhibitors: mechanisms and potential applications in cancer therapy. *Cancer Treat Rev.* 60, 139–151. doi: 10.1016/j.ctrv.2017.08.013

Caudell, J. J., Torres-Roca, J. F., Gillies, R. J., Enderling, H., Kim, S., Rishi, A., et al. (2017). The future of personalised radiotherapy for head and neck cancer. *Lancet Oncol.* 18, e266–e273. doi: 10.1016/s1470-2045(17)30252-30258

Chen, H., Jin, L., Zhou, L., and Huang, J. M. (2018). Overexpressed miR-128a enhances chemoradiotherapy to laryngeal cancer cells and its correlation with BMI1. *Future Oncol.* 14, 611–620. doi: 10.2217/fon-2017-2542

Chen, L., Wen, Y., Zhang, J., Sun, W., Lui, V. W. Y., Wei, Y., et al. (2018). Prediction of radiotherapy response with a 5-microRNA signature-based nomogram in head and neck squamous cell carcinoma. *Cancer Med.* 7, 726–735. doi: 10.1002/cam4.1369

Chen, L., Zhou, H., and Guan, Z. (2019). CircRNA_000543 knockdown sensitizes nasopharyngeal carcinoma to irradiation by targeting miR-9/platelet-derived growth factor receptor B axis. *Biochem. Biophys. Res. Commun.* 512, 786–792. doi: 10.1016/j.bbrc.2019.03.126

Chen, L. L. (2016). The biogenesis and emerging roles of circular RNAs. *Nat. Rev. Mol. Cell Biol.* 17, 205–211. doi: 10.1038/nrm.2015.32

Dai, F., Dai, L., Zheng, X., Guo, Y., Zhang, Y., Niu, M., et al. (2020). Non-coding RNAs in drug resistance of head and neck cancers: a review. *Biomed. Pharmacother* 127:110231. doi: 10.1016/j.biopha.2020.110231

de Jong, M. C., Ten Hoeve, J. J., Grénman, R., Wessels, L. F., Kerkhoven, R., Te Riele, H., et al. (2015). Pretreatment microRNA expression impacting on epithelial-to-mesenchymal transition predicts intrinsic radiosensitivity in head and neck cancer cell lines and patients. *Clin. Cancer Res.* 21, 5630–5638. doi: 10.1158/1078-0432.Ccr-15-0454

Doronkin, S., Djagaeva, I., and Beckendorf, S. K. (2002). CSN5/Jab1 mutations affect axis formation in the Drosophila oocyte by activating a meiotic checkpoint. *Development* 129, 5053–5064.

Economopoulou, P., Kotsantis, I., and Psyrri, A. (2016). The promise of immunotherapy in head and neck squamous cell carcinoma: combinatorial immunotherapy approaches. *ESMO Open* 1:e000122. doi: 10.1136/esmoopen-2016-2122

Emerson, C. H., and Bertuch, A. A. (2016). Consider the workhorse: nonhomologous end-joining in budding yeast. *Biochem. Cell Biol.* 94, 396–406. doi: 10.1139/bcb-2016-2011

Feng, L., Zhang, J., Sun, M., Qiu, F., Chen, W., and Qiu, W. (2020). Tumor suppressor LINC02487 inhibits oral squamous cell carcinoma cell migration and invasion through the USP17-SNAI1 Axis. *Front. Oncol.* 10:559808. doi: 10.3389/fonc.2020.559808

Feng, Q., Zhang, H., Yao, D., Chen, W. D., and Wang, Y. D. (2019). Emerging role of non-coding RNAS in esophageal squamous cell carcinoma. *Int. J. Mol. Sci.* 21:258. doi: 10.3390/ijms21010258

Feng, X., Lv, W., Wang, S., and He, Q. (2018). miR-495 enhances the efficacy of radiotherapy by targeting GRP78 to regulate EMT in nasopharyngeal carcinoma cells. *Oncol. Rep.* 40, 1223–1232. doi: 10.3892/or.2018.6538

Ferlay, J., Soerjomataram, I., Dikshit, R., Eser, S., Mathers, C., Rebelo, M., et al. (2015). Cancer incidence and mortality worldwide: sources, methods and major patterns in GLOBOCAN 2012. *Int. J. Cancer* 136, E359–E386. doi: 10.1002/ijc.29210

Gao, W., Lam, J. W., Li, J. Z., Chen, S. Q., Tsang, R. K., Chan, J. Y., et al. (2017a). MicroRNA-138-5p controls sensitivity of nasopharyngeal carcinoma to radiation by targeting EIF4EBP1. *Oncol. Rep.* 37, 913–920. doi: 10.3892/or.2017.5354

Gao, W., Li, Z. H., Chen, S., Chan, J. Y., Yin, M., Zhang, M. J., et al. (2017b). Epstein-Barr virus encoded microRNA BART7 regulates radiation sensitivity of nasopharyngeal carcinoma. *Oncotarget* 8, 20297–20308. doi: 10.18632/oncotarget.15526

Gehrmann, M., Specht, H. M., Bayer, C., Brandstetter, M., Chizzali, B., Duma, M., et al. (2014). Hsp70–a biomarker for tumor detection and monitoring of outcome of radiation therapy in patients with squamous cell carcinoma of the head and neck. *Radiat Oncol.* 9:131. doi: 10.1186/1748-717x-9-131

Gou, C., Han, P., Li, J., Gao, L., Ji, X., Dong, F., et al. (2020). Knockdown of lncRNA BLACAT1 enhances radiosensitivity of head and neck squamous cell carcinoma cells by regulating PSEN1. *Br. J. Radiol.* 93:20190154. doi: 10.1259/bjr.20190154

Gu, X., Wang, L., Coates, P. J., Boldrup, L., Fåhraeus, R., Wilms, T., et al. (2020). Transfer-RNA-Derived fragments are potential prognostic factors in patients with squamous cell carcinoma of the head and neck. *Genes (Basel)* 11:1344. doi: 10.3390/genes11111344

Haimovitz-Friedman, A., Kan, C. C., Ehleiter, D., Persaud, R. S., McLoughlin, M., Fuks, Z., et al. (1994). Ionizing radiation acts on cellular membranes to generate ceramide and initiate apoptosis. *J. Exp. Med.* 180, 525–535. doi: 10.1084/jem.180.2.525

Han, Q., Li, L., Liang, H., Li, Y., Xie, J., and Wang, Z. (2017). Downregulation of lncRNA X Inactive Specific Transcript (XIST) suppresses cell proliferation and enhances radiosensitivity by upregulating mir-29c in nasopharyngeal carcinoma cells. *Med. Sci. Monit.* 23, 4798–4807. doi: 10.12659/msm.905370

Hanai, R., Yazu, M., and Hieda, K. (1998). On the experimental distinction between ssbs and dsbs in circular DNA. *Int. J. Radiat. Biol.* 73, 475–479. doi: 10.1080/095530098142013

He, Y., Jing, Y., Wei, F., Tang, Y., Yang, L., Luo, J., et al. (2018). Long non-coding RNA PVT1 predicts poor prognosis and induces radioresistance by regulating DNA repair and cell apoptosis in nasopharyngeal carcinoma. *Cell Death Dis.* 9:235. doi: 10.1038/s41419-018-0265-y

Hess, A. K., Müer, A., Mairinger, F. D., Weichert, W., Stenzinger, A., Hummel, M., et al. (2017). MiR-200b and miR-155 as predictive biomarkers for the efficacy of chemoradiation in locally advanced head and neck squamous cell carcinoma. *Eur. J. Cancer* 77, 3–12. doi: 10.1016/j.ejca.2017.02.018

Hu, X., Jiang, H., and Jiang, X. (2017). Downregulation of lncRNA ANRIL inhibits proliferation, induces apoptosis, and enhances radiosensitivity in nasopharyngeal carcinoma cells through regulating miR-125a. *Cancer Biol. Ther.* 18, 331–338. doi: 10.1080/15384047.2017.1310348

Huang, N. S., Lei, B. W., Tan, L. C., Yu, P. C., Shi, X., Wang, Y., et al. (2020). Mitotically associated long non-coding RNA is a tumor promoter in anaplastic thyroid cancer. *Ann. Transl. Med.* 8:1226. doi: 10.21037/atm-20-4530

Huang, S., Zhan, Z., Li, L., Guo, H., Yao, Y., Feng, M., et al. (2019). LINC00958-MYC positive feedback loop modulates resistance of head and neck squamous cell carcinoma cells to chemo- and radiotherapy in vitro. *Onco Targets Ther.* 12, 5989–6000. doi: 10.2147/ott.S208318

Huang, T., Yin, L., Wu, J., Gu, J. J., Wu, J. Z., Chen, D., et al. (2016). MicroRNA-19b-3p regulates nasopharyngeal carcinoma radiosensitivity by targeting TNFAIP3/NF-κB axis. *J. Exp. Clin. Cancer Res.* 35:188. doi: 10.1186/s13046-016-0465-461

Huang, Y., Tan, D., Xiao, J., Li, Q., Zhang, X., and Luo, Z. (2018). miR-150 contributes to the radioresistance in nasopharyngeal carcinoma cells by targeting glycogen synthase kinase-3β. *J. Cancer Res. Ther.* 14, 111–118. doi: 10.4103/jcrt.JCRT_682_17

Jackson, S. P. (2002). Sensing and repairing DNA double-strand breaks. *Carcinogenesis* 23, 687–696. doi: 10.1093/carcin/23.5.687

Jarvis, W. D., Fornari, F. A. Jr., Browning, J. L., Gewirtz, D. A., Kolesnick, R. N., et al. (1994a). Attenuation of ceramide-induced apoptosis by diglyceride in human myeloid leukemia cells. *J. Biol. Chem.* 269, 31685–31692. doi: 10.1016/s0021-9258(18)31750-2

Jarvis, W. D., Kolesnick, R. N., Fornari, F. A., Traylor, R. S., Gewirtz, D. A., and Grant, S. (1994b). Induction of apoptotic DNA damage and cell death by activation of the sphingomyelin pathway. *Proc. Natl. Acad. Sci. U S A.* 91, 73–77. doi: 10.1073/pnas.91.1.73

Jiang, Y., Cao, W., Wu, K., Qin, X., Wang, X., Li, Y., et al. (2019). LncRNA LINC00460 promotes EMT in head and neck squamous cell carcinoma by facilitating peroxiredoxin-1 into the nucleus. *J. Exp. Clin. Cancer Res.* 38:365. doi: 10.1186/s13046-019-1364-z

Kang, M., Xiao, J., Wang, J., Zhou, P., Wei, T., Zhao, T., et al. (2016). MiR-24 enhances radiosensitivity in nasopharyngeal carcinoma by targeting SP1. *Cancer Med.* 5, 1163–1173. doi: 10.1002/cam4.660

Kangboonruang, K., Wongtrakoongate, P., Lertsuwan, K., Khachonkham, S., Changkaew, P., Tangboonduangjit, P., et al. (2020). MALAT1 decreases the sensitivity of head and neck squamous cell carcinoma cells to radiation and cisplatin. *Anticancer Res.* 40, 2645–2655. doi: 10.21873/anticanres.14235

Kong, L., Wei, Q., Hu, X., Chen, L., and Li, J. (2019). miR-193a-3p promotes radioresistance of nasopharyngeal cancer cells by targeting SRSF2 gene and hypoxia signaling pathway. *Med. Sci. Monit. Basic Res.* 25, 53–62. doi: 10.12659/msmbr.914572

Lacas, B., Bourhis, J., Overgaard, J., Zhang, Q., Grégoire, V., Nankivell, M., et al. (2017). Role of radiotherapy fractionation in head and neck cancers (MARCH): an updated meta-analysis. *Lancet Oncol.* 18, 1221–1237. doi: 10.1016/s1470-2045(17)30458-30458

Leemans, C. R., Snijders, P. J. F., and Brakenhoff, R. H. (2018). The molecular landscape of head and neck cancer. *Nat. Rev. Cancer* 18, 269–282. doi: 10.1038/nrc.2018.11

Lewanski, C. R., and Gullick, W. J. (2001). Radiotherapy and cellular signalling. *Lancet Oncol.* 2, 366–370. doi: 10.1016/s1470-2045(00)00391-390

Li, B. Y., Luo, Y., Zhao, W. S., Zhang, L., Zhou, H. J., Zou, Y. C., et al. (2017). MicroRNA-210 negatively regulates the radiosensitivity of nasopharyngeal carcinoma cells. *Mol. Med. Rep.* 16, 1401–1408. doi: 10.3892/mmr.2017.6694

Li, L. N., Xiao, T., Yi, H. M., Zheng, Z., Qu, J. Q., Huang, W., et al. (2017). MiR-125b increases nasopharyngeal carcinoma radioresistance by targeting A20/NF-κB signaling pathway. *Mol. Cancer Ther.* 16, 2094–2106. doi: 10.1158/1535-7163.Mct-17-0385

Li, G., Liu, Y., Su, Z., Ren, S., Zhu, G., Tian, Y., et al. (2013). MicroRNA-324-3p regulates nasopharyngeal carcinoma radioresistance by directly targeting WNT2B. *Eur. J. Cancer* 49, 2596–2607. doi: 10.1016/j.ejca.2013.03.001

Li, J., Liu, X., Nan, S., and Xu, C. (2020). Silencing of long non-coding RNA LINC00520 promotes radiosensitivity of head and neck squamous cell carcinoma cells. *Free Radic Res.* 54, 254–270. doi: 10.1080/10715762.2020.1752373

Lin, T., Zhou, F., Zhou, H., Pan, X., Sun, Z., and Peng, G. (2015). MicroRNA-378g enhanced radiosensitivity of NPC cells partially by targeting protein tyrosine phosphatase SHP-1. *Int. J. Radiat. Biol.* 91, 859–866. doi: 10.3109/09553002.2015.1096028

Maia, D., de Carvalho, A. C., Horst, M. A., Carvalho, A. L., Scapulatempo-Neto, C., and Vettore, A. L. (2015). Expression of miR-296-5p as predictive marker for radiotherapy resistance in early-stage laryngeal carcinoma. *J. Transl. Med.* 13:262. doi: 10.1186/s12967-015-0621-y

Mansour, W. Y., Bogdanova, N. V., Kasten-Pisula, U., Rieckmann, T., Köcher, S., Borgmann, K., et al. (2013). Aberrant overexpression of miR-421 downregulates ATM and leads to a pronounced DSB repair defect and clinical hypersensitivity in SKX squamous cell carcinoma. *Radiother Oncol.* 106, 147–154. doi: 10.1016/j.radonc.2012.10.020

Marie-Egyptienne, D. T., Lohse, I., and Hill, R. P. (2013). Cancer stem cells, the epithelial to mesenchymal transition (EMT) and radioresistance: potential role of hypoxia. *Cancer Lett.* 341, 63–72. doi: 10.1016/j.canlet.2012.11.019

Mattick, J. S., and Makunin, I. V. (2006). Non-coding RNA. *Hum. Mol. Genet.* 15, R17–R29. doi: 10.1093/hmg/ddl046

Mitchell, P. S., Parkin, R. K., Kroh, E. M., Fritz, B. R., Wyman, S. K., Pogosova-Agadjanyan, E. L., et al. (2008). Circulating microRNAs as stable blood-based markers for cancer detection. *Proc. Natl. Acad. Sci. U S A.* 105, 10513–10518. doi: 10.1073/pnas.0804549105

Nakashima, H., Yoshida, R., Hirosue, A., Kawahara, K., Sakata, J., Arita, H., et al. (2019). Circulating miRNA-1290 as a potential biomarker for response to chemoradiotherapy and prognosis of patients with advanced oral squamous cell carcinoma: a single-center retrospective study. *Tumour Biol.* 41:1010428319826853. doi: 10.1177/1010428319826853

Nastasi, C., Mannarino, L., and D'Incalci, M. (2020). DNA damage response and immune defense. *Int. J. Mol. Sci.* 21:7504. doi: 10.3390/ijms21207504

Nichols, A. C., Theurer, J., Prisman, E., Read, N., Berthelet, E., Tran, E., et al. (2019). Radiotherapy versus transoral robotic surgery and neck dissection for oropharyngeal squamous cell carcinoma (ORATOR): an open-label, phase 2, randomised trial. *Lancet Oncol.* 20, 1349–1359. doi: 10.1016/s1470-2045(19)30410-30413

Obeid, L. M., Linardic, C. M., Karolak, L. A., and Hannun, Y. A. (1993). Programmed cell death induced by ceramide. *Science* 259, 1769–1771. doi: 10.1126/science.8456305

Pan, Y., Zhang, Q., Atsaves, V., Yang, H., and Claret, F. X. (2013). Suppression of Jab1/CSN5 induces radio- and chemo-sensitivity in nasopharyngeal carcinoma through changes to the DNA damage and repair pathways. *Oncogene* 32, 2756–2766. doi: 10.1038/onc.2012.294

Pan, Y., Zhang, Q., Tian, L., Wang, X., Fan, X., Zhang, H., et al. (2012). Jab1/CSN5 negatively regulates p27 and plays a role in the pathogenesis of nasopharyngeal carcinoma. *Cancer Res.* 72, 1890–1900. doi: 10.1158/0008-5472.Can-11-3472

Pasi, F., Corbella, F., Baio, A., Capelli, E., De Silvestri, A., Tinelli, C., et al. (2020). Radiation-induced circulating miRNA expression in blood of head and neck cancer patients. *Radiat Environ. Biophys.* 59, 237–244. doi: 10.1007/s00411-020-00832-833

Pignon, J. P., le Maître, A., Maillard, E., and Bourhis, J. (2009). Meta-analysis of chemotherapy in head and neck cancer (MACH-NC): an update on 93 randomised trials and 17,346 patients. *Radiother Oncol.* 92, 4–14. doi: 10.1016/j.radonc.2009.04.014

Plavc, G., Jesenko, T., Oražem, M., and Strojan, P. (2020). Challenges in combining immunotherapy with radiotherapy in recurrent/metastatic head and neck cancer. *Cancers (Basel)* 12:3197. doi: 10.3390/cancers12113197

Qu, C., Liang, Z., Huang, J., Zhao, R., Su, C., Wang, S., et al. (2012). MiR-205 determines the radioresistance of human nasopharyngeal carcinoma by directly targeting PTEN. *Cell Cycle* 11, 785–796. doi: 10.4161/cc.11.4.19228

Qu, J. Q., Yi, H. M., Ye, X., Li, L. N., Zhu, J. F., Xiao, T., et al. (2015a). MiR-23a sensitizes nasopharyngeal carcinoma to irradiation by targeting IL-8/Stat3 pathway. *Oncotarget* 6, 28341–28356. doi: 10.18632/oncotarget.5117

Qu, J. Q., Yi, H. M., Ye, X., Zhu, J. F., Yi, H., Li, L. N., et al. (2015b). MiRNA-203 reduces nasopharyngeal carcinoma radioresistance by targeting IL8/AKT signaling. *Mol. Cancer Ther.* 14, 2653–2664. doi: 10.1158/1535-7163.Mct-15-0461

Rothkamm, K., and Löbrich, M. (2003). Evidence for a lack of DNA double-strand break repair in human cells exposed to very low x-ray doses. *Proc. Natl. Acad. Sci. U S A.* 100, 5057–5062. doi: 10.1073/pnas.0830918100

Sher, D. J., Pham, N. L., Shah, J. L., Sen, N., Williams, K. A., Subramaniam, R. M., et al. (2020a). Prospective phase II study of radiotherapy dose and volume de-escalation for elective neck treatment of oropharyngeal and laryngeal cancer. *Int. J. Radiat. Oncol. Biol. Phys.* doi: 10.1016/j.ijrobp.2020.09.063 [Epub ahead of print].

Sher, D. J., Yan, J., Day, A. T., Khan, S., and Zhu, H. (2020b). Comparative cost analysis between definitive radiotherapy and transoral surgery for oropharyngeal squamous cell carcinoma: a SEER-Medicare analysis. *Oral Oncol.* 112:105029. doi: 10.1016/j.oraloncology.2020.105029

Shiiba, M., Shinozuka, K., Saito, K., Fushimi, K., Kasamatsu, A., Ogawara, K., et al. (2013). MicroRNA-125b regulates proliferation and radioresistance of oral squamous cell carcinoma. *Br. J. Cancer* 108, 1817–1821. doi: 10.1038/bjc.2013.175

Shuai, M., and Huang, L. (2020). High expression of hsa_circRNA_001387 in nasopharyngeal carcinoma and the effect on efficacy of radiotherapy. *Onco Targets Ther.* 13, 3965–3973. doi: 10.2147/ott.S249202

Slack, F. J. (2006). Regulatory RNAs and the demise of ' junk '. DNA. *Genome Biolo.* 7:328. doi: 10.1186/gb-2006-7-9-328

Suh, Y. E., Raulf, N., Gäken, J., Lawler, K., Urbano, T. G., Bullenkamp, J., et al. (2015). MicroRNA-196a promotes an oncogenic effect in head and neck cancer cells by suppressing annexin A1 and enhancing radioresistance. *Int. J. Cancer* 137, 1021–1034. doi: 10.1002/ijc.29397

Sun, Q., Liu, T., Zhang, T., Du, S., Xie, G. X., Lin, X., et al. (2015). MiR-101 sensitizes human nasopharyngeal carcinoma cells to radiation by targeting stathmin 1. *Mol. Med. Rep.* 11, 3330–3336. doi: 10.3892/mmr.2015.3221

Sur, S., Nakanishi, H., Steele, R., Zhang, D., Varvares, M. A., and Ray, R. B. (2020). Long non-coding RNA ELDR enhances oral cancer growth by promoting ILF3-cyclin E1 signaling. *EMBO Rep.* 21, e51042. doi: 10.15252/embr.202051042

Symington, L. S., and Gautier, J. (2011). Double-strand break end resection and repair pathway choice. *Annu. Rev. Genet.* 45, 247–271. doi: 10.1146/annurev-genet-110410-132435

Tao, Y., Aupérin, A., Sun, X., Sire, C., Martin, L., Coutte, A., et al. (2020). Avelumab-cetuximab-radiotherapy versus standards of care in locally advanced squamous-cell carcinoma of the head and neck: the safety phase of a randomised phase III trial GORTEC 2017-01 (REACH). *Eur. J. Cancer* 141, 21–29. doi: 10.1016/j.ejca.2020.09.008

Tian, Y., Yan, M., Zheng, J., Li, R., Lin, J., Xu, A., et al. (2019). miR-483-5p decreases the radiosensitivity of nasopharyngeal carcinoma cells by targeting DAPK1. *Lab Invest.* 99, 602–611. doi: 10.1038/s41374-018-0169-166

Vahabi, M., Pulito, C., Sacconi, A., Donzelli, S., D'Andrea, M., Manciocco, V., et al. (2019). miR-96-5p targets PTEN expression affecting radio-chemosensitivity of HNSCC cells. *J. Exp. Clin. Cancer Res.* 38:141. doi: 10.1186/s13046-019-1119-x

Vo, D. T., Karanam, N. K., Ding, L., Saha, D., Yordy, J. S., Giri, U., et al. (2019). miR-125a-5p functions as tumor suppressor microRNA And is a marker of locoregional recurrence and poor prognosis in head and neck cancer. *Neoplasia* 21, 849–862. doi: 10.1016/j.neo.2019.06.004

Wang, R., Ma, Z., Feng, L., Yang, Y., Tan, C., Shi, Q., et al. (2018). LncRNA MIR31HG targets HIF1A and P21 to facilitate head and neck cancer cell proliferation and tumorigenesis by promoting cell-cycle progression. *Mol. Cancer* 17:162. doi: 10.1186/s12943-018-0916-918

Wang, S., Pan, Y., Zhang, R., Xu, T., Wu, W., Zhang, R., et al. (2016). Hsa-miR-24-3p increases nasopharyngeal carcinoma radiosensitivity by targeting both the 3'UTR and 5'UTR of Jab1/CSN5. *Oncogene* 35, 6096–6108. doi: 10.1038/onc.2016.147

Wang, S., Zhang, R., Claret, F. X., and Yang, H. (2014). Involvement of microRNA-24 and DNA methylation in resistance of nasopharyngeal carcinoma to ionizing radiation. *Mol. Cancer Ther.* 13, 3163–3174. doi: 10.1158/1535-7163.Mct-14-0317

Wang, S. S., Lv, Y., Xu, X. C., Zuo, Y., Song, Y., Wu, G. P., et al. (2019). Triptonide inhibits human nasopharyngeal carcinoma cell growth via disrupting Lnc-RNA THOR-IGF2BP1 signaling. *Cancer Lett.* 443, 13–24. doi: 10.1016/j.canlet.2018.11.028

Wang, Z., Mao, J. W., Liu, G. Y., Wang, F. G., Ju, Z. S., Zhou, D., et al. (2019). MicroRNA-372 enhances radiosensitivity while inhibiting cell invasion and metastasis in nasopharyngeal carcinoma through activating the PBK-dependent p53 signaling pathway. *Cancer Med.* 8, 712–728. doi: 10.1002/cam4.1924

Wang, Y., Wang, S., Ren, Y., and Zhou, X. (2020). The role of lncRNA crosstalk in leading cancer metastasis of head and neck squamous cell carcinoma. *Front. Oncol.* 10:561833. doi: 10.3389/fonc.2020.561833

Weber, A. M., and Ryan, A. J. (2015). ATM and ATR as therapeutic targets in cancer. *Pharmacol. Therapeut.* 149, 124–138. doi: 10.1016/j.pharmthera.2014.12.001

Weng, J. H., Yu, C. C., Lee, Y. C., Lin, C. W., Chang, W. W., and Kuo, Y. L. (2016). miR-494-3p induces cellular senescence and enhances radiosensitivity in human oral squamous carcinoma cells. *Int. J. Mol. Sci.* 17:1092. doi: 10.3390/ijms17071092

Wills, W. K. (1904). The present position of radiotherapy in therapeutics. *Bristol. Med. Chir. J. (1883)* 22, 39–46.

Wu, H., Yang, L., and Chen, L. L. (2017). The diversity of long noncoding RNAs and their generation. *Trends Genet.* 33, 540–552. doi: 10.1016/j.tig.2017.05.004

Wu, H., Zheng, J., Deng, J., Zhang, L., Li, N., Li, W., et al. (2015). LincRNA-uc002yug.2 involves in alternative splicing of RUNX1 and serves as a predictor for esophageal cancer and prognosis. *Oncogene* 34, 4723–4734. doi: 10.1038/onc.2014.400

Wu, S. Y., Wu, A. T., and Liu, S. H. (2016). MicroRNA-17-5p regulated apoptosis-related protein expression and radiosensitivity in oral squamous cell carcinoma caused by betel nut chewing. *Oncotarget* 7, 51482–51493. doi: 10.18632/oncotarget.9856

Wu, W., Chen, X., Yu, S., Wang, R., Zhao, R., and Du, C. (2018). microRNA-222 promotes tumor growth and confers radioresistance in nasopharyngeal carcinoma by targeting PTEN. *Mol. Med. Rep.* 17, 1305–1310. doi: 10.3892/mmr.2017.7931

Xu, J., Ai, Q., Cao, H., and Liu, Q. (2015). MiR-185-3p and miR-324-3p Predict radiosensitivity of nasopharyngeal carcinoma and modulate cancer cell growth and apoptosis by targeting SMAD7. *Med. Sci. Monit.* 21, 2828–2836. doi: 10.12659/msm.895660

Yang, T., Li, S., Liu, J., Yin, D., Yang, X., and Tang, Q. (2018). lncRNA-NKILA/NF-κB feedback loop modulates laryngeal cancer cell proliferation, invasion, and radioresistance. *Cancer Med.* 7, 2048–2063. doi: 10.1002/cam4.1405

Yao, R. W., Wang, Y., and Chen, L. L. (2019). Cellular functions of long noncoding RNAs. *Nat. Cell Biol.* 21, 542–551. doi: 10.1038/s41556-019-0311-318

Yi, L., Ouyang, L., Wang, S., Li, S. S., and Yang, X. M. (2019). Long noncoding RNA PTPRG-AS1 acts as a microRNA-194-3p sponge to regulate radiosensitivity and metastasis of nasopharyngeal carcinoma cells via PRC1. *J. Cell Physiol.* 234, 19088–19102. doi: 10.1002/jcp.28547

Yu, M., Lu, B., Zhang, J., Ding, J., Liu, P., and Lu, Y. (2020). tRNA-derived RNA fragments in cancer: current status and future perspectives. *J. Hematol. Oncol.* 13:121. doi: 10.1186/s13045-020-00955-956

Zhang, J. X., Qian, D., Wang, F. W., Liao, D. Z., Wei, J. H., Tong, Z. T., et al. (2013). MicroRNA-29c enhances the sensitivities of human nasopharyngeal carcinoma to cisplatin-based chemotherapy and radiotherapy. *Cancer Lett.* 329, 91–98. doi: 10.1016/j.canlet.2012.10.033

Zhang, L. M., Su, L. X., Hu, J. Z., Wang, M., Ju, H. Y., Li, X., et al. (2020). Epigenetic regulation of VENTXP1 suppresses tumor proliferation via miR-205-5p/ANKRD2/NF-kB signaling in head and neck squamous cell carcinoma. *Cell Death Dis.* 11:838. doi: 10.1038/s41419-020-03057-w

Zhao, B., Rothenberg, E., Ramsden, D. A., and Lieber, M. R. (2020). The molecular basis and disease relevance of non-homologous DNA end joining. *Nat. Rev. Mol. Cell Biol.* 21, 765–781. doi: 10.1038/s41580-020-00297-298

Zhao, L., Tang, M., Hu, Z., Yan, B., Pi, W., Li, Z., et al. (2015). miR-504 mediated down-regulation of nuclear respiratory factor 1 leads to radioresistance in nasopharyngeal carcinoma. *Oncotarget* 6, 15995–16018. doi: 10.18632/oncotarget.4138

Zhao, X., Wei, C., Li, J., Xing, P., Li, J., Zheng, S., et al. (2017). Cell cycle-dependent control of homologous recombination. *Acta Biochim. Biophys. Sin (Shanghai)* 49, 655–668. doi: 10.1093/abbs/gmx055

Conflict of Interest: The authors declare that the research was conducted in the absence of any commercial or financial relationships that could be construed as a potential conflict of interest.

frontiers in Cell and Developmental Biology

ORIGINAL RESEARCH
published: 20 April 2021
doi: 10.3389/fcell.2021.636178

PprA Protein Inhibits DNA Strand Exchange and ATP Hydrolysis of *Deinococcus* RecA and Regulates the Recombination in Gamma-Irradiated Cells

Yogendra Singh Rajpurohit[1,2]*, *Dhirendra Kumar Sharma*[1,2] *and Hari S. Misra*[1,2]*

[1] Molecular Biology Division, Bhabha Atomic Research Centre, Mumbai, India, [2] Homi Bhabha National Institute (DAE-Deemed University), Mumbai, India

OPEN ACCESS

Edited by:
Rosa Maria Bermudez-Cruz, Centro de Investigaciones y Estudios Avanzados, Instituto Politécnico Nacional de México (CINVESTAV), Mexico

Reviewed by:
Issay Narumi, Toyo University, Japan
Kaiying Cheng, Hangzhou Normal University, China
Sangyong Lim, Korea Atomic Energy Research Institute (KAERI), South Korea

***Correspondence:**
Yogendra Singh Rajpurohit
ysraj@barc.gov.in
Hari S. Misra
hsmisra@barc.gov.in

Specialty section:
This article was submitted to Molecular and Cellular Oncology, a section of the journal Frontiers in Cell and Developmental Biology

Received: 18 December 2020
Accepted: 23 March 2021
Published: 20 April 2021

Citation:
Rajpurohit YS, Sharma DK and Misra HS (2021) PprA Protein Inhibits DNA Strand Exchange and ATP Hydrolysis of Deinococcus RecA and Regulates the Recombination in Gamma-Irradiated Cells. Front. Cell Dev. Biol. 9:636178. doi: 10.3389/fcell.2021.636178

DrRecA and PprA proteins function are crucial for the extraordinary resistance to γ-radiation and DNA strand break repair in *Deinococcus radiodurans*. DrRecA mediated homologous recombination help in DNA strand break repair and cell survival, while the PprA protein confers radio-resistance *via* its roles in DNA repair, genome maintenance, and cell division. Genetically *recA* and *pprA* genes interact and constitute an epistatic group however, the mechanism underlying their functional interaction is not clear. Here, we showed the physical and functional interaction of DrRecA and PprA protein both *in solution* and inside the cells. The absence of the *pprA* gene increases the recombination frequency in gamma-irradiated *D. radiodurans* cells and genomic instability in cells growing under normal conditions. PprA negatively regulates the DrRecA functions by inhibiting DrRecA mediated DNA strand exchange and ATPase function *in vitro*. Furthermore, it is shown that the inhibitory effect of PprA on DrRecA catalyzed DNA strand exchange was not due to sequestration of homologous dsDNA and was dependent on PprA oligomerization and DNA binding property. Together, results suggest that PprA is a new member of recombination mediator proteins (RMPs), and able to regulate the DrRecA function in γ-irradiated cells by protecting the *D. radiodurans* genome from hyper-recombination and associated negative effects.

Keywords: PprA, DrRecA, *Deinococcus radiodurans*, DNA repair, ATPase

INTRODUCTION

An astounding gamma radiation resistance of *Deinococcus radiodurans* has been attributed to its efficient DNA double-strand break (DSB) repair supported by the Extended Synthesis Dependent Strand Annealing (ESDSA) mechanism and the ability to protect its biomolecules from oxidative damage (Zahradka et al., 2006; Slade et al., 2009; Misra et al., 2013). In bacteria, RecA plays an important role in homologous recombination (Bell and Kowalczykowski, 2016) and thus becomes integral to macromolecular events responsible for DNA strand break repair by homologous recombination and genome integrity (Heyer, 2015). RecA plays a deterministic role in both RecBC and RecF pathways of homologous recombination and several interacting proteins

may involve in the regulation of RecA functions, viz. RecBC, RecF, RecO, RecR, DinI, RecX, RdgC, PsiB, and UvrD at multiple levels (Cox, 2007). In *Escherichia coli*, the expression of RecA is under the control of SOS regulon while the C-terminal region of RecA protein autoregulates its functions (Little and Mount, 1982). For bacterium *D. radiodurans,* DNA DSB repair and cell survival are heavily relying on RecA-mediated homologous (Daly et al., 1994; Daly and Minton, 1996; Zahradka et al., 2006; Slade et al., 2009). *D. radiodurans* lacks the LexA/RecA mediated canonical SOS regulation as DrRecA expression and/or activity is not under the control of either LexA proteins or its operon partners (CinA and LigT) (Narumi et al., 2001; Bonacossa de Almeida et al., 2002; Jolivet et al., 2006; Satoh et al., 2006). Nonetheless, two transcriptional regulators; IrrE and DdrO are shown to be a transcriptional regulator of *the recA* gene in the gamma-irradiated *D. radiodurans* cells (Earl et al., 2002), while DrRRA is shown to be a positive regulator during normal growth (Wang et al., 2008). Recently, phosphorylation mediated regulation of DrRecA function has been suggested, where it was shown that a radiation responsive RqkA kinase phosphorylates at Y77 and T318 amino acid and these sites phosphorylation has a substantial impact on nucleotide preference and DNA affinity of DrRecA (Rajpurohit et al., 2016) and the conformational stability, dynamics of DrRecA (Sharma et al., 2020). RecX of *D. radiodurans* is a negative regulator of *recA* expression as well could directly inhibit RecA activities like DNA strand exchange, ATPase activity, and LexA cleavage (Sheng et al., 2005). Interestingly, RecX does not seems to be a regulator of DrRecA under gamma radiation conditions as radiation resistance of *recX*$^{-}$ mutant was similar to that of wild-type *D. radiodurans* (Sheng et al., 2005). *D. radiodurans* cells also lack many known RecA protein regulators (RecB, RecC, RecE, and RecT) as known for *E. coli* (Slade and Radman, 2011). Thus, it is likely that some new protein regulators or other novel mechanisms may regulate DrRecA activity in the gamma-irradiated cells.

PprA (Pleiotropic protein promoting DNA repair) is a unique DNA repair protein contributing to ionizing radiation and desiccation resistance as transcription of this gene induced multi-fold when *D. radiodurans* cells exposed to gamma radiation and by desiccation (Liu et al., 2003; Narumi et al., 2004). Biochemically, it stimulates ATP and NAD-dependent DNA ligases and protects DNA ends from exonucleolytic degradation (Narumi et al., 2004). It also binds with double-strand DNA ends to promote DNA looping (Adachi et al., 2014). The *pprA*$^{-}$ mutant of *D. radiodurans* grows slowly and displays high sensitivity to UV-A radiation (Bauermeister et al., 2009), ionizing γ- radiation, and mitomycin C (Narumi et al., 2004). Interestingly, the γ-radiation sensitivity level of *the pprA*$^{-}$ mutant is much lesser compare to the *recA*$^{-}$ mutant. The γ-radiation survival of double mutant of *pprA* and *recA* genes (*pprA*$^{-}$*recA*$^{-}$*)* did not show additive sensitive phenotype (Tanaka et al., 2004), suggesting that both the proteins seem to contribute to radioresistance of *D. radiodurans* through common pathways and epistatic. However, the precise nature of *recA* and *pprA* interaction at a cellular and genetic level is not known and would be worth unveiling. Here, we report the physical and functional interaction of PprA with DrRecA and demonstrated that the role of PprA in the regulation of DrRecA biochemical properties and the recombination frequencies in the γ-irradiated *D. radiodurans*. The *pprA*$^{-}$ mutant showed an increased recombination frequency in γ-treated cells and increased genomic instability in cells grown under normal conditions. Further, we showed that the inhibitory effect of PprA on DrRecA catalyzed DNA strand exchange activity was independent of PprA capability of sequestration of homologous DNA but dependent on PprA oligomerization and its DNA binding property. Together, results highlight the importance of PprA-DrRecA interaction in the regulation of DrRecA function under γ-irradiated conditions perhaps by protecting the genome from hyper-recombination and associated negative effect during post-irradiation recovery of *D. radiodurans.*

RESULTS

PprA Protein Interacts With DrRecA

PprA protein assists in DNA repair and cell survival of *D. radiodurans* recovering from ionizing radiation, and included in the DrRecA epistatic group (Narumi et al., 2004; Tanaka et al., 2004). The physical interaction of PprA and DrRecA protein was monitored using a bacterial two-hybrid system in surrogate *E. coli* BTH101, co-expressing T18 tagged PprA and T25 tagged DrRecA and also with tag swapped version of these proteins (**Figure 1A**). In the *E. coli* BTH101 cells, a functional gain of β-galactosidase activity due to interaction of tagged proteins (here DrRecA and PprA). The *in vivo* functional interaction of tagged proteins monitored as a function of β-galactosidase enzyme activity (Karimova et al., 2000). The nature and relative strength of the interaction between DrRecA-C18 and PprA-C25 was comparable to positive control where inter-subunit of RecA-RecA interaction was measured (**Figures 1A,B**). Similarly, in the tag swapped experiment, where RecA-C25 and PprA-C18 protein expressed in BTH cells, the interaction strength and β-galactosidase activity were comparable to DrRecA-C18 and PprA-C25 interaction results (**Figures 1A,B**). The β-galactosidase activity was minimal in the negative control, where T18 and T25 tags were expressed in BTH101 (**Figures 1A,B**).

The interaction of these proteins was also assayed in *D. radiodurans* by Co-immunoprecipitation (Co-IP) and by cellular co-localization. For Co-IP, DrRecA (poly His-tagged) and PprA (T18 tagged) were expressed either alone or together in *D. radiodurans* cells. Tag swap experiment was also done where DrRecA (T18 tagged) and PprA (poly His-tagged) together expressed in *D. radiodurans* cells (**Supplementary Figure 1**). Results showed that cells expressing alone DrRecA (T18 tagged) or PprA (poly His-tagged) did not produce a signal on blot when Co-IP was done with anti-His antibody (Ab) followed by detection by Anti-T18 Ab (**Figure 1C**). Similarly, in tag swapped experiment when PprA (T18 tagged) alone expressed and Co-IP was done with anti-T18 Ab followed by detection by Anti-His Ab (**Figure 1C**). The immunoprecipitate from cells expressing both proteins (T18 tagged DrRecA and poly His-tagged PprA) produce a band of molecular mass of ∼56 kDa (a

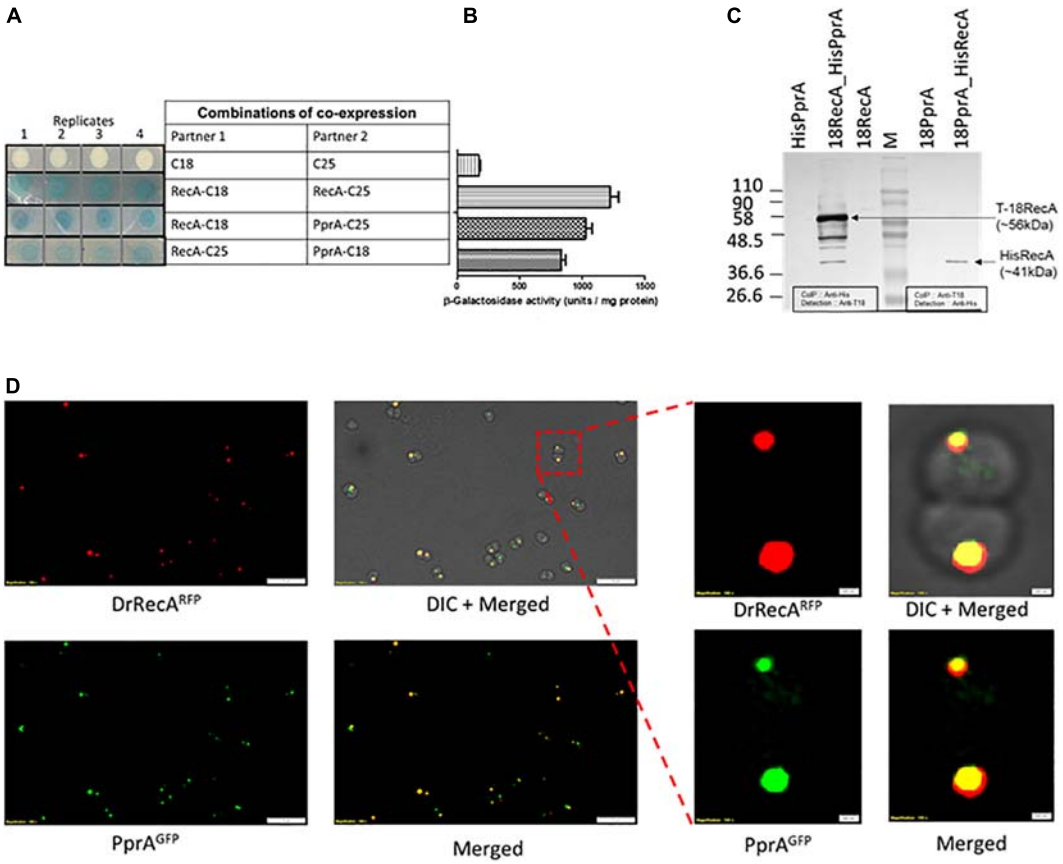

FIGURE 1 | DrRecA and PprA interaction studies in surrogate *E. coli* and *D. radiodurans* cells. **(A,B)** T18 and T25 domains of adenylate cyclase were tagged with the PprA and RecA of *D. radiodurans* by cloning in BACTH plasmids. These plasmids were transformed into an *E. coli* BTH101 host. The interaction of proteins tagged with T18 and T25 were monitored as white-blue colonies **(A)** and β-galactosidase expression in liquid culture **(B)**. RecA-C18 and RecA-C25 were used as positive control while C18 and C25 tags expressing cells were used as a negative control. **(C)** Cell-free extracts of *D. radiodurans* cells co-expressing C18-RecA and His-PprA or C18-PprA and His-RecA from respective pVHSM and pRAD plasmid co-transformed in *D. radiodurans* cells, used for immunoprecipitation assay. An immunoprecipitation done using anti-His/anti-T18 antibody (Ab) and immunoprecipitates were separated on SDS-PAGE followed by immunoblot detection using antibodies against T18 domain of CyaA (anti-T18) or antibodies against histidine-tag (anti-His) antibody (Ab) as detailed in Materials and Methods. Data in panels **(A,C)** are representative of results from a reproducible independent experiment repeated three times, while data in panel **(B)** represent means ± SD (n = 9). **(D)** Fluorescence microscopy of *D. radiodurans* cells expressing DrRecA^{RFP} and PprA^{GFP} grown to logarithmic phase was carried out. The expression of DrRecA is visualized in the RFP channel (DrRecA^{RFP}), GFP channel (PprA^{GFP}), and under bright field (DIC). Merged images depict the colocalization of RFP and GFP fluorescence. Inset shows the single diplococci of *D. radiodurans* cells expressing DrRecA^{RFP} and PprA^{GFP} and their merged image along with DIC image. Scale and magnification are given in images.

theoretical size of T18 tagged DrRecA) Co-IP carried by anti-His antibody (Ab) and detection by Anti-T18 Ab (**Figure 1C**). The tag swapped experiment (poly His-tagged DrRecA and T18 tagged PprA) produces a band of molecular mass of ∼41 kDa (a theoretical size of poly His-DrRecA) (**Figure 1C**). Results of Co-IP data suggest that DrRecA and PprA interact with each other and could able to form a relatively stable complex which can be pulled down using Ab against one partner and the presence of an interacting partner in immunoprecipitant could be detected using Ab specific to another partner (**Figure 1C**). To further validate the interaction of DrRecA-PprA proteins *in solution*, the equimolar concentration of both proteins mixed and incubated for 10 min in the HEPES buffer followed by cross-linking of the interacting complex by glutaraldehyde and complex separated on SDS-PAGE. Results showed that both proteins form a stable complex and appeared a high molecular mass complex on SDS-PAGE gel (**Supplementary Figure 2**, PprA^{wt}). Interestingly, though the presence of linear dsDNA induces the complex formation. However, later removal of DNA by DNAase treatment or using PprA mutant either lacking DNA binding (**Supplementary Figure 2**, PprA^{R166A}) or defective in oligomerization (**Supplementary Figure 2**, PprA^{R212A}) did not lose the ability of the physical interaction of proteins, together suggestive of physical interaction of DrRecA-PprA protein *in solution* which may further be supported by the presence of linear dsDNA (**Supplementary Figure 2**). Additionally, co-localization of DrRecA and PprA proteins was also ascertained by co-expressing of GFP-PprA and RFP-DrRecA fusion proteins in *D. radiodurans* cells and observation of fluorescence under a fluorescence microscope. The majority of cells expressing the

GFP-PprA and RFP-DrRecA fusion proteins form definitive foci and a large number of foci showed colocalization in *D. radiodurans* cells (**Figure 1D**). Since both proteins were shown to be DNA repair proteins and showed cellular colocalization together support the observation of physical interaction of DrRecA and PprA protein in *D. radiodurans.*

PprA Contributes to Recombination Frequency and Genetic Stability in *Deinococcus radiodurans*

Radiation resistance of *pprA*$^{-}$ mutant and PprA overexpressing *D. radiodurans* cells were monitored (**Supplementary Figure 3**). As reported earlier, *pprA*$^{-}$ mutant showed sensitivity to gamma radiation, but the overexpression of PprA in the wild type did not change its response to gamma radiation (**Supplementary Figure 3**). Although, DrRecA plays an important role in *D. radiodurans* resistance to genotoxic effects of radiation, desiccation, and oxidative stress (Jolivet et al., 2006; Schlesinger, 2007; Slade et al., 2009; Rajpurohit et al., 2016), its unregulated functions might result to hyper recombination leading to genomic instability in bacteria (Sander et al., 2003; Sheng et al., 2005).

PprA protein could able to interact with DrRecA physically *in solution* and *in vivo* (**Figure 1**), therefore, we tested the role of PprA in the modulation of DrRecA functions in the normal and γ-stressed *D. radiodurans* cells. The effects of PprA on recombination and genomic stability were monitored by measuring the recombination frequency of the *nptII* gene (pNOKpqq plasmid confer Kan^{R}) in either *pprA*$^{-}$ mutant or PprA overexpressing *D. radiodurans* grew under normal and gamma stressed conditions (**Figures 2B,C**). Since the transformation efficiency of *pprA*$^{-}$ mutant was ∼10-fold less than wild type *D. radiodurans* (**Figure 2A**), the recombination frequency normalized with transformation efficiency and normalized recombination frequency did not change significantly in both the *pprA*$^{-}$ mutant or PprA overexpressing wild type cells grown under normal condition (**Figure 2B**). However, the irradiated (3kGy) *D. radiodurans* cells showed ∼10% normalized recombination frequency in the absence of *the pprA* gene while this frequency is ∼5% in the wild type and ∼1% in the cells overexpressing PprA (**Figure 2C**). These results suggested that the presence of PprA protein in cells could negatively regulate the recombination in gamma-irradiated cells *in vivo* and cells lacking *the pprA* gene showed relatively higher recombination events compare to wild-type cells.

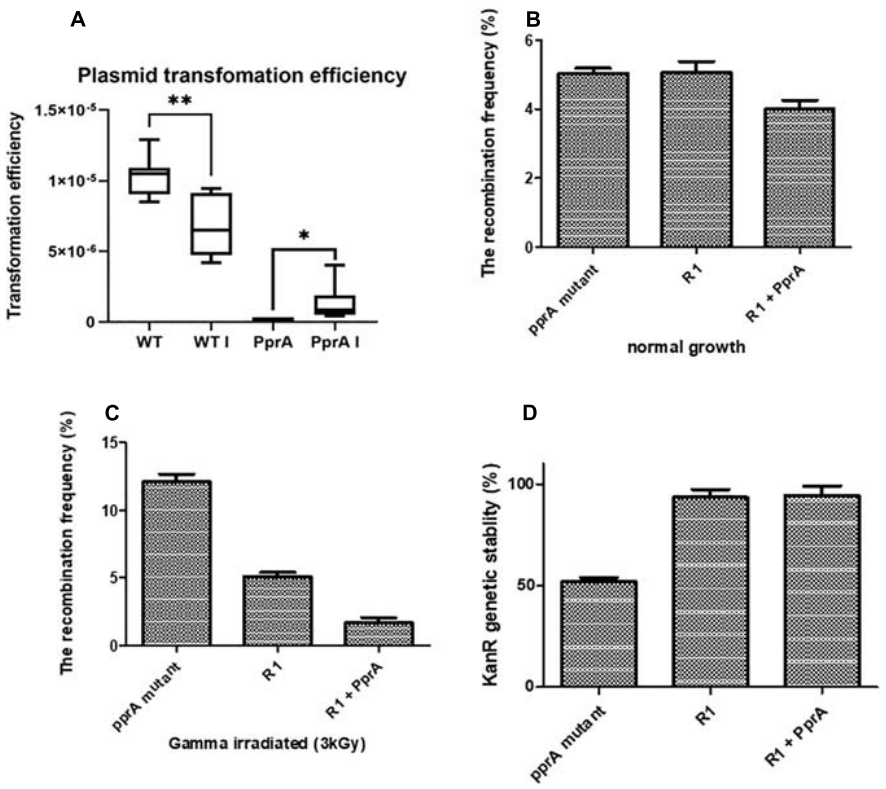

FIGURE 2 | Transformation efficiency, recombination frequency, and genomic stability. **(A)** Plasmid pVHS559 was used to evaluate the transformation efficiency of γ-irradiated and unirradiated wild type and *pprA*$^{-}$ mutant of *D. radiodurans* cells. Transformants were selected on an appropriate antibiotic. Transformation efficiently calculated by calculating CFU/μg plasmid DNA used. **(B,C)** Recombination frequency of *nptII* gene (confer kanamycin resistance) in **(B)** growing normally, and **(C)** γ-irradiated cells of wild type (R1), *pprA*$^{-}$ mutant, and PprA over-expressed cells (R1 + PprA). **(D)** Genomic stability of nptII marker (confer kanamycin resistance) after 15th generations of wild type (R1), pprA- and PprA over-expressed cells (R1 + PprA). Data represented here is means ± SD ($n = 9$).

Genomic instability was also tested by scoring the kanamycin resistance of cells of different genetic backgrounds from the above experiment. A significant loss of kanamycin resistance gene (*nptII*) (∼50%) was observed in the *pprA*$^{-}$ mutant after the 15th generation of growth, while it did not change in the wild-type cells overexpressing PprA and was similar to wild type control (**Figure 2D**). This result emphasizes that the presence of PprA protein helps in maintaining the genomic stability in *D. radiodurans* cells while in *pprA*$^{-}$ mutant, the kanamycin resistance has lost progressively over the generation possibly due to genomic instability. Collectively, results about recombination and genomic stability suggested that the absence of the *pprA* gene alleviates the recombination frequency in the gamma-irradiated *D. radiodurans* cells and also impacts the genomic stability of the marker gene (*nptII*) in the cells growing normally.

PprA Inhibit Strand Exchange Promoted by DrRecA

The recombination events in gamma-irradiated *D. radiodurans* cells had increased significantly in *pprA*$^{-}$ genetic background (**Figure 2C**) suggestive of the possible inhibitory effects of PprA interaction on DrRecA functions *in vivo*. Therefore, the effect of PprA on recombination activity of DrRecA was examined in an assay using short (40 bp) and long homology (M13 DNA) at varying concentration of PprA (0.02–0.8 μM) and a fixed concentration of DrRecA (0.2 μM) as reaction scheme given in **Figure 3**. Results showed significant inhibition of heteroduplex formation with increasing concentration of PprA protein (**Figure 3A**, lane 2–7 and **Figure 3B**, lane 3–6). It may be noted that equimolar concentration of PprA (0.2 μM) could exert the maximum inhibitory effect (**Figure 3A**, lane 5 and **Figure 3B**, lane 4). PprA alone did not catalyze the heteroduplex formation (**Figure 3A**, lane 8 and **Figure 3B**, lane 7), while DrRecA without PprA showed an efficient DNA strand exchange activity (**Figure 3A**, lane 9 and **Figure 3B**, lane 2). These results together prove the inhibitory effect of PprA protein on DrRecA promoted DNA strand exchange reaction.

The Inhibitory Effect of PprA Protein Is Not Due to Sequestration of Homologous dsDNA During DNA Strand Exchange

To understand a mechanistic aspect of the PprA inhibition of DrRecA catalyzed DNA strand exchange reaction (SER), the SER assay was performed as discussed above and the PprA protein was added before and after the addition of homologous dsDNA (**Figure 4**). The pre-incubation of PprA with DrRecA led to complete inhibition of recombination reaction (**Figures 4A,B**). However, the inhibition was significantly less when PprA was added after the addition of dsDNA (**Figure 4**). A similar effect was observed in the strand exchange assay with a long homology substrate (**Figure 4B**). In the absence of PprA, DrRecA could efficiently catalyzed the reaction and recombinant product formation (**Figures 4A,B**). However, PprA addition after dsDNA addition in the reaction showed ∼70% substrate conversation to product compare to reaction lane where PprA did not add (**Figure 4**). The observation of the complete inhibition of recombinant product, when PprA protein added before dsDNA addition allows us to speculate that PprA physical interaction with DrRecA may affect DrRecA ability to either interact ssDNA or RecA polymerization during the formation of presynaptic filament. PprA is a non-specific dsDNA binding protein and has nearly negligible affinity for ssDNA (Narumi et al., 2004; Rajpurohit and Misra, 2013; Adachi et al., 2014). Thus, the possibility of homologous dsDNA sequestration

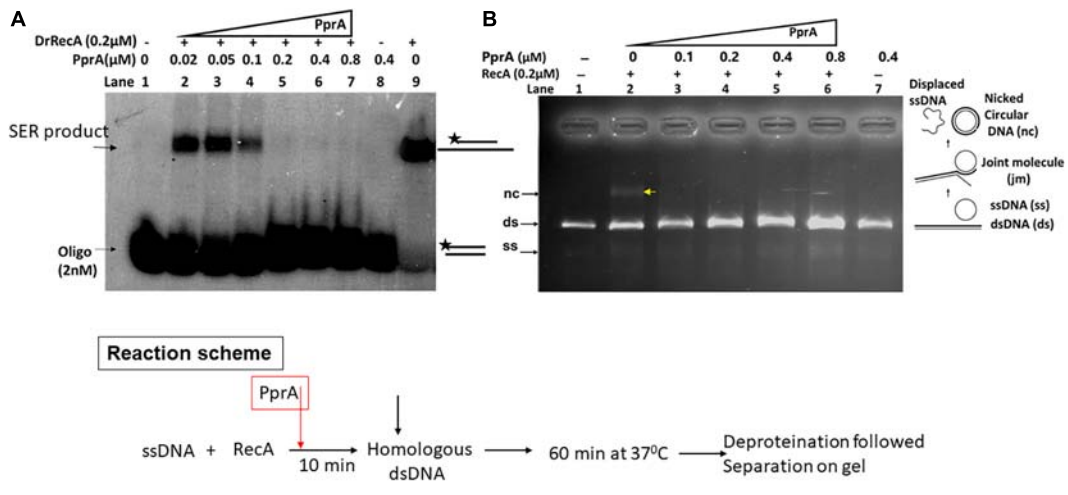

FIGURE 3 | Inhibitory effect of PprA protein on DrRecA catalyzed DNA strand exchange. **(A)** Oligo-based DNA strand exchange catalyzed by DrRecA and **(B)** DrRecA catalyzed DNA strand exchange between M13mp18 ssDNA and linear dsDNA. In both the experiments, an increasing concentration of PprA protein was added in the reaction to see the inhibitory effect of PprA protein on DrRecA function as detailed in methods.

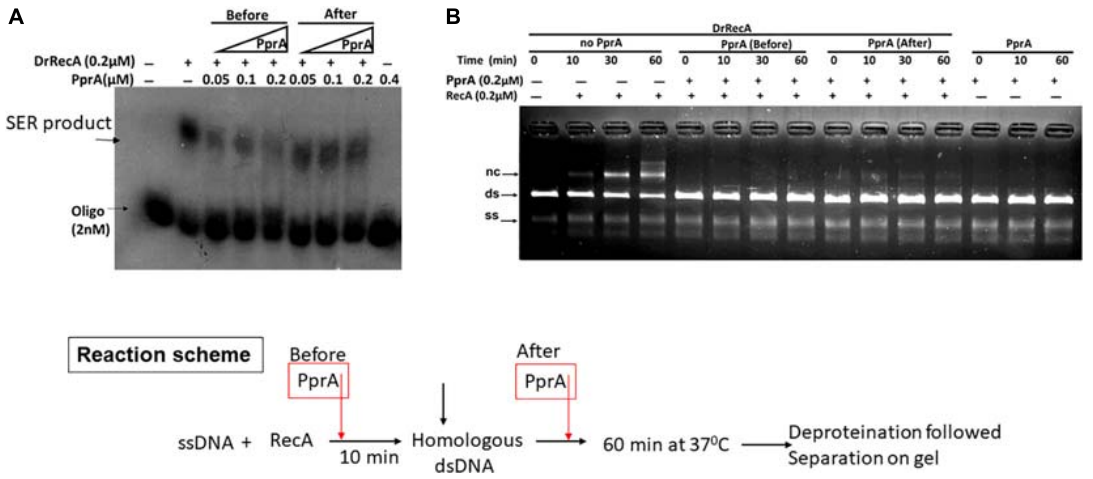

FIGURE 4 | Inhibitory effect of PprA protein when added before and after addition of dsDNA. An oligo and long homology M13-based DNA strand exchange assay was employed to see the inhibitory effect of PprA protein. **(A)** In oligo-based strand exchange increasing concentration of PprA protein (0.05–0.2 μM) added to the reaction mixture as mentioned in methods before and after the addition of dsDNA 40-mer and product formation visualized by autoradiogram. **(B)** M13mp18-based strand exchange reaction (SER) where reaction carried out as stated in methods without adding PprA (no PprA), the addition of PprA before M13 linear dsDNA (PprA before) or 0.2 μM PprA addition after M13 linear dsDNA (PprA after). As a control reaction 0.2 μM PprA protein was added without the addition of DrRecA protein. all reactions were incubated till 60 min and samples were drawn at the indicated time and separated on 0.8% agarose gel after deproteinization.

by PprA might affect the strand exchange activity of DrRecA was examined in the presence of 5–40-fold molar excess of non-specific dsDNA (**Figure 5**). The addition of an increasing concentration of non-specific dsDNA did not rescue DrRecA strand exchange activity from PprA led inhibition (**Figure 5A**). A similar observation was also confirmed using M13 substrates, where strand exchange reaction was performed in the presence of five molar excess of 1 kb non-specific dsDNA (**Figure 5B**). These findings together highlight the direct inhibitory effect of PprA on DrRecA catalyzed SER, however, this effect is not due to limiting the availability of homologs DNA by PprA during DNA strand exchange reaction.

PprA Protein Hamper the ssDNA Stimulated ATPase of DrRecA

How PprA inhibits the DrRecA catalyzed SER is not clear and hypothesized that PprA interaction with DrRecA may hamper either DrRecA functional biochemical activities such as access to DNA substrates, ATPase activity, or PprA may limit metal ion availability to DrRecA. PprA protein did not show binding with ssDNA, however able to bind with dsDNA and form a distinct DNA-PprA nucleoprotein complex than the DNA-DrRecA nucleoprotein complex (**Supplementary Figure 4**). Interestingly, PprA did not limit the access of DrRecA to DNA substrates as the binding of DrRecA to ssDNA and dsDNA with and without PprA protein was found to be similar (**Supplementary Figure 4**). This observation was further supported by data presented in **Figure 5**, where the addition of molar excess non-specific dsDNA did not rescue the inhibitory effect of PprA (**Figure 5**). Next, we checked the possibilities of limiting the availability of ATP or metal ion by PprA when added in DrRecA catalyzed SER. For that, an assay was performed where PprA protein-mediated inhibition of DrRecA catalyzed DNA strand exchange (short homology oligo-based) was rescued by adding molar excess of ATP and metal ion ($MgCl_2$) (**Figure 6A**). Data showed in **Figure 6A** suggested that the addition of 5 mM ATP could able to restore the strand exchange product formation in the presence of PprA while excess metal ion (10 mM) did not restore the reaction (**Figure 6A**). A similar observation was also apparent in the M13 based SER (**Figure 6B**). No adverse effect of excess ATP (5 mM) was observed in DrRecA catalyzed strand exchange (**Supplementary Figure 5**). Collectively, these data conclude that PprA did not limit the binding of DrRecA to DNA as well as the availability of metal ions rather PprA may have an effect on either limiting the ATP hydrolysis or availability to DrRecA during strand exchange reaction as the addition of ATP (1–5 mM) could effectively reverse the inhibitory effect of PprA (**Figures 6B,C**). To address these possibilities, ssDNA-dependent ATPase activity of DrRecA was checked in the presence and absence of equimolar concentration of PprA protein. Results showed that DrRecA display strong ssDNA-dependent ATPase activity (**Figure 7A**). The addition of equimolar concentration of PprA protein resulted in strong inhibition of DrRecA ATPase and could not be restored till 30 min of reaction time (**Figure 7A**). PprA alone or BSA (negative control) did not hydrolyze the ATP (**Figure 7A**). The experiment results reveal the mechanistic proof of PprA protein led inhibition of DrRecA by limiting the DrRecA ATPase function. This observation was further corroborated by a fluorescent ATP (mant-ATP, sigma) binding assay. In this assay, binding of fluorescent ATP by DrRecA was found to be inhibited by increasing the concentration of PprA protein (0.1–0.4 μM) and this inhibition could be reversed by the addition of ATP (5 mM) (**Figure 7B**). Together, presented data suggested that PprA could impede the DrRecA

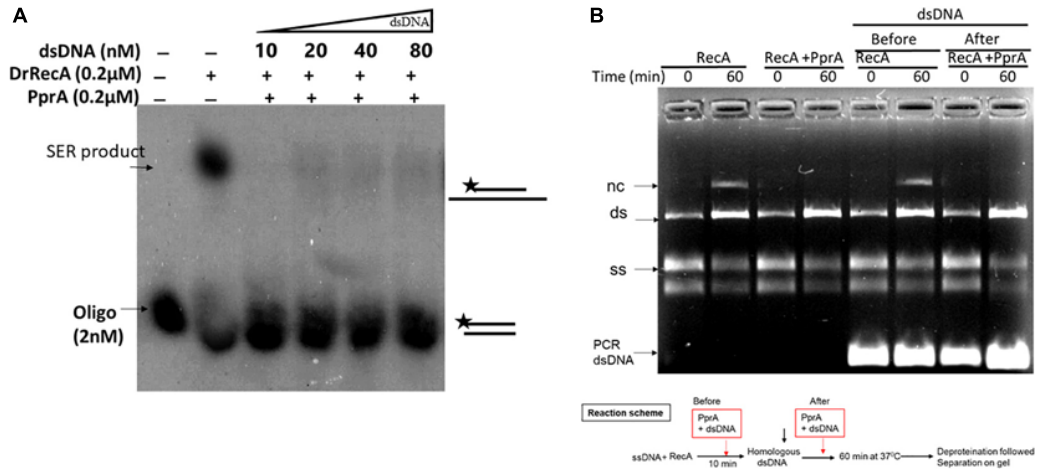

FIGURE 5 | PprA protein led inhibition of DrRecA DNA strand exchange is not due to sequestration of homologous DNA. **(A)** PprA protein was added to the reaction along with molar excess of dsDNA (5–40-fold). **(B)** SER reaction performed using M13 substrates, and addition of five molar excess of 1 kb non-specific dsDNA in the reaction after addition of specific dsDNA did not rescue the SER product formation, when PprA protein present. The products were analysed and visualized on gel and autoradiogram.

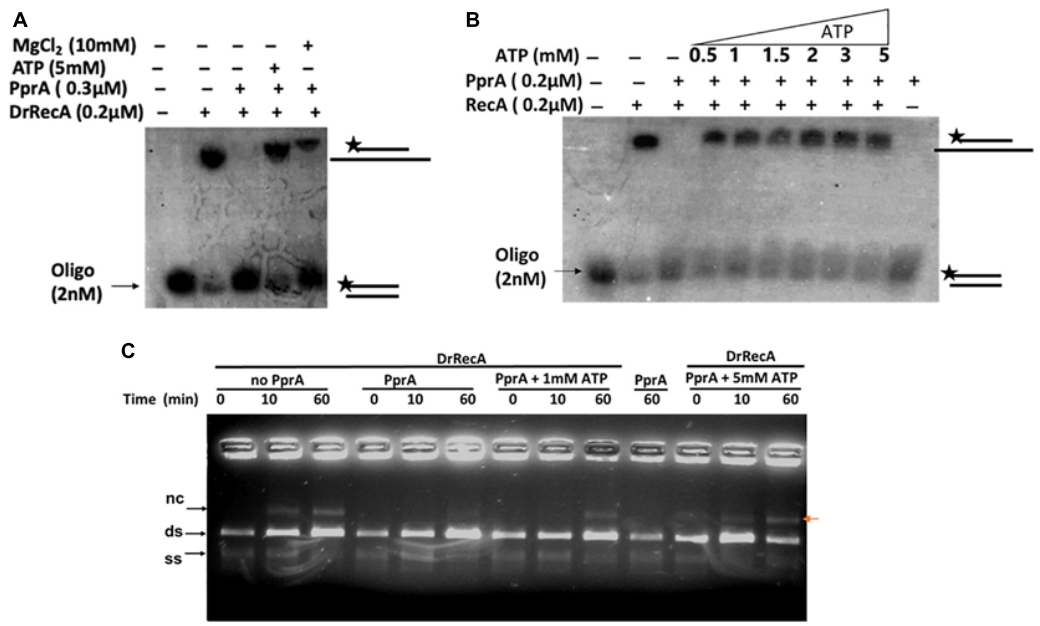

FIGURE 6 | Rescue effect of ATP and Mg^{2+} ion on PprA protein led inhibition of DrRecA DNA strand exchange. **(A)** 5 mM ATP and 10 mM $MgCl_2$ were added to overcome the inhibitory effect of PprA in oligo-based DNA strand exchange reaction. **(B)** Increasing concentration of ATP (0.5–5 mM) is used to counter the inhibitory effect of PprA in reaction. **(C)** 1 and 5 mM ATP addition in M13mp18-based DNA strand exchange reaction proves to be effective to counter PprA inhibitory effect. Whereas, the addition of PprA without the addition of additional ATP inhibits DrRecA function in DNA strand exchange.

by either sequestering the ATP in solution or by limiting ATP access to the nucleotide-binding pocket of DrRecA and consequently interfering with the ATP hydrolysis. Since PprA was not able to bind and hydrolyze ATP (**Figure 7A**), the possibilities of DrRecA's ATPase inhibition by PprA protein would possibly due to the inability of DrRecA filament to either bind or hydrolyze the ATP when it forms physical interaction with PprA.

PprA Mutants Lacking Oligomerization and DNA Binding Could Not Inhibit the DrRecA

PprA protein has both dsDNA binding and oligomerization properties (Narumi et al., 2004; Rajpurohit and Misra, 2013; Adachi et al., 2014). Our interest was to find out how do these properties contribute to PprA inhibition of DrRecA function.

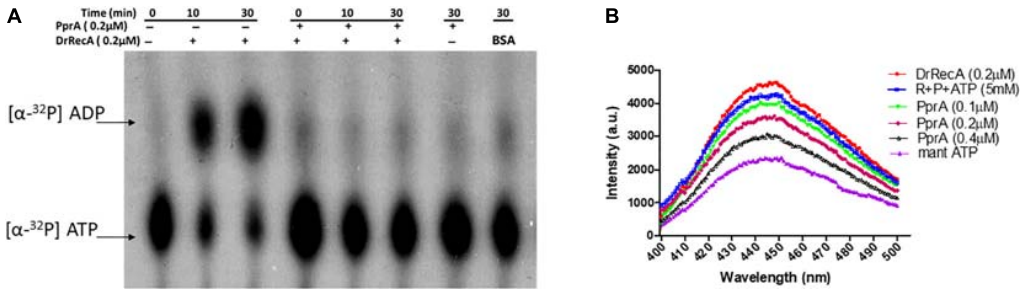

FIGURE 7 | Inhibitory effect of PprA protein on DrRecA ATPase and ATP binding. **(A)** The inhibitory effect of PprA protein on DrRecA ATPase was assayed by thin-layer chromatography (TLC). The hydrolysis of [α^{-32}P] ATP to [α^{-32}P] ADP monitored on a TLC plate followed by an autoradiogram. **(B)** ATP binding assay of DrRecA (0.2μM) was monitored with fluorescent ATP (Mant ATP) in the absence (DrRecA) and presence of PprA protein (0.1 to 0.4μM) separately and together with DrRecA + PprA + ATP (R + P + ATP). Data was recorded on Spectro-fluorimeter in the range of 400 to 500nm wavelength.

Previously, R208A and R212A mutants of PprA lacking both oligomerization and DNA binding properties, while K149A and R166A mutants lacking DNA binding activity but proficient in oligomerization were reported (Adachi et al., 2014). We have generated these mutants and their properties were verified and found to similar to as reported earlier (data not shown). The strand exchange reaction was monitored in the presence of PprA and its R208A, R212A, K149A, and R166A mutants Interestingly, all four mutants either defective in DNA binding activity (R208A, R212A, K149A, and R166A) or oligomerization (R208A and R212A) showed marginal inhibition on DrRecA catalyzed DNA strand exchange reaction (**Figure 8**), while wild type PprA having intact DNA binding and oligomerization properties was being able to efficiently inhibit DrRecA functions (**Figure 8**). Interestingly, DNA binding mutant (R166A) and oligomer mutant (R212A) of PprA retained their ability to interact with DrRecA similar to wild-type PprA (**Supplementary Figure 2**). However, these mutations of PprA protein (R166A and R212A) hamper their ability to interfere with DrRecA catalyzed SER raised the possibility of a more dynamic nature of the interaction of PprA interaction with DrRecA. Nonetheless, these results highlighted the crucial role of PprA DNA binding and oligomerization ability in the inhibition of DrRecA function *in vitro*.

DISCUSSION

Deinococcus radiodurans cells have an extraordinary DNA repair capability and can endure a high level of genetic perturbation caused by ionizing radiation, desiccation, and stress-induced by cold conditions (Cox and Battista, 2005; Slade et al., 2009; Misra et al., 2013). DrRecA mediated recombination repair required for radiation-resistant phenotype and *recA* mutant of *D. radiodurans* highly sensitive to gamma radiation, UV radiation, and MMC (mitomycin C) treatment (Moseley and Copland, 1975; Gutman et al., 1994; Rajpurohit et al., 2016). Moreover, radiation sensitivity directly correlated with reduced recombination frequency in *recA* mutant of *D. radiodurans* (Moseley et al., 1972; Daly et al., 1994; Daly and Minton, 1996). RecA and its homolog catalyzes homologous recombination repair (HRR) of the collapsed replication fork, DNA DSBs, and involve in the maintenance of genomic integrity (Li and Heyer, 2008). The regulation of bacterial RecA function is highly diverse and is regulated by many proteins. The regulatory proteins catalog affecting the function of bacterial RecA is increasing and many new candidates have been added to this list in the recent past (Cox, 2007). To add a new candidate to this list, the present study has brought forth a PprA protein as a negative regulator of DrRecA. In bacteria, canonical mechanisms of RecA regulation; is SOS regulatory mechanism and the same was found to be redundant in the case of regulation DrRecA (Narumi et al., 2001; Slade et al., 2009). Therefore, some new mechanisms that could regulate DrRecA expression have been suggested (Earl et al., 2002; Wang et al., 2008; Devigne et al., 2015; Blanchard et al., 2017). Phosphorylation-mediated regulation of DrRecA activity and structure dynamics has been recently shown (Rajpurohit et al., 2016; Sharma et al., 2020). *D. radiodurans,* RecFOR proteins that help the loading of RecA on DNA substrate were shown to be crucial for DrRecA function (Slade et al., 2009; Bentchikou et al., 2010), while RecX is shown to be a negative regulator of DrRecA and causes net disassembly of RecA nucleoprotein filament through physical interaction and mitigating the possibilities of hyper recombination that would be deleterious for the genome integrity under normal growth of this bacterium (Sheng et al., 2005). The present study has provided evidence to suggest the regulatory role of PprA protein in the regulation of DrRecA functions and possible underlying mechanisms to explain the epistatic natures of *pprA* and *recA* genes in *D. radiodurans*, particularly in γ-irradiated cells. The data presented in this study supported the following conclusions, (1) DrRecA and PprA protein interact physically, (2) PprA role is crucial in minimizing the deleterious effect of DrRecA due to possible hyper recombination activity in the cells recovering from gamma irradiation and for the genomic stability of the cells growing normally, (3) PprA protein could interfere DrRecA catalyzed strand exchange reaction is due to impediment of the ATPase function of DrRecA, but not due to sequestration of homologous dsDNA, and (4) PprA The oligomerization and DNA binding properties crucial for PprA led inhibition of DrRecA function.

PprA and DrRecA could physically interact *in vitro* and *in vivo* (**Figure 1**). This observation is not surprising as the

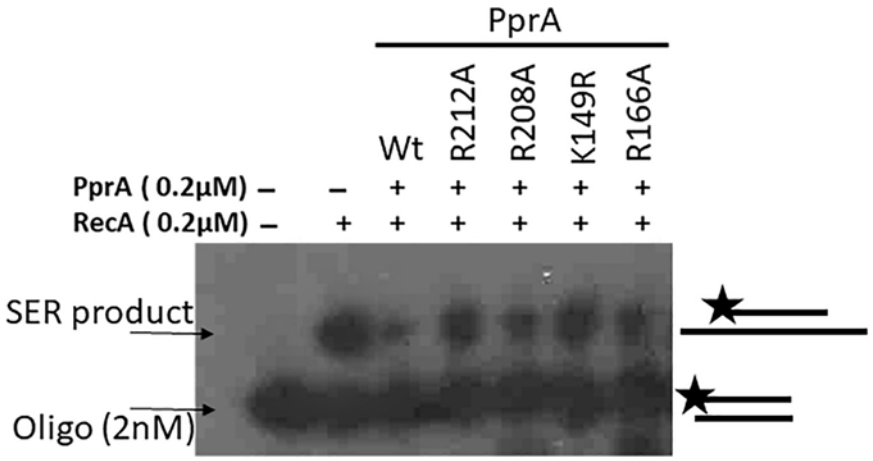

FIGURE 8 | An inhibitory effect of PprA and its mutants on SER of DrRecA. The inhibitory effect of PprA and its mutants on SER of DrRecA was evaluated using an oligo-based DNA in the presence of PprA and its DNA binding (K149A, and R166A) and oligomerization (R208A, and R212A) mutants. Products were analyzed on gel and visualized on autoradiogram.

epistatic nature of these protein and the ability of PprA protein to interact with other DNA metabolic protein (DNA ligase, DNA gyrase, and topoisomerase IB) and DNA replication related proteins (DnaA and DnaB) due to its pleiotropic functions (Kota and Misra, 2008; Devigne et al., 2015; Maurya and Misra, 2020). The presence of dsDNA further augments the interaction of both proteins (**Supplementary Figure 2**) and was further supported by the inability of PprA mutants (lacking DNA binding and oligomerization properties) to exert an inhibitory effect on DrRecA catalyzed SER (**Figure 8**). The requirement of intact DNA binding and oligomerization properties of PprA protein for the maximum inhibitory effect on DrRecA catalyzed DNA strand exchange (**Figure 8**) is intriguing and raises the possibility that DNA might function as a mediator for this interaction. PprA protein has dsDNA binding properties but lacking ssDNA binding (Adachi et al., 2014), while DrRecA has both ssDNA and dsDNA binding properties with more affinity toward dsDNA in the absence of nucleotide cofactor (Warfel and LiCata, 2015; Rajpurohit et al., 2016; Sharma et al., 2020). The binding of DrRecA to ssDNA and dsDNA was least affected by the presence of an equimolar concentration of PprA (**Supplementary Figure 4**). Thus, it is likely that PprA may suppress the DrRecA activity by possible interdependent mechanisms; where direct binding of PprA to DrRecA may have further augmented by DNA binding ability of PprA protein to make a stable complex with DrRecA (**Figure 8** and **Supplementary Figure 4**). RecA promoted DNA strand exchange reaction begins with the loading of RecA on the single-stranded DNA (ssDNA) to form nucleoprotein filament which searches for homologs double-strand DNA (dsDNA) and facilitate the strand exchange (Shan and Cox, 1997; Yu et al., 2001). Interestingly, ATP hydrolysis is not required for the formation of heteroduplex complex during DNA strand exchange reaction as RecA may able to perform a search for homologs DNA even in the presence of a non-hydrolyzable ATP analog; ATPγS or in the presence of ADP-AlF4 analog (Menetski et al., 1990). Therefore, it was proposed that RecA unsaturated nucleoprotein filament propel the DNA exchange until the newly formed heteroduplex molecule keeps releasing from triple-helix nucleoprotein complex during SER (strand exchange reaction) and this function is being facilitated by ATP hydrolysis. Therefore, ATP hydrolysis by nucleoprotein filament is crucial for propelling the strand exchange reaction in the forward direction (Kowalczykowski et al., 1987). The established hypothesis about RecA mediated DNA strand exchange suggest that nucleoprotein filaments adopt a stretched, rigid, under-wound B-DNA-like conformation (Chen et al., 2008), and the discontinuities in RecA nucleoprotein filaments would terminate the strand exchange and start homology search (Shan and Cox, 1997). Thus, ATP hydrolysis by RecA nucleoprotein filament offers dynamics to the RecA nucleoprotein filaments (van Loenhout et al., 2009). Data from the present study suggest that PprA protein interaction with DrRecA causes severe inhibition of ATPase function of DrRecA nucleoprotein filament (**Figure 7**) and inhibition of DNA strand exchange (**Figure 3**). The PprA led inhibition of DrRecA strand exchange was could not be rescued by adding molar excess of dsDNA or metal ion suggest that the inhibitory effect of PprA is not indirect rather through direct interaction with DrRecA filament and inhibition of ATPase function. The exact mechanism and the nature of this interaction are not clear but PprA interaction with DrRecA nucleoprotein filament interaction may likely either freeze the domain motion of nucleoprotein filament of DrRecA assisted by its ATPase activity or may limit the access the ATP to DrRecA nucleoprotein. Since PprA alone did not have ATPase and neither it can bind with ATP, thus former possibility is more likely. Recently, the functional implications of RecA unsaturated and saturated nucleoprotein filaments formation and the role of RecA ATPase function to regulate the dynamic equilibrium was probed by Zhao et al. (2017) by capillary electrophoresis-laser-induced fluorescence polarization assay (CE-LIFP) and suggest that RecA unsaturated nucleoprotein filaments predominate under

physiologically relevant conditions over long saturated RecA nucleoprotein filaments and these unsaturated nucleoprotein filaments are key driver scaffolds for the DNA strand exchange and homologous recombination (Zhao et al., 2017). Therefore, ATPase function is not only required for the removal of RecA from heteroduplex complex but also facilitates the formation of unsaturated nucleoprotein filament continuously to propel the DNA strand exchange reaction in a forward direction (Kowalczykowski et al., 1987; Zhao et al., 2017). The ATPase function of DrRecA nucleoprotein filaments may exist in an inactive default state under the condition when protein is bound to dsDNA. However, the inactive state changes to an active ATPase state when ssDNA is added to the reaction or in the presence of lower pH or by volume exclusion agents (Ngo et al., 2013). In general, the ATPase function of RecA gives mechanical power for nucleoprotein filament remodeling and dysfunctional ATPase would hamper the remodeling capacity of RecA filament and resultant no strand exchange product will be formed. Thus, data presented in the present study suggested that inhibition of ATPase of DrRecA by PprA may directly lead to an imbalance in DrRecA saturated and unsaturated nucleoprotein filament and resultant inhibition of DNA strand exchange.

The activity of RecA is supposed to be highly regulated because unregulated RecA function may lead to hyper-recombination situations and could be deleterious for cell survival. Therefore, numerous protein regulator (RecBCD, RecFOR, SSB, LexA, UmuD, DinI, PsiB, RdgC, and RecX proteins) known to regulate bacterial RecA activity (Lusetti et al., 2004, 2006; Drees et al., 2006; Spies and Kowalczykowski, 2006; Cox, 2007). Here our data suggest that the PprA protein of *D. radiodurans* is a new regulator of RecA function, especially in the irradiated cells. Earlier it was shown that DrRecA could catalyzes the DNA strand exchange through unique inverse strand exchange and able to complement the RecA functions in *E. coli*. However, *E. coli* RecA could only complement partially the DrRecA functions suggesting that RecA regulatory network operates in *D. radiodurans* are different from *E. coli* (Narumi et al., 1999). Interestingly, the existence of PprA protein was reported only in the *Deinococcaceae* family, and no homolog was reported outside this family (Narumi et al., 2004), suggesting that RecA activity regulation by PprA protein may be limited to the *Deinococcaceae* family. However, it would be interesting to see the inhibitory effect of PprA on RecA from other bacteria like *E. coli*. The ectopic expression *pprA* gene in *E. coli* induces the catalase function and oxidative stress resistance but its interaction with *E. coli* RecA not studied (Kota and Misra, 2006). How does PprA precisely contributes to the regulation of recombination repair and DrRecA function in *D. radiodurans* needs further careful and thorough study. Nonetheless, the present study hitherto brought forth interesting observations about the negative regulation of DrRecA activities and recombination by PprA. The recombination frequency increases in *pprA*$^{-}$ mutant cells after irradiation but, little change in recombination compare to wild-type cells in PprA overexpressing cells after irradiation could be due to very high overexpression *pprA* gene itself in wild type cells after irradiation (**Figure 2**). On the mechanistic front, we propose that DrRecA activity inhibition by PprA by impeding the ATPase function of DrRecA and altered nucleoprotein filament function which effectively diminishes the homology search and DNA strand exchange function of DrRecA (**Figure 9**). Zahradka et al. (2006) showed that DNA repair in *D. radiodurans* follows biphasic repair kinetics following exposure to extreme radiation, in phase I, massive DNA synthesis followed by assembly of DNA fragments occurs, which is dependent on DNA polymerase I activity and termed extended synthesis-dependent strand annealing (ESDSA) repair (Zahradka et al., 2006). Though the DrRecA level increased in the ESDSA phase, its function was primarily required in the later stage of repair where DrRecA mediated homologous recombination using substrate from ESDSA repair to produces full-length chromosomes (Liu et al., 2003; Slade and Radman, 2011). We believe that the implications of our finding of DrRecA and PprA interaction may help in allowing ESDSA repair by minimizing the DrRecA induced recombination events during ESDSA repair after acute doses of γ-radiation (Zahradka et al., 2006; Slade et al., 2009). Together, based on data presented here allow us to speculate that even though PprA work as an inhibitor of DrRecA by impeding its ATPase function but this inhibitory effect of PprA protein may well help *D. radiodurans* cells to efficiently repair shattered genome with the highest precision and thus help in maintaining genomic integrity.

MATERIALS AND METHODS

Bacterial Strains, Growth Medium, and Plasmids

Wild type bacterium *D. radiodurans* R1 used from lab stock (ATCC 13939). *pprA*$^{-}$ mutant was a generous gift from I. Narumi, Japan (Narumi et al., 2004). Wild type *D. radiodurans* and its mutant were gro*wn* in TGY medium (1% Bacto tryptone, 0.1% glucose, 0.5% yeast extract) with appropriate antibiotic as described earlier (Rajpurohit and Misra, 2010). For the cloning and maintenance of plasmids; *E. coli* Novablue strain was used while *E. coli* BTH101 (lacking cyaA, referred here as BTH101) was used for the coexpression of cloned proteins on BACTH plasmids for *in vivo* protein-protein interaction studies and grown at 30°C (Maurya et al., 2018). pUT18, pKNT25, and pET28a (+) plasmids and their derivatives were maintained in *E. coli* cells (Nova blue) in the presence of the required antibiotics. Shuttle vector for *E. coli* and *D. radiodurans* pVHS559 and their derivatives were maintained in the presence of spectinomycin *D. radiodurans* (70 μg/ml) and *E. coli* (150 μg/ml) (Maurya et al., 2018). Standard molecular biology techniques were used as described (Green and Sambrook, 2012). Antibodies against the T18 (SC-13582) and T25 (SC-33620) domains of CyaA of Bordetella pertussis were procured commercially (Santa Cruz Biotechnology, Inc.), an antibody (Ab) against Anti-His purchased from New England Biolabs (United States). Molecular biology grade chemicals, enzymes, and other salts used in this study were procured from different manufactures like Sigma Chemicals Company, United States; Roche Biochemicals, Mannheim, Germany; New England Biolabs (United States); and Merck India Pvt. Ltd., India. Radiolabeled nucleotides were obtained from the Board of Radiation and Isotope Technology (BRIT), Department of

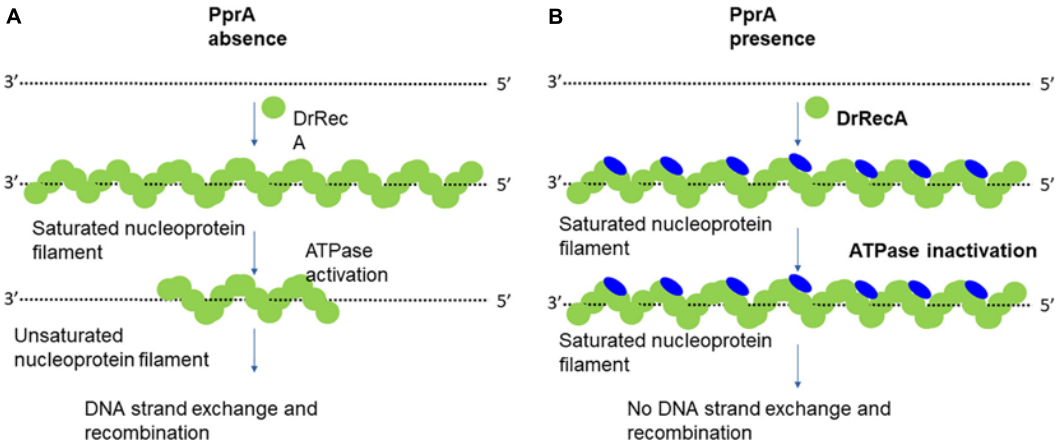

FIGURE 9 | Model explains the working hypothesis of PprA protein-mediated inhibitory effect on DrRecA functions. **(A)** In the absence of PprA protein, DrRecA protein forms nucleoprotein filament on ssDNA. This RecA saturated nucleoprotein filament (inactive filament) converted to unsaturated nucleoprotein filament (active filament) by ATPase function of DrRecA. This dynamics facilitates the homology search by DrRecA for a successful SER. **(B)** PprA interaction with DrRecA inhibits its ATPase function of DrRecA nucleoprotein filament by either interfering with ATP binding that affects the dynamics of active and inactive filament nucleoprotein filament interchange and impairment of SER activity of DrRecA.

Atomic Energy, India. All the bacterial strains and plasmids used in this study are listed in **Supplementary Table 1**.

Construction of Recombinant Plasmids and Protein Purification

List of plasmids and primers used in this study given in **Supplementary Table 1**. The transnational fusion of DrRecA and PprA protein with T18 tag and T25 tag obtained by cloning of coding sequence of *recA* and *pprA* gene in pUT18 and pKNT25 plasmids at the restriction sites indicated in **Supplementary Table 1**. Obtained plasmids for *recA* gene (pUTDr*recA* and pKNDr*recA*) and *pprA* gene (pUT*pprA* and pKNDr*pprA*) were transformed to *E. coli* BTH101. Coding sequences of polyhistidine-tagged DrRecA and PprA were PCR amplified using pETHisFw and pETHisRw primers from their respective pET28a (+) clones as a template (Kota and Misra, 2006; Rajpurohit et al., 2016), and were sub-cloned in shuttle plasmid pRADgro at *Apa*I and *Xba*I sites, yielding pRadHisrecA and pRadHispprA respectively. Similarly, the T18-tagged *recA* gene was PCR amplified using primers (BTH*recA*-F and BTH*recA*-R) and T18-tagged *pprA* genes using primers (BTH*pprA*-F and BTH*pprA*-R) and cloned in pVHS559 shuttle vector at *Nde*I-*Xho*I sites for coimmunoprecipitation studies in *D. radiodurans* (**Supplementary Table 1**). Expression of all fusion proteins was confirmed by Western blotting using antibodies against the T18 domain of C18-tag and polyhistidine-tag (**Supplementary Figure 2**). pVHpprA^{GFP} expressing PprA-GFP fusion protein constructed earlier and used here (Kota et al., 2014). For the construction of the DrRecA-RFP expression plasmid, the coding sequence of DrRecA was cloned at pDSred plasmid (Clontech) at *Kpn*I and *Bam*HI sites, yield pDSrecA^{RFP}. The rfp–recA region was PCR amplified from pDSrecA and cloned at *Apa*I and *Eco*RV sites in pRAD plasmid and pRADrecA^{RFP} plasmid was obtained. Both pRADrecA^{RFP} and pVHpprA^{GFP} plasmids were transformed into *D. radiodurans* transformants were screened on TYG agar plates supplemented with spectinomycin (75 μg/ml) and chloramphenicol (7 μg/ml). Recombinant GFP-PprA was expressed by inducing the culture with 10 mM IPTG in the case of *D. radiodurans* while RFP-DrRecA expresses constitutively.

Recombinant plasmids pET*recA* and pET*pprA* used in this study were constructed earlier and described previously (Rajpurohit and Misra, 2013; Rajpurohit et al., 2016). Recombinant DrRecA and PprA were expressed in *E. coli* BL21(DE3) pLysS. Both proteins were purified as described previously (Rajpurohit and Misra, 2013; Rajpurohit et al., 2016). In brief, *E. coli* BL21(DE3) pLysS expressing recombinant proteins were harvested after 3 h post-induction by IPTG. The cell pellet was suspended in buffer A (20 mM Tris–HCl; pH 7.6, 150 mM NaCl) containing 10 mM imidazole, 0.5 mg/ml lysozyme, 1 mM phenylmethylsulfonyl fluoride (PMSF), 0.2% Triton X-100, and 10% glycerol and incubated at 37°C for 30 min. A protease inhibitor cocktail was added to the reaction mixture, and the cells were sonicated for 10 min using 5-s pulses with intermittent cooling for 10 s at 35% amplitude. The cell lysate was centrifuged at 12,000 rpm for 30 min at 4°C. The cell extract was loaded onto a $NiCl_2$ charged-fast-flow-chelating Sepharose column (GE Healthcare) equilibrated with buffer A (20 mM Tris–HCl; pH 7.6, 300 mM NaCl, 10% glycerol). The column was washed with 20 column volumes of buffer A containing 20 mM imidazole until proteins stopped coming from the column. Recombinant proteins were eluted with buffer A containing 250 mM imidazole. Fractions were analyzed by SDS-PAGE, and those containing nearly pure proteins were pooled and their his-tag removed by incubating proteins with Factor-Xa (NEB). Untagged protein comes out in flow-through when loaded on Ni-NTA agarose column following the protocols described by the manufacturer (Qiagen, Inc.). Unbound proteins were further purified on Q-sepharose,

Heparin, and Superdex-200 column. Proteins fractions free from detectable nuclease contamination and has more than 95% purity, were polled and precipitated by ammonium sulfate precipitation followed by dialysis in buffer B; 10 mM Tris–HCl (pH7.6), 50 mM KCl, 50% glycerol, and 1 mM PMSF and stored at −20°C Proteins.

Protein-Protein Interaction Studies, Western Blotting, and Coimmunoprecipitation

A bacterial two-hybrid system (BACTH) is employed to ascertain the *in vivo* protein-protein interaction in *E. coli* as detailed elsewhere (Battesti and Bouveret, 2012; Siddiqui et al., 2017). BTH101 *E. coli* cells were transformed with different plasmids expressing target proteins with T18 tags or T25 tags at the C-terminus of target proteins, respectively. Empty vectors in BTH101 cells used as controls. The cells in quadruplet spotted on LB agar plates containing 5-bromo-4-chloro-3-indolyl-β-D-galactopyranoside (X-Gal) (40 μg/ml), IPTG (0.5 mM), and antibiotics as required. After overnight incubation of plates at 30°C, the appearance of white-blue colored colonies was recorded. In parallel, an aliquot of the same culture was grown overnight with 0.5 mM IPTG and appropriate antibiotics, and β-galactosidase activity was measured from liquid cultures as described earlier (Maurya et al., 2018). In brief, diluted culture (1:4) into LB medium with OD_{600} normalized. Cultures (100 μl) were mixed with 1 μl Z-buffer (60 mM Na_2HPO_4, 40 mM NaH_2PO_4, 10 mM KCl, 10 mM $MgSO_4$, 50 mM β-mercaptoethanol, pH 7.0) followed by the addition of, 0.01% SDS and 20 μl chloroform to permeabilize the cells, and cell debris was removed. Enzyme activity was measured in triplicate with 50 μl of supernatant using 0.4% *O*-nitrophenyl-β-D-galactopyranoside (ONPG) as a substrate. The β-galactosidase activity was calculated in Miller units as described previously (Battesti and Bouveret, 2012). The interaction of DrRecA and PprA proteins *in solution* was assayed by a glutaraldehyde-assisted cross-linking experiment. In brief, both proteins (approx. 5 μg each) were mixed in HEPES buffer (pH 7.6) and allowed to interact for 10 min followed by addition of 0.5% glutaraldehyde added and reaction incubated for another 10 min reaction terminated by adding 2X SDS dye and samples analyzed on SDS-PAGE. 1 kb dsDNA was added to see DNA-assisted protein interaction. For the western blotting and coimmunoprecipitation studies, different derivatives of pVHS559 and pRAD plasmids expressing C-18 tag (18DrRecA and 18PprA) and His-tag (HisRecA and HisPprA) fusion proteins were co-transformed in different combinations into *D. radiodurans*. The recombinant cells co-expressing these proteins were induced with 0.5 mM IPTG, and harvested cell washed with 70% ethanol followed by lysed in the buffer (50 mM Tris base, 150 mM NaCl, 5 mM EDTA) containing 0.5% Triton X-100, 1 mM PMSF, 1 mM dithiothreitol (DTT), supplemented with 0.5 mg/ml lysozyme, and 50 μg of a protease inhibitor cocktail tablet followed by sonication. The clear cell-free extracts (CFE) were obtained by centrifugation at 12000 × *g* for 30 min. CFE used for immunoprecipitation using polyclonal antibodies against either T18 or Anti-His tag antibody (Ab) and precipitated immunoprecipitates were separated on a 10% SDS-PAGE gel, blotted onto a polyvinylidene difluoride (PVDF) membrane, and hybridized with monoclonal antibodies against the either T18 or Anti-His tag antibody (Ab) as required. Hybridization signals were detected using anti-mouse secondary antibodies conjugated with alkaline phosphatase using BCIP/NBT (5-bromo-4-chloro-3-indolylphosphate/nitroblue tetrazolium) substrates (Roche Biochemical, Mannheim, Germany).

The Measure of Cell Survival, Recombination Frequency, Genomic Stability, and Transformation Efficiency

Wild type and its mutants (*recA*$^-$ and *pprA*$^-$) were treated with different doses of γ-radiation as described previously (Rajpurohit et al., 2008). In brief, mutant and wild-type *D. radiodurans* cells were grown in TGY medium to the late log phase at 32°C. The cells were suspended in sterile phosphate-buffered saline (PBS) and exposed to different doses of γ-radiation (GC500; ^{60}CO; Board of Radiation and Isotopes Technology, Department of Atomic Energy, India). Appropriate dilutions were plated on TGY agar plates and incubated at 32°C. The numbers of CFU were recorded after 48 h of incubation at 32°C.

For recombination frequency estimation *pNOKpqq* plasmid was used (Rajpurohit et al., 2008). This suicidal vector-only survives when integrated at *the pqq* locus of the chromosomal site of host *D. radiodurans* cells. Recombination frequency was estimated for normal growth and γ-irradiated cells as discussed earlier (Vierling et al., 2000). Briefly, 10^6 *D. radiodurans* R1 cells were mixed with 5 μg *pNOKpqq* plasmid, incubated on ice for 20 min and at 32°C for 50 min followed by dilution in 5 ml TGY medium overnight. Appropriate serial dilutions were plated on TGY plates with or without Kanamycin (8 μg/ml) and incubated at 32°C for 72 h to count colony-forming units (CFU). The recombination ability was calculated by the following formula: recombination efficiency (%) = (CFU with Kam/CFU without Kam) × 100, Here, Kam stands for kanamycin antibiotic. Genomic stability assayed as described earlier (Sheng et al., 2005). In brief, *nptII* gene stability was examined by genomic PCR using Npt-F and Npt-R primers (**Supplementary Table 1**). Homozygous cells incubated at 32°C in TGY medium till stationary phase and subcultured to fresh TGY medium. each subculture considered as a new generation. For each generation, approximately one thousand clones from every sample plated on TGY plates with and without antibiotics and plates incubated at 32°C. The formula applied for genetic stability (%) calculation [Genetic stability (%) = (CFU with Kam/CFU without Kam) × 100]. Plasmid pVHS559 was used to evaluate the transformation efficiency of γ-irradiated and unirradiated wild-type and *pprA* mutant cells. Transformants were selected on an appropriate antibiotic. 10 OD (A_{600}) cells resuspended in fresh TGY medium and irradiated for a 6kGy dose. Unirradiated sham controls were plated parallelly. 30 mM $CaCl_2$ is used to assist transformation. Appropriate dilution

plated and transformation efficiently calculated by calculating CFU/μg plasmid DNA used.

DNA Binding Assay

DNA binding activity of DrRecA and PprA protein was checked using electrophoretic gel mobility shift assay (EMSA) as described earlier (Rajpurohit et al., 2016). In brief, 40 nucleotides long random sequence oligonucleotide (Oligo40-F, **Supplementary Table 1**) was used as ssDNA substrate and dsDNA substrate was made by annealing it with its complementary strand (Oligo40-R, **Supplementary Table 1**). Both ssDNA and dsDNA were labeled with [^{32}P]-γ-ATP using polynucleotide kinase and purified by G-25 column. The 0.2 pmole of the labeled probe (ssDNA and dsDNA) was incubated with increasing concentrations of DrRecA (0.5–2 μg) in 10 μl of reaction mixture containing 10 mM Tris-HCl, pH 7.5, 50 mM NaCl and 1 mM DTT for 10 min at 37°C. 2 μg PprA protein used with DrRecA or alone. Products were analyzed on a 12.5% native polyacrylamide gel, dried and signals were recorded by autoradiography.

DNA Strand Exchange Reaction

Long homology-dependent RecA-dependent DNA strand exchange was carried out using circular M13mp18 ssDNA and linear dsDNA as described earlier (Kim and Cox, 2002). Reaction carried out in buffer (25 mM Tris-acetate, 1 mM DTT, 5% glycerol, 3 mM potassium glutamate, 10 mM magnesium acetate, and an ATP-regenerating system (10 units/ml of pyruvate kinase/3.3 mM phosphoenolpyruvate or 10 units/ml creatine kinase/12 mM phosphocreatine). 2.5 μM *E. coli* SSB (NEB), ATP, DrRecA, and PprA protein concentrations are indicated for each experiment. The reaction began with a pre-incubation of 6 μM ssDNA^{nt} with DrRecA protein at 37°C for 10 min. followed by the addition of ATP and SSB protein. After incubation of 10-min, linear 5 μM dsDNA^{nt} was added to start the DNA strand exchange reactions. PprA protein was added before and after the addition of dsDNA (when required). The reactions were stopped by the addition of 5 μl of gel loading buffer (0.125% bromophenol blue/25 mM EDTA/25% glycerol/5% SDS) and samples were electrophoresed in a 0.8% agarose gel with TAE buffer. Gel stained with ethidium bromide and photographed in Gel doc system (Syngene).

For the oligo-based DNA strand exchange reaction, firstly, 1 μl of 0.1 μM concentration Oligo40-F was labeled at 5′ end using polynucleotide kinase enzyme (PNK, NEB) using reaction buffer (70 mM Tris–HCl, pH 7.6, 10 mM $MgCl_2$, and 5 mM DTT) and 1 μM [^{32}P]-γ-ATP for 1 hr. Unused [^{32}P]-γ-ATP removed by passing reaction mixture from G-25 column. To obtain dsDNA equal molar concentration of [^{32}P]-labeled Oligo40-F and its complementary oligo Oligo40-R mixed in 50 μl reaction volume supplemented with 1X buffer (10 mM Tris–HCl, pH 7.6, 50 mM NaCl, and 1 mM EDTA) (**Supplementary Table 1**). Reaction sample heated for 5 min at 95°C and allowed for slow cooling to room temperature for annealing purpose. To perform the assay, indicated concentration of DrRecA incubated with oligo167-mer (2.5 μM nucleotides, **Supplementary Table 1**) in 10 μl of buffer (25 mM Tris–HCl, pH 7.5, 1 mM DTT, 2.5 mM $MgCl_2$, 0.25 mM KCl) containing 1 mM ATP for 5 min., after this ^{32}P-labeled oligo40-mer dsDNA oligonucleotide (2.5 μM nucleotides, **Supplementary Table 1**) added. PprA protein was added as and when required with indicated concentration. At the indicated times, a 2.5 μl aliquot was removed and mixed with an equal volume of 1% SDS containing proteinase K (1 mg/ml) and incubated at 37°C for 20 min. The samples were analyzed on 10% PAGE, dried gel exposed to x-ray, and autoradiogram developed.

ATPase Assay

[α-^{32}P] ATP (Board of Radiation and Isotope Technology, Dept. of Atomic Energy, India) was used for TLC, and the release of [α-^{32}P]ADP was measured as described earlier (Modi et al., 2014). In brief, purified recombinant DrRecA (0.2 μM) was incubated in the buffer (25 mM Tris–HCl, pH 7.5, 1 mM DTT, 2.5 mM $MgCl_2$, 1 mM ATP, 25 mM KCl, 2 nM ssDNA^{nt}) added with 30 nM of [α^{-32}P] ATP. DrRecA incubated with increasing concentration of PprA to check PprA effect on ATPase of DrRecA. Reaction mixtures were incubated at 37°C for 10 min. The reaction was stopped by the addition of 10 mM EDTA. Further, 1 μl of the reaction mixture was spotted on polyethyleneimine (PEI)-cellulose TLC sheets. Spots were air-dried, components were separated on a solid support in a buffer system in 0.75 M KH_2PO_4/H_3PO_4 (pH 3.5), and an autoradiogram was developed.

ATP Binding Assay

ATP binding assay to DrRecA performed as described earlier (Rohn et al., 1999). In brief, 100 nM of fluorescent Mant-ATP (sigma) and 0.2 μM DrRecA was added in an assay buffer (20 mM Tris–HCl, 50 mM KCl, 1 mM DTT and 5 mM $MgCl_2$) in a cuvette (final volume 0.4 ml). The samples were then analyzed on FLS980 Spectrometer, Edinburg Instruments, United Kingdom at room temperature using an excitation wavelength of 355 nm and recording the emission spectra from 400 to 500 nm. The baseline buffer spectrum was subtracted from all spectra shown. To check the PprA protein effect, PprA protein added in reaction with increasing concentration as indicated. ATP (5 mM) was added for the competition assays.

Site-Directed Mutagenesis

PprA protein mutants were generated using a site-directed mutagenesis kit (New England Biolabs) following the kit manufacturer's protocols. Details of primers used for site-directed mutagenesis are given in **Supplementary Table 1**.

Evaluation of Transformation Efficiency

For the evaluation of transformation efficiency, 5 μg pVHSM plasmid was used to transform the wild-type and *pprA*$^{-}$ mutant cells. Transformants were selected on spectinomycin antibiotic (100 μg/ml). For the gamma-irradiated cells, 10 OD (A_{600}) cells were resuspended in a fresh TGY medium and irradiated for a 6kGy dose. Unirradiated sham controls were plated parallelly. 30 mM $CaCl_2$ is used to assist transformation. Appropriate dilution plated and transformation efficiently calculated by calculating CFU/μg plasmid DNA used.

DATA AVAILABILITY STATEMENT

The original contributions presented in the study are included in the article/**Supplementary Material**, further inquiries can be directed to the corresponding author/s.

AUTHOR CONTRIBUTIONS

YR: hypothesized, design of experiments, execution, and manuscript writing and editing. DS: design and execution of experiments. HM: manuscript writing, editing, and discussion. All authors contributed to the article and approved the submitted version.

ACKNOWLEDGMENTS

The authors are thankful to Dr. Rajani Kant, BARC, India for helping in carrying ATP binding assay and Dr. Ganesh Kumar Maurya, Banaras Hindu University, UP, India for helping in the construction of recombinant plasmids.

SUPPLEMENTARY MATERIAL

The Supplementary Material for this article can be found online at: https://www.frontiersin.org/articles/10.3389/fcell.2021.636178/full#supplementary-material

REFERENCES

Adachi, M., Hirayama, H., Shimizu, R., Satoh, K., Narumi, I., and Kuroki, R. (2014). Interaction of double-stranded DNA with polymerized PprA protein from *Deinococcus radiodurans*. *Protein Sci.* 23, 1349–1358. doi: 10.1002/pro.2519

Battesti, A., and Bouveret, E. (2012). The bacterial two-hybrid system based on adenylate cyclase reconstitution in *Escherichia coli*. *Methods* 58, 325–334. doi: 10.1016/j.ymeth.2012.07.018

Bauermeister, A., Bentchikou, E., Moeller, R., and Rettberg, P. (2009). Roles of PprA, IrrE, and RecA in the resistance of *Deinococcus radiodurans* to germicidal and environmentally relevant UV radiation. *Arch. Microbiol.* 191, 913–918. doi: 10.1007/s00203-009-0522-7

Bell, J. C., and Kowalczykowski, S. C. (2016). Mechanics and single-molecule interrogation of DNA recombination. *Annu. Rev. Biochem.* 85, 193–226. doi: 10.1146/annurev-biochem-060614-034352

Bentchikou, E., Servant, P., Coste, G., and Sommer, S. (2010). A major role of the RecFOR pathway in DNA double-strand-break repair through ESDSA in *Deinococcus radiodurans*. *PLoS Genet.* 6:e1000774. doi: 10.1371/journal.pgen.1000774

Blanchard, L., Guerin, P., Roche, D., Cruveiller, S., Pignol, D., Vallenet, D., et al. (2017). Conservation and diversity of the IrrE/DdrO-controlled radiation response in radiation-resistant *Deinococcus* bacteria. *Microbiologyopen* 6:e00477. doi: 10.1002/mbo3.477

Bonacossa de Almeida, C., Coste, G., Sommer, S., and Bailone, A. (2002). Quantification of RecA protein in *Deinococcus radiodurans* reveals involvement of RecA, but not LexA, in its regulation. *Mol. Genet. Genom.* 268, 28–41. doi: 10.1007/s00438-002-0718-x

Chen, Z., Yang, H., and Pavletich, N. P. (2008). Mechanism of homologous recombination from the RecA-ssDNA/dsDNA structures. *Nature* 453, 484–489.

Cox, M. M. (2007). Regulation of bacterial RecA protein function. *Crit. Rev. Biochem. Mol. Biol.* 42, 41–63. doi: 10.1080/10409230701260258

Cox, M. M., and Battista, J. R. (2005). *Deinococcus radiodurans* - the consummate survivor. *Nat. Rev. Microbiol.* 3, 882–892. doi: 10.1038/nrmicro1264

Daly, M. J., and Minton, K. W. (1996). An alternative pathway of recombination of chromosomal fragments precedes recA-dependent recombination in the radioresistant bacterium *Deinococcus radiodurans*. *J. Bacteriol.* 178, 4461–4471. doi: 10.1128/jb.178.15.4461-4471.1996

Daly, M. J., Ouyang, L., Fuchs, P., and Minton, K. W. (1994). In vivo damage and recA-dependent repair of plasmid and chromosomal DNA in the radiation-resistant bacterium *Deinococcus radiodurans*. *J. Bacteriol.* 176, 3508–3517. doi: 10.1128/jb.176.12.3508-3517.1994

Devigne, A., Ithurbide, S., Bouthier de la Tour, C., Passot, F., Mathieu, M., Sommer, S., et al. (2015). DdrO is an essential protein that regulates the radiation desiccation response and the apoptotic-like cell death in the radioresistant *Deinococcus radiodurans* bacterium. *Mol. Microbiol.* 96, 1069–1084. doi: 10.1111/mmi.12991

Drees, J. C., Chitteni-Pattu, S., McCaslin, D. R., Inman, R. B., and Cox, M. M. (2006). Inhibition of RecA protein function by the RdgC protein from *Escherichia coli*. *J. Biol. Chem.* 281, 4708–4717. doi: 10.1074/jbc.M513592200

Earl, A. M., Mohundro, M. M., Mian, I. S., and Battista, J. R. (2002). The IrrE protein of *Deinococcus radiodurans* R1 is a novel regulator of recA expression. *J. Bacteriol.* 184, 6216–6224. doi: 10.1128/jb.184.22.6216-6224.2002

Green, M. R., and Sambrook, J. (2012). *Molecular Cloning: A Laboratory Manual*. Cold Spring Harbor, N.Y: Cold Spring Harbor Laboratory Press.

Gutman, P. D., Carroll, J. D., Masters, C. I., and Minton, K. W. (1994). Sequencing, targeted mutagenesis and expression of a recA gene required for the extreme radioresistance of *Deinococcus radiodurans*. *Gene* 141, 31–37. doi: 10.1016/0378-1119(94)90124-4

Heyer, W. D. (2015). Regulation of recombination and genomic maintenance. *Cold Spring Harb. Perspect. Biol.* 7:a016501. doi: 10.1101/cshperspect.a016501

Jolivet, E., Lecointe, F., Coste, G., Satoh, K., Narumi, I., Bailone, A., et al. (2006). Limited concentration of RecA delays DNA double-strand break repair in *Deinococcus radiodurans* R1. *Mol. Microbiol.* 59, 338–349. doi: 10.1111/j.1365-2958.2005.04946.x

Karimova, G., Ullmann, A., and Ladant, D. (2000). A bacterial two-hybrid system that exploits a cAMP signaling cascade in *Escherichia coli*. *Methods Enzymol.* 328, 59–73. doi: 10.1016/s0076-6879(00)28390-0

Kim, J. I., and Cox, M. M. (2002). The RecA proteins of *Deinococcus radiodurans* and *Escherichia coli* promote DNA strand exchange via inverse pathways. *Proc. Natl. Acad. Sci. U.S.A.* 99, 7917–7921. doi: 10.1073/pnas.122218499

Kota, S., Charaka, V. K., Ringgaard, S., Waldor, M. K., and Misra, H. S. (2014). PprA contributes to *Deinococcus radiodurans* resistance to nalidixic acid, genome maintenance after DNA damage and interacts with deinococcal topoisomerases. *PLoS One* 9:e85288. doi: 10.1371/journal.pone.0085288

Kota, S., and Misra, H. S. (2006). PprA, A protein implicated in radioresistance of *Deinococcus radiodurans* stimulates catalase activity in *Escherichia coli*. *Appl. Microbiol. Biotechnol.* 72, 790–796. doi: 10.1007/s00253-006-0340-7

Kota, S., and Misra, H. S. (2008). Identification of a DNA processing complex from *Deinococcus radiodurans*. *Biochem. Cell. Biol.* 86, 448–458. doi: 10.1139/o08-122

Kowalczykowski, S. C., Clow, J., and Krupp, R. A. (1987). Properties of the duplex DNA-dependent ATPase activity of *Escherichia coli* RecA protein and its role in branch migration. *Proc. Natl. Acad. Sci. U.S.A.* 84, 3127–3131. doi: 10.1073/pnas.84.10.3127

Li, X., and Heyer, W. D. (2008). Homologous recombination in DNA repair and DNA damage tolerance. *Cell Res.* 18, 99–113. doi: 10.1038/cr.2008.1

Little, J. W., and Mount, D. W. (1982). The SOS regulatory system of *Escherichia coli*. *Cell* 29, 11–22. doi: 10.1016/0092-8674(82)90085-x

Liu, Y., Zhou, J., Omelchenko, M. V., Beliaev, A. S., Venkateswaran, A., Stair, J., et al. (2003). Transcriptome dynamics of *Deinococcus radiodurans* recovering from ionizing radiation. *Proc. Natl. Acad. Sci. U.S.A.* 100, 4191–4196. doi: 10.1073/pnas.0630387100

Lusetti, S. L., Voloshin, O. N., Inman, R. B., Camerini-Otero, R. D., and Cox, M. M. (2004). The DinI protein stabilizes RecA protein filaments. *J. Biol. Chem.* 279, 30037–30046. doi: 10.1074/jbc.M403064200

Lusetti, S. L., Hobbs, M. D., Stohl, E. A., Chitteni-Pattu, S., Inman, R. B., Seifert, H. S., et al. (2006). The RecF protein antagonizes RecX function via direct interaction. *Mol. Cell* 21, 41–50. doi: 10.1016/j.molcel.2005.11.011

Maurya, G. K., and Misra, H. S. (2020). PprA interacts with replication proteins and affects their physicochemical properties required for replication initiation in *Deinococcus radiodurans*. *bioRxiv* [Preprint]. doi: 10.1101/2020.03.25.007906

Maurya, G. K., Modi, K., Banerjee, M., Chaudhary, R., Rajpurohit, Y. S., and Misra, H. S. (2018). Phosphorylation of FtsZ and FtsA by a DNA damage-responsive Ser/Thr protein kinase affects their functional interactions in *Deinococcus radiodurans*. *mSphere* 3:e00325-18.

Menetski, J. P., Bear, D. G., and Kowalczykowski, S. C. (1990). Stable DNA heteroduplex formation catalyzed by the *Escherichia coli* RecA protein in the absence of ATP hydrolysis. *Proc. Natl. Acad. Sci. U.S.A.* 87, 21–25. doi: 10.1073/pnas.87.1.21

Misra, H. S., Rajpurohit, Y. S., and Kota, S. (2013). Physiological and molecular basis of extreme radioresistance in *Deinococcus radiodurans*. *Curr. Sci.* 104, 194–205.

Modi, K. M., Tewari, R., and Misra, H. S. (2014). FtsZDr, a tubulin homologue in radioresistant bacterium *Deinococcus radiodurans* is characterized as a GTPase exhibiting polymerization/depolymerization dynamics in vitro and FtsZ ring formation in vivo. *Int. J. Biochem. Cell Biol.* 50, 38–46. doi: 10.1016/j.biocel.2014.01.015

Moseley, B. E., and Copland, H. J. (1975). Isolation and properties of a recombination-deficient mutant of *Micrococcus radiodurans*. *J. Bacteriol.* 121, 422–428. doi: 10.1128/jb.121.2.422-428.1975

Moseley, B. E., Mattingly, A., and Copland, H. J. (1972). Sensitization to radiation by loss of recombination ability in a temperature-sensitive DNA mutant of *Micrococcus radiodurans* held at its restrictive temperature. *J. Gen. Microbiol.* 72, 329–338. doi: 10.1099/00221287-72-2-329

Narumi, I., Kikuchi, M., Funayama, T., Kitayama, S., Yanagisawa, T., Watanabe, H., et al. (1999). Molecular analysis of the *Deinococcus radiodurans* recA locus and identification of a mutation site in a DNA repair-deficient mutant, rec30. *Mutat. Res.* 435, 233–243. doi: 10.1016/s0921-8777(99)00048-8

Narumi, I., Satoh, K., Cui, S., Funayama, T., Kitayama, S., and Watanabe, H. (2004). PprA, a novel protein from *Deinococcus radiodurans* that stimulates DNA ligation. *Mol. Microbiol.* 54, 278–285. doi: 10.1111/j.1365-2958.2004.04272.x

Narumi, I., Satoh, K., Kikuchi, M., Funayama, T., Yanagisawa, T., Kobayashi, Y., et al. (2001). The LexA protein from *Deinococcus radiodurans* is not involved in RecA induction following gamma irradiation. *J. Bacteriol.* 183, 6951–6956. doi: 10.1128/jb.183.23.6951-6956.2001

Ngo, K. V., Molzberger, E. T., Chitteni-Pattu, S., and Cox, M. M. (2013). Regulation of *Deinococcus radiodurans* RecA protein function via modulation of active and inactive nucleoprotein filament states. *J. Biol. Chem.* 288, 21351–21366. doi: 10.1074/jbc.m113.459230

Rajpurohit, Y. S., Bihani, S. C., Waldor, M. K., and Misra, H. S. (2016). Phosphorylation of *Deinococcus radiodurans* RecA regulates its activity and may contribute to radioresistance. *J. Biol. Chem.* 291, 16672–16685. doi: 10.1074/jbc.m116.736389

Rajpurohit, Y. S., Gopalakrishnan, R., and Misra, H. S. (2008). Involvement of a protein kinase activity inducer in DNA double strand break repair and radioresistance of *Deinococcus radiodurans*. *J. Bacteriol.* 190, 3948–3954. doi: 10.1128/jb.00026-08

Rajpurohit, Y. S., and Misra, H. S. (2010). Characterization of a DNA damage-inducible membrane protein kinase from *Deinococcus radiodurans* and its role in bacterial radioresistance and DNA strand break repair. *Mol. Microbiol.* 77, 1470–1482. doi: 10.1111/j.1365-2958.2010.07301.x

Rajpurohit, Y. S., and Misra, H. S. (2013). Structure-function study of deinococcal serine/threonine protein kinase implicates its kinase activity and DNA repair protein phosphorylation roles in radioresistance of *Deinococcus radiodurans*. *Int. J. Biochem. Cell Biol.* 45, 2541–2552. doi: 10.1016/j.biocel.2013.08.011

Rohn, T. T., Nelson, L. K., Davis, A. R., and Quinn, M. T. (1999). Inhibition of GTP binding to Rac2 by peroxynitrite, potential role for tyrosine modification. *Free Radic. Biol. Med.* 26, 1321–1331. doi: 10.1016/s0891-5849(98)00332-3

Sander, P., Bottger, E. C., Springer, B., Steinmann, B., Rezwan, M., Stavropoulos, E., et al. (2003). A recA deletion mutant of Mycobacterium bovis BCG confers protection equivalent to that of wild-type BCG but shows increased genetic stability. *Vaccine* 21, 4124–4127. doi: 10.1016/s0264-410x(03)00434-1

Satoh, K., Ohba, H., Sghaier, H., and Narumi, I. (2006). Down-regulation of radioresistance by LexA2 in *Deinococcus radiodurans*. *Microbiology* 152, 3217–3226. doi: 10.1099/mic.0.29139-0

Schlesinger, D. J. (2007). Role of RecA in DNA damage repair in *Deinococcus radiodurans*. *FEMS Microbiol. Lett.* 274, 342–347. doi: 10.1111/j.1574-6968.2007.00862.x

Shan, Q., and Cox, M. M. (1997). RecA filament dynamics during DNA strand exchange reactions. *J. Biol. Chem.* 272, 11063–11073. doi: 10.1074/jbc.272.17.11063

Sharma, D. K., Siddiqui, M. Q., Gadewal, N., Choudhary, R. K., Varma, A. K., Misra, H. S., et al. (2020). Phosphorylation of deinococcal RecA affects its structural and functional dynamics implicated for its roles in radioresistance of *Deinococcus radiodurans*. *J. Biomol. Struct. Dyn.* 38, 114–123. doi: 10.1080/07391102.2019.1568916

Sheng, D., Liu, R., Xu, Z., Singh, P., Shen, B., and Hua, Y. (2005). Dual negative regulatory mechanisms of RecX on RecA functions in radiation resistance, DNA recombination and consequent genome instability in *Deinococcus radiodurans*. *DNA Repair.* 4, 671–678. doi: 10.1016/j.dnarep.2005.02.006

Siddiqui, M. Q., Rajpurohit, Y. S., Thapa, P. S., Maurya, G. K., Banerjee, K., Khan, M. A., et al. (2017). Studies of protein-protein interactions in Fanconi anemia pathway to unravel the DNA interstrand crosslink repair mechanism. *Int. J. Biol. Macromol.* 104, 1338–1344. doi: 10.1016/j.ijbiomac.2017.05.166

Slade, D., Lindner, A. B., Paul, G., and Radman, M. (2009). Recombination and replication in DNA repair of heavily irradiated *Deinococcus radiodurans*. *Cell* 136, 1044–1055. doi: 10.1016/j.cell.2009.01.018

Slade, D., and Radman, M. (2011). Oxidative stress resistance in *Deinococcus radiodurans*. *Microbiol. Mol. Biol. Rev.* 75, 133–191. doi: 10.1128/mmbr.00015-10

Spies, M., and Kowalczykowski, S. C. (2006). The RecA binding locus of RecBCD is a general domain for recruitment of DNA strand exchange proteins. *Mol. Cell* 21, 573–580. doi: 10.1016/j.molcel.2006.01.007

Tanaka, M., Earl, A. M., Howell, H. A., Park, M. J., Eisen, J. A., Peterson, S. N., et al. (2004). Analysis of *Deinococcus radiodurans*'s transcriptional response to ionizing radiation and desiccation reveals novel proteins that contribute to extreme radioresistance. *Genetics* 168, 21–33. doi: 10.1534/genetics.104.029249

van Loenhout, M. T., van der Heijden, T., Kanaar, R., Wyman, C., and Dekker, C. (2009). Dynamics of RecA filaments on single-stranded DNA. *Nucleic Acids Res.* 37, 4089–4099. doi: 10.1093/nar/gkp326

Vierling, S., Weber, T., Wohlleben, W., and Muth, G. (2000). Transcriptional and mutational analyses of the *Streptomyces lividans* recX gene and its interference with RecA activity. *J. Bacteriol.* 182, 4005–4011. doi: 10.1128/jb.182.14.4005-4011.2000

Wang, L., Xu, G., Chen, H., Zhao, Y., Xu, N., Tian, B., et al. (2008). DrRRA, a novel response regulator essential for the extreme radioresistance of *Deinococcus radiodurans*. *Mol. Microbiol.* 67, 1211–1222. doi: 10.1111/j.1365-2958.2008.06113.x

Warfel, J. D., and LiCata, V. J. (2015). Enhanced DNA binding affinity of RecA protein from *Deinococcus radiodurans*. *DNA Repair.* 31, 91–96. doi: 10.1016/j.dnarep.2015.05.002

Yu, X., Jacobs, S. A., West, S. C., Ogawa, T., and Egelman, E. H. (2001). Domain structure and dynamics in the helical filaments formed by RecA and Rad51 on DNA. *Proc. Natl. Acad. Sci. U.S.A.* 98, 8419–8424. doi: 10.1073/pnas.111005398

Zahradka, K., Slade, D., Bailone, A., Sommer, S., Averbeck, D., Petranovic, M., et al. (2006). Reassembly of shattered chromosomes in *Deinococcus radiodurans*. *Nature* 443, 569–573. doi: 10.1038/nature05160

Zhao, B., Zhang, D., Li, C., Yuan, Z., Yu, F., Zhong, S., et al. (2017). ATPase activity tightly regulates RecA nucleofilaments to promote homologous recombination. *Cell Discov.* 3:16053.

Conflict of Interest: The authors declare that the research was conducted in the absence of any commercial or financial relationships that could be construed as a potential conflict of interest.

frontiers in Oncology

REVIEW
published: 25 May 2021
doi: 10.3389/fonc.2021.673154

GLI1: A Therapeutic Target for Cancer

Justin T. Avery[1†], *Ruowen Zhang*[2†] *and Rebecca J. Boohaker*[1*]

[1] Oncology Department, Drug Discovery Division, Southern Research, Birmingham, AL, United States, [2] Department of Medicine, Stony Brook University, Stony Brook, NY, United States

GLI1 is a transcriptional effector at the terminal end of the Hedgehog signaling (Hh) pathway and is tightly regulated during embryonic development and tissue patterning/differentiation. GLI1 has low-level expression in differentiated tissues, however, in certain cancers, aberrant activation of GLI1 has been linked to the promotion of numerous hallmarks of cancer, such as proliferation, survival, angiogenesis, metastasis, metabolic rewiring, and chemotherapeutic resistance. All of these are driven, in part, by GLI1's role in regulating cell cycle, DNA replication and DNA damage repair processes. The consequences of GLI1 oncogenic activity, specifically the activity surrounding DNA damage repair proteins, such as NBS1, and cell cycle proteins, such as CDK1, can be linked to tumorigenesis and chemoresistance. Therefore, understanding the underlying mechanisms driving GLI1 dysregulation can provide prognostic and diagnostic biomarkers to identify a patient population that would derive therapeutic benefit from either direct inhibition of GLI1 or targeted therapy towards proteins downstream of GLI1 regulation.

Keywords: hedgehog, GLI1, therapeutic resistance, DNA damage repair, cancer

OPEN ACCESS

Edited by:
José Díaz-Chávez, National Institute of Cancerology (INCAN), Mexico

Reviewed by:
Chinnadurai Mani, Texas Tech University Health Sciences Center, United States
Kai Jiang, University of Kentucky, United States

***Correspondence:**
Rebecca J. Boohaker
RBoohaker@southernresearch.org

†These authors have contributed equally to this work and share first authorship

Specialty section:
This article was submitted to Molecular and Cellular Oncology, a section of the journal Frontiers in Oncology

Received: *26 February 2021*
Accepted: *30 April 2021*
Published: *25 May 2021*

Citation:
Avery JT, Zhang R and Boohaker RJ (2021) GLI1: A Therapeutic Target for Cancer. Front. Oncol. 11:673154. doi: 10.3389/fonc.2021.673154

GLI AND THE HEDGEHOG PATHWAY

GLI1 is an effector transcriptional factor distal to both the canonical and non-canonical Hedgehog (Hh) signaling pathways. The Hh family of proteins contains three subfamilies: sonic hedgehog (SHh), desert hedgehog (DHh) and Indian hedgehog (IHh) (1). IHh and DHh are reported to be involved in normal tissue development, such as bone formation (2). SHh, first discovered in Drosophila, has been found to be highly conserved across many different vertebrate species including human, mouse, rat, frog, fish, and chicken, and is the most studied member of the hedgehog family (3). SHh plays a critical role in the embryonic development that is necessary for certain cell differentiation and maintenance of tissue polarity (4). Due to its conserved nature, and apparent critical functionality across organisms, SHh and the downstream pathway members have evolved to serve vastly diverse roles in both embryonic and non-embryonic cellular homeostasis. Herein, we focus specifically on our current understanding of SHh-GLI pathway and its clinical significance in human development and the consequences of its dysregulation in disease progression (5–8).

SHh-mediated transduction is initiated *via* extracellular SHh ligand binding to the 12-span transmembrane receptor, PATCHED-1 (PTCH-1) or the redundant receptor PTCH-2, in target cells (9, 10). In the absence of SHh, PTCH-1 and, redundantly, PTCH-2, catalytically inhibit

downstream signaling activity with seven-transmembrane G-protein-coupled receptor, Smoothened (SMO) (11–13). Upon SHh binding to PTCH, the inhibitory interaction is terminated through internalization of PTCH, releasing SMO and allowing for phosphorylation to transduce signal into the cytoplasm (14). The resultant signal leads to the component dissociation of a large protein complex comprising of Sufu and GLIs in the cytoplasm, releasing the GLI transcription factors. Finally, the released GLI transcription factors translocate into the nucleus to execute transcriptional activation of specific target genes (15). Aberrant activation of the hedgehog pathway has been shown to promote oncogenic activities, such as metastasis, DNA damage repair, stem-ness, and chemotherapeutic resistance, in a variety of types of cancer (16–26).

There are two models for the over-activation of the Hh pathway in cancer: (a) ligand-dependent model: tumors are able to over-activate SHh-GLI pathway *via* autocrine signaling to produce high level of SHh ligands (18, 27–31). This can be observed in several epithelial originating tumors such as small cell lung cancer (SCLC), pancreatic, colon, and prostate cancer, and glioblastomas, and medulloblastomas. (b) Ligand-independent model: Clinical observations have found mutations of PTCH-1 and PTCH-2 in basal cell carcinomas and in medulloblastomas, resulting in dysregulated GLI signaling due to ineffective sequestration of SMO signaling, regardless of SHh ligand levels. Mutant PTCH often results in SMO constitutive activation, subsequently promoting cell transformation and tumorigenesis (32). Inactivation of PTCH-1 due to gene mutation has also been reported in trichoepitheliomas (33), esophageal squamous cell carcinomas (34), and transitional cell carcinomas of the bladder (35). In both models, the commonality is a failure to stifle SMO signal transduction.

Regardless of how SHh-GLI pathway is activated, all biological function of these upstream proteins such as SHh, PTCH and SMO depends on the transcriptional effectors at the distal end of the pathway: the GLI proteins. There are three GLI transcriptional proteins in this family, two which act as transcriptional activators (GLI1 and GLI2) and one transcriptional repressor (GLI3) (36). GLI1 was initially found to transcriptionally regulate specific target genes involved in mammalian development, such as patterning in the central nervous system, proliferation, differentiation, and survival (37). However, increased expression in terminally differentiated cells is a known oncogenic biomarker for numbers cancer subtypes (38–40), making it an ideal drug discovery target.

GLI1 AS A TRANSCRIPTION FACTOR

GLI1 (1106 amino acids; MW 117.9kDa) was originally identified as an amplified gene product in a malignant glioma (41) and was the first member described in the human GLI gene family. GLI1-DNA binding is mediated by five highly conserved tandem C2-H2 zinc finger (ZF) domains and a consensus histidine-cysteine linker sequence between zinc fingers (42). While ZF1-3 interacts with the phosphate backbone and contributes to binding stability and recruitment of co-regulatory factors, ZF4-5 regulates transcription, recognizing the consensus sequence 5'-GACCACCCA-3' in the promoter region of target genes. The two cytosine-pairs flanking the central adenine within the consensus site are critical for GLI binding, whereas the other positions can tolerate a certain degree of flexibility (43). In addition to the transcriptional ZF domain, the GLI proteins contain both nuclear export sequence (NES) and a nuclear localization signal (NLS), which facilitate the nucleo-cytoplasmic shuttling of GLI (44). GLI1 also contains a single SUFU-interacting site located at the N-terminus (SIN) (45), which is responsible for SUFU-mediated cytoplasmic retention of GLI1. The positioning of the SIN is unique to GLI1; GLI2 and GLI3 also have a SUFU-interacting site though it is located in the C-terminus (SIC) (45, 46). The GLI1 C-terminal region possesses a transactivation domain (TAD) which remodels chromatin and interacts with histone acetyltransferase (HAT), histone deacetylase (HDAC); SWI-SNF5; SWI/SNF-like Brg/Brm-associated factor; and the TFIID TATA box-binding protein-associated factor, TAFII31 (26). Like the SIN domain, all GLI proteins also possess a TAD, but GLI2 and GLI3 have an additional N-terminal repressor domain, which is lacking on GLI1. Therefore, GLI1 performs as a strong transcriptional activator (47), whereas full-length GLI2 is generally a weak activator since the fully activated form requires significant truncation of its N-terminus and C-terminus (48–51), and GLI3 has been reported as a strong repressor in most settings (52).

Two additional isoforms of GLI1, N-terminal deletion variant (GLI1ΔN) and truncated GLI1 (tGLI1), have been identified. GLI1ΔN is generation is the result of a 128-amino acid deletion on its N-terminus (47). This deletion results in loss of the lone critical suppressive SUFU-binding domain on the GLI1 protein sequence, while preserving the ZNF domains, NLS and NES, and the transactivation domain. As would be expected, this isoform of GLI1 functions as a constitutively active protein, with activity comparable to full-length GLI1 (GLI1FL) but surprisingly does not show a preferential expression in cancer tissues (53, 54). tGLI1 originates from a splicing of exon 3 and part of exon 4 of the GLI1 gene, resulting in the deletion of 41 amino acids (55). All functional domains are retained in tGLI1, and this isoform is observed specifically in tumor expression. It has been shown to regulate an additional set of target genes involved in EMT, invasion and metastasis (56). All three GLI1 isoforms (GLI1FL, GLI1ΔN, and tGLI1) could be activated by SHh ligand stimulation, but whether they induce differently transcriptional targets has not yet been determined.

NON-CANONICAL ACTIVATION OF GLI1

Over-activation of Hh promotes the tumor microenvironment through pro-inflammatory mechanisms, angiogenesis, genome instability, mutation, resistance to cell death, energy imbalance, and is involved in invasion and metastasis (57, 58). Some studies,

however, fail to observe a positive correlation between the Hh signaling pathway and the development/progression of cancer (59–61). For instance, Li discovered that SMO expression was not statistically correlated with CRC-specific or overall survival; the same results were reported by Stefanius, where no correlation between Hh and colorectal serrated adenocarcinomas was observed (62, 63). Our lab, like many others, observed a positive correlation between GLI1 expression and disease severity (64). We also demonstrated that both GLI1 and one of its transcriptional targets, NBS1, negatively correlate with CRC patient 5-year survival, driving chemotherapeutic resistance by overcoming FOLFOX induced DNA damage (standard of care treatment). The difference lies in the way GLI1 is activated—whether it be through canonical activation (PTCH/SMO) or non-canonical (RAS/RAF, etc) (**Figure 1**). Elevated levels of GLI1 in cancer are often driven by non-canonical pathways. As such, this explains why Vismodegib, the first SMO inhibitor to be approved by the FDA for the treatment of BCC (65), failed to demonstrate the effectiveness in clinical trials for the treatment of metastatic colorectal cancer where GLI expression is driven non-canonically (66). Therefore, it is important to determine how GLI1 is upregulated and its function in the initiation, progression, invasion and metastasis in order to develop a therapeutic target for new treatment schemes based on the inhibition, at different levels, of the Hh pathway (67–69).

RAS-RAF-MEK-ERK Pathway

The RAS-RAF-MEK-ERK pathway is the most common non-canonical mechanism involved both in transcriptional activation of GLI genes and in post-translational modifications of GLI-transcribed proteins. In colorectal cancer, constitutively activated mutant KRAS or altered stimulation of pathway components (mainly RAS, RAF, MEK) results in the hyperactivation of the mitogen-activated protein kinase (MAPK) extracellular signal-regulated kinase 1 and 2 (ERK1/2) and positively modulates tumor proliferation by increasing GLI1 transcriptional activity and expression of Hh target genes (54, 70, 71). This non-canonical activation pathway was confirmed in a study where EGF-induced stimulation of GLI is unaffected by SMO inhibition but was blocked by MEK1 inhibition (72). Similarly, the RAS-RAF pathway induces GLI1 and GLI2 transcriptional activity and increases mRNA and protein levels in a non-canonical manner in colon cancer cells (73). Pharmacological and genetic inhibition of GLI function is more effective in reducing tumor proliferation and inducing apoptosis than the inhibition of the canonical pathway at SMO level, suggesting that GLI activity is crucial for RAS/MEK-induced colon cancer proliferation (74, 75).

PI3K-AKT-mTOR Pathway

The PI3K-AKT-mTOR signaling pathway is another crucial non-canonical activator of GLI1, particularly evident in pancreatic cancers (76). Activation of PI3K-AKT signaling has been found to enhance GLI1 protein stability (77) since AKT is able to extend GLI proteins half-life in the cells by alleviating the inhibitory effect of PKA and facilitates nuclear translocation. Another mechanism of PI3K signaling activating GLI1 is *via* members of the ribosomal S6 kinase family (S6K/p70-S6K), which are the downstream effectors of the PI3K-AKT-mTOR axis. Activated S6K1 promotes GLI1 disassociation from SUFU by phosphorylating GLI1 at Serine residue at position 84, increasing GLI1 transcriptional activity (78). Additionally, p70-S6K2 has been shown to inhibit GSK3 by phosphorylating GLI1at Ser9, leading to decreases of GSK3b-mediated GLI1 degradation (79).

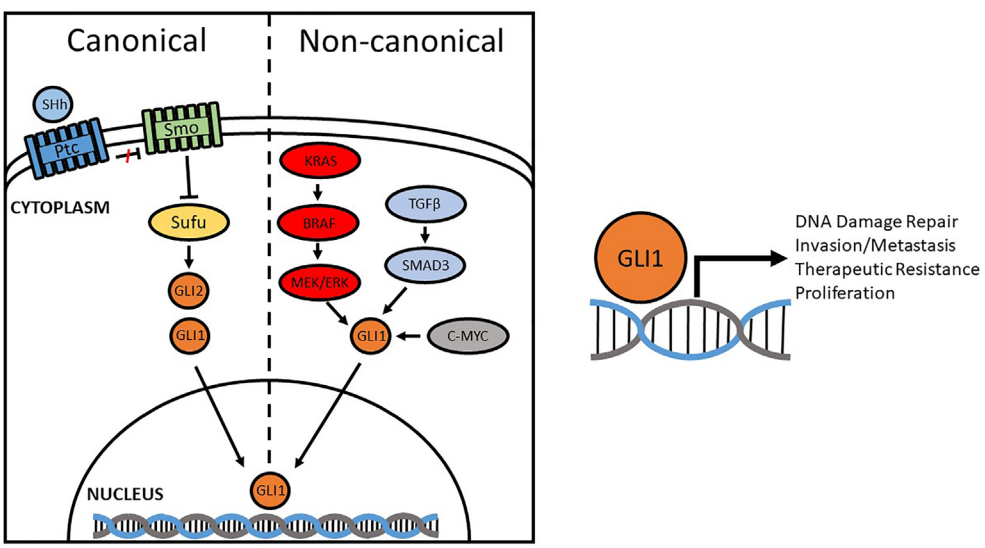

FIGURE 1 | Canonical and Non-canonical activation of GLI1. Compounds originally designed to inhibit the Hedgehog pathway focused on canonical regulators, like SMO, but were found to be ineffective in some cancers due to non-canonical activation. Aberrant activation of GLI1 promotes DNA damage repair, invasion/metastasis, proliferation, and therapeutic resistance through transcriptional regulation of target genes.

TGFβ Pathway

TGFβ is a multifunctioning cytokine that has been implicated in nearly all the key steps of tumorigenesis, tumor maintenance and advanced metastasis (80). In brief, TGFβ is secreted as a latent complex and sequestered in the extracellular matrix until activated. Once biologically available to its target cells, TGFβ binds its type 2 receptor (TGFBR2), leading to the recruitment of its type 1 receptor (TGFBR1) and subsequent downstream signaling resulting in nuclear localization of the SMAD2/3/4 complex (81). In advanced pancreatic cancer, TGFβ signaling contributes to a metastatic phenotype (82). GLI1 as an effector of TGFβ signaling as it interacts with SMAD proteins to induce a subset of TGFβ-inducible target genes, including BCL2, IL7, and Cyclin D1 (83). In the mouse model of PDAC, SMO-independent GLI1 activation promotes transformation and requires both TGFβ and KRAS signaling (84) where inhibition of TGFβ by TbRI antagonist SD208 significantly reduces tumor burden and increases infiltration of lymphocytes.

Other Pathways

C-MYC, which is frequently over-amplified in colorectal cancer, has been confirmed to be another oncogene that activates GLI1 independently from Hh ligand-mediated signaling (85). C-MYC is a transcriptional activator of GLI1. C-MYC-GLI1 activated pathway could be blocked by small molecule inhibitors targeting either protein, downregulating GLI1 expression and, in turn, inducing cell apoptosis of colorectal cells. Similarly, aberrant expression of oncogenic EGFR, which is responsible for the over-activation of GLI1 through RAS-RAF-MEK pathway, promotes colorectal cancer metastasis and chemotherapeutic resistance. In triple negative breast cancer, elevated expression of GLI1 is driven by VEGF/NRP2 and α6β1 pathway results in an autocrine feedback loop with GLI1 enhancing the expression of NRP2 (86). Atypical protein kinase C iota/lambda (aPKC) has been identified as a novel regulator of GLI, and like the VEGF/NRP2 pathway, results in a positive feedback loop enhancing GLI1 overexpression in basal cell carcinoma (87) and has been also observed in drosophila (88). An interesting connection between GLI1 and p53 has also been reported because of loss of p53 results in aberrant GLI1 expression (89). Genetic mutations of aforementioned pathway genes have been shown to drive GLI1 expression in multiple types of cancer and cancer precursor diseases (90–95). An interesting GLI1 genetic translocation was first noted in 2004 when five pericytomas had an ACTB-GLI fusion transcript t(7;12) (96), with an additional three patients reported on 15 years later (97). Additional fusions were later observed with ACTB1/MALAT1/PTCH1-GLI1, which were associated with metastasis to the lung/lymph node in three of the patients (98).

GLI1 IN CANCER

While GLI1 and GLI2 are both transcriptional activators, GLI1 can be thought of as the primary effector of Hh signaling since GLI1 is a transcriptional target of GLI2, which may amplify Hh-induced, GLI2-mediated transcription of GLI1 target genes (99–102). As previously stated, GLI1 induced by Hh signaling is important in the regulation of cellular proliferation, stemness, cell fate determination, and cellular survival in a variety of organs (36, 103); however, its aberrant activation has been associated with many human cancers (104). For example, GLI1 is amplified in glioma (37), osteosarcoma, and rhabdomyosarcoma (105). Mutations in PTCH or SMO are also prevalent in basal cell carcinomas, medulloblastomas, and cancers of the esophagus and bladder (102), and sustained and activated Hh-Gli signaling has led to the development of medulloblastomas in PTCH heterozygous mice (106). Melanomas and carcinomas of the prostate have further demonstrated a need for elevated Hh-Gli signaling, since inhibition by cyclopamine (a SMO inhibitor) can result in reduction for these types of cancers (107, 108).

Although GLI1 plays a key role in canonically activated Hh cancers (103, 109), non-canonical oncogenic activation (CMYC, RAS/RAF, TGFβ, etc) is critical to address as well (110). For example, in gastrointestinal (GI) cancers, over-activation of GLI1 is driven by KRAS/BRAF mutation (102). It has recently been suggested that oncogenic GLI1 progresses during colon carcinogenesis (111, 112) and in metastatic disease (31), whereas in normal colonic tissue, Hh-GLI is strictly involved in differentiation (59, 113).

Cancer Stem Cells and Colorectal Cancer

Colorectal cancer (CRC) is still one of the most common gastrointestinal cancers worldwide and results in approximately 33% mortality rate, despite several therapeutic advancements (114). The most important prognostic indicator is stage at diagnosis. The 5-year relative survival of patients diagnosed with CRC is 90% for patients with localized disease (non-metastatic), whereas clinical statistics shows less than 5% 5-year survival for metastatic CRC (115, 116). Therefore, oncogenic drivers of metastasis promote a significant problem to both CRC patients and clinicians (63, 117). The mechanism for CRC progression toward metastasis is multifactorial, with age, dietary habits, genetic alteration (mutational activation of oncogenes and inhibition of several tumor suppressor genes), intensity of epithelial-to-mesenchymal transformation (EMT), angiogenesis in tumor growth, and response to the therapeutic treatment all playing roles in the progression of disease (118, 119). Various gene mutations (KRAS, MYB, and BRAF) and gene abnormal amplification (CMYC and EGFR) have been associated with the molecular mechanisms underlying the development of CRC, all of which can result in non-canonical activation of GLI1 (120, 121). Another complication for studying and treating CRC is the heterogeneity of the disease. This heterogeneity is driven by the by pluripotent, self-renewing cancer stem cells (CSCs) which have unlimited self-renewal through symmetric cell division, and have the ability to give rise to progeny cells through asymmetric division, and an innate resistance to cytotoxic therapeutics (122). Additionally, may publications have implicated Wnt, Notch, Hh, and/or TGFβ signaling pathways in proliferation and maintenance of CSCs, and dysregulation of these pathways might cause the development of CRC (123–127). All of these pathways drive

GLI1 expression, defining GLI1 as a cancer stem cell marker in multiple types of cancer, including colorectal (128–131).

Metastasis and Pancreatic Cancer

Pancreatic ductal adenocarcinoma (PDAC) is one of the deadliest types of cancer in the United States, with a 5-year survival rate of less than 3.5% (132, 133). Removal of the tumor is the only potentially curative treatment to date, but this is not achievable for over 85% patients due to non-resectable cases like early-stage metastasis or complicated primary site (80). KRAS over-activation mutations play a major role in initiating the transformation from precursor lesions termed "pancreatic intraepithelial neo-plasias" (PanINs) to PDAC and promote cancer development and metastasis (134–136). In pancreatic cancer, KRAS mutations are present in 90% of cases (137). Multiple mutation types exist, with codon-13 (G13D) or -61 (Q61L or Q61H) occurring less frequently and 95% of KRAS mutations occurring at codon-12. Single-nucleotide mutations on codon-12 result in eight different amino acid substitutions, with G12D the predominant mutation (51%), G12V (30%), G12R (12%), G12C (2%), G12S (2%), G12A (2%), G12L/F (1%) (11, 14). These missense mutations enhance the level of GTP-bound active KRAS due to impairing intrinsic and GTPase-activating protein-mediated GTP hydrolysis, resulting in over-activating downstream signaling, increasing cell growth and survival, leading to neoplastic transformation (138–140). For patients with locally advanced and/or metastatic PDAC, a G12D KRAS mutation within the primary tumor is an independent prognostic factor that results in significantly decreased overall survival, including those within the subgroup that receive chemotherapy (141). Pancreatic cancer with activating mutations in KRAS or BRAF occur frequently, and oncogenic pathways like RAS/RAF/MEK/ERK, the PI3K-AKT-mTOR, and TGFβ signaling converge on the activation of GLI1, promoting cellular proliferation, tumor progression, chemotherapeutic resistance, and early metastasis (142, 143).

Radiosensitivity, Heterogeneity, and Brain Cancer

Glioblastoma multiforme (GBM) is the most aggressive and most common type of brain tumor. The standard of care for patients with GBM is maximum safe surgical resection followed by concurrent temozolamide (TMZ) and radiation therapy (144). TMZ is an alkylating agent that results in the transport of methyl groups to guanine and adenine, resulting in DNA damage and eventual cell cycle arrest and apoptosis. TMZ also acts as a radiation-sensitizer to enhance the DNA damage induced by the ionizing radiation. Individuals receiving this standard treatment have a median survival time between 12 and 15 months and have an average 5-year survival of 5% in the United States. Unfortunately, approximately 50% of patients do not respond to the standard of care regimen (145). Most of these cases are the result of overexpression of O6-methylguanine-DNA methyl-transferase (MGMT), a protein that directly counters the methyl damage caused by TMZ (146). In fact, hypomethylation of the MGMT promoter is a biomarker for aggressiveness of disease and poor response to therapy (147). GLI1 was recently identified as positive regulator of MGMT, having several putative binding sites in the MGMT promoter region (148). Aberrant activation of GLI family members has been linked to chemotherapeutic resistance to TMZ (69). Data set analysis from the Chinese Glioma Genome Atlas (CGGA) indicates that individuals with lower expression of GLI1 (149) have a statistically greater median survival when compared to GLI1 high-expressing patients. Several studies have examined the effect of GLI inhibition in GBM cells *in vitro* and found that treatment with GLI inhibitors, like GANT61, results in decreased expression of MGMT and re-sensitization to TMZ (148, 150, 151).

Neuroblastoma accounts for roughly 8% of all childhood malignancies and up to 15% of all pediatric cancer deaths (152). It is a heterogeneous solid tumor, and the heterogeneity is partially driven by the generation of extrachromosomal circular DNA (eccDNA) (153). eccDNA formation has been linked to the dysregulation of the double-stranded break (DSB) repair mechanism, specifically that which drives non-homologous end-joining (NHEJ) and is produced through R-loop defects or circularization of gene fragments (154). Oncogenic GLI1 drives R-loop formation, and treatment with GANT61 has been shown to decrease the generation of R-loop formation (155), likely additionally reducing the generation of eccDNAs.

IMPACT OF GLI1 ON BIOLOGICAL PROCESSES

Metastasis and Epithelial-Mesenchymal Transition

EMT is considered to be an important feature in cancer development. This process allows the epithelial cells to undergo various biological changes, transforming them to a mesenchymal cell phenotype characterized by enhanced migration, invasiveness, and resistance to apoptosis. EMT markers, such as snail family of zinc-finger transcription factor 1 (SNAIL1), vimentin, and E-cadherin, are three of the primary factors that regulate the EMT transition. GLI1 can initiate cancer cell EMT by increasing expression of SNAIL1 and vimentin but decreasing E-cadherin, causing β-catenin to migrate into the nucleus and act as a transcription factor, inducing cell transformation (156, 157). Since β-catenin is an important member of the WNT signaling pathway, this results in cross-talk between WNT pathway and Hh pathway, resulting in GLI1 activation (158). Overexpression of GLI1 in colorectal cancer cells induces more invasive growth in organoid 3D cultures as well as in soft agar colony formation (159).

DNA Damage Repair Response

GLI1 activation has been linked to the DNA damage response (DDR) and promotes chemotherapeutic resistance. Recent studies have demonstrated that loss of either non-homologous end joining (NHEJ) gene DNA Ligase IV (Lig4), or genes involved in homologous recombination (HR) like X-ray cross complementation 2 (XRCC2),

and breast cancer growth suppressor protein 2 (BRCA2), or (Lig4/XRCC2) in combination with p53 deficiency results in PTCH-1 downregulation and GLI1 activation (69, 160). DNA damaging agents, such as doxorubicin and cisplatin, induced concomitant expression of p53 and downregulation of GLI1 and its target genes (161). In response to damage, p53-induced cell cycle checkpoints prevents proliferation of damaged cells and provides sufficient time for repair, which is the opposite response that GLI1 promotes (69).

Specific inhibition of GLI1 induces extensive cell death while the inhibition of Hh signaling at the level of SMO did not in colorectal cancers (161). In HT29 cells, inhibition of GLI1 by siRNAs or GANT61 (a small molecule inhibitor) showed increased DNA damage and cell cycle arrest at G1–S and in early S-phase, resultant of down-regulation of cell cycle genes, such as E2F2, cyclin E2, Cdc25a, Cdk2 and cyclin A2, Cdc25c, cyclinB2, Cdc20, Cdc2. Inhibition of GLI1 induces serious DNA damage because it pauses DNA synthesis by impairing the ensemble of DNA licensing pre-complex and accumulates conflicts by head-to-head jam made by DNA and RNA synthesis machinery due to cell cycle arrest (155). Additionally, inhibition of GLI1 not only promotes cell cycle arrest it also impairs cell innate DNA damage response procedure. The DDR machinery is comprised of multiple sensors and repair enzymes that are deployed at various stages of the cell cycle to ensure the maintenance of chromosomal integrity and replicative fidelity. Numerous reports of overexpression of critical DDR component proteins in oncogenic environments indicate that chemo-resistance can arise due to over-activation of the MRE11, Rad50, NBS1 (MRN) complex. A critical component of the MRN complex is the Nijmegen breakage syndrome-1 (NBS1; p95, nibrin) protein, produced by NBS gene. Complexing with MRE11 and RAD50, NBS1 is the first factor to detect and bind to histone H2AX at the site of a DNA lesion which subsequently forms the multimeric MRN complex, initiating the process of DSBs repair (162–164). Overexpression of individual components of the MRN complex has been significantly associated with adverse clinical outcomes due to chemotherapeutic resistance. Therefore, induced novel therapeutic avenue would be to inhibit the DDR mechanism, allowing chemotherapeutic mechanisms that target DNA damage to work more effectively. The challenge, however, is to specifically eliminate DDR in cancer cells without affecting the normal and necessary functions of DDR in non-cancerous cells.

Ataxia-telangiectasia mutated (ATM) is a kinase that regulates a number of substrates, including the phosphorylation of NBS1, which is required to initiate and enhance NBS1's DDR activity. As such, several programs have attempted to develop various ATM inhibitors aimed to inhibit DDR (165). Unfortunately, ATM itself is not a specific therapeutic target because of its multiple domained nature, critical kinase function in normal cellular processes, and essential role in the maintenance of chromosome integrity at all phases of the cell cycle (166). Some studies reported that the level of phosphorylated NBS1 (Ser343), which is regulated by its upstream kinase ATM/ATR, is a critical phosphorylation status thought to increases DNA damage response and promotes cell survival. To test this theory, our lab overexpressed wild type NBS1, domain-negative NBS1 (S343A), or phospho-mimic NBS1 (S343E) in HT29 cells. Overexpression of any NBS1 vector rescued ~25% of cells from apoptosis mediated by GLI inhibition. Surprisingly, the overexpression of S343E, S343A, or total NBS1 was not statistically different from one another, indicating that total levels of NBS1, elevated by GLI1 transcription, rather than the phosphorylation status, were responsible for protection from GLI inhibition-induced apoptosis (64). Since GLI1 is not typically expressed by differentiated cells, targeting oncogenic expression of GLI1 would result in fewer off-target effects and provide a specific therapeutic strategy.

GLI1 INHIBITORS

Most of the efforts to-date have typically focused on targeting GLI inhibition through the canonical Hh pathway, targeting upstream regulators like SMO, and subsequently sequestering GLI1 in the cytoplasm. Five SMO inhibitors have been approved by the FDA for clinical trials: vismodegib (GDC-0449), sonidegib (NPV-LDE-225), saridegib (IPI-926), BMS-833923, glasdegib (PF-04449913), and taladegib (LY2940680) (167). Variable success using SMO inhibitors has been demonstrated across a variety of different cancer types in preclinical models (30, 31, 107, 168–171) and clinical models (172–177). This is due to the predominant dependence of certain types of human cancers on canonical Hh signaling, such as basal cell carcinoma (173, 177), and medulloblastoma (172). However, clinical trials in most solid tumors have failed, likely because of aforementioned non-canonical activation pathways (i.e., RAS-ERK, PI3K-AKT-mTORS6K1 signaling, p53 loss, epigenetic alterations, etc.). Therefore, direct targeting of GLI might represent a better choice to improve the antitumor activity of these drugs in such cases.

The library of GLI1 antagonists is not as extensive as that for SMO. The most commonly used small molecules are GANT58 and GANT61, which were identified in a cell-based GLI-dependent luciferase screening system (178). These two compounds belong to different chemical classes, with GANT61 being a hexahydropyrimidine derivative and GANT58 possessing a thiophene core with four pyridine rings. Compared to GANT58, GANT61 is more specific toward GLI proteins and effectively reduces GLI1 and GLI2 DNA-binding ability, inhibiting the Hh pathway with a half maximal effective concentration (EC50) of 5 μM in GLI1-expressing HEK293T cells (26). GANT61 binds to the GLI1 protein between ZF2 and ZF3, by interacting with Glu119 and Glu167, as demonstrated by *in silico* docking on the crystal structure of the ZF domain of GLI1 bound to DNA (119). Experimental analysis shows that mutation of the predicted binding sites significantly reduces GANT61-GLI binding affinity. The GANT61 binding site is different from the GLI DNA-binding region, and the inhibitor is not able to bind to other ZF transcription factors such as KLF4 or TFIIβ (26, 119). Unfortunately, GANT61 is not usable as a translational therapeutic as it is unstable and has poor PK properties (179).

Using GANT61 as an initial scaffold, Southern Research has recently developed a novel GLI1 inhibitor (SRI-38832) that has better PK properties and has shown efficacy *in vivo* (64). Additionally, there are several promising compounds showing the biological activity of GLI inhibition (180), arsenic trioxide (ATO), originally approved by the FDA for the treatment of acute promyelocytic leulemia, has been shown to inhibit GLI proteins by binding to GLI proteins and enhancing degradation (181). ATO is currently being tested in multiple clinical trials ranging from phase I to phase IV for either solid tumors and hematologic malignancies. However, recent reports indicate lack of efficacy against small cell lung cancer (182). Polyunsaturated fatty acids (PUFAs) have also been reported to repress GLI1 expression by stimulating GLI1 suppressor, nuclear factor of activated T cells 1 (NFATc1) expression (183). Glabrescione B (GlaB), an isoflavone naturally found in the seeds of Derris glabrescens, is able to bind the GLI1 ZF domain, thereby diminishing GLI1/DNA interaction (184). Leadiant Biosciences used Glabrescione B as their scaffold for generating a pool of compounds for GLI1 inhibition (185, 186). Computational modeling of the DNA/GLI1 protein interaction has also been used to develop an 8-hydroxyquinolines as a GLI1 inhibitors, with similar scaffolds as Lediant Bioscience's compounds (187). Finally, the Hedgehog pathway inhibitors (HPIs) including HPI-1, HPI-2, HPI-3, and HPI-4, were identified with a high-throughput screening for compounds capable of abolishing the Hh target gene expression induced by the SMO agonist SAG (188). HPI-1 can suppress Hh pathway activation, likely through targeting a posttranslational modification of the GLI proteins and/or an interaction between the transcription factor and a co-factor (189). The detailed mechanisms of action have not yet been completely unraveled.

One specific problem often encountered is the non-specificity of developed compounds claiming to be specific for GLI1 (i.e., also inhibit GLI2 and decrease GLI2 protein/messenger expression). The homology of GLI1 and GLI2, along with the similarities in the promotor recognition sequence makes it difficult to design an inhibitor of one without inadvertently targeting the other. Computational modeling and structural biology (NMR; crystallography) can help to resolve the challenge of non-specificity.

CONCLUSIONS

GLI1 exists at the conjunction of multiple oncogenic pathways outside of the canonically understood hedgehog pathway. In the scope of oncogenesis, GLI1 activation is particularly dominant in subsets of a number of cancer types because parallel non-canonical pathways outside of hedgehog signaling influence GLI1 function. Additionally, the list of GLI1 transcriptional targets continues to expand, encompassing cell cycle regulators (Cdt1), DNA damage repair proteins (NBS1), and proliferation (FOXM1). In certain cancers, it promotes a dedifferentiation to a more stem-like phenotype. Because of GLI1's regulatory fluidity, targeting upstream pathway members is often an exercise in futility, as seen by the failure of SMO inhibitors, for example. For this reason, GLI1 is a significant therapeutic target for the treatment of multiple cancer types.

Whether overexpressed due to canonical, non-canonical, or genetic mutation, elevated GLI1 expression drives several of the hallmarks of cancer including DNA damage repair, cell proliferation, and metastasis. Rather than target upstream regulators of GLI, targeting the distal effector provides the greatest potential for therapeutic benefit. Since GLI1 is canonically active in embryonic development, with minimal basal expression in differentiated cells, it 1) serves as a biomarker for de-differentiation in cancer cells, particularly those refractory to treatment and 2) provides a prominent target not readily expressed in most non-cancerous tissue. As such, by targeting the downstream effector (GLI1) rather than upstream activators, we can effectively inhibit the oncogenesis driven by aberrant GLI1 activation, and promote cancer-specific DNA damage. While many promising drug discovery campaigns are developing and looking for novel GLI1 inhibitors, more work needs to be done to develop a potent, specific inhibitory compound.

AUTHOR CONTRIBUTIONS

JA and RZ compiled the information and wrote the manuscript. RB reviewed and corrected the manuscript. JA and RZ have contributed equally to this work and share first authorship. All authors contributed to the article and approved the submitted version.

FUNDING

This work was supported by The National Institutes of Health [5RO1CA183921-05].

REFERENCES

1. Kumar S, Balczarek KA, Lai ZC. Evolution of the Hedgehog Gene Family. *Genetics* (1996) 142(3):965–72. doi: 10.1093/genetics/142.3.965
2. McMahon AP. More Surprises in the Hedgehog Signaling Pathway. *Cell* (2000) 100(2):185–8. doi: 10.1016/s0092-8674(00)81555-x
3. Ingham PW, Nakano Y, Seger C. Mechanisms and Functions of Hedgehog Signalling Across the Metazoa. *Nat Rev Genet* (2011) 12(6):393–406. doi: 10.1038/nrg2984
4. Mohler J. Requirements for Hedgehog, a Segmental Polarity Gene, in Patterning Larval and Adult Cuticle of Drosophila. *Genetics* (1988) 120 (4):1061–72. doi: 10.1093/genetics/120.4.1061
5. Belloni E, Muenke M, Roessler E, Traverso G, Siegel-Bartelt J, Frumkin A, et al. Identification of Sonic Hedgehog as a Candidate Gene Responsible for Holoprosencephaly. *Nat Genet* (1996) 14(3):353–6. doi: 10.1038/ng1196-353
6. Villavicencio EH, Walterhouse DO, Iannaccone PM. The Sonic Hedgehog-Patched-Gli Pathway in Human Development and Disease. *Am J Hum Genet* (2000) 67(5):1047–54. doi: 10.1016/S0002-9297(07)62934-6

7. Gritli-Linde A, Bei M, Maas R, Zhang XM, Linde A, McMahon AP. Shh Signaling Within the Dental Epithelium is Necessary for Cell Proliferation, Growth and Polarization. *Development* (2002) 129(23):5323–37. doi: 10.1242/dev.00100
8. Collins RT, Cohen SM. A Genetic Screen in Drosophila for Identifying Novel Components of the Hedgehog Signaling Pathway. *Genetics* (2005) 170 (1):173–84. doi: 10.1534/genetics.104.039420
9. Stone DM, Hynes M, Armanini M, Swanson TA, Gu Q, Johnson RL, et al. The Tumour-Suppressor Gene Patched Encodes a Candidate Receptor for Sonic Hedgehog. *Nature* (1996) 384(6605):129–34. doi: 10.1038/384129a0
10. Smyth I, Narang MA, Evans T, Heimann C, Nakamura Y, Chenevix-Trench G, et al. Isolation and Characterization of Human Patched 2 (PTCH2), a Putative Tumour Suppressor Gene Inbasal Cell Carcinoma and Medulloblastoma on Chromosome 1p32. *Hum Mol Genet* (1999) 8 (2):291–7. doi: 10.1093/hmg/8.2.291
11. Murone M, Rosenthal A, de Sauvage FJ. Sonic Hedgehog Signaling by the Patched-Smoothened Receptor Complex. *Curr Biol* (1999) 9(2):76–84. doi: 10.1016/s0960-9822(99)80018-9
12. Taipale J, Cooper MK, Maiti T, Beachy PA. Patched Acts Catalytically to Suppress the Activity of Smoothened. *Nature* (2002) 418(6900):892–7. doi: 10.1038/nature00989
13. Casali A, Struhl G. Reading the Hedgehog Morphogen Gradient by Measuring the Ratio of Bound to Unbound Patched Protein. *Nature* (2004) 431(7004):76–80. doi: 10.1038/nature02835
14. Pasca di Magliano M, Hebrok M. Hedgehog Signalling in Cancer Formation and Maintenance. *Nat Rev Cancer* (2003) 3(12):903–11. doi: 10.1038/nrc1229
15. Hegde GV, Munger CM, Emanuel K, Joshi AD, Greiner TC, Weisenburger DD, et al. Targeting of Sonic hedgehog-GLI Signaling: A Potential Strategy to Improve Therapy for Mantle Cell Lymphoma. *Mol Cancer Ther* (2008) 7 (6):1450–60. doi: 10.1158/1535-7163.MCT-07-2118
16. Goodrich LV, Milenkovic L, Higgins KM, Scott MP. Altered Neural Cell Fates and Medulloblastoma in Mouse Patched Mutants. *Science* (1997) 277 (5329):1109–13. doi: 10.1126/science.277.5329.1109
17. Oro AE, Higgins KM, Hu Z, Bonifas JM, Epstein EHJr., Scott MP. Basal Cell Carcinomas in Mice Overexpressing Sonic Hedgehog. *Science* (1997) 276 (5313):817–21. doi: 10.1126/science.276.5313.817
18. Watkins DN, Berman DM, Burkholder SG, Wang B, Beachy PA, Baylin SB. Hedgehog Signalling Within Airway Epithelial Progenitors and in Small-Cell Lung Cancer. *Nature* (2003) 422(6929):313–7. doi: 10.1038/nature01493
19. Bowman RV, Yang IA, Semmler AB, Fong KM. Epigenetics of Lung Cancer. *Respirology* (2006) 11(4):355–65. doi: 10.1111/j.1440-1843.2006.00859.x
20. Clement V, Sanchez P, de Tribolet N, Radovanovic I, Ruiz i Altaba A. Hedgehog-GLI1 Signaling Regulates Human Glioma Growth, Cancer Stem Cell Self-Renewal, and Tumorigenicity. *Curr Biol* (2007) 17(2):165–72. doi: 10.1016/j.cub.2006.11.033
21. Dierks C, Beigi R, Guo GR, Zirlik K, Stegert MR, Manley P, et al. Expansion of Bcr-Abl-positive Leukemic Stem Cells is Dependent on Hedgehog Pathway Activation. *Cancer Cell* (2008) 14(3):238–49. doi: 10.1016/j.ccr.2008.08.003
22. Goel A, Boland CR. Epigenetics of Colorectal Cancer. *Gastroenterology* (2012) 1431442–1460(6):e1441. doi: 10.1053/j.gastro.2012.09.032
23. Seeber LM, van Diest PJ. Epigenetics in Ovarian Cancer. *Methods Mol Biol* (2012) 863:253–69. doi: 10.1007/978-1-61779-612-8_15
24. Ozen C, Yildiz G, Dagcan AT, Cevik D, Ors A, Keles U, et al. Genetics and Epigenetics of Liver Cancer. *N Biotechnol* (2013) 30(4):381–4. doi: 10.1016/j.nbt.2013.01.007
25. Rimkus TK, Carpenter RL, Qasem S, Chan M, Lo HW. Targeting the Sonic Hedgehog Signaling Pathway: Review of Smoothened and GLI Inhibitors. *Cancers (Basel)* (2016) 8(2):22. doi: 10.3390/cancers8020022
26. Mastrangelo E, Milani M. Role and Inhibition of GLI1 Protein in Cancer. *Lung Cancer (Auckl)* (2018) 9:35–43. doi: 10.2147/LCTT.S124483
27. Zurawel RH, Allen C, Chiappa S, Cato W, Biegel J, Cogen P, et al. Analysis of PTCH/SMO/SHH Pathway Genes in Medulloblastoma. *Genes Chromosomes Cancer* (2000) 27(1):44–51. doi: 10.1002/(sici)1098-2264(200001)27:1<44::aid-gcc6>3.0.co;2-v
28. Pola R, Ling LE, Silver M, Corbley MJ, Kearney M, Blake Pepinsky R, et al. The Morphogen Sonic Hedgehog is an Indirect Angiogenic Agent Upregulating Two Families of Angiogenic Growth Factors. *Nat Med* (2001) 7(6):706–11. doi: 10.1038/89083
29. Walsh PC. Hedgehog Signalling in Prostate Regeneration, Neoplasia and Metastasis. *J Urol* (2005) 173(4):1169. doi: 10.1097/01.ju.0000156734.69186.57
30. Stecca B, Mas C, Clement V, Zbinden M, Correa R, Piguet V, et al. Melanomas Require HEDGEHOG-GLI Signaling Regulated by Interactions Between GLI1 and the RAS-MEK/AKT Pathways. *Proc Natl Acad Sci USA* (2007) 104(14):5895–900. doi: 10.1073/pnas.0700776104
31. Varnat F, Duquet A, Malerba M, Zbinden M, Mas C, Gervaz P, et al. Human Colon Cancer Epithelial Cells Harbour Active HEDGEHOG-GLI Signalling That is Essential for Tumour Growth, Recurrence, Metastasis and Stem Cell Survival and Expansion. *EMBO Mol Med* (2009) 1(6-7):338–51. doi: 10.1002/emmm.200900039
32. Xie J, Murone M, Luoh SM, Ryan A, Gu Q, Zhang C, et al. Activating Smoothened Mutations in Sporadic Basal-Cell Carcinoma. *Nature* (1998) 391(6662):90–2. doi: 10.1038/34201
33. Vorechovsky I, Unden AB, Sandstedt B, Toftgard R, Stahle-Backdahl M. Trichoepitheliomas Contain Somatic Mutations in the Overexpressed PTCH Gene: Support for a Gatekeeper Mechanism in Skin Tumorigenesis. *Cancer Res* (1997) 57(21):4677–81.
34. Maesawa C, Tamura G, Iwaya T, Ogasawara S, Ishida K, Sato N, et al. Mutations in the Human Homologue of the Drosophila Patched Gene in Esophageal Squamous Cell Carcinoma. *Genes Chromosomes Cancer* (1998) 21(3):276–9. doi: 10.1002/(SICI)1098-2264(199803)21:3<276::AID-GCC15>3.0.CO;2-N
35. McGarvey TW, Maruta Y, Tomaszewski JE, Linnenbach AJ, Malkowicz SB. PTCH Gene Mutations in Invasive Transitional Cell Carcinoma of the Bladder. *Oncogene* (1998) 17(9):1167–72. doi: 10.1038/sj.onc.1202045
36. Ruiz i Altaba A, Mas C, Stecca B. The Gli Code: An Information Nexus Regulating Cell Fate, Stemness and Cancer. *Trends Cell Biol* (2007) 17 (9):438–47. doi: 10.1016/j.tcb.2007.06.007
37. Kinzler KW, Bigner SH, Bigner DD, Trent JM, Law ML, O'Brien SJ, et al. Identification of an Amplified, Highly Expressed Gene in a Human Glioma. *Science* (1987) 236(4797):70–3. doi: 10.1126/science.3563490
38. Gupta S, Takebe N, Lorusso P. Targeting the Hedgehog Pathway in Cancer. *Ther Adv Med Oncol* (2010) 2(4):237–50. doi: 10.1177/1758834010366430
39. Skoda AM, Simovic D, Karin V, Kardum V, Vranic S, Serman L. The Role of the Hedgehog Signaling Pathway in Cancer: A Comprehensive Review. *Bosn J Basic Med Sci* (2018) 18(1):8–20. doi: 10.17305/bjbms.2018.2756
40. Yao Z, Han L, Chen Y, He F, Sun B, Kamar S, et al. Hedgehog Signalling in the Tumourigenesis and Metastasis of Osteosarcoma, and its Potential Value in the Clinical Therapy of Osteosarcoma. *Cell Death Dis* (2018) 9(6):701. doi: 10.1038/s41419-018-0647-1
41. Wong AJ, Bigner SH, Bigner DD, Kinzler KW, Hamilton SR, Vogelstein B. Increased Expression of the Epidermal Growth Factor Receptor Gene in Malignant Gliomas is Invariably Associated With Gene Amplification. *Proc Natl Acad Sci USA* (1987) 84(19):6899–903. doi: 10.1073/pnas.84.19.6899
42. Ruppert JM, Kinzler KW, Wong AJ, Bigner SH, Kao FT, Law ML, et al. The GLI-Kruppel Family of Human Genes. *Mol Cell Biol* (1988) 8(8):3104–13. doi: 10.1128/mcb.8.8.3104
43. Winklmayr M, Schmid C, Laner-Plamberger S, Kaser A, Aberger F, Eichberger T, et al. Non-Consensus GLI Binding Sites in Hedgehog Target Gene Regulation. *BMC Mol Biol* (2010) 11:2. doi: 10.1186/1471-2199-11-2
44. Bauer NC, Doetsch PW, Corbett AH. Mechanisms Regulating Protein Localization. *Traffic* (2015) 16(10):1039–61. doi: 10.1111/tra.12310
45. Han Y, Shi Q, Jiang J. Multisite Interaction With Sufu Regulates Ci/Gli Activity Through Distinct Mechanisms in Hh Signal Transduction. *Proc Natl Acad Sci USA* (2015) 112(20):6383–8. doi: 10.1073/pnas.1421628112
46. Han Y, Xiong Y, Shi X, Wu J, Zhao Y, Jiang J. Regulation of Gli Ciliary Localization and Hedgehog Signaling by the PY-NLS/karyopherin-beta2 Nuclear Import System. *PloS Biol* (2017) 15(8):e2002063. doi: 10.1371/journal.pbio.2002063
47. Carpenter RL, Lo HW. Hedgehog Pathway and GLI1 Isoforms in Human Cancer. *Discovery Med* (2012) 13(69):105–13.
48. Roessler E, Ermilov AN, Grange DK, Wang A, Grachtchouk M, Dlugosz AA, et al. A Previously Unidentified Amino-Terminal Domain Regulates Transcriptional Activity of Wild-Type and Disease-Associated Human GLI2. *Hum Mol Genet* (2005) 14(15):2181–8. doi: 10.1093/hmg/ddi222

49. Speek M, Njunkova O, Pata I, Valdre E, Kogerman P. A Potential Role of Alternative Splicing in the Regulation of the Transcriptional Activity of Human GLI2 in Gonadal Tissues. *BMC Mol Biol* (2006) 7:13. doi: 10.1186/1471-2199-7-13
50. Grachtchouk M, Pero J, Yang SH, Ermilov AN, Michael LE, Wang A, et al. Basal Cell Carcinomas in Mice Arise From Hair Follicle Stem Cells and Multiple Epithelial Progenitor Populations. *J Clin Invest* (2011) 121(5):1768–81. doi: 10.1172/JCI46307
51. Pantazi E, Gemenetzidis E, Trigiante G, Warnes G, Shan L, Mao X, et al. GLI2 Induces Genomic Instability in Human Keratinocytes by Inhibiting Apoptosis. *Cell Death Dis* (2014) 5:e1028. doi: 10.1038/cddis.2013.535
52. Tsanev R, Tiigimagi P, Michelson P, Metsis M, Osterlund T, Kogerman P. Identification of the Gene Transcription Repressor Domain of Gli3. *FEBS Lett* (2009) 583(1):224–8. doi: 10.1016/j.febslet.2008.12.010
53. Shimokawa T, Tostar U, Lauth M, Palaniswamy R, Kasper M, Toftgard R, et al. Novel Human Glioma-Associated Oncogene 1 (GLI1) Splice Variants Reveal Distinct Mechanisms in the Terminal Transduction of the Hedgehog Signal. *J Biol Chem* (2008) 283(21):14345–54. doi: 10.1074/jbc.M800299200
54. Pietrobono S, Gagliardi S, Stecca B. Non-Canonical Hedgehog Signaling Pathway in Cancer: Activation of GLI Transcription Factors Beyond Smoothened. *Front Genet* (2019) 10:556. doi: 10.3389/fgene.2019.00556
55. Lo HW, Zhu H, Cao X, Aldrich A, Ali-Osman F. A Novel Splice Variant of GLI1 That Promotes Glioblastoma Cell Migration and Invasion. *Cancer Res* (2009) 69(17):6790–8. doi: 10.1158/0008-5472.CAN-09-0886
56. Cao X, Geradts J, Dewhirst MW, Lo HW. Upregulation of VEGF-A and CD24 Gene Expression by the tGLI1 Transcription Factor Contributes to the Aggressive Behavior of Breast Cancer Cells. *Oncogene* (2012) 31(1):104–15. doi: 10.1038/onc.2011.219
57. Justilien V, Fields AP. Molecular Pathways: Novel Approaches for Improved Therapeutic Targeting of Hedgehog Signaling in Cancer Stem Cells. *Clin Cancer Res* (2015) 21(3):505–13. doi: 10.1158/1078-0432.CCR-14-0507
58. Hanna A, Shevde LA. Hedgehog Signaling: Modulation of Cancer Properies and Tumor Mircroenvironment. *Mol Cancer* (2016) 15:24. doi: 10.1186/s12943-016-0509-3
59. van den Brink GR, Bleuming SA, Hardwick JC, Schepman BL, Offerhaus GJ, Keller JJ, et al. Indian Hedgehog is an Antagonist of Wnt Signaling in Colonic Epithelial Cell Differentiation. *Nat Genet* (2004) 36(3):277–82. doi: 10.1038/ng1304
60. Taniguchi H, Yamamoto H, Akutsu N, Nosho K, Adachi Y, Imai K, et al. Transcriptional Silencing of Hedgehog-Interacting Protein by CpG Hypermethylation and Chromatic Structure in Human Gastrointestinal Cancer. *J Pathol* (2007) 213(2):131–9. doi: 10.1002/path.2216
61. Shi T, Mazumdar T, Devecchio J, Duan ZH, Agyeman A, Aziz M, et al. cDNA Microarray Gene Expression Profiling of Hedgehog Signaling Pathway Inhibition in Human Colon Cancer Cells. *PloS One* (2010) 5(10):E13054. doi: 10.1371/journal.pone.0013054
62. Stefanius K, Kantola T, Tuomisto A, Vahteristo P, Karttunen TJ, Aaltonen LA, et al. Downregulation of the Hedgehog Receptor PTCH1 in Colorectal Serrated Adenocarcinomas is Not Caused by PTCH1 Mutations. *Virchows Arch* (2011) 458(2):213–9. doi: 10.1007/s00428-010-1031-4
63. Li T, Liao X, Lochhead P, Morikawa T, Yamauchi M, Nishihara R, et al. SMO Expression in Colorectal Cancer: Associations With Clinical, Pathological, and Molecular Features. *Ann Surg Oncol* (2014) 21(13):4164–73. doi: 10.1245/s10434-014-3888-y
64. Zhang R, Ma J, Avery JT, Sambandam V, Nguyen TH, Xu B, et al. Gli1 Inhibitor Sri-38832 Attenuates Chemotherapeutic Resistance by Downregulating Nbs1 Transcription in BRAF(V600E) Colorectal Cancer. *Front Oncol* (2020) 10:241. doi: 10.3389/fonc.2020.00241
65. Dlugosz A, Agrawal S, Kirkpatrick P. Vismodegib. *Nat Rev Drug Discov* (2012) 11(6):437–8. doi: 10.1038/nrd3753
66. Berlin J, Bendell JC, Hart LL, Firdaus I, Gore I, Hermann RC, et al. A Randomized Phase II Trial of Vismodegib Versus Placebo With FOLFOX or FOLFIRI and Bevacizumab in Patients With Previously Untreated Metastatic Colorectal Cancer. *Clin Cancer Res* (2013) 19(1):258–67. doi: 10.1158/1078-0432.CCR-12-1800
67. Taipale J, Chen JK, Cooper MK, Wang B, Mann RK, Milenkovic L, et al. Effects of Oncogenic Mutations in Smoothened and Patched can be Reversed by Cyclopamine. *Nature* (2000) 406(6799):1005–9. doi: 10.1038/35023008
68. Das S, Samant RS, Shevde LA. Nonclassical Activation of Hedgehog Signaling Enhances Multidrug Resistance and Makes Cancer Cells Refractory to Smoothened-targeting Hedgehog Inhibition. *J Biol Chem* (2013) 288(17):11824–33. doi: 10.1074/jbc.M112.432302
69. Palle K, Mani C, Tripathi K, Athar M. Aberrant GLI1 Activation in DNA Damage Response, Carcinogenesis and Chemoresistance. *Cancers (Basel)* (2015) 7(4):2330–51. doi: 10.3390/cancers7040894
70. Samatar AA, Poulikakos PI. Targeting RAS-ERK Signalling in Cancer: Promises and Challenges. *Nat Rev Drug Discov* (2014) 13(12):928–42. doi: 10.1038/nrd4281
71. Rovida E, Stecca B. Mitogen-Activated Protein Kinases and Hedgehog-GLI Signaling in Cancer: A Crosstalk Providing Therapeutic Opportunities? *Semin Cancer Biol* (2015) 35:154–67. doi: 10.1016/j.semcancer.2015.08.003
72. Seto M, Ohta M, Asaoka Y, Ikenoue T, Tada M, Miyabayashi K, et al. Regulation of the Hedgehog Signaling by the Mitogen-Activated Protein Kinase Cascade in Gastric Cancer. *Mol Carcinog* (2009) 48(8):703–12. doi: 10.1002/mc.20516
73. Schnidar H, Eberl M, Klingler S, Mangelberger D, Kasper M, Hauser-Kronberger C, et al. Epidermal Growth Factor Receptor Signaling Synergizes With Hedgehog/GLI in Oncogenic Transformation *Via* Activation of the MEK/ERK/JUN Pathway. *Cancer Res* (2009) 69(4):1284–92. doi: 10.1158/0008-5472.CAN-08-2331
74. Schneider P, Bayo-Fina JM, Singh R, Kumar Dhanyamraju P, Holz P, Baier A, et al. Identification of a Novel Actin-Dependent Signal Transducing Module Allows for the Targeted Degradation of GLI1. *Nat Commun* (2015) 6:8023. doi: 10.1038/ncomms9023
75. Savona MR, Pollyea DA, Stock W, Oehler VG, Schroeder MA, Lancet J, et al. Phase Ib Study of Glasdegib, a Hedgehog Pathway Inhibitor, in Combination With Standard Chemotherapy in Patients With AML or High-Risk Mds. *Clin Cancer Res* (2018) 24(10):2294–303. doi: 10.1158/1078-0432.CCR-17-2824
76. Riobo NA, Lu K, Ai X, Haines GM, Emerson CPJr. Phosphoinositide 3-Kinase and Akt are Essential for Sonic Hedgehog Signaling. *Proc Natl Acad Sci U.S.A.* (2006) 103(12):4505–10. doi: 10.1073/pnas.0504337103
77. Singh R, Dhanyamraju PK, Lauth M. DYRK1B Blocks Canonical and Promotes non-Canonical Hedgehog Signaling Through Activation of the mTOR/AKT Pathway. *Oncotarget* (2017) 8(1):833–45. doi: 10.18632/oncotarget.13662
78. Wang Y, Ding Q, Yen CJ, Xia W, Izzo JG, Lang JY, et al. The Crosstalk of mTOR/S6K1 and Hedgehog Pathways. *Cancer Cell* (2012) 21(3):374–87. doi: 10.1016/j.ccr.2011.12.028
79. Mizuarai S, Kawagishi A, Kotani H. Inhibition of p70S6K2 Down-Regulates Hedgehog/GLI Pathway in non-Small Cell Lung Cancer Cell Lines. *Mol Cancer* (2009) 8:44. doi: 10.1186/1476-4598-8-44
80. Jones S, Zhang X, Parsons DW, Lin JC, Leary RJ, Angenendt P, et al. Core Signaling Pathways in Human Pancreatic Cancers Revealed by Global Genomic Analyses. *Science* (2008) 321(5897):1801–6. doi: 10.1126/science.1164368
81. Principe DR, DeCant B, Mascarinas E, Wayne EA, Diaz AM, Akagi N, et al. Tgfbeta Signaling in the Pancreatic Tumor Microenvironment Promotes Fibrosis and Immune Evasion to Facilitate Tumorigenesis. *Cancer Res* (2016) 76(9):2525–39. doi: 10.1158/0008-5472.CAN-15-1293
82. Grusch M, Petz M, Metzner T, Ozturk D, Schneller D, Mikulits W. The Crosstalk of RAS With the TGF-beta Family During Carcinoma Progression and its Implications for Targeted Cancer Therapy. *Curr Cancer Drug Targets* (2010) 10(8):849–57. doi: 10.2174/156800910793357943
83. Nye MD, Almada LL, Fernandez-Barrena MG, Marks DL, Elsawa SF, Vrabel A, et al. The Transcription Factor GLI1 Interacts With SMAD Proteins to Modulate Transforming Growth Factor Beta-Induced Gene Expression in a p300/CREB-binding Protein-Associated Factor (PCAF)-Dependent Manner. *J Biol Chem* (2014) 289(22):15495–506. doi: 10.1074/jbc.M113.545194
84. Nolan-Stevaux O, Lau J, Truitt ML, Chu GC, Hebrok M, Fernandez-Zapico ME, et al. GLI1 is Regulated Through Smoothened-independent Mechanisms in Neoplastic Pancreatic Ducts and Mediates PDAC Cell Survival and Transformation. *Genes Dev* (2009) 23(1):24–36. doi: 10.1101/gad.1753809
85. Yoon JW, Gallant M, Lamm ML, Iannaccone S, Vieux KF, Proytcheva M, et al. Noncanonical Regulation of the Hedgehog Mediator GLI1 by c-MYC

in Burkitt Lymphoma. *Mol Cancer Res* (2013) 11(6):604–15. doi: 10.1158/1541-7786.MCR-12-0441
86. Goel HL, Pursell B, Chang C, Shaw LM, Mao J, Simin K, et al. GLI1 Regulates a Novel neuropilin-2/alpha6beta1 Integrin Based Autocrine Pathway That Contributes to Breast Cancer Initiation. *EMBO Mol Med* (2013) 5(4):488–508. doi: 10.1002/emmm.201202078
87. Atwood SX, Li M, Lee A, Tang JY, Oro AE. GLI Activation by Atypical Protein Kinase C Iota/Lambda Regulates the Growth of Basal Cell Carcinomas. *Nature* (2013) 494(7438):484–8. doi: 10.1038/nature11889
88. Jiang K, Liu Y, Fan J, Epperly G, Gao T, Jiang J, et al. Hedgehog-regulated Atypical PKC Promotes Phosphorylation and Activation of Smoothened and Cubitus Interruptus in Drosophila. *Proc Natl Acad Sci USA* (2014) 111 (45):E4842–50. doi: 10.1073/pnas.1417147111
89. Stecca B, Ruiz i Altaba A. A GLI1-p53 Inhibitory Loop Controls Neural Stem Cell and Tumour Cell Numbers. *EMBO J* (2009) 28(6):663–76. doi: 10.1038/emboj.2009.16
90. Sjoblom T, Jones S, Wood LD, Parsons DW, Lin J, Barber TD, et al. The Consensus Coding Sequences of Human Breast and Colorectal Cancers. *Science* (2006) 314(5797):268–74. doi: 10.1126/science.1133427
91. Lees CW, Zacharias WJ, Tremelling M, Noble CL, Nimmo ER, Tenesa A, et al. Analysis of Germline GLI1 Variation Implicates Hedgehog Signalling in the Regulation of Intestinal Inflammatory Pathways. *PloS Med* (2008) 5 (12):e239. doi: 10.1371/journal.pmed.0050239
92. Liu JA, Lai FP, Gui HS, Sham MH, Tam PK, Garcia-Barcelo MM, et al. Identification of GLI Mutations in Patients With Hirschsprung Disease That Disrupt Enteric Nervous System Development in Mice. *Gastroenterology* (2015) 1491837-1848(7):e1835. doi: 10.1053/j.gastro.2015.07.060
93. Lucchesi C, Khalifa E, Laizet Y, Soubeyran I, Mathoulin-Pelissier S, Chomienne C, et al. Targetable Alterations in Adult Patients With Soft-Tissue Sarcomas: Insights for Personalized Therapy. *JAMA Oncol* (2018) 4 (10):1398–404. doi: 10.1001/jamaoncol.2018.0723
94. Newell F, Kong Y, Wilmott JS, Johansson PA, Ferguson PM , Cui C, et al. Whole-Genome Landscape of Mucosal Melanoma Reveals Diverse Drivers and Therapeutic Targets. *Nat Commun* (2019) 10(1):3163. doi: 10.1038/s41467-019-11107-x
95. Wilmott JS, Johansson PA, Newell F, Waddell N, Ferguson P, Quek C, et al. Whole Genome Sequencing of Melanomas in Adolescent and Young Adults Reveals Distinct Mutation Landscapes and the Potential Role of Germline Variants in Disease Susceptibility. *Int J Cancer* (2019) 144(5):1049–60. doi: 10.1002/ijc.31791
96. Dahlen A, Mertens F, Mandahl N, Panagopoulos I. Molecular Genetic Characterization of the Genomic ACTB-GLI Fusion in Pericytoma With T(7;12). *Biochem Biophys Res Commun* (2004) 325(4):1318–23. doi: 10.1016/j.bbrc.2004.10.172
97. Kerr DA, Pinto A, Subhawong TK, Wilky BA, Schlumbrecht MP, Antonescu CR, et al. Pericytoma With T(7;12) and ACTB-GLI1 Fusion: Reevaluation of an Unusual Entity and its Relationship to the Spectrum of GLI1 Fusion-Related Neoplasms. *Am J Surg Pathol* (2019) 43(12):1682–92. doi: 10.1097/PAS.0000000000001360
98. Antonescu CR, Agaram NP, Sung YS, Zhang L, Swanson D, Dickson BC. A Distinct Malignant Epithelioid Neoplasm With Gli1 Gene Rearrangements, Frequent S100 Protein Expression, and Metastatic Potential: Expanding the Spectrum of Pathologic Entities With Actb/Malat1/Ptch1-GLI1 Fusions. *Am J Surg Pathol* (2018) 42(4):553–60. doi: 10.1097/PAS.0000000000001010
99. Bai CB, Auerbach W, Lee JS, Stephen D, Joyner AL. Gli2, But Not Gli1, is Required for Initial Shh Signaling and Ectopic Activation of the Shh Pathway. *Development* (2002) 129(20):4753–61. doi: 10.1242/dev.129.20.4753
100. Ikram MS, Neill GW, Regl G, Eichberger T, Frischauf AM, Aberger F, et al. GLI2 is Expressed in Normal Human Epidermis and BCC and Induces GLI1 Expression by Binding to its Promoter. *J Invest Dermatol* (2004) 122 (6):1503–9. doi: 10.1111/j.0022-202X.2004.22612.x
101. Thiyagarajan S, Bhatia N, Reagan-Shaw S, Cozma D, Thomas-Tikhonenko A, Ahmad N, et al. Role of GLI2 Transcription Factor in Growth and Tumorigenicity of Prostate Cells. *Cancer Res* (2007) 67(22):10642–6. doi: 10.1158/0008-5472.CAN-07-2015
102. Katoh Y, Katoh M. Hedgehog Target Genes: Mechanisms of Carcinogenesis Induced by Aberrant Hedgehog Signaling Activation. *Curr Mol Med* (2009) 9 (7):873–86. doi: 10.2174/156652409789105570
103. Kasper M, Schnidar H, Neill GW, Hanneder M, Klingler S, Blaas L, et al. Selective Modulation of Hedgehog/GLI Target Gene Expression by Epidermal Growth Factor Signaling in Human Keratinocytes. *Mol Cell Biol* (2006) 26(16):6283–98. doi: 10.1128/MCB.02317-05
104. Ruiz i Altaba A. Gli Proteins Encode Context-Dependent Positive and Negative Functions: Implications for Development and Disease. *Development* (1999) 126(14):3205–16. doi: 10.1242/dev.126.14.3205
105. Khatib ZA, Matsushime H, Valentine M, Shapiro DN, Sherr CJ, Look AT. Coamplification of the CDK4 Gene With MDM2 and GLI in Human Sarcomas. *Cancer Res* (1993) 53(22):5535–41.
106. Zurawel RH, Allen C, Wechsler-Reya R, Scott MP, Raffel C. Evidence That Haploinsufficiency of Ptch Leads to Medulloblastoma in Mice. *Genes Chromosomes Cancer* (2000) 28(1):77–81. doi: 10.1002/(SICI)1098-2264(200005)28:1<77::AID-GCC9>3.0.CO;2-Y
107. Sanchez P, Hernandez AM, Stecca B, Kahler AJ, DeGueme AM, Barrett A, et al. Inhibition of Prostate Cancer Proliferation by Interference With SONIC Hedgehog-GLI1 Signaling. *Proc Natl Acad Sci USA* (2004) 101 (34):12561–6. doi: 10.1073/pnas.0404956101
108. Hu X, Lai D, Chen W, Zi S, Li J, Du P, et al. Differential Expression Profiles of the Hedgehog Signaling Pathway Between Microsatellite-Stable and Microsatellite-Unstable Colorectal Cancers. *Mol Med Rep* (2011) 4(5):873–7. doi: 10.3892/mmr.2011.529
109. Kasper M, Regl G, Frischauf AM, Aberger F. GLI Transcription Factors: Mediators of Oncogenic Hedgehog Signalling. *Eur J Cancer* (2006) 42 (4):437–45. doi: 10.1016/j.ejca.2005.08.039
110. Eichberger T, Sander V, Schnidar H, Regl G, Kasper M, Schmid C, et al. Overlapping and Distinct Transcriptional Regulator Properties of the GLI1 and GLI2 Oncogenes. *Genomics* (2006) 87(5):616–32. doi: 10.1016/j.ygeno.2005.12.003
111. Yoshikawa K, Shimada M, Miyamoto H, Higashijima J, Miyatani T, Nishioka M, et al. Sonic Hedgehog Relates to Colorectal Carcinogenesis. *J Gastroenterol* (2009) 44(11):1113–7. doi: 10.1007/s00535-009-0110-2
112. Mazumdar T, DeVecchio J, Shi T, Jones J, Agyeman A, Houghton JA. Hedgehog Signaling Drives Cellular Survival in Human Colon Carcinoma Cells. *Cancer Res* (2011) 71(3):1092–102. doi: 10.1158/0008-5472.CAN-10-2315
113. Varnat F, Zacchetti G, Ruiz i Altaba A. Hedgehog Pathway Activity is Required for the Lethality and Intestinal Phenotypes of Mice With Hyperactive Wnt Signaling. *Mech Dev* (2010) 127(1-2):73–81. doi: 10.1016/j.mod.2009.10.005
114. Wu C, Zhu X, Liu W, Ruan T, Tao K. Hedgehog Signaling Pathway in Colorectal Cancer: Function, Mechanism, and Therapy. *Onco Targets Ther* (2017) 10:3249–59. doi: 10.2147/OTT.S139639
115. N IJ, Rijnierse A, de Wit N, Jonker-Termont D, Dekker J, Muller M, et al. Dietary Haem Stimulates Epithelial Cell Turnover by Downregulating Feedback Inhibitors of Proliferation in Murine Colon. *Gut* (2012) 61 (7):1041–9. doi: 10.1136/gutjnl-2011-300239
116. Song J, Zhang J, Wang J, Wang J, Guo X, Dong W. Beta1 Integrin Mediates Colorectal Cancer Cell Proliferation and Migration Through Regulation of the Hedgehog Pathway. *Tumour Biol* (2015) 36(3):2013–21. doi: 10.1007/s13277-014-2808-x
117. Gulino A, Ferretti E, De Smaele E. Hedgehog Signalling in Colon Cancer and Stem Cells. *EMBO Mol Med* (2009) 1(6-7):300–2. doi: 10.1002/emmm.200900042
118. Chowdhury S, Pradhan RN, Sarkar RR. Structural and Logical Analysis of a Comprehensive Hedgehog Signaling Pathway to Identify Alternative Drug Targets for Glioma, Colon and Pancreatic Cancer. *PloS One* (2013) 8(7): e69132. doi: 10.1371/journal.pone.0069132
119. Agyeman A, Jha BK, Mazumdar T, Houghton JA. Mode and Specificity of Binding of the Small Molecule GANT61 to GLI Determines Inhibition of GLI-DNA Binding. *Oncotarget* (2014) 5(12):4492–503. doi: 10.18632/oncotarget.2046
120. Ciucci A, De Stefano I, Vellone VG, Lisi L, Bottoni C, Scambia G, et al. Expression of the Glioma-Associated Oncogene Homolog 1 (gli1) in Advanced Serous Ovarian Cancer is Associated With Unfavorable Overall Survival. *PloS One* (2013) 8(3):e60145. doi: 10.1371/journal.pone.0060145
121. Chung JH, Larsen AR, Chen E, Bunz F. A PTCH1 Homolog Transcriptionally Activated by p53 Suppresses Hedgehog Signaling. *J Biol Chem* (2014) 289(47):33020–31. doi: 10.1074/jbc.M114.597203

122. Ramasamy TS, Ayob AZ, Myint HH, Thiagarajah S, Amini F. Targeting Colorectal Cancer Stem Cells Using Curcumin and Curcumin Analogues: Insights Into the Mechanism of the Therapeutic Efficacy. *Cancer Cell Int* (2015) 15:96. doi: 10.1186/s12935-015-0241-x
123. Curtin JC, Lorenzi MV. Drug Discovery Approaches to Target Wnt Signaling in Cancer Stem Cells. *Oncotarget* (2010) 1(7):563–77. doi: 10.18632/oncotarget.191
124. Roy S, Majumdar AP. Signaling in Colon Cancer Stem Cells. *J Mol Signal* (2012) 7(1):11. doi: 10.1186/1750-2187-7-11
125. Ramirez A, Boulaiz H, Morata-Tarifa C, Peran M, Jimenez G, Picon-Ruiz M, et al. HER2-Signaling Pathway, JNK and ERKs Kinases, and Cancer Stem-Like Cells are Targets of Bozepinib Small Compound. *Oncotarget* (2014) 5 (11):3590–606. doi: 10.18632/oncotarget.1962
126. So JY, Suh N. Targeting Cancer Stem Cells in Solid Tumors by Vitamin D. *J Steroid Biochem Mol Biol* (2015) 148:79–85. doi: 10.1016/j.jsbmb.2014.10.007
127. Zhang X, Zhang SS, Wei GJ, Deng ZM, Hu Y. Dysregulation of Hedgehog Signaling Pathway Related Components in the Evolution of Colonic Carcinogenesis. *Int J Clin Exp Med* (2015) 8(11):21379–85.
128. Miyazaki Y, Matsubara S, Ding Q, Tsukasa K, Yoshimitsu M, Kosai K, et al. Efficient Elimination of Pancreatic Cancer Stem Cells by Hedgehog/GLI Inhibitor GANT61 in Combination With mTOR Inhibition. *Mol Cancer* (2016) 15(1):49. doi: 10.1186/s12943-016-0534-2
129. Yang Z, Cui Y, Ni W, Kim S, Xuan Y. Gli1, a Potential Regulator of Esophageal Cancer Stem Cell, is Identified as an Independent Adverse Prognostic Factor in Esophageal Squamous Cell Carcinoma. *J Cancer Res Clin Oncol* (2017) 143(2):243–54. doi: 10.1007/s00432-016-2273-6
130. Lv L, Yang Z, Ma T, Xuan Y. Gli1, a Potential Cancer Stem Cell Marker, is Strongly Associated With Prognosis in Prostate Cancer. *Int J Clin Exp Pathol* (2018) 11(10):4957–66.
131. Yang Z, Zhang C, Qi W, Cui Y, Xuan Y. GLI1 Promotes Cancer Stemness Through Intracellular Signaling Pathway PI3K/Akt/NFkappaB in Colorectal Adenocarcinoma. *Exp Cell Res* (2018) 373(1-2):145–54. doi: 10.1016/j.yexcr.2018.10.006
132. Li D, Xie K, Wolff R, Abbruzzese JL. Pancreatic Cancer. *Lancet* (2004) 363 (9414):1049–57. doi: 10.1016/S0140-6736(04)15841-8
133. Stathis A, Moore MJ. Advanced Pancreatic Carcinoma: Current Treatment and Future Challenges. *Nat Rev Clin Oncol* (2010) 7(3):163–72. doi: 10.1038/nrclinonc.2009.236
134. Grutzmann R, Pilarsky C, Ammerpohl O, Luttges J, Bohme A, Sipos B, et al. Gene Expression Profiling of Microdissected Pancreatic Ductal Carcinomas Using High-Density DNA Microarrays. *Neoplasia* (2004) 6(5):611–22. doi: 10.1593/neo.04295
135. Lim KH, Counter CM. Reduction in the Requirement of Oncogenic Ras Signaling to Activation of PI3K/AKT Pathway During Tumor Maintenance. *Cancer Cell* (2005) 8(5):381–92. doi: 10.1016/j.ccr.2005.10.014
136. Collins MA, Bednar F, Zhang Y, Brisset JC, Galban S, Galban CJ, et al. Oncogenic Kras is Required for Both the Initiation and Maintenance of Pancreatic Cancer in Mice. *J Clin Invest* (2012) 122(2):639–53. doi: 10.1172/JCI59227
137. Hahn SA, Schmiegel WH. Recent Discoveries in Cancer Genetics of Exocrine Pancreatic Neoplasia. *Digestion* (1998) 59(5):493–501. doi: 10.1159/000007526
138. Scheffzek K, Ahmadian MR, Kabsch W, Wiesmuller L, Lautwein A, Schmitz F, et al. The Ras-RasGAP Complex: Structural Basis for GTPase Activation and its Loss in Oncogenic Ras Mutants. *Science* (1997) 277(5324):333–8. doi: 10.1126/science.277.5324.333
139. Scheidig AJ, Burmester C, Goody RS. The Pre-Hydrolysis State of p21(ras) in Complex With GTP: New Insights Into the Role of Water Molecules in the GTP Hydrolysis Reaction of Ras-Like Proteins. *Structure* (1999) 7(11):1311–24. doi: 10.1016/s0969-2126(00)80021-0
140. Kim ST, Lim DH, Jang KT, Lim T, Lee J, Choi YL, et al. Impact of KRAS Mutations on Clinical Outcomes in Pancreatic Cancer Patients Treated With First-Line Gemcitabine-Based Chemotherapy. *Mol Cancer Ther* (2011) 10 (10):1993–9. doi: 10.1158/1535-7163.MCT-11-0269
141. Kotoula V, Charalambous E, Biesmans B, Malousi A, Vrettou E, Fountzilas G, et al. Targeted KRAS Mutation Assessment on Patient Tumor Histologic Material in Real Time Diagnostics. *PloS One* (2009) 4(11):e7746. doi: 10.1371/journal.pone.0007746
142. Tuveson DA, Shaw AT, Willis NA, Silver DP, Jackson EL, Chang S, et al. Endogenous Oncogenic K-ras(G12D) Stimulates Proliferation and Widespread Neoplastic and Developmental Defects. *Cancer Cell* (2004) 5 (4):375–87. doi: 10.1016/s1535-6108(04)00085-6
143. Ji Z, Mei FC, Xie J, Cheng X. Oncogenic KRAS Activates Hedgehog Signaling Pathway in Pancreatic Cancer Cells. *J Biol Chem* (2007) 282(19):14048–55. doi: 10.1074/jbc.M611089200
144. Fabian D, Guillermo Prieto Eibl MDP, Alnahhas I, Sebastian N, Giglio P, Puduvalli V, et al. Treatment of Glioblastoma (GBM) With the Addition of Tumor-Treating Fields (Ttf): A Review. *Cancers (Basel)* (2019) 11(2):174. doi: 10.3390/cancers11020174
145. Lee SY. Temozolomide Resistance in Glioblastoma Multiforme. *Genes Dis* (2016) 3(3):198–210. doi: 10.1016/j.gendis.2016.04.007
146. Jiapaer S, Furuta T, Tanaka S, Kitabayashi T, Nakada M. Potential Strategies Overcoming the Temozolomide Resistance for Glioblastoma. *Neurol Med Chir (Tokyo)* (2018) 58(10):405–21. doi: 10.2176/nmc.ra.2018-0141
147. Wick W, Weller M, van den Bent M, Sanson M, Weiler M, von Deimling A, et al. MGMT Testing–the Challenges for Biomarker-Based Glioma Treatment. *Nat Rev Neurol* (2014) 10(7):372–85. doi: 10.1038/nrneurol.2014.100
148. Wang K, Chen D, Qian Z, Cui D, Gao L, Lou M. Hedgehog/Gli1 Signaling Pathway Regulates MGMT Expression and Chemoresistance to Temozolomide in Human Glioblastoma. *Cancer Cell Int* (2017) 17:117. doi: 10.1186/s12935-017-0491-x
149. Yan W, Zhang W, You G, Zhang J, Han L, Bao Z, et al. Molecular Classification of Gliomas Based on Whole Genome Gene Expression: A Systematic Report of 225 Samples From the Chinese Glioma Cooperative Group. *Neuro Oncol* (2012) 14(12):1432–40. doi: 10.1093/neuonc/nos263
150. Li J, Cai J, Zhao S, Yao K, Sun Y, Li Y, et al. GANT61, a GLI Inhibitor, Sensitizes Glioma Cells to the Temozolomide Treatment. *J Exp Clin Cancer Res* (2016) 35(1):184. doi: 10.1186/s13046-016-0463-3
151. Melamed JR, Morgan JT, Ioele SA, Gleghorn JP, Sims-Mourtada J, Day ES. Investigating the Role of Hedgehog/GLI1 Signaling in Glioblastoma Cell Response to Temozolomide. *Oncotarget* (2018) 9(43):27000–15. doi: 10.18632/oncotarget.25467
152. Zafar A, Wang W, Liu G, Wang X, Xian W, McKeon F, et al. Molecular Targeting Therapies for Neuroblastoma: Progress and Challenges. *Med Res Rev* (2020) 41(2):961–1021. doi: 10.1002/med.21750
153. Koche RP, Rodriguez-Fos E, Helmsauer K, Burkert M, MacArthur IC, Maag J, et al. Extrachromosomal Circular DNA Drives Oncogenic Genome Remodeling in Neuroblastoma. *Nat Genet* (2020) 52(1):29–34. doi: 10.1038/s41588-019-0547-z
154. Ain Q, Schmeer C, Wengerodt D, Witte OW, Kretz A. Extrachromosomal Circular Dna: Current Knowledge and Implications for CNS Aging and Neurodegeneration. *Int J Mol Sci* (2020) 21(7):2477. doi: 10.3390/ijms21072477
155. Zhang R, Wu J, Ferrandon S, Glowacki KJ, Houghton JA. Targeting GLI by GANT61 Involves Mechanisms Dependent on Inhibition of Both Transcription and DNA Licensing. *Oncotarget* (2016) 7(49):80190–207. doi: 10.18632/oncotarget.13376
156. Li X, Deng W, Lobo-Ruppert SM, Ruppert JM. Gli1 Acts Through Snail and E-cadherin to Promote Nuclear Signaling by Beta-Catenin. *Oncogene* (2007) 26(31):4489–98. doi: 10.1038/sj.onc.1210241
157. Zheng X, Song T, Dou C, Jia Y, Liu Q. CtBP2 is an Independent Prognostic Marker That Promotes GLI1 Induced Epithelial-Mesenchymal Transition in Hepatocellular Carcinoma. *Oncotarget* (2015) 6(6):3752–69. doi: 10.18632/oncotarget.2915
158. Liao X, Siu MK, Au CW, Chan QK, Chan HY, Wong ES, et al. Aberrant Activation of Hedgehog Signaling Pathway Contributes to Endometrial Carcinogenesis Through Beta-Catenin. *Mod Pathol* (2009) 22(6):839–47. doi: 10.1038/modpathol.2009.45
159. Harrison W, Cochrane B, Neill G, Philpott M. The Oncogenic GLI Transcription Factors Facilitate Keratinocyte Survival and Transformation Upon Exposure to Genotoxic Agents. *Oncogene* (2014) 33(19):2432–40. doi: 10.1038/onc.2013.199
160. Frappart PO, Lee Y, Russell HR, Chalhoub N, Wang YD, Orii KE, et al. Recurrent Genomic Alterations Characterize Medulloblastoma Arising From DNA Double-Strand Break Repair Deficiency. *Proc Natl Acad Sci USA* (2009) 106(6):1880–5. doi: 10.1073/pnas.0806882106

161. Mazumdar T, Devecchio J, Agyeman A, Shi T, Houghton JA. Blocking Hedgehog Survival Signaling at the Level of the GLI Genes Induces DNA Damage and Extensive Cell Death in Human Colon Carcinoma Cells. *Cancer Res* (2011) 71(17):5904–14. doi: 10.1158/0008-5472.CAN-10-4173
162. Varon R, Vissinga C, Platzer M, Cerosaletti KM, Chrzanowska KH, Saar K, et al. Nibrin, a Novel DNA Double-Strand Break Repair Protein, is Mutated in Nijmegen Breakage Syndrome. *Cell* (1998) 93(3):467–76. doi: 10.1016/s0092-8674(00)81174-5
163. Kobayashi J, Antoccia A, Tauchi H, Matsuura S, Komatsu K. NBS1 and its Functional Role in the DNA Damage Response. *DNA Repair (Amst)* (2004) 3 (8-9):855–61. doi: 10.1016/j.dnarep.2004.03.023
164. Antoccia A, Kobayashi J, Tauchi H, Matsuura S, Komatsu K. Nijmegen Breakage Syndrome and Functions of the Responsible Protein, NBS1. *Genome Dyn* (2006) 1:191–205. doi: 10.1159/000092508
165. Ronco C, Martin AR, Demange L, Benhida R. Atm, ATR, Chk1, CHK2 and WEE1 Inhibitors in Cancer and Cancer Stem Cells. *Medchemcomm* (2017) 8 (2):295–319. doi: 10.1039/c6md00439c
166. Boohaker RJ, Xu B. The Versatile Functions of ATM Kinase. *BioMed J* (2014) 37(1):3–9. doi: 10.4103/2319-4170.125655
167. Pietrobono S, Stecca B. Targeting the Oncoprotein Smoothened by Small Molecules: Focus on Novel Acylguanidine Derivatives as Potent Smoothened Inhibitors. *Cells* (2018) 7(12):272. doi: 10.3390/cells7120272
168. Ecke I, Rosenberger A, Obenauer S, Dullin C, Aberger F, Kimmina S, et al. Cyclopamine Treatment of Full-Blown Hh/Ptch-associated RMS Partially Inhibits Hh/Ptch Signaling, But Not Tumor Growth. *Mol Carcinog* (2008) 47 (5):361–72. doi: 10.1002/mc.20394
169. Robarge KD, Brunton SA, Castanedo GM, Cui Y, Dina MS, Goldsmith R, et al. Gdc-0449-a Potent Inhibitor of the Hedgehog Pathway. *Bioorg Med Chem Lett* (2009) 19(19):5576–81. doi: 10.1016/j.bmcl.2009.08.049
170. Sarangi A, Valadez JG, Rush S, Abel TW, Thompson RC, Cooper MK. Targeted Inhibition of the Hedgehog Pathway in Established Malignant Glioma Xenografts Enhances Survival. *Oncogene* (2009) 28(39):3468–76. doi: 10.1038/onc.2009.208
171. Mas C, Ruiz i Altaba A. Small Molecule Modulation of HH-GLI Signaling: Current Leads, Trials and Tribulations. *Biochem Pharmacol* (2010) 80 (5):712–23. doi: 10.1016/j.bcp.2010.04.016
172. Rudin CM, Hann CL, Laterra J, Yauch RL, Callahan CA, Fu L, et al. Treatment of Medulloblastoma With Hedgehog Pathway Inhibitor GDC-0449. *N Engl J Med* (2009) 361(12):1173–8. doi: 10.1056/NEJMoa0902903
173. Von Hoff DD, LoRusso PM, Rudin CM, Reddy JC, Yauch RL, Tibes R, et al. Inhibition of the Hedgehog Pathway in Advanced Basal-Cell Carcinoma. *N Engl J Med* (2009) 361(12):1164–72. doi: 10.1056/NEJMoa0905360
174. De Smaele E, Ferretti E, Gulino A. Vismodegib, a Small-Molecule Inhibitor of the Hedgehog Pathway for the Treatment of Advanced Cancers. *Curr Opin Investig Drugs* (2010) 11(6):707–18.
175. Dierks C. Gdc-0449–targeting the Hedgehog Signaling Pathway. *Recent Results Cancer Res* (2010) 184:235–8. doi: 10.1007/978-3-642-01222-8_17
176. Low JA, de Sauvage FJ. Clinical Experience With Hedgehog Pathway Inhibitors. *J Clin Oncol* (2010) 28(36):5321–6. doi: 10.1200/JCO.2010.27.9943
177. LoRusso PM, Rudin CM, Reddy JC, Tibes R, Weiss GJ, Borad MJ, et al. Phase I Trial of Hedgehog Pathway Inhibitor Vismodegib (GDC-0449) in Patients With Refractory, Locally Advanced or Metastatic Solid Tumors. *Clin Cancer Res* (2011) 17(8):2502–11. doi: 10.1158/1078-0432.CCR-10-2745
178. Lauth M, Bergstrom A, Shimokawa T, Toftgard R. Inhibition of GLI-mediated Transcription and Tumor Cell Growth by Small-Molecule Antagonists. *Proc Natl Acad Sci USA* (2007) 104(20):8455–60. doi: 10.1073/pnas.0609699104
179. Calcaterra A, Iovine V, Botta B, Quaglio D, D'Acquarica I, Ciogli A, et al. Chemical, Computational and Functional Insights Into the Chemical Stability of the Hedgehog Pathway Inhibitor GANT61. *J Enzyme Inhib Med Chem* (2018) 33(1):349–58. doi: 10.1080/14756366.2017.1419221
180. Peer E, Tesanovic S, Aberger F. Next-Generation Hedgehog/GLI Pathway Inhibitors for Cancer Therapy. *Cancers (Basel)* (2019) 11(4):538. doi: 10.3390/cancers11040538
181. Beauchamp EM, Ringer L, Bulut G, Sajwan KP, Hall MD, Lee YC, et al. Arsenic Trioxide Inhibits Human Cancer Cell Growth and Tumor Development in Mice by Blocking Hedgehog/GLI Pathway. *J Clin Invest* (2011) 121(1):148–60. doi: 10.1172/JCI42874
182. Owonikoko TK, Zhang G, Kim HS, Stinson RM, Bechara R, Zhang C, et al. Patient-Derived Xenografts Faithfully Replicated Clinical Outcome in a Phase II Co-Clinical Trial of Arsenic Trioxide in Relapsed Small Cell Lung Cancer. *J Transl Med* (2016) 14(1):111. doi: 10.1186/s12967-016-0861-5
183. Comba A, Almada LL, Tolosa EJ, Iguchi E, Marks DL, Vara Messler M, et al. Nuclear Factor of Activated T Cells-Dependent Down-regulation of the Transcription Factor Glioma-associated Protein 1 (Gli1) Underlies the Growth Inhibitory Properties of Arachidonic Acid. *J Biol Chem* (2016) 291 (4):1933–47. doi: 10.1074/jbc.M115.691972
184. Infante P, Mori M, Alfonsi R, Ghirga F, Aiello F, Toscano S, et al. Gli1/DNA Interaction is a Druggable Target for Hedgehog-dependent Tumors. *EMBO J* (2015) 34(2):200–17. doi: 10.15252/embj.201489213
185. Giannini G, Taddei M, Manetti F, Petricci E, Stecca B. Gli1 Inhibitors and Uses Thereof. (2017).
186. Manetti F, Stecca B, Santini R, Maresca L, Giannini G, Taddei M, et al. Pharmacophore-Based Virtual Screening for Identification of Negative Modulators of GLI1 as Potential Anticancer Agents. *ACS Med Chem Lett* (2020) 11(5):832–8. doi: 10.1021/acsmedchemlett.9b00639
187. Dash RC, Wen J, Zaino AM, Morel SR, Chau LQ, Wechsler-Reya RJ, et al. Structure-Based Virtual Screening Identifies an 8-Hydroxyquinoline as a Small Molecule GLI1 Inhibitor. *Mol Ther Oncolytics* (2021) 20:265–76. doi: 10.1016/j.omto.2021.01.004
188. Chen JK, Taipale J, Young KE, Maiti T, Beachy PA. Small Molecule Modulation of Smoothened Activity. *Proc Natl Acad Sci USA* (2002) 99 (22):14071–6. doi: 10.1073/pnas.182542899
189. Hyman JM, Firestone AJ, Heine VM, Zhao Y, Ocasio CA, Han K, et al. Small-Molecule Inhibitors Reveal Multiple Strategies for Hedgehog Pathway Blockade. *Proc Natl Acad Sci USA* (2009) 106(33):14132–7. doi: 10.1073/pnas.0907134106

Conflict of Interest: The authors declare that the research was conducted in the absence of any commercial or financial relationships that could be construed as a potential conflict of interest.

frontiers in Cell and Developmental Biology

ORIGINAL RESEARCH
published: 01 July 2021
doi: 10.3389/fcell.2021.652325

NTNG1 Modulates Cisplatin Resistance in Epithelial Ovarian Cancer Cells via the GAS6/AXL/Akt Pathway

*Shanyu Fang, Yuanyuan Luo, Ying Zhang, Houmei Wang, Qianfen Liu, Xinya Li and Tinghe Yu**

Laboratory of Obstetrics and Gynecology, The Second Affiliated Hospital, Chongqing Medical University, Chongqing, China

Cisplatin resistance is a challenge in the treatment of epithelial ovarian cancer. Here, clinical data showed that the level of netrin-G1 (NTNG1) in cisplatin-resistant cancer was higher than that in cisplatin-sensitive cancer (2.2-fold, $p = 0.005$); patients with a high NTNG1 level in cancer tissues had shorter progression-free survival (11.0 vs. 25.0 months, $p = 0.010$) and platinum-free interval (5.0 vs. 20.0 months, $p = 0.021$) compared with patients with a low level. Category- or stage-adjusted analyses demonstrated that the association between the NTNG1 level and prognosis occurred in type II or FIGO III/IV cancer. The basal level of NTNG1 in SKOV3/DDP cells (a cisplatin-resistant subline) was higher than that in SKOV3 cells; therefore, NTNG1 was overexpressed in SKOV3 cells, or silenced in SKOV3/DDP cells. Knocking in NTNG1 reduced the action of cisplatin to decrease cell death and apoptosis of SKOV3 cells, accompanied by upregulation of p-AXL, p-Akt and RAD51; however, opposite effects were observed in SKOV3/DDP cells after knocking down NTNG1. Co-immunoprecipitation demonstrated that NTNG1 bound GAS6/AXL. Silencing NTNG1 enhanced cisplatin effects *in vivo*, decreasing tumor volume/mass. These data suggested that a high NTNG1 level can result in cisplatin resistance in ovarian cancer cells via the GAS6/AXL/Akt pathway and that NTNG1 may be a useful target to overcome resistance.

Keywords: NTNG1, cisplatin resistance, ovarian cancer, Axl, DNA repair

OPEN ACCESS

Edited by:
David Y. Lee,
University of New Mexico,
United States

Reviewed by:
Tuan Zea Tan,
National University of Singapore,
Singapore
Jareer Kassis,
Bien-Etre Labs, LLC, United States

****Correspondence:***
Tinghe Yu
yutinghe@hotmail.com;
yutinghe@cqmu.edu.cn

Specialty section:
This article was submitted to Molecular and Cellular Oncology, a section of the journal Frontiers in Cell and Developmental Biology

Received: *12 January 2021*
Accepted: *13 April 2021*
Published: *01 July 2021*

Citation:
Fang S, Luo Y, Zhang Y, Wang H, Liu Q, Li X and Yu T (2021) NTNG1 Modulates Cisplatin Resistance in Epithelial Ovarian Cancer Cells via the GAS6/AXL/Akt Pathway. Front. Cell Dev. Biol. 9:652325. doi: 10.3389/fcell.2021.652325

INTRODUCTION

Ovarian cancer is the most lethal gynecologic malignancy worldwide; epithelial cancer (EOC) accounts for >85% of cases. The standard treatment for EOC is cytoreductive surgery, followed by cisplatin (CDDP)-based chemotherapy. However, the 5-year survival rate is <40%, since the gradually increasing cisplatin resistance during treatment leads to treatment failure (Christie and Bowtell, 2017; Coburn et al., 2017).

Mechanisms of cisplatin resistance are only partially understood. Cisplatin commonly attacks DNA leading to apoptosis; therefore, an increase in DNA repair and activation of survival pathways can result in cisplatin resistance, and numerous candidate genes have been identified

(Gasparri et al., 2018; Damia and Broggini, 2019). Understanding the functions of these molecules will help identify targets to overcome cisplatin resistance.

Netrin-G1 (NTNG1, also known as laminet-1) belongs to the family of netrins and interacts with diverse single-pass surface receptors to mediate cell repulsion, attraction, and adhesion (Sun et al., 2011). NTNG1 contains an extracellular N-terminal laminin-like domain and a C-terminal glycosylphosphatidylinositol (GPI) anchor; NTNG1 predominantly tethers to the membrane through the GPI anchor, promoting outgrowth of thalamocortical axons (Yin et al., 2002; Lin et al., 2003). It has been shown that abnormal expression of the NTNG1 gene plays a role in the occurrence and recurrence of colorectal cancer, and that an alteration in NTNG1 activity is related to poor prognosis via disruption of the extracellular matrix (Yi et al., 2011; Sho et al., 2017). However, the role of NTNG1 in ovarian cancer remains unclear.

The receptor tyrosine kinase AXL triggers cancer progression. AXL interacts with its ligand growth arrest-specific 6 (GAS6), promoting cell adhesion, survival, and proliferation via activation of the ERK or Akt pathway (Graham et al., 2014). Recent data have indicated that AXL may participate in cisplatin resistance. AXL can prevent DNA damage due to drugs and promote DNA repair by upregulating the expression of RAD51, a key protein for homologous recombination (HR) (Balaji et al., 2017; Kim et al., 2017; Rose et al., 2020). High expression of AXL is associated with lower therapeutic responses and poorer prognosis in ovarian cancer; thus, AXL is a candidate molecule to conquer cisplatin resistance (Kim et al., 2015; Suh et al., 2015; Tian et al., 2021). However, underlying mechanisms are poorly understood.

Our protein interaction analysis showed that NTNG1 can interact with GAS6, suggesting that the role of NTNG1 may correlate with AXL. Here, the correlation between the expression level of NTNG1 and cisplatin response in ovarian cancer was evaluated using online datasets, and the role of NTNG1 in cisplatin resistance was explored with knock-in and knockdown experiments. Preliminary data indicated that NTNG1 bound GAS6/AXL to activate the Akt pathway, thereby modulating the response of ovarian cancer cells to cisplatin.

MATERIALS AND METHODS

Bioinformatic Analyses

GSE45553 and GSE73935 datasets from the Gene Expression Omnibus (GEO) that contained mRNA profiles of cisplatin-sensitive and -resistant human ovarian cancer cell lines were analyzed. The GSE45553 dataset was for OVCAR-8 and OVCAR-8C, and GSE73935 was for A2780 and A2780-C; OVCAR-8C and A2780-C were cisplatin-resistant sublines. Interactions of the target gene and proteins were analyzed in the Biological General Repository for Interaction Datasets (BioGRID)[1] (Oughtred et al., 2019).

The KM plotter[2] was used to explore the relationship between the expression level of the target gene and progression-free survival (PFS) in patients with ovarian cancer (Zhou et al., 2019).

Patients and Cancer Tissues

The use of human tissues was ethically approved by the local Institutional Review Board. Paraffin-embedded tumor tissues were collected from 67 EOC patients, who underwent cytoreductive surgery followed by cisplatin-based chemotherapy at the Second Affiliated Hospital, Chongqing Medical University (Chongqing, China) from August 2009 to June 2018. Clinical data (i.e., age, pathological type/grade, FIGO stage, therapeutic responses, and survival) were recorded. Resistance was defined as tumors that recurred or progressed within 6 months of the last dose, and sensitivity was defined as tumors that relapsed after 6 months (Matsuura et al., 2017). The therapeutic outcome was reflected using PFS and the platinum-free interval (PFI). PFS was the interval from the date of initial surgery to the date of progression/recurrence or last contact (censored), and PFI was the interval from the end of cisplatin treatment to the date of progression/recurrence or last contact (censored). PFS/PFI received stage- or category-adjusted analyses. Type I cancer included low-grade serous, clear cell, and endometrioid cancers; type II was high-grade serous cancer (Salazar et al., 2018).

Detection of NTNG1 in Cancer Tissues With an Immunohistochemical Assay

An immunohistochemical assay was performed to detect NTNG1 in cancer tissues with a streptavidin–peroxidase kit (ZSGB-BIO, Beijing, China), using an anti-NTNG1 antibody (GeneTex, Irvine, CA, United States). The expression level of NTNG1 was quantified using the software Image-Pro Plus (Media Cybernetics, Rockville, MD, United States) and was expressed with the mean density (i.e., integrated absorbance/area). The cutoff value of a high/low expression level was determined using the receiver operator characteristic curve.

Cells

Human EOC cell lines SKOV3 and SKOV3/DDP (identified by STR; Cell Bank, Type Culture Collect., Chin. Acad. Sci., Shanghai, China) were cultured in RPMI 1640 medium (Gibco, Beijing, China) enriched with 10% fetal bovine serum (Biol. Ind., Kibbutz Beit Haemek, Israel) at 37°C and 5% CO_2. SKOV3/DDP was a resistant subline that can grow in the presence of 0.75 μg/mL of cisplatin (Yunnan Phytopharm., Kunming, China); cells were transferred to cisplatin-free medium for 5 days before performing experiments to avoid interference induced by residual drugs (Yu et al., 2015, 2016; Qian et al., 2019; Liu et al., 2020).

Cell Viability

Cells were seeded in a 96-well plate (5.0×10^3 cells per well) and then exposed to cisplatin (0, 0.5, 1.0, 2.0, 4.0, 8.0, and 16.0 μg/mL). Cell viability was determined with a CCK-8 assay

[1] https://thebiogrid.org

[2] http://kmplot.com/analysis/

(Dojindo Lab., Kumamoto, Japan) after 48 h. The half-maximal inhibition concentration (IC_{50}) was calculated using the probit regression. For transfected cells, cells were subjected to cisplatin (IC_{50}) and cell viability was determined after 24, 48, and 72 h.

Cell Transfection

A lentiviral vector of shNTNG1 (GenePharma, Shanghai, China) was used to downregulate NTNG1 in SKOV3/DDP cells, and a lentiviral vector of NTNG1 (GenePharma) was adopted to upregulate NTNG1 in SKOV3 cells. shNTNG1, shNC, NTNG1, or NC was transferred into cells with the Polybrene kit (GenePharma). Puromycin (Solarbio Life Sci., Beijing, China) was added into the medium to remove uninfected cells, thereby obtaining stably transfected cells. The siRNA sequences were as follows: shNTNG1, 5′-CCAAGCCTCTCCAGGTTAA-3′, and shNC, 5′-TTCTCCGAACGTGTCACGT-3′. NC was the negative control (i.e., empty vector).

Western Blotting

Proteins were extracted after cells were exposed to cisplatin (IC_{50}) for 48 h using ice-cold RIPA buffer (Beyotime, Chongqing, China) supplemented with phenylmethanesulfonyl fluoride (PMSF); the concentration was determined with a BCA kit (Beyotime). Proteins were separated by SDS-PAGE and transferred to a PVDF membrane (Merck Millipore, Billerica, MA, United States). Primary antibodies were as follows: anti-NTNG1 (GeneTex), anti-RAD51 (Abcam, Cambridge, United Kingdom), anti-AXL/p-AXL (Cell Signaling Technology, Danvers, MA, United States), anti-Akt/p-Akt (Cell Signaling Technol.), anti-GAS6 (Bioss Biotechnology, Beijing, China), and anti-β-actin (Proteintech, Wuhan, China). The secondary antibody was a goat anti-rabbit IgG antibody (Abcam). Bands were analyzed with the software Image Lab (Bio-Rad Lab., Hercules, CA, United States). The density ratio was used to calibrate the level of a target protein, with β-actin as the reference.

To detect the expression level of NTNG1 after cisplatin exposure, proteins were extracted after SKOV3 or SKOV3/DDP cells were exposed to cisplatin (IC_{50} or $0.5 \times IC_{50}$) for 48 h, or after SKOV3/DDP cells were cultured in cisplatin-free medium for 3, 5, 7, and 9 days.

Cell Apoptosis

Cells were treated with cisplatin (IC_{50}), and then apoptotic cells were detected using an Annexin V assay (Elabscience, Wuhan, China) after 48 h.

Detection of γ-H2A.X Using an Immunofluorescent Assay

Cells were exposed to cisplatin (IC_{50}) for 48 h, fixed with 4% paraformaldehyde for 30 min, blocked with 10% BSA for 1 h, and incubated with anti-γ-H2A.X antibody (Alexa Fluor-647 conjugate; Abcam) overnight at 4°C in the dark. Nuclei were counterstained with DAPI (Beyotime). Cells were observed under a confocal microscope (Nikon, Tokyo, Japan), and the fluorescence intensity was determined with Image-Pro Plus.

Co-immunoprecipitation

Co-immunoprecipitation (coIP) was performed to validate the interaction between NTNG1 and GAS6/AXL. Protein A/G beads (MedChemExpress, Monmouth Junction, NJ, United States) were incubated with the primary antibody against NTNG1 (Santa Cruz Biotechnol., Dallas, TX, United States) with shaking for 1 h. NTNG1/NC-transfected SKOV3 cells were lysed in prechilled RIPA buffer supplemented with PMSF, protein A/G beads were added, and the mixture was shaken for 1 h. The beads were washed, and the eluted proteins were subjected to western blotting to detect NTNG1, GAS6, AXL, and p-AXL.

In vivo Therapies

The use of laboratory animals was ethically and scientifically approved by the local Institutional Review Board in compliance with the Care and Use of Laboratory Animals. A total of 1.0×10^6 NC− or NTNG1-transfected SKOV3 cells, and shNC− or shNTNG1-transfected SKOV3/DDP cells, were subcutaneously injected into the left armpit of 4-week-old female BALB/c nude mice (Cavens Lab. Anim., Changzhou, China), with five animals in each group. Cisplatin (10 mg/kg) was injected via a tail vein every 4 days at four times in groups NC + CDDP and NTNG1 + CDDP for SKOV3 tumors, and in groups shNC + CDDP and shNTNG1 + CDDP for SKOV3/DDP tumors; mice in the remaining groups received normal saline. The tumor volume was calibrated every 4 days [(length × width^2)/2]. Animals were euthanized 4 days after

TABLE 1 | Clinicopathological characteristics and their associations with the expression level of NTNG1 in ovarian cancer tissues.

Clinicopathological variables	Case no.	NTNG1 expression level		*p*-value
		Low (*n* = 39)	High (*n* = 28)	
Age (year)				
<50	23	13 (56.5%)	10 (43.5%)	0.840
≥50	44	26 (59.1%)	18 (40.9%)	
Histological type				
Serous	59	34 (57.6%)	25 (42.4%)	0.386
Clear cell	7	5 (71.4%)	2 (28.6%)	
Endometrioid	1	0 (0.0%)	1 (100.0%)	
Pathological grade				
1/2	25	12 (48.0%)	13 (52.0%)	0.191
3	42	27 (64.3%)	15 (35.7%)	
Category				
Type I	32	17 (53.1%)	15 (46.9%)	0.420
Type II	35	22 (62.9%)	13 (37.1%)	
FIGO stage				
I/II	22	15 (68.2%)	7 (31.8%)	0.247
III/IV	45	24 (53.3%)	21 (46.7%)	
Cisplatin response*				
Resistant	23	7 (30.4%)	16 (69.6%)	0.001
Sensitive	44	32 (72.7%)	12 (27.3%)	

**Resistance was that tumors recurred or progressed within 6 months from the last dose, and sensitivity was that tumors relapsed after 6 months.*

the last dose; tumors were removed, weighed, and pathologically examined. NTNG1 and RAD51 proteins in tumor tissues were immunohistochemically detected.

Statistics

Data were processed with the SPSS software (IBM, Armonk, NY, United States). Analysis of variance was used, and multiple comparisons were performed with the *t*-test. The correlation between the NTNG1 level and clinicopathological variables was analyzed with the chi-square test. PFS and PFI were evaluated with the Kaplan–Meier method. The difference was significant if the *p*-value was <0.05.

RESULTS

A High Expression Level of NTNG1 in Cancer Tissues Indicated Chemoresistance and a Poorer Prognosis

Bioinformatic analyses of the GSE45553 and GSE73935 datasets indicated that NTNG1 was a candidate gene involved in cisplatin resistance in ovarian cancer; the BioGRID demonstrated an interaction between NTNG1 and GAS6. The expression level of NTNG1 in cisplatin-resistant cell lines was higher than in cisplatin-sensitive cell lines ($\log_2$ fold change, 2.3–4.0). The KM plotter indicated that a higher expression level of the NTNG1 gene was related to a shorter PFS of ovarian cancer patients in overall as well as in the subgroup that received cisplatin treatments ($p = 0.005$, $p < 0.001$) (**Supplementary Figures 1, 2**).

To verify the aforementioned results, the correlation between the expression level of NTNG1 protein in cancer tissues and clinicopathological variables in 67 EOC cases was explored (**Table 1**). The NTNG1 level was higher in resistant cancers compared with sensitive cancers (0.0124 ± 0.0021 vs. 0.0056 ± 0.0009, $p = 0.005$) (**Figures 1A,B**); the cutoff value was 0.0066. Predictive values were 57.1% (95% confidence interval [CI]: 37.6–76.7%) and 82.1% (95% CI: 69.4–94.7%) when using a high level for resistance and a low level for sensitivity, respectively ($p = 0.032$). Patients with a high NTNG1 level in cancer tissues had shorter PFS [median: 11.0 (95% CI 8.9–13.0) vs. 25.0 (95% CI: 17.1–32.9) months, $p = 0.010$] and PFI [median: 5.0 (95% CI: 2.7–7.3) vs. 20.0 (95% CI: 13.9–26.1) months, $p = 0.021$], compared with those with a low level (**Figures 1C,D**). Adjusted analyses showed that the correlation between the high NTNG1 level and the poorer prognosis was observed in type II and FIGO III/IV cancers (**Supplementary Figure 3**). Overall, the data demonstrated that a high level of NTNG1 in cancer tissues indicated poorer therapeutic responses and outcomes.

A High NTNG1 Level Caused Cisplatin Resistance

The IC_{50} values were 1.4 and 4.2 μg/mL for SKOV3 and SKOV3/DDP cells, respectively, confirming the resistance

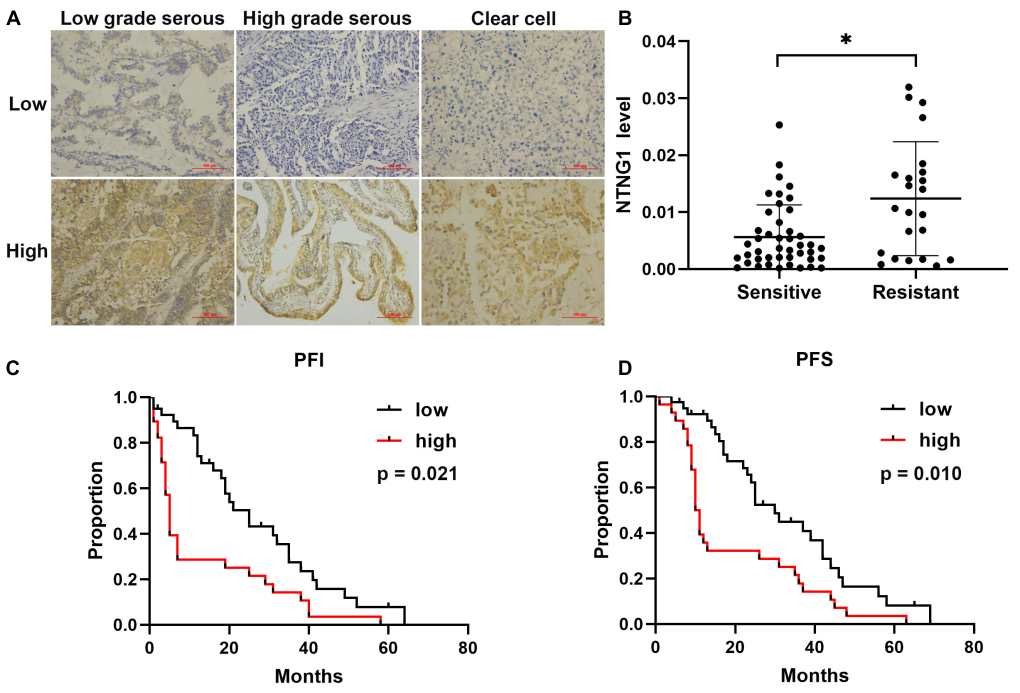

FIGURE 1 | Level of correlated with cisplatin response and prognosis in patients with ovarian cancer ($n = 67$). **(A)** Representative immunohistochemical images of NTNG1 protein in cancer tissues; scale = 100 μm. **(B)** Expression level of NTNG1 in cisplatin-sensitive or -resistant cancer tissues; a higher level was observed in resistant cancers. **(C,D)** Kaplan–Meier analyses of platinum-free interval (PFI) and progression-free survival (PFS); patients with a high NTNG1 level in cancer tissues had shorter PFI and PFS compared with those with a low level. $^*p < 0.05$.

phenotype of SKOV3/DDP (**Figure 2A**). NTNG1 was detected in both cell lines, and the basal expression level in SKOV3/DDP was higher than that in SKOV3 (2.1-fold, $p < 0.001$) (**Figure 2B**). Therefore, SKOV3 and SKOV3/DDP were used for knock-in and knockdown experiments, respectively.

Following exposure to cisplatin, the level of NTNG1 dose-dependently increased in SKOV3 (2.6- to 4.2-fold, $p < 0.001$) and SKOV3/DDP (1.6- to 2.0-fold, $p < 0.001$) cells (**Figure 2C**). In SKOV3/DDP cells, this increased level gradually decreased to the basal level following the removal of cisplatin ($p = 0.007$) (**Figure 2D**).

Overexpression of NTNG1 decreased the percentages of dead and apoptotic cells induced by cisplatin in SKOV3 cells ($p = 0.006$–0.030, $p = 0.004$) (**Figures 3A,C,E,F**). These percentages were increased in SKOV3/DDP cells after silencing NTNG1 ($p = 0.004$–0.018, $p = 0.011$) (**Figures 3B,D,E,G**). Cisplatin-induced expression of NTNG1 was also observed following knock-in or knockdown. The findings demonstrated that NTNG1 was involved in cisplatin resistance.

NTNG1 Promoted DNA Repair

DNA damage/repair was assayed by detecting γ-H2A.X and RAD51. γ-H2A.X was involved in the retention of repair complexes at sites of DNA damage, and RAD51 was a key molecule for HR (Bonner et al., 2008; Zhao et al., 2017). Cisplatin induced the formation of γ-H2A.X foci and an increase in the RAD51 level in both cell lines, i.e., initiating DNA repair. Overexpressing NTNG1 increased the RAD51 level in SKOV3 cells ($p = 0.002$), while the γ-H2A.X level decreased ($p = 0.023$) (**Figures 4A,B,E**). Silencing NTNG1 reduced the RAD51 level in SKOV3/DDP cells ($p = 0.001$), but the γ-H2A.X level was increased ($p = 0.025$) (**Figures 4C,D,F**). These data showed that NTNG1 upregulated the expression of RAD51, favoring DNA repair.

NTNG1 Improved DNA Repair Through the AXL/Akt Pathway

The BioGRID database indicated an interaction between NTNG1 and GAS6, suggesting that NTNG1 can activate the AXL/Akt pathway to enhance DNA repair. Cisplatin caused DNA damage, inducing phosphorylation of AXL/Akt; the levels of p-Akt and p-AXL were increased in SKOV3 cells following overexpression of NTNG1 ($p = 0.012$, $p = 0.013$) (**Figures 5A–C**), but were decreased in SKOV3/DDP cells following silencing of NTNG1 ($p = 0.001$, $p = 0.002$) (**Figures 5D–F**).

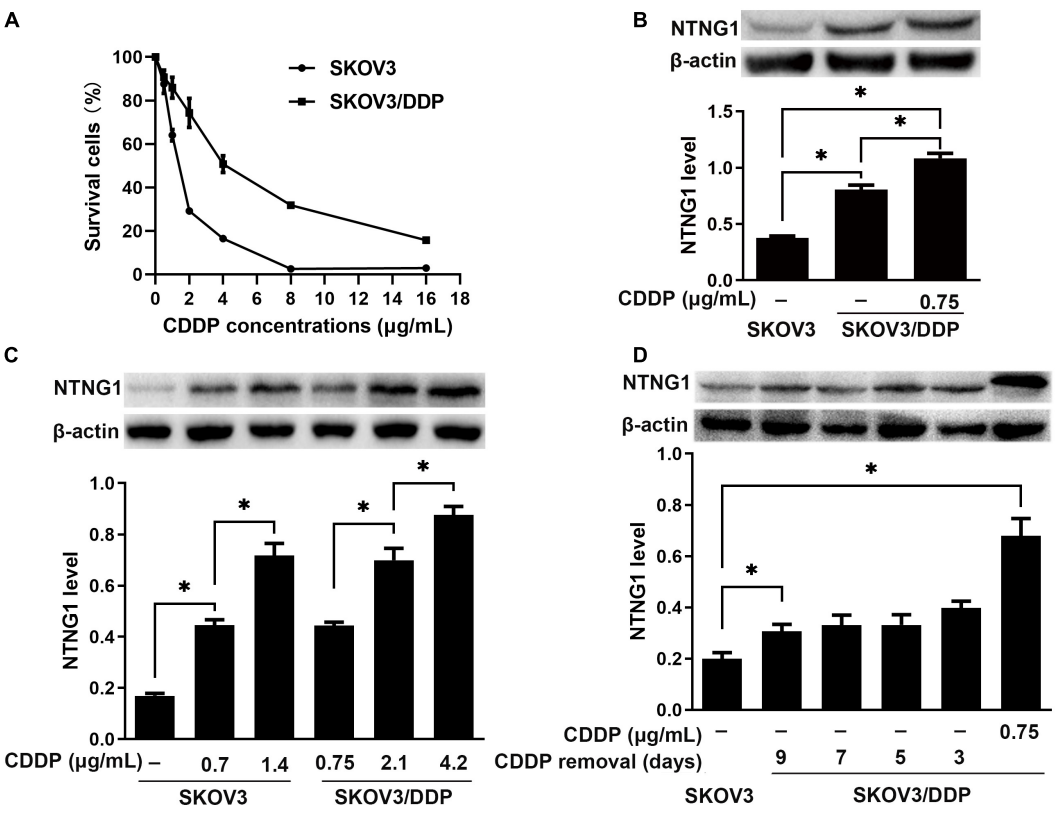

FIGURE 2 | The level of NTNG1 was increased in cisplatin-resistant ovarian cancer cells ($n = 3$). **(A)** Cell survival (%) following cisplatin exposure; higher values were noted in SKOV3/DDP cells, confirming the resistance phenotype. **(B)** Expression level of NTNG1 was assayed by western blotting; the basal level in SKOV3/DDP cells (determined 5 days after cisplatin removal) was higher than that in SKOV3 cells; cisplatin induced its expression in SKOV3/DDP cells. **(C)** The level of NTNG1 increased with increasing concentration of cisplatin in SKOV3 and SKOV3/DDP cells. **(D)** The expression level of NTNG1 in SKOV3/DDP cells gradually decreased to the basal level following cisplatin removal. CDDP, cisplatin. *$p < 0.05$.

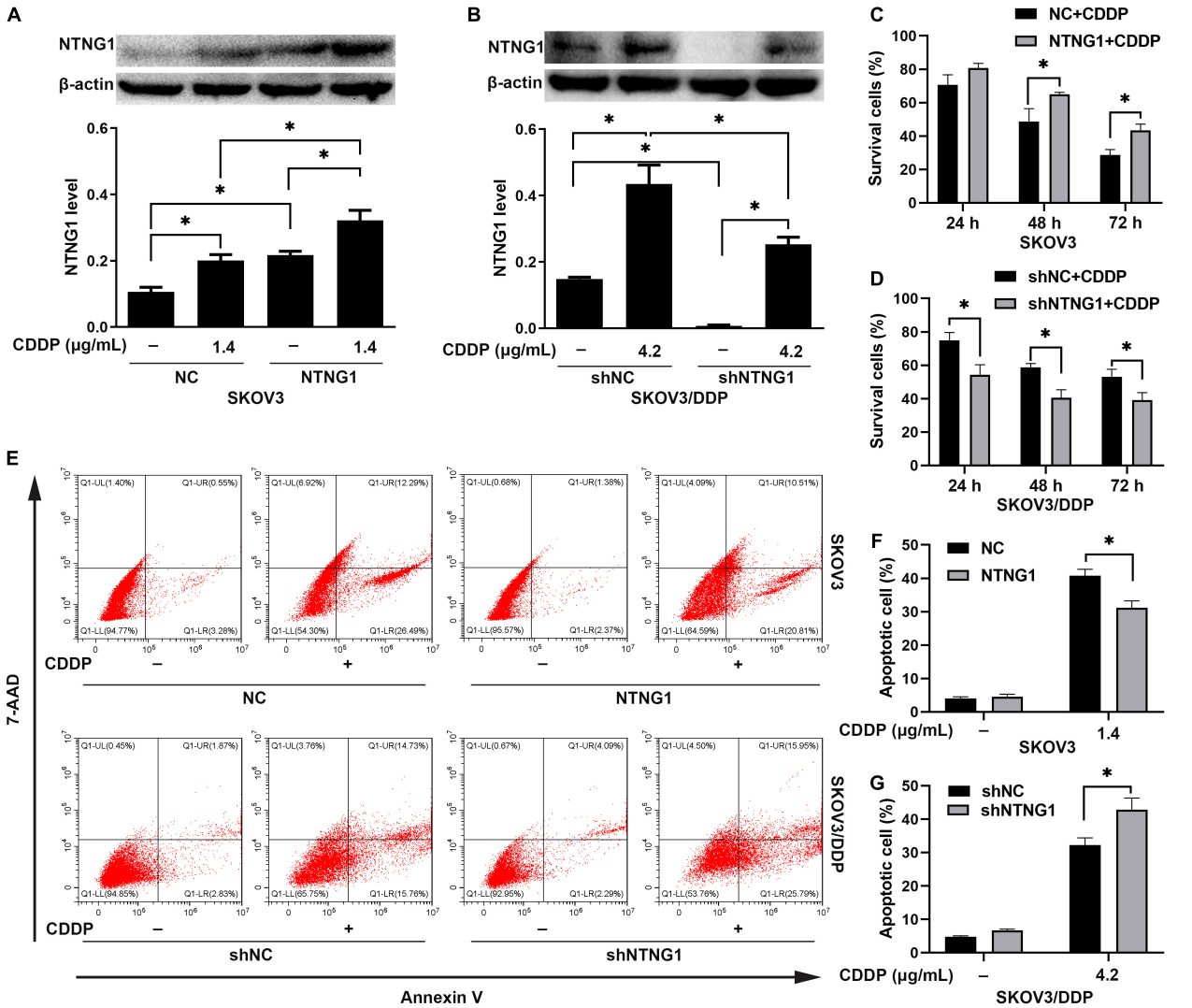

FIGURE 3 | NTNG1 enhanced the action of cisplatin *in vitro* ($n = 3$). **(A,C)** The level of NTNG1 was increased in NTNG1-transfected SKOV3 cells; overexpression of NTNG1 increased the cell-survival percentage following cisplatin exposure. **(B,D)** The NTNG1 level was decreased in shNTNG1-transfected SKOV3/DDP cells; silencing NTNG1 decreased the cell-survival percentage following cisplatin treatment. **(E–G)** Apoptosis induced by cisplatin; the percentage of apoptotic SKOV3 cells decreased following overexpression of NTNG1, but increased in SKOV3/DDP cells after silencing NTNG1. CDDP, cisplatin. *$p < 0.05$.

To understand the mechanism of NTNG1 regulation of the AXL/Akt pathway, the interaction of NTNG1 and GAS6/AXL was validated by a coIP assay. The immunoprecipitate obtained from lysates of SKOV3 cells contained NTNG1, GAS6, and AXL/p-AXL; overexpression of NTNG1 increased the levels of GAS6 and AXL/p-AXL (**Figure 5G**). These data indicated that NTNG1 directly bound GAS6/AXL to activate the AXL/Akt pathway.

NTNG1 Modulated the Action of DNA *in vivo*

To determine the effect of NTNG1 on the action of cisplatin *in vivo*, NTNG1- or shNTNG1-transfected cells were injected into mice to form tumors. In SKOV3 tumors, overexpression of NTNG1 did not affect the tumor; tumor volume and mass in group NTNG1 + CDDP were greater than those in group NC + CDDP ($p = 0.030$, $p = 0.029$) (**Figures 6A–C**). In SKOV3/DDP tumors, silencing NTNG1 did not inhibit the tumor; smaller tumors were detected in group shNTNG1 + CDDP compared with group shNC + CDDP ($p = 0.021$, $p = 0.009$) (**Figures 6A,D,E**).

NTNG1 and RAD51 in tumor tissues were analyzed. These two proteins were present at a higher level in SKOV3/DDP tumors compared with SKOV3 tumors, and cisplatin treatment induced an increase in both tumor types. In SKOV3 tumors, levels of NTNG1 and RAD51 in group NTNG1 + CDDP were higher than those in group NC + CDDP ($p < 0.001$, $p = 0.003$) (**Figures 6F,H,I**); however, in SKOV3/DDP tumors, levels in group shNTNG1 + CDDP were lower than those in group shNC + CDDP ($p < 0.001$, $p = 0.001$) (**Figures 6G–I**). These data confirmed that the

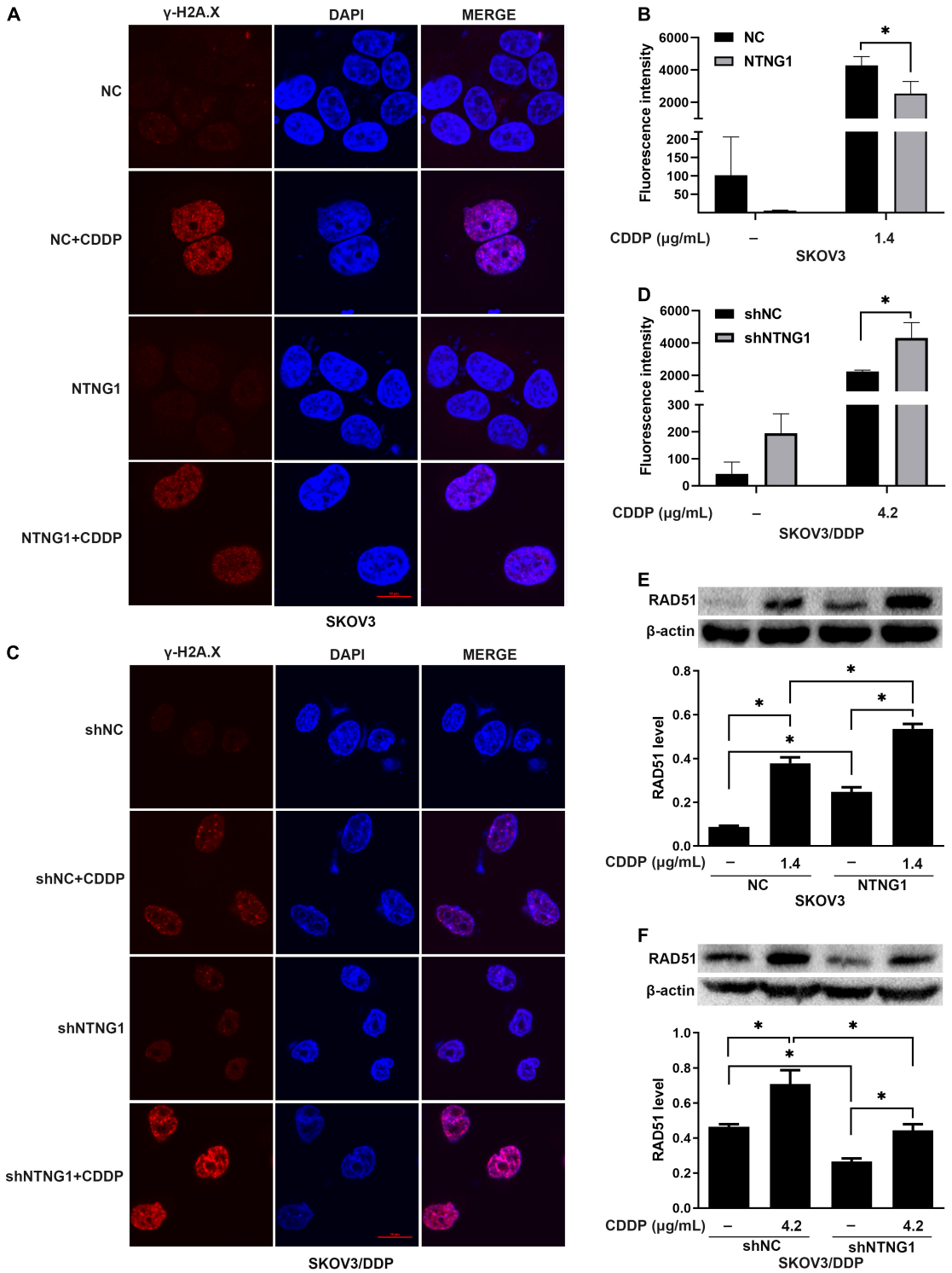

FIGURE 4 | Effects of NTNG1 on DNA damage/repair ($n = 3$). **(A–D)** Immunofluorescent detection of γ-H2A.X; the level was increased in SKOV3 and SKOV3/DDP cells following cisplatin exposure; after cisplatin treatment, the level in NTNG1-transfected SKOV3 cells was lower than that in NC-transfected cells, but a higher level was observed in shNTNG1-transfected SKOV3/DDP cells compared with shNC-transfected cells; scale = 10 μm. **(E,F)** Cisplatin induced the expression of RAD51; following cisplatin exposure, a higher level was noted in NTNG1-transfected SKOV3 cells compared with NC-transfected cells, but a lower level was detected in shNTNG1-transfected SKOV3/DDP cells compared with shNC-transfected cells. CDDP, cisplatin. *$p < 0.05$.

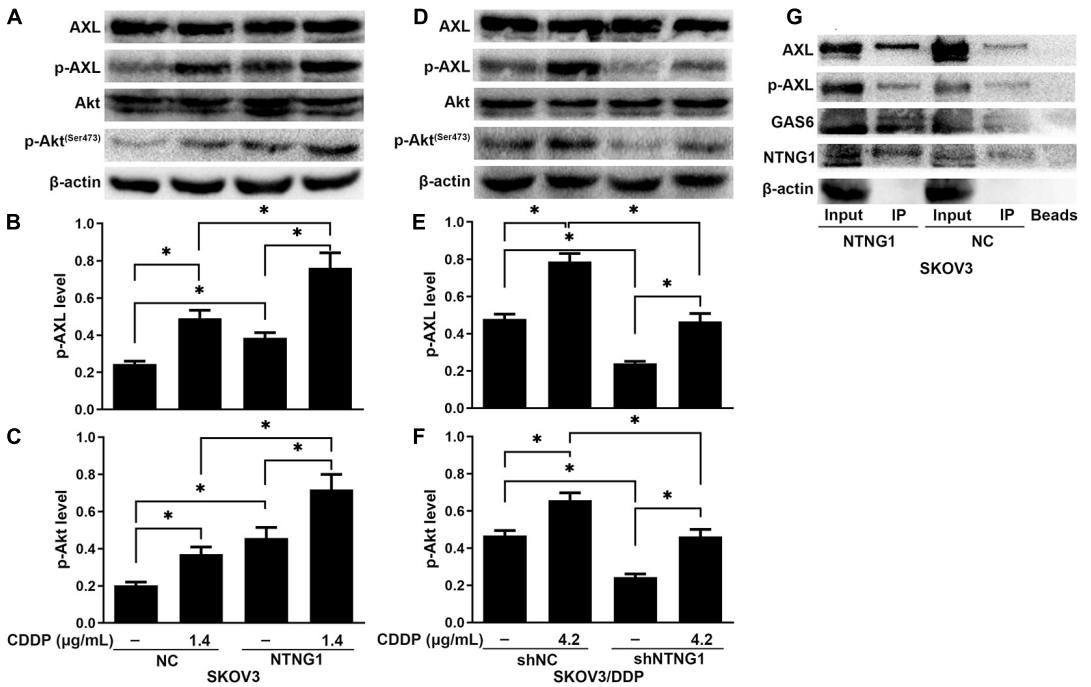

FIGURE 5 | NTNG1 bound GAS6/AXL to activate the AXL/Akt pathway (n = 3). **(A–F)** AXL, p-AXL, Akt, and p-Akt were assayed by western blotting; the levels of p-AXL and p-Akt were increased following cisplatin exposure, indicating these molecules were involved in cell survival; such an inductive effect was enhanced in SKOV3 cells following overexpression of NTNG1 but was suppressed in SKOV3/DDP cells after silencing NTNG1. **(G)** Co-immunoprecipitation in SKOV3 cells; proteins were assayed by western blotting; the immunoprecipitate contained NTNG1, GAS6, and AXL/p-AXL; higher levels were noted following overexpression of NTNG1, confirming an interaction between NTNG1 and GAS6/AXL. CDDP, cisplatin. *$p < 0.05$.

level of NTNG1 in tumor tissues determined the efficacy of cisplatin treatment.

DISCUSSION

Clinical data indicated that patients with a low NTNG1 level in cancer tissues had longer PFI and PFS and that cancers exhibiting a low NTNG1 level were sensitive to cisplatin. The NTNG1 level did not correlate with other clinicopathological variables. Thus, longer PFI and PFS resulted from a better therapeutic response. Category- or stage-adjusted analyses demonstrated that the correlation between a high NTNG1 level and poorer prognosis occurred only in type II or FIGO III/IV cancers. These two results were consistent. Here, type II cancer was high-grade serous cancer, which was frequently detected at stage III/IV (Garces et al., 2015). Type II cancer had gene mutations (e.g., TP53 and BRCA) and copy amplifications (e.g., MYC and CCNE1), which can cause cisplatin resistance (Brachova et al., 2013; Rojas et al., 2016; Singh et al., 2019; Gorski et al., 2020). The sample size was small, and therefore the present results should be validated in larger trials. Using a low level to show sensitivity had a higher predictive value compared with using a high level to indicate resistance, i.e., a low NTNG1 level can provide more information for clinical decisions.

Cisplatin attacked DNA to cause breaks, and double-strand breaks (DSBs) led to cell death via apoptosis; enhancing DSBs was a strategy to modulate cisplatin treatment and to overcome resistance (He et al., 2014; Wan et al., 2018; Qian et al., 2019). The γ-H2A.X foci formed at the DSB sites to favor an accumulation of repair molecules and were therefore used to monitor DSB repair (Liu et al., 2016). HR was the major pathway employed to repair DSBs induced by cisplatin; RAD51 was a key molecule in this pathway (Sugiyama and Kantake, 2009; Helleday, 2010; Lee et al., 2019). Levels of γ-H2A.X and RAD51 were upregulated following cisplatin exposure, i.e., cisplatin caused DSBs, initiating HR. Overexpression of NTNG1 increased the RAD51 level in SKOV3 cells, boosting HR; silencing NTNG1 decreased the RAD51 level in SKOV3/DDP cells, debasing HR; the expression pattern of NTNG1 determined the cells' response to cisplatin. These results were consistent with alterations of the percentages of dead and apoptotic cells following knock-in or knockdown of NTNG1. The γ-H2A.X foci disappear after DSBs were repaired (Pintado-Berninches et al., 2019). Consequently, a lower level of γ-H2A.X was observed following overexpression of NTNG1, but a higher level was detected after silencing NTNG1. The present data showed that NTNG1 modulated sensitivity to cisplatin by adjusting HR capability.

Survival pathways were necessary for cell survival and may be involved in chemoresistance. The Akt pathway was such a pathway to prevent apoptosis (Zhang et al., 2016). Activation of Akt can induce the expression of RAD51 to enhance DNA repair, while inactivation of Akt downregulated RAD51 to augment the action of DNA-damaging drugs (Ko et al., 2016; Boichuk et al., 2020). AXL, highly expressed in multiple cancer types, can activate Akt to favor cell

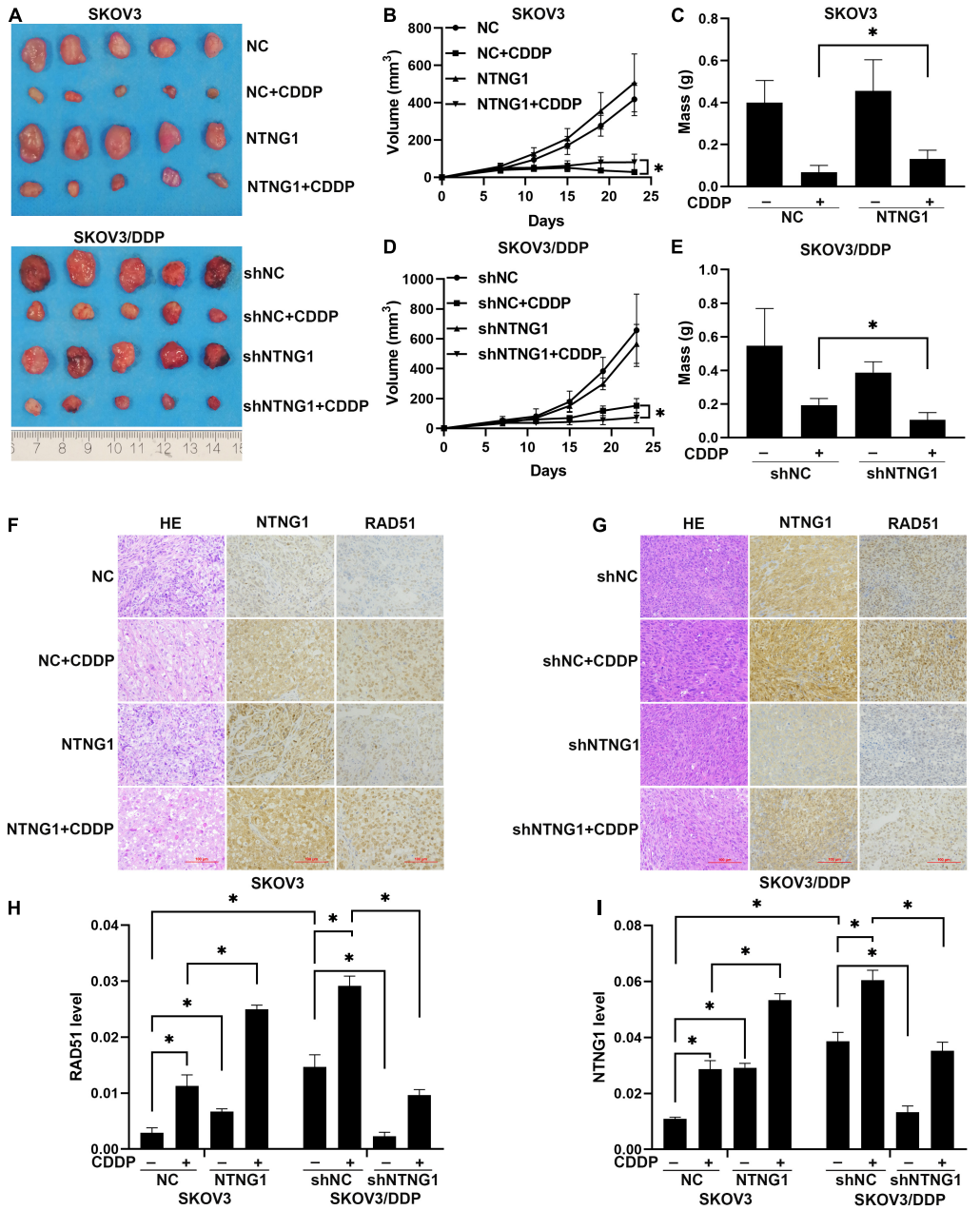

FIGURE 6 | NTNG1 modulated the action of cisplatin in xenograft tumors (n = 5). **(A)** Image of SKOV3 and SKOV3/DDP tumors. **(B,C)** Volume and mass of SKOV3 tumors; values in group NTNG1 + CDDP were greater than those in group NC + CDDP, indicating a decrease in antitumor efficacy. **(D,E)** Volume and mass of SKOV3/DDP tumors; values in group shNTNG1 + CDDP were less than those in group shNC + CDDP, demonstrating a stronger anticancer action. **(F,G)** Immunohistochemical images of NTNG1 and RAD51 proteins in tumor tissues; scale = 100 μm. **(H,I)** Levels of NTNG1 and RAD51 proteins; cisplatin treatment induced the expression of RAD51; in SKOV3 tumors, levels of NTNG1 and RAD51 in group NTNG1 + CDDP were higher than those in group NC + CDDP; in SKOV3/DDP tumors, lower levels were detected in group shNTNG1 + CDDP compared with group shNC + CDDP. CDDP, cisplatin. *$p < 0.05$.

proliferation and chemoresistance (Li et al., 2014; Tian et al., 2016). AXL was the only known ligand of GAS6; binding of GAS6 to AXL activated the kinase domain of AXL, and downstream signaling pathways such as the Akt and ERK pathways were activated (Wang et al., 2016; Antony et al., 2018; Li et al., 2019). Activation of Akt and AXL was realized via phosphorylation. The BioGRID suggested that GAS6 be a target protein of NTNG1. This was supported by our coIP results, which demonstrated an interaction between NTNG1 and GAS6/AXL. Cisplatin induced an increase in the level of p-AXL and p-Akt, confirming their roles in cisplatin resistance of ovarian cancer cells; the inductive effect was amplified in SKOV3 cells following overexpression of NTNG1, and an opposite result was observed

in SKOV3/DDP cells when silencing NTNG1. These findings suggested the following mechanism: NTNG1 interacted with GAS6/AXL, activating the Akt pathway, which upregulated the expression of RAD51 and improved the HR capacity, ultimately leading to cisplatin resistance.

In vivo data demonstrated that NTNG1 determined the therapeutic outcome of cisplatin: upregulation of NTNG1 decreased the therapeutic efficacy, but downregulation enhanced the anticancer action. These data were consistent with the results of *in vitro* therapies. The expression pattern of RAD51 protein displayed a similar trend. Thus, NTNG1 modulated the action of cisplatin by affecting HR. The therapeutic efficacy should be verified on an orthotopic ovarian cancer model to improve the clinical relevancy (Zhang et al., 2017; Liu et al., 2020). SKOV3/DDP represented acquired resistance, but resistance can be intrinsic in refractory ovarian cancer (Luvero et al., 2014; Cornelison et al., 2017). Thus, the role of NTNG1 in intrinsic cisplatin resistance should be explored.

Overall, the level of NTNG1 was higher in cisplatin-resistant ovarian cancer tissues compared with cisplatin-sensitive ones; patients with a high NTNG1 level in cancer tissues had shorter PFS and PFI. NTNG1 directly bound GAS6/AXL to regulate phosphorylation of AXL and Akt, upregulated the expression of RAD51, enhanced DSB repair, and eventually resulted in cisplatin resistance. Thus, NTNG1 was a target for ovarian cancer treatment, and inhibiting NTNG1 may be a useful strategy to overcome cisplatin resistance.

DATA AVAILABILITY STATEMENT

The original contributions presented in the study are included in the article/**Supplementary Material**, further inquiries can be directed to the corresponding author/s.

ETHICS STATEMENT

The studies involving human participants were reviewed and approved by the Institutional Review Board of The Second Affiliated Hospital, Chongqing Medical University. Written informed consent for participation was not required for this study in accordance with the national legislation and the institutional requirements. The animal study was reviewed and approved by the Ethics Committee of Chongqing Medical University Approval.

AUTHOR CONTRIBUTIONS

SF designed the study and performed the experiments. YL, YZ, HW, and QL performed the experiments. SF and XL drafted the manuscript. TY designed the study and checked the manuscript. All authors have given approval to the final version of the manuscript.

FUNDING

This work was supported by The Second Affiliated Hospital, Chongqing Medical University (2017-74 and CYB20152).

SUPPLEMENTARY MATERIAL

The Supplementary Material for this article can be found online at: https://www.frontiersin.org/articles/10.3389/fcell.2021.652325/full#supplementary-material

REFERENCES

Antony, J., Zanini, E., Kelly, Z., Tan, T. Z., Karali, E., Alomary, M., et al. (2018). The tumour suppressor OPCML promotes AXL inactivation by the phosphatase PTPRG in ovarian cancer. *EMBO Rep.* 19:e45670. doi: 10.15252/embr.201745670

Balaji, K., Vijayaraghavan, S., Diao, L., Tong, P., Fan, Y., Carey, J. P., et al. (2017). AXL inhibition suppresses the DNA damage response and sensitizes cells to PARP inhibition in multiple cancers. *Mol. Cancer Res.* 15, 45–58. doi: 10.1158/1541-7786.MCR-16-0157

Boichuk, S., Bikinieva, F., Nurgatina, I., Dunaev, P., Valeeva, E., Aukhadieva, A., et al. (2020). Inhibition of AKT-signaling sensitizes soft tissue sarcomas (STS) and gastrointestinal stromal tumors (GIST) to doxorubicin via targeting of homology-mediated DNA repair. *Int. J. Mol. Sci.* 21:8842. doi: 10.3390/ijms21228842

Bonner, W. M., Redon, C. E., Dickey, J. S., Nakamura, A. J., Sedelnikova, O. A., Solier, S., et al. (2008). γH2AX and cancer. *Nat. Rev. Cancer* 8, 957–967. doi: 10.1038/nrc2523

Brachova, P., Thiel, K. W., and Leslie, K. K. (2013). The consequence of oncomorphic TP53 mutations in ovarian cancer. *Int. J. Mol. Sci.* 14, 19257–19275. doi: 10.3390/ijms140919257

Christie, E. L., and Bowtell, D. D. L. (2017). Acquired chemotherapy resistance in ovarian cancer. *Ann. Oncol.* 28, viii13–viii15. doi: 10.1093/annonc/mdx446

Coburn, S. B., Bray, F., Sherman, M. E., and Trabert, B. (2017). International patterns and trends in ovarian cancer incidence, overall and by histologic subtype. *Int. J. Cancer* 140, 2451–2460. doi: 10.1002/ijc.30676

Cornelison, R., Llaneza, D. C., and Landen, C. N. (2017). Emerging therapeutics to overcome chemoresistance in epithelial ovarian cancer: a mini-review. *Int. J. Mol. Sci.* 18:2171. doi: 10.3390/ijms18102171

Damia, G., and Broggini, M. (2019). Platinum resistance in ovarian cancer: role of DNA repair. *Cancers* 11:119. doi: 10.3390/cancers11010119

Garces, ÁH. I., Dias, M. S. F., Paulino, E., Moreira, C. G., and de Melo, A. C. (2015). Treatment of ovarian cancer beyond chemotherapy: are we hitting the target? *Cancer Chemother. Pharmacol.* 75, 221–234. doi: 10.1007/s00280-014-2581-y

Gasparri, M. L., Besharat, Z. M., Farooqi, A. A., Khalid, S., Taghavi, K., Besharat, R. A., et al. (2018). MiRNAs and their interplay with PI3K/AKT/mTOR pathway in ovarian cancer cells: a potential role in platinum resistance. *J. Cancer Res. Clin. Oncol.* 144, 2313–2318. doi: 10.1007/s00432-018-2737-y

Gorski, J. W., Ueland, F. R., and Kolesar, J. M. (2020). CCNE1 amplification as a predictive biomarker of chemotherapy resistance in epithelial ovarian cancer. *Diagnostics* 10:279. doi: 10.3390/diagnostics10050279

Graham, D. K., DeRyckere, D., Davies, K. D., and Earp, H. S. (2014). The TAM family: phosphatidylserine sensing receptor tyrosine kinases gone awry in cancer. *Nat. Rev. Cancer* 14, 769–785. doi: 10.1038/nrc3847

He, H., Huang, H., and Yu, T. (2014). Detection of DNA damage in sonochemotherapy against cisplatin-resistant human ovarian cancer cells using the modified comet assay. *Int. J. Radiat. Biol.* 90, 897–902. doi: 10.3109/09553002.2014.922721

Helleday, T. (2010). Homologous recombination in cancer development, treatment and development of drug resistance. *Carcinogenesis* 31, 955–960. doi: 10.1093/carcin/bgq064

Kim, N. Y., Lee, H. Y., and Lee, C. (2015). Metformin targets Axl and Tyro3 receptor tyrosine kinases to inhibit cell proliferation and overcome chemoresistance in ovarian cancer cells. *Int. J. Oncol.* 47, 353–360. doi: 10.3892/ijo.2015.3004

Kim, S., Kim, K. C., and Lee, C. (2017). Mistletoe (*Viscum album*) extract targets Axl to suppress cell proliferation and overcome cisplatin- and erlotinib-resistance in non-small cell lung cancer cells. *Phytomedicine* 36, 183–193. doi: 10.1016/j.phymed.2017.09.017

Ko, J. C., Chen, J. C., Wang, T. J., Zheng, H. Y., Chen, W. C., Chang, P. Y., et al. (2016). Astaxanthin down-regulates Rad51 expression via inactivation of AKT kinase to enhance mitomycin C-induced cytotoxicity in human non-small cell lung cancer cells. *Biochem. Pharmacol.* 105, 91–100. doi: 10.1016/j.bcp.2016.02.016

Lee, J. O., Kang, M. J., Byun, W. S., Kim, S. A., Seo, I. H., Han, J. A., et al. (2019). Metformin overcomes resistance to cisplatin in triple-negative breast cancer (TNBC) cells by targeting RAD51. *Breast Cancer Res.* 21:115. doi: 10.1186/s13058-019-1204-2

Li, M., Ye, J., Zhao, G., Hong, G., Hu, X., Cao, K., et al. (2019). Gas6 attenuates lipopolysaccharide-induced TNF-α expression and apoptosis in H9C2 cells through NF-κB and MAPK inhibition via the Axl/PI3K/Akt pathway. *Int. J. Mol. Med.* 44, 982–994. doi: 10.3892/ijmm.2019.4275

Li, Y., Jia, L., Ren, D., Liu, C., Gong, Y., Wang, N., et al. (2014). Axl mediates tumor invasion and chemosensitivity through PI3K/Akt signaling pathway and is transcriptionally regulated by slug in breast carcinoma. *IUBMB Life* 66, 507–518. doi: 10.1002/iub.1285

Lin, J. C., Ho, W. H., Gurney, A., and Rosenthal, A. (2003). The netrin-G1 ligand NGL-1 promotes the outgrowth of thalamocortical axons. *Nat. Neurosci.* 6, 1270–1276. doi: 10.1038/nn1148

Liu, Q., Zhong, X., Zhang, Y., Li, X., Qian, G., and Yu, T. (2020). Ultrasound enhances ZD2767P-carboxypeptidase G2 against chemoresistant ovarian cancer cells by altering the intracellular pharmacokinetics of ZD2767D. *Mol. Pharm.* 17, 1922–1932. doi: 10.1021/acs.molpharmaceut.0c00008

Liu, Y., Long, Y. H., Wang, S. Q., Li, Y. F., and Zhang, J. H. (2016). Phosphorylation of H2A.X^{Tyr39} positively regulates DNA damage response and is linked to cancer progression. *FEBS J.* 283, 4462–4473. doi: 10.1111/febs.13951

Luvero, D., Milani, A., and Ledermann, J. A. (2014). Treatment options in recurrent ovarian cancer: latest evidence and clinical potential. *Ther. Adv. Med. Oncol.* 6, 229–239. doi: 10.1177/1758834014544121

Matsuura, K., Huang, N. J., Cocce, K., Zhang, L., and Kornbluth, S. (2017). Downregulation of the proapoptotic protein MOAP-1 by the UBR5 ubiquitin ligase and its role in ovarian cancer resistance to cisplatin. *Oncogene* 36, 1698–1706. doi: 10.1038/onc.2016.336

Oughtred, R., Stark, C., Breitkreutz, B. J., Rust, J., Boucher, L., Chang, C., et al. (2019). The BioGRID interaction database: 2019 update. *Nucleic Acids Res.* 47, D529–D541. doi: 10.1093/nar/gky1079

Pintado-Berninches, L., Fernandez-Varas, B., Benitez-Buelga, C., Manguan-Garcia, C., Serrano-Benitez, A., Iarriccio, L., et al. (2019). GSE4 peptide suppresses oxidative and telomere deficiencies in ataxia telangiectasia patient cells. *Cell Death Differ.* 26, 1998–2014. doi: 10.1038/s41418-018-0272-7

Qian, G., Dai, L., and Yu, T. (2019). Thioridazine sensitizes cisplatin against chemoresistant human lung and ovary cancer cells. *DNA Cell Biol.* 38, 718–724. doi: 10.1089/dna.2019.4715

Rojas, V., Hirshfield, K. M., Ganesan, S., and Rodriguez-Rodriguez, L. (2016). Molecular characterization of epithelial ovarian cancer: implications for diagnosis and treatment. *Int. J. Mol. Sci.* 17:2113. doi: 10.3390/ijms17122113

Rose, M., Burgess, J. T., O'Byrne, K., Richard, D. J., and Bolderson, E. (2020). PARP inhibitors: clinical relevance, mechanisms of action and tumor resistance. *Front. Cell Dev. Biol.* 8:564601. doi: 10.3389/fcell.2020.564601

Salazar, C., Campbell, I. G., and Gorringe, K. L. (2018). When is "type I" ovarian cancer not "type I"? Indications of an out-dated dichotomy. *Front. Oncol.* 8:654. doi: 10.3389/fonc.2018.00654

Sho, S., Court, C. M., Winograd, P., Russell, M. M., and Tomlinson, J. S. (2017). A prognostic mutation panel for predicting cancer recurrence in stages II and III colorectal cancer. *J. Surg. Oncol.* 116, 996–1004. doi: 10.1002/jso.24781

Singh, A., Gupta, S., and Sachan, M. (2019). Epigenetic biomarkers in the management of ovarian cancer: current prospectives. *Front. Cell Dev. Biol.* 7:182. doi: 10.3389/fcell.2019.00182

Sugiyama, T., and Kantake, N. (2009). Dynamic regulatory interactions of Rad51, Rad52, and replication protein-A in recombination intermediates. *J. Mol. Biol.* 390, 45–55. doi: 10.1016/j.jmb.2009.05.009

Suh, Y. A., Jo, S. Y., Lee, H. Y., and Lee, C. (2015). Inhibition of IL-6/STAT3 axis and targeting Axl and Tyro3 receptor tyrosine kinases by apigenin circumvent taxol resistance in ovarian cancer cells. *Int. J. Oncol.* 46, 1405–1411. doi: 10.3892/ijo.2014.2808

Sun, K. L. W., Correia, J. P., and Kennedy, T. E. (2011). Netrins: versatile extracellular cues with diverse functions. *Development* 138, 2153–2169. doi: 10.1242/dev.044529

Tian, M., Chen, X. S., Li, L. Y., Wu, H. Z., Zeng, D., Wang, X. L., et al. (2021). Inhibition of AXL enhances chemosensitivity of human ovarian cancer cells to cisplatin via decreasing glycolysis. *Acta Pharmacol. Sin.* 42, 1180–1189. doi: 10.1038/s41401-020-00546-8

Tian, Y., Zhang, Z., Miao, L., Yang, Z., Yang, J., Wang, Y., et al. (2016). Anexelekto (AXL) increases resistance to EGFR-TKI and activation of AKT and ERK1/2 in non-small cell lung cancer cells. *Oncol. Res.* 24, 295–303. doi: 10.3727/096504016X14648701447814

Wan, B., Dai, L., Wang, L., Zhang, Y., Huang, H., Qian, G., et al. (2018). Knockdown of BRCA2 enhances cisplatin and cisplatin-induced autophagy in ovarian cancer cells. *Endocr. Relat. Cancer* 25, 69–82. doi: 10.1530/ERC-17-0261

Wang, C., Jin, H., Wang, N., Fan, S., Wang, Y., Zhang, Y., et al. (2016). Gas6/Axl axis contributes to chemoresistance and metastasis in breast cancer through Akt/GSK-3β/β-catenin signaling. *Theranostics* 6, 1205–1219. doi: 10.7150/thno.15083

Yi, J. M., Dhir, M., Van Neste, L., Downing, S. R., Jeschke, J., Glöckner, S. C., et al. (2011). Genomic and epigenomic integration identifies a prognostic signature in colon cancer. *Clin. Cancer Res.* 17, 1535–1545. doi: 10.1158/1078-0432.CCR-10-2509

Yin, Y., Miner, J. H., and Sanes, J. R. (2002). Laminets: laminin- and netrin-related genes expressed in distinct neuronal subsets. *Mol. Cell. Neurosci.* 19, 344–358. doi: 10.1006/mcne.2001.1089

Yu, T., Luo, L., and Wang, L. (2016). Ultrasound as a cancer chemotherapy sensitizer: the gap between laboratory and bedside. *Expert Opin. Drug Deliv.* 13, 37–47. doi: 10.1517/17425247.2015.1083008

Yu, T., Yang, Y., Zhang, J., He, H., and Ren, X. (2015). Circumvention of cisplatin resistance in ovarian cancer by combination of cyclosporin A and low-intensity ultrasound. *Eur. J. Pharm. Biopharm.* 91, 103–110. doi: 10.1016/j.ejpb.2015.02.003

Zhang, D., Piao, H. L., Li, Y. H., Qiu, Q., Li, D. J., Du, M. R., et al. (2016). Inhibition of AKT sensitizes chemoresistant ovarian cancer cells to cisplatin by abrogating S and G2/M arrest. *Exp. Mol. Pathol.* 100, 506–513. doi: 10.1016/j.yexmp.2016.05.003

Zhang, Y., Li, J., and Yu, T. (2017). Pharmacokinetic profiles of cancer sonochemotherapy. *Expert Opin. Drug Deliv.* 14, 745–753. doi: 10.1080/17425247.2016.1232248

Zhao, W., Steinfeld, J. B., Liang, F., Chen, X., Maranon, D. G., Jian, M. C., et al. (2017). BRCA1-BARD1 promotes RAD51-mediated homologous DNA pairing. *Nature* 550, 360–365. doi: 10.1038/nature24060

Zhou, J., Hui, X., Mao, Y., and Fan, L. (2019). Identification of novel genes associated with a poor prognosis in pancreatic ductal adenocarcinoma via a bioinformatics analysis. *Biosci. Rep.* 39:BSR20190625. doi: 10.1042/BSR20190625

Conflict of Interest: The authors declare that the research was conducted in the absence of any commercial or financial relationships that could be construed as a potential conflict of interest.

frontiers in Oncology

MINI REVIEW
published: 24 September 2021
doi: 10.3389/fonc.2021.743556

Exosomes: A New Pathway for Cancer Drug Resistance

Yunbin Zhong[1†], Haibo Li[2†], Peiwen Li[2], Yong Chen[3], Mengyao Zhang[2], Zhendong Yuan[1], Yufang Zhang[4], Zhijie Xu[5], Geng Luo[1], Yuan Fang[2,6‡] and Xu Li[2*‡]*

[1] Hand, Foot Vascular Surgery, Tungwah Hospital to Sun Yet-sen University, Dongguan, China, [2] Department of Plastic Surgery, The Third Xiangya Hospital, Central South University, Changsha, China, [3] Dermatology Department, The First Hospital of Changsha, Changsha, China, [4] Anyang Tumor Hospital, The Fourth Affiliated Hospital of Henan University of Science and Technology, Anyang, China, [5] Department of Pathology, Xiangya Hospital, Central South University, Changsha, China, [6] Department of Plastic and Reconstructive Surgery, Shanghai Ninth People's Hospital, Shanghai Jiao Tong University School of Medicine, Shanghai, China

OPEN ACCESS

Edited by:
José Díaz-Chávez, National Institute of Cancerology (INCAN), Mexico

Reviewed by:
Simona Bernardi, University of Brescia, Italy
Stefano Fais, National Institute of Health (ISS), Italy

***Correspondence:**
Yuan Fang
jingji5996@163.com
Xu Li
1090787456@qq.com

[†]These authors have contributed equally to this work and share first authorship

[‡]These authors have contributed equally to this work

Specialty section:
This article was submitted to Molecular and Cellular Oncology, a section of the journal Frontiers in Oncology

Received: *18 July 2021*
Accepted: *06 September 2021*
Published: *24 September 2021*

Citation:
Zhong Y, Li H, Li P, Chen Y, Zhang M, Yuan Z, Zhang Y, Xu Z, Luo G, Fang Y and Li X (2021) Exosomes: A New Pathway for Cancer Drug Resistance. Front. Oncol. 11:743556. doi: 10.3389/fonc.2021.743556

Exosomes are extracellular vesicles (EVs) that are secreted into body fluids by multiple cell types and are enriched in bioactive molecules, although their exact contents depend on the cells of origin. Studies have shown that exosomes in the tumor microenvironment affect tumor growth, metastasis and drug resistance by mediating intercellular communication and the transport of specific molecules, although their exact mechanisms of action need to be investigated further. In this review, we have summarized current knowledge on the relationship between tumor drug resistance and exosomes, and have discussed the potential applications of exosomes as diagnostic biomarkers and therapeutic targets.

Keywords: exosomes, cancer, chemoresistance, drug resistance, tumor microenvironment, signal transmission

INTRODUCTION

Exosomes were discovered by Pan et al. while studying the transition of reticulocytes to mature red blood cells (1), and were later defined by Johnstone et al. as vesicles that containing non-essential proteins that are expelled from cells (2) following the fusion of microvesicles with the cell membranes (3). Subsequent studies showed that exosomes are released from blood cells, tumor cells, epithelial cells, mesenchymal stem cells and neuronal cells into the blood, saliva, urine and other body fluids (4–7). Exosomes were first considered to be "garbage bags" that remove waste proteins and metabolites. However, recent studies have shown that the exosomal cargo is biologically active (8) and mediates intercellular communication (9). Several exosomes-enriched proteins, including cytoskeletal proteins, fusion-related proteins, tetrapeptides (CD9, CD63, CD81 and CD82) and membrane connectins (10, 11), as well as oncoproteins (12), have been reported on in recent years. Furthermore, exosomes are also known to transport nucleic acids, such as DNA and coding and non-coding RNAs (13), including micro RNAs (miRNAs) and circular RNAs (circRNAs) (14), that regulate various aspects of tumor development, including immunosuppression, angiogenesis, cell migration and invasion (15–17). Electron microscopy studies have revealed that exosomes measure 50-150 nm in diameter and have a "dish-like" or "cup-shaped" morphology. In addition, several surface exosomal proteins, such as the lysosomal protein Lamp2b, heat shock protein Hsp70 and others (18, 19) that serve as diagnostic markers have also been identified.

Chemotherapeutic drug resistance is a major challenge in cancer treatment. Tumor cells are either naturally resistant to drugs or acquire resistance over the course of treatment (20). Acquired drug resistance is the result of mutations, polymorphisms and splicing variations in genes related to drug metabolism and toxicity (21). A major mechanism of drug resistance in tumor cells is the overexpression of membrane transporters, in particular the ATP binding box (ABC) transporter protein, which rapidly expel drugs and thus reduces their intracellular levels. Furthermore, mutations in drug targets can decrease the efficacy and toxicity of drugs. Interestingly, studies have shown that exposure to chemotherapy drugs significantly increases mutation rates in cancer cells, which may be partially attributed to the activation of pro-survival and anti-apoptotic pathways (22). Furthermore, tumor cells have a higher DNA repair rate compared with normal cells, which neutralizes any DNA damage induced by chemotherapeutic drugs and generates drug-resistant clones. Given that exosomes are involved in the aforementioned signaling pathways, it is important to explore their role in the development of drug resistance (23). In this review, we have summarized the common mechanisms of the genesis of chemoresistance in cancer cells and have also discussed the possible involvement of exosomes.

EXOSOMAL-MEDIATED TUMOR RESISTANCE

Exosomes Participate in Tumor Microenvironment Regulation

The tumor microenvironment (TME) is comprised of fibroblasts, stromal cells and the extracellular matrix that aid in the survival, proliferation and metastasis of tumor cells (24, 25). Exosomes mediate cell-to-cell communication in the TME by shuttling signaling molecules, lipids, proteins, nucleic acids and metabolites. In addition, exosomes released from the tumor cells and stromal cells can regulate drug resistance by directly interacting with drug molecules, altering the transcriptome of cancer cells and influencing the immune response (26). The extracellular acidity of tumors markedly affects exosome release by tumors in terms of both the amounts of released exosomes and the make-up of the exosomes (27–30). As shown in **Figure 1** (31), exosomes release active molecules, such as ncRNAs and proteins into target cells following receptor ligand interactions, membrane fusion, as well as puffing, phagocytosis, or receptor-mediated endocytosis, which then regulates tumor cell proliferation, invasion, metastasis and drug resistance (32, 33).

Tumor cells induce adaptive changes in distant organs to create a "pre-metastatic" environment that is conducive to their growth, and the formation of the secondary metastatic foci (34). Zhou et al. showed that exosomes derived from highly metastatic breast cancer cells express high levels of miR-105 (35). Absorption of these exosomes by pulmonary microvascular endothelial cells leads to the significant downregulation of ZO-1, which increases vascular permeability and facilitates the colonization of lung tissues by the tumor cells. Likewise, Yu et al. found that tumor cell-derived exosomes induced the formation of a pre-metastatic niche in the liver of a mouse model of pancreatic cancer, which enhanced metastasis and primary tumor growth. In addition, Costa-Silva et al. found that pancreatic cancer cells release exosomes loaded with macrophage migration inhibitory factors that are absorbed by the hepatic Kupffer cells. This promotes TGF-βD secretion and up-regulates the fibronectin level, and increases the metastasis of tumor cells to the liver. Evidence also indicates that the TME plays a role in drug resistance (36, 37). PGP transported by exosomes can fuse with the plasma membrane of osteosarcoma cells, and P-glycoprotein (P-gp) transporters that enrich tumor cells, resulting in pharmacological desensitization (38). In addition, exosomal P-gp in the serum of prostate cancer patients is a potential biomarker of docetaxel resistance (39).

Exosomes Participate in Tumor Local Immune Microenvironment Regulation

The TME harbors multiple immune cells including T lymphocytes, neutrophils, NK cells and the tumor-associated macrophages (TAMs). The T cells and TAMs in particular play a significant role in tumor genesis, development and drug resistance, while exosomes in the TME for instrumental in the interactions between immune cells and cancer cells. Exosomes released by the CD8+ T cells contain O-GlcNAc transferase, which upregulates PD-1 in the recipient cells and creates an immunosuppressive environment (40). Previous studies have shown that cancer cell-derived exosomes not only promote anti-tumor immunity but also enhance tumor immune escape (41). Binenbaum et al. demonstrated that when macrophage-derived exosomes expressing miR-365 are internalized by pancreatic ductal adenocarcinoma (PDAC) cells, the tri-phospho-nucleotide pool in cancer cells increases and activates cytidine deaminase, which then inducing resistance to gemcitabine (42).

Signal Transmission Between Drug-Resistant Cells and Sensitive Cells

Given the highly heterogeneous nature of tumors, individual cells of the same tumor mass differ in their response to chemotherapeutic drugs. Interestingly, chemoresistance or chemosensitivity can be transferred between cells *via* exosomes (see **Table 1**). For instance, exosomes derived from cisplatin-resistant lung cancer cells induced drug resistance in recipient cells *via* miRNA-100-5p, which altered mTOR expression levels (43). Fu X et al. showed that multidrug-resistant liver cells transferred miRNA-32-5p to sensitive cells through exosomes, which then activated phosphatidylinositol kinase *via* the protein kinase B (Akt) pathway and induced drug resistance (44). Compared with chemo-sensitive breast cancer cell lines such as MCF-7, the resistant strains express significantly higher levels of miRNA-222. The exosomes secreted by azithromycin-resistant breast cancer cells can confer drug resistance to sensitive recipient cells *via* miR-222, which is known to regulate cell cycle and apoptosis-related genes (45). Zhang et al. showed that colon cancer cells-derived exosomes promoted cetuximab resistance by downregulating human chromosome 10 phosphatase (PTEN) and increasing phosphorylated Akt levels (46). Furthermore, the exosomes released by gemcitabine-resistant cancer cells delivered miRNA-222-3p to recipient cells through endocytosis, which promote drug resistance and malignant

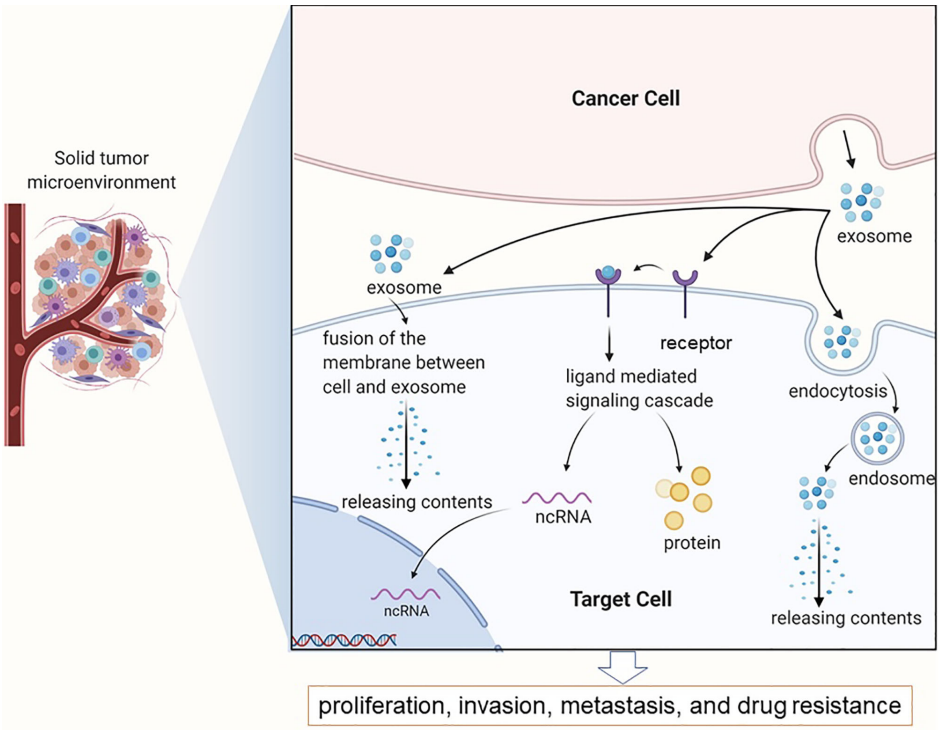

FIGURE 1 | Exosomes in the tumor microenvironment mainly complete information exchange and material transportation between tumor cells.

TABLE 1 | Signal transmission between drug-resistant cells and sensitive cells.

Disease	Cells	Drug resistance	Exosomal RNA	Mechanism/pathway	References
Lung cancer		Cisplatin	miR-100-5p	mTOR	(43)
Hepatocellular carcinoma	Bel/5-FU Bel7402	Multidrug resistance	miR-32-5p	PTEN/PI3K/Akt	(44)
Breast cancer	MCF-7	Adriamycin	miR-222		(45)
Colon cancer	RKO Caco-2	Cetuximab		PTEN/Akt	(46)
non-small cell lung cancer	A549-GR	Gemcitabine	miR-222-3p	SOCS3	(47)
Hepatocellular carcinoma	HepG2 PLC-PRF5	Sorafenib	linc-RoR	TGFβ	(48)
Renal Cancer		Sunitinib	lncARSR	miR-34/miR-449 AXL/c-MET	(49)

progression by targeting SOCS3 (47). Takahashi et al. found that sorafenib-resistant liver cancer cells expressed high levels of the lncRNA RoR that modulates the TGF-β signaling pathway. Furthermore, the co-culture of sensitive liver cancer cells with lncRNA-RoR exosomes released by drug-resistant cells was able to induce sorafenib resistance (48). Qu et al. found that exosomal lncARSR induced sunitinib resistance in renal cancer cells by sponging miR-34 and miR-449 and upregulating receptor tyrosine kinase (AXL) and c-MET (49).

Signal Transmission Between Stromal Cells and Tumor Cells

Exosomes derived from stromal cells can also induce drug resistance (**Table 2**). Zheng et al. showed that exosomes derived from M2 macrophages conferred cisplatin resistance to gastric cancer cells through miRNA-21, which inhibited apoptosis by downregulating PTEN and activating the PI3K/Akt signaling pathway (50, 55). Likewise, Ji et al. found that exosomes derived from mesenchymal stem cells (MSCs) induced fluorouracil resistance in gastric cancer cells by activating the CaMKs/Raf/MEK/ERK pathway (51). In addition, exosomes secreted by bone marrow matrix cells induced bortezomib resistance in myeloma cells (52), whereas colon tumors in mice developed resistance to fluorouracil or oxaliplatin in the presence of fibroblast-derived exosomes (53). Boelens et al. found that matrix cells in breast tumors trigger drug resistance in a paracrine manner through exosomal RNAs that activate the NOTCH3 signaling pathway (54).

TABLE 2 | Signal transmission between stromal cells and tumor cells.

Disease	Stromal cells	Drug resistance	Exosomal RNA	Mechanism/pathway	References
Gastric cancer	M2 macrophages	Cisplatin	miR-21	PTEN-PI3K- Akt	(50)
Gastric cancer	MSCs	5-fluorouracil		CaM-Ks/Raf/MEK/ERK	(51)
Multiple myeloma	Patients' peripheral blood	Bortezomib	FFAR1/SP9/HIST1H2BG/ ITIH2	mTOR/cAMP/PI3K-Akt	(52)
Colorectal cancer	Fibroblasts	5-fluorouracil Oxaliplatin		Promoted percentage, clonogenicity and tumor growth	(53)
Breast cancer	Stromal cells		5'-triphosphate exoRNA	STAT1/NOTCH3	(54)

As shown through the introduction to this section, exosomes play an important role in various types of transmissions, including the transmission of cisplatin and therapeutic antibodies (56–58). Exosomes with functional enzyme molecules can also be detected in human plasma and may play a pivotal guiding role in cancer progression (59). Exosomes carry molecules with the dual functions of being tracers and therapeutic molecules indicating their diagnostic and therapeutic potential (57). Exosomes are involved in regulating the direction material movement. Recently, researchers have also used exosomes to transfer nano materials (60). Therefore, the potential applications of exosomes are not only limited to its role in the development of tumor drug resistance.

THE ROLE AND MECHANISM OF ACTION OF EXOSOMES IN THE DEVELOPMENT OF TUMOR RESISTANCE

Regulation of Neoplastic Growth and Metastasis

Cancer stem cells (CSCs) are the source of primary and metastatic tumors, as well as the basis of chemo- and radio-resistance, which leads to tumor recurrence (61). Studies have shown that CSCs often reappear after chemotherapy and express the ATP binding cassette subfamily B member 5 (ABCB5) protein, which mediates multidrug resistance in multiple cancers. The stem cell-derived exosomes express pluripotency-related transcription factors such as Nanog, Oct-4, HOXB4, Rex-1, and Wnt-3, which can endow recipient cells with "stemness" features, such as self-renewal, expansion and differentiation into progenitor cells (62). In addition, exosomes secreted by the cancer-associated fibroblasts (CAFs) express Snail1, which can induce the epithelial-mesenchymal transition of recipient lung cancer cells (63). A recent study showed that tumor cells cultured in a conditioned medium of CAFs showed a higher proliferation rates in the presence of 5-fluorouracil or oxaliplatin, compared with cells grown in normal culture medium (53). Thus, drugs that target the CAFs can potentially sensitize tumor cells to chemotherapy. Furthermore, exosomes secreted by CSCs promote tumor growth and metastasis through paracrine and endocrine modes. The inhibition of exosome secretion can slow clonal expansion and tumor growth (64).

Expression of Transcription Factors

MiR-210 is expressed at significantly higher levels in colorectal cancer (CRC) tissues compared with that of normal colon tissues, and is associated with an increased level of metastasis. The exosomes secreted by the primary CRC cell line, HCT-8, induced 5-fluorouracil and folate resistance in the chemo-sensitive cells by delivering miR-210, which significantly increased sib levels (65). Non-small cell lung cancer (NSCLC) is usually of one of two types, either chemotherapeutic resistance or tumor rapid metastasis and spread. It is generally believed that this resistance is caused by mesenchymal NSCLC cells, but the mechanism of metastasis is unclear. R. J. et al. suggested that exosomes release by these transformed mesenchymal phenotype cancer cells could induce drug resistance in parental EPC and increased the expression of ZEB1 mRNA in receptor cells (66). Furthermore, T cell-derived exosomes triggered the epithelial mesenchymal transition (EMT) of esophageal cancer cells (67), and the exosomes released from CAFs promoted cancer cell growth and EMT *via* miR-21, miR-378e and miR-143 (68).

Cell Cycle and Apoptosis

MiR-21 is transferred from resident fat cells or fibroblasts in ovarian tumors to the cancer cells, and can induce drug resistance by inhibiting APAF1-mediated apoptosis (69). In addition, the exosomes secreted by the M2 polarized macrophages can induce cisplatin resistance in gastric cancer cells by directly delivering miR-21 into the recipient cells (50). Furthermore, Her2+ breast cancer cells-derived exosomes can promote trastuzumab resistance *via* lncSNHG14 that targets the Bcl-2/BAX apoptotic pathway (70). The PLX-4720 BRAF inhibitor–resistant melanoma cells were able to activate of PI3K/AKT signaling and inhibition of the MAPK pathway (71). A recent study showed that exosomes containing miR-32-5p induced multi-drug resistance by activating the PI3K/AKT pathway and inhibiting PTEN (44).

Drug Efflux and Metabolism

The concentration of drugs used for the treatment of cancer cells can be reduced to therapeutically sub-optimal levels by decreasing its permeability through the cell membrane and/or increasing its active efflux. L.V. et al. found that exosomes can efficiently transfer p-glycoprotein (p-gp) from chemo-resistant breast cancer cells to sensitive cells, thus inducing resistance in the latter through increased drug efflux (72). Based on these

findings, p-gp was hypothesized to be a drug efflux pump encoded by the ABCB1 gene (73). The experiment conducted by L.V. et al. indicated that when adding MCF-7/DOC that extract of supernatant fluid secretion body (DOC/exobiology) for culture, MCF-7/S resistance can be induced, and to join the MCF-7/S exosomes (S/exobiology) training, MCF-7/S did not acquire resistance. When MCF-7/S and DOC/exo was co-cultured, the level of p-glycoprotein expression raised based on the number of exosomes. Similar to the finding of the above mentioned studies, Ning et al. confirmed that exosomes secreted by MCF7/ADM carried UCH-L1 and p-glycoprotein (74). Taken together, the above mentioned findings indicate that drug-resistant breast cancer cells can secrete exosomes containing p-gp, and confer chemoresistance to the more sensitive recipients. The exosomes secreted by the docetaxel-sensitive DU145 prostate cancer cells (DU145 tax-sen) are enriched in MDR1 (ABCB1), mdr-3, endophilin-a2, and PABP4, which are potential biomarkers of docetaxel resistance (75).

In conclusion, exosomes secreted by tumor related cells can promote tumor growth and metastasis through a variety of action pathways. At the same time, some small RNA molecules can affect cell apoptosis, so as to achieve the effect of drug resistance. If the exosome carrier is no longer small RNA, but a drug, it can induce drug resistance in the process of endocytosis and exocytosis. The ability of exosomes to repair DNA or block the process of transferring mRNA can increase the sensitivity of chemotherapy and radiotherapy and achieve better therapeutic effect.

THE ROLE OF EXOSOMES IN TUMOR DRUG RESISTANCE

Based on the available research, exosomes have shown to be promising nanocarriers that can be used for the reversal of tumor drug resistance. For instance, Wang et al. sensitized cisplatin-resistant gastric cancer cells by directly delivering anti-miRNA-214 to the recipient cells through exosomes (76). Rapamycin and U18666A can sensitize B lymphoma cells to rituximab *via* the inhibition of exosome release by interfering with the synthesis of MVBs and the incorporation of cholesterol into cell membranes. Some researchers have found that β-elemene can act on targeted genes in breast cancer cell lines to alter the expression of resistance-related miRNAs in exosomes, thereby reducing the level of resistance transmission through exosomes and enhancing the sensitivity to chemotherapy (77) (see **Figure 2**).

Targeting Exosomes to Reverse Chemoresistance

In recent years, several studies have demonstrated that exosomes can be targeted to prevent the development and reverse the chemoresistance of cancer cells. For instance, Cao et al. showed that the neutral sphingomyelinase (NSM) inhibitor, GW4869, sensitized cisplatin-resistant ovarian cancer cells, indicating the therapeutic potential of this novel drug in the recalcitrant cancer patients (78). Furthermore, studies have shown that ketotifen,

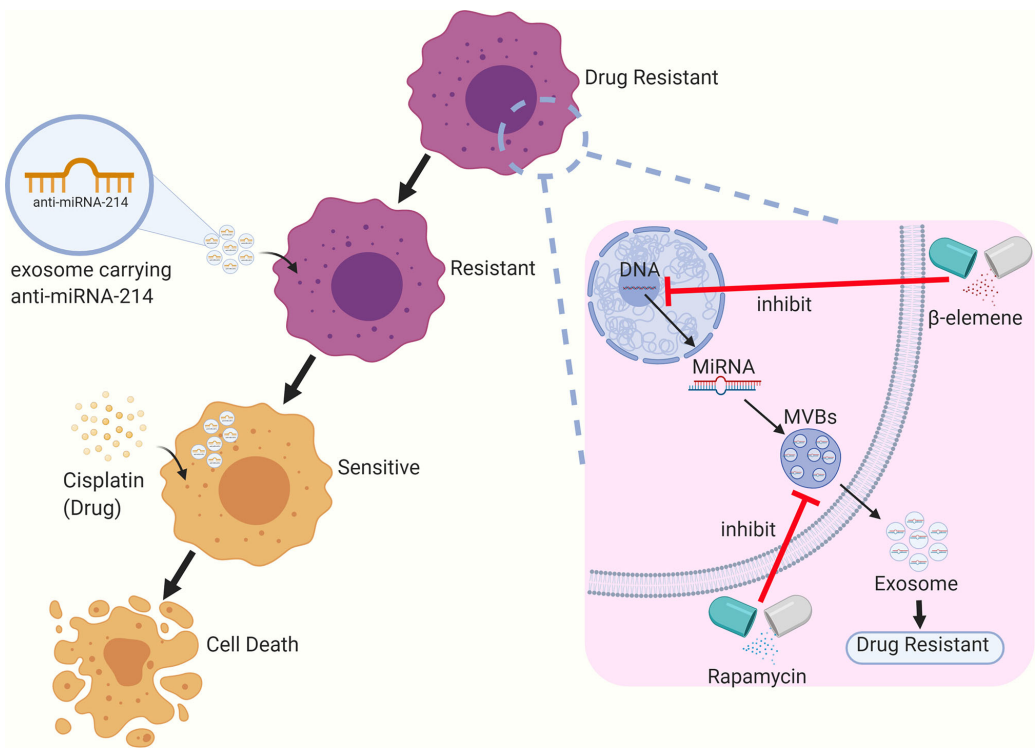

FIGURE 2 | The role of exosomes in the treatment of tumor drug resistance.

cannabinol (CBD) and psoralen can sensitize tumor cells to chemotherapeutic drugs by reducing exosome secretion from these cells. Likewise, rhamnose-emodin can reduce exosome secretion from the doxorubicin-resistant breast cancer cells and downregulate the expression of exosomal miRNAs involved in chemoresistance, reversing drug resistance. The exosomes secreted by human umbilical cord mesenchymal cells (hUC-MSC-Exo) can sensitize myelogenous leukemia K562 cells to imatinib by activating the caspase signaling pathway (79). Therefore, the combination of imatinib and hUC-MSC-Exo is a promising therapeutic strategy against chronic myelogenous leukemia (CML) (79). Li et al. found that the exosome-specific miRNA-770 reversed doxorubicin resistance in triple negative breast cancer (TNBC) cells by regulating apoptosis pathways and the TME (80). In addition, Akt inhibitors could reverse the chemoresistance of sensitive cancer cells induced by exosomes derived from the drug-resistant cells (81). Wang B. et al. found that the IC50 of cisplatin in chemo-sensitive TNBC cells increased 2.24 times after being co-cultured with a chemo-resistant cell line but decreased upon treatment with the compound, Yiqi (82).

Exosome and Tumor Chemotherapy Resistance Markers

Exosomes can be isolated from various biological fluids, such as blood, urine and saliva. The blood of healthy individuals may contain over 2000 trillion exosomes, whereas that of cancer patients contains 4000 trillion exosomes. Thus, tumor cells may produce and secrete more exosomes compared with normal cells, and can be used as potential diagnostic biomarkers (83). Yuwen et al. correlated lower serum levels of exosomal miRNA-146a-5p in patients with advanced NSCLC with a higher recurrence rate (84). In addition, serum exosomal miRNA-146a-5p is a novel biomarker that can be used to predict and monitor cisplatin resistance in NSCLC patients. Likewise, the serum exosomes enrichment of in TAG72 indicates a high probability of 5-FU resistance in CRC cells (85), and that of exosomal miRNA-222-3p predicts gemcitabine sensitivity in NSCLC patients (47). TRPC5 expression in breast cancer tissues and patient response to chemotherapy are significantly correlated with the level of cirExo-TRPC5 in peripheral blood. Since cirExo-TRPCS levels increase after chemotherapy, it can be used as a promising biomarker for the image-based detection of chemo-resistance (86). High expression of GSTP1 in circulating exosomes may indicate an increase of chemo-resistance. A clinical study showed that the level of miRNA-151a in cerebrospinal fluid (CSF)-derived exosomes reflects potential chemo-resistance of glioblastoma multiforme (GBM) patients (87). In addition, Leukemia-derived exosomes induced IL-8 production in bone marrow stromal cells, which can protect acute myeloid leukemia cells from chemotherapy drug induced apoptosis (88). The content of exosomes secreted by tumor cells changes along with the level of cellular stress induced by anticancer therapy, which leads to the metastasis of drug resistant phenotypes in breast cancer (72, 82). This leads to the transfer of drug resistance mediated by exosomes between drug resistant cells and sensitive breast cancer cells (89). Moreover, the selective isolation of circulating subsets of exosomes enriched in tumor sources could effectively improve the sensitivity and specificity of detection (90).

Then, according to the above, we boldly speculate that in the future, it can be separated from various human biological liquids, such as blood, urine and salivary blood, which could directly detect some disease-related exosomes bio-markers, so as to predict the condition and curative effect of patients at this stage. Then, some drugs are used to target the corresponding exosomes to reverse the drug resistance. This may be a simple, convenient and universal treatment in the future.

CONCLUSION AND PROSPECTS

Exosomes mediate intercellular communication in the TME, and can induce drug resistance in tumor cells by transferring specific mRNAs, ncRNAs or proteins (91). The differential expression of these molecules in exosomes are useful clinical markers of tumor drug resistance (92). Therefore, there is a clear need to further elucidate the role of exosomes in tumor drug resistance to improve prognostic prediction and therapeutic efficacy.

Exosomes in the TME have increasingly been identified as the vectors of oncogenesis, drug resistance and metastasis, although the exact pathways and mechanisms involved are still unclear. A deeper understanding of these mechanisms will provide new insights into tumor heterogeneity, and significant differences in the chemotherapeutic responses of individual cancer patients. Furthermore, exosomes are also promising nanocarriers for the targeted delivery of drugs to tumor cells. Given that the prognosis of cancer patients is closely associated with natural or acquired chemo-resistance of the tumor cells, early identification of recalcitrant patients can help formulate individualized optimal treatment regimens. Tumor patients have a higher level of plasmatic exosomes compared with healthy individuals, independently of tumor histology. This difference indicates that exosomes released by tumors during chemotherapy may deliver cytotoxic drugs to healthy organs, thus inducing harmful effects (29, 93, 94). Several ncRNAs that can regulate tumor cell proliferation, metastasis, chemoresistance and recurrence have been identified in recent years. Circulating exosomes that contain cancer-specific miRNAs and lncRNAs are promising diagnostic/prognostic biomarkers and therapeutic targets in cancer, although their underlying mechanisms of action remain to be clarified.

AUTHOR CONTRIBUTIONS

YF and XL performed the research. HL, YF, and XL designed the research study. PL and YFZ contributed essential reagents or tools. YF, HL, and YC helped to analyze the data. XL wrote the article. YF, ZY, and GL revised the article. ZX modified the language. YBZ provided financial assistance. All authors contributed to the article and approved the submitted version.

FUNDING

This work was supported by a grant from National Major Science and Technology Projects of Hunan Province (2020JJ4633).

ACKNOWLEDGMENTS

Thank you to all members of the Yunbin Zhong's team for your special support.

REFERENCES

1. Pan BT, Teng K, Wu C, Adam M, Johnstone RM. Electron Microscopic Evidence for Externalization of the Transferrin Receptor in Vesicular Form in Sheep Reticulocytes. *J Cell Biol* (1985) 101(3):942–8. doi: 10.1083/jcb.101.3.942
2. Johnstone RM, Adam M, Hammond JR, Orr L, Turbide C. Vesicle Formation During Reticulocyte Maturation. Association of Plasma Membrane Activities With Released Vesicles (Exosomes). *J Biol Chem* (1987) 262(19):9412–20.
3. Mohd Ali N, Yeap SK, Ho WY, Boo L, Ky H, Satharasinghe DA, et al. Adipose Mscs Suppress MCF7 and MDA-MB-231 Breast Cancer Metastasis and EMT Pathways Leading to Dormancy *via* Exosomal-Mirnas Following Co-Culture Interaction. *Pharmaceuticals (Basel)* (2020) 14(1):8. doi: 10.3390/ph14010008
4. Boriachek K, Islam MN, Moller A, Salomon C, Nguyen NT, Hossain MSA, et al. Biological Functions and Current Advances in Isolation and Detection Strategies for Exosome Nanovesicles. *Small* (2018) 14(6). doi: 10.1002/smll.201702153
5. Jiang L, Gu Y, Du Y, Liu J. Exosomes: Diagnostic Biomarkers and Therapeutic Delivery Vehicles for Cancer. *Mol Pharm* (2019) 16(8):3333–49. doi: 10.1021/acs.molpharmaceut.9b00409
6. Yan L, Liu G, Wu X. Exosomes Derived From Umbilical Cord Mesenchymal Stem Cells in Mechanical Environment Show Improved Osteochondral Activity *via* Upregulation of Lncrna H19. *J Orthop Translat* (2021) 26:111–20. doi: 10.1016/j.jot.2020.03.005
7. Wang X, Yang G. Bone Marrow Mesenchymal Stem Cells-Derived Exosomes Reduce Abeta Deposition and Improve Cognitive Function Recovery in Mice With Alzheimer's Disease by Activating Sphingosine Kinase/Sphingosine-1-Phosphate Signaling Pathway. *Cell Biol Int* (2020) 45(4):775–84. doi: 10.1002/cbin.11522
8. Fenselau C, Ostrand-Rosenberg S. Molecular Cargo in Myeloid-Derived Suppressor Cells and Their Exosomes. *Cell Immunol* (2021) 359:104258. doi: 10.1016/j.cellimm.2020.104258
9. Bai S, Xiong X, Tang B, Ji T, Li X, Qu X, et al. Exosomal Circ_DLGAP4 Promotes Diabetic Kidney Disease Progression by Sponging MiR-143 and Targeting ERBB3/NF-KappaB/MMP-2 Axis. *Cell Death Dis* (2020) 11 (11):1008. doi: 10.1038/s41419-020-03169-3
10. Yunusova NV, Tugutova EA, Tamkovich SN, Kondakova IV. [The Role of Exosomal Tetraspanins and Proteases in Tumor Progression]. *BioMed Khim* (2018) 64(2):123–33. doi: 10.18097/PBMC20186402123
11. Tamkovich SN, Yunusova NV, Tugutova E, Somov AK, Proskura KV, Kolomiets LA, et al. Protease Cargo in Circulating Exosomes of Breast Cancer and Ovarian Cancer Patients. *Asian Pac J Cancer Prev* (2019) 20 (1):255–62. doi: 10.31557/APJCP.2019.20.1.255
12. Miles J, Andre M, Caobi A, Ruiz M, Nair M, Raymond AD. Bioengineered Exosomal Extracellular Vesicles in Cancer Therapeutics. *Crit Rev BioMed Eng* (2020) 48(3):177–87. doi: 10.1615/CritRevBiomedEng.2020034847
13. Pan S, Zhao X, Shao C, Fu B, Huang Y, Zhang N, et al. STIM1 Promotes Angiogenesis by Reducing Exosomal Mir-145 in Breast Cancer MDA-MB-231 Cells. *Cell Death Dis* (2021) 12(1):38. doi: 10.1038/s41419-020-03304-0
14. Lin S, Xiong W, Liu H, Pei L, Yi H, Guan Y. Profiling and Integrated Analysis of Differentially Expressed Circular Rnas in Plasma Exosomes as Novel Biomarkers for Advanced-Stage Lung Adenocarcinoma. *Onco Targets Ther* (2020) 13:12965–77. doi: 10.2147/OTT.S279710
15. McLaughlin M, Patin EC, Pedersen M, Wilkins A, Dillon MT, Melcher AA, et al. Inflammatory Microenvironment Remodelling by Tumour Cells After Radiotherapy. *Nat Rev Cancer* (2020) 20(4):203–17. doi: 10.1038/s41568-020-0246-1
16. Kim H, Kim EH, Kwak G, Chi SG, Kim SH, Yang Y. Exosomes: Cell-Derived Nanoplatforms for the Delivery of Cancer Therapeutics. *Int J Mol Sci* (2020) 22(1):14. doi: 10.3390/ijms22010014
17. Ho M, Chen T, Liu J, Dowling P, Hideshima T, Zhang L, et al. Targeting Histone Deacetylase 3 (HDAC3) in the Bone Marrow Microenvironment Inhibits Multiple Myeloma Proliferation by Modulating Exosomes and IL-6 Trans-Signaling. *Leukemia* (2020) 34(1):196–209. doi: 10.1038/s41375-019-0493-x
18. Li Z, Zhou X, Gao X, Bai D, Dong Y, Sun W, et al. Fusion Protein Engineered Exosomes for Targeted Degradation of Specific Rnas in Lysosomes: A Proof-of-Concept Study. *J Extracell Vesicles* (2020) 9(1):1816710. doi: 10.1080/20013078.2020.1816710
19. Gastpar R, Gehrmann M, Bausero MA, Asea A, Gross C, Schroeder JA, et al. Heat Shock Protein 70 Surface-Positive Tumor Exosomes Stimulate Migratory and Cytolytic Activity of Natural Killer Cells. *Cancer Res* (2005) 65(12):5238–47. doi: 10.1158/0008-5472.CAN-04-3804
20. Fodor A, Abate BA, Deak P, Fodor L, Gyenge E, Klein MG, et al. Multidrug Resistance (MDR) and Collateral Sensitivity in Bacteria, With Special Attention to Genetic and Evolutionary Aspects and to the Perspectivs of Antimicrobial Peptides-A Review. *Pathogens* (2020) 9(7):522. doi: 10.3390/pathogens9070522
21. Lin Y, Luo Y, Sun Y, Guo W, Zhao X, Xi Y, et al. Genomic and Transcriptomic Alterations Associated With Drug Vulnerabilities and Prognosis in Adenocarcinoma at the Gastroesophageal Junction. *Nat Commun* (2020) 11 (1):6091. doi: 10.1038/s41467-020-19949-6
22. He L, Chen Y, Ke Z, Pang M, Yang B, Feng F, et al. Exosomes Derived From Mirna-210 Overexpressing Bone Marrow Mesenchymal Stem Cells Protect Lipopolysaccharide Induced Chondrocytes Injury *via* the NF-KappaB Pathway. *Gene* (2020) 751:144764. doi: 10.1016/j.gene.2020.144764
23. Zheng X, Liu J, Li X, Tian R, Shang K, Dong X, et al. Angiogenesis Is Promoted by Exosomal DPP4 Derived From 5-Fluorouracil-Resistant Colon Cancer Cells. *Cancer Lett* (2021) 497:190–201. doi: 10.1016/j.canlet.2020.10.009
24. Ilkhani K, Bastami M, Delgir S, Safi A, Talebian S, Alivand MR. The Engaged Role of Tumor Microenvironment in Cancer Metabolism: Focusing on Cancer-Associated Fibroblast and Exosome Mediators. *Anticancer Agents Med Chem* (2021) 21(2):254–66. doi: 10.2174/1871520620666200910123428
25. Farc O, Cristea V. An Overview of the Tumor Microenvironment, From Cells to Complex Networks (Review). *Exp Ther Med* (2021) 21(1):96. doi: 10.3892/etm.2020.9528
26. Kalluri R, LeBleu VS. The Biology, Function, and Biomedical Applications of Exosomes. *Science* (2020) 367(6478):eaau6977. doi: 10.1126/science.aau6977
27. Logozzi M, Capasso C, Di Raimo R, Del Prete S, Mizzoni D, Falchi M, et al. Prostate Cancer Cells and Exosomes in Acidic Condition Show Increased Carbonic Anhydrase IX Expression and Activity. *J Enzyme Inhib Med Chem* (2019) 34(1):272–8. doi: 10.1080/14756366.2018.1538980
28. Logozzi M, Mizzoni D, Angelini DF, Di Raimo R, Falchi M, Battistini L, et al. Microenvironmental Ph and Exosome Levels Interplay in Human Cancer Cell Lines of Different Histotypes. *Cancers (Basel)* (2018) 10(10):370. doi: 10.3390/cancers10100370
29. Logozzi M, De Milito A, Lugini L, Borghi M, Calabro L, Spada M, et al. High Levels of Exosomes Expressing CD63 and Caveolin-1 in Plasma of Melanoma Patients. *PloS One* (2009) 4(4):e5219. doi: 10.1371/journal.pone.0005219
30. Logozzi M, Angelini DF, Iessi E, Mizzoni D, Di Raimo R, Federici C, et al. Increased PSA Expression on Prostate Cancer Exosomes in *In Vitro* Condition and in Cancer Patients. *Cancer Lett* (2017) 403:318–29. doi: 10.1016/j.canlet.2017.06.036
31. Feng C, Xiong Z, Wang C, Xiao W, Xiao H, Xie K, et al. Folic Acid-Modified Exosome-PH20 Enhances the Efficiency of Therapy *via* Modulation of the Tumor Microenvironment and Directly Inhibits Tumor Cell Metastasis. *Bioact Mater* (2021) 6(4):963–74. doi: 10.1016/j.bioactmat.2020.09.014
32. Kugeratski FG, Kalluri R. Exosomes as Mediators of Immune Regulation and Immunotherapy in Cancer. *FEBS J* (2021) 288(1):10–35. doi: 10.1111/febs.15558
33. Qian M, Chen Z, Guo X, Wang S, Zhang Z, Qiu W, et al. Exosomes Derived From Hypoxic Glioma Deliver Mir-1246 and Mir-10b-5p to Normoxic Glioma Cells to Promote Migration and Invasion. *Lab Invest* (2021) 101 (5):612–24. doi: 10.1038/s41374-020-00522-0

34. Yuan X, Qian N, Ling S, Li Y, Sun W, Li J, et al. Breast Cancer Exosomes Contribute to Pre-Metastatic Niche Formation and Promote Bone Metastasis of Tumor Cells. *Theranostics* (2021) 11(3):1429–45. doi: 10.7150/thno.45351
35. Zhou W, Fong MY, Min Y, Somlo G, Liu L, Palomares MR, et al. Cancer-Secreted MiR-105 Destroys Vascular Endothelial Barriers to Promote Metastasis. *Cancer Cell* (2014) 25(4):501–15. doi: 10.1016/j.ccr.2014.03.007
36. Hanahan D, Weinberg RA. The Hallmarks of Cancer. *Cell* (2000) 100(1):57–70. doi: 10.1016/s0092-8674(00)81683-9
37. Hanahan D, Weinberg RA. Hallmarks of Cancer: The Next Generation. *Cell* (2011) 144(5):646–74. doi: 10.1016/j.cell.2011.02.013
38. Torreggiani E, Roncuzzi L, Perut F, Zini N, Baldini N. Multimodal Transfer of MDR by Exosomes in Human Osteosarcoma. *Int J Oncol* (2016) 49(1):189–96. doi: 10.3892/ijo.2016.3509
39. Kato T, Mizutani K, Kameyama K, Kawakami K, Fujita Y, Nakane K, et al. Serum Exosomal P-Glycoprotein Is a Potential Marker to Diagnose Docetaxel Resistance and Select a Taxoid for Patients With Prostate Cancer. *Urol Oncol* (2015) 33(9):385.e15–20. doi: 10.1016/j.urolonc.2015.04.019
40. Yuan Y, Wang L, Ge D, Tan L, Cao B, Fan H, et al. Exosomal O-Glcnac Transferase From Esophageal Carcinoma Stem Cell Promotes Cancer Immunosuppression Through Up-Regulation of PD-1 in CD8(+) T Cells. *Cancer Lett* (2021) 500:98–106. doi: 10.1016/j.canlet.2020.12.012
41. Zhou C, Wei W, Ma J, Yang Y, Liang L, Zhang Y, et al. Cancer-Secreted Exosomal MiR-1468-5p Promotes Tumor Immune Escape *via* the Immunosuppressive Reprogramming of Lymphatic Vessels. *Mol Ther* (2020) 29(4):1512–28. doi: 10.1016/j.ymthe.2020.12.034
42. Binenbaum Y, Fridman E, Yaari Z, Milman N, Schroeder A, Ben David G, et al. Transfer of MiRNA in Macrophage-Derived Exosomes Induces Drug Resistance in Pancreatic Adenocarcinoma. *Cancer Res* (2018) 78(18):5287–99. doi: 10.1158/0008-5472.CAN-18-0124
43. Qin X, Yu S, Zhou L, Shi M, Hu Y, Xu X, et al. Cisplatin-Resistant Lung Cancer Cell-Derived Exosomes Increase Cisplatin Resistance of Recipient Cells in Exosomal Mir-100-5p-Dependent Manner. *Int J Nanomed* (2017) 12:3721–33. doi: 10.2147/ijn.S131516
44. Fu X, Liu M, Qu S, Ma J, Zhang Y, Shi T, et al. Exosomal MicroRNA-32-5p Induces Multidrug Resistance in Hepatocellular Carcinoma *via* the PI3K/Akt Pathway. *J Exp Clin Cancer Res* (2018) 37(1):52. doi: 10.1186/s13046-018-0677-7
45. Yu DD, Wu Y, Zhang XH, Lv MM, Chen WX, Chen X, et al. Exosomes From Adriamycin-Resistant Breast Cancer Cells Transmit Drug Resistance Partly by Delivering MiR-222. *Tumour Biol* (2016) 37(3):3227–35. doi: 10.1007/s13277-015-4161-0
46. Zhang S, Zhang Y, Qu J, Che X, Fan Y, Hou K, et al. Exosomes Promote Cetuximab Resistance *via* the PTEN/Akt Pathway in Colon Cancer Cells. *Braz J Med Biol Res* (2017) 51(1):e6472. doi: 10.1590/1414-431x20176472
47. Wei F, Ma C, Zhou T, Dong X, Luo Q, Geng L, et al. Exosomes Derived From Gemcitabine-Resistant Cells Transfer Malignant Phenotypic Traits *via* Delivery of MiRNA-222-3p. *Mol Cancer* (2017) 16(1):132. doi: 10.1186/s12943-017-0694-8
48. Takahashi K, Yan IK, Kogure T, Haga H, Patel T. Extracellular Vesicle-Mediated Transfer of Long Non-Coding RNA ROR Modulates Chemosensitivity in Human Hepatocellular Cancer. *FEBS Open Bio* (2014) 4:458–67. doi: 10.1016/j.fob.2014.04.007
49. Qu L, Ding J, Chen C, Wu ZJ, Liu B, Gao Y, et al. Exosome-Transmitted Lncarsr Promotes Sunitinib Resistance in Renal Cancer by Acting as a Competing Endogenous RNA. *Cancer Cell* (2016) 29(5):653–68. doi: 10.1016/j.ccell.2016.03.004
50. Zheng P, Chen L, Yuan X, Luo Q, Liu Y, Xie G, et al. Exosomal Transfer of Tumor-Associated Macrophage-Derived Mir-21 Confers Cisplatin Resistance in Gastric Cancer Cells. *J Exp Clin Cancer Res* (2017) 36(1):53. doi: 10.1186/s13046-017-0528-y
51. Ji R, Zhang B, Zhang X, Xue J, Yuan X, Yan Y, et al. Exosomes Derived From Human Mesenchymal Stem Cells Confer Drug Resistance in Gastric Cancer. *Cell Cycle* (2015) 14(15):2473–83. doi: 10.1080/15384101.2015.1005530
52. Tang JX, Chen Q, Li Q, He YH, Xiao D. Exosomal mRNAs and Lncrnas Involved in Multiple Myeloma Resistance to Bortezomib. *Cell Biol Int* (2020) 45(5):965–75. doi: 10.1002/cbin.11540
53. Hu Y, Yan C, Mu L, Huang K, Li X, Tao D, et al. Fibroblast-Derived Exosomes Contribute to Chemoresistance Through Priming Cancer Stem Cells in Colorectal Cancer. *PloS One* (2015) 10(5):e0125625. doi: 10.1371/journal.pone.0125625
54. Boelens MC, Wu TJ, Nabet BY, Xu B, Qiu Y, Yoon T, et al. Exosome Transfer From Stromal to Breast Cancer Cells Regulates Therapy Resistance Pathways. *Cell* (2014) 159(3):499–513. doi: 10.1016/j.cell.2014.09.051
55. Hou Y, Liu Y, Liang S, Ding R, Mo S, Yan D, et al. The Novel Targetexosoms Derived From M2 Macrophage. *Int Rev Immunol* (2020), 40(3):183-196. doi: 10.1080/08830185.2020.1800687
56. Federici C, Petrucci F, Caimi S, Cesolini A, Logozzi M, Borghi M, et al. Exosome Release and Low Ph Belong to a Framework of Resistance of Human Melanoma Cells to Cisplatin. *PloS One* (2014) 9(2):e88193. doi: 10.1371/journal.pone.0088193
57. Kusuzaki K, Matsubara T, Murata H, Logozzi M, Iessi E, Di Raimo R, et al. Natural Extracellular Nanovesicles and Photodynamic Molecules: Is There a Future for Drug Delivery? *J Enzyme Inhib Med Chem* (2017) 32(1):908–16. doi: 10.1080/14756366.2017.1335310
58. Logozzi M, Di Raimo R, Properzi F, Barca S, Angelini DF, Mizzoni D, et al. Nanovesicles Released by OKT3 Hybridoma Express Fully Active Antibodies. *J Enzyme Inhib Med Chem* (2021) 36(1):175–82. doi: 10.1080/14756366.2020.1852401
59. Logozzi M, Mizzoni D, Capasso C, Del Prete S, Di Raimo R, Falchi M, et al. Plasmatic Exosomes From Prostate Cancer Patients Show Increased Carbonic Anhydrase IX Expression and Activity and Low Ph. *J Enzyme Inhib Med Chem* (2020) 35(1):280–8. doi: 10.1080/14756366.2019.1697249
60. Logozzi M, Mizzoni D, Bocca B, Di Raimo R, Petrucci F, Caimi S, et al. Human Primary Macrophages Scavenge Aunps and Eliminate It Through Exosomes. A Natural Shuttling for Nanomaterials. *Eur J Pharm Biopharm* (2019) 137:23–36. doi: 10.1016/j.ejpb.2019.02.014
61. Schott DS, Pizon M, Pachmann U, Pachmann K, Schobert R, Wittig A, et al. Influence of Adjuvant Radiotherapy on Circulating Epithelial Tumor Cells and Circulating Cancer Stem Cells in Primary Non-Metastatic Breast Cancer. *Transl Oncol* (2021) 14(3):101009. doi: 10.1016/j.tranon.2021.101009
62. Ratajczak J, Miekus K, Kucia M, Zhang J, Reca R, Dvorak P, et al. Embryonic Stem Cell-Derived Microvesicles Reprogram Hematopoietic Progenitors: Evidence for Horizontal Transfer of Mrna and Protein Delivery. *Leukemia* (2006) 20(5):847–56. doi: 10.1038/sj.leu.2404132
63. You J, Li M, Cao LM, Gu QH, Deng PB, Tan Y, et al. Snail1-Dependent Cancer-Associated Fibroblasts Induce Epithelial-Mesenchymal Transition in Lung Cancer Cells *via* Exosomes. *QJM* (2019) 112(8):581–90. doi: 10.1093/qjmed/hcz093
64. Domenis R, Cesselli D, Toffoletto B, Bourkoula E, Caponnetto F, Manini I, et al. Systemic T Cells Immunosuppression of Glioma Stem Cell-Derived Exosomes Is Mediated by Monocytic Myeloid-Derived Suppressor Cells. *PloS One* (2017) 12(1):e0169932. doi: 10.1371/journal.pone.0169932
65. Bigagli E, Luceri C, Guasti D, Cinci L. Exosomes Secreted From Human Colon Cancer Cells Influence the Adhesion of Neighboring Metastatic Cells: Role of Microrna-210. *Cancer Biol Ther* (2016) 17(10):1062–9. doi: 10.1080/15384047.2016.1219815
66. Lobb RJ, van Amerongen R, Wiegmans A, Ham S, Larsen JE, Moller A. Exosomes Derived From Mesenchymal Non-Small Cell Lung Cancer Cells Promote Chemoresistance. *Int J Cancer* (2017) 141(3):614–20. doi: 10.1002/ijc.30752
67. Min H, Sun X, Yang X, Zhu H, Liu J, Wang Y, et al. Exosomes Derived From Irradiated Esophageal Carcinoma-Infiltrating T Cells Promote Metastasis by Inducing the Epithelial-Mesenchymal Transition in Esophageal Cancer Cells. *Pathol Oncol Res* (2018) 24(1):11–8. doi: 10.1007/s12253-016-0185-z
68. Donnarumma E, Fiore D, Nappa M, Roscigno G, Adamo A, Iaboni M, et al. Cancer-Associated Fibroblasts Release Exosomal Micrornas That Dictate an Aggressive Phenotype in Breast Cancer. *Oncotarget* (2017) 8(12):19592–608. doi: 10.18632/oncotarget.14752
69. Au Yeung CL, Co NN, Tsuruga T, Yeung TL, Kwan SY, Leung CS, et al. Exosomal Transfer of Stroma-Derived Mir21 Confers Paclitaxel Resistance in Ovarian Cancer Cells Through Targeting APAF1. *Nat Commun* (2016) 7:11150. doi: 10.1038/ncomms11150
70. Dong H, Wang W, Chen R, Zhang Y, Zou K, Ye M, et al. Exosome-Mediated Transfer of Lncrnasnhg14 Promotes Trastuzumab Chemoresistance in Breast Cancer. *Int J Oncol* (2018) 53(3):1013–26. doi: 10.3892/ijo.2018.4467

71. Vella LJ, Behren A, Coleman B, Greening DW, Hill AF, Cebon J. Intercellular Resistance to BRAF Inhibition can be Mediated by Extracellular Vesicle-Associated Pdgfrbeta. *Neoplasia* (2017) 19(11):932–40. doi: 10.1016/j.neo.2017.07.002
72. Lv MM, Zhu XY, Chen WX, Zhong SL, Hu Q, Ma TF, et al. Exosomes Mediate Drug Resistance Transfer in MCF-7 Breast Cancer Cells and a Probable Mechanism Is Delivery of P-Glycoprotein. *Tumour Biol* (2014) 35(11):10773–9. doi: 10.1007/s13277-014-2377-z
73. Williams MS, Basma NJ, Amaral FMR, Williams G, Weightman JP, Breitwieser W, et al. Targeted Nanopore Sequencing for the Identification of ABCB1 Promoter Translocations in Cancer. *BMC Cancer* (2020) 20 (1):1075. doi: 10.1186/s12885-020-07571-0
74. Ning K, Wang T, Sun X, Zhang P, Chen Y, Jin J, et al. UCH-L1-Containing Exosomes Mediate Chemotherapeutic Resistance Transfer in Breast Cancer. *J Surg Oncol* (2017) 115(8):932–40. doi: 10.1002/jso.24614
75. Kharaziha P, Chioureas D, Rutishauser D, Baltatzis G, Lennartsson L, Fonseca P, et al. Molecular Profiling of Prostate Cancer Derived Exosomes May Reveal a Predictive Signature for Response to Docetaxel. *Oncotarget* (2015) 6 (25):21740–54. doi: 10.18632/oncotarget.3226
76. Wang X, Zhang H, Bai M, Ning T, Ge S, Deng T, et al. Exosomes Serve as Nanoparticles to Deliver Anti-Mir-214 to Reverse Chemoresistance to Cisplatin in Gastric Cancer. *Mol Ther* (2018) 26(3):774–83. doi: 10.1016/j.ymthe.2018.01.001
77. Zhang J, Zhang HD, Yao YF, Zhong SL, Zhao JH, Tang JH. Beta-Elemene Reverses Chemoresistance of Breast Cancer Cells by Reducing Resistance Transmission *via* Exosomes. *Cell Physiol Biochem* (2015) 36(6):2274–86. doi: 10.1159/000430191
78. Cao YL, Zhuang T, Xing BH, Li N, Li Q. Exosomal DNMT1 Mediates Cisplatin Resistance in Ovarian Cancer. *Cell Biochem Funct* (2017) 35 (6):296–303. doi: 10.1002/cbf.3276
79. Liu Y, Song B, Wei Y, Chen F, Chi Y, Fan H, et al. Exosomes From Mesenchymal Stromal Cells Enhance Imatinib-Induced Apoptosis in Human Leukemia Cells *via* Activation of Caspase Signaling Pathway. *Cytotherapy* (2018) 20(2):181–8. doi: 10.1016/j.jcyt.2017.11.006
80. Li Y, Liang Y, Sang Y, Song X, Zhang H, Liu Y, et al. MiR-770 Suppresses the Chemo-Resistance and Metastasis of Triple Negative Breast Cancer *via* Direct Targeting of STMN1. *Cell Death Dis* (2018) 9(1):14. doi: 10.1038/s41419-017-0030-7
81. Liu X, Jiang T, Li X, Zhao C, Li J, Zhou F, et al. Exosomes Transmit T790M Mutation-Induced Resistance in EGFR-Mutant NSCLC by Activating PI3K/AKT Signalling Pathway. *J Cell Mol Med* (2020) 24(2):1529–40. doi: 10.1111/jcmm.14838
82. Wang B, Zhang Y, Ye M, Wu J, Ma L, Chen H. Cisplatin-Resistant MDA-MB-231 Cell-Derived Exosomes Increase the Resistance of Recipient Cells in an Exosomal MiR-423-5p-Dependent Manner. *Curr Drug Metab* (2019) 20 (10):804–14. doi: 10.2174/1389200220666190819151946
83. Melo SA, Luecke LB, Kahlert C, Fernandez AF, Gammon ST, Kaye J, et al. Glypican-1 Identifies Cancer Exosomes and Detects Early Pancreatic Cancer. *Nature* (2015) 523(7559):177–82. doi: 10.1038/nature14581
84. Yuwen DL, Sheng BB, Liu J, Wenyu W, Shu YQ. MiR-146a-5p Level in Serum Exosomes Predicts Therapeutic Effect of Cisplatin in Non-Small Cell Lung Cancer. *Eur Rev Med Pharmacol Sci* (2017) 21(11):2650–8.
85. Kang KW, Jung JH, Hur W, Park J, Shin H, Choi B, et al. The Potential of Exosomes Derived From Chronic Myelogenous Leukaemia Cells as a Biomarker. *Anticancer Res* (2018) 38(7):3935–42. doi: 10.21873/anticanres.12679
86. Wang T, Ning K, Lu TX, Sun X, Jin L, Qi X, et al. Increasing Circulating Exosomes-Carrying TRPC5 Predicts Chemoresistance in Metastatic Breast Cancer Patients. *Cancer Sci* (2017) 108(3):448–54. doi: 10.1111/cas.13150
87. Yang SJ, Wang DD, Li J, Xu HZ, Shen HY, Chen X, et al. Predictive Role of GSTP1-Containing Exosomes in Chemotherapy-Resistant Breast Cancer. *Gene* (2017) 623:5–14. doi: 10.1016/j.gene.2017.04.031
88. Chen T, Zhang G, Kong L, Xu S, Wang Y, Dong M. Leukemia-Derived Exosomes Induced IL-8 Production in Bone Marrow Stromal Cells to Protect the Leukemia Cells Against Chemotherapy. *Life Sci* (2019) 221:187–95. doi: 10.1016/j.lfs.2019.02.003
89. Dong X, Bai X, Ni J, Zhang H, Duan W, Graham P, et al. Exosomes and Breast Cancer Drug Resistance. *Cell Death Dis* (2020) 11(11):987. doi: 10.1038/s41419-020-03189-z
90. Foroni C, Zarovni N, Bianciardi L, Bernardi S, Triggiani L, Zocco D, et al. When Less Is More: Specific Capture and Analysis of Tumor Exosomes in Plasma Increases the Sensitivity of Liquid Biopsy for Comprehensive Detection of Multiple Androgen Receptor Phenotypes in Advanced Prostate Cancer Patients. *Biomedicines* (2020) 8(5):131. doi: 10.3390/biomedicines8050131
91. Qiao L, Liu X, Tang Y, Zhao Z, Zhang J, Liu H. Knockdown of Long non-Coding RNA Prostate Cancer-Associated Ncrna Transcript 1 Inhibits Multidrug Resistance and C-Myc-Dependent Aggressiveness in Colorectal Cancer Caco-2 and HT-29 Cells. *Mol Cell Biochem* (2018) 441(1-2):99–108. doi: 10.1007/s11010-017-3177-8
92. Santos JC, Lima NDS, Sarian LO, Matheu A, Ribeiro ML, Derchain SFM. Exosome-Mediated Breast Cancer Chemoresistance *via* MiR-155 Transfer. *Sci Rep* (2018) 8(1):829. doi: 10.1038/s41598-018-19339-5
93. Osti D, Del Bene M, Rappa G, Santos M, Matafora V, Richichi C, et al. Clinical Significance of Extracellular Vesicles in Plasma From Glioblastoma Patients. *Clin Cancer Res* (2019) 25(1):266–76. doi: 10.1158/1078-0432.CCR-18-1941
94. Rodriguez Zorrilla S, Perez-Sayans M, Fais S, Logozzi M, Gallas Torreira M, Garcia Garcia A. A Pilot Clinical Study on the Prognostic Relevance of Plasmatic Exosomes Levels in Oral Squamous Cell Carcinoma Patients. *Cancers (Basel)* (2019) 11(3):429. doi: 10.3390/cancers11030429

Conflict of Interest: The authors declare that the research was conducted in the absence of any commercial or financial relationships that could be construed as a potential conflict of interest.

Publisher's Note: All claims expressed in this article are solely those of the authors and do not necessarily represent those of their affiliated organizations, or those of the publisher, the editors and the reviewers. Any product that may be evaluated in this article, or claim that may be made by its manufacturer, is not guaranteed or endorsed by the publisher.

frontiers in Cell and Developmental Biology

ORIGINAL RESEARCH
published: 03 November 2021
doi: 10.3389/fcell.2021.710721

Effect of Photodynamic Therapy on Gemcitabine-Resistant Cholangiocarcinoma *in vitro* and *in vivo* Through KLF10 and EGFR

Yang Yang[1,2†], Jigang Li[1†], Lei Yao[3] and Lile Wu[2]*

[1] Department of Clinical Pathology, Hunan Cancer Hospital, Changsha, China, [2] Department of Hepatobiliary Surgery, The Affiliated Hospital of Southwest Medical University, Luzhou, China, [3] Academician Expert Workstation of Sichuan Province, The Affiliated Hospital of Southwest Medical University, Luzhou, China

Cholangiocarcinoma is a relatively rare neoplasm with increasing incidence. Although chemotherapeutic agent such as gemcitabine has long been used as standard treatment for cholangiocarcinoma, the interindividual variability in target and drug sensitivity and specificity may lead to therapeutic resistance. In the present study, we found that photodynamic therapy (PDT) treatment inhibited gemcitabine-resistant cholangiocarcinoma cells *via* repressing cell viability, enhancing cell apoptosis, and eliciting G1 cell cycle arrest through modulating Cyclin D1 and caspase 3 cleavage. *In vivo*, PDT treatment significantly inhibited the growth of gemcitabine-resistant cholangiocarcinoma cell-derived tumors. Online data mining and experimental analyses indicate that KLF10 expression was induced, whereas EGFR expression was downregulated by PDT treatment; KLF10 targeted the EGFR promoter region to inhibit EGFR transcription. Under PDT treatment, EGFR overexpression and KLF10 silencing attenuated the anti-cancer effects of PDT on gemcitabine-resistant cholangiocarcinoma cells by promoting cell viability, inhibiting apoptosis, and increasing S phase cell proportion. Importantly, under PDT treatment, the effects of KLF10 silencing were significantly reversed by EGFR silencing. In conclusion, PDT treatment induces KLF10 expression and downregulates EGFR expression. KLF10 binds to EGFR promoter region to inhibit EGFR transcription. The KLF10/EGFR axis participates in the process of the inhibition of PDT on gemcitabine-resistant cholangiocarcinoma cells.

Keywords: cholangiocarcinoma, gemcitabine resistance, photodynamic therapy (PDT), KLF10, EGFR, cell cycle 3

OPEN ACCESS

Edited by:
José Díaz-Chávez, National Institute of Cancerology (INCAN), Mexico

Reviewed by:
Fei Han, Army Medical University, China
Wunchana Seubwai, Khon Kaen University, Thailand

***Correspondence:**
Lile Wu
wbm_bigcat@hotmail.com

† These authors have contributed equally to this work

Specialty section:
This article was submitted to Molecular and Cellular Oncology, a section of the journal Frontiers in Cell and Developmental Biology

Received: *17 May 2021*
Accepted: *16 September 2021*
Published: *03 November 2021*

Citation:
Yang Y, Li J, Yao L and Wu L (2021) Effect of Photodynamic Therapy on Gemcitabine-Resistant Cholangiocarcinoma in vitro and in vivo Through KLF10 and EGFR. Front. Cell Dev. Biol. 9:710721. doi: 10.3389/fcell.2021.710721

INTRODUCTION

Cholangiocarcinoma is a diverse group of malignancies arising from the biliary epithelium and a relatively rare neoplasm in developed countries; however, the incidence of cholangiocarcinoma is increasing globally (Siegel et al., 2019). Due to the difficulty of prognostic accuracy, at least half of patients are diagnosed with unresectable tumors and progress to an advanced stage (Blechacz and Gores, 2008; Kim et al., 2017). Thus, advanced, or metastatic disease patients present an overall survival of less than 6 months and a 5-year survival rate of less than 10% (Marin et al., 2018).

Systemic chemotherapy, as well as single-agent molecular targeted therapy are the conventional treatments for cholangiocarcinoma. For example, gemcitabine, one of the most widely used chemotherapeutic drugs for treating cholangiocarcinoma, is a nucleoside deoxycytidine analog that can enter cells *via* nucleoside receptors and then activate deoxycytosine kinases to bind DNA (Thongprasert, 2005; Alvarellos et al., 2014; Fan et al., 2017). Gemcitabine leads to apoptosis *via* blocking cell cycle progression at the G1/S phase boundary (Plunkett et al., 1995; Gilbert et al., 2006; Fan et al., 2017). However, patients with advanced cholangiocarcinoma often obtain chemoresistance and show poor response to chemotherapy (Park et al., 2015; Morizane et al., 2019). For example, patients with inoperable cholangiocarcinoma received gemcitabine therapy only obtained relatively low 5-year survival rates (Valle et al., 2010; Razumilava and Gores, 2013; Rizvi and Gores, 2013). The interindividual variability in target and drug sensitivity and specificity may lead to therapeutic resistance. According to the understanding of the cell mechanism related to cholangiocarcinoma growth and drug reaction, multimodal therapies including combined treatment have emerged as a reasonable method to promote the therapeutic efficacy.

Photodynamic therapy (PDT) employs light activation of tissue-localized photosensitizer in an oxygen-dependent process (the most convenient light source is a laser). In the first stage of PDT, a tumor selective photosensitizer is administered (Dougherty et al., 1998; Bown et al., 2002), followed after some time by the illumination with visible light, which, in the presence of oxygen, leads to the generation of cytotoxic species and consequently to cell death and tissue destruction (Dougherty et al., 1998; Dolmans et al., 2003; Ayaru et al., 2007). PDT has been reported to be used upon skin lesions or hollow organ walls, and in recent years more attention has been paid to its potential in the treatment of solid organ lesions and digestive tract dysplasia and early cancerous lesions (Evrard et al., 1991; Schuitmaker et al., 1996; Bown et al., 2002), including cholangiocarcinoma (Kahaleh, 2012; McCaughan et al., 1991; Talreja et al., 2011). Although the synergetic anti-tumor effects of PDT/gemcitabine combination have been reported within cholangiocarcinoma (Chen et al., 2014; Hong et al., 2014; Wentrup et al., 2016; Kim et al., 2018), the mechanism underlying the synergetic anticancer effect remains unclear.

Previous studies indicated that PDT might induce cancer cell survival pathway activation. For example, within perihilar cholangiocarcinoma (QBC939) cells, sublethal PDT (LC50) led to the alteration of survival signaling pathways such as HIF-1, NF-κB, AP-1, and heat shock factor (HSF) (Luna et al., 1994; Broekgaarden et al., 2015; Weijer et al., 2015, 2016). PDT-treated QBC939 cell line also exhibited decreased protein levels related to the EGFR pathway, especially at LC90 (Weijer et al., 2017). Notably, HIF-1 induction within Het-1a, a human esophageal squamous epithelial cell line, decreased 5-ALA-PDT-induced cell death and apoptosis; the pro-survival response of HIF-1 showed to be inhibited after siRNA-mediated knockdown of HIF-1, thereby increasing PDT efficacy within the Het-1a cell line (Ji et al., 2006). Verteporfin-PDT induced EGFR and STAT3 expression in OVCAR-5 and H460 cancer cells, whereas the EGFR or STAT-3 silencing with siRNA augmented PDT efficacy (Edmonds et al., 2012). Thus, identifying PDT-targeted survival pathways might provide an in-depth understanding of the synergetic anticancer effect of PDT and gemcitabine.

Herein, the study firstly constructed cholangiocarcinoma cells with resistance to gemcitabine and examined the specific effects of PDT exposure on regular and gemcitabine-resistant cholangiocarcinoma cell viability, apoptosis, and cell cycle distribution. The *in vivo* effects of PDT treatment on regular and gemcitabine-resistant cholangiocarcinoma cell-derived implanted tumor growth were also investigated. Then, bioinformatics analyses were performed using online datasets to identify differentially expressed transcription factors and genes after PDT treatment and KLF10 and EGFR were found. The predicted binding and regulation between KLF10 and EGFR were verified, and the specific effects of KLF10 and EGFR upon the synergetic anti-tumor effects of PDT/gemcitabine combination were examined, respectively and combinedly. In conclusion, we identified transcription factors and signaling that might participate in PDT reversing cholangiocarcinoma resistance to gemcitabine.

MATERIALS AND METHODS

Cell Resource

The human cholangiocarcinoma cell line RBE and QBC939 was obtained from Xiangya Cell Bank (Changsha, China) and cultured in RPMI1640 medium (Invitrogen, Carlsbad, CA, United States) supplemented with 10% FBS (Invitrogen). All cells were cultured at 37°C in 5% CO_2.

Induction of Gemcitabine-Resistant Cholangiocarcinoma Cell Lines

RBE and QBC939 cells were exposed to the graded concentrations of gemcitabine, as described previously (De Angelis et al., 2004). Generally, a total of 1×10^5 cells was cultured in 25-cm^2 flasks for 24 h and exposed to gemcitabine (0.25, 0.5, 1, 2, 4, 8, 16, 32, and 64 μM) for 72 h. Surviving cells were cultured in drug-free medium to allow cells to attain 80% confluence. Then, the cells were cultured at this drug concentration until they grew steadily and the IC50 values were determined by the MTT assay. These surviving cells were then exposed to gemcitabine at twofold increase of IC50 concentration for six rounds. Two gemcitabine-resistant cell lines, RBE-R and QBC939-R were obtained after 8 months of culture. All two gemcitabine-resistant cell lines were grown in drug-free medium for 2 weeks then harvested, frozen in the liquid nitrogen, and stored at −80°C until analyzed.

MTT for Cell Viability

Cells were seeded in 96-well plates at a density of 5×10^3 cells/well and treated with gemcitabine for 72 h or PDT treatment. Cell viability was evaluated with the 3-(4,5-dimethylthiazol-2yl)-2,5-diphenyltetrazolium bromide (MTT) assay (AMRESCO, Solon, OH, United States). Half-maximal inhibitory concentration (IC50) was analyzed relative

to the DMSO control. Values are shown as the means of triplicate wells from three independent experiments for each drug concentration.

Flow Cytometry for Cell Cycle and Cell Apoptosis

For cell cycle analysis, cells were plated in 6-well plates at a density of 1×10^5 cells/well for 24 h. After treatment and/or transfection, cells were harvested, washed twice with cold PBS, fixed overnight in 70% ethanol at 4°C, incubated for 30 min in the dark with RNase A and propidium iodide (PI) (final concentration 2.4 μg/ml) at room temperature. The cell cycle distribution was examined using an ACEA NovoCyte flow cytometer (Becton-Dickinson, San Jose, CA, United States), and the data were analyzed using FlowJo software.

For cell apoptosis, an Annexin V-FLUOS staining kit (Roche Diagnostic, Mannheim, Germany) was used. Cells were plated in 6-well plates at a density of 1×10^5 cells/well for 24 h. After treatment and/or transfection, floating and adherent cells were collected, washed twice with cold PBS, resuspended in 100 μl binding buffer containing 2 μl Annexin V-FITC and 2 μl PI (50 μg/ml) and incubated at room temperature for 15 min in the dark. Then, cell apoptosis was analyzed using a FACScanto^{TM} II flow cytometer (Becton-Dickinson), and the data were analyzed using FACS Diva^{TM} software (Becton-Dickinson).

Immunoblotting

Target cells were lysed with the iced hypotonic buffer. After estimating the protein concentrations, the samples containing the proteins were loaded and separated on SDS–PAGE. Then, the blots were transferred to a PVDF membrane and incubated with the primary antibodies for 24 h at 4°C. The following antibodies were used: anti-ki67 (27309-1-AP; Proteintech, Wuhan, China), anti-Cyclin D1 (60186-1-Ig, Proteintech), anti-cleaved-caspase 3 (ab2302; Abcam, Cambridge, MA, United States), anti-caspase 3 (19677-1-AP, Proteintech), anti-EGFR (CSB-PA10279A0Rb; CUSABIO, Houston, TX, United States), Erk1/2 (67170-1-Ig, Proteintech), p-Erk1/2 (sc-81492; Santa Cruz, Dallas, TX, United States), anti-Akt (Y409094; ABM, Richmond, BC, Canada), anti-p-Akt (Y011054, ABM), anti-VEGF (CSB-PA07529A0Rb, CUSABIO), anti-KLF10 (ab73537, Abcam), and anti-GAPDH (ab8245, Abcam). After that, the membrane was incubated with HRP-conjugated secondary antibody (1:1000) for 1 h at 37°C. The visualization of the proteins was achieved by the enhanced chemiluminescence (ECL) reagent.

Subcutaneously Implanted Tumor Model in Nude Mouse

Gemcitabine-resistant QBC939-R/REB-R or gemcitabine-sensitive QBC939/REB cells were implanted into 5-week-old BALB/c nude mice. Briefly, the cells (2×10^6) in 100 μl of serum-free RPMI were injected subcutaneously into the flank of the mice. Mice bearing human cholangiocarcinoma cells-derived xenograft tumors were treated or non-treated with PDT. Tumor size and tumor weight were measured every 3 days, and volumes were determined using the formula volume = length × width^2/2. At day 35, the mice were sacrificed. The tumor tissues were collected and the protein levels of ki67, CyclinD1, and cleaved-caspase3/caspase3 were examined in tumor tissues. All procedures were approved by the Institutional Animal Care and Use Committee (IACUC) of The Affiliated Hospital of Southwest Medical University in accordance with the "Principles of Laboratory Animal Care" (NIH, Bethesda, MD, United States).

Mice Photodynamic Therapy

After tumor diameter of nude mice reached over 6 mm for about 15 days, mice bearing QBC939/REB- or QBC939-R/REB-R-derived tumors were randomized to divide into 8 groups, including QBC939 (n = 6), QBC939 + PDT (n = 6), QBC939-R (n = 6), QBC939-R + PDT (n = 6), REB (n = 6), REB + PDT (n = 6), REB-R (n = 6), REB-R + PDT (n = 6). Mice received intratumoral administration of 20% 5-ALA (Sigma Chemical Co.) at a dose of 100 mg/kg, following by PDT for 5 min at 4 h later (630 nm, 100 J/cm^2, 100 mW/cm^2). The diameter of the irradiating laser beam entirely covered the tumor. At 14 days after irradiation, the mice were sacrificed. Tumor sizes and weights were analyzed statistically.

RT-qPCR

RNA was extracted from target cells and cDNA was prepared using the oligo-dT-based Transcriptor first-strand cDNA synthesis kit (Roche Diagnostics, Basel, Switzerland) with an input of 500 ng total RNA according to the manufacturer's instructions and diluted in RNAse-free H_2O to obtain a final concentration of 5 ng/μl. The RT-qPCR assays were performed using a Power SYBR Green PCR Master Mix (Life Technologies, Carlsbad, CA, United States) in an ABI Prism 7900HT instrument (Applied Biosystems, Carlsbad, CA, United States). The relative expression levels were calculated using the $2^{-\Delta\Delta Ct}$ method, taking the GAPDH mRNA level as an internal reference.

Bioinformatics Analysis

The expression and clinical data were acquired from The Cancer Genome Atlas (TCGA)-cholangiocarcinoma (CHOL) data and the Gene Expression Omnibus (GEO) data with accession numbers GSE84756 and GSE68292. The GSE84756 dataset includes the whole genome expression profiling of biliary adenocarcinoma cells (SK-ChA-1) while were treated with the buffer (control group), dark toxicity (DT group), 50% lethal concentration of 500-mW laser light (LC50) group) or super lethal concentration of 500-mW laser light (LC90 group). The GSE68292 dataset includes the gene expression of hilar cholangiocarcinoma (SK-ChA-1) cells which were treated with PBS (control group), dark (0 mW group), 50-mW laser light (50 mW group), or 500-mW laser light (500 mW group). The TCGA-CHOL dataset includes the gene expression data of 9 normal control tissues and 36 cholangiocarcinoma tissues.

The online tool UALCAN (Chandrashekar et al., 2017)[1] was used for KLF10 expression, overall survival, disease-specific survival and progression-free interval analysis. The analysis for the microarrays GSE84756 and GSE68292 were analyzed by R language Limma package (Ritchie et al., 2015) with the condition of $|\log2 \text{ (fold change)}| \geq 0.56$, $P < 0.05$.

Chromatin Immunoprecipitation Assay

Chromatin immunoprecipitation assays were performed by using the Magna ChIP Kit (Millipore, Bedford, MA, United States) following the manufacturer's directions. QBC939 cells were treated with formaldehyde to generate DNA-protein cross-links. Cell lysates were sonicated to generate chromatin fragments of 200–300 bp, and the lysates were immunoprecipitated with anti-KLF10 or anti-IgG (internal reference). The precipitated chromatin DNA was recovered and measured by qPCR.

Dual-Luciferase Reporter Assay

To verify the binding between KLF10 and the EGFR promoter, we generated psicheck2-proEGFR and psicheck2-proEGFR-mut luciferase reporter plasmids. The plasmids were then co-transfected into 293T cells with a negative control vector or KLF10-overexpressing vector (vector/KLF10); 48 h after the transfection, the luciferase activity was determined using the Dual-Luciferase Assay Kit (Promega, ıMadison, WI, United States).

Statistical Analysis

Statistical analyses were performed using GraphPad (GraphPad Software, Inc., La Jolla, CA, United States). Significant differences between groups were evaluated by a Student's *t*-test. The results are reported as the means ± standard deviation (SD) based on at least three replicates.

RESULTS

Effects of Photodynamic Therapy on Cholangiocarcinoma Gemcitabine Resistance

To investigate the specific functions of PDT exposure upon cholangiocarcinoma gemcitabine resistance to gemcitabine, we firstly established two gemcitabine-resistant cholangiocarcinoma cells, RBE-R and QBC939-R, as described. After 8 months induction, the IC50 values of regular RBE and QBC939 cell lines were increased from 3.011, 4.501 to 14.44, 18.19 μM, respectively (**Figure 1A**), suggesting that the gemcitabine-resistant cancer cells were successfully constructed. Secondly, these cholangiocarcinoma cells were exposed or non-exposed to PDT treatment and examined for the cell viability. **Figure 1B** showed that RBE-R, and QBC939-R cell viability was higher than that of regular RBE, and QBC939 cell; PDT exposure significantly inhibited the cell viability of all cancer cells and RBE-R, and QBC939-R cell viability more inhibited. Then, RBE-R and QBC939-R cell lines showed to be exposed or non-exposed to PDT treatment and examined for the cell apoptosis and cell cycle distribution. Compared with RBE and QBC939 cell line, respectively, the apoptosis of RBE-R and QBC939-R cell line was significantly inhibited; PDT significantly promoted apoptosis of these cell lines (**Figure 1C** and **Supplementary Figure 1A**). Compared with RBE and QBC939 cells, respectively, RBE-R and QBC939-R cell cycle tended to distribute in S phase; PDT exposure induced cell cycle in G1 phase within these cell lines (**Figure 1D** and **Supplementary Figure 1B**). As for the proliferating and apoptotic markers, the protein levels of ki67 and Cyclin D1 were significantly increased, whereas cleaved-caspase 3/caspase 3 was decreased in RBE-R and QBC939-R cells; PDT exposure significantly reversed the changes in these proteins in these cell lines (**Figure 1E**). These data suggest that PDT exposure exhibited cytotoxicity on regular RBE and QBC939 cell line and gemcitabine-resistant RBE-R and QBC939-R cell line.

Photodynamic Therapy Treatment Inhibits Gemcitabine-Resistant Cholangiocarcinoma Cells Xenotransplanted Tumors

To further confirm the *in vitro* findings, we established a xenotransplanted tumor model in nude mice by injecting regular RBE and QBC939 cell lines or gemcitabine-resistant RBE-R and QBC939-R cell lines. Mice bearing tumors derived from regular RBE and QBC939 cell line or gemcitabine-resistant RBE-R and QBC939-R cell line showed to be treated or non-treated with PDT. Twenty-eight days after transplanting, the tumor volume (**Figure 2A**) and tumor weight (**Figure 2B**) of RBE-R or QBC939-R-derived tumors were significantly larger than those of the RBE or QBC939-derived tumors, respectively. For both types of tumors, PDT treatment significantly reduced the tumor volume and tumor weight (**Figures 2A,B**). Moreover, the protein levels of ki67, Cyclin D1, cleaved-caspase 3, and caspase 3 were examined in tumor tissues. Consistent with *in vitro* findings, ki67 and Cyclin D1 proteins showed to be dramatically increased, whereas cleaved-caspase 3/caspase 3 was decreased in RBE-R or QBC939-R-derived tumors, compared with those in RBE or QBC939-derived tumors, respectively (**Figure 2C**). PDT exposure significantly reversed the alterations in these proteins in both types of tumors (**Figure 2C**). These *in vivo* findings suggest that PDT treatment exhibits anti-tumor effects on gemcitabine-resistant cell-derived tumors.

Identification of Differentially Expressed Genes That Could Participate in Photodynamic Therapy Reversing the Resistance of Cholangiocarcinoma Cells to Gemcitabine

Transcription factors are at the core of gene expression regulation. To investigate the mechanism underlying PDT reversing cholangiocarcinoma gemcitabine resistance, we performed online data mining to identify transcription factors

[1] http://ualcan.path.uab.edu/index.html

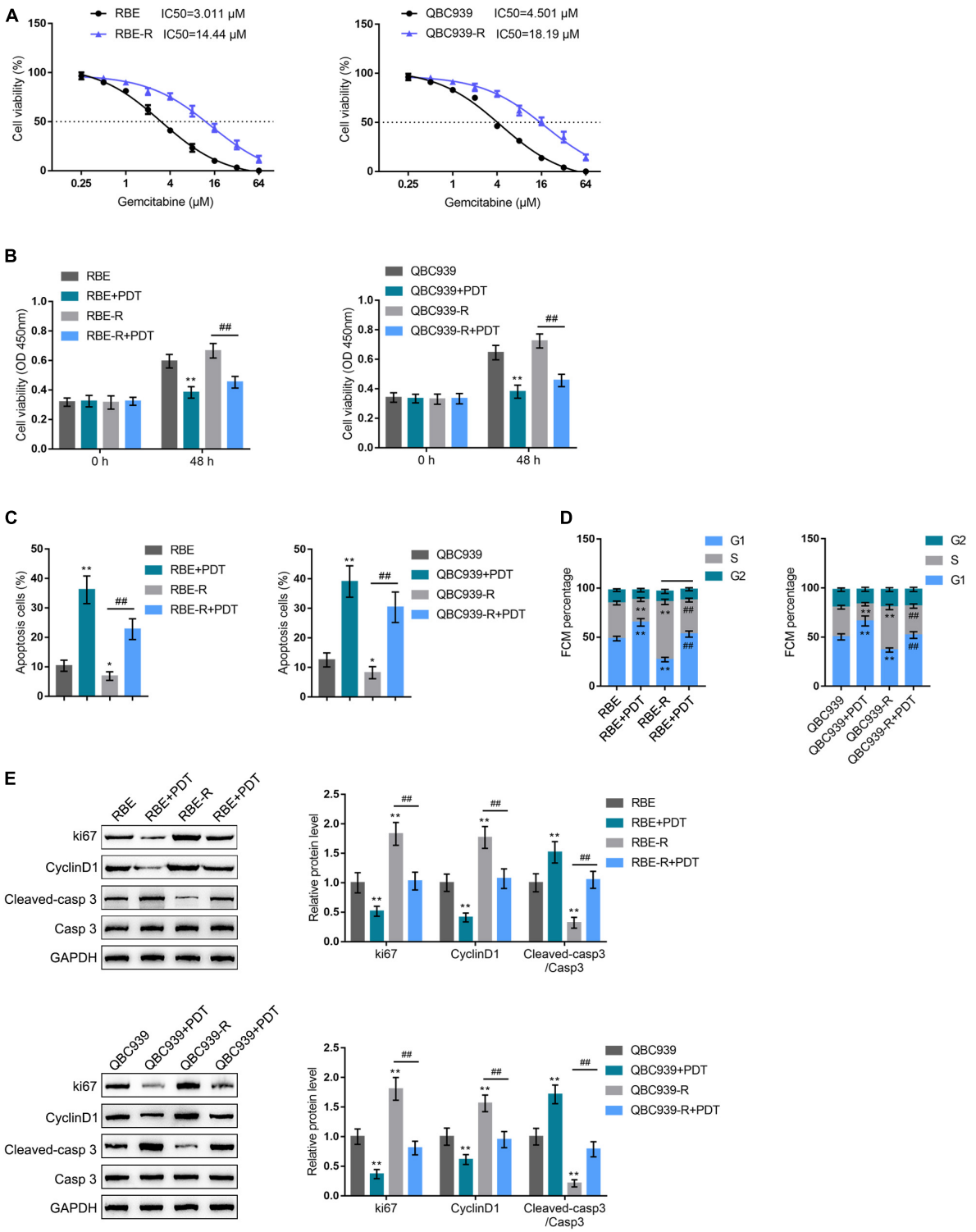

FIGURE 1 | Effects of PDT on gemcitabine-resistant cholangiocarcinoma cells. **(A)** Gemcitabine-resistant cholangiocarcinoma cell lines, RBE-R and QBC939-R were established as described; the cell viability was determined by MTT assays and shown as the IC50 values. **(B)** Regular and gemcitabine-resistant cholangiocarcinoma cell lines were exposed or non-exposed to PDT treatment and examined for the cell viability by MTT assays. Then, RBE, QBC939, RBE-R, and QBC939-R cells were exposed or non-exposed to PDT treatment and examined for the cell apoptosis by Flow cytometry **(C)**; cell cycle distribution by Flow cytometry **(D)**; the protein levels of ki67, Cyclin D1, cleaved-caspase 3, and caspase 3 by Immunoblotting **(E)**. $^{*}P < 0.05$, $^{**}P < 0.01$, $^{\#\#}P < 0.01$.

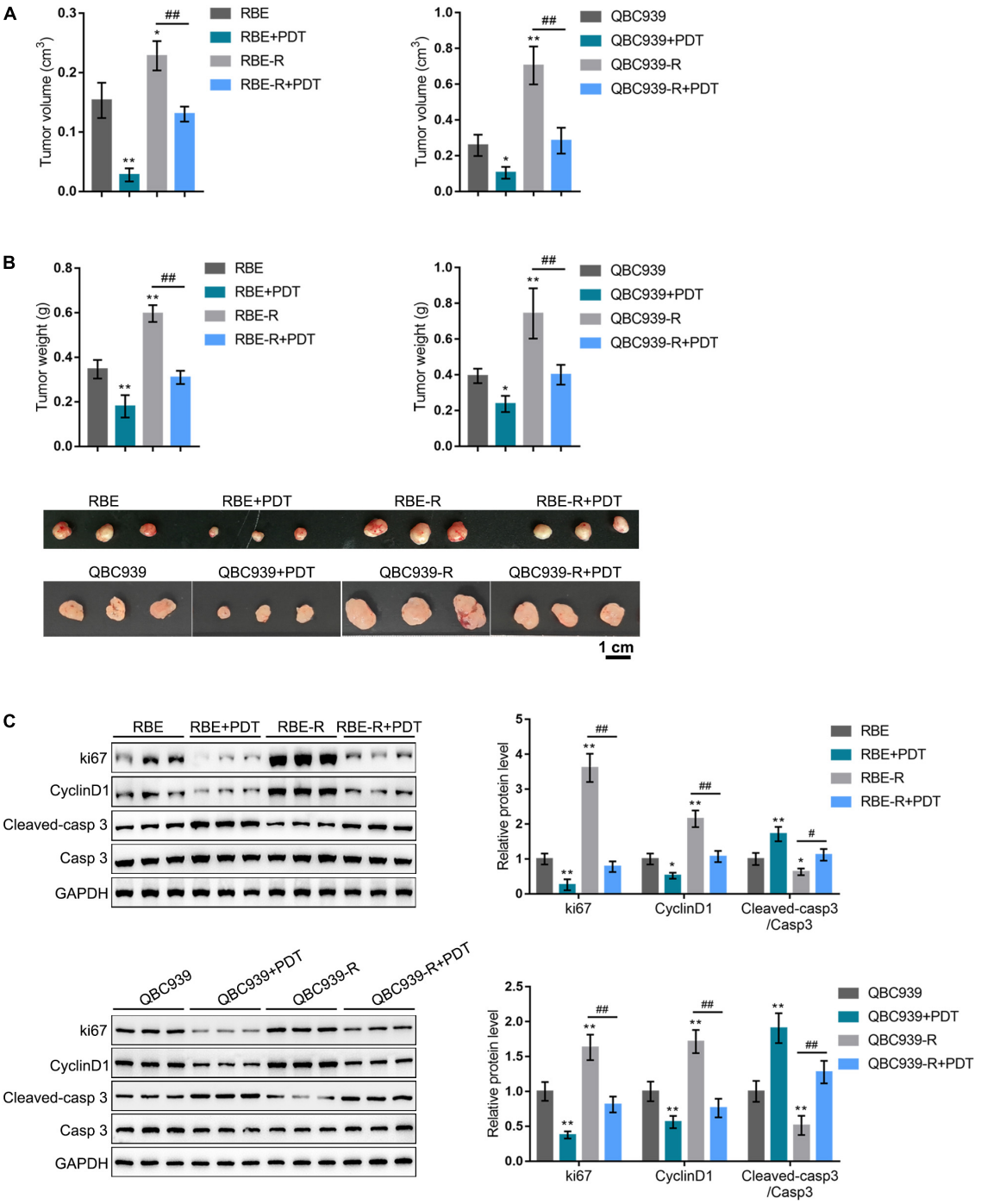

FIGURE 2 | PDT treatment inhibits gemcitabine-resistant cholangiocarcinoma cells xenotransplanted tumors. **(A,B)** Xenotransplanted tumor model derived from regular RBE and QBC939 or gemcitabine-resistant RBE-R and QBC939-R cells was established in nude mice as described in section "Materials and Methods." Twenty-eight days after transplanting, the tumors were undergone PDT treatment. Fourteen days later, the tumor size was measured and the tumor volume was calculated **(A)**; the tumor weight was measured **(B)**; **(C)** the protein levels of ki67, Cyclin D1, cleaved-caspase 3, and caspase 3 in tumor tissues were examined by Immunoblotting. $^{*}P < 0.05$, $^{**}P < 0.01$, $^{\#\#}P < 0.01$.

altered by PDT treatment by bioinformatics analyses. GSE84756 and GSE68292 datasets were compared, and found that these two datasets intersected in 31 differentially expressed transcription factors (11 downregulated and 20 upregulated) within PDT-subjected QBC939 cell line (**Supplementary Table 1**). Among the 20 upregulated transcription factors,

CEBPD, CSRNP1, and KLF10 were regularly underexpressed in cholangiocarcinoma but upregulated by PDT treatment. According to TCGA- CHOL data, KLF10 expression was significantly downregulated in cholangiocarcinoma tissues (**Supplementary Figure 2A**). Moreover, also according to TCGA-CHOL data, cholangiocarcinoma patients with lower KLF10 expression predicted poorer overall survival (**Supplementary Figure 2B**), disease-specific survival (**Supplementary Figure 2C**), and progression-free survival (**Supplementary Figure 2D**). Thus, KLF10 might participate in the process of PDT reversing cholangiocarcinoma gemcitabine resistance.

As for the downstream signaling involved, also based on GSE84756 and GSE68292, a total of 147 genes were upregulated and 181 downregulated after PDT treatment. These deregulated genes were applied for DAVID KEGG signaling enrichment annotation, and 17 were enriched in tumor signaling, including 11 downregulated (EGFR, AXIN2, WNT7B, ADCY1, GNG12, GNAI1, ITGB1, ITGA6, LAMB1, LAMC1, and RUNX1) and 6 upregulated (CXCL8, FOS, MYC, JUN, NFKB2, and TRAF4) by PDT. Then, KLF10 targeted signaling was predicted and EGFR was among the KLF10 targeted genes. According to GSE84756 and GSE68292, KLF10 expression was significantly upregulated, whereas EGFR expression was downregulated by PDT treatment (**Figures 3A–D**). In tissue samples, KLF10 and EGFR expression were negatively correlated (**Figures 3E,F**). Thus, we hypothesize that KLF10 might target the EGFR promoter region to inhibit EGFR transcription. KLF10 and EGFR might be involved in the process of PDT reversing cholangiocarcinoma gemcitabine resistance.

KLF10 Inhibits EGFR Transcription by Binding the Promoter Region

Before investigating the roles of KLF10 and EGFR in PDT reversing cholangiocarcinoma gemcitabine resistance, we first examined the predicted KLF10 binding and negative regulation of EGFR. RBE and gemcitabine-resistant RBE-R cell line showed to be exposed or non-exposed to PDT treatment and examined for KLF10 mRNA expression and protein levels. KLF10 expression was downregulated within RBE-R cells compared with RBE cells. Moreover, consistent with online microarray expression profiles, PDT treatment significantly induced KLF10 mRNA expression and protein levels in both REB and REB-R cells (**Figures 4A,B**). Then, KLF10 overexpression or silencing was achieved in RBE-R cells by transfecting KLF10-overexpressing vector or small interfering RNA targeting KLF10. The transfection efficiency was verified using Immunoblotting (**Figure 4C**). In RBE-R cells, EGFR mRNA expression and protein levels were significantly downregulated by KLF10 overexpression, whereas upregulated by KLF10 silencing (**Figures 4D,E**). These data confirmed that KLF10 negatively regulates EGFR expression.

To confirm the binding of KLF10 to EGFR promoter, we transfected RBE-R cells with KLF10 or empty vector and performed ChIP assay using anti-KLF10 or anti-IgG (negative control). We employed real-time qPCR to examine the EGFR promoter levels in the immunoprecipitate. **Figure 4F** showed that the EGFR promoter levels were significantly increased within the immunoprecipitate of anti-KLF10 compared with that in anti-IgG group; moreover, KLF10-overexpressing cells obtained higher EGFR promoter levels compared with that in cells transfected with empty expression vector. Next, dual-luciferase reporter assay was performed by constructing wild-type psicheck2-proEGFR and mutant type psicheck2-proEGFR-mut luciferase reporter plasmids and co-transfected them in 293T cells with KLF10 or empty vector. **Figure 4G** showed that KLF10 overexpression dramatically repressed psicheck2-proEGFR plasmid luciferase activity; when co-transfected with psicheck2-proEGFR-mut, KLF10 overexpression failed to alter the luciferase activity. In summary, KLF10 could inhibit EGFR transcription *via* directly binding to the EGFR promoter region.

EGFR Might Participate in Photodynamic Therapy Reversing Cholangiocarcinoma Gemcitabine Resistance

After confirming KLF10 negative regulation of EGFR, next, the specific effects of these two factors on the process of PDT reversing cholangiocarcinoma gemcitabine resistance were investigated. RBE or gemcitabine-resistant RBE-R cell lines showed to be exposed or non-exposed to PDT treatment and examined for EGFR mRNA and protein expression. EGFR mRNA and protein expression showed to be significantly upregulated within RBE-R cell line compared with RBE cell line; PDT treatment significantly downregulated the mRNA and protein expression of EGFR within these two cell lines (**Figures 5A,B**). Next, EGFR overexpression was achieved within RBE-R cell line under PDT treatment by transfecting the EGFR-overexpressing vector (EGFR). The transfection efficiency was verified using real-time qPCR (**Figure 5C**). Under PDT treatment, EGFR overexpression significantly promoted RBE-R cell viability (**Figure 5D**), inhibited cell apoptosis (**Figure 5E**), and increased the proportion of S phase cells (**Figure 5F**). As for the proliferating and apoptotic markers, under PDT treatment, EGFR overexpression significantly increased EGFR and VEGF proteins, as well as the ratio of p-Erk1/2/Erk1/2 and p-Akt/Akt (**Figure 5G**). These data suggest that EGFR overexpression could attenuate gemcitabine-resistant cholangiocarcinoma cell response to PDT treatment.

KLF10 Silencing Attenuates the Effects of Photodynamic Therapy on Gemcitabine-Resistant Cells

Considering that PDT significantly induces KLF10 expression, next, KLF10 silencing was achieved in RBE-R cells under PDT treatment by transfecting si-KLF10 or si-NC (negative control). Similar to EGFR overexpression, under PDT treatment, KLF10 silencing significantly promoted RBE-R cell viability (**Figure 6A**), repressed cell apoptosis (**Figure 6B**), and increased the proportion of S phase cells (**Figure 6C**). As for the proliferating and apoptotic markers, under PDT treatment, KLF10 silencing decreased the protein levels of KLF10, whereas increased EGFR and VEGF protein levels and the ratio of p-Erk1/2/Erk1/2 and p-Akt/Akt significantly (**Figure 6D**).

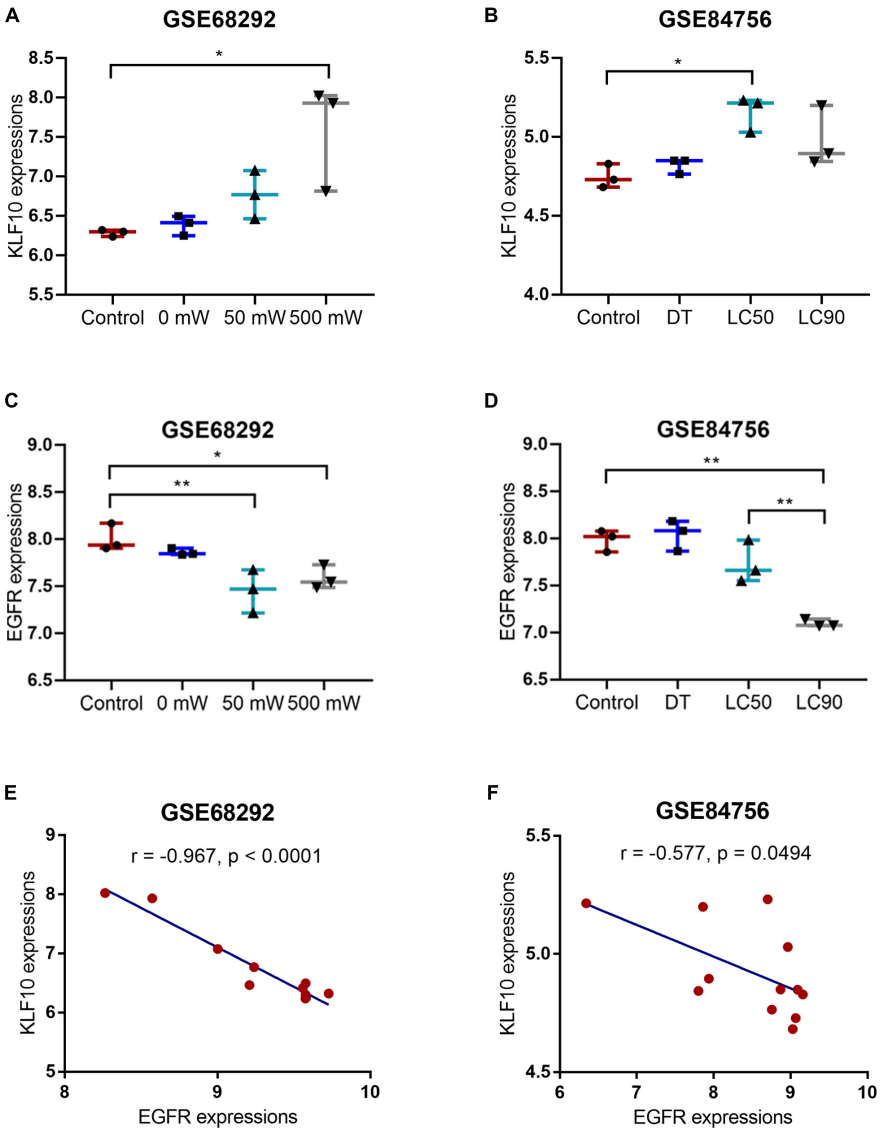

FIGURE 3 | KLF10 expression and correlation with EGFR. **(A)** KLF10 expression under the control, 0, 50, or 500 mW PDT exposure, according to GSE68292. **(B)** KLF10 expression under the control, dark toxicity (DT), LC50, or LC90 PDT exposure, according to GSE84756. **(C)** EGFR expression under the control, 0, 50, or 500 mW PDT exposure, according to GSE68292. **(D)** EGFR expression under the control, dark toxicity (DT), LC50, or LC90 PDT exposure, according to GSE84756. **(E)** The correlation between KLF10 and EGFR expression, according to GSE68292. **(F)** The correlation between KLF10 and EGFR expression, according to GSE84756. *$P < 0.05$, **$P < 0.01$.

KLF10 Modulates Photodynamic Therapy Reversing Cholangiocarcinoma Gemcitabine Resistance Through EGFR

To investigate whether the KLF10/EGFR axis plays a dynamic role in the process of PDT reversing cholangiocarcinoma gemcitabine resistance, we co-transfected RBE-R cells with si-KLF10 and si-EGFR, exposed the cells to PDT treatment, and examined for the mRNA expression of KLF10 and EGFR. As shown in **Figures 7A,B**, under PDT treatment, si-KLF10 transfection downregulated KLF10 expression and upregulated EGFR expression, and si-EGFR transfection caused no alteration in KLF10 expression and downregulated EGFR expression; the effects of si-KLF10 transfection on EGFR expression was significantly reversed by si-EGFR transfection (**Figures 7A,B**). As for the cellular functions, KLF10 silencing promoted cell viability, repressed cell apoptosis, and increased the proportion of S phase cells (**Figures 7C–E**); on the contrary, EGFR silencing inhibited cell viability, enhanced cell apoptosis, and elicited G1 cell cycle arrest (**Figures 7C–E**). The effects of KLF10 silencing on cell phenotype were reversed by EGFR silencing (**Figures 7C–E**). As for the proliferating and apoptotic markers, KLF10 silencing increased EGFR and VEGF proteins and the ratio of p-Erk1/2/Erk1/2 and p-Akt/Akt (**Figure 7F**); on the

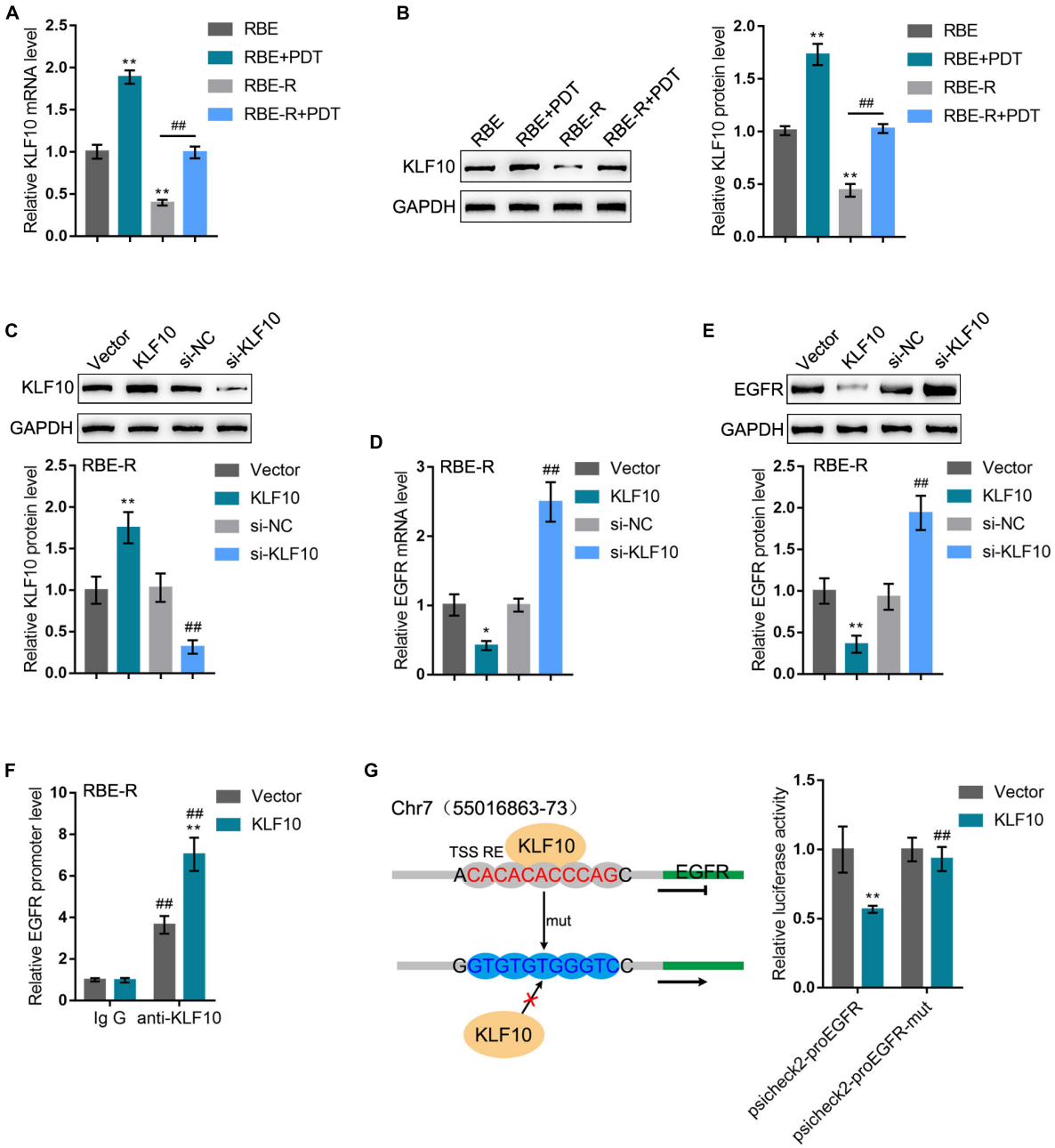

FIGURE 4 | KLF10 inhibits EGFR transcription by binding the promoter region. **(A)** RBE and RBE-R cells were treated or non-treated with PDT and examined for KLF10 mRNA expression by real-time qPCR. **(B)** RBE and RBE-R cells were treated or non-treated with PDT and examined for KLF10 protein levels by Immunoblotting. **(C)** KLF10 overexpression or silencing was achieved in RBE-R cells by transfecting KLF10-overexpressing vector or small interfering RNA targeting KLF10. The transfection efficiency was verified using Immunoblotting. Then, RBE-R cells were transfected with KLF10 or si-KLF10 and examined for the mRNA expression of EGFR by real-time qPCR **(D)** and the protein levels of EGFR by Immunoblotting **(E)**. **(F)** RBE-R cells were transfected with KLF10 or empty vector and ChIP assay was performed using anti-KLF10 or anti-IgG (negative control). The EGFR promoter levels in the immunoprecipitate was examined using real-time qPCR. **(G)** Wild-type psicheck2-proEGFR and mutant type psicheck2-proEGFR-mut luciferase reporter plasmids were constructed and co-transfected in 293T cells with KLF10 or empty vector. The luciferase activity was examined by a dual-luciferase reporter assay. $^{*}P < 0.05$, $^{**}P < 0.01$, $^{\#\#}P < 0.01$.

contrary, EGFR silencing reduced EGFR and VEGF proteins and the ratio of p-Erk1/2/Erk1/2 and p-Akt/Akt (**Figure 7F**). The effects of KLF10 silencing on these markers were reversed by EGFR silencing.

DISCUSSION

In the present study, we found that PDT treatment inhibited gemcitabine-resistant cholangiocarcinoma cells *via* repressing

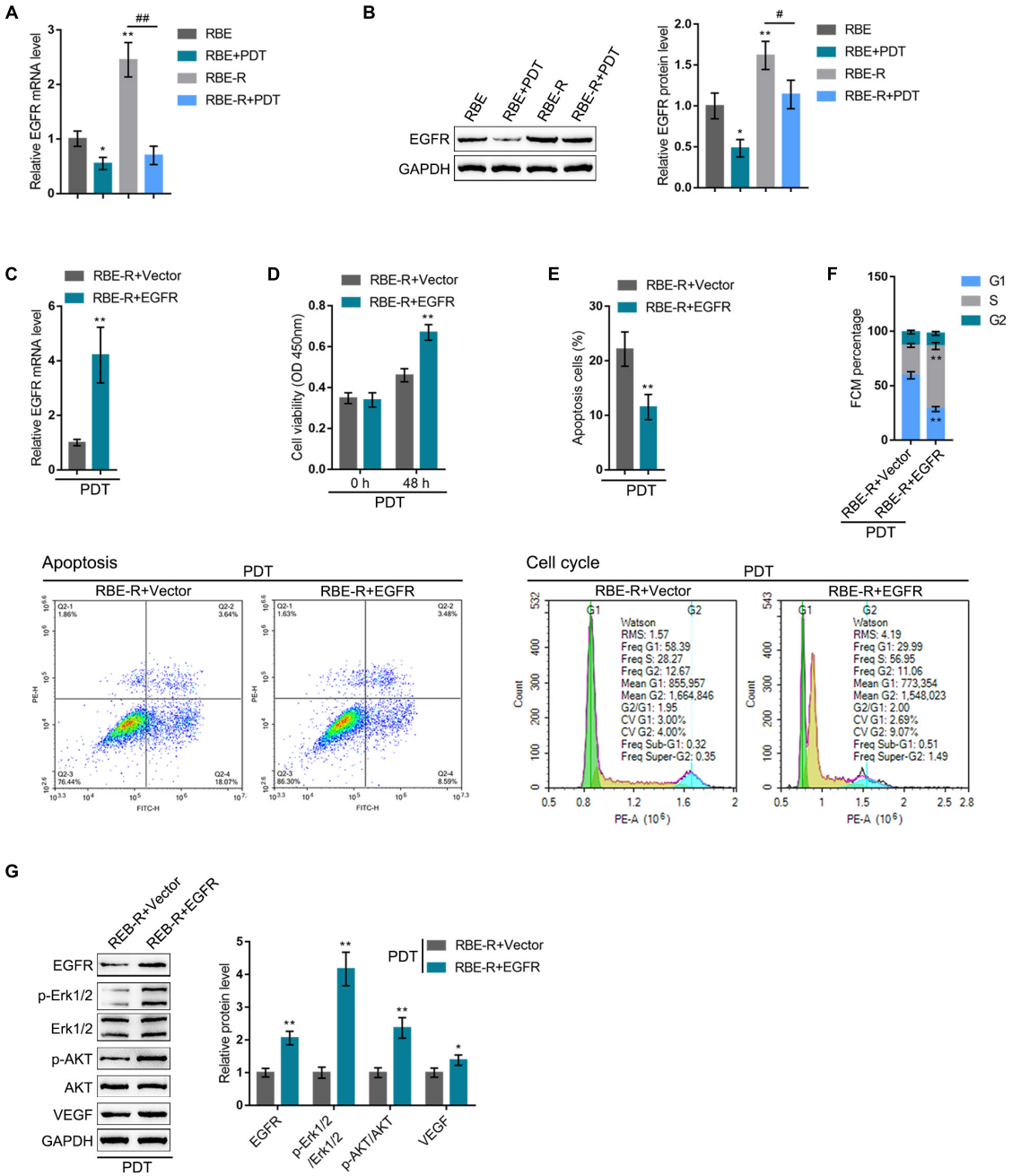

FIGURE 5 | EGFR might participate in PDT reversing cholangiocarcinoma gemcitabine resistance. RBE or gemcitabine-resistant RBE-R cells were treated or non-treated with PDT and examined for EGFR mRNA expression by real-time qPCR **(A)** and the protein levels of EGFR by Immunoblotting **(B)**. **(C)** EGFR overexpression was achieved in RBE-R cells by transfecting EGFR-overexpressing vector (EGFR). The transfection efficiency was verified using real-time qPCR. Then, RBE-R cells were transfected with EGFR or empty vector (negative control), exposed to PDT treatment, and examined for cell viability by MTT assay **(D)**; cell apoptosis by Flow cytometry **(E)**; cell cycle distribution by Flow cytometry **(F)**; the protein levels of EGFR, Erk1/2, p-Erk1/2, Akt, p-Akt, and VEGF by Immunoblotting **(G)**. $^{*}P < 0.05$, $^{**}P < 0.01$, $^{\#}P < 0.05$, $^{\#\#}P < 0.01$.

cell viability, enhancing cell apoptosis, and eliciting G1 cell cycle arrest through modulating Cyclin D1 and caspase 3 cleavage. *In vivo*, PDT treatment significantly inhibited the growth of gemcitabine-resistant cholangiocarcinoma cell-derived tumors. Online data mining and experimental analyses indicate that KLF10 expression was induced, whereas EGFR expression was downregulated by PDT treatment; KLF10 targeted the EGFR promoter region to inhibit EGFR transcription. Under PDT treatment, EGFR overexpression and KLF10 silencing attenuated the anti-cancer effects of PDT on gemcitabine-resistant

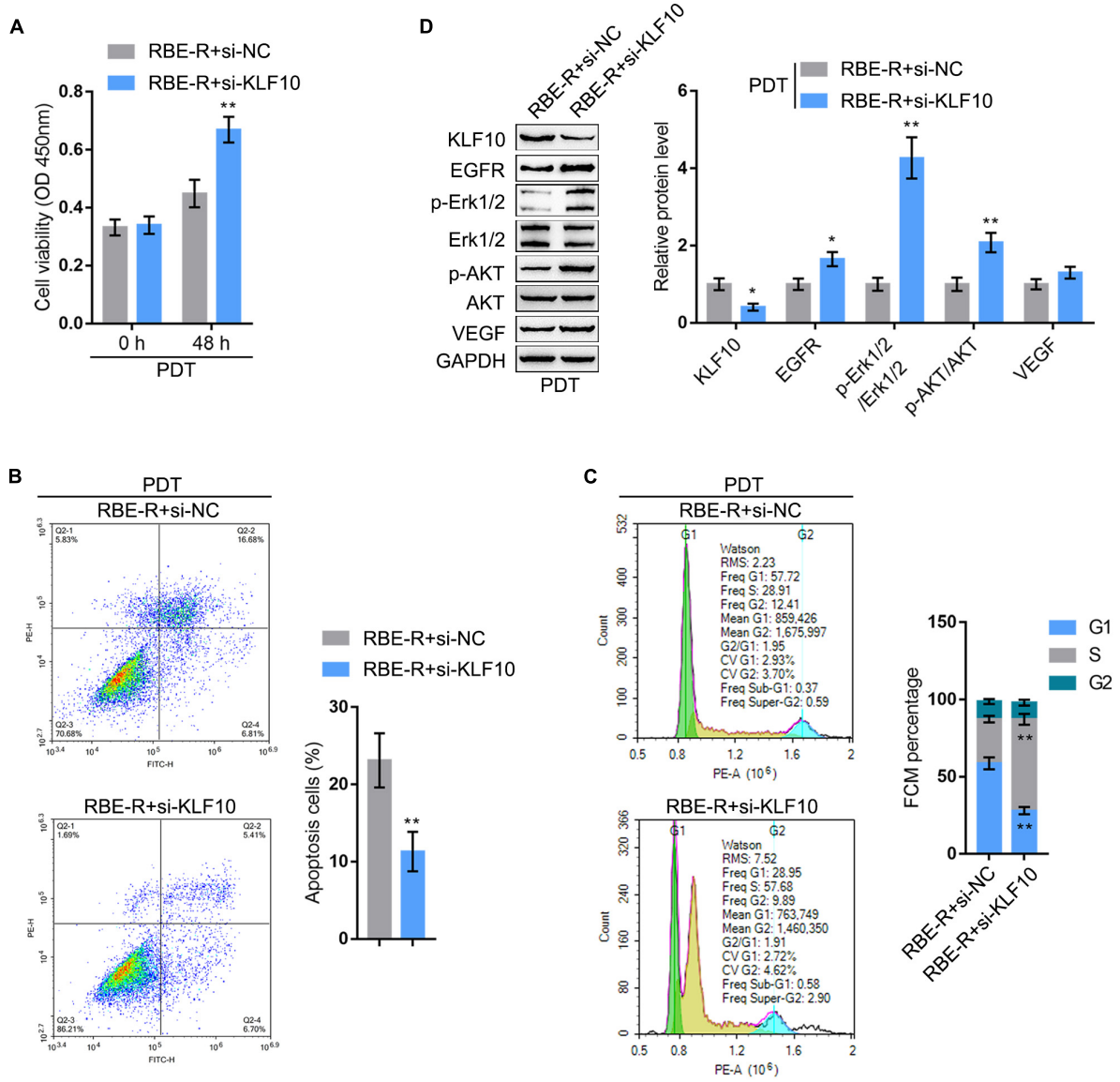

FIGURE 6 | KLF10 silencing attenuates the effects of PDT on gemcitabine-resistant cells. RBE-R cells were transfected with si-KLF10 or si-NC (negative control), exposed to PDT treatment, and examined for the cell viability by MTT assay **(A)**; cell apoptosis by Flow cytometry **(B)**; cell cycle distribution by Flow cytometry **(C)**; the protein levels of KLF10, EGFR, p-Erk1/2, Erk1/2, p-Akt, Akt, and VEGF by Immunoblotting **(D)**. $^{*}P < 0.05$, $^{**}P < 0.01$.

cholangiocarcinoma cells by promoting cell viability, inhibiting apoptosis, and increasing S phase cell proportion. Importantly, under PDT treatment, the effects of KLF10 silencing were significantly reversed by EGFR silencing.

The use of PDT with concomitant chemotherapy is frequently seen in the treatment of cancers. Nevertheless, limited data are available to analyze PDT combined with chemotherapy. Several prospective and retrospective studies were performed comparing the outcome of PDT combined with chemotherapy vs. PDT alone (Hong et al., 2014; Park et al., 2014; Wentrup et al., 2016). Another retrospective study was performed to compare the overall survival of PDT combined with chemotherapy vs. chemotherapy alone, and PDT/chemotherapy combination was found to present the potential of survival benefits, nevertheless, the difference did not reach statistically significant ($P = 0.47$) (Knuppel et al., 2012). Gonzalez-Carmona et al. (2019) first indicated that PDT/chemotherapy combination could lead to an obviously higher overall survival in patients with unresectable cholangiocarcinoma than chemotherapy alone ($P = 0.022$). Herein, the study constructed gemcitabine-resistant cholangiocarcinoma cells and found that PDT exposure indeed inhibited these cells, as manifested as inhibited cell viability, enhanced cell apoptosis, and G1 cell cycle arrest. Moreover, PDT treatment inhibited the growth of the tumor derived from gemcitabine-resistant cholangiocarcinoma cells. Despite previous prospective and retrospective studies and our present findings, the specific molecular mechanism

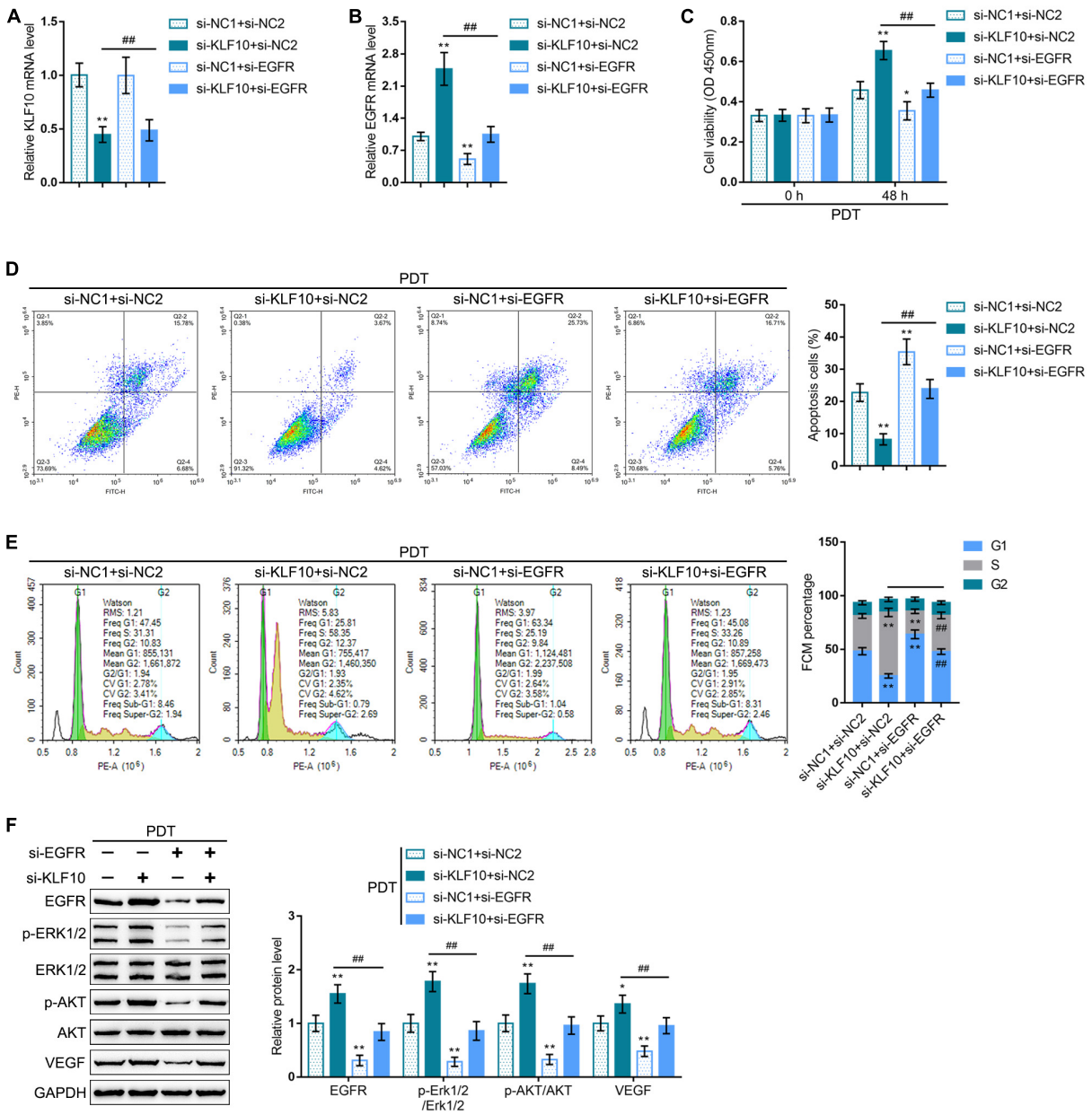

FIGURE 7 | KLF10 modulates PDT reversing cholangiocarcinoma gemcitabine resistance through EGFR. RBE-R cells were co-transfected with si-KLF10 and si-EGFR, exposed to PDT treatment, and examined for the mRNA expression of KLF10 **(A)** and EGFR **(B)** by real-time qPCR; cell viability by MTT assay **(C)**; cell apoptosis by Flow cytometry **(D)**; cell cycle distribution by Flow cytometry **(E)**; the protein levels of KLF10, EGFR, p-Erk1/2, Erk1/2, p-Akt, Akt, and VEGF by Immunoblotting **(F)**. $^{*}P < 0.05$, $^{**}P < 0.01$, compared with the si-NC1 + si-NC2 group; $^{\#\#}P < 0.01$, compared with the si-KLF10 + si-NC2 group.

underlying the synergetic anti-tumor effects of PDT/ gemcitabine combination remain unclear.

Indeed, PDT treatment could alter a range of survival pathways, including HIF-1, NF-κB, AP-1, HSF, and EGFR (Luna et al., 1994; Broekgaarden et al., 2015; Weijer et al., 2015, 2016, 2017). In the present study, by cross-checking online microarray expression profiles reporting PDT-altered genes, we found that KLF10, a transcription factor, could be significantly induced by PDT treatment, which was further evidenced by the observation that PDT treatment upregulated KLF10 mRNA expression and protein levels in gemcitabine-resistant cholangiocarcinoma cells. The KLF transcription factor family performs a variety of biological functions (McConnell and Yang, 2010), and several members of KLF family are found to be associated with certain aspects of tumor cell biology, such as cell growth, cell apoptosis, cell differentiation and cell migration (Tetreault et al., 2013; Cheng et al., 2019; Zhang et al., 2020). KLF10 enhances human leukemia cell death by upregulating Bim and Bax pro-apoptotic proteins (Jin et al., 2007). Within cholangiocarcinoma, KLF10 could be regulated by miR-106b and

might participate in the anti-apoptotic effects of miR-106b on cholangiocarcinoma cells (Wehrkamp et al., 2018). Thus, KLF10 might be involved in the inhibition of PDT on gemcitabine-resistant cholangiocarcinoma cells.

Considering that transcription factors are at the core of gene expression regulation, we also searched for possible target genes of KLF10. Notably, EGFR was in the intersection of KLF10 target genes and PDT treatment-downregulated genes. EGFR was overexpressed in multiple cancer types (Herbst and Shin, 2002), such as perihilar cholangiocarcinoma (Harder et al., 2009; Yang et al., 2014), and was affected by PDT using liposome bound ZnPc (Weijer et al., 2017). EGFR is an emerging therapeutic target for treating cancers, and the approval of monoclonal cetuximab and panitumumab and the kinase inhibitors gefitinib and erlotinib is evidence of this (Joseph et al., 2012). In the present study, EGFR mRNA expression and protein levels in gemcitabine-resistant cholangiocarcinoma cells were significantly downregulated by PDT treatment. Since KLF10 targets the promoter region of EGFR and inhibits EGFR transcription, we speculate that KLF10 might play a role in the synergetic anti-tumor effects of PDT/gemcitabine combination through inhibiting EGFR.

Gemcitabine was phosphorylated into gemcitabine monophosphate by deoxycytidine kinase (dCK) after an influx of nucleoside transporters into cell membranes, which underwent a complex intracellular transformation to gemcitabine diphosphate (dFdCDP) and triphosphate (dFdCTP), responsible for its cytotoxicity, thereby leading to inhibition of DNA synthesis and induction of apoptosis *via* blocking cell cycle progression at the G1/S phase boundary (Heinemann et al., 1995; Plunkett et al., 1995; Galmarini et al., 2002). As we observed in the present study, PDT treatment on gemcitabine-resistant cholangiocarcinoma cell lines elicited G1 cell cycle arrest, repressed cell viability, and enhanced cell apoptosis through modulating the cell cycle regulator and apoptosis-associated Cyclin D1 and caspase 3. As speculated, KLF10 silencing or EGFR overexpression attenuated the anti-cancer effects of PDT on gemcitabine-resistant cholangiocarcinoma cells by increasing S phase cell proportion, promoting cell viability, and inhibiting cell apoptosis. More importantly, when co-transfected to gemcitabine-resistant cholangiocarcinoma cells, the effects of si-KLF10 were significantly reversed by EGFR silencing, indicating that KLF10 participates in the inhibition of PDT on gemcitabine-resistant cholangiocarcinoma cells through EGFR.

CONCLUSION

In conclusion, PDT treatment induces KLF10 expression and downregulates EGFR expression. KLF10 binds to the EGFR promoter region to inhibit EGFR transcription. The KLF10/EGFR axis participates in the process of the inhibition of PDT on gemcitabine-resistant cholangiocarcinoma cells growth. These occurrences forebode that PDT treatment could be deemed as a newfangled strategy for the treatment of gemcitabine chemoresistance cholangiocarcinoma. However, in clinical chemotherapy of cholangiocarcinoma, gemcitabine and platinum-based drug combination is the first-line treatment (Abdel-Rahman et al., 2018). Multidrug resistance is one of the major challenges in cholangiocarcinoma treatment (Gonzalez-Carmona et al., 2019). Therefore, the function and mechanism of PDT in multidrug-resistant cholangiocarcinoma need to be investigated in the future.

DATA AVAILABILITY STATEMENT

The original contributions presented in the study are included in the article/**Supplementary Material**, further inquiries can be directed to the corresponding author.

ETHICS STATEMENT

All procedures were approved by the Institutional Animal Care and Use Committee (IACUC) of The Affiliated Hospital of Southwest Medical University in accordance with the "Principles of Laboratory Animal Care" (NIH, Bethesda, MD, United States).

AUTHOR CONTRIBUTIONS

LW designed the study and critically revised the manuscript. YY led the animal experiments and drafted the manuscript. JL and LY performed experiments on animal and cells, collected the samples, and analyzed the samples and data. All authors edited the manuscript and approved the final manuscript.

FUNDING

This study was supported by the Changsha Municipal Natural Science Foundation (kq2014210), Scientific Research Project of Hunan Health Commission (20201713), and Hunan Provincial Natural Science Foundation of China (2021JJ70100).

SUPPLEMENTARY MATERIAL

The Supplementary Material for this article can be found online at: https://www.frontiersin.org/articles/10.3389/fcell.2021.710721/full#supplementary-material

Supplementary Figure 1 | Effects of PDT on gemcitabine-resistant cholangiocarcinoma cells apoptosis and cycle. RBE, QBC939, RBE-R, and QBC939-R cells were exposed or non-exposed to PDT treatment and examined for the cell apoptosis by Flow cytometry **(A)**; cell cycle distribution by Flow cytometry **(B)**.

Supplementary Figure 2 | Correlation of KLF10 expression with the prognosis of patients with cholangiocarcinoma. **(A)** KLF10 expression in normal (n = 9) and cholangiocarcinoma (n = 36) tissues, according to TCGA-cholangiocarcinoma (CHOL) database. Then, cases from TCGA-CHOL were divided into high and low KLF10 expression groups using the median value of KLF10 expression as cut-off, and the correlation between KLF10 expression and the overall survival **(B)**, disease-specific survival **(C)**, progression-free interval **(D)** in patients with cholangiocarcinoma was analyzed using a Cox proportional hazard regression model and log-rank analysis. Results were shown as Kaplan–Meier curves.

Supplementary Table 1 | Differentially expressed transcription factors in cholangiocarcinoma QBC939 cells treated by PDT based on GSE84756 and GSE68292.

REFERENCES

Abdel-Rahman, O., Elsayed, Z., and Elhalawani, H. (2018). Gemcitabine-based chemotherapy for advanced biliary tract carcinomas. *Cochrane Database Syst. Rev.* 4:CD011746. doi: 10.1002/14651858.CD011746.pub2

Alvarellos, M. L., Lamba, J., Sangkuhl, K., Thorn, C. F., Wang, L., Klein, D. J., et al. (2014). PharmGKB summary: gemcitabine pathway. *Pharmacogenet. Genomics* 24, 564–574. doi: 10.1097/FPC.0000000000000086

Ayaru, L., Wittmann, J., Macrobert, A. J., Novelli, M., Bown, S. G., and Pereira, S. P. (2007). Photodynamic therapy using verteporfin photosensitization in the pancreas and surrounding tissues in the Syrian golden hamster. *Pancreatology* 7, 20–27. doi: 10.1159/000101874

Blechacz, B., and Gores, G. J. (2008). Cholangiocarcinoma: advances in pathogenesis, diagnosis, and treatment. *Hepatology* 48, 308–321. doi: 10.1002/hep.22310

Bown, S. G., Rogowska, A. Z., Whitelaw, D. E., Lees, W. R., Lovat, L. B., Ripley, P., et al. (2002). Photodynamic therapy for cancer of the pancreas. *Gut* 50, 549–557. doi: 10.1136/gut.50.4.549

Broekgaarden, M., Weijer, R., van Gulik, T. M., Hamblin, M. R., and Heger, M. (2015). Tumor cell survival pathways activated by photodynamic therapy: a molecular basis for pharmacological inhibition strategies. *Cancer Metastasis Rev.* 34, 643–690. doi: 10.1007/s10555-015-9588-7

Chandrashekar, D. S., Bashel, B., Balasubramanya, S. A. H., Creighton, C. J., Ponce-Rodriguez, I., Chakravarthi, B., et al. (2017). UALCAN: a portal for facilitating tumor subgroup gene expression and survival analyses. *Neoplasia (New York, NY)* 19, 649–658. doi: 10.1016/j.neo.2017.05.002

Chen, M. H., Liang, P. C., Chang, K. C., Huang, J. Y., Chang, Y. T., Chang, F. Y., et al. (2014). Prototype of biliary drug-eluting stent with photodynamic and chemotherapy using electrospinning. *Biomed. Eng. Online* 13:118. doi: 10.1186/1475-925X-13-118

Cheng, L., Shi, L., and Dai, H. (2019). Bioinformatics analysis of potential prognostic biomarkers among Kruppel-like transcription Factors (KLFs) in breast cancer. *Cancer Biomark* 26, 411–420. doi: 10.3233/CBM-190199

De Angelis, P. M., Kravik, K. L., Tunheim, S. H., Haug, T., and Reichelt, W. H. (2004). Comparison of gene expression in HCT116 treatment derivatives generated by two different 5-fluorouracil exposure protocols. *Mol. Cancer* 3:11. doi: 10.1186/1476-4598-3-11

Dolmans, D. E., Fukumura, D., and Jain, R. K. (2003). Photodynamic therapy for cancer. *Nat. Rev. Cancer* 3, 380–387. doi: 10.1038/nrc1071

Dougherty, T. J., Gomer, C. J., Henderson, B. W., Jori, G., Kessel, D., Korbelik, M., et al. (1998). Photodynamic therapy. *J. Natl. Cancer Inst.* 90, 889–905. doi: 10.1093/jnci/90.12.889

Edmonds, C., Hagan, S., Gallagher-Colombo, S. M., Busch, T. M., and Cengel, K. A. (2012). Photodynamic therapy activated signaling from epidermal growth factor receptor and STAT3: targeting survival pathways to increase PDT efficacy in ovarian and lung cancer. *Cancer Biol. Ther.* 13, 1463–1470. doi: 10.4161/cbt.22256

Evrard, S., Aprahamian, M., Miehe, J., Damge, C., Sultan, R., and Marescaux, J. (1991). [Photodynamic therapy in oncological digestive tract surgery]. *Presse Med.* 20, 1892–1898.

Fan, Y., Wang, Q., Lin, G., Shi, Y., Gu, Z., and Ding, T. (2017). Combination of using prodrug-modified cationic liposome nanocomplexes and a potentiating strategy via targeted co-delivery of gemcitabine and docetaxel for CD44-overexpressed triple negative breast cancer therapy. *Acta Biomater.* 62, 257–272. doi: 10.1016/j.actbio.2017.08.034

Galmarini, C. M., Mackey, J. R., and Dumontet, C. (2002). Nucleoside analogues and nucleobases in cancer treatment. *Lancet Oncol.* 3, 415–424. doi: 10.1016/S1470-2045(02)00788-X

Gilbert, J. A., Salavaggione, O. E., Ji, Y., Pelleymounter, L. L., Eckloff, B. W., Wieben, E. D., et al. (2006). Gemcitabine pharmacogenomics: cytidine deaminase and deoxycytidylate deaminase gene resequencing and functional genomics. *Clin. Cancer Res.* 12, 1794–1803. doi: 10.1158/1078-0432.CCR-05-1969

Gonzalez-Carmona, M. A., Bolch, M., Jansen, C., Vogt, A., Sampels, M., Mohr, R. U., et al. (2019). Combined photodynamic therapy with systemic chemotherapy for unresectable cholangiocarcinoma. *Aliment. Pharmacol. Ther.* 49, 437–447. doi: 10.1111/apt.15050

Harder, J., Waiz, O., Otto, F., Geissler, M., Olschewski, M., Weinhold, B., et al. (2009). EGFR and HER2 expression in advanced biliary tract cancer. *World J. Gastroenterol.* 15, 4511–4517. doi: 10.3748/wjg.15.4511

Heinemann, V., Schulz, L., Issels, R. D., and Plunkett, W. (1995). Gemcitabine: a modulator of intracellular nucleotide and deoxynucleotide metabolism. *Semin. Oncol.* 22, 11–18.

Herbst, R. S., and Shin, D. M. (2002). Monoclonal antibodies to target epidermal growth factor receptor-positive tumors: a new paradigm for cancer therapy. *Cancer* 94, 1593–1611. doi: 10.1002/cncr.10372

Hong, M. J., Cheon, Y. K., Lee, E. J., Lee, T. Y., and Shim, C. S. (2014). Long-term outcome of photodynamic therapy with systemic chemotherapy compared to photodynamic therapy alone in patients with advanced hilar cholangiocarcinoma. *Gut Liver* 8, 318–323. doi: 10.5009/gnl.2014.8.3.318

Ji, Z., Yang, G., Shahzidi, S., Tkacz-Stachowska, K., Suo, Z., Nesland, J. M., et al. (2006). Induction of hypoxia-inducible factor-1alpha overexpression by cobalt chloride enhances cellular resistance to photodynamic therapy. *Cancer Lett.* 244, 182–189. doi: 10.1016/j.canlet.2005.12.010

Jin, W., Di, G., Li, J., Chen, Y., Li, W., Wu, J., et al. (2007). TIEG1 induces apoptosis through mitochondrial apoptotic pathway and promotes apoptosis induced by homoharringtonine and velcade. *FEBS Lett.* 581, 3826–3832. doi: 10.1016/j.febslet.2007.07.008

Joseph, S. O., Wu, J., and Muggia, F. M. (2012). Targeted therapy: its status and promise in selected solid tumors. Part II: impact on selected tumor subsets, and areas of evolving integration. *Oncology (Williston Park)* 26, 1021–30, 1035.

Kahaleh, M. (2012). Photodynamic therapy in cholangiocarcinoma. *J. Natl. Compr. Canc. Netw.* 10(Suppl. 2), S44–S47. doi: 10.6004/jnccn.2012.0174

Kim, B. J., Hyung, J., Yoo, C., Kim, K. P., Park, S. J., Lee, S. S., et al. (2017). Prognostic factors in patients with advanced biliary tract cancer treated with first-line gemcitabine plus cisplatin: retrospective analysis of 740 patients. *Cancer Chemother. Pharmacol.* 80, 209–215. doi: 10.1007/s00280-017-3353-2

Kim, D. H., Im, B. N., Hwang, H. S., and Na, K. (2018). Gemcitabine-loaded DSPE-PEG-PheoA liposome as a photomediated immune modulator for cholangiocarcinoma treatment. *Biomaterials* 183, 139–150. doi: 10.1016/j.biomaterials.2018.08.052

Knuppel, M., Kubicka, S., Vogel, A., Malek, N. P., Schneider, M., Papendorf, F., et al. (2012). Combination of conservative and interventional therapy strategies for intra- and extrahepatic cholangiocellular carcinoma: a retrospective survival analysis. *Gastroenterol. Res. Pract.* 2012:190708. doi: 10.1155/2012/190708

Luna, M. C., Wong, S., and Gomer, C. J. (1994). Photodynamic therapy mediated induction of early response genes. *Cancer Res.* 54, 1374–1380.

Marin, J. J. G., Lozano, E., Herraez, E., Asensio, M., Di Giacomo, S., Romero, M. R., et al. (2018). Chemoresistance and chemosensitization in cholangiocarcinoma. *Biochim. Biophys. Acta. Mol. Basis Dis.* 1864, 1444–1453. doi: 10.1016/j.bbadis.2017.06.005

McCaughan, J. S. Jr., Mertens, B. F., Cho, C., Barabash, R. D., and Payton, H. W. (1991). Photodynamic therapy to treat tumors of the extrahepatic biliary ducts. A case report. *Arch. Surg.* 126, 111–113. doi: 10.1001/archsurg.1991.01410250119022

McConnell, B. B., and Yang, V. W. (2010). Mammalian Kruppel-like factors in health and diseases. *Physiol. Rev.* 90, 1337–1381. doi: 10.1152/physrev.00058.2009

Morizane, C., Okusaka, T., Mizusawa, J., Katayama, H., Ueno, M., Ikeda, M., et al. (2019). Combination gemcitabine plus S-1 versus gemcitabine plus cisplatin for advanced/recurrent biliary tract cancer: the FUGA-BT (JCOG1113) randomized phase III clinical trial. *Ann. Oncol.* 30, 1950–1958. doi: 10.1093/annonc/mdz402

Park, D. H., Lee, S. S., Park, S. E., Lee, J. L., Choi, J. H., Choi, H. J., et al. (2014). Randomised phase II trial of photodynamic therapy plus oral fluoropyrimidine S-1, versus photodynamic therapy alone for unresectable hilar cholangiocarcinoma. *Eur. J. Cancer* 50, 1259–1268. doi: 10.1016/j.ejca.2014.01.008

Park, J. O., Oh, D. Y., Hsu, C., Chen, J. S., Chen, L. T., Orlando, M., et al. (2015). Gemcitabine plus cisplatin for advanced biliary tract cancer: a systematic review. *Cancer Res. Treat.* 47, 343–361. doi: 10.4143/crt.2014.308

Plunkett, W., Huang, P., Xu, Y. Z., Heinemann, V., Grunewald, R., and Gandhi, V. (1995). Gemcitabine: metabolism, mechanisms of action, and self-potentiation. *Semin. Oncol.* 22, 3–10.

Razumilava, N., and Gores, G. J. (2013). Classification, diagnosis, and management of cholangiocarcinoma. *Clin. Gastroenterol. Hepatol.* 11, 13–21.e1; quiz e3–4. doi: 10.1016/j.cgh.2012.09.009

Ritchie, M. E., Phipson, B., Wu, D., Hu, Y., Law, C. W., Shi, W., et al. (2015). Limma powers differential expression analyses for RNA-sequencing and microarray studies. *Nucleic Acids Res.* 43:e47. doi: 10.1093/nar/gkv007

Rizvi, S., and Gores, G. J. (2013). Pathogenesis, diagnosis, and management of cholangiocarcinoma. *Gastroenterology* 145, 1215–1229. doi: 10.1053/j.gastro.2013.10.013

Schuitmaker, J. J., Baas, P., van Leengoed, H. L., van der Meulen, F. W., Star, W. M., and van Zandwijk, N. (1996). Photodynamic therapy: a promising new modality for the treatment of cancer. *J. Photochem. Photobiol. B* 34, 3–12. doi: 10.1016/1011-1344(96)07342-3

Siegel, R. L., Miller, K. D., and Jemal, A. (2019). Cancer statistics, 2019. *CA Cancer J. Clin.* 69, 7–34. doi: 10.3322/caac.21551

Talreja, J. P., DeGaetani, M., Sauer, B. G., and Kahaleh, M. (2011). Photodynamic therapy for unresectable cholangiocarcinoma: contribution of single operator cholangioscopy for targeted treatment. *Photochem. Photobiol. Sci.* 10, 1233–1238. doi: 10.1039/c0pp00259c

Tetreault, M. P., Yang, Y., and Katz, J. P. (2013). Kruppel-like factors in cancer. *Nat. Rev. Cancer* 13, 701–713. doi: 10.1038/nrc3582

Thongprasert, S. (2005). The role of chemotherapy in cholangiocarcinoma. *Ann. Oncol.* 16(Suppl. 2), ii93–ii96. doi: 10.1093/annonc/mdi712

Valle, J., Wasan, H., Palmer, D. H., Cunningham, D., Anthoney, A., Maraveyas, A., et al. (2010). Cisplatin plus gemcitabine versus gemcitabine for biliary tract cancer. *N. Engl. J. Med.* 362, 1273–1281. doi: 10.1056/NEJMoa0908721

Wehrkamp, C. J., Natarajan, S. K., Mohr, A. M., Phillippi, M. A., and Mott, J. L. (2018). miR-106b-responsive gene landscape identifies regulation of Kruppel-like factor family. *RNA Biol.* 15, 391–403. doi: 10.1080/15476286.2017.1422471

Weijer, R., Broekgaarden, M., Krekorian, M., Alles, L. K., van Wijk, A. C., Mackaaij, C., et al. (2016). Inhibition of hypoxia inducible factor 1 and topoisomerase with acriflavine sensitizes perihilar cholangiocarcinomas to photodynamic therapy. *Oncotarget* 7, 3341–3356. doi: 10.18632/oncotarget.6490

Weijer, R., Broekgaarden, M., van Golen, R. F., Bulle, E., Nieuwenhuis, E., Jongejan, A., et al. (2015). Low-power photodynamic therapy induces survival signaling in perihilar cholangiocarcinoma cells. *BMC Cancer* 15:1014. doi: 10.1186/s12885-015-1994-2

Weijer, R., Clavier, S., Zaal, E. A., Pijls, M. M., van Kooten, R. T., Vermaas, K., et al. (2017). Multi-OMIC profiling of survival and metabolic signaling networks in cells subjected to photodynamic therapy. *Cell. Mol. Life Sci.* 74, 1133–1151. doi: 10.1007/s00018-016-2401-0

Wentrup, R., Winkelmann, N., Mitroshkin, A., Prager, M., Voderholzer, W., Schachschal, G., et al. (2016). Photodynamic therapy plus chemotherapy compared with photodynamic therapy alone in hilar nonresectable cholangiocarcinoma. *Gut Liver* 10, 470–475. doi: 10.5009/gnl15175

Yang, X., Wang, W., Wang, C., Wang, L., Yang, M., Qi, M., et al. (2014). Characterization of EGFR family gene aberrations in cholangiocarcinoma. *Oncol. Rep.* 32, 700–708. doi: 10.3892/or.2014.3261

Zhang, J., Li, G., Feng, L., Lu, H., and Wang, X. (2020). Kruppel-like factors in breast cancer: function, regulation and clinical relevance. *Biomed. Pharmacother.* 123:109778. doi: 10.1016/j.biopha.2019.109778

Conflict of Interest: The authors declare that the research was conducted in the absence of any commercial or financial relationships that could be construed as a potential conflict of interest.

Publisher's Note: All claims expressed in this article are solely those of the authors and do not necessarily represent those of their affiliated organizations, or those of the publisher, the editors and the reviewers. Any product that may be evaluated in this article, or claim that may be made by its manufacturer, is not guaranteed or endorsed by the publisher.

frontiers in Oncology

REVIEW
published: 24 November 2021
doi: 10.3389/fonc.2021.718636

Biological Adaptations of Tumor Cells to Radiation Therapy

Angeles Carlos-Reyes[1], *Marcos A. Muñiz-Lino*[2], *Susana Romero-Garcia*[1], *César López-Camarillo*[3] *and Olga N. Hernández-de la Cruz*[3]*

[1] Department of Chronic-Degenerative Diseases, National Institute of Respiratory Diseases "Ismael Cosío Villegas", Mexico City, Mexico, [2] Laboratorio de Patología y Medicina Bucal, Universidad Autónoma Metropolitana Unidad Xochimilco, Mexico City, Mexico, [3] Posgrado en Ciencias Genómicas, Universidad Autónoma de la Ciudad de México, Mexico City, Mexico

OPEN ACCESS

Edited by:
José Díaz-Chávez, National Institute of Cancerology (INCAN), Mexico

Reviewed by:
Subhayan Das, Indian Institute of Technology Kharagpur, India
Emer Bourke, National University of Ireland Galway, Ireland

***Correspondence:**
Olga N. Hernández-de la Cruz
ediacara79@yahoo.com.mx

Specialty section:
This article was submitted to Molecular and Cellular Oncology, a section of the journal Frontiers in Oncology

Received: *01 June 2021*
Accepted: *28 October 2021*
Published: *24 November 2021*

Citation:
Carlos-Reyes A, Muñiz-Lino MA, Romero-Garcia S, López-Camarillo C and Hernández-de la Cruz ON (2021) Biological Adaptations of Tumor Cells to Radiation Therapy. Front. Oncol. 11:718636. doi: 10.3389/fonc.2021.718636

Radiation therapy has been used worldwide for many decades as a therapeutic regimen for the treatment of different types of cancer. Just over 50% of cancer patients are treated with radiotherapy alone or with other types of antitumor therapy. Radiation can induce different types of cell damage: directly, it can induce DNA single- and double-strand breaks; indirectly, it can induce the formation of free radicals, which can interact with different components of cells, including the genome, promoting structural alterations. During treatment, radiosensitive tumor cells decrease their rate of cell proliferation through cell cycle arrest stimulated by DNA damage. Then, DNA repair mechanisms are turned on to alleviate the damage, but cell death mechanisms are activated if damage persists and cannot be repaired. Interestingly, some cells can evade apoptosis because genome damage triggers the cellular overactivation of some DNA repair pathways. Additionally, some surviving cells exposed to radiation may have alterations in the expression of tumor suppressor genes and oncogenes, enhancing different hallmarks of cancer, such as migration, invasion, and metastasis. The activation of these genetic pathways and other epigenetic and structural cellular changes in the irradiated cells and extracellular factors, such as the tumor microenvironment, is crucial in developing tumor radioresistance. The tumor microenvironment is largely responsible for the poor efficacy of antitumor therapy, tumor relapse, and poor prognosis observed in some patients. In this review, we describe strategies that tumor cells use to respond to radiation stress, adapt, and proliferate after radiotherapy, promoting the appearance of tumor radioresistance. Also, we discuss the clinical impact of radioresistance in patient outcomes. Knowledge of such cellular strategies could help the development of new clinical interventions, increasing the radiosensitization of tumor cells, improving the effectiveness of these therapies, and increasing the survival of patients.

Keywords: radioresistance, radiotherapy, cancer, DNA-damage response, DNA repair pathways

INTRODUCTION

Radiotherapy (RT) is an effective treatment against different types of solid tumors detected in early stages, while it is also used as a palliative treatment in metastatic stages. Over 50% of cancer patients are treated with RT and, depending on the type of cancer and the location and size of the tumor, the application can be external or internal (1). The main objective of the RT is to kill tumor cells through DNA damage. However, the damage is detected by tumor cells through a DNA damage response (DDR) mechanism that promotes the activation of cell cycle checkpoints and induces the arrest, or delay, of the cell cycle, inducing the activation of the different DNA repair mechanisms (2). The DDR promotes several cell death pathways, including apoptosis, mitotic catastrophe, necrosis, and necroptosis, activated by death receptors dependent on kinases (RIPK1, RIPK3) (3, 4). The main radiation-activated DNA damage repair pathways are base excision repair (BER), non-homologous end joining (NHEJ), and homologous recombination (HR) (2). However, an increased tumor volume, low oxygen tension, and dysregulation of key genes can lead to tolerance and clonal selection of tumor cells to radiation, thus reducing sensitivity to radiotherapy, leading to tumor recurrence and therapy resistance (2, 5, 6). In addition, the radiation stimulates biological changes like chromatin remodeling, global changes in gene expression, metabolic reprogramming, epithelial-mesenchymal transition (EMT), and disturbances of circadian rhythms, among others (7–14). All changes induced by radiation promote an adaptation biological of tumor cells to the tumor microenvironment, which contributes to aggressiveness and radioresistance of tumors, exacerbating the cancer hallmarks, such as proliferation, migration, invasion, and metastasis (11, 15).

In this review, we describe strategies that tumor cells use to respond to radiation stress, to adapt, and proliferate, promoting the appearance of tumor radioresistance, and highlight strategies that target genes to enhance radiosensitivity in various cancer types.

RADIATION THERAPY IN CLINICAL PRACTICE

In clinical practice, radiotherapy (RT) treatment uses two ionizing radiation types: electromagnetic (like X-rays) and Gamma-rays. Radiotherapy aims to kill cancer cells during the treatment. The affected tissues absorb this energy, and its amount applicated is by the unit weight of the organ or tissue and is expressed in units of gray (Gy) (3, 16). Radiation therapy can be delivered externally (teletherapy) or internally (brachytherapy), or both in combination; its use depends on factors such as type of cancer, size of the tumor, tumor location in the body, and regional extent, as well as anatomic area implicated in the geometric accuracy to apply the calculated radiation dose. The efficacy of radiotherapy is established by the therapeutic index of radiation that will be used; this is established by the relationship between the tolerance of the normal tissue surrounding the tumor (NTT) and the lethal dose against the tumor (TLD), whose objective is to erase the tumor and prevent its regression in the affected area (17–20). **Table 1** summarizes the different types of RT currently used in clinical practice and their advantages and disadvantages.

TUMOR CELLS ACTIVATE SIGNALING PATHWAYS INVOLVED IN DNA-DAMAGE RESPONSE TO SURVIVE IONIZING RADIATION

Despite the recent technological advances in treatments against cancer, some tumors develop acquired resistance or have intrinsic resistance, which is a problem in the fight against cancer (36). In addition, the tumor heterogeneity can promote innate response favorable to radiation. However, the tumor heterogeneity induces the development of intratumoral resistance to radiation through clonal selection (37, 38).

Ionizing radiation (IR) produces DNA lesions, among them double-strand breaks (DSBs), the most lethal form of DNA damage, and single-strand breaks (SSBs). Ionizing radiation can, directly and indirectly, damage DNA, causing ionization of the atoms or breaking its bonds in the DNA molecules or by the production of highly reactive free radicals, which can interact with the DNA. DNA damage by exogenous agents like radiation is sensed by DNA damage response (DDR), mediated by activation of the DNA repair pathways (12, 18).

DDR also induces the cell cycle arrest through regulation checkpoint kinases and promotes apoptosis when DNA damage repair mechanisms fail (39, 40). Damage to DNA is repaired by activation of various repair pathways, like base excision repair (BER), non-homologous end joining (NHEJ), and homologous recombination (HR) (41, 42). **Figure 1** shows some proteins involved in DNA repair pathways modulated in response to radiation.

BER Pathway

This mechanism can repair more than 90% of radiation-generated DNA damage, which includes injuries on nitrogenated bases caused by oxidation, alkylation, deamination, and depurination, as well as SSBs (43). Briefly, this repair route detects and removes damaged bases through specialized DNA glycosylases, which are constantly scanning the damaged DNA. The UNG glycosylase hydrolyzes the N-glycosylic bond between the DNA base and sugar-phosphate backbone to produce a basic site. Then, APE1 endonuclease cleaves the phosphodiester bond to generate an SSB. DNA polymerase β (pol β) acts as an AP lyase, removing the sugar attached to the 5′ phosphate, and DNA polymerase adds nucleotides to the end of SSB. Finally, a DNA ligase seals the nicks (44).

It has been reported that key factors for the BER pathway are overexpressed or activated in radioresistant cells. For example, the CUX1 transcription factor is overexpressed in colorectal

TABLE 1 | Types of radiotherapy used in clinical practice for the treatment of different types of cancer.

Teletherapy (applied externally)						
Protocol type	**Characteristics**	**Cancer treated**	**Example of protocol**	**Advantage**	**Disadvantages**	**References**
Three-dimensional conformal radiotherapy (3D-CRT)	Radiation administered geometrically from the volume to be treated	Prostate, spine, esophagus, lung, bladder, pancreas, head and neck cancer	Adjuvant (additional to chemotherapy) for locally advanced non-small-cell lung cancer; 55 to 65 Gy administered in three sessions over approximately 4 weeks	Uses three-dimensional images for the geographic location of the tumor Radiation beam is tailored to target tumor Limits radiation dose to adjacent tissues	Requires very precise dosing and planning to minimize exposure of surrounding normal tissues to radiation dose Requires specialized equipment Long treatment	(17, 21–23)
Intensity-modulated radiation therapy (IMRT)	Controls the shape (similar to 3D-CRT) and also the intensity of each beam emitted Reduces the exposure of healthy tissue to radiation	Prostate, spine, lung, breast, kidney, pancreas, liver, tongue, and larynx cancer	In prostate cancer (PCa), 62 Gy in 20 fractions, over 4 weeks	Dose limitations of the target tumor and adjacent tissues Vary dose intensities in the treatment field	Requires very precise doses Long treatment Requires specialized equipment	(17, 21, 24, 25)
Stereotactic Body Radiation Therapy (SBRT) or Stereotactic Ablative Radiation Therapy (SABR)	Uses multiple beams of radiation, from many different directions, that converge into a very small volume Allows high doses of radiation to be delivered with little damage to surrounding healthy tissue	Used in the treatment of small tumors in the head and brain, also in lung, spine, and liver cancer	In PCa, 25 Gy in five fractions over the course of 1–2 weeks	Precise geographic location of the tumor Use high doses The treatment can be completed in a few fractions (1 to 5) and in a short time (1 to 5 days) Improves response to treatment Can be used in combination with chemotherapy A treatment for inoperable tumors	Difficult to manage Requires a lot of pressure Requires specialized equipment	(21, 24, 25)
Volumetric modulated arc therapy (VMAT)	Supplies the radiation beams by means of a 360° arc integrated into a linear accelerator Treatment cycles are very fast (less than 2 min) Provides very high doses of radiation with precision and speed.	In head and neck tumors, PCa, or central nervous system tumors.	Twenty Gy in a single dose for the treatment of brain metastasis	Radiation adapts to the shape of the tumor to minimize exposure to healthy structures Rapid treatment administration	Longer doses	(21, 26–28)
Brachytherapy (Applied internally)						
Protocol type	**Characteristics**	**Cancer treated**	**Example of protocol**	**Advantage**	**Disadvantages**	**References**
Interstitial	Administration within the tumor	Uterus and recurrence of vaginal cuff cancer	In uterus cancer, three or four 6 Gy fractions, one fraction per week	High doses in tumor and low in healthy tissue Allows the treatment of larger tumors	Invasive Formation of necrotic cavities	(29, 30)
Intracavitary	Administration inside a natural (as vagina or larynx) or surgically created cavity	Larynx, uterine, cervical, and endometrial cancer	In cervical cancer, 15 or 20 Gy in three or four fractions.	Uses anatomical pathways to place radioactive sources	Higher risk of error	(31, 32)

(Continued)

TABLE 1 | Continued

Teletherapy (applied externally)						
Protocol type	**Characteristics**	**Cancer treated**	**Example of protocol**	**Advantage**	**Disadvantages**	**References**
				Can be used without anesthesia You can use low dose, pulsed dose, or high dose		
Intraluminal	Application into the lumen of organs	Extrahepatic biliary duct cancer and esophagus cancer	For biliary duct cancer, 30 Gy for definitive dose	High doses of radiation to the tumor and minimize the dose to healthy adjacent organs Allows biliary drainage through the tumor Improve survival	May cause bleeding	(33, 34)
Intravenous	Venous administration of radioactive molecules	Hepatocellular carcinoma	For hepatic cancer, 100 Gy in a single dose	Little invasive Quick and easy administration Therapy targeting specific proteins on the surface of tumor cells	Long treatment May cause side effects	(35)

cancer (CRC) cell lines that exhibit high levels of ROS and is required for the activation of DDR using multiple transcriptional targets, such as ATR and ATM (45). In addition, CUX1 stimulates OGG1 expression, a DNA glycosylase involved in removing oxidative purine lesions (46). Naidu et al. found that cells with higher endogenous APE1 endonuclease are more radioresistant, and the APE1 ectopic expression in glioma cell lines has a dose-dependent effect, increasing radioresistance (RR) (47). Low expression of GADD45α, an APE1-binding protein, has been observed in radioresistant cancer cells and biopsies from radioresistant cancer patients. Li et al. reported that GADD45α subexpression protects from radiation-induced cell death and DNA damage contributing to the development of RR in cervical cancer (48).

On the other hand, Nickson et al. note that oropharyngeal squamous cell carcinoma (OPSCC) patients that are HPV-16 positive (+) have the most radiotherapy treatment sensitivity and survival, while HPV-16 negative (−) OPSCC patients have a lesser response to the same therapy. In addition, in *in vitro* studies in cell lines, HPV-16-positive cells and HPV-16 negative cells showed a relationship similar to that observed in OPSCC patients (HPV-16+/HPV-16−), related to the low efficacy of DNA repair mechanism in HPV-16 (−). Additionally, OPSCC HPV-16+ radiosensitive cells express high levels of the XRCC1, DNA polymerase β, PNKP, and PARP-1 proteins related to the BER and SSB repair mechanisms. At the same time, treating HPV-16 (−) cells with a PARP inhibitor (olaparib) and radiotherapy induces the most therapy radiosensitivity. The radiotherapy response is most effective in HPV-16 positive OPSCC patients compared to HPV-16 negative OPSCC patients (43). DSB is the most complex and lethal type of DNA damage. When DSBs occur during RT, proteins involved in the NHEJ and HR pathways are turned on to promote the survival of tumor cells against damage.

The NHEJ Pathway

In mammalian cells, most DSB lesions are repaired by the NHEJ pathway. This is a mechanism triggered in cells in any phase of the cell cycle and allows DSBs to rejoin. The initial step in the NHEJ pathway is to recognize and protect free DNA ends by Ku70/80 heterodimer. After, the Ku70/80 complex recruits additional members of the NHEJ pathway to the damage sites, such as DNA-PKcs, forming the complex know as DNA-PK. DNA-PKcs, activated by autophosphorylation or ATM, phosphorylates different factors required for DNA end-processing, including Artemis endonuclease, Mre11/Rad50/Nbs1 complex, and different polymerases. Finally, DNA ligase 4 (LIG4) is responsible for catalyzing the ligation of the DNA ends (49).

In radiotherapy-resistant prostate cancer cell lines (PC3, DU145, and LNCaP), the DNA damage by radiation promotes DSBs mediated by DNA NHEJ and HR repair mechanisms activation, increasing Ku70, Ku80, BRCA1, BRCA2, and Rad51 expression of proteins, respectively. The resistant cells showed cell cycle arrest in G0/G1 and S phase through an increase in p-p53 (p53 phosphorylated) and p21 by Chk1/2 activation. Besides, the activation of caspase 3 and 7, the decrease of PARP-1 and Bax protein expressions, as well as the expression high of Bcl-2 and Bcl-xl proteins promote the inhibition of apoptosis, as well as autophagy, through the increased expression of Beclin-1 and

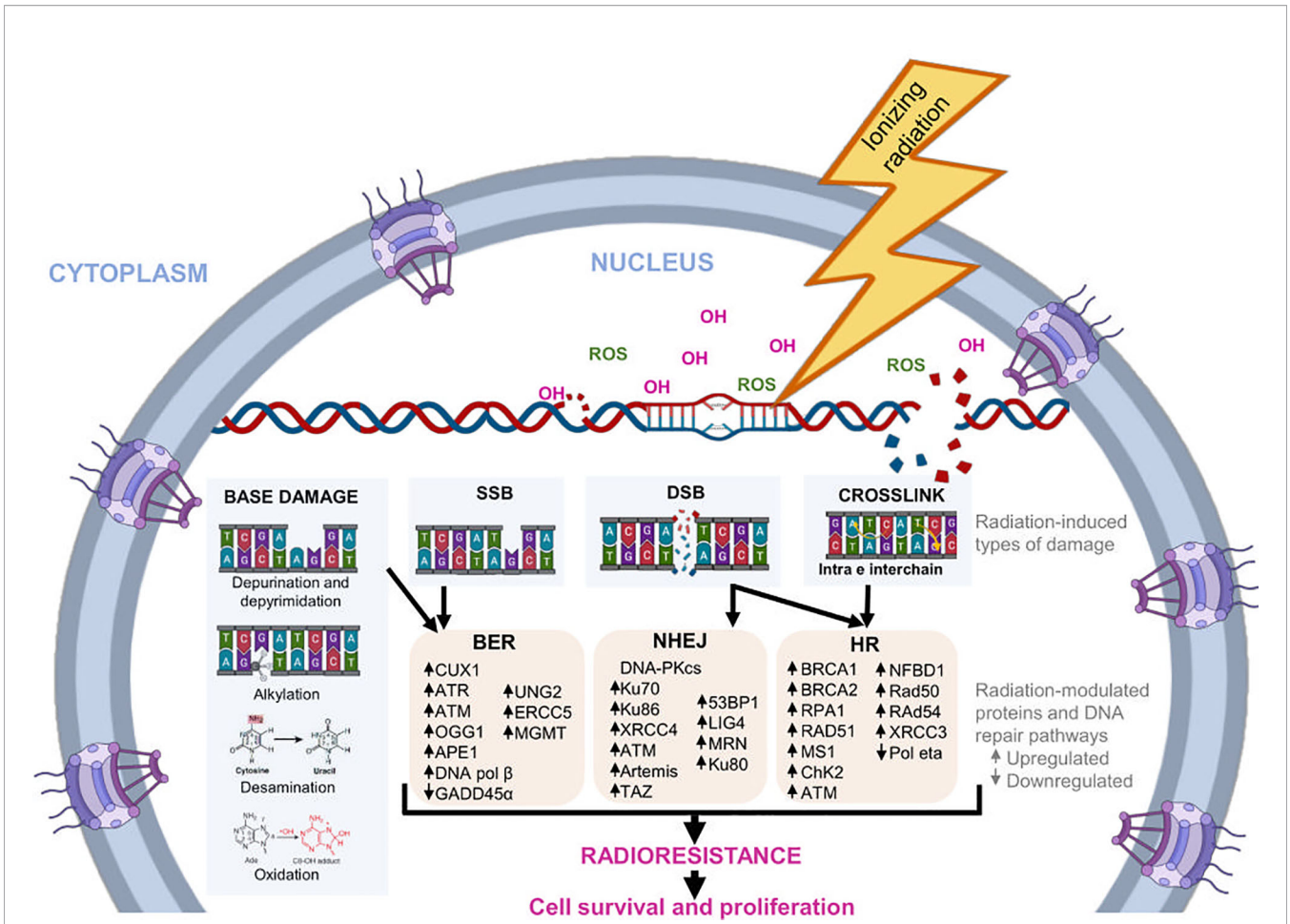

FIGURE 1 | DNA repair pathways induced by radiation. During radiotherapy, IR can alter the chemical structure of DNA directly or indirectly. Indirectly, it promotes the formation of molecules, such as the OH- ion and ROS, which bind to nucleotides and modify them structurally. The main modifications induced by radiation are base damage, crosslink, SSB, and DSB. In response, cells regulate the expression of several genes and proteins involved in different DNA repair pathways, such as BER, NHEJ, and HR. The activation of this pathways helps to reduce radiation-induced DNA damage, favoring the survival and proliferation of tumor cells, as well as cellular radioresistance.

LC3A/B (50). In another report, Beskow et al. showed an increased expression of genes involved in NHEJ (such as DNA-PKcs, Ku70, and Ku86) in the residual carcinoma from patients with cervical cancer after RT relative to corresponding primary tumors (51). Accordingly, low expression of Ku80 in cervical cancer patients also shows a better response to RT, and therefore a greater overall survival of patients (52). In agreement, low expression of Ku70 or XRCC4 proteins in hypopharyngeal squamous cell carcinoma patients was related to better locoregional control, suggesting a greater sensitivity to chemoradiotherapy (53). TAZ is a transcriptional coactivator upregulated in different types of cancer; its overexpression stimulates the expression of genes involved in NHEJ, such as TP53BP1 (53BP1), PRKDC (DNA-PKCs), and XRCC6 (Ku70), contributing to the radioresistant phenotype. It has been associated with clinicopathological features, poor prognosis, and radioresistance in esophageal cancer cells. Furthermore, TAZ overexpression increases various hallmarks of cancer, such as proliferation, migration, invasion, and decreased apoptosis (54).

In vitro studies have shown that radiation modulates the expression of different proteins involved in NHEJ. Bian et al. established a radioresistant breast cancer cell line (MD-PR) through prolonged and repeated exposure to radiation. After radiation, MD-PR presented higher expression of phosphorylated ATM and ATR than parental cells, resulting in higher efficiency in DDR and NHEJ. On the other hand, Artemis is rapidly hyperphosphorylated by ATM in response to radiation and subsequently recruited to the damaged sites together with 53BP1 to coordinate the binding of the DSBs (7). Other radiation-modulated proteins are DNA ligase IV (LIG 4) and TAZ. LIG 4 senses DSBs and facilitates cell survival following treatment with ionizing radiation. Lung cancer cells (LCCs) expressing mutant LIG4 are sensitive to ionizing radiation (55, 56). Additionally, the C-X-C motif chemokine ligand 1 (CXCL1) oncogene secreted by components of the tumor

microenvironment is highly expressed in various cancer types, promoting tumor angiogenesis, migration, invasion metastasis, tumor progression, and chemoresistance (57). In esophageal squamous cell carcinoma, the cancer-associated fibroblasts (CAFs) were found to produce high expression of chemokine CXCL1, which promotes radiotherapy resistance *in vitro* and *in vivo* in ESCC through an overregulated expression of DNA damage repair proteins (e.g., p-ATM, Rad50, p-Chk2, Ku80, and DNA-PKcs) and the Mek/Erk signaling pathway activation, as well as an increase of γ-H2AX protein. Besides, CXCL1 inhibits the expression of superoxide dismutase 1 (SOD1) and induces the accumulation of ROS-induced DNA damage repair pathways (27). In glioblastoma (GBM), the high expression of CXCL1 was related to poor prognosis of patients induced radiotherapy resistance through EMT event and using activation of NF-κB signaling (58).

The HR Pathway

HR is a complex pathway specifically triggered in later-S and G2/M phases of the cell cycle because a homologous sequence is used as a template to restore dsDNA breaks, DNA gaps, and DNA interstrand cross-links. Compared with the NHEJ pathway, HR is a process that provides high-fidelity, requires more proteins to repair, and reduces the probability of genome rearrangements and loss of genetic material. During HR, DSB ends are recognized and resected by nucleases (Mre11-Rad50-NBS1 complex, Exo1, Dna2, Sae2/CtIP) and a helicase (Sgs1/BLM) to form a terminal 3′-OH single-stranded DNA tail. Then, the RPA protein binds to the tail and inhibits the formation of secondary structures in the ssDNA chain. Rad51 recombinase is recruited onto ssDNA through mediator proteins and forms a nucleofilament called the presynaptic filament. The Rad51 nucleofilament must search the homologous sequence located in the intact sister chromatid and invade (synapsis), generating the displacement of the homologous DNA strand to form the so-called D-loop. After D-loop formation, the invading chain is elongated by a polymerase, thus synthesizing the information lost during the DSB, then released. Later, multiple subpathways can be used for the resolution and repair of the DSBs (59–61).

Multiple studies have shown that radioresistant cells have an increase in DNA repair by HR compared to radiosensitive cells (43, 62). In breast cancer, the treatment used for conserving of breasts (BCT) is surgery plus adjuvant radiation therapy. However, some patients experience tumor recurrence around the scar. In the use of intraoperative radiotherapy (IORT) with intensive radiation administered during surgery directly to the tumor bed while sparing normal surrounding tissue, it has been observed that IORT induces biological changes in the tumor microenvironment and the activity of surgical wound fluid (RT-SWF) of breast cancer. These RT-SWF promote a DDR in the MDA-MB-468 cells, inducing overregulation of ERCC2, ERCC8, and RAD51 of the repair mechanisms NER and HR, promoting the arrest cell cycle at the G2M phase and raise its glycolytic metabolism (63). Overexpression of BRCA1/BRCA2/RAD51/RPA1 proteins in the HR was detected in hypopharyngeal carcinoma cell radioresistance, promoting the S phase and G2 phase cell cycle arrest. However, the RPA1 deletion in these cells leads to sensitivity to radiation (64). A similar study in a nasopharyngeal carcinoma (NPC) (CNE2RR) cell line induced the expression of NFBD1, BRCA1, BRCA2, RPA1, and RAD51 proteins widely associated with HR and radioresistance (65). Another report on this cancer found that the interaction of RAD50 (recombinant) with Mre11 and Nbs1 leads to G2/M cell cycle arrest through decreased DSBs, inhibits colony formation, and promotes sensitivity to radiation (66).

High expression of MSI1, CHK2, and Rad51 and higher ATM phosphorylation was reported in radioresistant stem-like cells from patient-derived glioblastoma (GBM). Furthermore, the overexpression of MSI1, a stem-like marker, promoted an increase in survival, invasion, EMT-like phenotype, and maintenance of cancer stem properties after radiation, through hyperactivation of DDR and DNA repair by HR (67). Some DNA lesions may persist despite the efficient activation of the different repair pathways in response to damage. In these cases, the cells can turn on the translesion DNA synthesis (TLS) mechanism, where a low-fidelity polymerase (such as Pol eta) induces a bypass of DNA damage to ensure continued genome duplication and cell survival. Paradoxically, irradiated cells lacking Pol eta showed greater radioresistance and survival through inhibition of the TLS mechanism, increasing the number of DNA templates and stimulating DNA repair by HR (68).

DNA repair pathways can compete or work together and converge at some point because, potentially, all types of damage can be generated during the irradiation. However, many details are still unknown (69). For example, leukemia cells lacking DNA pol β cannot perform the BER pathway efficiently but can activate the NHEJ pathway to repair damage by alkylation (70).

Cells have developed multiple pathways to detect DNA damage and coordinate the response to DNA damage, so the cell fate (survival or death) depends on their ability to activate these pathways quickly and efficiently. After irradiating HT29 colon cancer cells, ATM is activated by phosphorylation, promoting the recruitment of multiple factors involved in DDR, such as MDC1 and 53BP1, into the γ-H2AX repair foci (71). Chk2, a DDR regulator activated by ATM in response to damage, interacts with p53 to modulate the cell cycle (72). DSBs also stimulate the activation of GSK-3β by ATM. Subsequently, it is translocated from the cytoplasm to the nucleus, where it participates in the recruitment of other repair factors to the site of damage. Examples of these factors involved in NHEJ are 53BP1 and MRN and UNG2 involved in BER (59). WNT proteins are overexpressed and activated by radiation and promote RR in several human cancers, such as CRC and intestinal stem cells through the Wnt/β-catenin signaling pathway. After irradiation, β-catenin is stabilized by Wnt; it is translocated to the nucleus, enhancing the expression of different gene targets, such as LIG4 (73). The Wnt canonical pathway has also been associated with survival and aggressiveness of tumor cells after radiation because it promotes the maintenance of CSCs, EMT, and apoptosis evasion, contributing to RR and relapse of cancer (74).

The hippo pathway has an important role in regulating cell proliferation, organ growth, and cell regeneration. It has been

reported that this occurs *via* a pivotal role in cell growth, invasion, metastasis, and its components could be therapeutic target potential in cancer (75, 76). In a glioma U251 cell line, irradiation induced cell apoptosis through high expression of c-caspase 3, caspase 3, and Bax. Irradiation also promoted a low expression of YAP and the inactivation of Hippo/YAP signaling through the ubiquitination mediated by RCHY1 ubiquitin ligase, as well as the high expression of Mst1, LATS1, MOB1, and SAVI (77). Whereas the medulloblastoma cells were irradiated, a YAP high expression was detected, which induced the cell proliferation through high-rise Cyclin D2 (CCND2), and phosphorylated H3 promoted the tumor aggressiveness and tumor recurrence. Besides, YAP promotes IGF2 expression, which promotes the activation of PI3K/Akt pathway signaling. Akt activity automatically induces ATM and Chk2 dephosphorylation, immediately the lock of the DDR mechanism, thereby favoring radioresistance (78).

The Brahma-related gene product 1 (BRG1) enzyme catalyzes the SWI/SNF chromatin remodeling complex activity. BRG1 participates in proliferation, migration, and cellular and cell cycle progression in cancer (79). BRDs are conserved molecules that bind the acetylated lysine residues of the histone tails, leading to the regulation of gene expression, participate as readers of chromatin state, and repair DNA damage by activating DDR mechanisms. In cancer, BRDs are dysregulated, promoting the cell cycle and metastasis (80, 81). In colon cancer, BRG1-BRD dimerization was detected to have a greater chromatin binding strength, leading to radiosensitivity through γ–H2AX foci formation block and DSB repair. Also, this interaction inhibits the accumulation of 53BP1 towards the DSB sites and no alteration of ATM, CHK2, and p53 activations (71). On the other hand, in radiotherapy-resistant cervical cancer cell line (HeLa), the expression of DNA Damage-inducible protein 45α (GADD45α) was detected, promoting the increase cytoplasmic APE1 levels in these cells through overregulation of nitric oxide (NO), and inducing the nuclear export of APE1 to the cytoplasm, promoting cell proliferation and inhibiting apoptosis (48).

DSBs are the most lethal type of DNA strand damage and constitute the most complex type of damage. Consequently, it has been extensively studied. When DSBs occur, two evolutionarily highly conserved repair pathways are turned on: NHEJ and HR. In the same way, factors involved in both repair pathways are key to promoting tumor cells' survival against radiation damage.

CELL CYCLE ADAPTATIONS IN RESPONSE TO RADIATION

During the cell cycle, the cell duplicates its genome, grows, and divides; these events are regulated through cyclin-dependent kinase (CDK) in the checkpoints in the phase difference. Loss of cell cycle control is one of the hallmarks of cancer (82). The biological alterations in the cell cycle by radiation show changes in the phases of the cell cycle; for instance, in cervical cancer cell line HeLa irradiated with Gy (Gray) x-ray in different doses was observed an important G2/M retardation of these cells, decreased CDK1 protein expression, and increased CHK1 expression. Furthermore, the radiation promotes DNA damage by DSBs and a high γ-H2AX expression and production of ROS after radiation (83). Other research, in an oral cancer cell line SCC4 treated with RAD001 (an inhibitor of mTOR) plus radiation, reduced mTOR-S6 and 4EBP1 activation was detected, as well as the arrest in the G2/M cell cycle phase. This phenomenon was induced through CHK1 activation due to phosphorylation in Ser345 position and inhibition of CDC2-cyclin B1 complex and high levels of histone H2AX phosphorylation, thus inhibiting the proliferation of these cells (84). On the other hand, Chang and coworkers showed that PI3K/Akt/mTOR signaling pathway inhibitors (BEZ235 or PI103), in combination with radiotherapy in resistant prostate cancer cell lines (PC-3RR, DU145RR and LNCaPRR), promote distribution of cell cycle toward (G2/M) phase and decrease of G0/G1 and S phases through reduced protein phosphorylation of p-CDK1, p-Chk1, p-Chk2, and p-Rb. Moreover, apoptosis was induced by activating caspase-3 and caspase-7, with the split-off PARP-1, high γH2AX expression, and a decrease of repair proteins Ku70 and Ku80 BRCA-1, BRCA-2, and Rad-51 of NHEJ and HR, respectively, increasing to radiosensitivity in this cancer (50). Multiple studies have reported that tyrosine phosphatase (SHP1) is a negative regulator of cancer cell proliferation, EMT, migration, invasion, and cell cycle (85). In lung cancer, resistant cell lines (A549S1 and S549S2) show high levels of expression of SHP1, CDK4, and CylinD1 and low p16 expression. SHP1 promotes resistance to radiotherapy through regulating G0/G1 phase arrest of the cell cycle (86).

In another study, comparing two methods of radiation, one with carbon ions and the other X-irradiation in prostate cancer and colon cancer (PC3 and Caco-2 cell lines), it was observed that the carbon ions induce a higher γH2AX foci formation in colon cancer than in prostate cancer. X-radiation promotes lesser γH2AX foci formation, which is dose dependent, in both types of cancer. Furthermore, low doses of carbon ions trigger the G2/M arrest phase continuously, whereas high doses of radiation-X can keep the G2/M arrest phase in these cell lines and promote radiosensitivity (87). Radiotherapy promotes accumulation in the G2/M phase of the cell cycle in the different cancer types.

CHROMATIN REMODELING AS A MECHANISM OF RADIATION ADAPTATION

The genome of eukaryotes is located in a highly compacted core in chromatin form; this is a dynamic structure that maintains genomic stability and regulates gene expression and DNA repair. Chromatin remodeling is done through covalent modification of histones and the catalytic activity of remodeling proteins (88). For more than two decades, it has been reported that structural changes in the chromatin organization can contribute to the RR of tumor cells (89). The chromatin supercoiled (heterochromatin) configuration is more susceptible to developing radiotherapy

resistance than the relaxed chromatin (euchromatin) of tumor cells (90). For instance, in colon cancer, heterochromatin formation and histones methylation were observed in the irradiated subpopulation of cancer stem cells; both could promote radioresistance in this cancer (91).

Another study in a lung cancer cell line and head and neck squamous carcinoma cell line reported that more condensation of heterochromatin of irradiated cells is observed in 3D cultures than with 2D cultures, through decreased histone H3 acetylation and HP1a expression and fewer DSBs, promoting resistance toward radiotherapy (92). It has been described that genome compaction is a protective mechanism deployed by irradiated cells to protect the integrity of DNA against ionizing and other damaging agents. Takata et al. demonstrated that after γ-irradiation, the frequency of occurrence of DSBs is 5–50 times less in compact chromatin than in decondensed chromatin. However, they observed that this effect is a consequence of a lower chromatin opening rather than an increase in the concentration of associated proteins (14, 93).

Interestingly, the protective effect extends to other irradiation sources, such as carbon ion (C-ion), and chemical agents, such as cisplatin, both used in cancer therapies. Consistent with this, Sato et al. observed that cells subjected to different doses of X-rays can develop RR not only to X-rays but also to C-ion. It has also been reported that resistant C-ion cells may be sensitive to X-rays. These data suggest that resistance mechanisms to different sources may overlap. In the same report, they showed for the first time that the degree of RR correlates directly with the number of heterochromatic domains present in cells, so this characteristic could be used as an indicator of RR (14, 93).

Mund et al. (94) reported that after γ-irradiation of human bone osteoblastoma cancer cells, SPOC1 protein is recruited to DSBs-repair foci in an ATM-dependent manner. At repair sites, SPOC1 interacts with chromatin and chromatin remodeling factors, stimulating heterochromatinization and DDR (94).

Wang et al. also reported that EGFR is another protein involved in chromatin compaction after radiation in non-small-cell lung cancer (NSCLC) cells, and its inhibition can induce cellular senescence, increase the number of DSB, and radiosensitization, so it has been proposed as a therapeutic target for this cancer (95, 96).

The formation of highly condensed and ordered chromatin can reduce the exposure of DNA to OH and ROS radicals and decrease the direct ionization of DNA, thus increasing cell survival. On the other hand, heterochromatinization can promote the DNA repair activity of tumor cells through a greater restriction in molecular diffusion and thus promotes the detection of lesions. The latter is of great importance during HR repair since the colocalization and stability of the sister chromatids and the mechanical components are favored for rapid and accurate rejoining. The compaction of chromatin in response to radiation, and other stressors, has been reported in several species, so it appears to be a highly conserved adaptation mechanism (97).

However, highly compact chromatin constitutes a barrier limiting the access of proteins that participate in DDR to DNA damage. Therefore, regions to repair must be locally reconfigured towards more relaxed chromatin to promote efficient repair and after repackaged again into nucleosomes (98). Chromatin remodeling proteins facilitate the recruitment of essential factors required during DNA repair. Brahma-related gene-1 (BRG1), the central catalytic subunit of many chromatin-modifying enzymatic complexes such as SWI/SFN, has been implicated in the ATP-dependent local alteration of chromatin structure after radiation. After DSBs formation, the ATM protein is activated and phosphorylates H2A histone family member X (H2AX) located at the damage sites, resulting in the formation of γ-H2AX-containing nucleosomes. Subsequently, BRG1 is recruited to damage sites through its interaction with acetylated histones H3 of γ-H2AX nucleosomes, where it promotes the disruption of histone-DNA contacts, thus increasing the local accessibility of DNA to repair proteins, stimulating DDR and apoptosis evasion (71, 99). On the other hand, Andrade et al. reported that by protein-RNA interactions in breast cancer cells, HuR stabilizes the ARID1A mRNA, a subunit of the SWI/SNF chromatin remodeling complex, reducing radiation-induced DNA fragmentation, possibly through NHEJ pathway stimulation, thus reducing DSBs accumulation and conferring RR (100).

CHANGES IN THE PLASMA MEMBRANE THAT FAVOR RADIORESISTANCE

The plasma membrane is a semipermeable lipid bilayer associated with different proteins and carbohydrates; their composition and organization largely determine its role within different biological processes. The plasma membrane helps maintain cell homeostasis by serving as a barrier between the intracellular and extracellular environment, regulating the transport of molecules, and is involved in cell communication and cell signaling in cell movements. After radiation, tumor cells can alter the expression of genes that promote changes in the composition of lipids and membrane proteins, thus promoting their reorganization and increasing the RR phenotype (101).

Astrocytoma cells can rearrange their plasma membrane and form thin and ultralong (up to hundreds of micrometers) protrusions, also called tumor microtubes (TMs), in response to radiation. The formation of these TMs may support brain invasion, proliferation, and multicellular communication over long distances; importantly, TMs-interconnected tumor cells were more resistant to RT. On the other hand, an increase of intracellular calcium has been reported to promote the sensitization of tumor cells to radiation (101). Osswald et al. have reported that intracellular calcium levels increase in cells that TMs do not connect after radiation. However, cells interconnected by TMs present more homogeneous calcium levels, similar to those of non-irradiated cells. The formation of TMs favors the cellular interconnections and the maintenance of calcium homeostasis since they could serve as bridges for the distribution and homogenization of calcium between cells and protect cells from cell death. Few proteins involved in the formation and function of TMs have been identified; one of

them is the growth-associated protein 43 (GAP-43), a protein associated with neuronal growth and plasticity. After radiation, GAP-43 is overexpressed, stimulating TMs formation, increasing cellular interconnectivity, and forming a communication network within the tumor (102). By gene-expression microarray analysis, Jung et al. identified the Tweety-homolog 1 (Ttyh1) protein as a new TM-relevant factor. Ttyh1 is a plasma membrane protein associated with neuronal development that colocalizes with integrin α5 and is highly expressed in invasive cells with one or two TMs, compared to less invasive cells with more than two TMs. However, although Ttyh1 expression is important for TMs formation, Ttyh1-deficient cells with more than two TMs showed higher TMs interconnectivity, leading to increased RR of tumor cells (103).

Both reports agree that radioresistant tumor cells presented more interconnecting TMs. In breast cancer, Chignola et al. reported that the formation of intercellular cytoplasmic bridges and the presence of multinucleated giant cells increase in response to radiation and significantly stimulate tumor RR. An increase in cytoplasmic bridges formation, and greater communication between cells within a tumor population, is stimulated by the action of Syncytin-1 homologous protein (SyHP). Syncytin-1 is a viral protein involved in fusogenic events between viral and cell membranes. After radiation, a portion of the cell population begins to die, exposing the SyHP protein on its surface. SyHP exposure on dead cells serves as a stimulus for the formation of cytoplasmic bridges and the induction of fusion events between the surviving cells, resulting in syncytia formation and increase of the tumor population survival (104). In CRC cell lines, the radiation triggers plasma membrane alterations, such as loss of polarity, spindle-cell shape, intercellular separation, and the emergence of pseudopodia; these changes increase invasion, migration, and survival of the radiated cells (105).

In the plasma membrane, ASMase hydrolyzes sphingomyelin generating ceramide; this process is carried out especially in lipid rafts, sphingomyelin-rich membrane microdomains involved in cell signaling. Ceramide-rich lipid rafts rearrange and fuse, forming large lipid platforms (106, 107). Ketteler et al. showed that stress by radiation stimulates changes in the lipid composition of plasma membranes, promoting their reorganization, altering downstream cell signaling, and affecting the RR of PCa cells. After radiation, epithelial cells (EC) stimulate the activation and translocation (from the lysosome to the plasma membrane) of the ASMase enzyme and decrease the expression of caveolin-1 (CAV1), increasing apoptosis. However, CAV1 overexpression has been reported in malignant EC of different types of solid tumors; tumor cells could increase CAV1 expression as a mechanism for evasion of apoptosis and RR (108).

ENDOPLASMIC RETICULUM ADAPTATIONS TO RADIATION

The endoplasmic reticulum (ER) is an endomembrane system that participates in multiple cellular functions, mainly related to synthesis, folding, modification, and transport of proteins (109). Radiation and chemotherapeutic drugs can perturb cellular homeostasis and generate stress in the ER; numerous evidences indicate that said stress (ERS) plays an important role in activating resistance mechanisms to radiation and drugs (110). The accumulation of unfolded or misfolded proteins in ER lumen after radiation activates a cytoprotective unfolded protein response (UPR) that maintains ER homeostasis. However, the UPR pathway can induce cell death if stress is severe and persistent (13).

RR in oropharyngeal carcinoma cells (OPCCs) is regulated by protein kinase R-like endoplasmic reticulum kinase (PERK), one of the main sensors and transducers of the ERS pathway. After radiation, PERK is autophosphorylated and phosphorylates to the eukaryotic initiation factor-2 (eIF2α) factor, which subsequently inhibits the global synthesis of proteins, reducing translocation and accumulation of misfolded proteins in the ER lumen. At the same time, phosphorylated eIF2α activates NF-kB, which is translocated to the nucleus and promotes the transactivation of its target genes. This process inhibits G2/M cell cycle arrest and apoptosis, as well as stimulates DNA DSB repair (110). Additionally, NF-κB confers RR in lymphoma cells by, at least in part, inducing the aberrant expression of HIF-1 (111). IRE1 is another principal sensor of ERS pathway, and its overexpression in HPV-negative OPCC patients treated with RT has been correlated with poor outcomes. IRE1 promotes IL-6 activation, enhancing X-ray-induced DNA DSB and cell apoptosis (112). Another mechanism that activates ERS signaling is the activation of EGFR conferring RR in OSCC. The EGFR inhibition improves therapy in non-response OPCC patients by inhibiting PERK-eIF2α-GRP94 and IRE1α-GRP78 (113).

The ERS pathway also stimulates chaperones' expression to assist protein folding; the chaperone glucose-regulated protein 78 (GRP78) has been reported to increase its expression in response to radiation. Furthermore, the high expression of GRP78 in different types of cancers has been associated with RR. GRP78 overexpression increases DSB DNA repair and autophagy, as well as decreases apoptosis of tumor cells (13). Cetuximab is a monoclonal antibody used for the inhibition of EGFR and radiosensitization of tumor cells. However, it can also decrease the GRP78 expression of OPCC (13).

CSCs constitute a tumoral subpopulation with a high capacity for DNA repair, self-renewal, and differentiation towards other cell types and have been implicated in the recurrence of different types of tumors (114). CSCs present different mechanisms that have high resistance to different oncological therapies, including RT (115). In glioblastoma stem cells (GSC), an increase in ER luminal diameter, the activation of the UPR pathway, and the expression of proteins involved folding protein (such as GRP78 and GPR94) have been reported as mechanisms to avoid radiation-induced damage. Another survival mechanism in this tumor subpopulation is the activation of autophagy, which participates in the elimination of damaged cell fractions (116). The use of 2-deoxy-D-glucose (2-DG) may potentiate radiation-induced ERS to cytotoxic levels, inactivating the survival pathway and activating apoptosis (116).

Hypoxia is a feature frequently found in tumors, and its contribution to malignancy and treatment resistance has been demonstrated (117). Severe hypoxia also activates ER stress signaling. Particularly, the survival of a subset of hypoxic cells that determine tumor RR is dependent on the eIF2α-associated arm of the UPR. The eIF2α signaling promotes the synthesis of glutathione, cysteine uptake, and protection against ROS produced during periods of cycling hypoxia (118). In contrast, it has been reported that the enhancement of endoplasmic reticulum stress response under hypoxic conditions increases radiosensitivity in pancreatic and breast cancer cell lines *via* the stimulation of the insulin-like growth factor (IGF) signaling pathway and subsequent activation of the PI3K-mTOR pathway (119).

MITOCHONDRIAL ADAPTATIONS TO RADIATION

Mitochondria generate the chemical energy that cells need to carry out their biochemical functions through oxidative phosphorylation, the most efficient cellular pathway for the generation of ATP (120). The structure and function of mitochondria are compromised during different types of stress, including RT, so mitochondria respond through different adaptive mechanisms to support RR and maintain organellar and cellular homeostasis (**Figure 2**).

Lebeau et al. reported that acute stress in ER can also alter the mitochondria structure, promoting elongation and fragmentation. In response to ERS, mitochondria turn on a prosurvival mechanism called stress-induced mitochondrial hyperfusion (SIMH), avoiding premature fragmentation, stimulating metabolic activity, and facilitating adaptation and recovery during stress periods. In SIMH, ERS inhibits PERK-dependent eIF2α phosphorylation, decreasing translation, translocation, and accumulation of misfolded or damaged proteins in the mitochondrial lumen, thus maintaining cellular proteostasis (121).

Lynam et al. compared two esophageal adenocarcinoma cell lines with the same origin but with different degrees of RR, OE33 R, and OE33 P, to identify mitochondrial alterations associated with RR. They observed that the resistant subline OE33 R presented an increase in ROS levels and more DNA mitochondrial mutations than the parental line OE33 P, an increase in the number and mass of mitochondria, and more elongated and condensed mitochondria. Likewise, OE33 R presented bioenergetic alterations, such as increased mitochondrial respiration and oxidative phosphorylation and increased levels of intracellular ATP. Additionally, five genes involved in energy metabolism (ATP5G1, ATP5G3, ATPV0A2, NDUFC2, and NDUFS3) were overexpressed in OE33 R cells, supporting increased metabolic activity in these cells. Interestingly, radioresistant cells show an increase in their metabolic plasticity, changing from glycolysis to oxidative phosphorylation pathways, accompanied by enhanced survival (122). In head and neck cancer cells, preservation of mitochondrial functions after radiation has also been associated with a change from a glycolytic to more oxidative metabolism, increased mitochondria number, and a higher mtDNA content (123). Recently, Montenegro et al. also reported that radiation-induced changes that favor oxidative metabolism and an increase in ATP production in breast cancer cells were mediated by S-adenosylmethionine SAM. SAM is a donor of methyl groups in transmethylation reactions, so an increase in its cellular concentration stimulates the activity of different cellular methylases and promotes the hypermethylation of other cellular proteins. In this way, protein arginine methyltransferase 1 (PRMT1) methylates the BRCA1 protein after radiation and stimulates its nuclear translocation favoring DSBs repair *via* HR and inhibiting apoptosis. Thus, protein methylation also plays an important role in defense of tumor cells against IR (124).

However, exposure of tumor cells to a brief low-oxygen environment (7% O2 for 3 h) decreases mitochondrial respiration, resulting in exacerbated glycolysis, high lactate concentrations, and an increase in RR. During acute hypoxic stress, tumor cells adapt their metabolism through HIF-1α, which modulates glycolytic genes, making them less dependent on oxygen and increasing survival (125). The survival of HIF-1α knockdown tumor cells under hypoxia conditions is lower and increases their response to RT because they maintain a more oxidative metabolism that requires oxygen consumption, and since there is not enough oxygen, they are more likely to die. Importantly, HIF-1α inhibition altered tumor metabolism in mice exposed to a low oxygen environment (7% O2 for 3 h), enhancing RT response but having minimal effect on tumors in air-breathing animals (10). Epperly et al. reported that after irradiation of tumor cells, the expression of HIF-1α, c-Myc, and Glucose transporter 1 (GLUT1) increased in a dose-dependent manner, promoting the transport of glucose into the cell and stimulating glycolysis (126).

The signal transducer and activator of transcription 1 (STAT1), in addition to its role as a transmitter of interferon (INF) signaling and pro-apoptotic tumor suppressor, has been associated with energy metabolism regulation. The STAT1 overexpression pathway confers RR and INF resistance. In contrast, STAT1 knockdown in tumors alters the expression of genes and proteins of oxidative phosphorylation, the citrate cycle, and glycolysis/gluconeogenesis (127). In STAT1 knockdown tumor xenografts, radiation predominantly suppresses the glycolysis/gluconeogenesis pathway without significant change in STAT1 wildtype tumor xenografts. The IR-induced energy deprivation of proliferating STAT1-suppressed tumor cells constitutes a potential mechanism of tumor radiosensitization (128).

A determining point for the performance of oxidative phosphorylation in the cell is the transport of cytoplasmic pyruvate to the mitochondria. Mitochondrial pyruvate carrier (MPC) is the protein responsible for pyruvate transport to the mitochondria (129), and the subexpression of this carrier in pancreatic cancer and CRC cell lines induces changes associated with EMT and RR. MPC1-suppressed cells change their morphology from oval to spindle shape, the levels of E-cadherin transcript decreased, fibronectin increased, and migration and their ability to withstand radiation increased. When MPC1-suppressed cells were cultured in a glutamine-

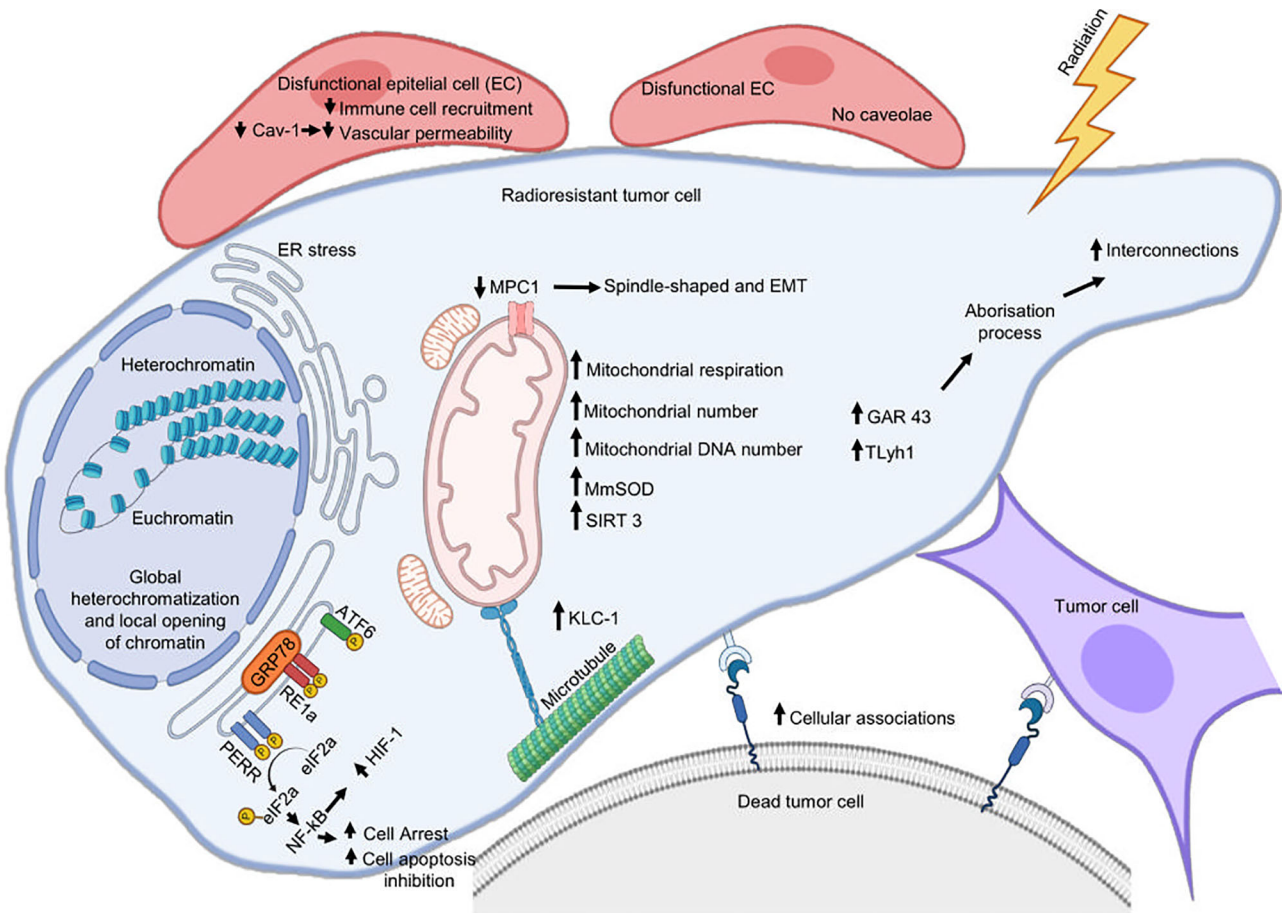

FIGURE 2 | Cellular mechanisms associated with radioresistance. Cytoplasmic membrane, reticulum endoplasmic, and mitochondria are the main organelles where tumor cells assemble a response to develop radioresistance. Radiation can damage the endoplasmic reticulum (ER) homeostatic state and cause ER stress that will favor radioresistance. This last is also supported by mitochondrial alterations, metabolic remodeling, and by an increase in plasma membrane interconnections favoring the formation of cytoplasmic bridges. Cetuximab promotes radioresistance involving ERS pathway IRE1α/ATF6-GRP78. Silencing GRP78 inhibits the cooperative effects of radiotherapy and cetuximab inhibiting DSB repair and autophagy in OPCC. IRE1 promotes radioresistance in HPV-negative OPCC through IL-6 activation. Decreased MPC1 expression favors EMT and promotes radioresistance of cancer.

deficient medium, the changes in the EMT markers were suppressed; this suggests that EMT-like phenotype can be stimulated with alternative use of energy substrates, such as glutamine, when the entry of pyruvate into the mitochondria is reduced, thus compensating for ATP production (130).

Mitochondrial permeability transition pore (MPTP) is a non-specific pore located in the inner mitochondrial membrane, which opens under stress conditions resulting in alterations in oxidative phosphorylation, ATP depletion, and cell death (131). In a mouse model, Zhang et al. observed that after radiation to the whole body, liver cells from radiosensitive mouse strain (BALB/c) showed lower mitochondrial copy number, and MPTP opened sooner than radioresistant mouse strain (C57BL/6). Interestingly, they also showed that radiation response was maternally inherited (132).

The exact role that mitophagy plays in response to radiation is still debated. However, some authors have proposed that this mechanism may help cells eliminate mitochondria damaged by treatment (133). Zheng et al. reported that Parkin-mediated mitophagy plays a relevant role in cellular homeostasis maintenance and RR of breast cancer cells under hypoxic conditions. Under normal conditions, Parkin protein accumulation in dysfunctional mitochondria initiates the process of mitophagy. However, this process is inhibited by p53 protein. Parkin-p53 interaction inhibits the translocation of Parkin to the mitochondria, disrupting the protective mitophagy process and radiosensitizing cells significantly. However, in different types of tumors, there is a dysfunction of p53 (mutation or silencing), and so an increase in mitophagy (134). Additionally, mitophagy was markedly increased by low oxygen tension. Thus, these two facts could explain why p53-deficient cells adapt better to hypoxic stress conditions and are more radioresistant (134).

Kinesins are motor proteins associated with microtubules of the cytoskeleton involved in the intracellular transport of

different cellular components, such as organelles and vesicles. Loss of Kinesin light chain 4 (KLC4) promotes apoptotic cell death and a decreased tumor growth in a mouse xenograft model. Also, downregulated-KLC4 cells have mitochondrial dysfunction through impaired mitochondrial respiration and an increase in ROS and mitochondrial calcium uptake. Because KLC4 is overexpressed in radioresistant lung cancer cell lines and tissues from lung cancer patients, it could be favoring mitochondrial homeostasis and the survival of tumor cells (135).

Mitochondria is the major source of ROS, which can cause oxidative damage to a wide range of molecules affecting cellular homeostasis; additionally, as we already mentioned, RT can also promote ROS generation (74). Manganese superoxide dismutase (MnSOD) is the major ROS-detoxifying enzyme located in the mitochondria; alterations in this enzyme generate mitochondrial and cellular dysfunction (136). Miar et al. have reported a higher expression of MnSOD compared to non-tumor samples in multiple tumor types, such as colon and lung, and an increase in MnSOD in middle-stage tumors of PCa. In addition, they also found high levels of MnSOD in all the metastatic tumors they analyzed, so overexpression of this enzyme may be involved in stimulating cancer hallmarks, such as migration and invasion, promoting thus carcinogenesis (137). Interestingly, it has been reported that MnSOD activity increases significantly after irradiation, contributing to the ROS neutralization and maintaining the cellular redox balance. In addition, irradiated cancer cells that overexpress MnSOD show an increase in the activation of the G2 phase of the cell cycle, so they can survive and divide despite the stress generated by radiation (126, 138).

On the other hand, it has been shown that higher doses of radiation generate lower mitochondrial membrane potential. Since the mitochondria use this membrane potential to generate energy in ATP form, its prolonged decrease can generate adverse effects on cells and lead to cell death (139). Epperly et al. reported that MnSOD overexpression in cancer cells stabilizes the initial changes in membrane potential generated by radiation, where another antioxidant enzyme, mitochondrial catalase, could maintain homeostasis at later times (83, 126).

Another mechanism of RR mediated by IL6 was studied by Tamari et al. comparing rat glioma cell lines (C6) as tumor cells against a rat astrocyte cell line (RNB) as a non-tumor cell. After irradiation, the addition of IL-6 reduces ROS levels and superoxide concentration in mitochondria, thus increasing C6 cell survival (140).

Additionally, there are other mitochondrial and epigenetic mechanisms associated with tumor RR. SIRT3 is a mitochondrial NAD (+)-dependent deacetylase that promotes deacetylation of other mitochondrial proteins to maintain metabolic homeostasis and prevent cell aging. Liu et al. reported that the SIRT3 promoter is overexpressed in radiation-treated tumor cells, and the NF-κB transcription factor mediates their transactivation. After radiation, SIRT3 and Cyclin B1/CDK1 are overexpressed and translocated to the mitochondrial matrix, where SIRT3 is phosphorylated and activated by Cyclin B1/CDK1, thus promoting the deacetylation of mitochondrial proteins, such as MnSOD, p53, and NADUFA9. In this way, SIRT3 maintains the mitochondrial homeostasis and increases survival and adaptive RR in tumor cells (141).

EXTRACELLULAR ADAPTATIONS OF TUMOR CELLS TO RADIATION

The behavior, progression, and response to different therapies of tumor cells are influenced by the type of molecules, cells, and conditions present in their surrounding environment, that is, by the tumor microenvironment (TME) (142). TME is very heterogeneous and consists of multiple elements, such as a diversity of infiltrating cells of the host, stroma cells, the vascular system, extracellular matrix (ECM), secreted soluble factors, and different surrounding types of non-malignant cells. Dynamic interactions of these components can promote tumor progression, migration, invasion, metastasis, and survival of tumor cells (143). Generally, solid tumor cells (e.g., ovary, lung, cervical, and colon) can be subjected to an oxygen concentration gradient, where low concentrations (hypoxia) can stimulate the malignant characteristics of tumor cells and resistance to RT (144). On the other hand, it has been described that acidic pH, lack of nutrients, and low oxygen concentrations promote deficient blood perfusion and, consequently, hypoxia within the TME (145). Hypoxia promotes sustained angiogenesis and the activation of new neovascularization mechanisms, such as vasculogenic mimicry, the latter induced through EMT phenotype and changes in gene expression (144–146).

EMT is a complex mechanism that allows solid tumor cells to suppress their epithelial characteristics and acquire a mesenchymal phenotype. During EMT, cells show morphological changes and adhesion and migration capacity, facilitating their detachment from the primary tumor and the invasion of other body regions, thus favoring metastasis and tumor progression. Interestingly, an association between EMT and the generation of CSCs has been widely reported, promoting the formation of new tumors (147).

In CRC cell lines, the radiation triggers molecular changes consistent with EMT, such as low expression of the epithelial marker E-cadherin and high expression of mesenchymal markers, such as vimentin, fibronectin, and the Snail Family Transcriptional Repressor 2 (SNAI2), increasing invasion, migration, and survival of the radiated cells (105). Another report, using the ESCC KYSE-150 cell line and a xenograft tumor model, showed that the irradiation of KYSE-150 cells stimulated the EMT phenotype and the acquisition of stemness-like properties. In addition, those cells undergo morphological changes from cuboidal to spindle-like shape and show high expression of WNT1 inducible signaling pathway (WISP1), a signaling protein associated with the ECM, which plays a role in the development of the EMT phenotype and RR through regulation of genes associated with EMT (148).

The ECM is a dynamic three-dimensional network of proteins (collagen, proteoglycans, laminin, and fibronectin) and non-cellular components of tissue (water, minerals) that serve, among other things, as a cellular niche, as the organizer of

TME components, and provides scaffolding for intercellular communication (149). When growing surrounded or embedded in the ECM, tumor cells are highly influenced by their matrix components. Inversely, tumor cells induce changes in their surrounding ECM to modulate its development, progression, and response to therapy (150). As mentioned already, tumor cells grown in a 3D environment have increased resistance to stressors, such as IR, compared to 2D cultures; this phenomenon is known as cell-adhesion mediated radioresistance (CAM-RR). It has been observed in several cell lines from different types of cancer that IR stimulates changes in the plasma membrane components. For example, after radiation, fibronectin and β1-integrin are overexpressed. Also, the β1-integrin is reorganized into clusters. Therefore, these two components can interact, stimulating cell-matrix interactions; consequently, RR and survival are increased (151–153). These interactions also influence chromatin structure, stimulate heterochromatinization with the aforementioned implications, and promote changes in gene expression and cellular response to environmental stimuli (92). Bai et al. compared the gene expression patterns of sarcoma cells grown in 2D and 3D by microarray analysis. These authors also observed that genes involved in tumor cell adhesion (N- and E-cadherin), gap junction (connexins Cx26, Cx43, Cx45), and ECM remodeling (COL1A1, LOX, FN1, SNED1, ITGB1, and LAMA4) were overexpressed in 3D cultures, and so are potentially involved in RR (154).

The lysyl oxidase-like 2 (LOXL2) is a protein that catalyzes the cross-linking of collagen and elastin components in the ECM and has been reported to contribute to the development and progression of several cancer types. A high expression of LOXL2 has been observed in DU145 and PC3 androgen-independent cell lines (from castration-resistant PCa), compared to LNCaP and 22Rv1 androgen-dependent cell lines. LOXL2 inhibition promotes radiosensitivity in prostate cells and xenograft tumors by EMT reversion and increased apoptosis by caspase-3 activation (155). PC-3, DU145, and LNCaP cancer prostate cell lines treated with radiation acquire characteristics of the EMT phenotype and stemness-like properties and show structural changes, such as loss of the glandular morphology, vacuolated cytoplasm, pleomorphic nuclei, and enlarged cell size. Furthermore, they increase the activation of p-Chk1 and p-Chk2 proteins and turn on the PI3K/Akt/mTOR signaling pathway; both processes can contribute to the repair of radiation-induced damage in tumor cells (156). Another study performed in poorly differentiated hepatocellular carcinoma (HCC) showed an association between PI3K/AKT/mTOR signaling pathway activation through the protein 3-phosphoinositide-dependent protein kinase 1 (PDPK1) and an increase in stemness characteristics, EMT, metastasis, DDR, and RR (157). Konge et al. demonstrated that TGF-β-induced mammary epithelium cells promote EMT and CSCs generation, which are more radioresistant compared to breast cancer non-stem cells. In addition, CSCs populations present very few polyploid cells, a G2/M arrest phase cell cycle, free radical scavengers, and activation of the death receptor pathways (FasL, TRAIL, and TNF-α), contributing to acquired RR during EMT (158).

On the other hand, although RT is a localized treatment, it promotes cytokine expression and systemic release. Cytokines are small proteins secreted by multiple cell types, which fundamentally modulate the immune and inflammatory response, and as already mentioned, they could mediate the survival of tumors to radiation. Ellsworth et al. conducted a prospective study to evaluate changes in cytokine expression patterns in NSCLC patients undergoing radiation therapy and found that different cytokines changed their expression during RT, including sCD40l, IP-10, MIP-1β, CX3CL1, VEGF, GM-CSF, IL-12, IFN-γ, IL-1a, and VEGF, which could participate in the promotion, growth, and progression of tumors by suppressing factors of the immune system, adding thus another layer to the complex response to the IR (159).

POTENTIAL MOLECULAR TARGETS TO ENHANCE RADIOSENSITIVITY OF CANCER CELLS

There is no universal method to detect RR in patients. However, after RT, if a reduction in tumor volume is not observed in the expected response time or even increases, RR is suspected. RR can also be clinically deduced in cases of tumor recurrence, that is if tumor reappearance is detected after RT (15, 20). Depending on the type of tumor, stage of development, and location, other clinical manifestations associated with RR may be observed in patients. For example, in PCa, if symptoms of urinary obstruction continue after treatment, or if in a laboratory test the patient again shows elevated serum prostatic antigen levels, RR is also suspected (160).

The knowledge generated in recent decades on the mechanisms of tumor resistance to RT has made it possible to identify different molecules that can be used as molecular markers of RR or as therapeutic targets to increase radiosensitivity. Different research groups have focused on the search for markers of resistance to RT; some traits proposed as RR predictors include the presence of oxidative stress markers, such as some reactive oxygen species that are produced during therapy, tissue hypoxia which is evidenced by vascularity and central necrosis in some tumors, presence of cancer cells close to blood vessels, as well as the expression of specific interleukins, such as IL-8 (161). More specific molecular markers related to mechanisms of cellular adaptation and resistance to radiation have been proposed. TME and EMT signatures, TGF-β, poly ADP-ribose polymerase (PARP-1), or certain chaperone proteins have been found in radiologically resistant PCa. Analysis of these markers in patients can allow oncologists to assess the initial response to therapy and propose a more appropriate therapeutic strategy for each patient (160, 161).

As previously mentioned, RR is the main obstacle to the success of radiotherapies, so different research groups are constantly working in the search for strategies that allow reducing the resistance of tumor cells to radiation, and thus be

able to increase the success of therapies and favorably impact on the quality of life and survival of cancer patients. Because one of the main mechanisms of RR in different types of tumors is the overexpression of molecules involved in DDR and DNA repair, these molecules are among the most explored therapeutic targets. However, molecules that participate in other RR mechanisms, such as epigenetic modulation, chromatin remodeling, maintenance of organelle homeostasis, lipid and carbohydrate metabolism, apoptosis, EMT, and signal transduction, among others, have been identified. Decreasing these molecules during RT can be of great help to increase the response of patients to therapy.

In recent years, multiple molecule types have been developed (mainly chemical inhibitors or interference RNAs) that specifically inhibit or decrease the action of proteins involved in tumor RR, and when tested in preclinical studies (in cell cultures or animal models), have given promising results for the radiosensitization of cells from different tumor types, such as brain, lung, pancreas, colorectal, breast, oral, cervical, prostate, and liver (**Table 2**). Inhibitors could be applied to patients in combination with radiation to increase the response to RT; even the combination of protein inhibitors can help increase radiosensitization and the success of the therapies. Because RR is a complex process, where different cellular pathways and mechanisms are orchestrated to increase the survival and reproduction of tumor cells, strategies must be focused on combating multiple aspects of tumor cell biology. The inhibition of key RR players, that is, participating in different pathways or mechanisms, would be especially useful to interfere with the process from different angles. However, other aspects must be worked on in parallel, for example, the mechanisms of action of the inhibitors, activation and inactivation mechanisms, effective doses to increase their effectiveness and reduce possible collateral damage.

TABLE 2 | Potential molecular targets to enhance radiosensitivity of cancer cells.

Target	Process	Radiosensitization experiments	References
53BP1	Involved in DNA repair *via* the NHEJ and HR pathways.	53BP1 is knocked down using specific shRNAs in GBM cell lines.	(162)
AKT	Involved in cell survival, growth, cancer progression, and DNA damage repair.	Treatment of radioresistant lung cancer cells with Diosmetin, an AKT Pathway Inhibitor.	(163)
APE1	Involved in DNA repair *via* BER pathway.	Analysis of glioma and pancreas cells lacking APE1. Treatment of radioresistant pancreatic cancer cells with Lucanthone, an APE1 inhibitor. APE1 is knocked down using specific shRNAs in pancreatic cells.	(47)
Artemis	Involved in DNA repair *via* the NHEJ pathway	Mouse embryonic fibroblasts (MEFs) from DNA-PKcs mutant mice	(164)
β1 integrin	Signal transduction	GCS or patient-derived GBM cell cultures treated with AIIB2, a specific antibody against β1 integrin, and JNK inhibitor SP600125.	(165)
β-catenin	Wnt/β-catenin pathway	Treatment of radioresistant ESCC with iCRT14, an β-catenin inhibitor.	(74)
BRG1	Chromatin remodeling	BRG1 negative mutant overexpression in colon, breast, and lung cancer cells. Xenograft colon tumors that overexpress the BRG1 negative mutant.	(71)
Catalase	ROS detoxifying	32D cl 3, a hematopoietic progenitor cell line, was transfected with mt-catalase-plasmid, that overexpressing mitochondrial catalase. Intratracheal injection of mt-catalase plasmid-liposome complexes in C57BL/6NHsd female mice and subsequent thoracic irradiation.	(126)
CHOP (C/EBP homologous protein)	UPR pathway and Autophagy	CHOP is knocked by RNAi in breast cancer cells.	(166)
CUX1	DDR response	CUX1 is knocked by siRNAs in radioresistant breast cancer cells and MEFs (mouse embryonic fibroblasts).	(45)
CXCL1	Inflammation and DNA repair	CXCL1 is knocked by shRNAs in radioresistant GBM cell lines. Xenograft tumors of ESCC cells in combination with CAFs (XRCC1 producing cells) are implanted and after treated with an CXCL1 antibody.	(27, 58)
DNA-PKcs	Involved in DNA repair *via* the NHEJ pathway	MEFs analysis from DNA-PKcs mutant mice.	(164)
EGFR	Cell proliferation and survival	Radioresistant human lung carcinoma cells treated with erlotinib or cetuximab EGFR inhibitors.	(96)
EPOR (Erythropoietin Receptor)	Cell cycle arrest and grow	Erythropoietin-induced glioma and cervical cancer cells treated with tyrphostin B42, an inhibitor of JAK2 tyrosine kinase activity. JAK2 is an effector of EPOR. EPOR knockdown in GBM.	(167, 168)
FHIT	DNA methylation	Transfection of oral cancer cells using FHIT-overexpressing cDNA myc-tag plasmid. Generation of radioresistant mouse xenograft tumors that overexpress FHIT	(169)
GADD45α	BER	GADD45α overexpression in X-ray-resistant HeLa cell line, by transfection with GADD45α plasmid.	(48)
GAP-43	Neuronal differentiation	Glioblastoma cells grown under stem conditions (GBMSCs) with a genetic knockdown of GAP-43.	(102)

(Continued)

TABLE 2 | Continued

Target	Process	Radiosensitization experiments	References
G0S2 (G0/G1 Switch 2)	Lipid metabolism	Targeting G0S2 by shRNAs in GSCs.	(4)
GRP78	ERS endoplasmic reticulum stress	Targeting GRP78 by siRNAs in OPSCC cell lines. GRP78 upregulation with 2-Deoxy-D-Glucose (2-DG) in GSC.	(13, 116)
GSK-3β	Involved in DNA repair *via* the NHEJ and HR pathways.	Inhibition of GSK-3β in pancreatic cancer cells using LiCl, AR-A014418, or SB216763 GSK inhibitors. Targeting GSK-3β by siRNAs in pancreatic cancer cell lines.	(170, 171)
HDAC	Histone deacetylase	Inhibition of HDAC in human prostate cancer cell lines using suberoylanilide hydroxamic acid (SAHA). Inhibition of HDAC in radioresistant esophageal carcinoma cells lines using trichostatin A and sodium butyrate.	(172, 173)
HDAC6	Histone deacetylase	Inhibition of HDAC6 in radioresistant GSC using HDAC6i.	(174)
JNK (c-Jun N-terminal kinase)	UPR pathway and apoptosis	Inhibition of JNK in radioresistant breast cancer cell lines using SP600125.	(166)
KDMs containing a Jumomji C (JmjC) domain	DNA methylation	Inhibition of KDM in radioresistant lung cancer cell lines using JIB-04.	(175)
KLC4	Mitochondrial homeostasis	Targeting KLC4 by siRNAs in lung cancer cell lines. Generation of mouse xenograft tumors with lung cancer cells lacking KLC4.	(135)
Ku70	Involved in DNA repair *via* the NHEJ pathway	Ku70 negative mutant overexpression in embryonic stem cells.	(176)
LIG4	Involved in DNA repair *via* the NHEJ pathway	Inhibition of LIG4 in colorectal cancer cells using SCR7 inhibitor. Targeting LIG4 by shRNAs in colorectal cancer cell lines.	(55)
LOXL2	EMT phenotype	LOXL2 knockdown by shRNA in castration-resistant prostate cancer cells.	(155)
MGMT	DNA-methyltransferase	Targeting MGMT by siRNAs in breast cancer cells lines.	(177)
MnSOD	ROS detoxifying	Targeting MnSOD by siRNAs in human pancreatic cancer cell lines. Intratracheal injection of MnSOD-PL plasmid-liposome complexes (that overexpress MnSOD) in C57BL/6NHsd female mice and subsequent thoracic irradiation.	(126, 138)
MSI1	Involved in DNA repair *via* the HR pathway	Silencing of MSI1 by shRNA in MSI1-high-expressing radioresistant GBM cell line. Generation of mouse xenograft tumors with GMB cancer cells lacking MSI1.	(67)
NFBD1	Involved in DNA repair *via* the HR pathway	Silencing of NFBD1 by shRNA in radioresistant NPC cell line.	(65)
OGG1	Involved in DNA repair *via* the BER pathway	Silencing of OGG1 by siRNAs in CRC cell lines. Inhibition of OGG1 in CRC cell lines using Chembridge 5245457 and 5552704 inhibitors.	(46)
P53	Transcription	Transfection of NSCLC cells using p53-overexpressing pCDNA3.1-p53 plasmid.	(178, 179)
PARP-1	Involved in DNA repair *via* the BER pathway	Inhibition of PARP-1 in HPV- negative in OPSCC using Olaparib.	(43)
PDK1	Signal transduction	PDK1 inhibition by siRNAs in hepatocellular carcinoma (HCC). PDK1 inhibition by BX795 in HCC.	(157)
PERK	Endoplasmic reticulum stress	Silencing of PERK by siRNAs in OPCC cell lines.	(110)
PI3k/mTOR	Signaling pathway	Dual PI3K/mTOR inhibition with BEZ235 in patient-derived OSCC cells or prostate cancer cell lines. Treatment of OSCC cell lines with RAD001 inhibitor decreases the phosphorylation and activation of mTOR and increases the RR.	(50, 84)
PNKP (Polynucleotide Kinase 3'-Phosphatase)	Involved in DNA repair *via* the NHEJ pathway	Inhibition of PNKP in prostate adenocarcinoma cancer cell lines using A12B4C3 PNKP inhibitor.	(180)
Pol β	Involved in DNA repair *via* the BER pathway	Human adenocarcinoma cells or MEFs cell lines that grow in conditions of confluence and expressing a dominant negative of Pol β.	(181–183)
Rad51	Involved in DNA repair *via* the HR pathway	Cells treated with chronic hypoxia had a reduced RR. Knocking down Rad51 with siRNA to levels like the levels seen under chronic hypoxia also radiosensitizes human lung cancer cells.	(184)
RPA1	Involved in DNA repair *via* the HR pathway	Targeting RPA1 by shRNAs in radioresistant hypopharyngeal cancer cell.	(64)
SHP1	Cell cycle regulation	Targeting SHP1 by siRNAs in radioresistant NSCLC cells.	(86)
SOCS	Signal transduction	Ectopic expression of SOCS1 in GBM cells. Blocking SOCS3 expression (by expressing a dominant-negative STAT3) in GBM cells.	(185)
TGF-β receptor	Signal transduction	Inhibition of TGF-β receptor in radioresistant gastric cancer cells using LY2109761.	(186)
Topo II α (DNA Topoisomerase II α)	Replication and transcription	Treatment of radioresistant laryngeal squamous cancer cells with 5-aza-2'-deoxycytidine, a DNA methyltransferase inhibitor.	(187)
WISP1	EMT	ESCC KYSE-150R cell line was treated with WISP1-specific neutralizing antibody.	(148)
WntT7	Signal transduction	Overexpression of Wnt7a in NSCLC by pcDNA6-Wnt7a transfection.	(188)

CONCLUDING REMARKS

Cancer is a group of diseases that cause high rates of mortality and morbidity worldwide. For a long time, multiple treatments have been developed to combat different types of cancer. RT is applied in more than 50% of cancer patients due to its various advantages: non-invasive, painless, localized, and with high controllability. Despite its broad effectiveness, some patients show resistance to therapy and tumor recurrence, with negative implications on patients' quality of life and survival.

After radiation, tumor cells can turn on a complex molecular and cellular response to maintain the integrity of their genome and organelles. This response conjugates different signaling pathways, which allow sensing the lesions and activate a DNA damage response. Genes modulated in response to radiation can alter multiple biological events, mainly, a redistribution of the cell cycle, DNA repair pathways activation, reconfiguration (global and local) of chromatin, increase in their metabolic plasticity, changes in the lipid and protein composition of the plasma membrane, the formation of intercellular networks, a cytoprotective response to stress generated in organelles such as ER and mitochondria, apoptosis evasion, EMT, and CSCs generation. Simultaneously, changes in the tumor microenvironment and ECM reorganization can occur, increasing the probability of survival, reproduction, and adaptation to radiation of tumor populations. These events can stimulate the appearance of tumors with more aggressive characteristics that interfere with patients' response to treatments and promote tumor recurrence.

The clinical response of patients to radiation is very heterogeneous; it depends on the type of therapy applied, of the intrinsic heterogeneity between tumor types and subtypes, to the genetic variants present in patients that make them more or less susceptible to RT (189–192). The knowledge generated in recent decades has allowed us to propose different combined and personalized strategies to increase the success of RT. However, the translation of this information to clinical practice requires even more in-depth and comprehensive knowledge. Therefore, it is essential to continue with the molecular studies that allow us to identify the vulnerabilities of radioresistant cells.

AUTHOR CONTRIBUTIONS

ÁC-R, MM-L, SR-G, CL-C, and OH-C organized and wrote the manuscript. MM-L wrote Radiation Therapy in Clinical Practice section. OH, ÁC-R, and MM-L wrote Tumor Cells Activate Signaling Pathways Involved in DNA-Damage Response to Survive Ionizing Radiation section. ÁC-R and CL-C wrote Cell Cycle Adaptations in Response to Radiation. SR-G and OH-C wrote Chromatin Remodeling as a Mechanism of Radiation Adaptation, Changes in the Plasma Membrane That Favor Radioresistance, Endoplasmic Reticulum Adaptations to Radiation, and Mitochondrial Adaptations to Radiation sections. ÁC-R and CL-C wrote Extracellular Adaptations of Tumor Cells to Radiation section. OH-C and MM-L wrote Targeting to Enhance Radiosensitivity section. All authors revised the last version of manuscript. Figures and Tables were designed and produced by ÁC-R, MM-L, SR-G, and OH-C. All authors contributed to the article and approved the submitted version.

ACKNOWLEDGMENTS

The authors thank Instituto Nacional de Enfermedades Respiratorias Ismael Cosió Villegas, Universidad Autónoma Metropolitana Unidad Xochimilco, and Universidad Autónoma de la Ciudad de México.

REFERENCES

1. Halkett G, O'Connor M, Jefford M, Aranda S, Merchant S, Spry N, et al. RT Prepare: A Radiation Therapist-Delivered Intervention Reduces Psychological Distress in Women With Breast Cancer Referred for Radiotherapy. *Br J Cancer* (2018) 118(12):1549–58. doi: 10.1038/s41416-018-0112-z
2. Huang RX, Zhou PK. DNA Damage Response Signaling Pathways and Targets for Radiotherapy Sensitization in Cancer. *Signal Transduct Target Ther* (2020) 5(1):60. doi: 10.1038/s41392-020-0150-x
3. Baskar R, Lee KA, Yeo R, Yeoh KW. Cancer and Radiation Therapy: Current Advances and Future Directions. *Int J Med Sci* (2012) 9(3):193–9. doi: 10.7150/ijms.3635
4. Wang Y, Hou Y, Zhang W, Alvarez AA, Bai Y, Hu B, et al. Lipolytic Inhibitor G0S2 Modulates Glioma Stem-Like Cell Radiation Response. *J Exp Clin Cancer Res* (2019) 38(1):1–13. doi: 10.1186/s13046-019-1151-x
5. Arnold CR, Mangesius J, Skvortsova II, Ganswindt U. The Role of Cancer Stem Cells in Radiation Resistance. *Front Oncol* (2020) 10:164. doi: 10.3389/fonc.2020.00164
6. Barker HE, Paget JTE, Khan AA, Harrington KJ. The Tumour Microenvironment After Radiotherapy: Mechanisms of Resistance and Recurrence. *Nat Rev Cancer* (2015) 15(7):409–25. doi: 10.1038/nrc3958
7. Bian L, Meng Y, Zhang M, Guo Z, Liu F, Zhang W, et al. ATM Expression is Elevated in Established Radiation-Resistant Breast Cancer Cells and Improves DNA Repair Efficiency. *Int J Biol Sci* (2020) 16(7):1096–106. doi: 10.7150/ijbs.41246
8. Dakup PP, Porter KI, Gajula RP, Goel PN, Cheng Z, Gaddameedhi S. The Circadian Clock Protects Against Ionizing Radiation-Induced Cardiotoxicity. *FASEB J* (2020) 34(2):3347–58. doi: 10.1096/fj.201901850RR
9. Kim EH, Park AK, Dong SM, Ahn JH, Park WY. Global Analysis of CpG Methylation Reveals Epigenetic Control of the Radiosensitivity in Lung Cancer Cell Lines. *Oncogene* (2010) 29(33):4725–31. doi: 10.1038/onc.2010.223
10. Leung E, Cairns RA, Chaudary N, Vellanki RN, Kalliomaki T, Moriyama EH, et al. Metabolic Targeting of HIF-Dependent Glycolysis Reduces Lactate, Increases Oxygen Consumption and Enhances Response to High-Dose Single-Fraction Radiotherapy in Hypoxic Solid Tumors. *BMC Cancer* (2017) 17(1):418. doi: 10.1186/s12885-017-3402-6
11. Lin X, Qiu J, Hua K. Long non-Coding RNAs as Emerging Regulators of Epithelial to Mesenchymal Transition in Gynecologic Cancers. *Biosci Trends* (2018) 12(4):342–53. doi: 10.5582/bst.2018.01181
12. Mavragani IV, Nikitaki Z, Kalospyros SA, Georgakilas AG. Ionizing Radiation and Complex DNA Damage: From Prediction to Detection Challenges and Biological Significance. *Cancers* (2019) 11(11):1789. doi: 10.3390/cancers11111789
13. Sun C, Han C, Jiang Y, Han N, Zhang M, Li G, et al. Inhibition of GRP78 Abrogates Radioresistance in Oropharyngeal Carcinoma Cells After EGFR Inhibition by Cetuximab. *PloS One* (2017) 12(12):e0188932. doi: 10.1371/journal.pone.0188932
14. Takata H, Hanafusa T, Mori T, Shimura M, Iida Y, Ishikawa K, et al. Chromatin Compaction Protects Genomic DNA From Radiation Damage. *PloS One* (2013) 8(10):75622. doi: 10.1371/journal.pone.0075622

15. Seibold P, Auvinen A, Averbeck D, Bourguignon M, Hartikainen JM, Hoeschen C, et al. Clinical and Epidemiological Observations on Individual Radiation Sensitivity and Susceptibility. *Int J Radiat Biol* (2020) 96(3):324–39. doi: 10.1080/09553002.2019.1665209
16. Gianfaldoni S, Gianfaldoni R, Wollina U, Lotti J, Tchernev G, Lotti T. An Overview on Radiotherapy: From Its History to Its Current Applications in Dermatology. *Maced J Med Sci* (2017) 5(4):521–5. doi: 10.3889/oamjms.2017.122
17. Abshire D, Lang MK. The Evolution of Radiation Therapy in Treating Cancer. *Semin Oncol Nurs* (2018) 34(2):151–7. doi: 10.1016/j.soncn.2018.03.006
18. Desouky O, Ding N, Zhou G. Targeted and Non-Targeted Effects of Ionizing Radiation. *J Radiat Res Appl Sci* (2015) 8(2):247–54. doi: 10.1016/j.jrras.2015.03.003
19. Hughes JR, Parsons JL. Flash Radiotherapy: Current Knowledge and Future Insights Using Proton-Beam Therapy. *Int J Mol Sci* (2020) 21(18):1–14. doi: 10.3390/ijms21186492
20. Mehta SR, Suhag V, Semwal M, Sharma N. Radiotherapy: Basic Concepts and Recent Advances. *Med J Armed Forces India* (2010) 66(2):158–62. doi: 10.1016/S0377-1237(10)80132-7
21. Citrin DE. Recent Developments in Radiotherapy. *N Engl J Med* (2017) 377 (11):1065–75. doi: 10.1056/NEJMra1608986
22. Chun SG, Hu C, Choy H, Komaki RU, Timmerman RD, Schild SE, et al. Impact of Intensity-Modulated Radiation Therapy Technique for Locally Advanced Non-Small-Cell Lung Cancer: A Secondary Analysis of the NRG Oncology RTOG 0617 Randomized Clinical Trial. *J Clin Oncol* (2017) 35 (1):56–62. doi: 10.1200/JCO.2016.69.1378
23. Tipton K, Sullivan N, Bruening W, Inamdar R, Launders J, Uhl S, et al. Stereotactic Body Radiation Therapy. *J Am Coll Radiol* (2005) 2(8):676–80. doi: 10.1016/j.jacr.2005.01.002
24. Brand D, Tree A, Ostler P, van der Voet H, Loblaw A, Chu W, et al. Intensity-Modulated Fractionated Radiotherapy Versus Stereotactic Body Radiotherapy for Prostate Cancer (PACE-B): Acute Toxicity Findings From an International, Randomised, Open-Label, Phase 3, Non-Inferiority Trial. *Lancet Oncol* (2019) 20(11):1531–43. doi: 10.1016/S1470-2045(19)30569-8
25. Tiong SS, Dickie C, Haas RL, O'Sullivan B. The Role of Radiotherapy in the Management of Localized Soft Tissue Sarcomas. *Cancer Biol Med* (2016) 13 (3):373–83. doi: 10.20892/j.issn.2095-3941.2016.0028
26. Tran A, Zhang J, Woods K, Yu V, Nguyen D, Gustafson G, et al. Treatment Planning Comparison of IMPT, VMAT and 4π Radiotherapy for Prostate Cases. *Radiat Oncol* (2017) 12(1):10. doi: 10.1186/s13014-016-0761-0
27. Zhang H, Yue J, Jiang Z, Zhou R, Xie R, Xu Y, et al. CAF-Secreted CXCL1 Conferred Radioresistance by Regulating DNA Damage Response in a ROS-Dependent Manner in Esophageal Squamous Cell Carcinoma. *Cell Death Dis* (2017) 8(5):e2790. doi: 10.1038/cddis.2017.180
28. Sanda C, Sarafoleanu C. Advantages of VMAT-IMRT Technique in Nasopharyngeal Cancer. *Rom J Rhinol* (2016) 6(22):101–8. doi: 10.1515/rjr-2016-0012
29. Kunogi H, Hsu IC, Yamaguchi N, Kusunoki S, Nakagawa K, Sugimori Y, et al. CT-Guided Pelvic Lymph Nodal Brachytherapy. *Front Oncol* (2021) 10:532555. doi: 10.3389/fonc.2020.532555
30. Bretschneider T, Mohnike K, Hass P, Seidensticker R, Göppner D, Dudeck O, et al. Efficacy and Safety of Image-Guided Interstitial Single Fraction High-Dose-Rate Brachytherapy in the Management of Metastatic Malignant Melanoma. *J Contemp Brachytherapy* (2015) 7(2):154–60. doi: 10.5114/jcb.2015.51095
31. Kusada T, Toita T, Ariga T, Kudaka W, Maemoto H, Makino W, et al. Definitive Radiotherapy Consisting of Whole Pelvic Radiotherapy With No Central Shielding and CT-Based Intracavitary Brachytherapy for Cervical Cancer: Feasibility, Toxicity, and Oncologic Outcomes in Japanese Patients. *Int J Clin Oncol* (2020) 25(11):1977–84. doi: 10.1007/s10147-020-01736-4
32. Dieterich S, Ford E, Pavord D. Intracavitary Brachytherapy. *Pract Radiat Oncol Phys* (2016) 20(1):264–76. doi: 10.1016/B978-0-323-26209-5.00020-1
33. Autorino R, Bisiello S, Pappalardi B, Privitera V, Buwenge M, Piccolo F, et al. Intraluminal Brachytherapy in Unresectable Extrahepatic Biliary Duct Cancer: An Italian Pooled Analysis. *Anticancer Res* (2020) 40(6):3417–21. doi: 10.21873/anticanres.14326
34. Chigurupalli K, Vashistha A. Role of Intraluminal Brachytherapy as a Palliative Treatment Modality in Unresectable Cholangiocarcinomas. *J Cancer Res Ther* (2021) 17(1):10–2. doi: 10.4103/jcrt.JCRT_836_19
35. Facciorusso A, Bargellini I, Cela M, Cincione I, Sacco R. Comparison Between Y90 Radioembolization Plus Sorafenib and Y90 Radioembolization Alone in the Treatment of Hepatocellular Carcinoma: A Propensity Score Analysis. *Cancers* (2020) 12(4):897. doi: 10.3390/cancers12040897
36. Lippert TH, Ruoff HJ, Volm M. Intrinsic and Acquired Drug Resistance in Malignant Tumors: The Main Reason for Therapeutic Failure. *Arzneimittelforschung* (2008) 58(6):261–4. doi: 10.1055/s-0031-1296504
37. Alfonso JCL, Berk L. Modeling the Effect of Intratumoral Heterogeneity of Radiosensitivity on Tumor Response Over the Course of Fractionated Radiation Therapy. *Radiat Oncol* (2019) 14(1):88. doi: 10.1186/s13014-019-1288-y
38. Frame FM, Noble AR, Klein S, Walker HF, Suman R, Kasprowicz R, et al. Tumor Heterogeneity and Therapy Resistance - Implications for Future Treatments of Prostate Cancer. *J Cancer Metastasis Treat* (2017) 3(12):302. doi: 10.20517/2394-4722.2017.34
39. Campos A, Clemente-Blanco A. Cell Cycle and DNA Repair Regulation in the Damage Response: Protein Phosphatases Take Over the Reins. *Int J Mol Sci* (2020) 21(2):446. doi: 10.3390/ijms21020446
40. Hosoya N, Miyagawa K. Targeting DNA Damage Response in Cancer Therapy. *Cancer Sci* (2014) 105(4):370–88. doi: 10.1111/cas.12366
41. Santivasi WL, Xia F. Ionizing Radiation-Induced DNA Damage, Response, and Repair. *Antioxid Redox Signal* (2014) 21(2):251–9. doi: 10.1089/ars.2013.5668
42. Biau J, Chautard E, Verrelle P, Dutreix M. Altering DNA Repair to Improve Radiation Therapy: Specific and Multiple Pathway Targeting. *Front Oncol* (2019) 9:1009(SEP). doi: 10.3389/fonc.2019.01009
43. Nickson CM, Moori P, Carter RJ, Rubbi CP, Parsons JL. Misregulation of DNA Damage Repair Pathways in HPV-Positive Head and Neck Squamous Cell Carcinoma Contributes to Cellular Radiosensitivity. *Oncotarget* (2017) 8(18):29963–75. doi: 10.18632/oncotarget.16265
44. Wallace SS. Base Excision Repair: A Critical Player in Many Games. *DNA Repair* (2014) 19:14–26. doi: 10.1016/j.dnarep.2014.03.030
45. Vadnais C, Davoudi S, Afshin M, Harada R, Dudley R, Clermont PL, et al. CUX1 Transcription Factor is Required for Optimal ATM/ATR-Mediated Responses to DNA Damage. *Nucleic Acids Res* (2012) 40(10):4483–95. doi: 10.1093/nar/gks041
46. Ramdzan ZM, Ginjala V, Pinder JB, Chung D, Donovan CM, Kaur S, et al. The DNA Repair Function of CUX1 Contributes to Radioresistance. *Oncotarget* (2017) 8(12):19021–38. doi: 10.18632/oncotarget.14875
47. Naidu MD, Agarwal R, Pena LA, Cunha L, Mezei M, Shen M, et al. Lucanthone and its Derivative Hycanthone Inhibit Apurinic Endonuclease-1 (APE1) by Direct Protein Binding. *PloS One* (2011) 6(9): e23679. doi: 10.1371/journal.pone.0023679
48. Li Q, Wei X, Zhou ZW, Wang SN, Jin H, Chen KJ, et al. GADD45α Sensitizes Cervical Cancer Cells to Radiotherapy *via* Increasing Cytoplasmic APE1 Level Article. *Cell Death Dis* (2018) 9(5):524. doi: 10.1038/s41419-018-0452-x
49. Setton J, Bindra S, Powell S. DNA Double-Strand Repair by Nonhomologous End Joining and its Clinical Relevance. *DNA Repair Cancer Ther* (2016) 277–302. doi: 10.1016/B978-0-12-803582-5.00009-7
50. Chang L, Graham PH, Hao J, Ni J, Bucci J, Cozzi PJ, et al. PI3K/Akt/mTOR Pathway Inhibitors Enhance Radiosensitivity in Radioresistant Prostate Cancer Cells Through Inducing Apoptosis, Reducing Autophagy, Suppressing NHEJ and HR Repair Pathways. *Cell Death Dis* (2014) 5 (10):4–10. doi: 10.1038/cddis.2014.415
51. Beskow C, Skikuniene J, Holgersson A, Nilsson B, Lewensohn R, Kanter L, et al. Radioresistant Cervical Cancer Shows Upregulation of the NHEJ Proteins DNA-PKcs, Ku70 and Ku86. *Br J Cancer* (2009) 101(5):816–21. doi: 10.1038/sj.bjc.6605201
52. Harima Y, Sawada S, Miyazaki Y, Kin K, Ishihara H, Imamura M, et al. Expression of Ku80 in Cervical Cancer Correlates With Response to Radiotherapy and Survival. *Am J Clin Oncol* (2003) 26(4):e80–5. doi: 10.1097/01.COC.0000077938.48974.59
53. Hayashi J, Sakata KI, Someya M, Matsumoto Y, Satoh M, Nakata K, et al. Analysis and Results of Ku and XRCC4 Expression in Hypopharyngeal Cancer Tissues Treated With Chemoradiotherapy. *Oncol Lett* (2012) 4 (1):151–5. doi: 10.3892/ol.2012.674

54. Zhou W, Zhang L, Chen P, Li S, Cheng Y. Thymine DNA Glycosylase-Regulated TAZ Promotes Radioresistance by Targeting Nonhomologous End Joining and Tumor Progression in Esophageal Cancer. *Cancer Sci* (2020) 111(10):3613–25. doi: 10.1111/cas.14622
55. Jun S, Jung YS, Suh HN, Wang W, Kim MJ, Oh YS, et al. LIG4 Mediates Wnt Signalling-Induced Radioresistance. *Nat Commun* (2016) 7:1–13. doi: 10.1038/ncomms10994
56. Lee SL, Ryu H, Son AR, Seo B, Kim J, Jung SY, et al. TGF-β and Hypoxia/Reoxygenation Promote Radioresistance of A549 Lung Cancer Cells Through Activation of Nrf2 and EGFR. *Oxid Med Cell Longev* (2016) 2016:6823471. doi: 10.1155/2016/6823471
57. Acharyya S, Oskarsson T, Vanharanta S, Malladi S, Kim J, Morris PG, et al. A CXCL1 Paracrine Network Links Cancer Chemoresistance and Metastasis. *Cell* (2012) 150(1):165–78. doi: 10.1016/j.cell.2012.04.042
58. Alafate W, Li X, Zuo J, Zhang H, Xiang J, Wu W, et al. Elevation of CXCL1 Indicates Poor Prognosis and Radioresistance by Inducing Mesenchymal Transition in Glioblastoma. *CNS Neurosci Ther* (2020) 26(4):475–85. doi: 10.1111/cns.13297
59. Wright WD, Shah SS, Heyer WD. Homologous Recombination and the Repair of DNA Double-Strand Breaks. *J Biol Chem* (2018) 293(27):10524–35. doi: 10.1074/jbc.TM118.000372
60. Li X, Heyer WD. Homologous Recombination in DNA Repair and DNA Damage Tolerance. *Cell Res* (2008) 18(1):99–113. doi: 10.1038/cr.2008.1
61. Heyer WD, Ehmsen KT, Liu J. Regulation of Homologous Recombination in Eukaryotes. *Annu Rev Genet* (2010) 44:113–39. doi: 10.1146/annurev-genet-051710-150955
62. Velegzhaninov IO, Belykh ES, Rasova EE, Pylina YI, Shadrin DM, Klokov DY. Radioresistance, DNA Damage and DNA Repair in Cells With Moderate Overexpression of RPA1. *Front Genet* (2020) 11:855. doi: 10.3389/fgene.2020.00855
63. Piotrowski I, Kulcenty K, Murawa D, Suchorska W. Surgical Wound Fluids From Patients Treated With Intraoperative Radiotherapy Induce Radiobiological Response in Breast Cancer Cells. *Med Oncol* (2019) 36 (2):14. doi: 10.1007/s12032-018-1243-z
64. Liu C, Liao K, Gross N, Wang Z, Li G, Zuo W, et al. Homologous Recombination Enhances Radioresistance in Hypopharyngeal Cancer Cell Line by Targeting DNA Damage Response. *Oral Oncol* (2020) 100:104469. doi: 10.1016/j.oraloncology.2019.104469
65. Wang Z, Zuo W, Zeng Q, Li Y, Lu T, Bu Y, et al. The Homologous Recombination Repair Pathway is Associated With Resistance to Radiotherapy in Nasopharyngeal Carcinoma. *Int J Biol Sci* (2020) 16 (3):408–19. doi: 10.7150/ijbs.37302
66. Chang L, Huang J, Wang K, Li J, Yan R, Zhu L, et al. Targeting Rad50 Sensitizes Human Nasopharyngeal Carcinoma Cells to Radiotherapy. *BMC Cancer* (2016) 16(1):190. doi: 10.1186/s12885-016-2190-8
67. Lin JC, Tsai JT, Chao TY, Ma HI, Chien CS, Liu WH. MSI1 Associates Glioblastoma Radioresistance *via* Homologous Recombination Repair, Tumor Invasion and Cancer Stem-Like Cell Properties. *Radiother Oncol* (2018) 129(2):352–63. doi: 10.1016/j.radonc.2018.09.014
68. Nicolay NH, Carter R, Hatch SB, Schultz N, Prevo R, Mckenna WG, et al. Homologous Recombination Mediates S-Phase-Dependent Radioresistance in Cells Deficient in DNA Polymerase Eta. *Carcinogenesis* (2012) 33 (11):2026–34. doi: 10.1093/carcin/bgs239
69. Ingram SP, Warmenhoven JW, Henthorn NT, Smith EAK, Chadwick AL, Burnet NG, et al. Mechanistic Modelling Supports Entwined Rather Than Exclusively Competitive DNA Double-Strand Break Repair Pathway. *Sci Rep* (2019) 9(1):1–13. doi: 10.1038/s41598-019-42901-8
70. Kurosawa A, Kuboshima H, Adachi N. Complex Genetic Interactions Between DNA Polymerase β and the NHEJ Ligase. *FEBS J* (2020) 287 (2):377–85. doi: 10.1111/febs.15012
71. Kwon SJ, Lee SK, Na J, Lee SA, Lee HS, Park JH, et al. Targeting BRG1 Chromatin Remodeler *via* Its Bromodomain for Enhanced Tumor Cell Radiosensitivity *In Vitro* and *In Vivo*. *Mol Cancer Ther* (2015) 14(2):597–607. doi: 10.1158/1535-7163.MCT-14-0372
72. Squatrito M, Brennan CW, Helmy K, Huse JT, Petrini JH, Holland EC. Loss of ATM/Chk2/p53 Pathway Components Accelerates Tumor Development and Contributes to Radiation Resistance in Gliomas. *Cancer Cell* (2010) 18 (6):619–29. doi: 10.1016/j.ccr.2010.10.034
73. Lin J, Song T, Li C, Mao W. GSK-3β in DNA Repair, Apoptosis, and Resistance of Chemotherapy, Radiotherapy of Cancer. Biochimica Et Biophysica Acta. *Mol Cell Res* (2020) 1867(5):118659. doi: 10.1016/j.bbamcr.2020.118659
74. Zhao Y, Tao L, Yi J, Song H, Chen L. The Role of Canonical Wnt Signaling in Regulating Radioresistance. *Cell Physiol Biochem* (2018) 48(2):419–32. doi: 10.1159/000491774
75. Ansari D, Ohlsson H, Althini C, Bauden M, Zhou Q, Hu D, et al. The Hippo Signaling Pathway in Pancreatic Cancer. *Anticancer Res* (2019) 39(7):3317–21. doi: 10.21873/anticanres.13474
76. Misra JR, Irvine KD. The Hippo Signaling Network and Its Biological Functions. *Annu Rev Genet* (2018) 52:65–87. doi: 10.1146/annurev-genet-120417-031621
77. Xu X, Chen Y, Wang X, Mu X. Role of Hippo/Yap Signaling in Irradiation-Induced Glioma Cell Apoptosis. *Cancer Manag Res* (2019) 11:7577–85. doi: 10.2147/CMAR.S210825
78. Fernandez-L A, Squatrito M, Northcott P, Awan A, Holland EC, Taylor MD, et al. Oncogenic YAP Promotes Radioresistance and Genomic Instability in Medulloblastoma Through IGF2-Mediated Akt Activation. *Oncogene* (2012) 31(15):1923–37. doi: 10.1038/onc.2011.379
79. Giles KA, Gould CM, Achinger-Kawecka J, Page SG, Kafer GR, Rogers S, et al. BRG1 Knockdown Inhibits Proliferation Through Multiple Cellular Pathways in Prostate Cancer. *Clin Epigenet* (2021) 13(1):37. doi: 10.1186/s13148-021-01023-7
80. Fujisawa T, Filippakopoulos P. Functions of Bromodomain-Containing Proteins and Their Roles in Homeostasis and Cancer. *Nat Rev Mol Cell Biol* (2017) 18(4):246–62. doi: 10.1038/nrm.2016.143
81. Pérez-Salvia M, Esteller M. Bromodomain Inhibitors and Cancer Therapy: From Structures to Applications. *Epigenetics* (2017) 12(5):323–39. doi: 10.1080/15592294.2016.1265710
82. Barnum KJ, O'Connell MJ. Cell Cycle Regulation by Checkpoints. *Methods Mol Biol* (2014) 1170:29–40. doi: 10.1007/978-1-4939-0888-2_2
83. Zhao H, Zhuang Y, Li R, Liu Y, Mei Z, He Z, et al. Effects of Different Doses of X-Ray Irradiation on Cell Apoptosis, Cell Cycle, DNA Damage Repair and Glycolysis in HeLa Cells. *Oncol Lett* (2019) 17(1):42–54. doi: 10.3892/ol.2018.9566
84. Yu CC, Hung SK, Liao HF, Lee CC, Lin HY, Lai HC, et al. RAD001 Enhances the Radiosensitivity of SCC4 Oral Cancer Cells by Inducing Cell Cycle Arrest at the G2/M Checkpoint. *Anticancer Res* (2014) 34(6):2927–36.
85. Varone A, Spano D, Corda D. Shp1 in Solid Cancers and Their Therapy. *Front Oncol* (2020) 10:935. doi: 10.3389/fonc.2020.00935
86. Cao R, Ding Q, Li P, Xue J, Zou Z, Huang J, et al. SHP1-Mediated Cell Cycle Redistribution Inhibits Radiosensitivity of Non-Small Cell Lung Cancer. *Radiat Oncol* (2013) 8(1):178. doi: 10.1186/1748-717X-8-178
87. Suetens A, Konings K, Moreels M, Quintens R, Verslegers M, Soors E, et al. Higher Initial DNA Damage and Persistent Cell Cycle Arrest After Carbon Ion Irradiation Compared to X-Irradiation in Prostate and Colon Cancer Cells. *Front Oncol* (2016) 6:87(APR). doi: 10.3389/fonc.2016.00087
88. Ruiz-Velasco M, Zaugg JB. Structure Meets Function: How Chromatin Organization Conveys Functionality. *Curr Opin Syst Biol* (2017) 1:129–36. doi: 10.1016/j.coisb.2017.01.003
89. Gordon DJ, Milner AE, Beaney RP, Grdina DJ, Vaughan AT. Cellular Radiosensitivity in V79 Cells is Linked to Alterations in Chromatin Structure. *Int J Radiat Oncol Biol Phys* (1990) 19(5):1199–201. doi: 10.1016/0360-3016(90)90228-c
90. Woudstra EC, Roesink JM, Rosemann M, Brunsting JF, Driessen C, Orta T, et al. Chromatin Structure and Cellular Radiosensitivity: A Comparison of Two Human Tumour Cell Lines. *Int J Radiat Biol* (1996) 70(6):693–703. doi: 10.1080/095530096144581
91. Chen T, Zhang Y, Guo WH, Meng MB, Mo XM, Lu Y. Effects of Heterochromatin in Colorectal Cancer Stem Cells on Radiosensitivity. *Chin J Cancer* (2010) 29(3):270–6. doi: 10.5732/cjc.009.10694
92. Storch K, Eke I, Borgmann K, Krause M, Richter C, Becker K, et al. Three-Dimensional Cell Growth Confers Radioresistance by Chromatin Density Modification. *Cancer Res* (2010) 70(10):3925–34. doi: 10.1158/0008-5472.CAN-09-3848
93. Sato K, Imai T, Okayasu R, Shimokawa T. Heterochromatin Domain Number Correlates With X-Ray and Carbon-Ion Radiation Resistance in Cancer Cells. *Radiat Res* (2014) 182(4):408–19. doi: 10.1667/RR13492.1

94. Mund A, Schubert T, Staege H, Kinkley S, Reumann K, Kriegs M, et al. SPOC1 Modulates DNA Repair by Regulating Key Determinants of Chromatin Compaction and DNA Damage Response. *Nucleic Acids Res* (2012) 40(22):11363–79. doi: 10.1093/nar/gks868
95. Wang M, Kern AM, Hülskötter M, Greninger P, Singh A, Pan Y, et al. EGFR-Mediated Chromatin Condensation Protects Kras-Mutant Cancer Cells Against Ionizing Radiation. *Cancer Res* (2014) 74(10):2825–34. doi: 10.1158/0008-5472.CAN-13-3157
96. Wang M, Morsbach F, Sander D, Gheorghiu L, Nanda A, Benes C, et al. EGF Receptor Inhibition Radiosensitizes NSCLC Cells by Inducing Senescence in Cells Sustaining DNA Double-Strand Breaks. *Cancer Res* (2011) 71 (19):6261–9. doi: 10.1158/0008-5472.CAN-11-0213
97. Levin-Zaidman S, Englander J, Shimoni E, Sharma AK, Minton KW, Minsky A. Ringlike Structure of the Deinococcus Radiodurans Genome: A Key to Radioresistance? *Science* (2003) 299(5604):254–6. doi: 10.1126/science.1077865
98. Odell ID, Wallace SS, Pederson DS. Rules of Engagement for Base Excision Repair in Chromatin. *J Cell Physiol* (2013) 228(2):258–66. doi: 10.1002/jcp.24134
99. Trotter KW, Archer TK. The BRG1 Transcriptional Coregulator. *Nucl Recept Signaling* (2008) 6:e004. doi: 10.1621/nrs.06004
100. Andrade D, Mehta M, Griffith J, Oh S, Corbin J, Babu A, et al. Hur Reduces Radiation-Induced DNA Damage by Enhancing Expression of ARID1A. *Cancers* (2019) 11(12):2014. doi: 10.3390/cancers11122014
101. Billberg J, Frandsen SK, Gehl J, Mahmood F. The Effect of Concurrent Radiation and Calcium in Two Cancer Cell Lines. *Phys Med* (2016) 32 (3):269. doi: 10.1016/j.ejmp.2016.07.587
102. Osswald M, Jung E, Sahm F, Solecki G, Venkataramani V, Blaes J, et al. Brain Tumour Cells Interconnect to a Functional and Resistant Network. *Nature* (2015) 528(7580):93–8. doi: 10.1038/nature16071
103. Jung E, Osswald M, Blaes J, Wiestler B, Sahm F, Schmenger T, et al. Tweety-Homolog 1 Drives Brain Colonization of Gliomas. *J Neurosci* (2017) 37 (29):6837–50. doi: 10.1523/JNEUROSCI.3532-16.2017
104. Chignola R, Sega M, Molesini B, Baruzzi A, Stella S, Milotti E. Collective Radioresistance of T47D Breast Carcinoma Cells is Mediated by a Syncytin-1 Homologous Protein. *PloS One* (2019) 14(1):e0206713. doi: 10.1371/journal.pone.0206713
105. Kawamoto A, Yokoe T, Tanaka K, Saigusa S, Toiyama Y, Yasuda H, et al. Radiation Induces Epithelial-Mesenchymal Transition in Colorectal Cancer Cells. *Oncol Rep* (2012) 27(1):51–7. doi: 10.3892/or.2011.148
106. Corre I, Guillonneau M, Paris F. Membrane Signaling Induced by High Doses of Ionizing Radiation in the Endothelial Compartment. Relevance in Radiation Toxicity. *Int J Mol Sci* (2013) 14(11):22678–96. doi: 10.3390/ijms141122678
107. Silva LC, Futerman AH, Prieto M. Lipid Raft Composition Modulates Sphingomyelinase Activity and Ceramide-Induced Membrane Physical Alterations. *Biophys J* (2009) 96(8):3210–22. doi: 10.1016/j.bpj.2008.12.3923
108. Ketteler J, Wittka A, Leonetti D, Roy VV, Estephan H, Maier P, et al. Caveolin-1 Regulates the ASMase/ceramide-Mediated Radiation Response of Endothelial Cells in the Context of Tumor–Stroma Interactions. *Cell Death Dis* (2020) 11(4):228. doi: 10.1038/s41419-020-2418-z
109. Needham PG, Guerriero CJ, Brodsky JL. Chaperoning Endoplasmic Reticulum-Associated Degradation (ERAD) and Protein Conformational Diseases. *Cold Spring Harb Perspect Biol* (2019) 11(8):a033928. doi: 10.1101/cshperspect.a033928
110. Qiao Q, Sun C, Han C, Han N, Zhang M, Li G. Endoplasmic Reticulum Stress Pathway PERK-eIF2α Confers Radioresistance in Oropharyngeal Carcinoma by Activating NF-κB. *Cancer Sci* (2017) 108(7):1421–31. doi: 10.1111/cas.13260
111. Qiao Q, Nozaki Y, Sakoe K, Komatsu N, Kirito K. NF-κB Mediates Aberrant Activation of HIF-1 in Malignant Lymphoma. *Exp Hematol* (2010) 38 (12):1199–208. doi: 10.1016/j.exphem.2010.08.007
112. Lyu X, Zhang M, Li G, Cai Y, Li G, Qiao Q. Interleukin-6 Production Mediated by the IRE1-XBP1 Pathway Confers Radioresistance in Human Papillomavirus-Negative Oropharyngeal Carcinoma. *Cancer Sci* (2019) 110 (8):2471–84. doi: 10.1111/cas.14094
113. Zhang M, Han N, Jiang Y, Wang J, Li G, Lv X, et al. EGFR Confers Radioresistance in Human Oropharyngeal Carcinoma by Activating Endoplasmic Reticulum Stress Signaling PERK-eIF2α-GRP94 and IRE1α-XBP1-GRP78. *Cancer Med* (2018) 7(12):6234–46. doi: 10.1002/cam4.1862
114. Ayob AZ, Ramasamy TS. Cancer Stem Cells as Key Drivers of Tumour Progression. *J Biomed Sci* (2018) 25(1):20. doi: 10.1186/s12929-018-0426-4
115. Skvortsova I, Debbage P, Kumar V, Skvortsov S. Radiation Resistance: Cancer Stem Cells (CSCs) and Their Enigmatic Pro-Survival Signaling. *Semin Cancer Biol* (2015) 35:39–44. doi: 10.1016/j.semcancer.2015.09.009
116. Shah SS, Rodriguez GA, Musick A, Walters WM, de Cordoba N, Barbarite E, et al. Targeting Glioblastoma Stem Cells With 2-Deoxy-D-Glucose (2-DG) Potentiates Radiation-Induced Unfolded Protein Response (UPR). *Cancers* (2019) 11(2):159. doi: 10.3390/cancers11020159
117. Sørensen BS, Horsman MR. Tumor Hypoxia: Impact on Radiation Therapy and Molecular Pathways. *Front Oncol* (2020) 10:562. doi: 10.3389/fonc.2020.00562
118. Rouschop KM, Dubois LJ, Keulers TG, Van Den Beucken T, Lambin P, Bussink J, et al. PERK/eIF2α Signaling Protects Therapy Resistant Hypoxic Cells Through Induction of Glutathione Synthesis and Protection Against ROS. *Proc Natl Acad Sci U S A* (2013) 110(12):4622–7. doi: 10.1073/pnas.1210633110
119. Isohashi F, Endo H, Mukai M, Inoue T, Inoue M. Insulin-Like Growth Factor Stimulation Increases Radiosensitivity of a Pancreatic Cancer Cell Line Through Endoplasmic Reticulum Stress Under Hypoxic Conditions. *Cancer Sci* (2008) 99(12):2395–401. doi: 10.1111/j.1349-7006.2008.00970.x
120. Choi T, Kim S. Physiological Functions of Mitochondrial Reactive Oxygen Species in Free Radical Medicine and Biology. *IntechOpen* (2019) 1–24. doi: 10.5772/intechopen.88386
121. Lebeau J, Saunders JM, Moraes VWR, Madhavan A, Madrazo N, Anthony MC, et al. The PERK Arm of the Unfolded Protein Response Regulates Mitochondrial Morphology During Acute Endoplasmic Reticulum Stress. *Cell Rep* (2018) 22(11):2827–36. doi: 10.1016/j.celrep.2018.02.055
122. Lynam-Lennon N, Maher SG, Maguire A, Phelan J, Muldoon C, Reynolds JV, et al. Altered Mitochondrial Function and Energy Metabolism is Associated With a Radioresistant Phenotype in Oesophageal Adenocarcinoma. *PloS One* (2014) 9(6):100738. doi: 10.1371/journal.pone.0100738
123. Grasso D, Medeiros HCD, Zampieri LX, Bol V, Danhier P, van Gisbergen MW, et al. Fitter Mitochondria Are Associated With Radioresistance in Human Head and Neck SQD9 Cancer Cells. *Front Pharmacol* (2020) 11:263. doi: 10.3389/fphar.2020.00263
124. Montenegro MF, González-Guerrero R, Sánchez-del-Campo L, Piñero-Madrona A, Cabezas-Herrera J, Rodríguez-López JN. PRMT1-Dependent Methylation of BRCA1 Contributes to the Epigenetic Defense of Breast Cancer Cells Against Ionizing Radiation. *Sci Rep* (2020) 10(1):13275. doi: 10.1038/s41598-020-70289-3
125. Al Tameemi W, Dale TP, Al-Jumaily R, Forsyth NR. Hypoxia-Modified Cancer Cell Metabolism. *Front Cell Dev Biol* (2019) 7:4(4). doi: 10.3389/fcell.2019.00004
126. Epperly MW, Melendez JA, Zhang X, Nie S, Pearce L, Peterson J, et al. Mitochondrial Targeting of a Catalase Transgene Product by Plasmid Liposomes Increases Radioresistance *In Vitro* and *In Vivo*. *Radiat Res* (2009) 171(5):588–95. doi: 10.1667/RR1424.1
127. Khodarev NN, Roizman B, Weichselbaum RR. Molecular Pathways: Interferon/Stat1 Pathway: Role in the Tumor Resistance to Genotoxic Stress and Aggressive Growth. *Clin Cancer Res* (2012) 18(11):3015–21. doi: 10.1158/1078-0432.CCR-11-3225
128. Pitroda SP, Wakim BT, Sood RF, Beveridge MG, Beckett MA, MacDermed DM, et al. STAT1-Dependent Expression of Energy Metabolic Pathways Links Tumour Growth and Radioresistance to the Warburg Effect. *BMC Med* (2009) 5(7):68. doi: 10.1186/1741-7015-7-68
129. McCommis KS, Finck BN. Mitochondrial Pyruvate Transport: A Historical Perspective and Future Research Directions. *Biochem J* (2015) 466(3):443–54. doi: 10.1042/BJ20141171
130. Takaoka Y, Konno M, Koseki J, Colvin H, Asai A, Tamari K, et al. Mitochondrial Pyruvate Carrier 1 Expression Controls Cancer Epithelial-Mesenchymal Transition and Radioresistance. *Cancer Sci* (2019) 110 (4):1331–9. doi: 10.1111/cas.13980
131. Halestrap AP. What is the Mitochondrial Permeability Transition Pore? *J Mol Cell Cardiol* (2009) 46(6):821–31. doi: 10.1016/j.yjmcc.2009.02.021

132. Zhang SB, Maguire D, Zhang M, Tian Y, Yang S, Zhang A, et al. Mitochondrial DNA and Functional Investigations Into the Radiosensitivity of Four Mouse Strains. *Int J Cell Biol* (2014) 2014:850460. doi: 10.1155/2014/850460
133. Guan Y, Wang Y, Li B, Shen K, Li Q, Ni Y, et al. Mitophagy in Carcinogenesis, Drug Resistance and Anticancer Therapeutics. *Cancer Cell Int* (2021) 21(1):350. doi: 10.1186/s12935-021-02065-w
134. Zheng R, Yao Q, Xie G, Du S, Ren C, Wang Y, et al. TAT-ODD-P53 Enhances the Radiosensitivity of Hypoxic Breast Cancer Cells by Inhibiting Parkin-Mediated Mitophagy. *Oncotarget* (2015) 6(19):17417–29. doi: 10.18632/oncotarget.4002
135. Baek JH, Lee J, Yun HS, Lee CW, Song JY, Um HD, et al. Kinesin Light Chain-4 Depletion Induces Apoptosis of Radioresistant Cancer Cells by Mitochondrial Dysfunction *via* Calcium Ion Influx Article. *Cell Death Dis* (2018) 9(5):496. doi: 10.1038/s41419-018-0549-2
136. Holley AK, Bakthavatchalu V, Velez-Roman JM, St Clair DK. Manganese Superoxide Dismutase: Guardian of the Powerhouse. *Int J Mol Sci* (2011) 12 (10):7114–62. doi: 10.3390/ijms12107114
137. Miar A, Hevia D, Muñoz-Cimadevilla H, Astudillo A, Velasco J, Sainz RM, et al. Manganese Superoxide Dismutase (SOD2/MnSOD)/catalase and SOD2/GPx1 Ratios as Biomarkers for Tumor Progression and Metastasis in Prostate, Colon, and Lung Cancer. *Free Radical Biol Med* (2015) 85:45–55. doi: 10.1016/j.freeradbiomed.2015.04.001
138. Fisher CJ, Goswami PC. Mitochondria-Targeted Antioxidant Enzyme Activity Regulates Radioresistance in Human Pancreatic Cancer Cells. *Cancer Biol Ther* (2008) 7(8):1271–9. doi: 10.4161/cbt.7.8.6300
139. Zorova LD, Popkov VA, Plotnikov EY, Silachev DN, Pevzner IB, Jankauskas SS, et al. Mitochondrial Membrane Potential. *Anal Biochem* (2018) 552:50–9. doi: 10.1016/j.ab.2017.07.009
140. Tamari Y, Kashino G, Mori H. Acquisition of Radioresistance by IL-6 Treatment Is Caused by Suppression of Oxidative Stress Derived From Mitochondria After γ-Irradiation. *J Radiat Res* (2017) 58(4):412–20. doi: 10.1093/jrr/rrw084
141. Liu R, Fan M, Candas D, Qin L, Zhang X, Eldridge A, et al. CDK1-Mediated SIRT3 Activation Enhances Mitochondrial Function and Tumor Radioresistance. *Mol Cancer Ther* (2015) 14(9):2090–102. doi: 10.1158/1535-7163.MCT-15-0017
142. Jin MZ, Jin WL. The Updated Landscape of Tumor Microenvironment and Drug Repurposing. *Signal Transduct Target Ther* (2020) 5(1):166. doi: 10.1038/s41392-020-00280-x
143. Arneth B. Tumor Microenvironment. *Medicina (Kaunas Lithuania)* (2020) 56(1):15. doi: 10.3390/medicina56010015
144. Ackerman D, Simon MC. Hypoxia, Lipids, and Cancer: Surviving the Harsh Tumor Microenvironment. *Trends Cell Biol* (2014) 24(8):472–8. doi: 10.1016/j.tcb.2014.06.001
145. Hui L, Chen Y. Tumor Microenvironment: Sanctuary of the Devil. *Cancer Lett* (2015) 368(1):7–13. doi: 10.1016/j.canlet.2015.07.039
146. Ribeiro Franco PI, Rodrigues AP, de Menezes LB, Pacheco Miguel M. Tumor Microenvironment Components: Allies of Cancer Progression. *Pathol Res Pract* (2020) 216(1):152729. doi: 10.1016/j.prp.2019.152729
147. Ribatti D, Tamma R, Annese T. Epithelial-Mesenchymal Transition in Cancer: A Historical Overview. *Trans Oncol* (2020) 13(6):100773. doi: 10.1016/j.tranon.2020.100773
148. Zhang H, Luo H, Jiang Z, Yue J, Hou Q, Xie R, et al. Fractionated Irradiation-Induced EMT-Like Phenotype Conferred Radioresistance in Esophageal Squamous Cell Carcinoma. *J Radiat Res* (2016) 57(4):370–80. doi: 10.1093/jrr/rrw030
149. Yue B. Biology of the Extracellular Matrix: An Overview. *J Glaucoma* (2014) 23(8 Suppl 1):S20–3. doi: 10.1097/IJG.0000000000000108
150. Winkler J, Abisoye-Ogunniyan A, Metcalf KJ, Werb Z. Concepts of Extracellular Matrix Remodelling in Tumour Progression and Metastasis. *Nat Commun* (2020) 11(1):5120. doi: 10.1038/s41467-020-18794-x
151. Babel L, Grunewald M, Lehn R, Langhans M, Meckel T. Direct Evidence for Cell Adhesion-Mediated Radioresistance (CAM-RR) on the Level of Individual Integrin β1 Clusters. *Sci Rep* (2017) 7(1):1–13. doi: 10.1038/s41598-017-03414-4
152. Cordes N, Blaese MA, Meineke V, Van Beuningen D. Ionizing Radiation Induces Up-Regulation of Functional β1-Integrin in Human Lung Tumour Cell Lines *In Vitro*. *Int J Radiat Biol* (2002) 78(5):347–57. doi: 10.1080/09553000110117340
153. Cordes N, Meineke V. Cell Adhesion-Mediated Radioresistance (CAM-RR). Extracellular Matrix-Dependent Improvement of Cell Survival in Human Tumor and Normal Cells *In Vitro*. *Strahlenther Onkol* (2003) 179(5):337–44. doi: 10.1007/s00066-003-1074-4
154. Bai C, Yang M, Fan Z, Li S, Gao T, Fang Z. Associations of Chemo- and Radio-Resistant Phenotypes With the Gap Junction, Adhesion and Extracellular Matrix in a Three-Dimensional Culture Model of Soft Sarcoma. *J Exp Clin Cancer Res* (2015) 34(1):1–10. doi: 10.1186/s13046-015-0175-0
155. Xie P, Yu H, Wang F, Yan F, He X. Inhibition of LOXL2 Enhances the Radiosensitivity of Castration-Resistant Prostate Cancer Cells Associated With the Reversal of the EMT Process. *BioMed Res Int* (2019) 2019:4012590. doi: 10.1155/2019/4012590
156. Chang L, Graham PH, Hao J, Ni J, Bucci J, Cozzi PJ, et al. Acquisition of Epithelialmesenchymal Transition and Cancer Stem Cell Phenotypes Is Associated With Activation of the PI3K/Akt/mTOR Pathway in Prostate Cancer Radioresistance. *Cell Death Dis* (2013) 4(10):e875. doi: 10.1038/cddis.2013.407
157. Bamodu OA, Chang HL, Ong JR, Lee WH, Yeh CT, Tsai JT. Elevated PDK1 Expression Drives PI3K/AKT/MTOR Signaling Promotes Radiation-Resistant and Dedifferentiated Phenotype of Hepatocellular Carcinoma. *Cells* (2020) 9(3):746. doi: 10.3390/cells9030746
158. Konge J, Leteurtre F, Goislard M, Biard D, Morel-Altmeyer S, Vaurijoux A, et al. Breast Cancer Stem Cell-Like Cells Generated During Tgfβ-Induced EMT are Radioresistant. *Oncotarget* (2018) 9(34):23519–31. doi: 10.18632/oncotarget.25240
159. Ellsworth SG, Rabatic BM, Chen J, Zhao J, Campbell J, Wang W, et al. Principal Component Analysis Identifies Patterns of Cytokine Expression in non-Small Cell Lung Cancer Patients Undergoing Definitive Radiation Therapy. *PloS One* 12(9):e0183239. doi: 10.1371/journal.pone.0183239
160. Chaiswing L, Weiss HL, Jayswal RD, Clair D, Kyprianou N. Profiles of Radioresistance Mechanisms in Prostate Cancer. *Crit Rev Oncog* (2018) 23 (1-2):39–67. doi: 10.1615/CritRevOncog.2018025946
161. Ali MY, Oliva CR, Noman A, Allen BG, Goswami PC, Zakharia Y, et al. Radioresistance in Glioblastoma and the Development of Radiosensitizers. *Cancers* (2020) 12(9):2511. doi: 10.3390/cancers12092511
162. Squatrito M, Vanoli F, Schultz N, Jasin M, Holland EC. 53bp1 is a Haploinsufficient Tumor Suppressor and Protects Cells From Radiation Response in Glioma. *Cancer Res* (2012) 72(20):5250–60. doi: 10.1158/0008-5472.CAN-12-0045
163. Xu Z, Yan Y, Xiao L, Dai S, Zeng S, Qian L, et al. Radiosensitizing Effect of Diosmetin on Radioresistant Lung Cancer Cells *via* Akt Signaling Pathway. *PloS One* (2017) 12(4):1–14. doi: 10.1371/journal.pone.0175977
164. Rooney S, Alt FW, Lombard D, Whitlow S, Eckersdorff M, Fleming J, et al. Defective DNA Repair and Increased Genomic Instability in Artemis-Deficient Murine Cells. *J Exp Med* (2003) 197(5):553–65. doi: 10.1084/jem.20021891
165. Vehlow A, Klapproth E, Storch K, Dickreuter E, Seifert M, Dietrich A, et al. Adhesion- and Stress-Related Adaptation of Glioma Radiochemoresistance Is Circumvented by β1 Integrin/JNK Co-Targeting. *Oncotarget* (2017) 8 (30):49224–37. doi: 10.18632/oncotarget.17480
166. Li F, Zheng X, Liu Y, Li P, Liu X, Ye F, et al. Different Roles of CHOP and JNK in Mediating Radiation-Induced Autophagy and Apoptosis in Breast Cancer Cells. *Radiat Res* (2016) 185(5):539–48. doi: 10.1667/RR14344.1
167. Belenkov AI, Shenouda G, Rizhevskaya E, Cournoyer D, Belzile JP, Souhami L, et al. Erythropoietin Induces Cancer Cell Resistance to Ionizing Radiation and to Cisplatin. *Mol Cancer Ther* (2004) 3(12):1525–32.
168. Pérès EA, Gérault AN, Valable S, Roussel S, Toutain J, Divoux D, et al. Silencing Erythropoietin Receptor on Glioma Cells Reinforces Efficacy of Temozolomide and X-Rays Through Senescence and Mitotic Catastrophe. *Oncotarget* (2015) 6(4):2101–19. doi: 10.18632/oncotarget.2937
169. Lin HY, Hung SK, Lee MS, Chiou WY, Huang TT, Tseng CE, et al. DNA Methylome Analysis Identifies Epigenetic Silencing of FHIT as a Determining Factor for Radiosensitivity in Oral Cancer: An Outcome-Predicting and Treatment-Implicating Study. *Oncotarget* (2015) 6(2):915–34. doi: 10.18632/oncotarget.2821

170. Kitano A, Shimasaki T, Chikano Y, Nakada M, Hirose M, Higashi T, et al. Aberrant Glycogen Synthase Kinase 3β Is Involved in Pancreatic Cancer Cell Invasion and Resistance to Therapy. *PloS One* (2013) 8(2):e55289. doi: 10.1371/journal.pone.0055289
171. Ren J, Liu T, Han Y, Wang Q, Chen Y, Li G, et al. GSK-3β Inhibits Autophagy and Enhances Radiosensitivity in Non-Small Cell Lung Cancer. *Diagn Pathol* (2018) 13(1):1–10. doi: 10.1186/s13000-018-0708-x
172. Dong Q, Sharma S, Liu H, Chen L, Gu B, Sun X, et al. HDAC Inhibitors Reverse Acquired Radio Resistance of KYSE-150R Esophageal Carcinoma Cells by Modulating Bmi-1 Expression. *Toxicol Lett* (2014) 224(1):121–9. doi: 10.1016/j.toxlet.2013.10.014
173. Shi XY, Ding W, Li TQ, Zhang YX, Zhao SC. Histone Deacetylase (HDAC) Inhibitor, Suberoylanilide Hydroxamic Acid (SAHA), Induces Apoptosis in Prostate Cancer Cell Lines *via* the Akt/FOXO3a Signaling Pathway. *Med Sci Monit* (2017) 23:5793–802. doi: 10.12659/MSM.904597
174. Yang W, Liu Y, Gao R, Yu H, Sun T. HDAC6 Inhibition Induces Glioma Stem Cells Differentiation and Enhances Cellular Radiation Sensitivity Through the SHH/Gli1 Signaling Pathway. *Cancer Lett* (2018) 415:164–76. doi: 10.1016/j.canlet.2017.12.005
175. Bayo J, Tran TA, Wang L, Peña-Llopis S, Das AK, Martinez ED. Jumonji Inhibitors Overcome Radioresistance in Cancer Through Changes in H3K4 Methylation at Double-Strand Breaks. *Cell Rep* (2018) 25(4):1040–1050.e5. doi: 10.1016/j.celrep.2018.09.081
176. Gu Y, Jin S, Gao Y, Weaver DT, Alt FW. Ku70-Deficient Embryonic Stem Cells Have Increased Ionizing Radiosensitivity, Defective DNA End-Binding Activity, and Inability to Support V(D)J Recombination. *Proc Natl Acad Sci U S A* (1997) 94(15):8076–81. doi: 10.1073/pnas.94.15.8076
177. Chen C, Hua H, Han C, Cheng Y, Cheng Y, Wang Z, et al. Prognosis Value of MGMT Promoter Methylation for Patients With Lung Cancer: A Meta-Analysis. *Int J Clin Exp Pathol* (2015) 8(9):11560–4.
178. Cheng G, Kong D, Hou X, Liang B, He M, Liang N, et al. The Tumor Suppressor, P53, Contributes to Radiosensitivity of Lung Cancer Cells by Regulating Autophagy and Apoptosis. *Cancer Biother Radiopharm* (2013) 28 (2):153–9. doi: 10.1089/cbr.2012.1297
179. Menendez JA, Lupu R. RNA Interference-Mediated Silencing of the P53 Tumor-Suppressor Protein Drastically Increases Apoptosis After Inhibition of Endogenous Fatty Acid Metabolism in Breast Cancer Cells. *Int J Mol Med* (2005) 15(1):33–40. doi: 10.3892/ijmm.15.1.33
180. Srivastava P, Sarma A, Chaturvedi CM. Targeting DNA Repair With PNKP Inhibition Sensitizes Radioresistant Prostate Cancer Cells to High LET Radiation. *PloS One* (2018) 13(1):1–14. doi: 10.1371/journal.pone.0190516
181. Neijenhuis S, Begg AC, Vens C. Radiosensitization by a Dominant Negative to DNA Polymerase β Is DNA Polymerase β-Independent and XRCC1-Dependent. *Radiother Oncol* (2005) 76(2):123–8. doi: 10.1016/j.radonc.2005.06.020
182. Vens C, Dahmen-Mooren E, Verwijs-Janssen M, Blyweert W, Graversen L, Bartelink H, et al. The Role of DNA Polymerase β in Determining Sensitivity to Ionizing Radiation in Human Tumor Cells. *Nucleic Acids Res* (2002) 30 (13):2995–3004. doi: 10.1093/nar/gkf403
183. Vens C, Hofland I, Begg AC. Involvement of DNA Polymerase Beta in Repair of Ionizing Radiation Damage as Measured by *In Vitro* Plasmid Assays. *Radiat Res* (2007) 168(3):281–91. doi: 10.1667/RR0750.1
184. Chan N, Koritzinsky M, Zhao H, Bindra R, Glazer PM, Powell S, et al. Chronic Hypoxia Decreases Synthesis of Homologous Recombination Proteins to Offset Chemoresistance and Radioresistance. *Cancer Res* (2008) 68(2):605–14. doi: 10.1158/0008-5472.CAN-07-5472
185. Zhou H, Miki R, Eeva M, Fike FM, Seligson D, Yang L, et al. Reciprocal Regulation of SOCS1 and SOCS3 Enhances Resistance to Ionizing Radiation in Glioblastoma Multiforme. *Clin Cancer Res* (2007) 13(8):2344–53. doi: 10.1158/1078-0432.CCR-06-2303
186. Yang T, Huang T, Zhang D, Wang M, Wu B, Shang Y, et al. TGF-β Receptor Inhibitor LY2109761 Enhances the Radiosensitivity of Gastric Cancer by Inactivating the TGF-β/SMAD4 Signaling Pathway. *Aging* (2019) 11 (20):8892–910. doi: 10.18632/aging.102329
187. Kim JS, Kim SY, Lee M, Kim SH, Kim SM, Kim EJ. Radioresistance in a Human Laryngeal Squamous Cell Carcinoma Cell Line is Associated With DNA Methylation Changes and Topoisomerase II α. *Cancer Biol Ther* (2015) 16(4):558–66. doi: 10.1080/15384047.2015.1017154
188. Ai P, Xu X, Xu S, Wei Z, Tan S, Li J. Overexpression of Wnt7a Enhances Radiosensitivity of non-Smallcell Lung Cancer *via* the Wnt/JNK Pathway. *Biol Open* (2020) 9(6):bio050575. doi: 10.1242/bio.050575
189. Barnett GC, Thompson D, Fachal L, Kerns S, Talbot C, Elliott RM, et al. A Genome Wide Association Study (GWAS) Providing Evidence of an Association Between Common Genetic Variants and Late Radiotherapy Toxicity. *Radiother Oncol* (2014) 111(2):178–85. doi: 10.1016/j.radonc.2014.02.012
190. Grade M, Wolff HA, Gaedcke J, Ghadimi BM. The Molecular Basis of Chemoradiosensitivity in Rectal Cancer: Implications for Personalized Therapies. *Langenbecks Arch Surg* (2012) 397(4):543–55. doi: 10.1007/s00423-012-0929-5
191. Massi MC, Gasperoni F, leva F, Paganoni AM, Zunino P, Manzoni A, et al. A Deep Learning Approach Validates Genetic Risk Factors for Late Toxicity After Prostate Cancer Radiotherapy in a REQUITE Multi-National Cohort. *Front Oncol* (2020) 10:541281. doi: 10.3389/fonc.2020.541281
192. Xie X, Wang H, Jin H, Ouyang S, Zhou J, Hu J, et al. Expression of pAkt Affects P53 Codon 72 Polymorphism-Based Prediction of Response to Radiotherapy in Nasopharyngeal Carcinoma. *Radiat Oncol* (2013) 8(1):1–10. doi: 10.1186/1748-717X-8-117

Conflict of Interest: The authors declare that the research was conducted in the absence of any commercial or financial relationships that could be construed as a potential conflict of interest.

Publisher's Note: All claims expressed in this article are solely those of the authors and do not necessarily represent those of their affiliated organizations, or those of the publisher, the editors and the reviewers. Any product that may be evaluated in this article, or claim that may be made by its manufacturer, is not guaranteed or endorsed by the publisher.

frontiers in Cell and Developmental Biology

REVIEW
published: 11 March 2022
doi: 10.3389/fcell.2022.751367

The Influence of Oncogenic RAS on Chemotherapy and Radiotherapy Resistance Through DNA Repair Pathways

Rodrigo E. Cáceres-Gutiérrez[1], *Yair Alfaro-Mora*[1,2], *Marco A. Andonegui*[1], *José Díaz-Chávez*[1]* *and Luis A. Herrera*[1,2]*

[1]*Unidad de Investigación Biomédica en Cáncer, Instituto Nacional de Cancerología-Instituto de Investigaciones Biomédicas, UNAM, Mexico City, Mexico,* [2]*Instituto Nacional de Medicina Genómica, Mexico City, Mexico*

RAS oncogenes are chief tumorigenic drivers, and their mutation constitutes a universal predictor of poor outcome and treatment resistance. Despite more than 30 years of intensive research since the identification of the first RAS mutation, most attempts to therapeutically target RAS mutants have failed to reach the clinic. In fact, the first mutant RAS inhibitor, Sotorasib, was only approved by the FDA until 2021. However, since Sotorasib targets the KRAS G12C mutant with high specificity, relatively few patients will benefit from this therapy. On the other hand, indirect approaches to inhibit the RAS pathway have revealed very intricate cascades involving feedback loops impossible to overcome with currently available therapies. Some of these mechanisms play different roles along the multistep carcinogenic process. For instance, although mutant RAS increases replicative, metabolic and oxidative stress, adaptive responses alleviate these conditions to preserve cellular survival and avoid the onset of oncogene-induced senescence during tumorigenesis. The resulting rewiring of cellular mechanisms involves the DNA damage response and pathways associated with oxidative stress, which are co-opted by cancer cells to promote survival, proliferation, and chemo- and radioresistance. Nonetheless, these systems become so crucial to cancer cells that they can be exploited as specific tumor vulnerabilities. Here, we discuss key aspects of RAS biology and detail some of the mechanisms that mediate chemo- and radiotherapy resistance of mutant RAS cancers through the DNA repair pathways. We also discuss recent progress in therapeutic RAS targeting and propose future directions for the field.

Keywords: ras, oncogene-induced senescence, reactive oxygen species, DNA damage response, double strand breaks, cancer, chemotherapy and radiotherapy resistance

OPEN ACCESS

Edited by:
Kirill Afonin,
University of North Carolina at Charlotte, United States

Reviewed by:
Sezen Vatansever,
Icahn School of Medicine at Mount Sinai, United States
Samantha Messina,
Roma Tre University, Italy

***Correspondence:**
Luis A. Herrera
lherrera@inmegen.gob.mx
José Díaz-Chávez
jdiazchavez03@gmail.com

Specialty section:
This article was submitted to Molecular and Cellular Oncology, a section of the journal Frontiers in Cell and Developmental Biology

Received: *01 August 2021*
Accepted: *15 February 2022*
Published: *11 March 2022*

Citation:
Cáceres-Gutiérrez RE, Alfaro-Mora Y, Andonegui MA, Díaz-Chávez J and Herrera LA (2022) The Influence of Oncogenic RAS on Chemotherapy and Radiotherapy Resistance Through DNA Repair Pathways. Front. Cell Dev. Biol. 10:751367. doi: 10.3389/fcell.2022.751367

THE RAS ONCOGENES

The Ras superfamily is composed of structurally and mechanistically related small GTPase proteins organized in five major families named Ras, Rho, Arf, Ran, and Rab. In humans, the Ras family (20–29 kDa) encompasses 36 members of which KRAS, HRAS, NRAS, ERAS, RRAS, and MRAS are the archetypal elements (Rojas et al., 2012).

The main role of RAS proteins is the transduction of external stimuli into intracellular signaling cascades. These GTPases work as intracellular membrane-associated binary switches that trigger a

broad range of cell survival and proliferation events. These proteins cycle around active and inactive states through their intrinsic GTPase activity and their interaction with Guanine Nucleotide Exchange Factors (GEFs) and GTPase-Activating Proteins (GAPS), which promote the GTP-bound active, and GDP-bound inactive states, respectively (Simanshu et al., 2017).

Structurally, RAS proteins bear a G domain that binds and hydrolyzes guanine nucleotides, and two loops (switch 1 and switch 2) that drive the conformational changes that facilitate the binding of effectors, exchange factors, and activators. The C terminal region of RAS (25 amino acids) contains a hypervariable region (HVR) which is poorly conserved among the Ras family members. This HVR is targeted by several post-translational modifications and is crucial for insertion into and interaction with the plasma membrane (Prior and Hancock, 2001; Vetter and Wittinghofer, 2001; Hancock, 2003).

RAS activation relies on a plethora of membrane-associated receptors, like tyrosine kinase receptors, G-protein coupled receptors, integrins, or toll-like receptors (Cattaneo et al., 2014). When such receptors become activated by binding of their corresponding ligand, they recruit adaptor proteins and Guanine Exchange Factors (GEFs), which exchange RAS-associated GDP for GTP, thereby generating a conformational change in switch 1 and switch 2 loops. This conformational change exposes the residues necessary for RAS' interaction with its downstream effectors, including Y40 for PI3K, E37 for Ral-GEF, and T35 for RAF (Schlessinger, 2000; Shields et al., 2000; Vetter and Wittinghofer, 2001). RAS activity generates transient downstream signaling cascades that activate several effectors like the Raf/Mek/Erk, PI3K/Akt, RalGDS/Ral, and Mekk/Sek/Jnk pathways, which regulate multiple cellular events through gene transcription, among other mechanisms. Although RAS' GTP hydrolysis rate is intrinsically slow, its catalytic activity is importantly accelerated upon interaction with GTPase Activating Proteins (GAPs). GAPs can increase RAS GTPase activity about 10^5-fold by inserting an arginine finger into RAS' GTPase cleft. GTP hydrolysis leads RAS back to its inactive state (Drugan et al., 2000; Vetter and Wittinghofer, 2001; Pamonsinlapatham et al., 2009; Scheffzek and Shivalingaiah, 2019). In fact, the lifetime of active GTP-bound RAS is governed by the time of encounter with a GAP. Therefore, RAS-GAP inactivation or mutation, as well as RAS constitutive activation by inhibition of its GTP hydrolysis capacity, promotes sustained RAS signaling, which can ultimately lead to malignant transformation (Jett and Friedman, 2010).

The human RAS homologues of Harvey rat sarcoma viral oncogene (HRAS), Kirsten rat sarcoma viral oncogene (KRAS), and the neuroblastoma RAS viral oncogene (NRAS) become major disease drivers upon mutation: between 17 and 30% of all human tumors bear RAS mutations. Of these cancer-associated alterations, ~97% occur in codons 12, 13, and 61 of the distinct isoforms (Simanshu et al., 2017; Mo et al., 2018). More specifically, these mutations are present in 50% of colon cancer cases (Logsdon and Lu, 2016) and ~95% of pancreatic cancer cases, and are estimated to cause one million deaths per year worldwide (Simanshu et al., 2017). In addition, KRAS alterations are more frequently observed in lung, pancreatic, and colorectal malignancies, and NRAS mutations are present in hematological malignancies, while HRAS mutations are present in dermatological and head and neck malignancies (Pylayeva-Gupta et al., 2011). Overall, mutations in KRAS are the most common, accounting for ~85% of all RAS mutations, followed by 12% for NRAS, and 3% for HRAS (Simanshu et al., 2017).

These alterations lead to critical amino acid substitutions which generate a constitutively active RAS protein, due to the impairment of GAP binding or decreased GTP hydrolysis (Smith et al., 2013). KRAS, NRAS, and HRAS have different mutation frequencies among each of the mutational hotspots. The predominant point of mutations in KRAS is G12 (89%), followed by G13 (9%), and to a lesser extent, Q61 (1%). However, in NRAS, Q61 is the most commonly mutated hotspot (60%), followed by G12 (25%), and G13 (14%). For HRAS, the most prevalent mutation is G12 (55%), followed by Q61 (36%), and then G13 (8%) (Prior et al., 2012; Hobbs et al., 2016; Lu et al., 2016).

The RAS mutations mentioned above confer oncogenic properties to the cell, like uncontrolled proliferation, loss of contact inhibition, increased motility, altered metabolism, and loss of genome integrity (Yuan et al., 2018). Furthermore, these phenotypes are reflected in RAS mutant cancer's clinical behavior, which is associated with poorer outcomes, including decreased overall survival, bolstered by resistance to diverse chemotherapy and radiotherapy schemes (Lièvre et al., 2006; Jancík et al., 2010). Mutations in other codons of RAS are at the origin of milder conditions called RASopathies, which are characterized by distinctive craniofacial features, short stature, and learning disabilities, among other hallmarks (Mo et al., 2018).

Strategies to therapeutically target mutant RAS have met a tough road throughout the years. Approaches targeting posttranslational modifications of RAS that mediate its membrane localization or its signalling output have been overcome by the cell through multiple redundant feedback loops (Stephen et al., 2014). Moreover, in some cases, the use of more than one drug to tackle cancer cells' feedback loops has proven prohibitively toxic (Stephen et al., 2014; Singh et al., 2015).

On the other hand, RAS' three-dimensional conformation, which displays relatively shallow grooves, as well as its picomolar affinity for GTP/GDP, hampered the development of small molecule inhibitors (Grabocka et al., 2015; Esposito et al., 2019). However, in 2013, a new pocket was identified in KRAS that was not apparent in previous crystallographic structures (Ostrem et al., 2013). Based on this discovery, compounds were designed that covalently bind to the mutant cysteine of KRAS G12C and disrupt both switch 1 and switch 2 regions. As a consequence, KRAS G12C inhibitors thwart the GTPase's preference to favour GDP binding over GTP, concomitantly inhibiting its signalling activity by precluding RAS interaction with RAF (Ostrem et al., 2013). Notably, since these compounds target a mutant cysteine, they spare the WT protein, underscoring their suitability as cancer therapeutic agents (McCormick, 2020). Several new covalent

KRAS G12C inhibitors were rapidly developed, and this kind of molecules entered clinical trials only 6 years after the publication of the paper describing the new pocket and inhibitor (Goebel et al., 2020). One of them, AMG510, was approved in May 2021 after demonstrating an objective response rate of 36% with a median response duration of 10 months in a phase 2 trial in mutant advanced solid tumors (in combination with anti-PDL1 therapy and midazolam). AMG510 is currently commercialized by Amgen under the name Sotorasib and is evaluated in at least 13 trials. The other compound, MRTX849, is currently under scrutiny in phase 2 and phase 3 trials and was granted the breakthrough therapy designation by the FDA, which might expedite its approval.

Unfortunately, the percentage of patients that can benefit from KRAS G12C covalent inhibitors is relatively limited since this mutation represents no more than 14% of all KRAS mutations found in human tumors (Lu et al., 2016). For instance, KRAS G12C represents only 2% of all KRAS mutations in Pancreatic Ductal Adenocarcinoma (PDAC) (Kim et al., 2021). However, other efforts to target RAS GTPases are also yielding very promising results. Recent advances in screening technologies have prompted preclinical progress, resulting in the detection of RAS mutant cell vulnerabilities. One of the resulting approaches, termed synthetic lethality, consists of taking advantage of the exclusive dependence of mutant cells (RAS mutants in this case) on a second target (Singh et al., 2015). This will be discussed below for RAS, but the most commonly cited example in the literature is the therapeutic use of PARP inhibitors in BRCA1/2 mutant cancer (Marcotte et al., 2012).

RAS vulnerabilities present an extremely valuable resource for developing mutant RAS cancer therapies. In order to take advantage of this asset, it is crucial to understand the mechanisms that support mutant RAS cancer survival in the clinical setting. In the following sections, we explore the development of RAS-dependent chemotherapy and radiotherapy resistance through the DNA damage repair pathways; along the carcinogenic process, we expose mechanistic details of such resistance pathways and propose future directions of this exciting field.

RAS IN ONCOGENE-INDUCED SENESCENCE

RAS mutation is an early event in several tissues along the multistep carcinogenic process. In fact, several mouse models have been used to demonstrate that KRAS mutation alone is sufficient to initiate tumor development (Grabocka et al., 2014). Observations in human pancreatic cancer development provide further support to mutant RAS' early contribution to carcinogenesis. RAS alterations are commonly detected in early PanIN lesions, hyperplasias that precede the development of pancreatic intraepithelial neoplasia, one of the most, if not the most, lethal solid malignancy (Luo, 2021). However, early incipient cancer cells face the struggle of surviving in extremely adverse conditions since mutant RAS constant signalling leads to replicative, metabolic, and oxidative stress (Grabocka et al., 2015). For instance, constitutively active RAS abnormally increases the formation of replication forks on replisomes and promotes the generation of asymmetric replication forks (Di Micco et al., 2006). Also, the overexpression of RAS proteins decreases cellular dNTP concentration, which forces the premature termination of replication forks. This is a consequence of the downregulation of the ribonucleotide reductase subunit M2 (RRM2), mediated by RAS proteins, leading to DNA replication stress, cell cycle stress and senescence (Di Micco et al., 2007; Rai et al., 2011). Unresolved DNA replication stress can lead to DNA damage, giving rise to several types of mutations, including chromosomal rearrangements, and DNA amplifications or deletions (Sirbu and Cortez, 2013; Zeman and Cimprich, 2014; Gaillard et al., 2015; Blackford and Jackson, 2017).

As discussed above, the replicative, oxidative, and metabolic stresses resulting from RAS mutation represent an obvious drawback for incipient cancer cell proliferation and survival. In primary cells, much of this disadvantage is mediated by Oncogene-Induced Senescence (OIS), a state of permanent cell cycle arrest in the absence of telomere erosion, that prevents the proliferation of cells in which excessive damage could lead to a full malignant phenotype (Batsi et al., 2009). Current evidence suggests that OIS is the result of constant exposure to sublethal doses of stressors (Mijit et al., 2020). Depending on the intensity of the stress, cells may exceed a threshold that promotes programmed cell death instead of senescence, although other factors, such as the cell type and the type of stimulus, may tilt the balance towards either outcome (Mijit et al., 2020).

Several different pathways activate OIS in response to RAS signalling (Mijit et al., 2020). Among them, the best understood involves the DNA Damage Response (DDR). This pathway can be activated either by exposed stretches of single-stranded DNA caused by replication fork stalling or DNA breaks resulting thereof, or by DNA damage caused by ROS. Both initiating events have been listed as natural consequences of RAS-mediated oncogenic stress. DNA damage activates ATM/ATR kinases, which stabilize p53 through phosphorylation of its serine residues 15 and 20, and by inhibitory phosphorylation of its ubiquitin ligase MDM2 (Mijit et al., 2020). In turn, p53 upregulates the cyclin-dependent kinase inhibitors p21cip1 and p16INK4A, concomitantly preventing cell cycle progression (Mijit et al., 2020).

Alternative DDR-independent mechanisms of OIS have been elucidated, including the RAS-mediated NORE1A activation. NORE1A is a recently identified downstream RAS effector which, in conjunction with the kinase HIPK2, promotes p53 pro-senescence acetylation and inhibits its pro-apoptotic phosphorylation (Donninger et al., 2015). NORE1A can also form a complex with the phosphatase PP1A and promote the activation of the cell cycle progression inhibitor Rb, by dephosphorylation (Barnoud et al., 2016).

It has also been demonstrated that RAS G12V stimulates OIS in IMR-90 non-cancerous lung fibroblasts (Batsi et al., 2009). Mechanistically, the oncogenic stress instigated by RAS G12V promotes DNA double-strand breaks and the consequential

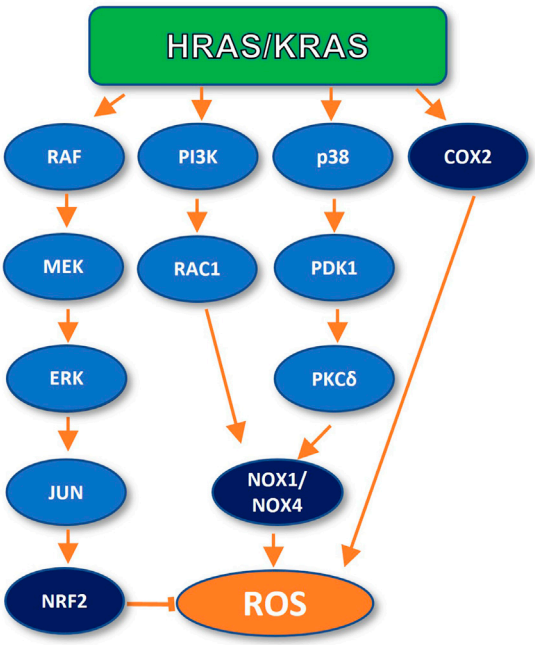

FIGURE 1 | Oncogenic RAS can inhibit and promote ROS generation. In early carcinogenesis, RAS inhibits ROS production by activating the NRF2 transcription factor. However, oncogenic RAS can also promote ROS generation through upregulation of NADPH oxidases (NOX1 and NOX4) and directly by COX2 activation.

activation of the DDR. Upon DDR activation, Chk1 and Chk2 activate p53. Among its multiple effects, p53 inhibits p65, one of the two subunits that compose the transcription factor NF-kB (Mijit et al., 2020). In unstimulated cells, NF-κB is localized to the cytoplasm in a complex with its inhibitor IκBα, which prevents NF-κB translocation to the nucleus. Upon stimulation with different external signals, such as TNF-α, the Iκκ complex phosphorylates IκBα, promoting its ubiquitylation and subsequent degradation. IκBα degradation allows for NF-κB translocation to the nucleus and transcriptional activity, which upregulates several genes associated with cell survival, chemotherapy and radiotherapy resistance, stromal adhesion molecules, and autocrine stimulation receptors (Xia et al., 2014). Remarkably, forced expression of the Iκκ subunit Iκκβca can relieve p53-induced inhibition of NF-κB, thereby delaying the onset of OIS (Batsi et al., 2009). Interestingly, the DDR itself promotes Iκκ activation through the action of ATM, but such endogenous activation can be overcome by wild-type p53 (Batsi et al., 2009). In fact, it has been shown in mouse embryonic fibroblasts expressing RAS G12D that p53 loss of heterozygosity (LOH) is required for sustained NF-κB nuclear localization. Furthermore, conditional p53 reactivation in human lung tumor cells has been demonstrated to restore p65 cytoplasmic localization (Meylan et al., 2009).

Once proliferating RAS mutant cells can bypass OIS, some mechanisms of genome fidelity safeguard become beneficial for cancer cell survival by mitigating the catastrophic effects of high stress levels and DNA damage (Gilad et al., 2010). This has been demonstrated for the tumor suppressor ATR, which is activated by oncogenic KRAS G12V-transformed murine embryonic fibroblasts. In this model, oncogenic transformation increases cellular reliance on the ATR-CHK2 pathway for survival. RNAi-mediated ATR targeting in $p53^{+/-}$cells leads to p53 LOH, bolstering tumorigenesis. Interestingly, when stronger ATR silencing is achieved, cells with the same genetic background (KRAS G12V/$p53^{+/-}$) attain intolerable levels of genomic instability, leading to decreased proliferation and cell death (Gilad et al., 2010). Similarly, a large shRNA screen performed in the colorectal cancer cell line DLD-1 identified synthetic lethality relations between RAS mutation and several components of the Base Excision Repair (BER) pathway, including NEIL2, XRCC1, Polymerase β (Pol-β), and the DNA ligase III (Luo et al., 2009). Therefore, OIS relies on the proper function of tumor suppressor genes, but tumor suppressors do not represent an eternally impervious barrier since such genes can suffer inactivating mutations and LOH. In this context, tightly regulated mechanisms of stress surveillance promote tumorigenesis.

RAS IN THE CELLULAR REDOX BALANCE

RAS has been shown to promote antioxidant as well as pro-oxidant programs in the cell (Lim and Leprivier, 2019) (**Figure 1**) The promotion of a RAS-dependent antioxidant response is supported by recent literature (Lim and Leprivier, 2019). It has been shown that endogenous expression of KRAS G12D in mouse embryonic fibroblasts promotes the activation of NRF2, a central player in the cellular antioxidant response, through the RAF/MEK/ERK/JUN pathway (DeNicola et al., 2011). In turn, NRF2 upregulates ROS-scavenging factors, such as Hmox1, Nqo1, Gclc, and Ggt1, to maintain the intracellular redox balance in check. Furthermore, genetic ablation of NRF2 impairs RAS-dependent tumor growth and proliferation (DeNicola et al., 2011). These findings argue for a role of RAS in limiting OIS during early tumor development.

The antioxidant response initiated by mutant RAS has also been shown to mediate chemotherapy resistance in established tumors. It has been reported that cisplatin induces mitochondrial ROS generation, increasing the stress levels present in cancer cells (Marullo et al., 2013). Platinum-based compounds like cisplatin, carboplatin, and oxaliplatin are chemotherapeutic agents widely used in cancer treatment. Such agents intercalate into DNA, interfering with RNA transcription and DNA replication by binding to N7 of guanine and adenosine residues, adduct formation, and subsequent apoptosis. However, platinum-based treatment can be overcome by cancer cells due to intrinsic resistance or acquired resistance through improved cell DNA repair and the overactivation of the anti-oxidative stress pathway (Oun et al., 2018). Tao and colleagues reported that cisplatin chemoresistance in non-small cell lung cancer cells and lung tumor tissue can be mediated by KRAS G12D-dependent activation of the transcription factor NRF2 pathway, by enhanced NRF2 mRNA expression and, therefore, increased gene expression of drug metabolizing enzymes,

antioxidant enzymes, and drug transporters, thereby limiting cisplatin toxicity in cancer cells (DeNicola et al., 2011; Tao et al., 2014). Furthermore, KRAS G12C mutants were found to be less sensitive to cisplatin treatment *in vitro* and *in vivo* as a result of DNA BER stimulation, which removes cisplatin from DNA before the formation of DNA adducts (Caiola et al., 2015).

On the other hand, most of the literature concerning the impact of RAS on cellular redox balance has shown a role for RAS in the generation of ROS (Lim and Leprivier, 2019), which promote multiple phenotypes associated with cancer development, such as increased DNA oxidation (Woo and Poon, 2004; Lim and Leprivier, 2019), increased proliferation (Irani et al., 1997; Ogrunc et al., 2014), chromosome breaks with concomitant chromosomal instability (Woo and Poon, 2004), anchor-independent growth (Weinberg et al., 2010), and increased DNA-repair upon cisplatin or UV-induced insults (Cho et al., 2002). As discussed above, although some of these effects are known to trigger OIS or cell death in tumor suppressor-proficient cells, loss of tumor suppressor genes constitutes a turning point in tumor development.

RAS has also been shown to play a central role in the ROS-dependent activation of the DDR, thereby preventing extreme genomic instability levels, and promoting resistance to chemotherapy and radiotherapy-induced cell death through DNA repair.

RAS proteins can promote ROS production and consequent stimulation of DNA repair through different pathways. For instance, mutant RAS expression promotes changes in cellular metabolism, increasing the intracellular levels of hydrogen peroxide (H_2O_2) and Reactive Oxygen Species (ROS), promoting the oxidation of the DNA, proteins, and lipids (Lee et al., 1999). In fact, the Qo site of the mitochondrial complex III has been identified as the main site of KRAS-driven ROS generation in a mouse model of lung cancer (Weinberg et al., 2010). It has also been observed that in mouse lung cells, KRAS mutant expression promotes ROS peroxide production through cyclooxygenase 2 (COX-2) (Maciag et al., 2004). Furthermore, Park and colleagues reported that KRAS induced ROS generation through a signalling axis specifically involving the p38 MAPK in normal human fibroblasts. KRAS induced activation of p38, which led to PDPK1 activation. Once active, PDPK1 interacts with and phosphorylates PKCδ which, in turns, interacts with and phosphorylates the SH3-N domain of p47phox, a subunit of the NADPH Oxidase 1 (NOX-1). This interaction mediates p47phox membrane translocation and activation of NADPH oxidase-1 (NOX-1) upregulating cellular ROS production (Park et al., 2014). Moreover, mutant KRAS has also been shown to upregulate Nox1, a homologue of the catalytic subunit of NOX-1 at the transcriptional level, through the MAPK pathway, in normal rat kidney epithelial cells. In this study, the specific inhibitor PD98059 was used to target p38, which demonstrated the participation of such signaling cascade in ROS generation, and the enhancement of cell growth and malignant transformation (Park et al., 2014).

On the other hand, it has been observed that oncogenic HRAS expression in NIH3T3 stimulates ROS production through the HRAS/PI3K/RAC1/NADPH oxidase signaling cascade. In this study, ROS promoted DNA repair upon challenge with cisplatin and UV light-induced insults. Furthermore, pre-treatment of the cells with the antioxidant N-acetyl-cysteine partially suppressed such enhanced DNA repair (Cho et al., 2002). A similar mechanism of ROS generation was observed in normal human fibroblasts, through NOX4, in an independent analysis (Ogrunc et al., 2014).

Overall, the relation of RAS with ROS may seem confusing since some reports show that RAS signaling antagonizes ROS, while others demonstrate that it promotes ROS generation. A reconciling model proposed that RAS plays distinct, sequential roles in the cellular redox balance along carcinogenesis (Lim and Leprivier, 2019), hypothesizing that mutant RAS activates antioxidant programs upon tumorigenic initiation; then, in a more advanced carcinogenic setting, amplified RAS signaling would activate pro-oxidant programs, enhancing the cellular capacity of DNA repair and proliferation. To test this model, it will be interesting to assess the alterations associated with anti- to pro-oxidant switching in terms of genetic, epigenetic, and tumor microenvironment along carcinogenesis.

INFLUENCE OF RAS IN DNA REPAIR PATHWAYS

RAS-dependent ROS stimulate DNA repair through the activation of NF-κB, an essential mediator of chemoresistance and radioresistance which promotes DNA repair and cancer cell survival (**Figure 2**). It has been shown that p65 loss compromises DNA repair and genome stability. Conversely, treatment with the NF-κB activator TNF-α enhances DSB repair, but this enhancement can be inhibited by overexpression of a degradation-resistant version of the NF-κB inhibitor IκBα. Specifically, p65 stimulates the Homologous Recombination (HR) repair pathway by upregulating ATM and BRCA2 at the transcriptional level, and by inducing the formation of a BRCA1 complex with the CtIP, which is required for DSB resection, necessary for single-strand ends in the process of HR (Volcic et al., 2012).

On the other hand, high intracellular H_2O_2 concentrations have been shown to upregulate poly (ADP-ribose) polymerase (PARP), which is required for DNA DSB repair (Ziemann et al., 1999). Moreover, ROS activate several transcription factors, such as AP-1, Sp1, NRF2, and p53 (Cho et al., 2002). Remarkably, several genes implicated in DNA repair bear redox-sensitive transcription factor binding motifs. For instance, the promoters of the XPA, XPB, XPC, and XPD genes, implicated in nucleotide excision repair XPA-XPD contain binding sites for the aforementioned Sp1, Ets1 (member of the AP-1-like family of transcription factors), and p53 transcription factors (Cho et al., 2002).

Therefore, RAS-mediated ROS enhancement promotes the activation of DNA repair through different mechanisms. This represents a major drawback for incipient cancer cells. However, once tumor cells have overcome the proliferation-counteracting OIS induction systems, RAS-mediated ROS-dependent activation

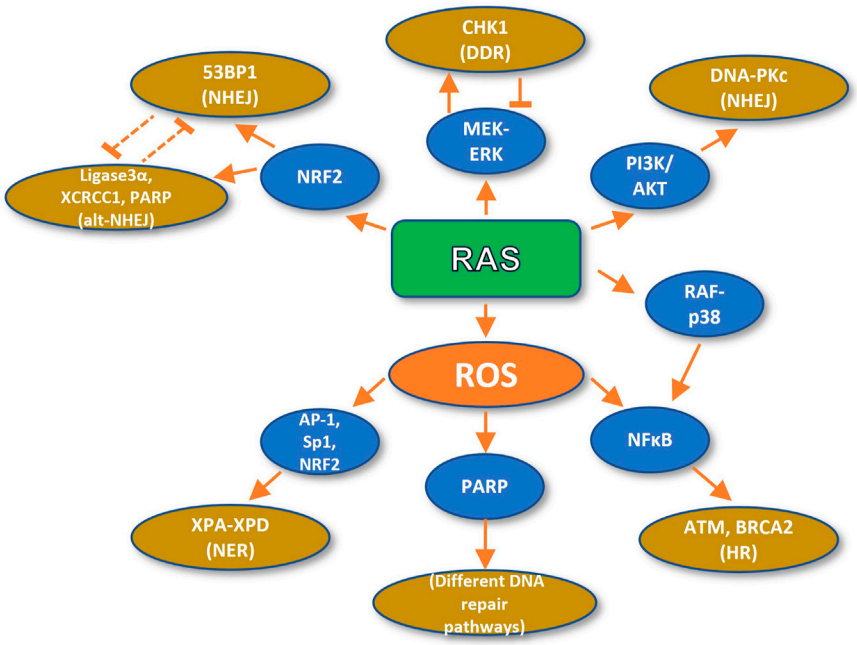

FIGURE 2 | Oncogenic RAS promotes DNA repair. RAS-dependent ROS formation stimulates DNA repair (HR and NER) and the DDR by the activity of NFkB, AP-1, Sp1, and NRF2 transcription factors and PARP activation. On the other hand, RAS fosters DNA repair (NHEJ and alt-NHEJ) directly through activation of MEK, PI3K, and p38 pathways and the NRF2 transcription factor.

promotes cell survival by preventing intolerable genomic instability, and provide the possibility to efficiently repair radiotherapy and chemotherapy-induced DNA damage.

Besides ROS, RAS can promote DNA repair and/or chemotherapy and radiotherapy resistance through several other pathways. This was evidenced by inhibition of HRAS prenylation in rodent cells, or inhibition of HRAS farnesylation in human tumor cells, which increased their radiosensitization (Miller et al., 1993; Bernhard et al., 1996, 1998). Also, the loss of an active RAS allele leads to a significant reduction in the survival of DLD-1 and HT1080 human cell lines upon radiation (Bernhard et al., 2000). Moreover, the inhibition of the PI3K pathway leads to radiosensitization of mutant RAS expressing cells treated with the PI3K inhibitor LY294002 (Gupta et al., 2001). Furthermore, in HCT-116 human colorectal cancer cells, mutant HRAS G12V expression increases the activation of the PI3K/AKT pathway and the activity of AKT upon radiation, promoting cell survival. However, this protective effect is abolished by AKT inhibition or by dominant-negative AKT expression, leading to increased radiation cell lethality (Carón et al., 2005).

In a recent study by Tago and colleagues, NF-κB was shown to be hyperactivated upon TNF-α stimulation of HRAS G12V expressing KF-8 mouse fibroblasts. NF-κB activation occurs through RAF/p38 MAPK-mediated p65 phosphorylation at serine 276 (Tago et al., 2019), which promotes NF-κB transcriptional activity. The authors of this study also reported higher levels of phosphorylated p65 in neoplastic tissue from mutant KRAS colorectal cancer samples. Furthermore, shRNA targeting of KRAS prevented the TNF-α hyperstimulation of NF-κB transcriptional activity in the A549 human lung cancer cell line, as measured by the abundance of its transcriptional targets COX2, ICAM1, and A20 (Tago et al., 2019).

Moreover, mutant KRAS has also been shown to promote autocrine stimulation of the MAPK pathway through the production of EGFR ligands. In response to radiation and under such autocrine stimulation, the PI3K/AKT pathway enhances DSB repair and concomitant radioresistance through phosphorylation of serine 2056 of DNA-PKc catalytic subunit, a critical regulator of the Non-Homologous End Joining DNA repair signalling cascade (Minjgee et al., 2011).

RAS/MEK signalling is also implicated in chemotherapy and radiotherapy resistance through the activation of the DNA damage response. It has been demonstrated that RAS signalling promotes CHK1 expression in human cancer cells, and that such expression can be abolished by MEK inhibition, through treatment with the specific MEK inhibitor cobimetinib (Lee et al., 2017). Furthermore, increased RAS/MEK/ERK signalling has been associated with resistance to the CHK1 inhibitor GDC-0425 (Lee et al., 2017). Nevertheless, MEK inhibition protects cells from reduced viability upon GDC-0425 treatment. Also, CHK1 decreases ERK activation in GDC-0425-sensitive cells. As in the case of ATR mentioned before, the authors of this study interpreted the data as a feed-forward and feedback loop between RAS and CHK1 which enables neoplastic cells to maximize growth without exceeding a threshold of intolerable DNA damage (Lee et al., 2017).

Similarly, another study demonstrated that the MEK inhibitor GSK1120212 radiosensitizes KRAS mutant pancreatic cancer cell lines MIAPaCa-2 and AsPC-1. Treatment with GSK1120212 delayed ɤH2AX foci disappearance and inhibited BRCA1 and RAD51 foci formation after radiation treatment. Furthermore, treatment with GSK1120212 also inhibited the disappearance of DNA-PKc and 53BP1 foci after radiation. Hence, it was concluded that MEK promotes radioresistance in pancreatic cancer cells through the activation of both the HR, and the NHEJ pathways (Poon et al., 2017). Interestingly, wild type HRAS and NRAS are also implicated in efficient Chk1 activation in mutant KRAS cells. Concordantly, the knockdown of wild type HRAS or NRAS specifically sensitizes KRAS mutant cells to DNA damaging agents (Grabocka et al., 2014).

Furthermore, it has also been demonstrated in colorectal cancer cell lines that KRAS G13D mutation can mediate radioresistance through the transcriptional upregulation of NRF2, followed by its nuclear translocation and the concomitant overexpression of 53BP1. 53BP1 translocates to the sites of DSB and promotes DNA repair through the NHEJ pathway. Interestingly, KRAS G13D was shown to accelerate DNA repair (measured by the disappearance of ɤH2AX foci) after irradiation, through the mentioned 53BP1 upregulation, while NRF2 or 53BP1 targeting radiosensitized the cells (Yang et al., 2021). Conversely, the same mutation upregulated the components of the alternative NHEJ (alt-NHEJ) pathway Ligase3α, XRCC1, and PARP1 in a different model, namely leukemic and lymphocytic cells. Interestingly, DNA repair showed delayed kinetics in response to radiation, which is a feature of alt-NHEJ (measured by the disappearance of ɤH2AX foci). Moreover, targeting alt-NHEJ components sensitized KRAS mutant cells to DNA damaging agents (Hähnel et al., 2014).

Furthermore, thymocytes derived from KRAS G12D knock in mice were shown to display increased repair through the alt-NHEJ pathway upon DNA damage with chemical agents or radiation, which was associated with an increased expression of Ligase3α, XRCC1, and PARP1 (Hähnel et al., 2014). The authors of this report proposed that the overexpression of alt-NHEJ components outcompeted classical NHEJ factors for DNA binding. Again, in a different tissue of the same animal (mouse embryonic fibroblasts) this mutation has been shown to upregulate NRF2, which, as mentioned above, promotes the NHEJ pathway through 53BP1 (DeNicola et al., 2011).

These results suggest that oncogenic RAS may have a distinct influence on the DSB repair pathway preference in tissues of different origins, underlying differences in clinical history and treatment response observed in hematological and solid neoplasms. Such differences could help guide the search for synthetic lethal interactions in cancers of different origins.

FUTURE PERSPECTIVES AND CONCLUDING REMARKS

Despite recent advances in targeting mutant RAS tumors, this field still faces important challenges. For example, G12C targeting with the recently approved covalent inhibitor Sotorasib is very specific for the mutant protein, but this brilliant approach's high selectivity comes at the price of benefiting a relatively small percentage of patients, as previously mentioned (Hansen et al., 2018; Kim et al., 2021). Therefore, new strategies are required to either attack RAS mutant cancer vulnerabilities or to develop new ways to directly target RAS itself.

Advances have been achieved in tackling RAS vulnerabilities by exploiting a recently discovered co-dependence between mutant KRAS and the component of the alternative NHEJ pathway PARP1. Interestingly, PARP1 is upregulated upon KRAS mutation (Hähnel et al., 2014) and, on the other hand, PARP1 resistance arises through the overactivation of RAS-MEK-ERK signaling (Sun et al., 2017). Thus, Sun and colleagues treated different types of tumor cells with combinations of MEK1/2 and PARP inhibitors both *in vitro* and *in vivo* and revealed a synergistic effect of these two kinds of drugs, specifically in KRAS mutants (Sun et al., 2017). Furthermore, their results prove that this synergy is associated with the overexpression of the transcription factor FOXO3a, which concomitantly promotes downregulation of the DDR components RAD51, BRCA1, and MRE11, while it promotes the upregulation of the proapoptotic factor BIM (Sun et al., 2017). As a result of the success obtained in the preclinical setting, a phase 1/2 clinical trial is now being conducted to test the efficacy of the combination of the two previously approved drugs Selumetinib (MEK1/2 inhibitor) and Olaparib (PARP1 inhibitor) in the treatment of ovarian and other solid malignancies with RAS pathway alterations (NCT03162627) (Sun et al., 2020).

Other notable efforts are aiming to inhibit components of the DDR chemically. Such is the case of a newly developed molecule (referred to as compound 14), that inhibits Pol-β (Yuhas et al., 2021). Pol-β is an essential component of the BER pathway which was previously shown to maintain a synthetic lethal relation with KRAS G13D in an RNAi screen. Compound 14 irreversibly inhibits the ability of Pol-β to bind to the DNA by covalently targeting two lysine residues while sparing other DNA polymerases. Remarkably, treatment with pro-14 (a prodrug derived from compound 14) promoted very low toxicity but could potentiate the cytotoxic effects of DNA damaging agents in mouse embryonic fibroblasts and HeLa cells (Yuhas et al., 2021). It will be interesting to test the ability of this new inhibitor to kill KRAS mutant cells as a mono-therapy (since Pol-β has been shown to be synthetic lethal with mutant KRAS), and to determine if this is a viable therapeutic strategy.

A different flourishing area in the RAS targeting endeavor involves RNA technology. RNAi against KRAS G12D, the most common RAS mutation in human cancer, holds the promise of very high specificity and efficient tumor killing. Recent advances in RNA delivery *in vivo* have prompted this approach to clinical trials. One of the studies is a phase 1/2a clinical trial in which a small biodegradable polymeric device directly implanted in locally advanced pancreatic tumors was used to slowly administer siRNAs against KRAS G12D over 4 months, with concomitant chemotherapy with DNA damaging agents. The treatment was shown to be safe and well tolerated, and 10/12

patients showed stable disease, and 2 showed partial response (Golan et al., 2015). These results fostered a still ongoing multinational phase 2 trial (NCT01676259) to determine the progression-free survival in patients with locally advanced pancreatic tumors receiving the treatment described above.

In another phase 1 clinical trial currently in progress (NCT03608631), exosomes containing siRNAs against KRAS G12D are being administered intraperitoneally to patients with metastatic pancreatic cancer. These exosomes are engineered to bear the CD47 surface protein, which helps to avoid clearance by monocytes, therefore increasing the stability of exosomes. This study relies on encouraging preclinical data in which these engineered exosomes showed a remarkable ability to suppress pancreatic cancer and significantly increase survival in mice when administered intraperitoneally (Kamerkar et al., 2017).

However, RNAi is not the only RNA system with potential clinical applications. Circular RNAs (circRNAs) are also capable of controlling the fate of mutant RAS cancer cells. This type of RNA was discovered several decades ago, but only recently started drawing researchers' attention (Kristensen et al., 2021). These transcripts consist of one or multiple exons of a coding gene covalently circularized in a process known as back-splicing (Kristensen et al., 2021). Interestingly, circRNAs can control several cellular events through their interaction with RNA-binding proteins, microRNAs, or with their genomic parent locus. It has been hypothesized that circRNAs are part of an RNA interaction network and compete with mRNAs for microRNA binding (Salmena et al., 2011). Therefore, circRNAs can, for instance, increase mRNA abundance by outcompeting mRNAs for microRNA binding. The regulation exerted by circRNAs can occur both in cis and in trans, but regulation in cis is expected to be quite common because both mRNAs and circRNAs can share microRNA Response Elements (MREs), since they are transcribed from the same gene.

Recent work has demonstrated interesting links between circRNA, the DDR, and oncogenic RAS. Experimental and bioinformatic evidence support the transcription of circRNAs from several DDR genes, including ATM, ATR, CHK1, CHK2, TP53BPP1, NBS1, MRE11, RAD50, and SMARCA5 (Papaspyropoulos et al., 2021). For most of these circRNAs, the microRNA targets remain to be validated, but the role of circSMARCA5 was recently elucidated. The SMARCA5 protein is a member of the SWI/SNF complex, a chromatin remodeler necessary for the recruitment of DDR components. Specifically, SMARCA5 promotes H2AX phosphorylation and ubiquitylation in response to DNA damage, and it is overexpressed in prostate and hepatic cancer (Xu et al., 2020). Conversely, circSMARCA5, the circular RNA produced from the SMARCA5 gene, is downregulated in the prostate, hepatic, and breast cancer. Mechanistically, circSMARCA5 interacts with its parent locus on the genomic DNA and promotes premature termination of the circSMARCA mRNA, ultimately leading to a truncated nonfunctional protein. Therefore, circSMARA5 expression indirectly decreases the DNA repair capacity, consequently increasing sensitivity to the DNA damaging agents cisplatin and bleomycin (Xu et al., 2020).

Interestingly, mutant KRAS decreases the expression of a large number of circRNAs, including circSMARCA5 (Dou et al., 2016). This kind of interactions could be exploited to target the DDR in cancer cells using novel RNA *in vivo* delivery methods to administer DDR-hindering RNAs such as circSMARCA5 in combination with DNA damaging agents. An advantage of RNA-based treatments is that different transcripts could be delivered at once, and tumor RNA profiles could be used to personalize RNA cocktails.

It is worth mentioning that therapies that target the DDR take advantage of the exacerbated genomic stress of RAS mutant tumors, leading to intolerable levels of genomic instability and subsequent cell death. Therefore, a possible strategy could consist of first specifically targeting the DDR in combination with genotoxic agents and then using RAS-inhibiting molecules to overcome resistance to DDR inhibitors and genotoxic agents, since resistance to treatment arises very fast in many RAS mutant cancers, including PDAC (Amrutkar and Gladhaug, 2017). Experimental testing should challenge this speculative rationale.

Mutations of the RAS oncogenes have a profound impact on multiple aspects of the cell. Their effects are so diverse that the literature has met controversies around the participation of RAS in cell biology. Such is the case of its impact on the cellular redox balance and association with stress and DNA damage surveillance mechanisms. However, a comprehensive understanding of the diverse mutant RAS effects in the context of the carcinogenic process will help solve such controversies, ultimately leading to solid foundations upon which new treatments could arise.

AUTHOR CONTRIBUTIONS

RC-G, LH, and JD-C contributed to the conception and design of the review. RC-G and YA-M wrote the first draft of the manuscript. RC-G, LH, JD-C, YA-M, and MA wrote sections of the manuscript. All authors reviewed the manuscript, read, and approved the submitted version.

REFERENCES

Amrutkar, M., and Gladhaug, I. (2017). Pancreatic Cancer Chemoresistance to Gemcitabine. *Cancers* 9, 157. doi:10.3390/cancers9110157

Barnoud, T., Donninger, H., and Clark, G. J. (2016). Ras Regulates Rb via NORE1A. *J. Biol. Chem.* 291, 3114–3123. doi:10.1074/jbc.M115.697557

Batsi, C., Markopoulou, S., Vartholomatos, G., Georgiou, I., Kanavaros, P., Gorgoulis, V. G., et al. (2009). Chronic NF-κB Activation Delays RasV12-Induced Premature Senescence of Human Fibroblasts by Suppressing the DNA Damage Checkpoint Response. *Mech. Ageing Dev.* 130, 409–419. doi:10.1016/j.mad.2009.04.002

Bernhard, E. J., Kao, G., Cox, A. D., Sebti, S. M., Hamilton, A. D., Muschel, R. J., et al. (1996). The Farnesyltransferase Inhibitor FTI-277 Radiosensitizes H-Ras-Transformed Rat Embryo Fibroblasts. *Cancer Res.* 56, 1727–1730.

Bernhard, E. J., McKenna, W. G., Hamilton, A. D., Sebti, S. M., Qian, Y., Wu, J. M., et al. (1998). Inhibiting Ras Prenylation Increases the Radiosensitivity of

Human Tumor Cell Lines with Activating Mutations of Ras Oncogenes. *Cancer Res.* 58, 1754–1761.

Bernhard, E. J., Stanbridge, E. J., Gupta, S., Gupta, A. K., Soto, D., Bakanauskas, V. J., et al. (2000). Direct Evidence for the Contribution of Activated N-Ras and K-Ras Oncogenes to Increased Intrinsic Radiation Resistance in Human Tumor Cell Lines. *Cancer Res.* 60, 6597–6600.

Blackford, A. N., and Jackson, S. P. (2017). ATM, ATR, and DNA-PK: The Trinity at the Heart of the DNA Damage Response. *Mol. Cel.* 66, 801–817. doi:10.1016/j.molcel.2017.05.015

Caiola, E., Salles, D., Frapolli, R., Lupi, M., Rotella, G., Ronchi, A., et al. (2015). Base Excision Repair-Mediated Resistance to Cisplatin in KRAS(G12C) Mutant NSCLC Cells. *Oncotarget* 6, 30072–30087. doi:10.18632/oncotarget.5019

Carón, R. W., Yacoub, A., Li, M., Zhu, X., Mitchell, C., Hong, Y., et al. (2005). Activated Forms of H-RAS and K-RAS Differentially Regulate Membrane Association of PI3K, PDK-1, and AKT and the Effect of Therapeutic Kinase Inhibitors on Cell Survival. *Mol. Cancer Ther.* 4, 257–270. doi:10.4161/cc.4.3.1249

Cattaneo, F., Guerra, G., Parisi, M., De Marinis, M., Tafuri, D., Cinelli, M., et al. (2014). Cell-Surface Receptors Transactivation Mediated by G Protein-Coupled Receptors. *Ijms* 15, 19700–19728. doi:10.3390/ijms151119700

Cho, H.-J., Jeong, H. G., Lee, J.-S., Woo, E.-R., Hyun, J.-W., Chung, M.-H., et al. (2002). Oncogenic H-Ras Enhances DNA Repair through the Ras/Phosphatidylinositol 3-Kinase/Rac1 Pathway in NIH3T3 Cells. *J. Biol. Chem.* 277, 19358–19366. doi:10.1074/jbc.M200933200

DeNicola, G. M., Karreth, F. A., Humpton, T. J., Gopinathan, A., Wei, C., Frese, K., et al. (2011). Oncogene-Induced Nrf2 Transcription Promotes ROS Detoxification and Tumorigenesis. *Nature* 475, 106–109. doi:10.1038/nature10189

Di Micco, R., Fumagalli, M., Cicalese, A., Piccinin, S., Gasparini, P., Luise, C., et al. (2006). Oncogene-Induced Senescence Is a DNA Damage Response Triggered by DNA Hyper-Replication. *Nature* 444, 638–642. doi:10.1038/nature05327

Di Micco, R., Fumagalli, M., and d'Adda di Fagagna, F. (2007). Breaking News: High-Speed Race Ends in Arrest–How Oncogenes Induce Senescence. *Trends Cel. Biol.* 17, 529–536. doi:10.1016/j.tcb.2007.07.012

Donninger, H., Calvisi, D. F., Barnoud, T., Clark, J., Schmidt, M. L., Vos, M. D., et al. (2015). NORE1A Is a Ras Senescence Effector that Controls the Apoptotic/senescent Balance of P53 via HIPK2. *J. Cel Biol.* 208, 777–789. doi:10.1083/jcb.201408087

Dou, Y., Cha, D. J., Franklin, J. L., Higginbotham, J. N., Jeppesen, D. K., Weaver, A. M., et al. (2016). Circular RNAs Are Down-Regulated in KRAS Mutant Colon Cancer Cells and Can Be Transferred to Exosomes. *Sci. Rep.* 6, 37982. doi:10.1038/srep37982

Drugan, J. K., Rogers-Graham, K., Gilmer, T., Campbell, S., and Clark, G. J. (2000). The Ras/p120 GTPase-Activating Protein (GAP) Interaction Is Regulated by the P120 GAP Pleckstrin Homology Domain. *J. Biol. Chem.* 275, 35021–35027. doi:10.1074/jbc.M004386200

Esposito, D., Stephen, A. G., Turbyville, T. J., and Holderfield, M. (2019). New Weapons to Penetrate the Armor: Novel Reagents and Assays Developed at the NCI RAS Initiative to Enable Discovery of RAS Therapeutics. *Semin. Cancer Biol.* 54, 174–182. doi:10.1016/j.semcancer.2018.02.006

Gaillard, H., García-Muse, T., and Aguilera, A. (2015). Replication Stress and Cancer. *Nat. Rev. Cancer* 15, 276–289. doi:10.1038/nrc3916

Gilad, O., Nabet, B. Y., Ragland, R. L., Schoppy, D. W., Smith, K. D., Durham, A. C., et al. (2010). Combining ATR Suppression with Oncogenic Ras Synergistically Increases Genomic Instability, Causing Synthetic Lethality or Tumorigenesis in a Dosage-dependent Manner. *Cancer Res.* 70, 9693–9702. doi:10.1158/0008-5472.CAN-10-2286

Goebel, L., Müller, M. P., Goody, R. S., and Rauh, D. (2020). KRasG12C Inhibitors in Clinical Trials: a Short Historical Perspective. *RSC Med. Chem.* 11, 760–770. doi:10.1039/d0md00096e

Golan, T., Khvalevsky, E. Z., Hubert, A., Gabai, R. M., Hen, N., Segal, A., et al. (2015). RNAi Therapy Targeting KRAS in Combination with Chemotherapy for Locally Advanced Pancreatic Cancer Patients. *Oncotarget* 6, 24560–24570. doi:10.18632/oncotarget.4183

Grabocka, E., Pylayeva-Gupta, Y., Jones, M. J. K., Lubkov, V., Yemanaberhan, E., Taylor, L., et al. (2014). Wild-type H- and N-Ras Promote Mutant K-Ras-Driven Tumorigenesis by Modulating the DNA Damage Response. *Cancer Cell* 25, 243–256. doi:10.1016/j.ccr.2014.01.005

Grabocka, E., Commisso, C., and Bar-Sagi, D. (2015). Molecular Pathways: Targeting the Dependence of Mutant RAS Cancers on the DNA Damage Response. *Clin. Cancer Res.* 21, 1243–1247. doi:10.1158/1078-0432.CCR-14-0650

Gupta, A. K., Bakanauskas, V. J., Cerniglia, G. J., Cheng, Y., Bernhard, E. J., Muschel, R. J., et al. (2001). The Ras Radiation Resistance Pathway. *Cancer Res.* 61, 4278–4282.

Hähnel, P. S., Enders, B., Sasca, D., Roos, W. P., Kaina, B., Bullinger, L., et al. (2014). Targeting Components of the Alternative NHEJ Pathway Sensitizes KRAS Mutant Leukemic Cells to Chemotherapy. *Blood* 123, 2355–2366. doi:10.1182/blood-2013-01-477620

Hancock, J. F. (2003). Ras Proteins: Different Signals from Different Locations. *Nat. Rev. Mol. Cel Biol.* 4, 373–385. doi:10.1038/nrm1105

Hansen, R., Peters, U., Babbar, A., Chen, Y., Feng, J., Janes, M. R., et al. (2018). The Reactivity-Driven Biochemical Mechanism of Covalent KRASG12C Inhibitors. *Nat. Struct. Mol. Biol.* 25, 454–462. doi:10.1038/s41594-018-0061-5

Hobbs, G. A., Der, C. J., and Rossman, K. L. (2016). RAS Isoforms and Mutations in Cancer at a Glance. *J. Cel. Sci.* 129, 1287–1292. doi:10.1242/jcs.182873

Irani, K., Xia, Y., Zweier, J. L., Sollott, S. J., Der, C. J., Fearon, E. R., et al. (1997). Mitogenic Signaling Mediated by Oxidants in Ras-Transformed Fibroblasts. *Science* 275, 1649–1652. doi:10.1126/science.275.5306.1649

Jančík, S., Drábek, J., Radzioch, D., and Hajdúch, M. (2010). Clinical Relevance of KRAS in Human Cancers. *J. Biomed. Biotechnol.* 2010, 1–13. doi:10.1155/2010/150960

Jett, K., and Friedman, J. M. (2010). Clinical and Genetic Aspects of Neurofibromatosis 1. *Genet. Med.* 12, 1–11. doi:10.1097/GIM.0b013e3181bf15e3

Kamerkar, S., LeBleu, V. S., Sugimoto, H., Yang, S., Ruivo, C. F., Melo, S. A., et al. (2017). Exosomes Facilitate Therapeutic Targeting of Oncogenic KRAS in Pancreatic Cancer. *Nature* 546, 498–503. doi:10.1038/nature22341

Kim, M. J., Chang, H., Nam, G., Ko, Y., Kim, S. H., Roberts, T. M., et al. (2021). RNAi-Based Approaches for Pancreatic Cancer Therapy. *Pharmaceutics* 13, 1638. doi:10.3390/pharmaceutics13101638

Kristensen, L. S., Jakobsen, T., Hager, H., and Kjems, J. (2021). The Emerging Roles of circRNAs in Cancer and Oncology. *Nat. Rev. Clin. Oncol.* 19, 188–206. doi:10.1038/s41571-021-00585-y

Lee, A. C., Fenster, B. E., Ito, H., Takeda, K., Bae, N. S., Hirai, T., et al. (1999). Ras Proteins Induce Senescence by Altering the Intracellular Levels of Reactive Oxygen Species. *J. Biol. Chem.* 274, 7936–7940. doi:10.1074/jbc.274.12.7936

Lee, H.-J., Cao, Y., Pham, V., Blackwood, E., Wilson, C., Evangelista, M., et al. (2017). Ras-MEK Signaling Mediates a Critical Chk1-Dependent DNA Damage Response in Cancer Cells. *Mol. Cancer Ther.* 16, 694–704. doi:10.1158/1535-7163.MCT-16-0504

Lièvre, A., Bachet, J.-B., Le Corre, D., Boige, V., Landi, B., Emile, J.-F., et al. (2006). KRAS Mutation Status Is Predictive of Response to Cetuximab Therapy in Colorectal Cancer. *Cancer Res.* 66, 3992–3995. doi:10.1158/0008-5472.CAN-06-0191

Lim, J. K. M., and Leprivier, G. (2019). The Impact of Oncogenic RAS on Redox Balance and Implications for Cancer Development. *Cell Death Dis.* 10, 955. doi:10.1038/s41419-019-2192-y

Logsdon, C. D., and Lu, W. (2016). The Significance of Ras Activity in Pancreatic Cancer Initiation. *Int. J. Biol. Sci.* 12, 338–346. doi:10.7150/ijbs.15020

Lu, S., Jang, H., Muratcioglu, S., Gursoy, A., Keskin, O., Nussinov, R., et al. (2016). Ras Conformational Ensembles, Allostery, and Signaling. *Chem. Rev.* 116, 6607–6665. doi:10.1021/acs.chemrev.5b00542

Luo, J., Emanuele, M. J., Li, D., Creighton, C. J., Schlabach, M. R., Westbrook, T. F., et al. (2009). A Genome-Wide RNAi Screen Identifies Multiple Synthetic Lethal Interactions with the Ras Oncogene. *Cell* 137, 835–848. doi:10.1016/j.cell.2009.05.006

Luo, J. (2021). KRAS Mutation in Pancreatic Cancer. *Semin. Oncol.* 48, 10–18. doi:10.1053/j.seminoncol.2021.02.003

Maciag, A., Sithanandam, G., and Anderson, L. M. (2004). Mutant K-rasV12 Increases COX-2, Peroxides and DNA Damage in Lung Cells. *Carcinogenesis* 25, 2231–2237. doi:10.1093/carcin/bgh245

Marcotte, R., Brown, K. R., Suarez, F., Sayad, A., Karamboulas, K., Krzyzanowski, P. M., et al. (2012). Essential Gene Profiles in Breast, Pancreatic, and Ovarian Cancer Cells. *Cancer Discov.* 2, 172–189. doi:10.1158/2159-8290.CD-11-0224

Marullo, R., Werner, E., Degtyareva, N., Moore, B., Altavilla, G., Ramalingam, S. S., et al. (2013). Cisplatin Induces a Mitochondrial-ROS Response that Contributes to Cytotoxicity Depending on Mitochondrial Redox Status and Bioenergetic Functions. *PLoS One* 8, e81162. doi:10.1371/journal.pone.0081162

McCormick, F. (2020). Sticking it to KRAS: Covalent Inhibitors Enter the Clinic. *Cancer Cell* 37, 3–4. doi:10.1016/j.ccell.2019.12.009

Meylan, E., Dooley, A. L., Feldser, D. M., Shen, L., Turk, E., Ouyang, C., et al. (2009). Requirement for NF-κB Signalling in a Mouse Model of Lung Adenocarcinoma. *Nature* 462, 104–107. doi:10.1038/nature08462

Mijit, M., Caracciolo, V., Melillo, A., Amicarelli, F., and Giordano, A. (2020). Role of P53 in the Regulation of Cellular Senescence. *Biomolecules* 10, 420. doi:10.3390/biom10030420

Miller, A. C., Kariko, K., Myers, C. E., Clark, E. P., and Samid, D. (1993). Increased Radioresistance of EJras-Transformed Human Osteosarcoma Cells and its Modulation by Lovastatin, an Inhibitor of P21ras Isoprenylation. *Int. J. Cancer* 53, 302–307. doi:10.1002/ijc.2910530222

Minjgee, M., Toulany, M., Kehlbach, R., Giehl, K., and Rodemann, H. P. (2011). K-RAS(V12) Induces Autocrine Production of EGFR Ligands and Mediates Radioresistance through EGFR-Dependent Akt Signaling and Activation of DNA-PKcs. *Int. J. Radiat. Oncol. Biol. Phys.* 81, 1506–1514. doi:10.1016/j.ijrobp.2011.05.057

Mo, S. P., Coulson, J. M., and Prior, I. A. (2018). RAS Variant Signalling. *Biochem. Soc. Trans.* 46, 1325–1332. doi:10.1042/BST20180173

Ogrunc, M., Di Micco, R., Liontos, M., Bombardelli, L., Mione, M., Fumagalli, M., et al. (2014). Oncogene-induced Reactive Oxygen Species Fuel Hyperproliferation and DNA Damage Response Activation. *Cell Death Differ.* 21, 998–1012. doi:10.1038/cdd.2014.16

Ostrem, J. M., Peters, U., Sos, M. L., Wells, J. A., and Shokat, K. M. (2013). K-Ras(G12C) Inhibitors Allosterically Control GTP Affinity and Effector Interactions. *Nature* 503, 548–551. doi:10.1038/nature12796

Oun, R., Moussa, Y. E., and Wheate, N. J. (2018). The Side Effects of Platinum-Based Chemotherapy Drugs: a Review for Chemists. *Dalton Trans.* 47, 6645–6653. doi:10.1039/c8dt00838h

Pamonsinlapatham, P., Hadj-Slimane, R., Lepelletier, Y., Allain, B., Toccafondi, M., Garbay, C., et al. (2009). p120-Ras GTPase Activating Protein (RasGAP): a Multi-Interacting Protein in Downstream Signaling. *Biochimie* 91, 320–328. doi:10.1016/j.biochi.2008.10.010

Papaspyropoulos, A., Hazapis, O., Lagopati, N., Polyzou, A., Papanastasiou, A. D., Liontos, M., et al. (2021). The Role of Circular Rnas in DNA Damage Response and Repair. *Cancers* 13, 5352. doi:10.3390/cancers13215352

Park, M.-T., Kim, M.-J., Suh, Y., Kim, R.-K., Kim, H., Lim, E.-J., et al. (2014). Novel Signaling axis for ROS Generation during K-Ras-Induced Cellular Transformation. *Cel Death Differ.* 21, 1185–1197. doi:10.1038/cdd.2014.34

Poon, E., Mullins, S., Watkins, A., Williams, G. S., Koopmann, J.-O., Di Genova, G., et al. (2017). The MEK Inhibitor Selumetinib Complements CTLA-4 Blockade by Reprogramming the Tumor Immune Microenvironment. *J. Immunother. Cancer* 5, 63. doi:10.1186/s40425-017-0268-8

Prior, I. A., and Hancock, J. F. (2001). Compartmentalization of Ras Proteins. *J. Cel. Sci.* 114, 1603–1608. doi:10.1242/jcs.114.9.1603

Prior, I. A., Lewis, P. D., and Mattos, C. (2012). A Comprehensive Survey of Ras Mutations in Cancer. *Cancer Res.* 72, 2457–2467. doi:10.1158/0008-5472.CAN-11-2612

Pylayeva-Gupta, Y., Grabocka, E., and Bar-Sagi, D. (2011). RAS Oncogenes: Weaving a Tumorigenic Web. *Nat. Rev. Cancer* 11, 761–774. doi:10.1038/nrc3106

Rai, P., Young, J. J., Burton, D. G. A., Giribaldi, M. G., Onder, T. T., and Weinberg, R. A. (2011). Enhanced Elimination of Oxidized Guanine Nucleotides Inhibits Oncogenic RAS-Induced DNA Damage and Premature Senescence. *Oncogene* 30, 1489–1496. doi:10.1038/onc.2010.520

Rojas, A. M., Fuentes, G., Rausell, A., and Valencia, A. (2012). The Ras Protein Superfamily: Evolutionary Tree and Role of Conserved Amino Acids. *J. Cel. Biol.* 196, 189–201. doi:10.1083/jcb.201103008

Salmena, L., Poliseno, L., Tay, Y., Kats, L., and Pandolfi, P. P. (2011). A ceRNA Hypothesis: the Rosetta Stone of a Hidden RNA Language? *Cell* 146, 353–358. doi:10.1016/j.cell.2011.07.014

Scheffzek, K., and Shivalingaiah, G. (2019). Ras-Specific GTPase-Activating Proteins-Structures, Mechanisms, and Interactions. *Cold Spring Harb Perspect. Med.* 9, a031500. doi:10.1101/cshperspect.a031500

Schlessinger, J. (2000). Cell Signaling by Receptor Tyrosine Kinases. *Cell* 103, 211–225. doi:10.1016/s0092-8674(00)00114-8

Shields, J. M., Pruitt, K., McFall, A., Shaub, A., and Der, C. J. (2000). Understanding Ras: 'it Ain't over 'til It's over'. *Trends Cel Biol.* 10, 147–154. doi:10.1016/s0962-8924(00)01740-2

Simanshu, D. K., Nissley, D. V., and McCormick, F. (2017). RAS Proteins and Their Regulators in Human Disease. *Cell* 170, 17–33. doi:10.1016/j.cell.2017.06.009

Singh, H., Longo, D. L., and Chabner, B. A. (2015). Improving Prospects for Targeting RAS. *Jco* 33, 3650–3659. doi:10.1200/jco.2015.62.1052

Sirbu, B. M., and Cortez, D. (2013). DNA Damage Response: Three Levels of DNA Repair Regulation. *Cold Spring Harbor Perspect. Biol.* 5, a012724. doi:10.1101/cshperspect.a012724

Smith, M. J., Neel, B. G., and Ikura, M. (2013). NMR-based Functional Profiling of RASopathies and Oncogenic RAS Mutations. *Proc. Natl. Acad. Sci.* 110, 4574–4579. doi:10.1073/pnas.1218173110

Stephen, A. G., Esposito, D., Bagni, R. K., and McCormick, F. (2014). Dragging Ras Back in the Ring. *Cancer Cell* 25, 272–281. doi:10.1016/j.ccr.2014.02.017

Sun, C., Fang, Y., Yin, J., Chen, J., Ju, Z., Zhang, D., et al. (2017). Rational Combination Therapy with PARP and MEK Inhibitors Capitalizes on Therapeutic Liabilities in RAS Mutant Cancers. *Sci. Transl. Med.* 9, eaal5148. doi:10.1126/scitranslmed.aal5148

Sun, C., Fang, Y., Labrie, M., Li, X., and Mills, G. B. (2020). Systems Approach to Rational Combination Therapy: PARP Inhibitors. *Biochem. Soc. Trans.* 48, 1101–1108. doi:10.1042/BST20191092

Tago, K., Funakoshi-Tago, M., Ohta, S., Kawata, H., Saitoh, H., Horie, H., et al. (2019). Oncogenic Ras Mutant Causes the Hyperactivation of NF-κB via Acceleration of its Transcriptional Activation. *Mol. Oncol.* 13, 2493–2510. doi:10.1002/1878-0261.12580

Tao, S., Wang, S., Moghaddam, S. J., Ooi, A., Chapman, E., Wong, P. K., et al. (2014). Oncogenic KRAS Confers Chemoresistance by Upregulating NRF2. *Cancer Res.* 74, 7430–7441. doi:10.1158/0008-5472.CAN-14-1439

Vetter, I. R., and Wittinghofer, A. (2001). The Guanine Nucleotide-Binding Switch in Three Dimensions. *Science* 294, 1299–1304. doi:10.1126/science.1062023

Volcic, M., Karl, S., Baumann, B., Salles, D., Daniel, P., Fulda, S., et al. (2012). NF-κB Regulates DNA Double-Strand Break Repair in Conjunction with BRCA1-CtIP Complexes. *Nucleic Acids Res.* 40, 181–195. doi:10.1093/nar/gkr687

Weinberg, F., Hamanaka, R., Wheaton, W. W., Weinberg, S., Joseph, J., Lopez, M., et al. (2010). Mitochondrial Metabolism and ROS Generation Are Essential for Kras-Mediated Tumorigenicity. *Proc. Natl. Acad. Sci. USA* 107, 8788–8793. doi:10.1073/pnas.1003428107

Woo, R. A., and Poon, R. Y. C. (2004). Activated Oncogenes Promote and Cooperate with Chromosomal Instability for Neoplastic Transformation. *Genes Dev.* 18, 1317–1330. doi:10.1101/gad.1165204

Xia, Y., Shen, S., and Verma, I. M. (2014). NF-κB, an Active Player in Human Cancers. *Cancer Immunol. Res.* 2, 823–830. doi:10.1158/2326-6066.CIR-14-0112

Xu, X., Zhang, J., Tian, Y., Gao, Y., Dong, X., Chen, W., et al. (2020). CircRNA Inhibits DNA Damage Repair by Interacting with Host Gene. *Mol. Cancer* 19, 128. doi:10.1186/s12943-020-01246-x

Yang, L., Shen, C., Estrada-Bernal, A., Robb, R., Chatterjee, M., Sebastian, N., et al. (2021). Oncogenic KRAS Drives Radioresistance through Upregulation of NRF2-53BP1-Mediated Non-homologous End-Joining Repair. *Nucleic Acids Res.* 49, 11067–11082. doi:10.1093/nar/gkab871

Yuan, T. L., Amzallag, A., Bagni, R., Yi, M., Afghani, S., Burgan, W., et al. (2018). Differential Effector Engagement by Oncogenic KRAS. *Cell Rep.* 22, 1889–1902. doi:10.1016/j.celrep.2018.01.051

Yuhas, S. C., Laverty, D. J., Lee, H., Majumdar, A., and Greenberg, M. M. (2021). Selective Inhibition of DNA Polymerase β by a Covalent Inhibitor. *J. Am. Chem. Soc.* 143, 8099–8107. doi:10.1021/jacs.1c02453

Zeman, M. K., and Cimprich, K. A. (2014). Causes and Consequences of Replication Stress. *Nat. Cel Biol.* 16, 2–9. doi:10.1038/ncb2897

Ziemann, C., Bürkle, A., Kahl, G. F., and Hirsch-Ernst, K. I. (1999). Reactive Oxygen Species Participate in Mdr1b mRNA and P-Glycoprotein Overexpression in Primary Rat Hepatocyte Cultures. *Carcinogenesis* 20, 407–414. doi:10.1093/carcin/20.3.407

Conflict of Interest: The authors declare that the research was conducted in the absence of any commercial or financial relationships that could be construed as a potential conflict of interest.

Advantages of publishing in Frontiers

OPEN ACCESS
Articles are free to read for greatest visibility and readership

FAST PUBLICATION
Around 90 days from submission to decision

HIGH QUALITY PEER-REVIEW
Rigorous, collaborative, and constructive peer-review

TRANSPARENT PEER-REVIEW
Editors and reviewers acknowledged by name on published articles

Frontiers
Avenue du Tribunal-Fédéral 34
1005 Lausanne | Switzerland

Visit us: www.frontiersin.org
Contact us: frontiersin.org/about/contact

REPRODUCIBILITY OF RESEARCH
Support open data and methods to enhance research reproducibility

DIGITAL PUBLISHING
Articles designed for optimal readership across devices

FOLLOW US
@frontiersin

IMPACT METRICS
Advanced article metrics track visibility across digital media

EXTENSIVE PROMOTION
Marketing and promotion of impactful research

LOOP RESEARCH NETWORK
Our network increases your article's readership